

Newcastle University

Effects of oxidative stress, exercise and cardiac rehabilitation on telomerase in T-lymphocytes

Nayef Mohammed AL Zhrany

Thesis submitted in fulfilment of requirements
of the regulation for the degree of Doctor of Philosophy

Newcastle University

Faculty of Medical Sciences

Institute of Genetic Medicine

May 2016

ABSTRACT

Effects of oxidative stress, exercise and cardiac rehabilitation on telomerase in T-lymphocytes

Myocardial infarction (MI) remains the primary cause of death worldwide, despite significant medical advances. Lymphocytes play a key role in both the pathogenesis of atherosclerosis and also the healing process following MI. It has been found however, that decreased lymphocyte telomere length correlates with greater risk of MI and worse outcomes. Atherosclerosis is causally linked with MI and can be triggered by myeloid and lymphoid cells, which destabilise and rupture lipid-rich plaques on the arterial wall. Atherosclerosis is also linked with elevated oxidative stress, increasing the risk of cardiovascular disease. Experiments *in-vitro* have shown that even mild oxidative stress caused telomere shortening and inhibits cell proliferation. Oxidative stress *in-vivo* can be caused by physical inactivity, which can contribute to atherosclerosis. Telomere length can be maintained by regular physical activity.

My results show that hyperoxia enhanced IFN- γ mRNA transcription in T-lymphocytes, whereas hypoxia significantly reduced inflammation. Oxidative stress suppressed a) *in-vitro* T-cell proliferation in a TERT-dependent way, b) telomerase activity and c) TERT expression in *mTert*-GFP $^+$ mice by 5-fold ($P<0.01$) compared to hypoxia. MAPK inhibition (MAPKi) down-regulated IFN- γ mRNA transcription and enhanced splenocyte proliferation equally under both hypoxia and hyperoxia. MAPKi enhanced telomerase activity under hyperoxia by day 10 in culture and significantly increased telomerase activity by day 14 compared to hypoxia. The effect of MAPKi seems to require the presence of TERT and interaction between cells. Voluntary wheel running led to increased telomerase activity in ApoE $^{-/-}$ *mTert*-GFP $^+$ mice on a high fat diet (HFD) compared to the no exercise group. HFD enhanced both telomerase activity and B-cell numbers under exercise compared to the same mice on a normal diet (ND). In humans, regulatory T-cells were elevated in the acute stage of MI and decreased by 7-fold ($P<0.001$) following cardiac rehabilitation. However, no significant effect was observed on telomerase activity.

DECLARATION

I hereby declare that this thesis presented my original research work and effort. Wherever contributions of others involved and other sources of information used have been specifically acknowledged.

Nayef Mohammed AL Zhrany Date: 31.05.2016

ACKNOWLEDGMENTS

I wish to extend my deepest gratitude to the many individuals who made this thesis possible. Without their help and inspiration this thesis would never have been completed.

Firstly, great thanks are due equally to: the Medical Services Department at the Ministry of Defence, represented at Prince Sultan Military Medical City (Saudi Arabia), and to Newcastle University, represented by the Institute of Genetic Medicine (IGM, UK), for giving me the opportunity to pursue my life's dream. I also wish to acknowledge the support given by the Royal Embassy of Saudi Arabia in the United Kingdom, represented by the Cultural Bureau in London.

After this four-year journey, no words can adequately express my gratitude to both of my supervisors, Prof. Ioakim Spyridopoulos and Dr. Gabriele Saretzki. Nevertheless, I am particularly indebted to these individuals for their guidance, mentorship and patience. Aside from the opportunities they gave me to participate in such a fascinating research project with its many different parts, they believed in me when my own self-belief was wavering – the times I needed their support the most. Their open-mindedness, encouragement and numerous creative discussions have made an enormous impact on my life, both within and outside this PhD. The University of Newcastle is made great by these individuals and people like them.

I am extremely grateful to my progress panel members, Dr. Kevin Marchbank and Dr. Simon Bamforth, as well as to the postgraduate coordinator team at IGM, Prof. Susan Lindsay, Dr. Joanna Elson and Dr. Helen Phillips, for their supportive ideas, suggestions, advice and encouragement.

Special thanks must also go to Prof. Deborah Henderson, Dr. Bill Chaudhry and their team, as well as to Prof. Djordje Jakovljevic and Dr. Sarah Charman for their unwavering support during the time I worked with them.

I would also like to thank all former and current members of the team led by Prof. Spyridopoulos for their help with this project.

To all the staff at the FGU, especially those who helped with the mouse work, I am forever indebted.

Finally, a big thank you is due to all the Newcastle University staff, both academic and administrative, as well as all those from other institutions who contributed to this thesis becoming a reality.

DEDICATION

Here, time stops, to turn to the other world, to the spirit of my father (Mohammed) and his father, my grandfather (Jamaan). Both passed into the hereafter during this study. I just would like to say, as I promised, I love and really miss both of you, and am sure my feelings and words will find you.

Now to return to the living; to the source of my existence, my inspiration and my perseverance. To my mum, the crown on my head and the light in my eyes; I am forever grateful to the woman who raised me, prepared me for this life and supported me to reach this point. I wish you the very best of health and happiness for a long and fulfilling future. As I promised.

To the flower of my life and Queen of my heart, who shares my life through good and bad; to my wife for loving me, supporting me and building my confidence throughout my studies. I love you dearly.

To my two great sons, Saeed and Mohammed, as well as my little princess, Neven, for giving me love, happiness and hope. I love you and wish you all a healthy and happy future.

Finally, to all my brothers, my sisters, and the rest of my family. I wish you health and happiness for all time.

PUBLICATION

Bennaceur, K., Atwill, M., Al Zhrany, N., Hoffmann, J., Keavney, B., Breault, D., Richardson, von Zglinicki, T., Saretzki, G., Spyridopoulos, I. (2014) 'Atorvastatin induces T cell proliferation by a telomerase reverse transcriptase (TERT) mediated mechanism', *Atherosclerosis*, 236(2), pp. 312–320.

TABLE OF CONTENTS

ABSTRACT	II
DECLARATION	III
ACKNOWLEDGMENTS	IV
DEDICATION	V
PUBLICATION	VI
Table of contents	VII
List of figures	XIII
List of tables	XVII
List of abbreviations	XVIII
CHAPTER 1	
INTRODUCTION	1
1.1 Functions of the immune system	1
1.1.1 Different cell types in the immune system	1
1.1.2 Acquired immunity	1
1.1.2.1 T-cells	1
1.1.2.2 B-cells	2
1.1.2.3 Monocytes	2
1.1.3 Regulation of the adaptive immune response	4
1.1.4 Role of T-lymphocytes in atherosclerosis	9
1.1.5 Regulatory T-cells (Tregs)	11
1.2 Atherosclerosis as an inflammatory disease	12
1.2.1 Pathobiology of atherosclerosis	12
1.2.2 Mediators of inflammation	12
1.2.3 Role of the immune system in inflammation and atherosclerosis	13
1.2.4 Oxidative stress	15
1.2.5 Role of the immune system in oxidative stress	19
1.2.6 Myocardial infarction as a complication of atherosclerosis	20
1.2.7 Immune response to myocardial infarction	22
1.3 Telomeres and telomerase	27
1.3.1 Biology of telomeres and telomerase	27
1.3.1.1 Telomeres	27
1.3.1.2 Telomerase	35
1.3.1.3 Telomerase expression	35
1.3.1.4 Telomerase functions	35
1.3.2 Role of telomerase and telomere length in cardiovascular disease	48
1.3.3 Role of telomerase and telomere length in T-lymphocytes	51
1.3.4 Interaction between oxidative stress and telomeres	53
1.4 Role of p38 MAP Kinase (MAPK) in inflammation and disease	54
1.4.1 Expression and function of MAPK	54
1.4.2 p38 MAPK Pathway	57
1.4.3 Role of MAPK inhibition/inhibitors (MAPKi) in cell death	57
1.4.4 Role of MAPKi in inflammation	58

1.4.5 Role of MAPKi in myocardial infarction	58
1.4.6 p38 MAPK knockout mice	59
1.5 Exercise and cardiac rehabilitation	61
1.5.1 Effects of exercise on the immune system	61
1.5.2 Exercise and atherosclerosis	63
1.5.3 Effects of exercise on telomerase activity and telomere length	64
1.5.4 Cardiac rehabilitation and its phases	65
1.6 Aims and hypothesis	68
CHAPTER 2	
MATERIAL AND METHODS	70
2.1 Materials	70
2.1.1 Plasticware	70
2.1.2 Media, antibodies and chemicals	70
2.2 Methods	71
2.2.1 Mouse lines and Ethics statements	71
2.2.1.1 TERT ^{+/+} (C57BL/6), TERT ^{-/-} and TERT ^{+/−} mice	71
2.2.1.2 <i>mTert</i> ^{+/+} GFP ⁺ mice	73
2.2.1.3 ApoE ^{-/-} <i>mTert</i> -GFP ⁺ mice	75
2.2.1.4 Mouse diet	76
2.2.2 Mouse dissection and isolation of spleen and thymus	76
2.2.3 Cryopreservation of cells	78
2.2.4 TCR stimulation	78
2.2.5 Mouse PBMNCs culture	79
2.2.5.1 Cell culture in 96-well plates	79
2.2.5.2 Cell culture in 24-well plates	79
2.2.5.3 Cell culture in 6-well plates	80
2.2.5.4 Cell culture in 25cm ² flask	80
2.2.6 Immunomagnetic sorting of mouse CD4 ⁺ T-cells	81
2.2.7 Long-term culture of splenocytes and CD4 ⁺ T-lymphocytes	82
2.2.8 Hypoxia, normoxia and hyperoxia	83
2.2.9 Quantification of TERT ^{+/+} and <i>mTert</i> -GFP ⁺ (cells) splenocytes, thymocytes and T-lymphocytes	83
2.2.9.1 Flow cytometry (FACS)	84
2.2.9.2 Strategy of FACS gating wild-type cells	87
2.2.9.3 Strategy of FACS gating of <i>mTert</i> -GFP ⁺ cells	87
2.2.10 Quantification of oxidative stress and mitochondrial membrane potential	88
2.2.11 Quantification of telomerase activity by TRAP-PCR ELISA	89
2.2.12 Total RNA isolation and cDNA synthesis	91
2.2.13 Quantitative Polymerase Chain Reaction (q-PCR)	93
2.2.14 Quantification of mouse regulatory T-cells	94
2.2.15 Voluntary wheel running of mice and quantification of running parameters with Spike2 (7.12) software	95

2.2.16 Patient recruitment, inclusion and exclusion criteria	96
2.2.17 Accelerometer and GENEActive software for the analysis of daily activity in patients with myocardial infarction (MI)	96
2.2.17.1 Accelerometer data processing and analysis	97
2.2.18 Cardiac rehabilitation programme	98
2.2.19 Human regulatory T-cells quantification	99
2.2.20 Human whole blood TruCount	101
2.2.21 Telomere length determination in human PBMNCs	102
2.2.22 Statistical analysis	102
 CHAPTER 3	
Effect of mild chronic oxidative stress on proliferation and regulation of telomerase in splenocytes and CD4⁺ T-lymphocytes	103
3.1 Introduction	103
3.2 Results	104
3.2.1 Hyperoxia induces oxidative stress and inflammation in lymphocytes	104
3.2.1.1 Hyperoxia induces oxidative stress in splenocytes and CD4⁺ T-cells	104
3.2.1.2 The effect of hyperoxia on mitochondrial membrane potential levels in splenocytes and CD4⁺ T-cells	104
3.2.1.3 Oxidative stress produces inflammation in mice splenocytes	105
3.2.2 Hyperoxia suppresses splenocyte proliferation by a telomerase dependent mechanism	109
3.2.2.1 Effects of telomerase and oxidative stress on splenocyte proliferation	109
3.2.2.2 Effect of telomerase and oxidative stress on proliferation of different splenocyte subsets	109
3.2.3 Role of telomerase in CD4⁺ T-cell proliferation	113
3.2.4 mTert-GFP⁺ (telomerase reporter) mice used to investigate the regulation of telomerase in lymphocytes	116
3.2.4.1 Effect of oxidative stress on splenocyte proliferation from transgenic mTert-GFP⁺ mice	116
3.2.4.2 Effect of oxidative stress on proliferation of subsets of transgenic mTert-GFP⁺ splenocytes	116
3.2.4.3 Oxidative stress downregulates transgenic mTert-GFP⁺ expression in splenocytes	118
3.2.4.4 Oxidative stress represses telomerase activity in splenocytes	119
3.2.5 Telomerase confers resistance to cell death in splenocytes	124
3.3 Discussion	127

CHAPTER 4	
Effect of MAPK inhibition on splenocytes and CD4⁺ T-lymphocytes under chronic mild oxidative stress	129
4.1 Introduction	129
4.2 Results	129
4.2.1 Effect of MAPKi on IFN-gamma mRNA transcription under oxidative stress	129
4.2.2 Effect of MAPK inhibition on splenocyte proliferation under oxidative stress	131
4.2.2.1 Effect of MAPK inhibition on lymphocyte proliferation under oxidative stress	131
4.2.2.2 Effect of MAPK inhibition on proliferation of lymphocyte subsets under oxidative stress	131
4.2.3 Effect of MAPK inhibition on splenocyte telomerase expression (<i>mTert</i> -GFP ⁺) and telomerase activity under oxidative stress	137
4.2.3.1 Effect of MAPK inhibition on <i>mTert</i> -GFP ⁺ /reporter lymphocyte proliferation under oxidative stress	137
4.2.3.2 Effect of MAPK inhibition on proliferation of lymphocyte subsets from <i>mTert</i> -GFP ⁺ mice under oxidative stress	138
4.2.3.3 Effect of MAPK inhibition on telomerase activation in splenocytes under oxidative stress	138
4.2.4 Effect of MAPK inhibition on the proliferation of activated pure CD4 ⁺ T-cells under oxidative stress	143
4.3 Discussion	145
CHAPTER 5	
Effect of voluntary exercise on telomerase and regulatory T-lymphocytes in mice	147
5.1 Introduction	147
5.2 Results	148
5.2.1 Effect of voluntary wheel running exercise on C57BL/6 wild-type mice	148
5.2.1.1 Variability and spatial pattern of speed and duration during voluntary wheel running exercise on C57BL/6 wild-type mice	148
5.2.1.2 Diurnal pattern of C57BL/6 wild-type mice on voluntary wheel running exercise	149
5.2.2 Effect of voluntary wheel running exercise on TERT ^{+/−} (heterozygous) mice	151
5.2.2.1 Variability and spatial pattern of speed and duration during voluntary wheel running exercise on TERT ^{+/−} (heterozygous) mice	151
5.2.2.2 Diurnal pattern of TERT ^{+/−} (heterozygous) mice on voluntary wheel running exercise	152

5.2.2.3	Effect of voluntary wheel running exercise on weight of TERT^{+/−} (heterozygous) mice	152
5.2.2.4	Effect of voluntary wheel running exercise on splenocyte numbers in TERT^{+/−} (heterozygous) mice	152
5.2.2.5	Effect of voluntary wheel running exercise on splenocyte subpopulations of TERT^{+/−} (heterozygous) mice	152
5.2.2.6	Effect of voluntary wheel running exercise on splenocyte regulatory T-cells of TERT^{+/−} mice	153
5.2.3	Effects of voluntary wheel running exercise on <i>mTert</i>-GFP⁺ mice	160
5.2.3.1	Variability and spatial pattern of speed and duration during voluntary wheel running exercise on <i>mTert</i>-GFP⁺ mice	160
5.2.3.2	Diurnal pattern of <i>mTert</i>-GFP⁺ mice on voluntary wheel running exercise	160
5.2.3.3	Effect of voluntary wheel running exercise on body weights of <i>mTert</i>-GFP⁺ mice	160
5.2.3.4	Effect of voluntary wheel running exercise on splenocyte numbers in <i>mTert</i>-GFP⁺ mice	161
5.2.3.5	Effect of voluntary wheel running exercise on splenocyte subpopulations of <i>mTert</i>-GFP⁺ mice	161
5.2.4	Effect of voluntary wheel running exercise on ApoE^{−/−}<i>mTert</i>-GFP⁺ mice	167
5.2.4.1	Variability and spatial pattern of speed and duration during voluntary wheel running exercise on ApoE^{−/−}<i>mTert</i>-GFP⁺ mice	167
5.2.4.2	Diurnal pattern of ApoE^{−/−}<i>mTert</i>-GFP⁺ mice on voluntary wheel running exercise	169
5.2.4.3	Effect of voluntary wheel running exercise on body weight of ApoE^{−/−}<i>mTert</i>-GFP⁺ mice	169
5.2.4.4	Effect of voluntary wheel running on telomerase activity in ApoE^{−/−}<i>mTert</i>-GFP⁺ mice	174
5.2.4.5	Effect of voluntary wheel running on splenocyte numbers in ApoE^{−/−}<i>mTert</i>-GFP⁺ mice	176
5.2.4.6	Effect of voluntary wheel running on B-cell numbers in ApoE^{−/−}<i>mTert</i>-GFP⁺ mice	176
5.2.4.7	Effect of voluntary wheel running on CD8⁺ T-cell numbers in ApoE^{−/−}<i>mTert</i>-GFP⁺ mice	177
5.2.4.8	Effect of voluntary wheel running on GFP⁺B-cell numbers in ApoE^{−/−}<i>mTert</i>-GFP⁺ mice	177
5.2.4.9	Effect of voluntary wheel running on other splenocyte subset numbers in ApoE^{−/−}<i>mTert</i>-GFP⁺ mice	178
5.2.4.10	Effect of voluntary wheel running on percentage of B-cells (thymocytes) in ApoE^{−/−}<i>mTert</i>-GFP⁺ mice	184
5.2.4.11	Effect of voluntary wheel running on percentage of total GFP⁺ (thymocytes) in ApoE^{−/−}<i>mTert</i>-GFP⁺ mice	184
5.2.4.12	Effect of voluntary wheel running on percentage of CD4⁺ T-cells (thymocytes) in ApoE^{−/−}<i>mTert</i>-GFP⁺ mice	185
5.2.4.13	Effect of voluntary wheel running on percentage of DP T-cells and other Thymocyte subsets in ApoE^{−/−}<i>mTert</i>-GFP⁺ mice	186

5.3. Discussion	192
CHAPTER 6	
Effect of cardiac rehabilitation on telomerase and regulatory T-lymphocytes in patients following acute myocardial infarction	198
6.1 Introduction	198
6.2 Results	199
6.2.1 Accelerometer-based physiological response to cardiac rehabilitation	199
6.2.1.1 Effect of cardiac exercise rehabilitation on patients' weight and BMI	199
6.2.1.2 Effect of cardiac rehabilitation on daily physical activity	199
6.2.1.3 Time spent per day in moderate to vigorous physical activity (MVPA)	200
6.2.1.4 Daily physical activity as acceleration distribution	200
6.2.2 Effect of cardiac rehabilitation on lymphocyte subsets	206
6.2.2.1 Effect of cardiac rehabilitation on T-lymphocytes	206
6.2.2.2 Effect of cardiac rehabilitation on CD4⁺ and CD8⁺ T-lymphocytes	206
6.2.2.3 Effect of cardiac rehabilitation on other lymphocyte subset	207
6.2.3. Effect of cardiac rehabilitation on regulatory T-cells	212
6.2.4 Effect of cardiac rehabilitation on telomerase activity and telomere length	215
6.2.4.1 Effect of cardiac rehabilitation on telomerase activity	215
6.2.4.2 Effect of cardiac rehabilitation on telomere length	215
6.3. Discussion	220
CHAPTER 7	
GENERAL DISCUSSION	223
7.1 Telomerase regulation under hyperoxia and hypoxia <i>in vitro</i>	223
7.2 Effects of mitogen-activated protein kinases inhibition (MAPKi) on telomerase under oxidative stress	225
7.3 Voluntary wheel running exercise increases telomerase activity in splenocytes in mice	227
7.4 Cardiac exercise rehabilitation reduces Tregs in PBMNCs after myocardial infarction (MI) in humans	233
7.5 Limitations of my study	236
7.6 Future experiments	237
REFERENCES	238

LIST OF FIGURES

Figure 1.1.	Illustration of the immune cells from origin to differentiation	3
Figure 1.2.	TCR signaling pathway to T-cell activation	6
Figure 1.3.	ROS formation and metabolism	17
Figure 1.4.	Telomere location and structure	29
Figure 1.5.	Structure of T and D loops	29
Figure 1.6.	Illustration of how the DNA damage response pathway leads to cellular senescence	34
Figure 1.7.	Telomerase function as a reverse transcriptase	37
Figure 1.8.	MAPK signaling pathway in normal and tumor cells.	56
Figure 1.9.	Interaction between exercise, cardiovascular system and the immune system.	63
Figure 2.1.	Illustration of wild type TERT gene and the TERT knockout construct	72
Figure 2.2.	Illustration of the <i>mTert</i> -GFP ⁺ construct	73
Figure 2.3.	A diagram illustrating the principle of a reporter gene	74
Figure 2.4.	ApoE ^{-/-} <i>mTert</i> -GFP ⁺ mouse generation	76
Figure 2.5.	Cell counting steps	77
Figure 2.6.	Two modes of splenocytes T-cell receptor activation in splenocytes	78
Figure 2.7.	CD4 ⁺ T-cell purification after expansion	82
Figure 2.8.	Flow cytometer principle	86
Figure 2.9.	Flow cytometry analysis on single cell level	86
Figure 2.10.	FACS gating strategy for wild-type cells	87
Figure 2.11.	FACS gating strategy for <i>mTert</i> -GFP ⁺ mice cells	88
Figure 2.12.	Illustration of the computer system for the mouse voluntary wheel running exercise	95
Figure 2.13.	GENEActive devices	98
Figure 2.14.	FACS gating strategy for human regulatory T-cells quantification	101
Figure 3.1.	Oxidative stress levels as measured by dihydroethidium (DHE) fluorescence.	106
Figure 3.2.	Mitochondrial membrane potential levels as measured by JC-1 fluorescence ratio.	107
Figure 3.3.	Oxidative stress enhanced transcription of IFN-gamma mRNA.	108
Figure 3.4.	Proliferation of splenocytes depends on the level of oxygen saturation and the presence of telomerase (TERT)	111
Figure 3.5.	Long-term culture and growth curves of different splenocyte subpopulations under different oxygen saturation levels	112
Figure 3.6.	The influence of TERT ^{+/+} and oxidative stress on long-term culture and growth curve of CD4 ⁺ T-cells	115
Figure 3.7.	Splenocytes from transgenic <i>mTert</i> -GFP ⁺ grow better under 3% than 40% oxygen saturation	120
Figure 3.8.	Long-term growth curves of different lymphocyte subsets from transgenic <i>mTert</i> -GFP ⁺ mice splenocytes under different oxygen saturation	121
Figure 3.9.	Number of GFP ⁺ cells in each splenocyte subset that express TERT gene from transgenic <i>mTert</i> -GFP ⁺ mice	122
Figure 3.10.	Telomerase activity in splenocytes from wild-type mice is higher under 3% than under 40% oxygen saturation	123

Figure 3.11.	Percentage of GFP ⁺ cells from <i>mTert</i> -GFP ⁺ mice that were cultured under different oxygen saturation, presented as a FACS dot plot	123
Figure 3.12.	Measurement of oxidative stress levels and mitochondrial membrane potential levels under 20% oxygen saturation.	125
Figure 3.13.	Telomerase positive cells survive better than telomerase negative cells under normoxia	126
Figure 4.1.	MAPKi regulate transcription of IFN-gamma mRNA in splenocytes under oxidative stress.	130
Figure 4.2.	Long-term culture and growth curve of splenocytes treated with 500nM MAPKi under different oxygen saturations	133
Figure 4.3.	Long-term culture and growth curve of splenocyte subsets treated with 500nM MAPKi under different oxygen saturations.	136
Figure 4.4.	Long-term culture and growth curve of splenocytes from transgenic <i>mTert</i> -GFP ⁺ mice treated with 500nM MAPKi under different oxygen saturations.	139
Figure 4.5.	Long-term growth curve of T-cells from transgenic <i>mTert</i> -GFP ⁺ mouse splenocytes treated with 500nM MAPKi under different oxygen saturations.	140
Figure 4.6.	MAPKi treatment rescues telomerase activity in wild-type mice splenocytes treated under hyperoxia	141
Figure 4.7.	MAPKi improves proliferation of pure CD4 ⁺ T-cells under 3% oxygen in a TERT dependent manner	144
Figure 5.1.	Daily running parameters for TERT ^{+/+} wild-type mice:	149
Figure 5.2	Diurnal pattern of average wheel rotations per hour for TERT ^{+/+} wild-type mice	150
Figure 5.3.	Daily running parameters for TERT ⁺⁻ (heterozygous) mice	154
Figure 5.4.	Diurnal pattern of average wheel rotations per hour for TERT ⁺⁻ (heterozygous) mice	155
Figure 5.5.	Body weight of TERT-heterozygous mice	156
Figure 5.6.	Splenocyte numbers of TERT ⁺⁻ heterozygous mice with and without exercise	157
Figure 5.7.	Percentage of splenocytes subset of TERT ⁺⁻ heterozygous mice with and with out exercise.	158
Figure 5.8.	Percentage of regulatory T-cells in TERT ⁺⁻ mice during exercise	159
Figure 5.9.	Daily running parameters for <i>mTert</i> -GFP ⁺ mice	162
Figure 5.10.	Diurnal pattern of average wheel rotations per hour for <i>mTert</i> -GFP ⁺ mice	163
Figure 5.11.	Body weight of <i>mTert</i> -GFP ⁺ mice with and without exercise	164
Figure 5.12.	Number of splenocytes from <i>mTert</i> -GFP ⁺ mice with and without exercise	165
Figure 5.13.	Percentage of splenocyte subpopulations in <i>mTert</i> -GFP ⁺ mice with and without exercise	166
Figure 5.14.	Daily running parameters for ApoE ^{-/-} <i>mTert</i> -GFP ⁺ mice	171
Figure 5.15.	Diurnal pattern of average wheel rotations per hour for ApoE ^{-/-} <i>mTert</i> -GFP ⁺ mice	172
Figure 5.16.	Body weight and calorie intake ApoE ^{-/-} <i>mTert</i> -GFP ⁺ and ApoE ^{+/+} <i>mTert</i> -GFP ⁺ mice on different diets with and without exercise	173

Figure 5.17.	Telomerase activity for ApoE ^{-/-} <i>mTert</i> -GFP ⁺ and ApoE ^{+/+} <i>mTert</i> -GFP ⁺ mice on different diets with and without exercise	175
Figure 5.18.	Splenocyte numbers for ApoE ^{-/-} <i>mTert</i> -GFP ⁺ and ApoE ^{+/+} <i>mTert</i> -GFP ⁺ mice on different diets with and without exercise	179
Figure 5.19.	B-cell (splenocytes) numbers for ApoE ^{-/-} <i>mTert</i> -GFP ⁺ and ApoE ^{+/+} <i>mTert</i> -GFP ⁺ mice on different diets with and without exercise	180
Figure 5.20.	CD8 ⁺ T-cell (splenocytes) numbers for ApoE ^{-/-} <i>mTert</i> -GFP ⁺ and ApoE ^{+/+} <i>mTert</i> -GFP ⁺ mice on different diets with and without exercise	181
Figure 5.21.	GFP ⁺ B-cell (splenocytes) numbers for ApoE ^{-/-} <i>mTert</i> -GFP ⁺ and ApoE ^{+/+} <i>mTert</i> -GFP ⁺ mice on different diets with and without exercise	182
Figure 5.22.	Number of other splenocyte subsets from ApoE ^{-/-} <i>mTert</i> -GFP ⁺ and ApoE ^{+/+} <i>mTert</i> -GFP ⁺ mice on different diets with and without exercise	183
Figure 5.23.	Percentage of B-cells in the thymus of ApoE ^{-/-} <i>mTert</i> -GFP ⁺ and ApoE ^{+/+} <i>mTert</i> -GFP ⁺ mice on different diets with and without exercise	187
Figure 5.24.	Percentage of total GFP ⁺ in the thymus of ApoE ^{-/-} <i>mTert</i> -GFP ⁺ and ApoE ^{+/+} <i>mTert</i> -GFP ⁺ mice on different diets with and without exercise	188
Figure 5.25.	Percentage of CD4 ⁺ T-cells in the thymus of ApoE ^{-/-} <i>mTert</i> -GFP ⁺ and ApoE ^{+/+} <i>mTert</i> -GFP ⁺ mice on different diets with and without exercise	189
Figure 5.26.	Percentage of DP T-cells in the thymus of ApoE ^{-/-} <i>mTert</i> -GFP ⁺ and ApoE ^{+/+} <i>mTert</i> -GFP ⁺ mice on different diets with and without exercise	190
Figure 5.27.	Percentages of other thymocyte subsets for ApoE ^{-/-} <i>mTert</i> -GFP ⁺ and ApoE ^{+/+} <i>mTert</i> -GFP ⁺ mice on different diets with and without exercise	191
Figure 6.1.	Cardiac patients' weight and BMI pre- and post-cardiac exercise rehabilitation.	201
Figure 6.2.	Acceleration for cardiac patients pre- and post-cardiac exercise rehabilitation	202
Figure 6.3.	Time spent per day in moderate to vigorous physical activity (MVPA) for pre- and Post-cardiac exercise rehabilitation.	203
Figure 6.4.	Acceleration distribution of time spent in 50 mg units-intensity for pre- and post-cardiac exercise rehabilitation.	204
Figure 6.5.	Acceleration distribution of time spent in 50 mg units-intensity for pre- and post-cardiac exercise rehabilitation.	205
Figure 6.6.	Total T-lymphocyte absolute numbers pre- and post-cardiac exercise rehabilitation	208
Figure 6.7.	Absolute numbers of CD4 ⁺ and CD8 ⁺ T-lymphocyte pre- and post-cardiac exercise rehabilitation	209
Figure 6.8.	DP T-lymphocytes absolute number and CD4 ⁺ /CD8 ⁺ T-cells ratio pre- and post-cardiac exercise rehabilitation	210
Figure 6.9.	Absolute numbers of other lymphocyte types pre- and post-cardiac exercise rehabilitation	211

Figure 6.10.	Percentage of regulatory T-cells pre- and post-cardiac exercise rehabilitation	213
Figure 6.11.	Illustration of the detection and gating the two levels of CD25 ⁺ expression	214
Figure 6.12.	Telomerase activity in PBMNCs for MI patients pre- and post-cardiac exercise rehabilitation	217
Figure 6.13.	Telomere length in PBMNCs for MI patients pre- and post-cardiac exercise rehabilitation.	218
Figure 6.14.	Relationship between telomere length (TL) and telomerase activity (TA) in PBMNCs for MI patients with pre- and post-cardiac exercise rehabilitation.	219

LIST OF TABLES

Table 2.1. Antibodies used in immuophenotyping of mouse splenocytes and thymocytes	85
Table 2.2. TRAP reaction protocol	90
Table 2.3. Different specificities of studied primers	93
Table 2.4. Aerobic exercise types	99
Table 2.5. Antibodies and reagents used with human regulatory T-cells	100
Table 4.1. Primary cell counts ($\times 10^6$) of splenocyte growth curve from TERT ^{+/+} mice cultured under 3% oxygen saturation.	134
Table 4.2. Primary cell counts ($\times 10^6$) of splenocyte growth curve from TERT ^{+/+} mice cultured under 40% oxygen saturation.	134
Table 4.3. Primary cell counts ($\times 10^6$) of splenocyte growth curve from TERT ^{-/-} mice cultured under 3% oxygen saturation.	135
Table 4.4. Primary cell counts ($\times 10^6$) of splenocyte growth curve from TERT ^{-/-} mice cultured under 40% oxygen saturation.	135
Table 4.5. Primary results of mouse splenocyte telomerase activity measured by TRAP-ELISA (absorbance 450nM)	142
Table 5.1. Groups of ApoE ^{-/-} <i>mTert</i> -GFP ⁺ and ApoE ^{+/+} <i>mTert</i> -GFP ⁺ mice	168
Table 5.2. Body weight of ApoE ^{-/-} <i>mTert</i> -GFP ⁺ and ApoE ^{+/+} <i>mTert</i> -GFP ⁺ mice	169

LIST OF ABBREVIATIONS

(ns)	no significant
%	Percentage
$^1\text{O}_2$	singlet oxygen
ACS	acute coronary syndrome
AIDS	acquired immune deficiency syndrome
AMI	acute myocardial infarction
AP1	activator protein 1
APC	Allophycocyanin
ApoE	Apolipoprotein E
ATM	ataxia-telangiectasia mutated
ATR	ATM- and Rad3-Related
B-cells	(named after the avian ‘bursa of Fabricius’)
BCRs	B-cell receptors
bHLHZ protein	basic-helix-loop-helix-zipper protein
BIRB 796	Doramapimod
BMC	bone marrow cell
C region	constant region
CAD	coronary artery disease
CCL5	Chemokine (C-C Motif) Ligand 5
CD4	Cluster of differentiation 4
CD8	Cluster of differentiation 8
cDNA	complementary deoxyribonucleic acid
CDRs	complementary determining regions
CED	Cambridge Electronic Design
CHD	coronary heart disease
ChIP	chromatin immunoprecipitation
Chk2	cell-cycle-checkpoint kinase 2

Cl ⁻	electronic configuration
CLTA-4	cytotoxic T-lymphocyte-associated protein 4
CMV	Cytomegalovirus
Con A	Concanavalin
COPD	chronic obstructive pulmonary disease
CRP	C-reactive protein
CVD	cardiovascular disease
DAG	Diacylglycerol
DCs	dendritic cells
DDR	dependent DNA damage response
DGK α and ζ	Diacylglycerol kinases alpha and zeta
DH	Department of Health
DHE	Dihydroethidium
DMSO	Dimethyl sulfoxide
DN	double negative
DNA	Deoxyribonucleic acid
DNA-PKcs	DNA-dependent protein kinase
dNTP	Deoxynucleotide
DP	double positive
dROMs	derivatives of reactive oxygen metabolites
EBV	Epstein-Barr virus
EDTA	ethylenediaminetetraacetic acid
EEE	exercise energy expenditure
ELISA	enzyme-linked immunosorbent assay
eNOS	endothelial nitric oxide synthase
ESC	embryonic stem cells
ESEs	exonic splicing enhances
ESSs	Silencers

FACS	fluorescence-activated cell sorting
FBS	Fetal Bovine Serum
Fc	Fragment-crystallizable
FISH	fluorescence in situ hybridization
FITC	Fluorescein isothiocyanate
FoxP3	forkhead box P3
FSC	forward-scattered
G	Gram
GDP	guanosine diphosphate
GFP	green fluorescent protein
GITR	glucocorticoid-induced tumor necrosis factor family receptor
GPCR	G protein-coupled receptors
GTP	guanosine triphosphate
H	Hour
H ₂ O ₂	hydrogen peroxide
HDL-C	high-density lipoprotein cholesterol
HERITAGE	HEalth, RIisk factors, exercise Training And Genetics
HFD	high fat diet
HIV	human immunodeficiency virus
HOCl	hypochlorous acid
HPV	Human papillomavirus
HSCs	hematopoietic stem cells
HSP	Heat shock protein
hTERT	human telomerase reverse transcriptase
hTR	human telomerase RNA
ICAM-1	intercellular adhesion molecule-1
Icos	Inducible costimulatory molecule
IFN- γ	Interferon Gamma

Ig	Immunoglobulin
IgM	immunoglobulin M
IGM	institute of genetic medicine
iGSH	intracellular glutathione
IL-	interleukin-
iNOS	inducible nitric oxide synthase enzyme
IP3	inositol triphosphate
ISEs	intronic splicing enhancers
ISS	Intronic splicing silencers
ITAMs	immunoreceptor tyrosine-based activation motifs
JNK	Jun kinase
Kbp	kilobase pairs
kCal/g	kilocalories per gram
Kg	Kilogram
KO	Knockout
LDL	low-density lipoprotein
LDL-C	low-density lipoprotein cholesterol
Ldlr-/-	lipoprotein receptor-deficient
LTL	leukocyte telomere length
M-CSF	macrophage colony stimulating factor
MACS	magnetic-activated cell sorting
Mad1	Mitotic spindle assembly checkpoint protein
MAPK	Mitogen-activated protein kinase
MCP-1	monocyte chemoattractant protein-1
MDA-LDL	Malondialdehyde Modified Low Density Lipoprotein
Sem	standard error of the mean
MEKK1	mitogen-activated protein kinase kinase kinase 1
Mg	acceleration unit, (mg is 1000 gal, gal is galileo = 1cm/sec ²).

mg/dL	milligrams per deciliter
MHCs	Histocompatibility Complexes
MI	myocardial infarction
miRNAs	microRNAs
MLS	mitochondrial localisation sequence
MMP/TIMP	matrix-metalloproteinases and their inhibitors
mRNA	messenger ribonucleic acid
mtDNA	mitochondrial DNA
<i>mTert</i>	mouse telomerase reverse transcriptase
mTOR	mammalian target of rapamycin
MVPA	moderate to vigorous physical activity
NADH/NADPH	nicotinamide adenine dinucleotide phosphate
ND	normal diet
Neo	neomycin-resistant gene
NES	nuclear export signal
NFAT	Nuclear factor of activated T-cells
NF κ B	nuclear factor kappa-light-chain-enhancer of activated B cells
ng	Nanogram
NHS	National Health Service
NICE	National Institute for Health and Care Excellence
NK	Natural Killer
NLS	nuclear localisation signal
nm	Nanometers
NO	Nitric Oxide
NRES	National Research Ethics Service
O ₂	Oxygen
O ₂ ⁻	Superoxide
OH	Hydroxyl

PA	phosphatidic acid
PBL	peripheral blood lymphocytes
PBMNCs	peripheral blood mononuclear cells
PBS	Phosphate Buffered Saline
PCI	percutaneous coronary intervention
PCR	Polymerase Chain Reaction
PD-L1	Programmed death-ligand 1
PE-Cy	Phycoerythrin with Cyanine
PerCP	Peridinin Chlorophyll Protein
PI	prodiuim iodide
PI3K	phosphoinositide 3-kinase
PKC θ	protein kinase C-theta
PKD	protein kinase D
PLC γ 1	phospholipase C, gamma 1
PMA	phorbol myristate acetate
PMT	photomultiplier tube
POT1	protection of telomeres 1
PPCI	percutaneous coronary intervention
q-PCR	Quantitative Polymerase Chain Reaction
Rag2	recombinase activating gene-2
RAP1	repressor/activator protein 1
RasGPR1	Ras guanyl-release protein
RNS	Reactive nitrogen species
ROS	Reactive Oxygen Species
RPMI 1640	Roswell Park Memorial Institute 1640
RT	reverse transcription
RTKs	receptor tyrosine kinases
S1P	sphingosine-1-phosphate

SCID	severe combined immunodeficiency
SD	standard deviation
shRNA	short hairpin RNA
SMCs	smooth muscle cells
snRNA	small nuclear RNA
SOD	Superoxide dismutase
SOS	Son of Sevenless
Sp3	specificity protein 3
Ss	single stranded
SSC	side-scattered
STATs	signal transducers and activators of transcription
STEMI	Segment Elevation Myocardial Infarction
TA	telomerase activity
TBP	TATA-box binding protein
Tc-cells	T cytotoxic cells
TCR	T-cell Receptor
TERC	Telomerase RNA component
TERT	telomerase reverse transcriptase
TGF	transforming growth factor
Th-cells	T helper cell
TIN2	TRF1-interacting nuclear protein 2
TL	telomere length
TNF	tumor necrosis factor
TNFR1	Tumor necrosis factor receptor 1
TPP1	TINT1, PTOP, PIP1
TRAP	Telomeric Repeat Amplification Protocol
Tregs	regulatory T-cells
TRF1	Telomere Repeat Binding Factor 1

TRF2	Telomere Repeat Binding Factor 2
Trx	thioredoxin
UK	United Kingdom
USA	United States of America
UV	Ultraviolet
V region	variable region
VCAM-1	vascular cell adhesion molecule-1
WBC	White blood cell
WT	wild type
WT1	Wilms' tumor 1
Xhol	enzyme restriction site
XO	xanthine oxidases
ZAP-70	Zeta-chain-associated protein kinase 70
µg	Microgram
µl	Microliter

CHAPTER 1. INTRODUCTION

1.1 Functions of the immune system

1.1.1 Different cell types in the immune system

The acquired, or adaptive, immune system is a subsystem of the immune system. It is the second of two immunity protection strategies, the other being the innate immune system (Rimer et al., 2014). The importance of the acquired immune system is due to its high specificity to pathogens and the long lasting protection it confers against different diseases. It is acquired over the lifetime of an organism through contact with specific pathogens, and is non-existent at birth (Nielsen et al., 2010).

Each type of antigen, whether a virus, bacteria or any foreign body, has unique molecular markers, in addition to lymphocytes with their own clearly recognizable proteins. Mitotic activity in lymphocytes (T and B cells) is stimulated when foreign proteins are discovered in an organism. The second generation of lymphocytes (T and B cells), produced after mitosis then becomes subdivided into effector cells and memory cells. Effector cells are fully differentiated, and they seek and destroy foreign cells. Memory cells are dormant, but respond rapidly into defence mode if a pathogen is re-encountered. On recognition of the specific antigen, memory T-cells produce a huge lymphocyte population after repeated mitosis. Memory T-cells have shorter telomere length than naïve T-cells, which is most likely a consequence of continuous proliferation compared to naïve T-cells (Akbar and Vukmanovic-Stejic, 2007).

1.1.2 Acquired immunity

1.1.2.1 T-cells

T-cells originate from stem cells (Figure 1.1) in the bone marrow hematopoietic stem cells (HSCs). They then travel to the thymus to mature and differentiate; it is from this location that the name ‘T-cell’ originates. Subsequently, having developed their own receptors, the T-cells are released into the bloodstream. Interleukins secreted by effector helper T cells ($CD4^+$) lead to division and differentiation of both T and B-cells. Effector ($CD8^+$) cytotoxic T-cells destroy the infected cells with pathogen inside the organism by secreting enzymes, which penetrate the infected cell, such that the cytoplasm leaks out. Finally the DNA and organelles are attacked by $CD8^+$ cytotoxicity, resulting in apoptosis.

CD4⁺ T-cells

Cluster of differentiation 4 (CD4) is a glycoprotein found on the surface of T helper cells (Th-cells). CD4 T-cells play an essential role in the immune system and can be classified into three main functional roles: memory, inflammatory and helper cells, depending on their cytokine production (Killar et al., 1987). Naïve CD4 T-cells differentiate into 4 sub-populations: Th1, Th2, Th17 and regulatory T-cells (Tregs) after stimulus and activation in the bloodstream (Zhu et al., 2006; Mosmann et al., 2009).

CD4 T-cells are mainly referred to as helper cells, as they primarily send signals to other types of immune cells, whereas CD8 T-cells are mainly known as killer cells since they actually destroy the infectious cells (Killar et al., 1987; Zhong et al., 2008).

CD8⁺ T-cells

Cluster of differentiation 8 (CD8) is a transmembrane glycoprotein found on the surface of T cytotoxic cells (Tc-cells). These cells play a crucial role in the immune system by producing and releasing cytotoxins (Perforin, granzymes and granzulysin), into the cytoplasm of infected cells, leading to apoptosis (Zhong et al., 2008).

1.1.2.2 B-cells

B-cells (named after the avian ‘bursa of Fabricius’) are produced and developed in the bone marrow from HSCs (Figure 1.1). They are covered by B-cell receptors (BCRs) and produce a single specific antibody, which targets and adheres to the surface of infected cells. When a specific antigen comes into contact with cells, or if an interleukin signal is sent by a helper T-cell, the B-cell will initiate replication. New B-cells differentiate into effector or memory cells. Effector B-cells produce vast quantities of free-floating antibodies, which travel through the bloodstream until they encounter a corresponding antigen, which is then ‘tagged for destruction’ by phagocytes.

1.1.2.3 Monocytes

Monocytes differentiate from hematopoietic stem cells after being produced in the bone marrow from precursor monoblasts (Figure 1.1). Monocytes play an important role in the immune system; using intermediary proteins (antibodies or complements) monocytes can coat the pathogen and destroy it by phagocytosis. They can also destroy the pathogen by antigen presentation or cytokine production (TNF, IL-1 and IL-12).

Altogether, $CD4^+$ (helper) T-cells produce memory and effector cells via the production and secretion of cytokines. $CD8^+$ (cytotoxic) T-cells play a role in the eradication of infected cells. Antibodies are produced by B-cells which stick to cell surfaces or are secreted into the blood. Monocytes use phagocytosis to engulf pathogens and secrete cytokines that attract T-lymphocytes to the affected site using specific antigens.

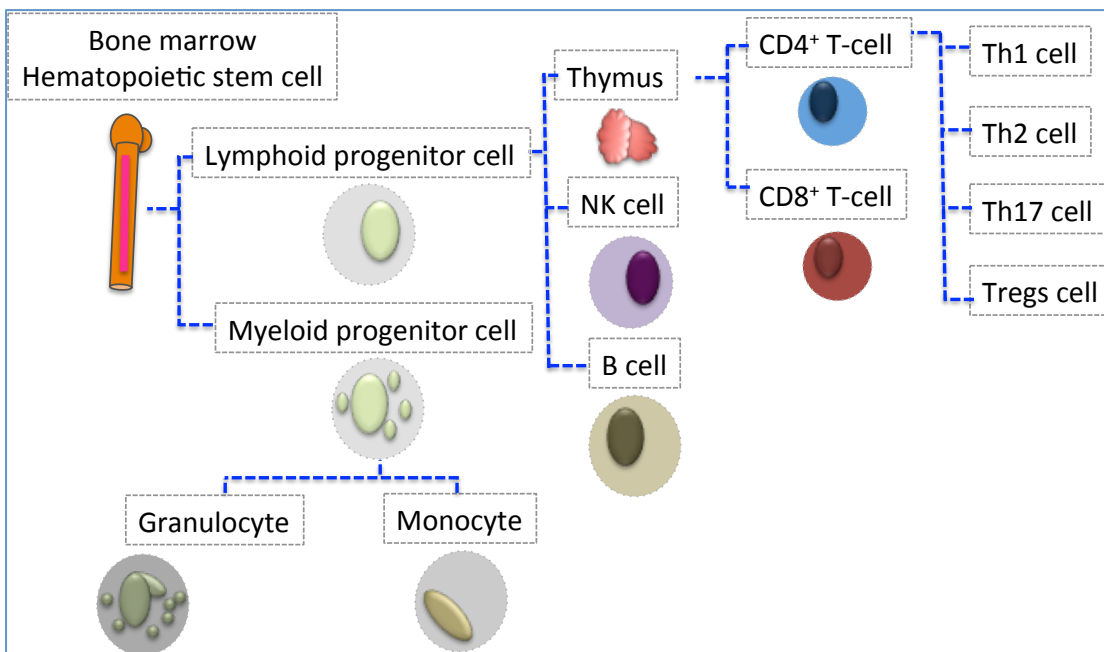


Figure 1.1. Illustration of the immune cells from origin to differentiation.

All lymphoid and myeloid blood cells arise from bone marrow-based hematopoietic stem cells (HSCs). Myeloid progenitors differentiate into monocytes and granulocytes within the bone marrow before travelling into the peripheral bloodstream where they exist for a few hours or days. Conversely, after differentiating in the bone marrow, lymphoid progenitors migrate to the thymus, where they mature into T-cells.

1.1.3 Regulation of the adaptive immune response

For adaptive immunity to develop, specific antigens must first be identified as non-self, which delays the process. The adaptive immune system relies entirely on the ability to differentiate between individual antigens (Bonilla and Oettgen, 2010). Over time, this produced the pool of clonal diversity, allowing dormant cells to remain inactive until such a time that they encounter any antigen for which they have a memory and can recognize. This ability is more effective in antigen removal than targeted immune responses.

The adaptive immune system is predominantly made up of T and B-cells, as well as antibodies. Within the T-cell population, various subtypes are present, including regulatory, cytotoxic, and pro- and anti-inflammatory helper (Th) T-cells. Pathogens which show resistance to neutrophils and macrophages are usually cleared by T-lymphocytes.

Following maturation in the thymus, both CD4 and CD8 are expressed by naïve T-cells, which are referred to as ‘double positive’ (DP). These cells reconfigure their TCR α chain, resulting in mature TCR $\alpha\beta$ expression. In its ability to distinguish between self- and non-self Major Histocompatibility Complexes (MHCs), the T-cell is rendered receptive to survival signals and positive selection (Naito and Taniuchi, 2010). The preference for MHC I or MHC II, as distinguished by the reconfigured TCR causes the T-cell to cease CD4 or CD8 expression accordingly, i.e. they become single positive. The Ras-Mek1 signalling pathway magnifies this process of positive selection (Alberola-Ila et al, 1996).

Following this positive selection process, the final stage in T-cell maturation involves negative selection, which is also governed by Ras signalling. Thymocytes are screened and those which express a TCR with a preference for self-MHC/peptide complexes are deleted (Robey, 1999). ERK1/2 is not required for negative selection, but Ras activated MAPK c-Jun kinase (JNK) is, which implies that Ras signalling plays a specific role in T-cell maturation (Robey, 1999). TCR interaction causes variations both quantitatively and temporally in TCR signaling, which can induce an instructional bias on CD4/CD8 lineage commitment, as well as kinase-assisted (Lck and ZAP70) downstream signal transduction events (Yasutomo et al, 2000).

CD3 and ζ -chains are phosphorylated by the Src kinase Lck when antigen presenting cells (APCs) are proximal to the TCR complex. This is due to an antigen/MHC complex bound to the surface of the APC. A conformational change is facilitated, which allows the TCR complex to bind with cytoplasmic tyrosine kinase Zap70, allowing Lck phosphorylation to take place (Smith-Garvin et al., 2009).

Consequently, one co-receptor is activated and the other is terminated, as required by the lineage commitment of that cell (Laky et al., 2006). CD8 is expressed when TCR activation is inhibited, in spite of any MHC II complex specificity, or if MHC I specific cells respond in the opposite way to TCR signalling. CD4 expression is intrinsic, although the nature of the TCR signalling, with regard to magnitude, frequency and duration, influences this lineage commitment. The role of Notch, a transmembrane receptor, has been implicated in the signalling within developing T-cells (Robey, 1999). The absence of Notch has been associated with increased CD8 $^{+}$ thymocyte generation and decreased CD4 $^{+}$ thymocyte generation (Xiong et al., 2011). A CD8 $^{+}$ phenotype commitment is therefore likely to be caused by Notch, since although MHC-mediated positive selection would not be affected, it is believed that Notch activation may cause diversion of MHCII dependent thymocytes from a CD4 to a CD8 lineage (Suzuki et al, 1997; Laky et al, 2006).

T-cell activation

Activation of naïve CD4 $^{+}$ and CD8 $^{+}$ T-cells is a two-stage process. When an APC yields an MHC/antigen complex, the T-cell's TCR is ligated with adjuvant co-stimulation (Smith-Garvin et al, 2009). Cytokines and adhesins, particularly in relation to the immune response, are critical to this process.

T-cell Receptor (TCR)

TCR comprises two immunoglobulin chains (thus rendering it a heterodimer), as well as other nuclear signalling-related proteins (Janeway, 1992). Pathogens are recognized and cleared by TCR via MHC-bound antigens, which stimulate intracellular signalling cascades (Figure 1.2). However, further stimuli are required due to the low affinity of TCR binding (Stone et al., 2009). TCRs comprise an α -chain, which is highly variable, and a more stable β -chain. These bond with invariant CD3 molecules via disulphide links. Being anchored to the membrane of the T-cell, stimulation by CD3 causes TCR signalling to the cells. 95% of T-cells express $\alpha\beta$ TCRs; the rest express $\gamma\delta$ TCR (Stone et al., 2009).

MHC/antigen complexes bind to the variable (V) region of the TCR chain, whilst the TCR is anchored to the cell membrane via the constant (C) region of the TCR chain (Rudolph et al., 2006). Three hyper-variable regions, or complementary determining regions (CDRs), make up the V domain of a TCR chain. In thymocyte development, activated RAG 1 and 2 recombination events cause stochastic rearrangement of CDRs, creating a vast range of TCR tertiary structures. The ability to achieve this wide variability is critical to recognizing and apprehending the broad array of antigens that will be encountered over an entire life span (Nikolich-Zugich et al, 2004). Recognition of processed antigens is generally mediated by CDR3, although some studies have demonstrated CDR1 and antigenic peptide also play a role.

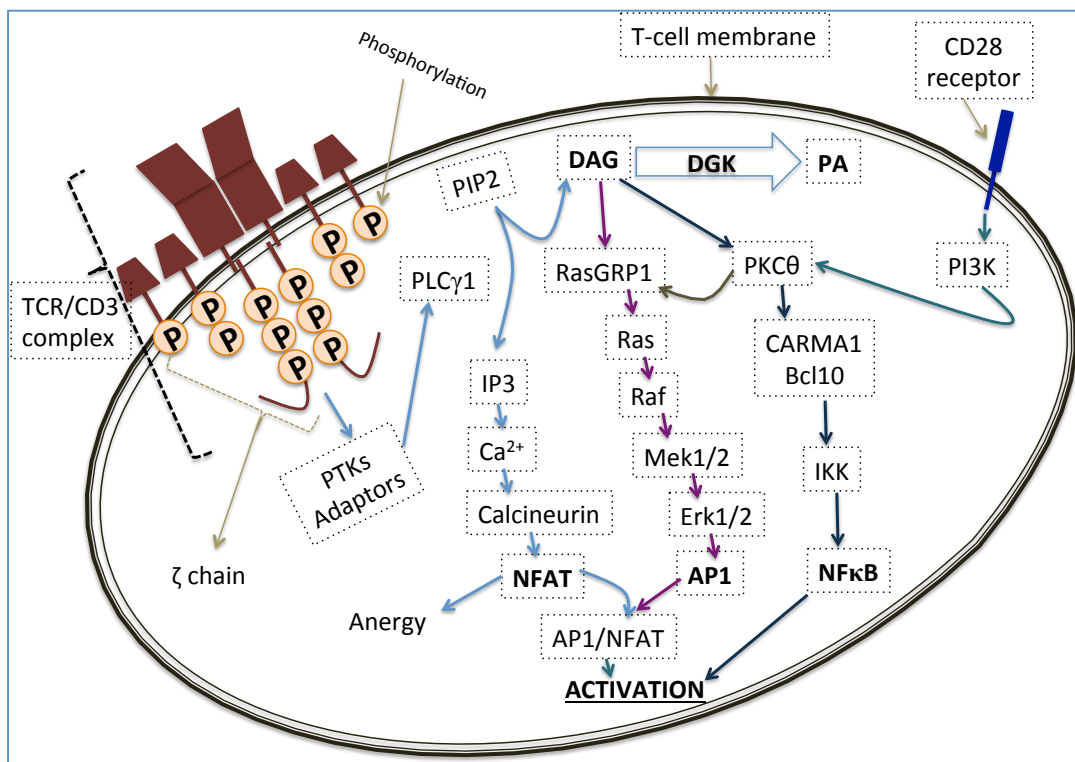


Figure 1.2. TCR signalling pathway to T-cell activation. (modified from Zhong et al., 2008)

Once the engagement of T-cell receptors (TCRs) has taken place, proximal tyrosine kinases and other adapter molecules trigger phospholipase C, gamma 1 (PLC γ 1) activation. This critical event stimulates triphosphate (IP3) and diacylglycerol (DAG) production, which triggers a number of pathways, including: Ca⁺⁺-calcineurin-NFAT activation; the protein kinase C-theta (PKCθ)-Carma1/Bcl10- nuclear factor kappa-light-chain-enhancer of activated B cells (NFκB) pathway; the Ras guanyl-release protein (RasGPR1)-Ras-Erk1/2- activator protein 1 (AP1) pathway; and protein kinase D (PKD). T-cell anergy may be caused by nuclear factor alone (in activated T-cells), which enhances the production of molecules such as DGK α , which promote anergy. Combined with DAG-mediated pathways, this cascade activates T-cells. Following this, TCR signalling is made more robust by CD28, leading to the activation of phosphoinositide 3-kinase (PI3K) and the downregulation of Diacylglycerol kinases alpha and zeta (DGK α and ζ) expression. Signalling mediated by DAG may be suppressed when DAG converts to phosphatidic acid (PA) via DGKs.

Antigen presenting cells and major histocompatibility complexes (MHCs)

A number of stages are involved in antigen processing before a cellular or humoral immune response becomes active. Specific fragments of antigen are phagocytosed by macrophages and dendritic cells before being presented for processing. The MHC uses tetrameric molecules to facilitate antigen presentation and also to mediate the distinction between self- and non-self-antigens. This is determined in both central and peripheral immunity by the level of interaction between TCRs and APC peptides.

MHC-I and MHC-II present processed antigens on the APC surface. The difference between class I and II MHC is in their constituent α and β chains. MHC-I molecules are characterized by small, endogenous antigens, primarily cytotoxic CD8 $^{+}$ T cells, whilst MHC-II are found on the membrane of specialized APCs and bind exogenous antigens via a small α -chain 'pocket'. MHC-I and II are heterodimeric glycoproteins, which exist on all human cells (except erythrocytes). Technically, any cell which expresses MHC is considered an APC. However, the three most effective types of 'professional' APC are B-cells, dendritic cells (DCs) and macrophages. Where other cells may only express MHC-II and co-stimulatory molecules in response to an inflammatory immune response or other physiological stress, DCs are particularly effective in their constitutive expression without the need for stress (Nickoloff and Turka, 1994). Consequently, DCs are the dominant human APC, enabling the differentiation and proliferation of specific T-cells.

The adaptive immune response is therefore highly dependent on the above activity in order to detect, capture and present antigens, migrate these to T-cell areas, then respond to external stimuli and differentiate accordingly. Although this does not constitute an innate immune response, it essentially provides the link between innate and adaptive immunity.

T cells and antigen presenting cells (APCs)

T-cell activation relies on interaction between MHC and TCR, as well as co-receptors for CD4 and CD8 (Rudolph et al., 2006). Evidence is emerging which suggests that CD4 and CD8 form a complex with the TCR, creating an antigen-bound MHC co-receptor (Rudolph et al., 2006). When TCR is not present, CD4 and CD8 ordinarily bind with the antigen presenting cell via its MHC I and II ligands. Downstream signal transduction in T-cell activation is also reliant on the presence of activated CD3 within the TCR complex (Smith-Garvin et al., 2009). The relationship between CD4 $^{+}$ and CD8 $^{+}$ T-cells is also critical: CD4 T-cells, as well as pro-inflammatory cytokines and increased numbers of co-stimulatory

molecules, all have a modulating effect on dendritic cells, leading to $CD8^+$ T-cell activation. In some cases, activation is the result of direct interaction; in others, it is the consequence of naïve CD8 precursor recruitment in lymphoid tissues.

Co-stimulation of T-cells

Co-stimulation is necessary for full T-cell activation. This is primarily achieved through TNF receptor (e.g. CD27 or CD40) and CD28 ligation (Acuto and Michel, 2003). When co-stimulation is not possible, TCR ligation causes T-cell anergy (Smith-Garvin et al., 2009; Valenzuela and Effros, 2002). Of interest to this study, T-cell proliferation relies heavily on CD80/86, which becomes bound by CD28. In the laboratory, monoclonal antibodies will be used to co-stimulate and bind CD3 on the TCR complex. The process of co-stimulation will also cause src kinase activation. In turn, ITAMs on the CD3 complex are phosphorylated, recruiting ZAP-70, causing integrin activation and cytoskeletal rearrangement (Acuto and Michel, 2003; Van der Merwe and Dushek, 2011).

Cytokines

Eukaryotic cells secrete autocrine, endocrine and paracrine regulators, including cytokines, during a normal immune response. Intercellular signalling cascades are triggered by ligation of each cytokine's corresponding cell-surface receptor. This causes the cell's phenotype and transcription factors to be altered, thus promoting an adaptation response to the cell's microenvironment. Monokines, lymphokines and interleukins express cytokine mRNA when their transcriptional activator is present and when an environmental change is detected in circulating cells. This is particularly true when subtle antagonistic or synergistic changes occur in the presence of cytokines.

Interleukin- 2 (IL-2)

IL-2 is produced via a CD28 canonical co-stimulatory signal (signal 2). TCR/CD3 engagement with MHC/antigen (signal 1) has lower affinity of signal to stimulate the T-cell receptor (Gaffen and Liu, 2004). IL-2 is mostly produced by $CD4^+$ T-cells. Non-specific activation also leads to about 60% of $CD4^+$ T-cells producing this cytokine. In pro-inflammatory T-cell responses, IL-2 is produced by Th1, and TCR ligation causes $CD8^+$ T-cells to produce IL-2 (Ho et al., 1999). When MHC/antigen complexes are presented to naïve cell TCRs, B-cells and dendritic cells also secrete IL-2 (Granucci et al., 2001; Gaffen and Liu, 2004).

Activated T-cells secrete a tiny α -helical cytokine (15kDa) with significant pleiotropic effects. The receptor of IL-2 is synthesized via TCR ligation, enabling effector T-cells to proliferate quickly. In humans and mice, the signalling role of IL-2 is significant; murine IL-2 is highly specific to its corresponding murine IL-2R α subunit, whereas human IL-2 can induce T-cells across the species (Liu, 1999; Mosmann et al., 2009). IL2-R production plays a critical role in the expansion of CD4 $^{+}$ and CD8 $^{+}$ T-cells which respond to specific antigens (Miyazaki et al., 1995; Gaffen and Liu, 2004). Both c-myc and c-fos signalling enable proliferation of activated T-cells, as well as anti-apoptotic signalling through Bcl. Both processes are reliant on IL-2 (Miyazaki et al, 1995).

Janus Kinase (JNK) signalling, and signal transducers and activators of transcription (STATs) are also activated through the action of IL-2 on cellular metabolism. This is more of a long-term T-cell proliferation effect, resulting in MAPK and ERK-Akt signalling pathways becoming activated. Nuclear factor of activated T-cells (NFAT) and the activator protein-1 (AP-1) transcription factor are also activated by IL-2 (Gaffen et al., 1996; Garrity et al., 1994). The presence of CD28 co-stimulatory signals supports this process, leading to robust T-cell activation through nuclear translocation of NF κ B (Kane et al, 2001).

Interferon Gamma (IFN- γ)

IFN- γ is produced by both Th1 CD4 $^{+}$ cells and cytotoxic CD8 $^{+}$ T-cells and, to a lesser degree, by NK cells. It is a soluble cytokine dimer and has critical importance to both innate and adaptive immunity. Not only are macrophages, NK cells and inducible nitric oxide synthase enzyme (iNOS) activated in the presence of IFN- γ , but it is also required for transcription factor activation, which, via a positive feedback loop, induces the Th1 lineage and suppresses Th2 differentiation. IFN- γ production is mediated by the APC cytokines IL-12 and IL-18 (Fukao et al, 2000; Otani et al, 1999) and suppressed by IL-4, IL-10 and TGF β , which are anti-inflammatory, whilst IFN- γ is a pro-inflammatory cytokine (Frostegård et al., 1999). It performs a number of other vital roles, including the facilitation of: leukocyte growth, maturation and differentiation (Young and Hardy, 1995; Boehm et al., 1997; Perussia et al., 2001); NK cell activity (Carnaud et al., 1990); and Ig class switching (Carnaud et al., 1990; Finkelman et al., 1988).

1.1.4 Role of T-lymphocytes in atherosclerosis

The role of T-cells in regulating the immune response is critical. Th-cells differentiate in response to antigens present at inflammation sites. Four lineages may develop: Th1 and Th2

eliminate pathogens, both within and outside of cells; Th17 cells promote inflammation and eliminate pathogens through neutrophil recruitment in peripheral tissues; and Treg-cells regulate immune hyperactivity through inflammation inhibition (Beyer and Schultz, 2006; Yu and Gaffen, 2008).

Healthy arteries attract T-cells into the aortic wall partly via L-selectin. In the aortic wall they localize primarily within the outermost connective tissue (Maffia et al., 2007). Of these T-cells, most are activated phenotype TCR $\alpha\beta^+$ CD4 $^+$ cells. Heat shock protein (HSP) is found in atherosclerotic plaques, alongside oxidized lipoprotein-specific T-cells. It is thought that lesion formation therefore causes local activation and clonal expansion (Rossmann et al., 2008) and the expression of V β 6 TCR, as opposed to V β and V α segments. Some studies have noted that oxidized LDL also yields T-cell responses dependent on CD80 $^-$, CD86 $^-$ and CD40-CD154 (Robertson and Hansson, 2006).

A number of phases are implicated in atherosclerotic inflammation. In the early stages, IFN- γ , IL-6 and IgG2a antibodies are produced by Th1 cells. T-bet is a transcription factor, which allows differentiation of Th1 and also plays a role in Th1 and Th2 regulation in response to inflammatory diseases. T-bet deficiency may reduce atherosclerosis, as well as altered T-cell dependent oxidized LDL-specific antibodies, increased B1-derived antibodies, reduced lesional SMCs and an HSP-60 response to Th2 (Zhou et al., 1998). Increased proinflammatory cytokines, increased antibodies, and B-cell function regulation indicate that atherosclerosis is at least in part caused by Th1. Indeed, atherosclerotic lesions in Apoe $^{-/-}$ mice with increased blood cholesterol exhibit a switch to a Th2 response and IL-4 production, but further atherosclerosis is not inhibited (Zhou et al., 1998).

Adoptive transfer into scid/scid Apoe $^{-/-}$ mice of CD4 $^+$ T-cells supports the proatherogenic role theory (Robertson and Hansson, 2006). There is evidence to suggest however, that CD4 $^+$ T-cell atheroprotection may occur following immunization against MDA-LDL, although the presence of an adjuvant negates this effect. Both local arterial and systemic actions, via secondary lymphoid organs, may be implicated in this effect. Lymphocyte proliferation and IFN- γ are both inhibited by FTY720, a sphingosine-1-phosphate (S1P) analogue. FTY720 also inhibits IL-6, IL-12 and CCL5 plasma levels and causes macrophages to switch to the M2 phenotype. Apoe is also inhibited in the presence of an adjuvant in Ldlr $^{-/-}$ and Apoe $^{-/-}$ mice (Nofer et al., 2007; Keul et al., 2007).

1.1.5 Regulatory T-cells (Tregs)

T-cells are initially double-negative CD4-CD8-TCR-cells, becoming double-positive for these 2 surface markers on reception of the appropriate signal. At this point, they become activated and proliferate into CD4⁺ and CD8⁺ T-cells. It has been suggested that atherosclerosis may be a form of autoimmune disease (Galkina and Ley, 2009; Foks et al., 2011). Tregs, which are critical to immunological tolerance, inhibit atherosclerosis development through avoiding inflammatory responses.

Th1 and Th2 responses are controlled by Tregs, which themselves respond to HSP-60 and LDL. This provides further support for the theory that atherosclerosis is an autoimmune disease (Sakaguchi et al., 2006). Consequently, if Tregs are either damaged or absent, this may promote the atherosclerotic proinflammatory response. Passive transfer of cognate peptide-specific Tregs (Tr1) inhibits the production of Th1 cytokine, IFN- γ and IgG2a in ApoE^{-/-} mice (Mallat et al., 2003). Indeed, recipient mice had less atherosclerosis and more IL-10. Adoptive transfer of CD4⁺CD25⁺Treg deficient bone marrow was found to increase lesion size in irradiated low-density lipoprotein receptor-deficient (Ldlr^{-/-}) donors (Ait-Oufella et al., 2006). Furthermore, in recombinase activating gene-2-deficient apolipoprotein E-deficient (Rag2^{-/-}ApoE^{-/-}) mice, lesion size doubled in response to the transfer of CD4⁺CD25⁺Treg deficient splenocytes, compared with wild-type splenocytes. This evidence implicates naturally occurring Tregs in playing a critical role in atheroprevention.

Inducible costimulatory molecule (Icos) affects Treg response. Indeed, Tregs found in inducible costimulatory molecule knockout (Icos^{-/-}) mice had far lower TGF- β -dependent suppression than their wild-type counterparts (Gotsman et al., 2006). CD31 also plays a role in Treg response, although the mechanism for this is not known (Grover et al., 2007). Treg number and functioning is increased by obesity, and Th1 polarisation is suppressed in low density lipoprotein knockout (Ldlr^{-/-}) mice with leptin deficiency (Taleb et al., 2007), resulting in improved Treg functioning and inhibited lesion development in atherosclerosis. Therefore, the immune response to atherosclerosis is also critically dependent on the leptin/leptin receptor pathway. IL-10 and TGF- β have also been implicated in the immune response to antigens in atherosclerosis (Van Puijvelde et al., 2007).

1.2 Atherosclerosis as an inflammatory disease

1.2.1 Pathobiology of atherosclerosis

Plaques, made up of blood substances including cholesterol, calcium and fats, may build up on arterial walls, causing atherosclerosis. Leukocytes, endothelial and smooth muscle cells may become inflamed, which can also lead to this arterial blood disease (Galkina and Ley, 2009). All arteries, including coronary arteries and the aorta are prone to atherosclerosis, and blood clots caused by plaques may cause partial or complete blockages. If blood flow to the heart muscles is prevented or reduced, this can result in angina pectoris or myocardial infarction (a heart attack). Elsewhere in the body, a stroke or the inflammatory disease ischemic gangrene may result. Despite its causes not being fully understood, risk factors have been identified: smoking, bad diet and lack of exercise – these factors are controllable; and age and genetic predisposition – these are uncontrollable. Atherosclerosis is particularly insidious, due to a lack of any physical signs or symptoms until the point of a stroke or heart attack.

Research into leukocyte recruitment mechanisms has shed some light on the causes of atherosclerosis. It has been observed that under an atherogenic (i.e. high fat) diet, leukocyte-binding selective adhesion molecules such as VCAM-1 are expressed in some areas of arterial endothelium, attracting white blood cells which do not ordinarily bind with endothelial cells. VCAM-1 also binds monocytes and T-lymphocytes (Li et al., 1993). Mice that had been modified to express defective VCAM-1 exhibited interrupted lesion formation (Cybulsky et al., 2001).

1.2.2 Mediators of inflammation

When tissue is injured, damaged or destroyed in some way, a localized inflammatory response is triggered, preventing further damage by attacking, diluting or otherwise blockading both the damaged area and the agent which caused the injury. In atherosclerosis, inflammation can cause blockages in the blood flow, leading to a heart attack. Studies have shown that inflammation in atherosclerosis indicates a heightened risk of cardiovascular complications. One study found multiple connections between atherosclerotic inflammation and other processes related to the cellular immune response, endothelium activation and altering of metabolic parameters (Galkina and Ley, 2009). It had been demonstrated that CD4+ T-cells play a vital role in the development of atherosclerosis (Galkina and Ley, 2009). It was later found that patients with coronary artery disease (CAD) exhibited reduced

inflammation after engaging in physical exercise (Swandfager et al., 2012) and that tissue damage is inhibited by control of the inflammatory response by T-reg (Gol-Ara et al., 2012).

Increased adhesion molecule expression in specific arterial sites tends to indicate a susceptibility to atheroma. Where blood flow is disrupted, particularly at branch points, atheroprotective mechanisms have been found to be damaged (Topper et al., 1996). It has been suggested that areas of decreased laminar stress produce less Nitric Oxide (NO), which would ordinarily have a dilatory and anti-inflammatory effect. NO also inhibits vascular cell adhesion molecule-1 (VCAM-1) expression on endothelial-leukocyte adhesion molecules (De Caterina et al., 1995). Other leukocyte adhesion molecules, e.g. intercellular adhesion molecule-1 (ICAM-1) and proteoglycans, cause inflammation by promoting oxidative modification of lipoproteins. These are also increased when blood flow is inhibited (Nagel et al., 1994).

1.2.3 Role of the immune system in inflammation and atherosclerosis

Chemoattractant molecules, including monocyte chemoattractant protein-1 (MCP-1) draw leukocytes from the endothelium into the intima. It has been suggested that this action is increased at lesion sites (Gu et al., 1998; Lee et al., 2001). Here, blood-derived inflammatory cells instigate an inflammatory response. Macrophages then produce scavenger receptors, which convert to foam cells through lipid ingestion. Inflammatory cytokines, IFN- γ and tumour necrosis factor (TNF- β), a lymphotoxin, are produced by macrophage colony stimulating factor (M-CSF) and T-cells, to stimulate smooth muscle cells (SMCs), macrophages, and vascular endothelial cells. Peptide growth factors and other fibrogenic mediators are secreted by arterial cells and activated leukocytes, causing SMCs to be replicated, leading to a dense extracellular matrix, or lesion (Smith et al., 1995).

Inflammatory responses as described above are implicated in both atheroma and other thrombotic complications. Most fatal heart attacks are caused by atherosclerotic plaque disruption (Mach et al., 1999). Plaques have a fibrous cap, which may be disrupted by proteolytic enzymes attacking its collagen and making it more vulnerable to rupture. IFN- γ inside the plaque may be released by T-lymphocytes to suppress collagen synthesis, which also weakens the structure (Libby et al., 1996). Finally, one major link between inflammation and thrombosis is a procoagulant tissue factor, secreted by macrophages and regulated by inflammatory mediators (Libby, 2001).

Atherosclerotic lesions exhibit components of adaptive immunity. Antigen-specific adaptive immune responses have been implicated in atherogenesis (Andersson et al., 2010). ApoE^{-/-} and Ldlr^{-/-} mice, combined with B- and T-cell deficient mice, exhibit significant adaptive immunity in response to atherosclerosis. Progeny from ApoE^{-/-} mice and lymphocyte deficient mice (also deficient in recombination activating gene (RAG) 1 or 2), or mice with severe combined immunodeficiency (SCID) exhibited significantly decreased atherosclerosis (Reardon et al., 2001; Zhou et al., 2000).

These results confirm the role of proinflammatory T-cells, but B-cells have also demonstrated a protective role. ApoE^{-/-} mice that have had their spleens removed exhibit aggravated atherosclerosis, but a protective effect was observed when these mice received splenetic B-cells from their aged counterparts (Caligiuri et al., 2002). B-cells have also been shown to have a protective effect when bone marrow was transferred to Ldlr^{-/-} mice from B-cell deficient mMT mice (Major et al., 2002). When the cytokine IL-5 is missing in bone marrow-chimeric Ldlr^{-/-} mice, lower amounts of immunoglobulin M (IgM) antibodies to phosphocholine are found, resulting in higher atherosclerosis (Binder et al., 2004). Other studies, by Ait-Oufella et al. (2010) and Kyaw et al. (2010) have suggested that varying effects on atherosclerosis are produced by different subsets of B-cells. Notably, anti-CD20, and B220^{lo}IgM⁺ B cells do not inhibit plasma cell production, and IgG-producing B cells are more significantly affected than IgM production is.

Atherosclerotic T-cells are memory-effectors and are $\alpha\beta$ T-cell antigen receptor (TCR) and CD4⁺ positive. Notwithstanding this, both TCR $\gamma\delta$ and CD8⁺ cells have also been found (Hansson and Libby, 2006). Lesions in both humans and ApoE^{-/-} mice have also exhibited T-cell clonal expansion (Paulsson et al., 2000; Liuzzo et al., 2000), suggesting the possibility that within lesions, antigen-specific reactions take place. Furthermore, interrupted CD40 ligation in Ldlr^{-/-} mice is associated with smaller lesions (Mach et al., 1998). CD4⁺ T-cells from atherosclerotic ApoE^{-/-} mice introduced to immunodeficient mice caused T-cells to be attracted to the lesion and increased atherosclerosis (Zhou et al., 2000). When an agonist to the tumour necrosis factor-like surface protein CD137 was injected into ApoE^{-/-} mice, CD8⁺ T-cells were stimulated. The same effect was observed when smooth muscle cells (SMCs) expressed an artificial antigen, increasing atherosclerosis (Olofsson et al., 2008; Ludewig et al., 2000). Programmed death-ligand 1 (PD-L1) and programmed death-ligand 2 (PD-L2) are inhibitory molecules, deficiency of which resulted in larger plaques and of CD8⁺ T-cells infiltrating the lesion and supporting the theory that programmed death-1 (PD-1) may play a role in controlling CD8⁺ T-cells (Gotsman et al., 2007; Hoffmann and Spyridopoulos, 2015).

1.2.4 Oxidative stress

Imbalances between the generation of Reactive Oxygen Species (ROS) in a living cell and that cell's ability to detoxify reactive intermediaries (or repair the damage they cause) results in oxidative stress. When a cell's redox state is disturbed, the resulting peroxides and free radicals produced can damage proteins, lipids and DNA, as well as other cell components. Oxidative stress, caused by oxidative metabolism can cause DNA strands to break as well as indirect damage to bases, for example in the form of the lesion 8-oxo-7,8-dihydro-2' - deoxyguanosine (8-oxodG) (Valavanidis et al., 2009). ROS include O_2^- (superoxide radical), OH (hydroxyl radical) and H_2O_2 (hydrogen peroxide) (Chandra et al., 2015), that are described below:

Different ROS types:

- 1. Singlet oxygen** reacts strongly with double bond-containing organic compounds. Singlet oxygen causes the oxidization of β -carotene into products which behave as secondary messengers. These play a role either in reducing the toxicity caused by singlet oxygen, or in the initiation of senescence (Foote et al., 1985; Holt et al., 2005).
- 2. Superoxide radical:** Electrons that leak from the mitochondrial electron transport chain can join molecular oxygen (O_2) to form the ROS, superoxide radical (O_2^-). This reaction is easily increased by the presence of exogenous components, such as redox cycling compounds. Superoxide radicals are initially produced in the internal mitochondrial membrane (by NADH ubiquinone reductase and ubiquinone cytochrome C reductase as complexes I and III of the electron transport chain (ETC)). Hydrogen peroxide (H_2O_2) is formed following reduction of this species by superoxide dismutase (SOD) (Sohal et al., 1995; Babcock, 1999). NADPH oxidases also generates superoxide radicals in the membranes of specialized cells such as macrophages and these are rapidly released in a respiratory (or oxidative) burst (Kotsias et al., 2013). These have a bactericidal function in combination with the phagocytic functions of macrophages. Superoxide radicals are also generated out of hypoxanthine and oxygen by the cytosolic enzyme xanthine oxidase, a flavin found in most tissues and also in milkfat globules. These particular superoxide radicals are thought to be one of the root causes of vascular pathologies (Sohal et al., 1995; Fridovich, 1995).
- 3. Hydroxyl radical**, via the Fenton reaction ($Fe^{2+} + H_2O_2 \rightarrow Fe^{3+} + \cdot OH + OH^-$), $\cdot OH$, a very reactive ROS, can be generated from hydrogen peroxide. This is one of the most prevalent reactions in all-biological systems and is responsible for the generation of numerous damaging lipid peroxidation products (Halliwell and Gutteridge, 1990).

·OH can be generated in a number of ways: Peroxinitrite or peroxinitrous acid can decay into hydroxyl radicals and ·NO₂. In neutrophils, myeloperoxidase and Cl⁻ ions are also able to produce ·OH during phagocytosis (Halliwell and Gutteridge, 2006).

4. Hydrogen peroxide, enzymatic reactions in microsomes, peroxysomes and mitochondria are the primary source of H₂O₂. This process is significant to a number of functions, even under conditions of normoxia and cellular H₂O₂ concentrations are maintained at between 10⁻⁹ and 10⁻⁷ M (Fransen et al., 2012).

H₂O₂ can be synthesized by O₂⁻ dismutation (via superoxide dismutase) in both plant and animal cells. This inhibits oxidative reactions. Cellular membranes are particularly porous to H₂O₂. The presence of both dismutase and catalase acts as a true cellular antioxidant by removing H₂O₂ (Fransen et al., 2012).

The term ROS can refer to any oxygen-containing chemically reactive chemical species. These are a normal byproducts of oxygen metabolism processes and are involved in cell signaling and homeostasis (Devasagayam et al., 2004). Environmental stressors, such as excessive heat, exposure to UV (Devasagayam et al., 2004), or exogenous sources such as ionizing radiation can cause ROS levels to significantly increase which in turn can result in cell damage (Sosa et al., 2015).

Exogenous ROS can be caused by drugs, smoke, radiation or other pollutants. Interaction between water and ionizing radiation – a process known as radiolysis - can result in damaging intermediaries. The probability of this happening in humans is high, due to the fact that the human body is 55-60% water. During radiolysis, water molecules lose an electron and become reactive. A three-step chain reaction follows, which involves water being sequentially converted to a hydroxyl radical (·OH), hydrogen peroxide (H₂O₂), a superoxide radical (·O₂⁻) and finally oxygen (O₂). Any molecules in the path of the hydroxyl radical are stripped of electrons to become a free radical. A chain reaction is thus propagated (Sosa et al., 2015).

Endogenous ROS can be produced intracellularly in numerous different ways, according to the cell type. (1) by ROS producers such as NADPH oxidase (NOX) complexes (7 distinct isoforms) in cell membranes, mitochondria, peroxisomes, and endoplasmic reticulum (Muller, 2000; Han et al., 2001). (2) As a by-product of oxidative phosphorylation in the mitochondria. Adenosine triphosphate (ATP) is generated by mitochondria to provide useable energy for cells. The process through which ATP is produced, oxidative phosphorylation, uses an

electron transport chain to convey protons across the inner mitochondrial membrane, which involves a series of oxidation-reduction reactions. Each successive acceptor protein has a higher reduction potential and the final destination for the electron being an oxygen molecule. Ordinarily, this molecule would be reduced to produce water, although 0.1-2% of electrons (the exact rate in live organisms is yet to be determined) which pass through the chain, oxygen is prematurely and incompletely reduced, resulting in a superoxide radical ($\cdot\text{O}_2^-$). In itself, $\cdot\text{O}_2^-$ is not particularly reactive, but in its protonated form, hydroperoxyl ($\text{HO}\cdot_2$), it can interfere with certain enzymes or initiate lipid peroxidation. At physiological pH, hydroperoxyl (whose pK_a is 4.8) mostly exists as a superoxide anion (Li et al., 2013).

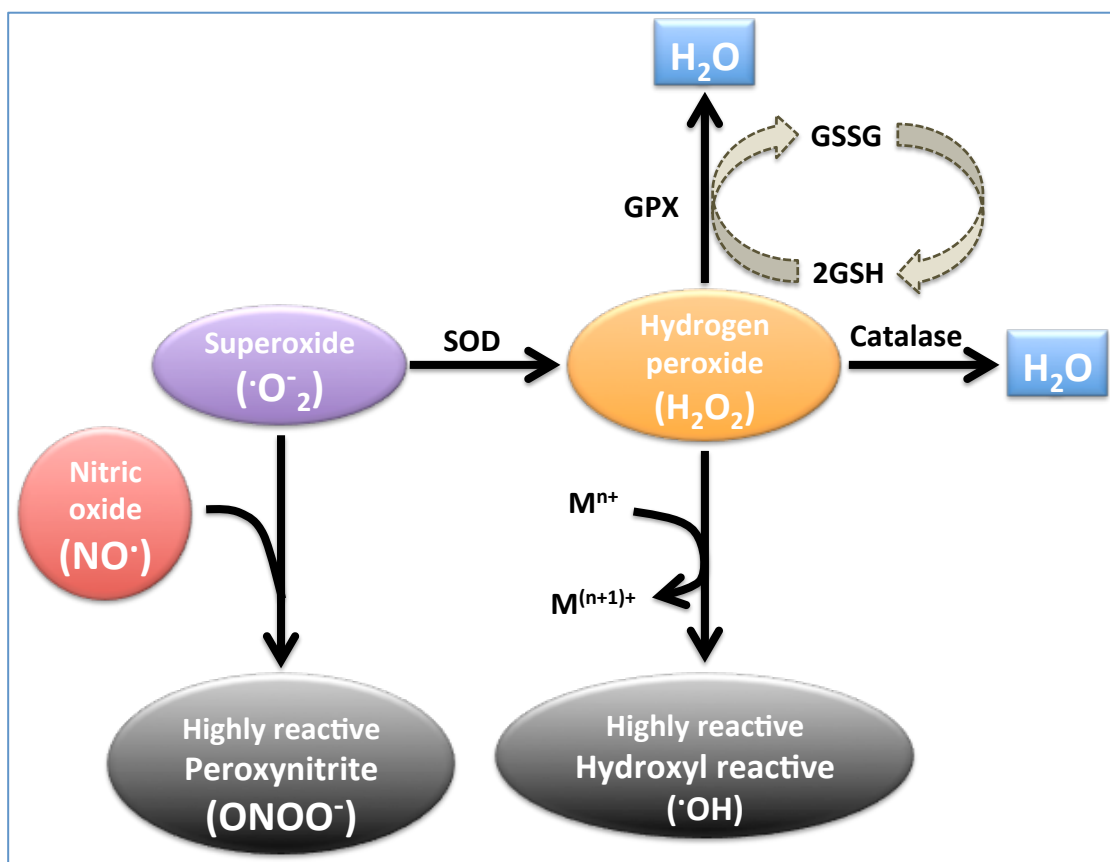


Figure 1.3. ROS formation and metabolism. Under normal conditions, superoxide ($\cdot\text{O}_2^-$) is formed by the mitochondrial respiratory chain. This can be dismutated by superoxide dismutase (SOD) into hydrogen peroxide (H_2O_2) which, through further reactions catalysed by transition metal (M^{n+}) can form the highly reactive hydroxyl radical ($\cdot\text{OH}$). Superoxide also reacts swiftly with nitric oxide (NO), generating peroxynitrite, which is also highly reactive (Modified from Sitte and von Zglinicki, 2003).

Antioxidants

1. Enzymatic

a) Superoxide dismutases (SOD) are a class of enzymes which play a critical role in the antioxidant defense of oxygen-exposed cells. These enzymes catalyze the dismutation of superoxide into O_2 and H_2O_2 (Benzie, 2000). Three forms of SOD exist in mammals and most chordates: SOD1, which is a dimer (two units), is mainly found in the cytoplasm and contains copper and zinc ions; SOD2, which is a tetramer, is mitochondrial and contains a manganese ion; and SOD3, an extracellular tetramer with copper and zinc ions. The genes are located on chromosomes 21, 6, and 4, respectively (21q22.1, 6q25.3 and 4p15.3-p15.1) (Benzie, 2000; Fransen et al., 2012).

b) Catalase, is an enzyme primarily located in the peroxisomes, but also, to a lesser extent, in mitochondria. The enzyme itself catalyzes the conversion of H_2O_2 into O_2 and H_2O ($2H_2O_2 \rightarrow 2H_2O + O_2$) and is a key player in the antioxidant defense mechanisms (Benzie, 2000). Glutathione peroxidase performs the same function and both enzymes reduce the toxicity of oxygen-reactive radicals through the catalysis of superoxide into H_2O_2 . Catalase is found in high concentrations in the liver, kidneys and red blood cells (Benzie, 2000).

c) Glutathione peroxidases, reactions involving glutathione and H_2O_2 and organic hydroperoxides are catalyzed by glutathione peroxidase. This enzyme can be either selenium dependent or selenium independent, and reduces peroxides, thereby protecting against free radical damage. The enzyme can be found within either the mitochondria or the cytosol of the cell, and is critical to the prevention of lipid peroxidation. This in turn maintains the integrity of biological membranes (Brigelius-Flohé and Maiorino, 2013).

2. Non-enzymatic. A number of small-molecule antioxidants are involved in antioxidant defense, as well as the antioxidant enzymes. These mainly function in the extracellular areas, such as the blood system, where there is a lower concentration of antioxidant enzymes. Two types of small-molecule antioxidants exist: lipid-soluble, which reside in cell membranes and lipoproteins, and water-soluble, which are present in bodily fluids such as blood and intercellular fluids (Nimse and Dilipkumar, 2015).

3. Vitamins. **Vitamin E**, tocopherol, is the most abundant natural antioxidant and is found in both plants and animals. At least eight structural isomers exist. Primary among these is alpha-tocopherol, which has particularly efficacy as an antioxidant. In cellular membranes, it reacts directly with oxy-radicals, superoxides and singlet oxygen, and protects against lipid

peroxidation (Darr et al., 1996). **Vitamin C**, ascorbic acid, is water-soluble (unlike vitamin E) and therefore has more efficacy in aqueous contexts. Both vitamins C and E work together to neutralize free radicals and singlet oxygen. The reduced antioxidant form of vitamin E (oxidized vitamin E) can also be regenerated, or recycled, by vitamin C. In its capacity as a reducing and antioxidant agent, vitamin C is able to process superoxide and hydroxyl free radicals, as well as lipid hydroperoxides through direct contact (Darr et al., 1996).

1.2.5 Role of the immune system in oxidative stress

Oxidative stress is caused by a disparity between oxidising and reducing agents (Sies, 1997), and can cause macromolecular damage over time, including lipid peroxidation, protein carbonylation and DNA oxidation. Increasingly however, the importance of Reactive Oxygen Species (ROS) in signalling is being acknowledged (Suzuki et al., 1997). Various examples can be provided: an ‘oxidative burst’ of neutrophil-generated ROS can destroy pathogens and thus benefit the immune systems in terms of antimicrobial protection (Dahlgren and Karlsson, 1999). Immune complexes with auto-antigens may result in overproduction of ROS, which can be damaging to macromolecules, can suppress T-cell proliferation and may cause apoptosis (Thoren et al., 2007). Reactive nitrogen species (RNS) peroxynitrite, when incubated with T-cells, has a similar effect that may lead to apoptosis after inhibiting the T-cell proliferation (Kasic et al., 2011). T-cells may also become hyper-responsive as a result of the susceptibility of TCR signalling to oxidative stress-induced modification of certain molecules such as CD3- ϵ , TCR- $\alpha\beta$ and TCR- ζ (Cemerski et al., 2003). Small amounts of ROS however, have been shown to be beneficial. Indeed, low levels of H₂O₂ induced nuclear factor kappa B (NF κ B) transcription, IL-2 gene expression and the IL-2 receptor chain-alpha in T-lymphoma cells (Los et al., 1995). It is proposed that changes in the cellular redox environment cause T-cells to react with ROS in different ways (Griffiths, 2005) and also to differentiate accordingly (King et al., 2006). When 2, 3-dimethoxy-1, 4-naphthoquinone, a ROS generator, was used to stimulate peripheral blood mononuclear cells (PBMC), Th2 phenotypes were observed to increase and Th1 were inhibited (King et al., 2006). When ROS are present, reactive carbonyls, such as 4-hydroxy-2-nonenal and malondialdehyde are generated at random on lipids and proteins, and these also lead to differentiation in favour of a Th2 phenotype (Moghaddam et al., 2011). These studies underline the importance of delicate ROS level regulation in order to maintain bacterial protection, immune response, or T-cell signalling in the cell maturation process.

Oxidative Stress and Regulatory T Cells

Tregs make up 5-10% of all CD4⁺ T-cells and their immunosuppressive function is dependent on oxidative stress (Zhu and Paul, 2008). The redox state between DC and naïve T-cells at the immune synapse is heavily influenced by Tregs, causing cysteine availability to naïve T-cells to be significantly reduced (Yan and Banerjee, 2010; Yan et al., 2010). Whilst not antigen-specific, this reduction is antigen dependent. Treg CLTA-4 and dendritic CD80/86 come into contact, stimulating a signal which suppresses the synthesis of DC iGSH and consequently extracellular cysteine synthesis (Yan et al., 2010). Furthermore, there is competition between Tregs and effector T-cells for this cysteine, which is then catabolized into sulphate, further limiting the amount of cysteine available (Yan et al., 2010). Effector T-cells consequently exhibit reduced intracellular glutathione (iGSH) levels and therefore fewer T-cells are activated and proliferation is reduced (Yan et al., 2010). The redox state at the immunological synapse is therefore critical. It has also been shown that, in comparison to other CD4⁺ T-cell subsets, Tregs have a higher tolerance for oxidative stress (Mougiakakos et al., 2009), making them far more adapted to immune response regulation. It has been found that Tregs secrete increased thioredoxin (Trx) which is an antioxidant enzyme, a 12 kDa oxidoreductase enzyme substrate containing a dithiol-disulfide, allowing it to scavenge ROS and metabolise H₂O₂ (Mougiakakos et al., 2011). Trx inhibition leads to decreased cell-surface thiols and, on addition of agent N-ethylmaleimide, a thiol depleting agent, Tregs became far more sensitive to H₂O₂ and died as a result (Mougiakakos et al., 2011). Furthermore, Trx was released when Tregs were exposed to tumour necrosis factor- α (TNF α) and the number of cell-surface thiols increased, resulting in greater H₂O₂ resistance.

1.2.6 Myocardial infarction as a complication of atherosclerosis

Restricted cardiac blood supply damages cardiomyocytes, causing myocardial infarction (MI). Clots, blockages, narrowing or arterial wall hardening may affect any cardiac or coronary artery, leading to poor blood supply. Heart function may be improved following MI by Tregs, which protect cardiomyocytes and reduce inflammation. A number of studies have been performed on animals with MI, investigating various inflammatory and/or vascular outcomes. One rat model study exhibited peak TNF- α , interleukin-1 β , and interleukin-6 levels one week following an induced MI, followed by a decline. These cytokines continued to be expressed at high levels, even in the unaffected myocardium, for a further 20 weeks.

It has been shown that MI can influence remote vascular processes (Takaoka et al., 2009), with implications for coronary restenosis following angioplasty or stent. A mouse model was studied, in which a spring wire was used to induce a smooth muscle cell-rich lesion in the femoral artery, mirroring stent-related restenosis. Four weeks later, neointimal hyperplasia was measured. It was found that the neointimal hyperplastic response was heightened if MI was induced at the same time as the injury. Green fluorescent protein (GFP) expressing mice had their bone marrow transplanted into the above mice. It was found that although neointimal hyperplasia was caused in part by GFP⁺ cells, the marrow itself was not implicated in the lesion's expanded area. Instead, in the injured arterial areas, a number of proinflammatory transcripts were found by cDNA arrays to have increased after the MI. Some of these were responsive to TNF α , so TNF α mRNA was measured and found to be augmented for up to 28 days after MI was induced. Back at the injury site, TNFR1 was found to be increased. The study team then successfully demonstrated that TNF α could be suppressed using pentoxifylline and consequently, the effects of the induced MI on neointima augmentation were significantly reduced. The paper therefore demonstrates a mechanism linking myocardial damage and the inflammatory pathways which increase the injury response at a remote vascular site. Studies of human MI patients with coronary stents have shown the monocyte subset (CD14⁺CD16⁺CX3CR1⁺) to be linked with restenosis (Liu et al., 2010). Consequently, adverse vascular events after MI may be caused by variation in peripheral blood monocytes.

In a more recent study, ApoE^{-/-} mice exhibited 50% increased plaque size three weeks after induced MI. Increased lesion protease activity was observed and CD11b⁺ myeloid cells, expressing increased levels of inflammatory genes, were found to occupy a larger area of that lesion. Increased monocyte levels in both blood and spleen – but not in bone marrow – were exhibited up to three months after MI. Humans who had died after acute myocardial infarction (AMI) also exhibited the same changes. It has been inferred therefore that the spleen may be involved in post-MI leukocytosis. It was found that atherosclerosis after MI slowed down following a splenectomy, although the bone marrow continued to release hematopoietic stem and progenitor cells, which seemed to accelerate atherosclerosis and support monocytosis (Katayama et al., 2006).

1.2.7 Immune response to myocardial infarction

Pathophysiology of acute myocardial infarction (AMI) is heavily influenced by the inflammatory response of the immune system. Previously I have described the adaptive immune system and its classification; below I am going to give some details about the response of the adaptive immune system subsequent to myocardial infarction.

Response of lymphocytes to MI

Inflammation is our most effective immune response. Threats are recognized, cells mobilized and instigators are removed from injury sites by the inflammatory response (Goronzy and Weyand, 2006). Lymphocytes (in comparison to neutrophils, whose existence is fleeting) survive for decades, and vary in accordance with the individual experience of the host. When an immune response is triggered, a clonal burst differentiates lymphocytes into a range of effector cells, which memorise the antigenic instigator (Hoffmann and Spyridopoulos, 2015; Caliguri and Nicoletti, 2006; Goronzy and Weyand, 2006; Ducloux et al., 2003) for future response. A range of factors, including age, gender, prior experience of infections, genetics and environment influence the repertoire of any given individual (Spyridopoulos et al., 2016; Hotchkiss and Karl, 2003).

Diseases with lymphopenia-mediated immunosuppression have been associated with increased incidents of cardiovascular events. AIDS patients, atomic bomb survivors or post-transplant immunosuppressed patients have all been observed to exhibit suppressed CD4 cells, leading to faster onset of atherosclerosis (Ducloux et al., 2003). In terms of ischemic heart disease development and prognosis, lymphocyte loss is implicated by these observations (Shmeleva et al., 2015).

AMI patients exhibit lymphopenia, but little is known of the implications of this. Low lymphocyte counts and high neutrophil to lymphocyte ratios were associated with increased cardiovascular events both in patients with AMI (Nuñez et al., 2008; Dragu et al., 2008) and without (Horne et al., 2005). A recent study of 1,037 AMI patients (68% ST-elevation AMI) found over a 23-month median follow up period that a low baseline lymphocyte count, adjusted for baseline characteristics, served as an independent mortality predictor (Dragu et al., 2008). Another study of 515 ST-elevation AMI patients found that acute phase AMI was associated with lymphopenia and furthermore, the higher ratio of neutrophils to lymphocytes also correlated with higher mortality (Nuñez et al., 2008).

It has not yet been proven whether this association is causative or simply correlational, but these studies certainly suggest that further understanding of alternative approaches to the pathophysiology of AMI is called for. These include novel therapies, such as those designed to prevent immune deregulation caused by an excess of proinflammatory T-cells and cytokines through mobilisation of Treg (Goronzy and Weyand, 2006; Caliguri and Nicoletti, 2006).

Effector T-cells response to MI

AMI risk can be more accurately indicated through lymphocyte count, which is a relatively easy measure to take. Whilst quick and easy to obtain however, lymphocyte count sheds little light on more complex cellular interactions. A deeper understanding of lymphocyte interaction and subtypes is required to gain useful therapeutic and pathophysiological knowledge.

CD4 lymphocytopenia is symptomatic of T-cell mediated immunodeficiency and is closely linked with atherosclerosis. Renal patients with higher CD4 cell counts ($>663/\text{ml}$) were found to be 1/10 as likely to suffer atherosclerotic events (Ducloux et al., 2003). AMI activates both CD4 (helper) and CD8 (cytotoxic) T-cells. The ratio between these is inverted on admission, and if this ratio is kept low over time, then the risk factor was observed to increase (Blum and Yeganeh, 2003).

Th1 and Th2 subsets are formed when CD4^+ cells are stimulated by an antigen and these produce specific cytokines. Pro-inflammatories, including $\text{INF}\gamma$, tumour necrosis factor- α , IL-2, IL-12 and IL-18 are released by Th1, whereas anti-inflammatories including IL-4, IL-5, IL-6, IL-9, IL-10 and IL-13 are produced by Th2. IL-10 in particular can suppress polarization of Th1 (Blum and Yeganeh, 2003; Steppich et al., 2007).

Th1 cells contribute to atherosclerotic growth as well as its destabilization, and can also lead to AMI in angina patients (Steppich et al., 2007; Methe et al., 2005). Both apoptosis of smooth muscle cells and increased synthesis of metalloproteinases are brought about by Th1, causing damage to the fibrous caps which form over atherosclerotic plaques, leading to rupture and potentially to thrombosis (Libby, 2001; Hansson, 2005). Unstable angina patients consistently exhibit increased Th1 levels compared with control groups (Steppich et al., 2007; Cheng et al., 2005; Methe et al., 2005).

Acute immune deregulation has been observed in AMI patients (Boag et al., 2015). A study involving 33 AMI patients found a proinflammatory imbalance between Th1 and Th2

compared to control groups. This was linked with left ventricular dilation, systolic dysfunction, and to a worse functional class (Cheng et al., 2005). Increased Th1 produces cytokines which activate endothelial cells and leukocytes, as well as inducing adhesion molecules (Cheng et al., 2005; Steppich et al., 2007). Furthermore, apoptosis of endothelial cells may be caused when blood supply returns, bringing with it various proinflammatory agents, causing a worsening of microvascular aggravation (Pasqui et al., 2003; Rössig et al., 2004). Pro-Th1 imbalance is implicated in AMI pathophysiology. IL-10, derived from Th2 is able to inhibit Th1 (Blum and Yeganeh, 2003; Steppich et al., 2007). It has been shown that mice which had been genetically manipulated to not produce IL-10 exhibited greater inflammatory response, higher TNF- α , higher neutrophil infiltration, increased intercellular adhesion molecules, increased infarct size and a higher death rate (Yang et al., 2000). In humans, as the ratio between pro- and anti-inflammatory cytokines increases, so does the frequency of cardiac events (Kilic et al., 2006).

Furthermore, AMI patients express a CD4 subset which lacks the marker for CD28. These CD4 $^+$ CD28null cells are cytolytic, expressing killer immunoglobulin-like receptors (Liuzzo et al., 2007; Zal et al., 2004). In AMI, CD4 $^+$ CD28null cells are very damaging; that they can be isolated from unstable plaques and also produce high levels of IFN- γ is a dangerous combination. These cells also recognize human HSP-60 (Zal et al., 2004), and are found in higher concentrations in patients with recurring acute coronary events (Liuzzo et al., 2007).

Regulatory T-cells response to MI

Physiological processes may become pathological if they are not effectively down-regulated, and immune responses are no exception (Caliguri and Nicoletti, 2006; Goronzy and Weyand, 2006; Mallat et al., 2007; Beissert et al., 2006). The previous ten years has seen increased scrutiny of the causes of AMI-related lymphocyte response. Both AMI patients and those with chronic atherosclerosis exhibit the same target antigenic stimuli, which means that coronary disease-related lymphocyte imbalances are not explained by the specific repertoire of target antigens alone (Caliguri and Nicoletti, 2006).

It has been suggested that defective T-lymphocyte compartment regulation may be responsible for a tolerance break, causing the pathological autoreactive immune response observed in AMI (Caliguri and Nicoletti, 2006; Goronzy and Weyand, 2006; Mallat et al., 2007). The idea of suppressor T-cells was first introduced in the 1970s, although the lack of more detailed characterization drew criticism (Gershon et al., 1972). By the mid-1980s, significant enquiry was focused on CD4 $^+$ CD25 $^+$ Treg (Sakaguchi, 2004), which use Foxp3

transcription factor and express cytotoxic T-lymphocyte antigen-4 (CTLA-4) and glucocorticoid-induced tumour necrosis factor family receptor (GITR).

It is thought that these natural suppressor cells come from a separate thymic lineage (Goronzy and Weyand, 2006). Their suppression of T-cells is antigen non-specific, although cell membrane contact must occur for this to happen. IL-2 has been implicated in $CD4^+CD25^+$ T-cell levels (Caliguri and Nicoletti, 2006; Goronzy and Weyand, 2006; Mallat et al., 2007; Beissert et al., 2006).

$CD4^+CD25^+$ T-cells have been shown to cause tryptophan deficiency by affecting dendritic cell metabolism in mice. Consequently, effector T-cells, which are stimulated by tryptophan, die off, potentially leading to lymphopenia (Beissert et al., 2006). Tregs function to protect against T-cell-derived proinflammatory cytokines being boosted in AMI. There appears to be a two-way relationship between dendritic and $CD4^+CD25^+$ T-cells. Tregs accumulate after being induced and expanded by dendritic cells, which present antigens in tissues (Beissert et al., 2006). In the presence of TGF- β and IL-10, $CD4^+CD25^+$ cells are also able to suppress $CD4^+$ T effector cells on contact (Beissert et al., 2006).

Other regulatory T-cells, including Tr1 and Th3 have been examined (Caliguri and Nicoletti, 2006; Goronzy and Weyand, 2006; Beissert et al., 2006). Tr1 produces TGF- β and IL-10 to inhibit a range of antigens. Th3 on the other hand, are non-antigen specific, and use primarily TGF- β to effect ‘bystander inhibition’. Th3 can be induced by oral administration of antigen and could, through this method, inhibit both Th1 and Th2 clone activation (Beissert et al., 2006). Treg activation is believed to be antigen-specific, but the suppressive effect of activated Tregs is non antigen-specific (Goronzy and Weyand, 2006; Beissert et al., 2006). Therefore, if deployed in therapy, these cells must be able to accurately target the affected organs in order to be used successfully (Beissert et al., 2006). Plaque inflammation and development also involves Tregs. $CD4^+CD25^+$ cells transfer into genetically modified mice prevented atherosclerosis induction and also inhibited plaque infiltration by T-cells and macrophages. The same study found that Treg depletion prevented collagen build up, making the plaque more vulnerable to infiltration, and also that lesion size increased (Mallat et al., 2007).

It has been suggested that AMI-related self-attacking lymphocyte behavior could be the result of a fault within the lymphocyte network itself. Despite sharing similar plaque structures and antigens, the distinction between stable and acute atherosclerosis might be explained by this fault within the regulatory lymphocyte network. Defective T-reg compartments were first

identified in AMI patients by Mor et al. (2006). It was found that patients with unstable angina exhibited oxidized LDL-specific T-lymphocytes, although this was not seen in chronic stable angina patients. The unstable angina patients exhibited fewer and less effective Tregs, and this has critical implications for potential therapeutic strategies (Mor et al., 2006).

This faulty regulation results in deviant behavior and, despite the cause being unknown, it is acknowledged that CD4⁺CD25⁺ T-cells are vital to the accurate modulation of the immune system. This knowledge yields great therapeutic potential as well as a deeper understanding of AMI pathophysiology (Caliguri and Nicoletti, 2006; Goronzy and Weyand, 2006).

Monocytes' Response to MI

Debris from damaged myocardial tissue is phagocytosed by neutrophils. Having been imported from the capillaries, monocytes then migrate to the extravascular space and become macrophages. 48-72 hours following the acute episode, the macrophages outnumber the neutrophils. They produce cytokines, which stimulate collagen production, and instigate moncytosis and fibroblast proliferation (Gibson and Gibson, 2006). The inflammatory marker CRP is produced in the liver, stimulated by macrophage and monocyte-secreted IL-6, and has undergone extensive investigation (Bodi et al., 2005; De Servi et al., 2005).

A study involving 238 primary angioplasty patients following acute ST-segment AMI was carried out, which used echocardiography to quantify systolic function, both at day 0 and at 6-months. White blood cell (WBC) subtypes were also measured. It was found that when reperfusion was inhibited, moncytosis was also reduced. Furthermore, these results correlated with decreased systolic recovery at 6 months (Mariani et al., 2006). These findings heavily implicate the role of monocytes in repair only after the hyperacute phase has passed.

It is still unknown whether moncytosis and neutrophilia are causal markers of necrosis, or they play a more direct role in injury related to reperfusion. It has been suggested that the association with more adverse angiographic outcomes is actually a two-way relationship (Gibson and Gibson, 2006). Pharmaceutical interventions including anticomplement antibodies, corticoids and neutrophil-blockers, which are designed to interrupt the inflammatory process, have not been successful in human studies (Gibson and Gibson, 2006; Nuñez et al., 2006). The conclusion from this is that elevated WBC is not a causative agent, but rather is merely a marker of negative clinical outcomes. Of course, a specific targeted ligand may not be involved at all; further investigation is required to identify the causal direction of this relationship.

1.3 Telomeres and Telomerase

Deoxyribonucleic acid (DNA) is a molecule whose coding determines most of the specific characteristics of living organisms. These long-chained molecules comprise proteins and ribonucleic acid and are folded into compact structures called chromosomes. In humans, 23 pairs of chromosomes can be found in the nucleus of every cell, making a total of 46 chromosomes. Each pair comprises one chromosome inherited from each parent and constitutes the means by which hereditary information is passed down each generation. Most cells have a limited life span and must replicate through cell division; this is known as the cell cycle. Each cell division requires the DNA to replicate in order to pass the same genetic code to each subsequent cell. This is critical for cells to share the same characteristics and therefore function correctly.

Linear chromosomes are capped at each end by a molecular structure called a telomere, which plays a vital role in chromosomal stability by preventing fusion events as well as chromosomal degradation due to exonucleases and oxidative stress. Every time a cell divides, replicating its chromosomes, the telomeres become slightly shorter. This continues in cells without telomerase until the telomeres emanate a DNA damage signal which halts the cell cycle and the cell cannot replicate, resulting eventually in cellular senescence since telomere damage can not be efficiently repaired (Petersen et al., 1998). This phenomenon is thought to function as a tumour suppressor mechanism for preventing cancer. Telomerase is an enzyme which uses its own RNA component to add telomeric repeats to the telomere structures, maintaining their length and preventing cellular senescence. Telomerase and its functions will be discussed in the forthcoming subchapters.

1.3.1 Biology of telomeres and telomerase

1.3.1.1 Telomeres

Telomeric DNA consists of repeating hexameric sequences ([TTAGGG]ⁿ) and is located at the ends of mammalian chromosomes (Figure 1.3). These specialised DNA structures are associated with the shelterin multiprotein complex, the human form of which contains six proteins: telomere repeat factors 1 and 2 (TRF1/TRF2), TRF1-interacting nuclear protein 2 (TIN2), TPP1, protection of telomeres 1 (POT1), and repressor/activator protein 1 (RAP1) (de Lange, 2005). In humans, telomere length ranges between 2-15 kilobase pairs (kbp) (Martens et al., 1998), whereas telomere length in laboratory mice can reach 40-80kbp (Blasco et al., 1997).

Telomeres and their associated proteins maintain chromosomal integrity in a number of ways. Chromosomal ends are protected by telomeres from enzymatic degradation, which prevents them from fusing with one another. This prevents chromosomal DNA from being recognised as a double-stranded break, which in turn inhibits the DNA damage response (de Lange, 2002).

T-loop and D-loop Structures

Telomeres form both T- and D-loops (Figure 1.4). The duplex part of the telomere is invaded by the single-stranded TTAGGG repeat tail. T-loop formation is dependent on DNA remodelling by architectural shelterin proteins (de Lange and Petrini, 2000).

T-loop formation with telomeric DNA substrates can be increased when TRF2 binds to tail-loop junctions *in vitro*. However, it is not yet known if TRF2 is responsible for stimulating T-loop formation. It may simply act as a stabilizing factor, for example, by preventing branch migration of T-loops, blocking their resolution. Irrespective of this, it is known that TRF2 inhibition *in vivo* may cause the T-loop to open, unfolding the telomere and resulting in the DNA being perceived as damaged (de Lange, 2005). Since chromosome ends are primarily protected by T-loops, the dynamics of such structures requires precise regulation in order for telomerase to access the telomere end without unravelling the chromosome ends (Griffith et al., 1999).

In a study on D-loops (displacement loops) of 100-200 base pairs, it has been shown that single-stranded DNA can invade homologous double-stranded regions and base pairs on one of the two strands. This indicates that a specific structure holds the D-loops in place, as opposed to simply random DNA looping. The TTAGGG G-strand telomere overhang in the D-loop is paired with internal CCCTAA tracts. This not only protects the DNA end, but is also structurally distinct from a broken DNA end (Griffith et al., 1999; Howard et al., 1991).

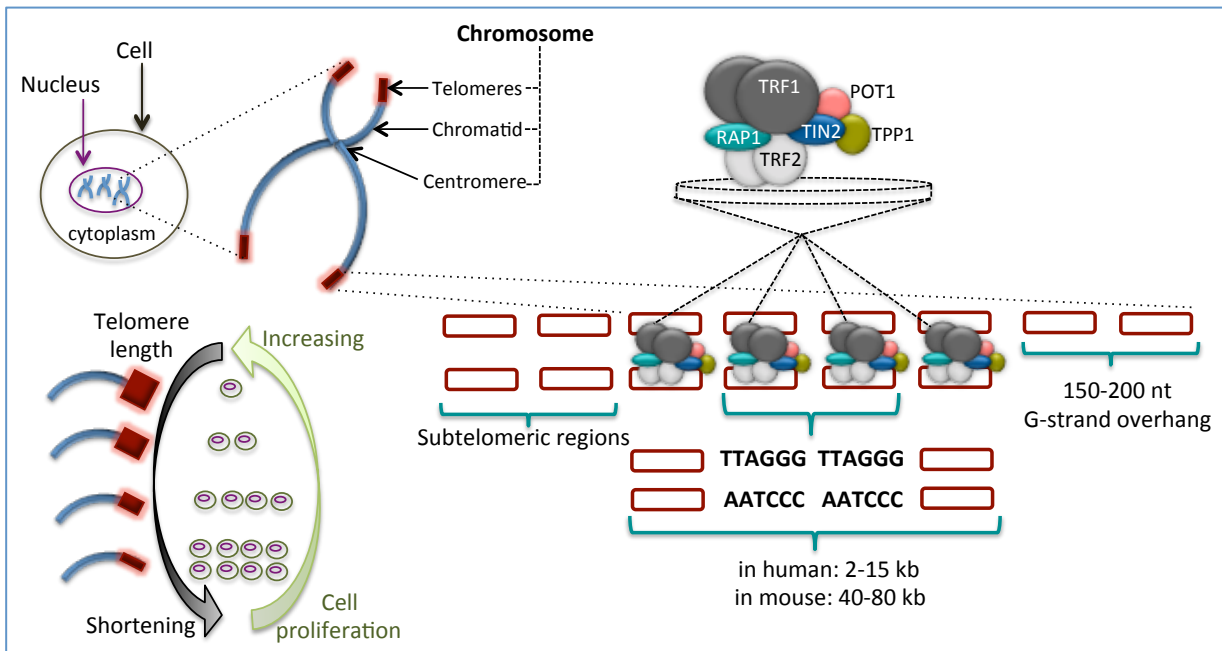


Figure 1.4. Telomere location and structure

Telomeres are located at the end of each chromosome's arm and shorten with each cell division. Protein complexes are linked to telomeres and are called telosome or shelterin (TRF1, TRF2, TIN2, POT1, TPP1 and RAP1). Heterodimer POT1/TPP is also linked to the G-strand (Modefied from Hoffmann and Spyridopoulos, 2011).

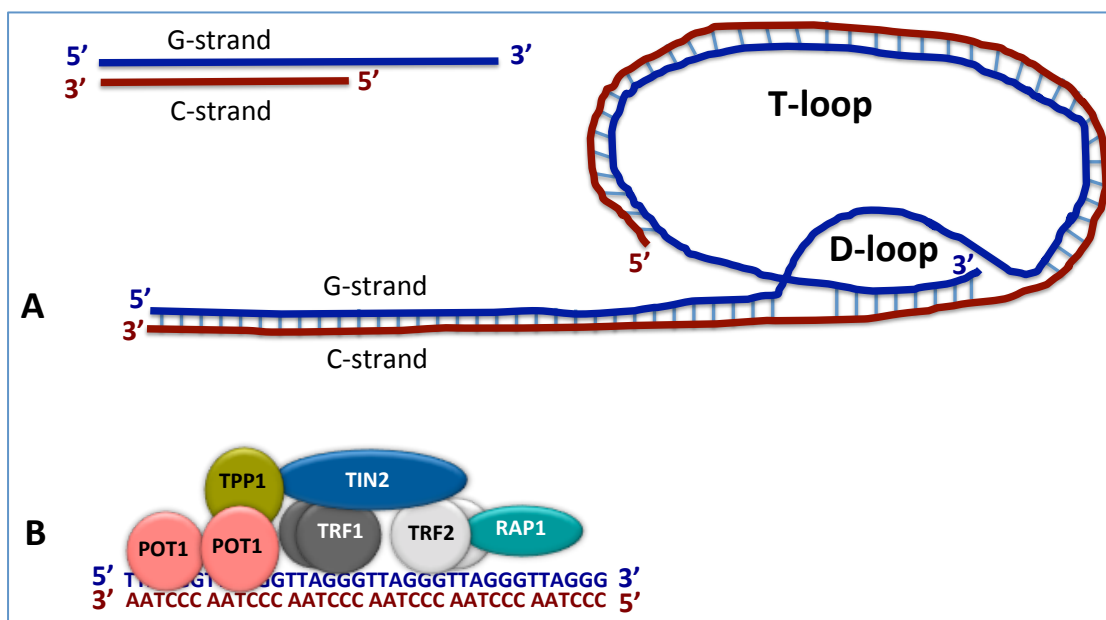


Figure 1.5. Structure of T and D loops

The T-loop as shown in **A**: is the big loop from double stranded telomere DNA and shelterin proteins. The invasion of the 3' single stranded (ss) overhang is the D-loop. The ss overhang also binds POT1. **B**: A telomere protection complex is formed by the sheltering proteins TRF1, TRF2, TPP1, POT1, TIN2 and RAP1. Modified from (Greider, 1999; de Lange and Petrini, 2000).

Telomere shortening is the product of both oxidative stress and the end replication problem, which occurs when the chromosomal ends are not fully replicated by DNA polymerase. This is called the “end replication problem” (Olovnikov, 1996). Mammalian DNA is replicated with DNA polymerases, which are only able to synthesise DNA in a 5’-3’ direction. A template is required for polymerases to begin the DNA synthesis, and the starting primer for this is an 8-12 RNA base segment. During this process, synthesis of the leading strand is uninterrupted, but the lagging strand is in short RNA-primed DNA segments known as Okazaki fragments. After DNA extension, the gaps are filled in by DNA polymerase priming from upstream DNA 3’ ends and the RNA segments are removed. Following removal of the outer 5’-RNA primer, a 3’ gap opens up, resulting in a daughter strand that is shorter than the parent strand (Watson, 1972; Levy et al., 1992).

Consequently, the terminal sequence – a short section of the telomere – is lost every time DNA replication occurs (Watson, 1972; Levy et al., 1992). Beyond a critical telomere length, the cell cycle is arrested due to the uncapped telomere ends signalling a DNA damage and replicative senescence is induced. The 3’-G-rich strand is recognised by telomerase and elongated with the TTAGGG telomeric repeats that are complementary to the RNA template on the TERC component (Blackburn, 2005). Oxidative stress significantly affects telomeric shortening (\approx 50-500bp) (von Zglinicki et al., 1995; Lorenz et al., 2001).

A finite number of cell divisions are therefore possible, known as the Hayflick limit (Allsopp et al., 1992; von Zglinicki et al., 1995; Blasco et al., 1997). In most somatic cells, where telomerase is not present, each cell division results in decreased telomere length, up to a critical limit, at which point, a p53-dependent DNA damage response (DDR) becomes activated, leading to cell senescence or apoptosis (Saretzki et al., 1999). DDR is caused by the activation of cell cycle checkpoint proteins (Ck1 and Ck2), which are triggered by sensor kinases (e.g. ATM/ATR or DNA PK), or phosphorylation of γ H2A.X. Ultimately, a p53/p21 pathway is initiated, resulting in cell-cycle arrest (d'Adda di Fagagna et al., 2003).

Telomere-independent DNA damage signalling (e.g. a non-telomeric DNA damage response, cyclin-dependent kinase inhibitor signalling, or altered mitogenic signalling) may also cause cellular senescence (Rodier and Campisi, 2011).

It has been suggested that telomere length may be a biomarker of human ageing, and in particular that telomere length is affected by oxidative stress and cellular senescence (von Zglinicki et al., 1995; von Zglinicki et al., 2005; Spyridopoulos and von Zglinicki, 2014). Further research into this concept has involved measuring the average leukocyte telomere

length (LTL) in relation to ageing and disease (Cawthon et al., 2003; von Zglinicki et al., 2000). A positive correlation was found between LTL and atherosclerosis and environmental factors linked with vascular ageing, such as smoking, high BMI, lack of exercise and insulin resistance (Samani et al., 2001). A recent longitudinal study by Huzen et al. (2014) found telomere attrition to be accelerated by smoking and metabolic syndrome variables including waist-hip ratio, cholesterol and blood glucose levels. Consequently, LTL may also indicate chronic immune activation, caused by oxidative stress and inflammation.

Telomere dysfunction and the induction of cell senescence.

Cellular senescence is defined as the “ultimate and irreversible loss of replicative capacity occurring in primary somatic cells” (Hayflick and Moorhead, 1961). It was found by these two authors that in a constant culture condition, after a reasonably specific number of population doublings (PDs), senescence was reached. This implies the concept of a ‘biological clock’ or ‘replication counter’, which uses cell divisions as a measure of biological time (Hayflick, 2000). After a certain number of divisions has been reached, then senescence is triggered, blocking any further cell division. Cellular senescence has numerous causes, but one very likely mechanism is through shortening of telomeres (Harley et al., 1990) or damage to telomeres (Hewitt et al., 2012).

Telomere shortening can be caused firstly by the end-replication problem, which occurs when the chromosomal ends are not fully replicated by DNA polymerase (Olovnikov, 1996). When the final RNA primer becomes detached from the OKASAKI fragment during telomere replication, a G-rich overhang is formed. Moreover, when telomeres are processed, C-rich strand degradation results in a single-stranded G-rich 3'-overhang at the end of each telomere (Wellinger et al., 1996; Makarov et al., 1997). Secondly, oxidative stress was found to accelerate senescence through increased telomere shortening (Von Zglinicki et al., 1995). It is thought that confluent cells, in spite of the fact that telomere length is maintained due to absence of cell division, may nevertheless exhibit telomere dysfunction due to accumulation of DNA damage such as single strand or double strand breaks (Sitte et al., 1998; Petersen et al., 1998; Hewitt et al., 2012). Thus, while telomere shortening requires cell division, DNA damage can also accumulate in telomeres of non-dividing cells and result in telomere dysfunction.

Reactive Oxygen Species (ROS) can cause significant damage to telomeres, resulting in their erosion and consequent signaling for senescence (Passos et al., 2007, 2010; Hewitt et al., 2012).

A DNA Damage Response (DDR) is induced via p53, p21, and ATM/ATR and Chk1/2 activation, caused by damaged or short telomeres (von Zglinicki et al., 2005). Telomeric damage is irreversible, so this process can eventually lead to senescence (permanent cell cycle arrest) (Hewitt et al., 2012; Nelson and von Zglinicki, 2013). Early events in DDR include signaling (Shilo, 2003) and recruitment of signaling kinases including ATR, ATM and potentially DNA-PK, to the damage site. When activated, these kinases cause the phosphorylation of Ser-139 at histone H2AX molecules (γ H2AX) proximal to the damage location. It has been suggested that histone H2AX phosphorylation assists in the focal assembly of MDC1/NFBD1, NBS1 and 53BP1, which are checkpoint and DNA repair factors. Further to this, histone H2AX phosphorylation plays a role in the activation of transducer kinases Chk1 and Chk2 via phosphorylation. These converge the signal onto p53. Studies have already demonstrated that growth arrest via ATM/ATR activation is caused by telomere dysfunction (Karlseder et al., 1999; Rouse and Jackson, 2002) and eventually through activation of p53 and p16 (observed in fibroblasts from humans, but not mice) (Smogorzewska and De Lange, 2002). Various groups have shown that senescence-associated DNA damage foci (SDFs) may be formed by uncapped telomeres, also called Telomere induced foci (TIF's) (Takai et al., 2003; d'Adda di Fagagna et al., 2003).

Mechanism of cellular senescence by dysfunctional telomeres

Through which mechanism is senescence caused by telomere shortening and age and telomere dysfunction? Telomere dysfunction can be caused by a) shortening of telomeres (von Zglinicki et al., 1995), b) uncapping of telomeres, for example by inhibition of TRF2 (Karlseder et al., 1999) and c) by DNA damage that occurs anywhere in the telomere (Hewitt et al., 2012). Von Zglinicki et al. (2005) describe that both telomere shortening and dysfunction induce senescence via the induction of a DNA damage response pathway. Telomere damage causes the DNA ends to become exposed, which may result in triggering of the DNA damage response. Telomeres have a 3' overhang, which forms a circular structure (a t-loop) by invading the double-stranded telomeric DNA. Binding proteins, including TRF1, TRF2 and Pot1 stabilize the t-loops (Smogorzewska and de Lange, 2004). However, TRF2 can become mutated and overexpression of mutated TRF2 results in t-loops becoming uncapped and eventually causing senescence or apoptosis (Karlseder et al., 1999). Mutant TRF2 overexpression has the interesting side effect of inducing γ H2AX foci (Takai et al., 2003), which are known to indicate DNA double strand breaks (DSBs). Increased γ H2AX foci at telomeres (TIF's or TAF's) are also seen in cells entering replicative senescence and in aged mice (Sedelnikova et al., 2004; Herbig et al., 2004; Hewitt et al., 2012). In addition, a

number of DNA damage factors, including MDC1, phospho-ATM, NBS1, Rad17 and 53BP1 are known to gather around mutant TRF2-induced foci (d'Adda di Fagagna et al., 2003). Consequently, it has been proposed that DNA damage responses are triggered by not only general DNA damage, but also by telomere shortening.

Two main pathways were identified, involving either p53 or Rb, in relation to the induction of cellular senescence. Inhibition of p53 and Rb by viral proteins causes human diploid fibroblasts to become immortal (Werness et al., 1990; Ide et al., 1983; Dyson et al., 1989). Rb is maintained in a hypophosphorylated form by p16INK4a, which inhibits CDK4/6. E2F activity is blocked by hypophosphorylated Rb, thereby inducing senescence. Senescent cells exhibit amplified P16INK4a levels, which in turn induces cellular cycle arrest (Hara et al., 1996; Alcorta et al., 1996). However, the DNA damage response pathway seems to play no role in regulating P16INK4a levels. Rather, P16INK4a can be upregulated by oncogenic signals, including overexpression of activated Ras. Conversely, the DNA damage response pathway includes p53 as one of its key downstream targets, therefore, when this pathway is triggered, p53 is stabilized and activated. P53 is activated by ATM through a number of routes (Kastan and Bartek, 2004) including: downstream activation of the kinases Chk1 and Chk2, causing p53 phosphorylation at Ser20, which stabilizes p53 by disrupting interaction between MDM2 and p53. MDM2 can also be phosphorylated directly by ATM, causing it to be downregulated. Lastly, p53 can be phosphorylated at Ser15 by ATM, triggering p53 transcriptional activity. There are numerous studies that have found evidence supporting a connection between p53 activity and cell cycle arrest. For example, heterozygous p53 truncation mutations are known to cause activation of abnormal p53, leading to premature senescence (Maier et al., 2004; Tyner et al., 2002). Similarly, there are several of ways to deactivate p53, including homozygous deletion of p53, dominant-negative p53 mutants, antisense oligonucleotide, anti-p53 antibodies and p53 peptide inhibitors, all of which cause DNA synthesis to reinitiate, preventing cellular senescence and thereby extending the cell's life span (Herbig and Sedivy, 2006). The evidence above underlines the key role played by p53 in cellular senescence induction.

P53 activation causes p53 target genes to be transcribed and upregulated. Within these, one major causal factor of p53-induced senescence is p21. p21 inhibits CDK's (cyclin dependent kinases), as does p16INK4a, leading to cell cycle arrest and consequently senescence. As the cells progress further into senescence, p21 increases (Alcorta et al., 1996) and it has been found that deleting the p21 gene in a targeted manner causes human fibroblasts to avoid senescence (Brown et al., 1997). The evidence collectively points to a role for the ATM-

Chk1/2- p53-p21 pathway in responding to DNA damage and telomere shortening by inducing senescence (Fig. 1.Q1).

If cellular senescence is genuinely caused by the DNA damage response pathway, then it should be reversed by inactivating that pathway, in theory causing the return of that cell to its normal replicative cycle. It has been observed that ATM/ATR and/or Chk1/Chk2 inhibition caused a significant amount of cells to return to the DNA synthesis phase, however without any real cell division occurring confirming the irreversibility of senescence (Herbig et al., 2004; d'Adda di Fagagna et al., 2003). Further to this, ATM and ATR inhibition by the protein kinase inhibitor 2-aminopurine (2-AP) was found to re-enable DNA replication in 40% of all cells (Herbig et al., 2004). A causal relationship is therefore confirmed linking the DNA damage response pathway and cell cycle arrest and that signal transduction pathways play an active role in maintaining cellular senescence (Passos et al., 2010).

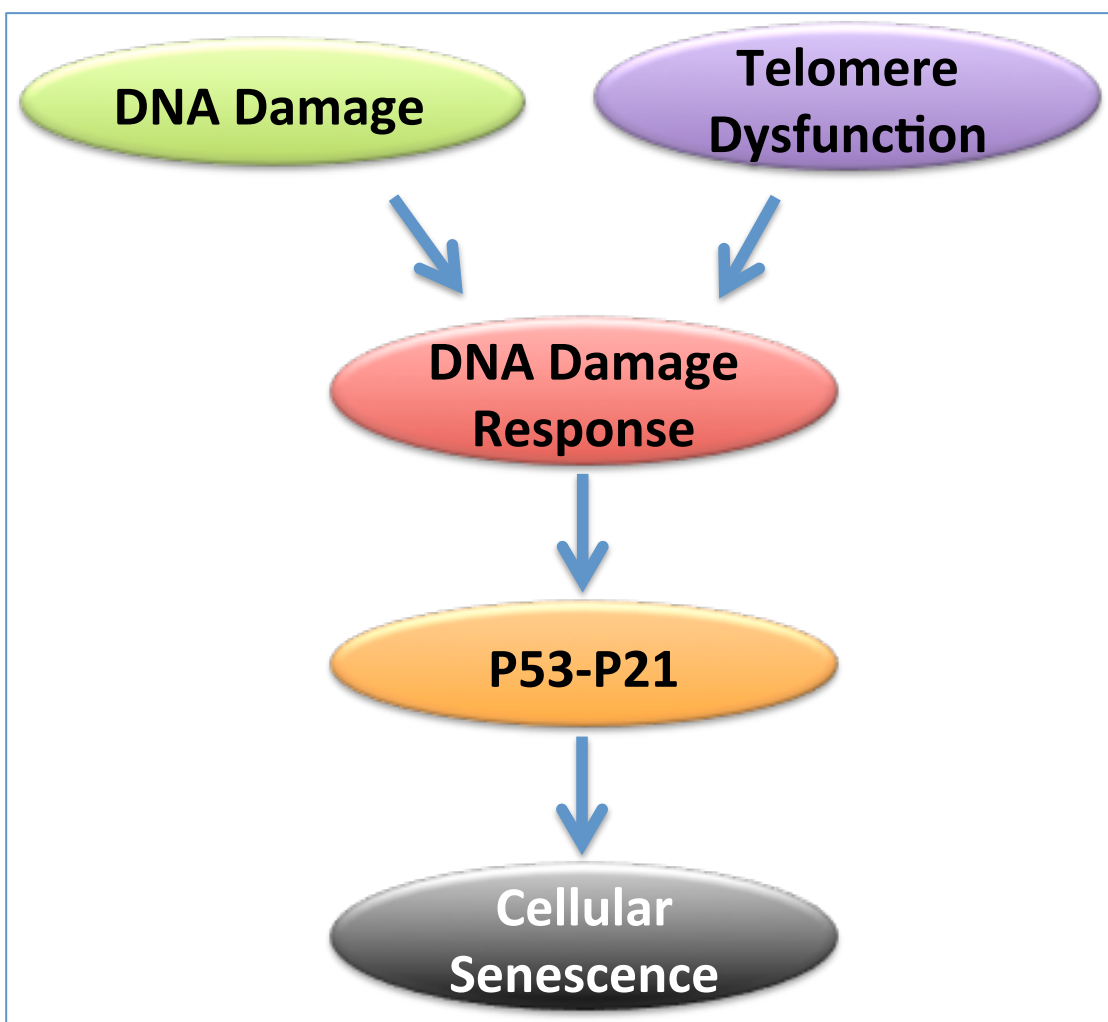


Figure 1.6. Illustration of how the DNA damage response pathway leads to cellular senescence (Modified from Lou and Chen, 2006).

1.3.1.2 Telomerase

Telomerase is a reverse transcriptase which in its canonical function extends telomere ends (Greider and Blackburn, 1989). It consists of the reverse transcriptase (TERT) catalytic subunit and the RNA part (TERC) containing the template, and is associated with various additional proteins (e.g. heat-shock protein hsp90 and dyskerin) (Lingner et al., 1997; Nakamura et al., 1997). TERT and TERC are both necessary and sufficient for the catalytic activity of telomere maintenance and elongation to take place (Lingner et al., 1997).

Both humans and mice share a similar TERT/TERC structure. The human TERT gene is located on chromosome 5, whereas in mice, it is found on chromosome 13 (Greenberg et al., 1998). TERT mRNA in mammals comprises 16 exons and 15 introns across 35kb (Cong et al., 1999), and both mouse and human TERT genes have comparable promoter regions in which its regulation differs (Pericuesta et al., 2006). In mammals, TERC comprises 451 nucleotides, while its template part complements the telomeric sequence, which comprises 11 nucleotides (5'-CUAACCCUAAC-3') (Feng et al., 1995; Egan and Collins, 2012). Mouse and human telomerase are also functionally similar. TERC knockout (KO) mouse cells (i.e. those which are telomerase-activity-deficient) have been transfected with human telomerase genes, resulting in fully restored telomerase. This leads to the conclusion that human and mouse telomerase is both functionally interchangeable and structurally conserved (Martín-Rivera et al., 1998).

1.3.1.3 Telomerase expression

Telomerase is expressed in a tissue-specific manner, and across their lifespan, telomerase activity is persistent in various mouse tissues, including lymphocytes, liver, muscles, testes and intestines (Breault et al., 2008). Telomerase is active in most human embryonic tissues until about week 20 of gestation, at which point its levels gradually decrease. Activity is still detectable in certain adult human cells, including lymphocytes, endothelial cells, stem cells and germ cells (Ulaner et al., 1998). In contrast, telomerase is active in most adult mouse somatic tissues (Martín-Rivera et al., 1998). Another important difference between telomerase activity in mouse and human cells is its different processivity which is much lower in mouse tissues (Chen and Greider, 2003).

1.3.1.4 Telomerase functions

Canonical as well as non-canonical functions have been described for telomerase (Figure 1.5). When functioning canonically, telomerase protects against chromosomal end fusion,

chromosomal instability and telomere erosion. Immortal cell proliferation requires an indefinite potential, such as that found in stem, germ, embryonic and cancer cells, and necessitates telomerase activity (Greenberg et al., 1998; Martín-Rivera et al., 1998).

Non-canonical (non-telomeric) telomerase functions have also been demonstrated. For example, TERT is increasingly implicated in a number of telomere-independent effects, cell survival and proliferation, mitochondrial function, regulation of gene expression, stem cell biology, chromatin remodelling and cellular transformation as well as a protective function against apoptosis and oxidative stress (Cong and Shay, 2008; Saretzki, 2014; Ahmed et al., 2008; Haendeler et al., 2009; Singhapol et al., 2013).

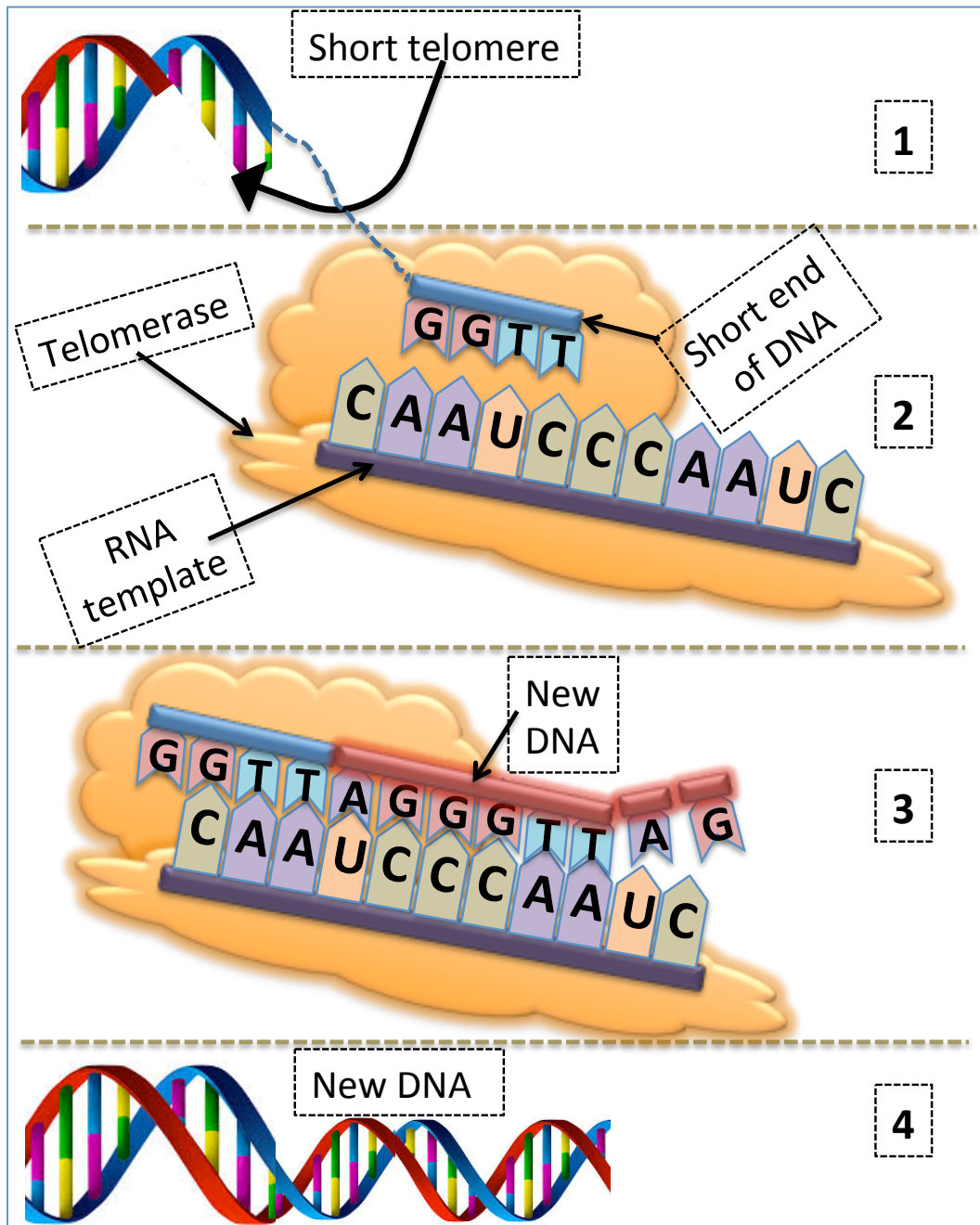


Figure 1.7. Telomerase functions as a reverse transcriptase

Telomeres are elongated by telomerase in the following way: 1. The telomere is short and un-replicated. 2. Telomerase extends the un-replicated end by annealing its RNA template to the DNA overhang. 3. The RNA template directs sequential nucleotide additions and anneals to the added sequence. 4. New DNA polymerase attaches the complementary strand (Modified from Sadava, 2007).

Regulation of telomerase

Telomerase is a highly regulated enzyme that synthesises telomeric repeats and maintains telomeres during late S-phase (Blackburn, 2005). Its activity is observed in human in highly proliferative cells, such as germ line, self-renewing stem cells and embryonic tissues, as well as lymphocytes and endothelial cells.

Telomerase regulation is achieved at various levels, including regulation by binding to and accessing telomeres, regulation of hTERT transcription, regulation of hTR, TERT splicing, post translational modification (phosphorylation), telomerase regulation by subcellular localization and cytokine regulation of telomerase activity in T-cells.

Telomerase regulation by binding to and accessing telomeres

Telomere tracts are not always maintained in all cells, despite the presence of active telomerase. One reason can be inaccessibility of telomeres by telomerase which affects level of regulation (Counter et al., 1998).

Telomerase accessibility is regulated by telomere-associated proteins (Evans and Lundblad, 2000); the first of these to be identified were TRF1 and TRF2 (TTAGGG repeat binding factors 1 and 2). These play a role in t-loop formation after having bound specifically to duplex telomeric DNA (Griffith et al., 1999). In this capacity, TRF1&2 negatively regulate telomere length (Smogorzewska et al., 2000; van Steensel and de Lange, 1997). In telomerase-positive cells, telomere elongation is subdued by TRF1&2 overexpression (Smogorzewska et al., 2000). It has also been suggested that the DNA damage repair complex, Rad50/MRE11/NBS1, interacts with TRF1&2 (Karlseder et al., 1999), implying that telomere integrity and DNA repair pathways interact at a molecular level. In vitro studies have shown that parallel pairing of telomeric DNA is promoted by TRF1 (Griffith et al., 1998). Furthermore, DNA polymerase-induced C-strand DNA synthesis is inhibited by TRF1 binding to duplex telomeric DNA (Smucker and Turchi, 2001), an observation supported by the role of TRF1 in telomere elongation inhibition (Ancelin et al., 2002). Endogenous TRF1 is removed by a dominant negative TRF1, causing telomeres to extend in telomerase-positive cells only (Karlseder et al., 2002). Telomerase is thought to be prevented from reaching the telomeres, because it is blocked by TRF1, which binds along the double-stranded telomeric DNA repeats. By this reasoning, more TRF1 is able to attach to longer telomeres, resulting in a negative feedback loop. This not only regulates telomere length, but also provides a potential explanation for why the shortest telomeres are preferentially elongated (Steinert et al., 2000). Two TRF1-associate partners have been identified: TIN2 (Kim et al., 1999) and tankyrase (Smith et al., 1998; Cook et al., 2002), which also both play roles in the negative feedback loop. PinX1, a TRF/Pin2-interacting protein that inhibits telomerase, has also been shown to directly interact with hTERT (Zhou and Lu, 2001).

The binding between some shelterin proteins and telomeres prevents telomerase from interacting with the end of chromosomes. This may lead to telomerase regulation (Venteicher

and Artandi, 2009) by the association between protection of telomeres 1 (POT1) and TPP1 (POT1 and TIN2 organizing protein 1) at the 3' end of telomeres. This prevents telomerase from binding to the end of the chromosome (de Lange, 2005). One study suggested that the physical links between the shelterin complex and telomerase is secondary to the affinity of POT1 to telomeric sDNA and TPP1 with telomerase, which also prevents telomerase from binding with the chromosome end. This may be one type of telomerase regulation (Xin et al., 2007; Chu et al., 2015).

TPP1 plays a role in the recruitment of telomerase to telomeres (Abreu et al., 2010). Super-telomerase HeLa cells (hTERT and hTR are overexpressed) have been used to investigate this phenomenon, using quantitative chromatin immunoprecipitation (ChIP) alongside immunofluorescence and fluorescence in situ hybridization (FISH). These methods are able to track hTR and hTERT relationships with telomeres. Reduced telomerase presence at telomeres has been found to be associated with the depletion of TPP1 and TIN2 on telomeres via the action of short hairpin RNA (shRNA). TPP1 binds to telomeres via TIN2 to regulate the presence of telomerase at the telomeres (Abreu et al., 2010).

TPP1-POT1 was found to be a stimulator for telomerase activity (Wang et al., 2007; Wang and Lei, 2011; Schmidt et al., 2014). A tripartite model which explains telomere length regulation has been proposed (Wang et al., 2007). This also appears to reconcile the apparently contradictory roles of TPP1 and POT1.

- 1) The 3'-terminus of the G-overhang is covered by POT1-TPP1, the telomere becomes occupied, preventing telomerase binding.
- 2) An as-yet unknown mechanism breaks the bond between POT1-TPP1 and the above site. This mechanism could involve disruption of the shelterin complex or post-translational modification.
- 3) During telomere extension, the POT1-TPP1 complex functions as a telomerase processivity factor.

The telomere then extends to a certain threshold, generating new repeats, to which shelterin complexes bind. Human telomeres could be maintained by one or more rounds of telomere extension per cell cycle. When POT1-TPP1 is present, telomerase processivity was in the region of four repeats, or 24 nucleotides. The new 3'-terminus then becomes rebound to POT1-TPP1, preventing further telomere extension (Wang et al., 2007; Nandakumar and Cech, 2013).

Regulation of hTERT transcription:

c-Myc is an oncogene which promotes growth, proliferation and apoptosis. c-Myc and Max (basic-helix-loop-helix-zipper (bHLHZ) protein) both form a heterodimer which binds with the E-box sequence 5'-TTAGGG-3' in the regulatory region of a target gene. Studies involving sequence analysis of the hTERT promoter have shown that the core region -34 and -242 nucleotides contain E-boxes, both upstream of the ATG (Cong et al., 2002).

The Sp1 transcription factor can potentially bind to one of five GC-boxes situated between two E-boxes on the hTERT core promoter (Kyo et al., 1997). Components within the general transcription mechanism, including TBP-associated factors and the TATA-box binding protein, interact with Sp1. Together, these associations assist in initiating the transcription of promoters lacking in TATA boxes (Emili et al., 1994; Hoey et al., 1993; Pugh and Tjian, 1991). The promoter for hTERT lacks TATA box (Cong et al., 1999; Kyo et al., 2000). It has been found within the core promoter that Sp1 sites are vital to hTERT promoter activity. Site mutations were seen to completely inhibit promoter activity in luciferase reporter assays (Cong and Bacchetti, 2000; Kyo et al., 1997).

Human papillomavirus (HPV) I6 E6 protein can induce telomerase activity in both mammary epithelial cells and primary human keratinocytes (Klingelhutz et al., 1996), mediated by hTERT transcription upregulation, itself the result of E6 and irrespective of p53 degradation and c-Myc induction (Gewin and Galloway, 2001; Oh et al., 2000; Veldman et al., 2001).

Telomerase activity in the human endometrium has a positive correlation with endometrial cell proliferation and is detected during the menstrual cycle (Kyo et al., 1997; Tanaka et al., 1998). This indicates a role for steroid sex hormones in telomerase activity regulation. Two possible oestrogen responses have been identified through hTERT promoter sequence analyses. The first contains a Sp1 site -950 bp upstream of the ATG. This is located in close proximity to an oestrogen response half-site that functions as an oestrogen response element. The second oestrogen response element is found at -2754 bp upstream of the ATG (Cong et al., 1999; Kyo et al., 1999). It has recently been shown that telomerase activation via oestrogen happens through direct transcriptional regulation of hTERT expression within tissues responsive to hormones (Kyo et al., 1999; Misiti et al., 2000).

Within 3h of 17 β -oestradiol treatment, human ovarian epithelial cells with oestrogen receptors exhibit telomerase activity running concurrently with hTERT induction and expression of mRNA and protein. In these cells, oestrogen activated hTERT transcription is

contingent on oestrogen receptor α , but not oestrogen receptor β . DNA footprinting has indicated that the -950 response element is modified in the oestrogen receptor. 17β -estradiol treatment indicates that this occurs in oestrogen receptor + cells, but not in oestrogen receptor - cells. Furthermore, the -950 response element has been shown via luciferase assays to cause hTERT transcription induction to be observed. Even when placed into the heterologous thymidine kinase promoter, the oestrogen response element maintains functionality (Misiti et al., 2000).

In addition to a transcriptional activation, there are also negative regulators of hTERT transcription, for example **Mad1**.

Normal cell growth and development depend on components of the c-Myc/Max/Mad transcription factors, which control various processes including differentiation, transformation and apoptosis (Grandori et al., 2000). These elements dimerize and, after binding to it, either activate or suppress E-box-containing promoter activity. Max is ubiquitous and dimerizes with both c-Myc and Mad. Gene expression is activated by E-box-bound c-Myc/Max heterodimers, whilst Mad/Max heterodimers act in competition for E-box-binding to repress transcription. Chromatin immunoprecipitation has shown hTERT promoter activity to have an antagonistic effect on HL60 cell differentiation (Xu et al., 2001). The hTERT promoter E-boxes of HL60 cells which proliferate exponentially and express both telomerase and hTERT become occupied by c-Myc/Max heterodimers. Telomerase activity is downregulated and hTERT transcription repressed as a consequence of changing from c-Myc/Max to Mad1/Max. In other words, c-Myc and Mad1 have opposite effects on hTERT transcription – but telomerase positive cells, including immortal and tumour cells, often exhibit increased c-Myc expression, whilst Mad1 expression remains relatively low. Most human somatic cells, as well as hTERT gene-repressed differentiated cells exhibit reversed c-Myc and Mad1 expression.

Wilms' tumour 1 (WT1) tumour suppressor

hTERT transcription suppression can also be caused by WT1 tumour suppressor (Oh et al., 1999). This works by interacting directly with the hTERT promoter, whose binding site can be found at -352 upstream of the ATG, in the core region. Mutation of this site causes 293 cells to exhibit increased hTERT promoter activity, but not HeLa cells. Expression of mRNA for hTERT, as well as 293 cell telomerase activity, are reduced in proportion to WT1 overexpression (Oh et al., 1999). WT1's role in the inhibition of hTERT is cell specific, since the WT1 gene is only expressed by kidney, gonad and spleen cells. It therefore significantly

affects kidney and gonad cell growth and differentiation (Englert, 1998). While differentiation is in progress, hTERT gene expression may be suppressed by WT1. Furthermore, WT1 inactivation may play a part in telomerase activation whilst tumours are forming in its target tissues.

Regulation of hTR

Telomerase is regulated in part by hTR levels, Sp1 and HIF-1 activate hTR transcription, while specificity protein 3 (Sp3) represses it by silencing the hTR promoter using MAPK signalling cues (reviewed in Cairney and Keith, 2008).

Mitogen-activated protein kinase (MAPK) signalling cascades are critical in the triggering of stress signals and extracellular growth. These processes play a role in modulating gene promoter transcription via mechanisms such as direct Sp1 phosphorylation. Binding sites for transcription factors such as AP-1, c-myc and Ets are effective in the core promoter and are involved in hTERT transcription regulation. A link has been suggested between Sp1-related regulation of hTR promoter activity, as shown by reporter assays, and the involvement of MAPK pathways in hTR transcription regulation (Cong et al., 2002; Janknecht, 2004; Kyo and Inoue, 2002).

Bilsland et al. (2006) recently reported that the mitogen-activated protein kinase kinase kinase 1 (MEKK1)/c-jun-NH₂-kinase (JNK) pathway plays a role in both Sp3 expression through binding and also hTR promoter activity repression. hTR promoter activity is induced by SP600125, the JNK inhibitor and this is dose-dependent. Having been shown in transient transfection assays as well as inducing endogenous levels of hTR at a concentration of 12.5 mmol/L, this implies that hTR may be repressed by JNK. These findings were verified by co-transfection of the constitutively active kinase domain MEKK1. Within the JNK pathway, MEKK1 is a significant MAP3K and this has been shown, in a panel of cancer cell lines, to strongly repress hTR promoter activity. It was also found that the repressive effect of MEKK1 could be suppressed by 12.5mmol/L SP600125 or JNK overexpression. However, the phosphoacceptor site mutant JNK2APK had no effect (Bilsland et al., 2006).

These findings inspired deeper investigation into the core promoter for JNK repression, particularly the role of the Sp1 binding sites. When these sites were mutated within the hTR core promoter, SP600125-induced promoter activity was slightly attenuated. This signposts the involvement of factors other than Sp1 binding in hTR induction via JNK inhibition. Sp3 is also bound at these sites and, as mentioned earlier, this can repress hTR promoter activity.

This effect can be achieved solely via Sp3 binding. However, it was found that when co-transfected with MEKK1, the effect is increased; ovarian carcinoma cell line A2780 exhibited basal activity levels reduced to 9%. It can be inferred from this that hTR promoter activity is repressed through collaboration between Sp3 and MEKK1 (Bilsland et al., 2006).

Regulation of TERT by alternative splicing

Complex genomes have vastly increased coding capacity due to the fact that 95% of genes in multicellular eukaryotes are affected by alternative splicing. Indeed, the phenomenon enables around 20,000 protein coding sequences to generate more than 100,000 proteins (Nilsen and Graveley, 2010). It has long been known that atypical alternative splicing is partially responsible for the regulation of hTERT expression, which may be a consequence of hTERT's low expression level (Ulaner and Giudice, 1997; Ulaner et al., 1998).

RNA splicing involves the removal of non-coding intron sequences, which allows exon sequences to join together. This is a co-transcriptional event, involving recruitment and assembly of a 'spliceosome' around the site of the splice, while pre-mRNA is transcribed by polymerase II (Schmidt et al., 2011; Goldstrohm et al., 2001). The spliceosome, a complex 'molecular machine' is a ribonucleoprotein made up of five small nuclear RNA (snRNA) particles (U1, U2, U4, U5, U6) in addition to around 300 other proteins (Jurica and Moore, 2003). These components are assembled in a specific sequence at every 30 and 50 splice site, polypyrimidine tract and branch point. From here, introns are formed into a lariat arrangement and removed, enabling exons to ligate (Beyer and Osheim, 1988; Tennyson et al., 1995).

Alternative splice variants are caused by the inclusion or exclusion of exons, which might always be present in a gene's mRNA (constitutive), or may only sometimes be present (alternative). Proximity of a splice site to cis-regulatory sequences (exonic splicing enhancers (ESEs) or silencers (ESSs), or intronic splicing enhancers (ISEs) or silencers (ISSs)) determines whether usage of that site is enhanced or suppressed (Roca et al 2013). In turn, these cis-regulatory sequences are bound by transacting factors or one of over 500 splicing factors which are able to play a role in alternative splicing.

Several unique elements are involved in the regulation of hTERT splicing. The hTERT gene is 42kb and is located in humans on chromosome 5p15.33. Numerous isoforms can be spliced from its 16 exons (Kilian et al., 1997), of which 22 have been identified so far (Hrdlickova et al., 2012). None of these isoforms however – with the exception of the full-length transcript, containing all 16 exons – are able to elongate telomeres, nor do they exhibit any reverse

transcriptase activity (Saeboe-Larsen et al., 2006; Yi et al., 2000). The reverse transcriptase domain of hTERT contains the following alternatively spliced isoforms: minus-alpha, minus-beta or minus alpha-beta. Exon 6 contains a splice acceptor site, resulting in a 36bp deletion, which allows minus-alpha to form an in-frame transcript. This becomes translated into a dominant-negative protein that does not exhibit reverse transcriptase activity (Saeboe-Larsen et al., 2006; Colgin et al., 2000).

Post-translational modification of TERT

The correlation between TERT mRNA levels and telomerase activity is not consistent, which suggests post-translational TERT regulation (Ulaner et al., 2000; Rohde et al., 2000; Oguchi et al., 2004).

Mammalian and plant TERT sequences exhibit sites for phosphorylation (Kang et al., 1999; Oguchi et al., 2004), which implicates at least two kinases in the phosphorylation of hTERT. C-Abl phosphorylates hTERT in the presence of ionizing radiation, resulting in telomerase being reduced to a third of its normal activity. An increase in telomerase activity has been observed in c-Abl deficient mice (Kharbanda et al., 2000). This result suggests that telomerase activity is negatively regulated by c-Abl. Conversely, hTERT phosphorylation by Akt increases telomerase activity. It is assumed that this is due to hTERT being translocated into the nucleus from the cytoplasm in lymphocytes (Kang et al., 1999; Minamino and Kourembanas, 2001).

Nuclear translocation and phosphorylation of hTERT involves its phosphorylation by Akt kinase, and it has been suggested that this also enhances telomerase activity (Kimura et al., 2004; Kawagoe et al., 2003). Serine residues 227 and 824 on the hTERT protein provide apparent sites for the phosphorylation of TERT by Akt (Kang et al., 1999).

A recent study has suggested that phosphorylation at serine 227 may cause nuclear localization of hTERT due to its location between two amino acid clusters in the bipartite nuclear localization signal (NLS) sequence. The study mutated serine residues at 227 and 824 to alanine (S227A, S824A, S227, 824A) – site-directed mutagenesis of hTERT. Following this, the 227 serine residue was replaced by glutamate (S227E), to create a mutant which would mimic phosphorylation. Mutant constructs, such as FLAG-hTERT were used to transfect H1299 cells, which were then analysed by immunofluorescence staining. The findings suggested that hTERT nuclear translocation is influenced by serine 227 (Chung et al., 2012).

Findings by Plunkett et al. (2007) support the observation that hTERT expression is not the

only regulator of telomerase activity in human T-cells. The authors also detected hTERT in every CD8⁺ T-cell subset following T-lymphocyte activation and that furthermore, the addition of IL-2 only caused a slight increase. The study suggests that as hTERT is a substrate for Akt, and hTERT should be phosphorylated to enable telomerase activity (Kang et al., 1999; Liu et al., 2001), then CD8⁺ T-cells might also have decreased hTERT phosphorylation. Consequently, it was found that a lack of Akt did not cause telomerase down-regulation in the CD8⁺CD28⁻CD27⁻ T-cell subset. None of the CD8⁺ T-cell subsets exhibited any changes in total Akt. In order for activation of telomerase to occur, Akt must be phosphorylated at both the Ser473 and Thr308 sites. In the CD8⁺CD28⁻CD27⁻ T-cell subset, a selective lack of Akt phosphorylation was found at the Ser473 site. Adding IL-2 did not reverse this (Plunkett et al., 2007). Data from this research indicates that when Akt fails to phosphorylate hTERT on the Ser227, there is a correlation with CD8⁺ T lymphocyte senescence.

Telomerase regulation by subcellular localization

It has been suggested that changes in subcellular localisation prevents the formation of new telomeres (Wong et al., 2002). TRF1, a component of human shelterin, interacts with PinX1, which has been implicated in telomerase regulation via sequestration (Lin et al., 2007). PinX1 binds directly to both hTERT and hTR in the nucleolus (Banik and Counter, 2004), which has been shown *in vitro* to reduce telomerase activity (Zhou and Lu, 2001). Est2 (TERT) and PinX1 have been shown to interact within yeast cells, also leading to nucleolus sequestration (Lin and Blackburn, 2004).

Nuclear exclusion mechanism

The molecular mechanism for hTERT nuclear exclusion follows both exogenous and endogenous oxidative stress (Haendeler et al., 2003a). A study by Haendeler et al. (2003b) found that Src kinase phosphorylation of the TERT protein on tyrosine 707 was required for nuclear exclusion to occur. In this instance, TERT and Ran GTPase associate together, then leave the nucleus in a leptomycin-sensitive manner via the nuclear pores. An antioxidant (e.g. N-acetylcysteine) is required to prevent this shuttling (Haendeler et al., 2003b; Haendeler et al., 2004). Nuclear TERT exclusion is therefore triggered primarily by oxidative stress. Both nuclear and mitochondrial telomerase locations have been modelled using organelle-specific localization vectors developed initially in Haendeler's research team (Haendeler et al., 2009; Haendeler et al., 2003b). It was recently established that two G-quadruplex ligands used to treat cancer cell lines induced hTERT shuttling into mitochondria and decreased TERT protein as well as telomerase activity (Zhuang and Yao, 2013).

TERT shuttling between nucleus and cytoplasm

It has been shown that a putative hTERT nuclear export signal (NES) is required to bind the 14-3-3 protein in order for nuclear localisation and hTERT accumulation to occur (Seimiya et al., 2000). Conversely, hTERT would localise in the cytoplasm if both proteins and NES mutations were interrupted, although telomerase activity continued uninterrupted even if 14-3-3 binding did not occur. Furthermore, hTERT-mediated apoptosis suppression may involve the 14-3-3 proteins (Zhang et al., 2003).

TERT shuttling in lymphocytes

In peripheral blood lymphocytes (PBL), telomerase is regulated through the PI3K/Akt/NF- κ B signalling pathways (Akiyama et al., 2003). This was demonstrated by Akiyama et al. (2004), who showed that PBL cytoplasmic telomerase activity could be induced by TNF α , then hTERT was translocated to the nucleus in the following hour. A specific inhibitor of NF- κ B translocation, SN-50, prevented TNF α -induced telomerase activity from translocating to the nucleus, but allowed it to continue in the cytoplasm. Instead, PBL cytoplasmic TNF α -induced telomerase activity was blocked by Wortmannin, a specific P13K suppressor, which also blocked TNF α -induced hTERT nuclear translocation (Akiyama et al., 2004).

Unstimulated T-lymphocytes contain cytoplasmic telomerase, which proceeds to the nucleus once the cells are activated (Liu et al., 2001). Nuclear translocation of hTERT is made possible by AKT-mediated phosphorylation of the nuclear localisation signal (NLS) at serine 227 of hTERT (amino acid residues 222-240) (Chung et al., 2012). Plunkett et al. (2007) have found that when Akt phosphorylation on serine 473, fails to happen telomerase is not activated and CD8 $^{+}$ T-cells proceeded to senescence. Telomerase activity is necessary for T-cells to proliferate following activation. However, once the ability to upregulate telomerase is lost leading to telomere shortening they enter senescence (Effros et al., 2003).

Mitochondrial localisation of hTERT

Human, mouse and rat TERT has been found to contain a specific N-terminal mitochondrial localisation sequence (MLS) (Santos et al., 2004). It is suggested that this sequence developed late in the enzyme's evolution, as it is not fully formed in plants and is lacking in yeast, ciliates and other simple organisms. TERT is directed towards the mitochondria by the mitochondrial localisation signal (MLS) and transported out of the nucleus via the nuclear exclusion signal (Seimiya et al., 2000). Following exposure to hydrogen peroxide and

etoposide, hTERT overexpressing human cells exhibited more mtDNA damage and higher apoptosis induction (Santos et al., 2004; Santos et al., 2006). However, other research has shown that when hTERT binds to mtDNA in vitro, or resides within mitochondria, then less mtDNA damage, ROS and apoptosis is observed (Ahmed et al., 2008; Haendeler et al., 2009). Furthermore, numerous other groups – including Santos’ – have established the benefits of mitochondrial TERT in various roles, including improved respiration, decreased mitochondrial superoxide, increased mitochondrial membrane potential and reduced apoptosis in both stressed and non-stressed conditions (Ahmed et al., 2008; Haendeler et al., 2009; Kovalenko et al., 2010). For hTERT shuttling between the nucleus and mitochondria, Src kinase phosphorylates tyrosine 707 in both the nucleus and in mitochondria, resulting in exclusion of hTERT from the nucleus and degradation of hTERT in mitochondria (Haendeler et al., 2003b; Buchner et al., 2010).

Cytokines regulate telomerase activity in T-cells.

Telomeres and telomerase regulation in T-lymphocytes have been examined from two perspectives. One study measured telomere length in different T-cell subpopulations and found longer telomeres in naïve T-cells compared with memory T-cells (Weng et al., 1995; Akbar and Vukmanovic-Stejic, 2007). Other studies establish a correlation between replicative senescence and telomere length in a selective single subpopulations (Fletcher et al., 2005; Vukmanovic-Stejic et al., 2006).

During absence of TCR signalling T-cell proliferation can be stimulated by specific cytokines. This process is called homeostatic proliferation (Surh and Sprent, 2005). Homeostatic cytokines induce proliferation of CD4 and CD8 lymphocytes (T-cells) without the need of antigen stimulation, i.e. infection. (Surh and Sprent, 2005; Wallace et al., 2006; Dunne et al., 2005; Weng et al., 2002). In this context, IL-7 is a homeostatic cytokine for CD4 T-cells, while IL-15 regulates CD8 T-cell proliferation. T-cell proliferation was activated *in vitro* by IL-7 and IL-15 (Wallace et al., 2006) and was found to be associated with telomerase activity induction and the prevention of telomere erosion in T lymphocytes. On the other hand, telomerase activity was inhibited by cytokines such as IFN- α , which increased CD4 $^{+}$ T-cell telomere loss *in vivo* (Reed et al., 2004). *In vitro*, CD4 $^{+}$ T-cell telomerase activity was inhibited by IFN- α secreted by cytomegalovirus (CMV) Ag-stimulated plasmacytoid dendritic cells (Fletcher et al., 2005). This means that cytokines may regulate T-cell telomerase activity.

IL-2 can stimulate hTERT localisation into the nucleus and telomerase activity activation. Furthermore, telomerase activity is regulated through the PI3K/Akt/Hsp90/mTOR/p70S6 kinase (S6K) pathway at the posttranslational level of hTERT in the human NK cell line (NK-92) when stimulated with IL-2 (Kawauchi et al., 2005).

1.3.2 Role of telomerase and telomere length in cardiovascular disease

A study of 25 coronary heart disease (CHD) patients aged 64 ± 3.4 years compared PBMNC telomere lengths in two control groups; 13 elderly (65 ± 2.1 year-old) and 14 young (26.7 ± 1.8 year-old) participants. The study found that patients with CHD had shorter telomere lengths in lymphoid and myeloid cells compared to control groups of the same age or younger (Spyridopoulos et al., 2009). Furthermore, coronary artery disease (CAD) patients were found to have shortened telomeres in bone marrow cells (BMCs), which was both age and CAD-dependent and was also linked with BMC functionality (Spyridopoulos et al., 2008).

Common carotid and internal carotid intima-media thickness were measured using ultrasound in the Cardiovascular Health Study ($n = 419$) (Fitzpatrick et al., 2007). In spite of the fact that leukocyte telomere length decreased as carotid stenosis increased, this was not significant ($p = 0.07$). Another study compared the incidence of carotid plaques against leukocyte telomere length among hypertensive patients ($n = 163$). 73 (44%) patients were found to have plaques (detected by ultrasound) as well as significantly shorter leukocyte telomere lengths (8.21kb vs. control 8.43kb, $p=0.03$). Mean lipid levels (high- and low-density lipids and total cholesterol) remained the same between groups, even after 55 patients on lipid reducing drugs were excluded (Benetos et al., 2004). These results indicate that shortened leukocyte telomeres may predict carotid plaques more accurately and may also play an as-yet undiscovered role in plaque development among hypertensive patients. A study of patients with type-2 diabetes ($n = 30$) and patients who did not exhibit either carotid or femoral plaques ($n = 30$) found that diabetics with plaques exhibited shorter telomere lengths (5.39, SEM 0.2kb) than those without (6.21, SEM 0.2kb). All patients were found to have shorter leukocyte telomeres than non-diabetics (8.7, SEM 0.5kb), although no distinction was made between femoral and carotid plaques (Adaikalakoteswari et al., 2007).

A study involving peripheral blood lymphocytes in *mTert*-GFP⁺ mice found that GFP⁺ cells expressed about 50% less telomerase compared between the ages of 2 and 5 months, suggesting that age-related decline in telomerase activity can occur *in vivo*. The study also found that low-density lipoprotein (LDL) cholesterol can inhibit both T-cell proliferation and telomerase activity *in vitro* (Bennaceur et al., 2014). Another study on mice investigated the

effects of Pioglitazone, an anti-diabetic drug which improved vascular function and slowed atherosclerotic progression. This study found that, in the presence of TERT, Pioglitazone also down-regulated p53 and p16 proteins as well as checkpoint kinase (Chk2). TERT^{-/-} mice did not exhibit this effect. The study also found that the drug up-regulated telomere-stabilising proteins, telomerase activity and therefore reduced vascular cell senescence (Werner et al., 2011).

Spyridopoulos et al. (2016) analysed PBMNCs from 749 85-year-olds. It was found that both CD4 and CD8 T-cell compartment senescence was a reliable predictor of cardiovascular mortality, myocardial infarction and stroke. A correlation has also been found between CD8 cell telomere erosion and left ventricular function deterioration. These results therefore demonstrate a link between cardiovascular disease and immunosenescence (Boag et al., 2015; Hoffmann et al., 2015).

Peripheral blood leukocytes from coronary heart disease (CHD) patients exhibit shorter telomere lengths (TL) than cells from age-matched healthy adults (Sakaguchi et al., 2014). It has also been demonstrated that CD8⁺ T-cell TL in chronic myocardial infarction (MI) patients is shorter compared to other myeloid and lymphoid leukocyte populations, as well those of age-matched seropositive non-MI individuals (Bentz and Yurochko, 2008; Hoffmann et al., 2015). It is therefore believed that the relationship between shortened TL in CD8⁺ T-cells and left ventricular function – which shows an inverse correlation – demonstrates a link between predisposition to immunosenescence and cardiovascular diseases (reviewed in Boag et al., 2015)

Apolipoprotein E-deficient (ApoE^{-/-}) mice as a model for atherosclerosis.

Apolipoprotein E-deficient (ApoE^{-/-}) mice are considered to be a good model for hyperlipidemia and atherosclerosis (cardiovascular phenotypes). The first gene-targeted mouse model of atherosclerosis was generated 20 years ago by inactivating the ApoE gene through homologous recombination (Plump et al., 1992; Piedrahita et al., 1992). ApoE^{-/-} mice are considered highly relevant to studies of atherosclerosis, due to their ability to develop spontaneous hypercholesterolemia and arterial lesions which resemble those found in humans (Plump et al., 1992; Piedrahita et al., 1992).

Phenotypic properties of ApoE^{-/-} mice:

1. As ApoE^{-/-} mice age, they develop hypercholesterolemia, as well as spontaneous atherosclerotic lesions, which can be found in both the carotid artery and the aortic

arch. In the plaque areas moderate lesions in the aortic arch of 4-month old ApoE^{-/-} mice were found. By 13-months, these plaques had increased considerably. By comparison, wild-type mice exhibited no such lesions (Ross, 1999).

2. ApoE^{-/-} mice exhibit some distinct phenotypes, including endothelial dysfunction. A study of isolated aortic rings *ex vivo* found that in 13-month old ApoE^{-/-} mice, endothelial nitric oxide (NO) dependent vasorelaxation was reduced when challenged with acetylcholine, although this was not observed in 4-month old mice, nor was it seen in wild-type mice at either age. The study concluded that endothelial dysfunction in ApoE^{-/-} mice is age-dependent (Wang et al., 2000), implicating NO deficiency in atherosclerosis (Anderson et al., 1995).
3. Atherosclerotic aged (18 months old) ApoE^{-/-} mice were found to have aortal vascular senescence, whereas their non-atherosclerotic aged wild type C57BL6 counterparts did not (Pereira et al., 2010). This suggests a connection between aortal vascular senescence and the development of vascular disease during ageing. This may be responsible for the observed endothelial dysfunction in this mouse model. Research with ApoE^{-/-} atherosclerotic mice may help to elucidate the interaction between vascular senescence and vascular endothelial dysfunction (Minamino et al., 2002; Matsushita et al., 2001).
4. Coronary systolic afterload stress is absorbed by the elasticity of the aorta. Therefore, the more rigid the aorta, the more stress is directed to the heart. One study shows that ApoE^{-/-} mice at 13-months were found to have increased heart weight, compared to their wild-type counterparts at the same age, although 7-month old mice exhibited no such difference (Wang, 2005). Using a non-invasive Doppler method to measure aortic flow velocity, also found that cardiac output increased significantly in 13-month old ApoE^{-/-} mice, compared to wild-type controls (Wang, 2005). This was accompanied by cardiac hypertrophy. Again, this result was not observed in 7-month old mice (Hartley et al., 2000). Niebauer et al. (1999) found that ApoE^{-/-} mice had reduced aerobic capacity in spite of an increased cardiac output during resting conditions. It was therefore concluded that these mice had compromised cardiac reserves. This may be caused by elevated cardiac hypertrophy due to an increase in cardiac afterload as a result of aortic stiffening in ApoE^{-/-} mice (Wang, 2005).

Why can ApoE knock out influence the regulation of telomerase?

Nothing has been reported in the literature so far about the regulation of telomerase activity in tissues from ApoE^{-/-} mice specifically. However, these ApoE^{-/-} mice are a good model of

atherosclerosis, which is known to be associated with increased oxidative stress and inflammation which may decreased telomerase activity in T-cells.

T-lymphocytes play a critical role in atherogenesis (Bennaceur et al., 2014). Our group has also shown that peripheral blood lymphocyte telomeres shorten faster than those in myeloid cells in coronary heart disease (CHD) patients (Spyridopoulos et al., 2008; Spyridopoulos et al., 2009). Given these two factors, it is thought that in T-cells, telomere length may be a factor influenced by atherosclerosis but it is also possible that it is causally involved in the disease formation by yet unknown mechanisms. Telomere length in T-cells is pre-dominantly maintained by telomerase (Plunkett et al., 2007). Therefore, interventions such as introducing the small molecule activator, TA-65, to restore telomerase activity (de Jesus et al., 2011; Harley et al., 2011), may prove extremely useful in slowing down telomere shortening in age-related diseases including atherosclerosis. Atherosclerosis has been implicated in diminishing telomerase activity, causing telomeres to shorten (Bennaceur et al., 2014). Our previous study has shown that treatment of activated human lymphocytes with LDL-cholesterol for 5 days decreases telomerase activity significantly as well as cell proliferation (Bennaceur et al., 2014). However, there are conflicting data around in the literature. Gizard et al. (2011) showed that in macrophages, atherosclerosis might increase telomerase activity via inflammation. This is due to the fact that the transcription factor NF κ B activates the TERT promoter and TERT expression as well as telomerase activity in response to inflammatory stimuli such as oxidized LDL (Gizard et al., 2011). Oxidized LDL can be caused by oxidative stress resulting in lipid peroxidation and cell damage (Pashkow, 2011; Minamino and Komuro, 2007). The same group fed a high fat diet (HFD) to LDLR $^{/-}$ mice and found a 13-fold increase in vascular telomerase activity after 3 months of this diet compared to a normal diet (Gizard et al., 2011).

Our study sought to establish a greater understanding of the cell-specific functions of telomerase in T-cells/splenocytes in regard to atherogenesis. Using the ApoE $^{/-}$ *mTert*-GFP $^{+}$ mouse model, we studied high fat diet (HFD)-fed ApoE $^{/-}$ x *mTert*-GFP $^{+}$ reporter mice.

1.3.3 Role of telomerase and telomere length in T-lymphocytes

Telomerase was not found to be particularly active in unstimulated peripheral blood T-cells (Akiyama et al. 2002; Kawauchi et al., 2005). However, telomerase plays a far greater role in T-cells after stimulation (Weng et al., 1998; Hathcock et al., 2005). All primary human

thymocyte subpopulations exhibit pronounced telomerase activity (Weng et al., 1996). CD4⁺ T-cells taken from chronic inflammation sites (for example, the tonsils) exhibit high telomerase activity levels, although not as high as that found in the thymus. High telomerase activity is also seen in antigen-specific T-cell stimulation *in vivo*. A study found that CD8⁺ T-cells which had reacted to the naturally occurring Epstein-Barr virus (EBV) were telomerase positive (Weng et al., 1996; Maini et al., 1999; Plunkett et al., 2001). Murine studies have shown an antigen-specific CD4⁺ T-cell telomerase activity in response to antigen challenge *in vivo* (Hathcock et al., 1998). Mice infected with lymphocytic choriomeningitis caused viral-peptide specific CD8⁺ T-cells and long-term memory cells to express telomerase. Combined, these studies and observations suggest that telomerase expression in response to acute immune response can be responsible for maintaining telomere lengths, replicative capacity and long-term memory in cells.

Human T-cell studies carried out *in vitro* also shed light on telomere length regulation. When the T-cell receptors CD3 and CD28 were stimulated with specific antibodies, T-cell proliferation was induced. Subsequently, T-cells expressed telomerase equally well from both old and young donors (Son et al., 2000). On the other hand, a study on CD8⁺ T-cells from human PBMNCs concluded that telomere lengths in CD8⁺ T-cells were shorter and that telomerase activity was lower in the older group compared to the younger group. These results also demonstrated that CD8⁺ T cell expression (CD28/CD27) was higher in the younger group (Plunkett et al., 2007). Antigen stimulation (Adibzadeh et al., 1996) or anti-receptor antibody stimulation (Weng et al., 1997) caused a proliferative response to be induced in T lymphocytes repeatedly, up to a point. At this point, the cells appeared senescent and no stimulus could induce further proliferation. Over the course of this long-term culture and repeated cell divisions, telomeres became progressively shorter. Critically, naïve T-cells have an increased potential for proliferation due to their longer telomeres than memory T-cells, which have undergone more cell divisions (Weng et al., 1995). Activated T-cells initially exhibited high levels of telomerase on stimulation, although this decreased at every cell division point, until senescence was reached and telomerase levels were very low. A correlation was found between telomerase activity and telomere shortening; telomeres did not shorten after initial cell division, but as telomerase decreased, the telomeres became progressively shorter (Weng et al., 1997; Akbar and Vukmanovic-Stejic, 2007; Plunkett et al., 2007).

Telomerase is implicated in telomere length maintenance, and as its activity decreases, telomeres begin to shorten in T cells. Telomere length also seemed to be related to the

proliferative capacity of T-cells (Plunkett et al., 2007). Therefore, telomerase might have an effect on T-cell division and senescence. Closer examination of this relationship has been carried out: The cDNA that codes for the expression of human TERT (hTERT) has been transfected into CD8⁺ T-cells. In the control group, the cells which expressed the least endogenous telomerase reached senescence more quickly, while the hTERT over-expressing experimental group had higher telomerase activity and divided far more readily (Hooijberg et al., 2000; Rufer et al., 2001).

1.3.4 Interaction between oxidative stress and telomeres

Telomere loss and the deceleration of replication can be caused by oxidative stress. This has been shown both in studies of human ageing (von Zglinicki et al., 2000) and *in vitro* (von Zglinicki et al., 1995). Guanine, which is found in abundance in telomeres, is particularly prone to the effects of oxidative stress (Wang et al., 2010). It is not fully known if this is merely a side-characteristic of telomeres, or if it is part of a functional process. Oxidative stress is implicated in telomere shortening and also causes damage to DNA through double and single-stranded breaks and through oxidising bases (Petersen et al., 1998; von Zglinicki et al., 1995). Cells enter replicative senescence via the tumour suppressor p53 in response to double-stranded breaks, telomere shortening or telomere dysfunction/uncapping (Shiloh, 2003, von Zglinicki et al., 1995; Takai et al., 2003, Hewitt et al., 2012). The ‘camouflage’ structure is created by a shelterin complex and is known as ‘telomere capping’. A DNA loop is created on the telomere end, disguising it from signalling and it is thought that oxidative stress results in a dysfunction of this loop on the telomere end. Each time the DNA replicates, a greater amount of the telomere is lost (von Zglinicki et al., 1995; Sitte et al., 1998). In addition, damage to telomeres can not be repaired (Petersen et al., 1998; Henle et al., 1999). While DNA damage foci within genomic regions are often repaired, telomeric damage (telomere associated foci, TAFs) are not (Hewitt et al., 2012, Nelson and von Zglinicki, 2013). However, the underlying mechanisms are not well understood yet.

Telomerase activity which combats telomere shortening through a specific and regulated re-elongation process might be also inhibited by oxidative stress (Saretzki, 2014). This has been observed in endothelial cells and is also implicated in the attrition of telomeres and consequent senescence. In addition, telomerase (TERT) shuttles out from the nucleus to the cytoplasm under oxidative stress, as shown by Ahmed et al (2008). There it enters the mitochondria, but is no longer able to extend telomeres (Saretzki, 2009).

1.4 Role of p38 MAP Kinase (MAPK) in inflammation and disease

1.4.1 Expression and function of MAPK

Mitogen-activated protein kinases (MAPK) are expressed in all eukaryotic cells and are activated in a number of ways, including cellular stress, neurotransmitters, hormones, growth factors and cytokines (Widmann et al., 1999). MAPK are serine-threonine protein kinases, whose sequential activation pathway is a three-component module conserved from yeast to humans. This is established through three kinases as follows: MAPK kinase kinase (MKKK), MAPK kinase (MKK), and MAPK. In mammalian cells, there are currently 14 MKKK, 7 MKK and 12 MAPK known, the latter of which subdivides into five distinct families, each with its own biological function: MAPKerk1/2, MAPKp38, MAPKjnk, MAPKerk3/4, and MAPKerk5. In the yeast *Saccharomyces cerevisiae*, five MAPaK pathways are responsible for mating, cell wall remodelling, nutrient deprivation, and stress responses (osmolarity changes). In mammalian cells, MAPK pathways are activated via a range of stimuli, indicated by the diversity of MKKK in MAPK modules (Widmann et al., 1999).

The MAPK signalling pathway in normal cells

MAP kinases, or MAPK, originate from the mitogen activated protein kinase protein family (Figure 1.6). The MAPK pathway is invoked when a ligand (e.g. EGF) binds with the extracellular component of a receptor tyrosine kinase (RTK) membrane-bound receptor, leading to two RTK sub-units being dimerised at the inner side, and catalysing phosphorylation at both sub-units. Next, growth factor receptor-bound protein binds temporarily to the phosphorylated RTKs. Son of Sevenless (SOS) genes, named after their homologues in *Drosophila*, are capable of binding to Ras. When dormant, Ras binds to guanosine diphosphate (GDP), allowing SOS to take advantage of the exchange between Ras-bound GDP and guanosine triphosphate (GTP), which causes Ras protein activation. Active Ras, bound to GTP can bind to a range of effector proteins. One critical effector is the kinase B-Raf, which phosphorylates, to activate the MEK 1 and 2 kinases. These go on to phosphorylate the ERK 1 and 2 kinases, ultimately leading to transcription factor activation of the activator protein-1 (AP-1) family (Meloche and Pouyssegur, 2007; Whitmarsh and Davis, 1996; Gille et al., 1995; Rouse et al., 1994; Widmann et al., 1999).

The Jun and Fos transcription factors are among the most widely known. Following activation, these migrate to the nucleus to form heterodimers which bind with AP-1 motifs and these are modulated by DNA. This caused expression of numerous genes, including growth factors, cytokines and cyclins. Consequently, normal cells proliferate, causing

deactivation of the Ras-GTP complex. This allows for a MAPK signalling pathway to be permanently activated, therefore avoiding undesirable effects. The GTPase activating protein (GAP) deactivates Ras-GTP, by binding to it and increasing its GTPase activity by several orders of magnitude. This is achieved by enabling a domain that allows Ras protein to hydrolyse GTP into GDP. When the GTP-bound Ras becomes inactive, the B-Raf bond is broken and the MAPK signalling pathway ends (Widmann et al., 1999; Robbins et al., 1993; Roux et al., 2007; Karnoub and Weinberg, 2008).

The MAPK signalling pathway in tumour cells with Ras mutation.

Ras gene mutation drastically effects cells. Mutated Ras protein behaves similarly to non-mutated Ras. It activates as normal and furthermore, active Ras-GTP complex, binds to and activates the B-Raf kinase. Critically however, the mutated Ras-GDP protein cannot be inactivated by GAP. While GAP still binds to Ras-GTP, the domain required for Ras GTPase is not available, so hydrolysis of GTP into GDP does not occur. Because of this, the mutated Ras-GDP is not deactivated and B-Raf kinase remains active and bound to Ras-GTP. MEK 1 and 2 proteins continue to be activated through B-Raf phosphorylation, leading to increased activation of ERK 1 and 2, and increased active Jun and Fos. The kinase cascade continues unabated, causing continuous proliferation, which is the determining characteristic of a tumour cell (Widmann et al., 1999; Melloni et al., 2012).

The MAPKp38 cascade can be found predominantly in endothelial, myocardial and renal cells, and is a key component in the initiation and progression of inflammatory diseases. Activating factors include: proinflammatory cytokines, pathogens, growth factors and environmental stimuli. LDL cholesterol, reactive oxygen species (e.g. peroxides), barotraumas and ischaemia are also implicated in MAPKp38 activation (Melloni et al., 2012).

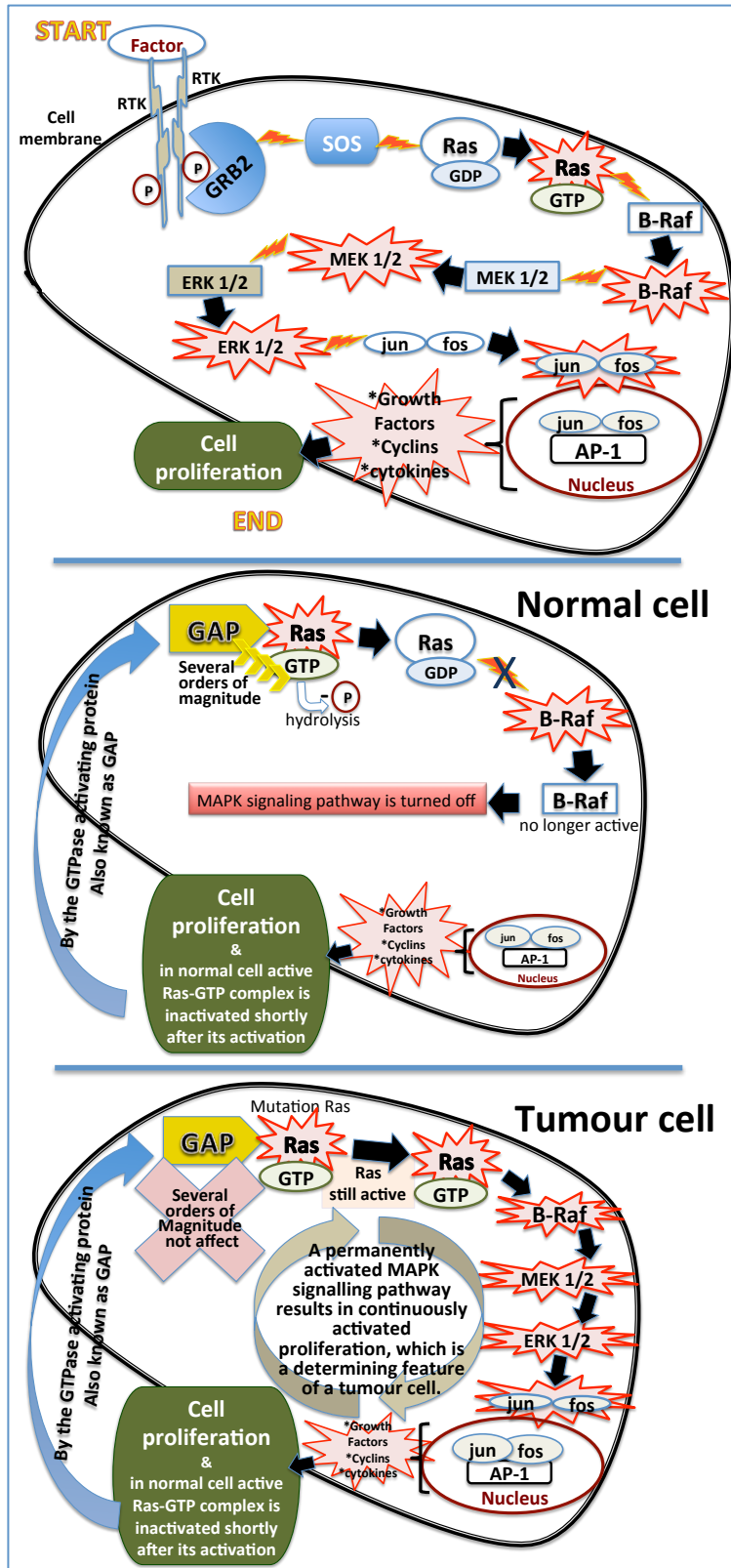


Figure 1.8. MAPK signalling pathway in normal and tumour cells.

The MAPK signalling pathway causes proliferation of normal cells. Following this, the active Ras-GTP complex becomes inactive, leading to the signalling pathway being deactivated. However, Ras-GTP remains active in tumour cells, consequently leaving the MAPK signalling pathway active and therefore leading to uncontrolled cell proliferation – the very definition of a tumour cell (Data from Widmann et al., 1999 and Melloni et al., 2012).

1.4.2 p38 MAPK Pathway

In mammals, the p38 MAPK family is made up of four homologous proteins, MAPKp38 α , β , γ and δ , which are activated by cellular stress (e.g. osmotic or heat shock, ultraviolet (UV) irradiation, protein synthesis inhibitors, lipopolysaccharides); certain cytokines; and G protein-coupled receptors (GPCR). Activation is via an ordered activation module of specific protein kinases, MKKK/MKK/MAPK. This is a similar mechanism to that found in the yeast MAPKhog1 (Singh et al., 2010).

MAPKp38 has the ability to phosphorylate numerous substrates. Within the Thr-Gly-Tyr activation motif, MAPKp38 can be activated through dual phosphorylation of Thr and Tyr. When MAPKp38 activity is engaged, the protein kinase 2 and 3 phosphorylates small heat-shock proteins such as 27-kDa (Widmann et al., 1999). As a substrate for MAPKp38, ATF2 can be phosphorylated at Thr-69 and Thr-71 within its amidogen-terminal activation domain, which enables greater transcription. Similarly, Elk1 is phosphorylated within its carboxylic acid-terminal activation domain. The C/EPB group of transcription factors includes GADD153 (chop), which MAPKp38 will phosphorylate on serine residues 78 and 81. This also increases transcriptional activity (Singh et al., 2010). MAPK p38 α includes a carboxylic acid-terminal truncated isoform, which binds with and phosphorylates the transcription factor Max. This forms a heterodimer with the MAPKerk substrate c-Myc, to increase potential for integration of MAPK Erk and MAPKp38 signalling pathways (Singh et al., 2010; Cargnello and Roux, 2011).

This ability points towards MAPKp38's involvement in a wide range of biological functions. The compound pyridinyl-imidazole [SmithKline Beecham (SB)-203580], a kinase inhibitor of MAPKp38, blocks production of cytokines (IL-1 and TNF- α) in stimulated monocytes. MAPKp38 appears to play a vital role in the production of cytokines in hematopoietic cells, since blocking MAPKp38 activity results in inhibited production of IL-2 in T cells. When MAPKp38 is inhibited by (SB)-203580, IL-2 and IL-7 driven proliferation is inhibited, which may indicate a vital role for MAPKp38 in cytokine stimulated cellular proliferation (Cargnello and Roux, 2011).

1.4.3 Role of MAPK inhibition/inhibitors (MAPKi) in cell death

Apoptosis, through cellular stress (e.g. UV irradiation, osmotic shock), can stimulate MAPKp38 kinase activity, as well as ligation of Fas and TNF receptors. This process is impaired by MAPKp38 activation blockage by pyridinyl-imidazole compounds. MAPKp38

and JNK MAPK activity induced by overexpression of MKKKask1 leads to apoptosis, whereas kinase dead MKKK Ask1 blocks TNF-induced apoptosis. Furthermore, administration of (SB)-203580 prevents sodium salicylate induced apoptosis and MAPKp38 activity. MAPKp38 may also be activated without apoptosis, inferring that its involvement in cell death is dependent on the induction method and cell type. MAPKp38's involvement in survival versus death responses can therefore be integrated into the sum of metabolic processes that determine caspase activation and by extension, commitment – or not – to apoptosis. (Deacon et al., 2003).

1.4.4 Role of MAPKi in inflammation

MAPKp38 signalling upregulates inflammation and, during chronic obstructive pulmonary disease (COPD), is increased. Administration of (SB)-239063, identified earlier as an inhibitor of MAPKp38 signalling, suppressed production of TNF. However, this effect was not observed with prednisolone, a corticosteroid. This implies a benefit for use alongside therapies which include inhaled corticosteroids, although long-term trials are required (Underwood et al., 2000).

A study by Ranjbaran et al. (2007) concluded that IL-12 plasma levels regulate an inflammatory pathway and this is associated with Th1 cell responses. Circulating IL-18 levels, which are linked with Th1 immune response may facilitate this. It is therefore suggested that the systemic IFN- γ axis may be involved in coronary atherosclerosis development. This has echoes of – although is not connected with – the IL-6/CRP cytokine cascade, which has already been studied extensively. Artery infiltration with T-cells and/or exacerbated Ag-driven T-cell responses may activate IFN- γ production through coronary arterial inflammatory stimuli. Consequently, IL-12 and IL-18 in circulation may be involved in atherosclerosis development by stimulating bystander activation of T-cells. Furthermore, IFN- γ secretion was decreased by p38 MAPKi *in vitro* when coronary artery segments were cultured.

1.4.5 Role of MAPKi in myocardial infarction

In mammalian cells, MAPKp38 inhibition has been observed to not only limit infarct cells, but also the atherogenic process itself (Melloni et al., 2012). Some studies demonstrated MAPKp38 inhibition as a key potential therapeutic approach in acute coronary syndrome (ACS). Its presence in the coronary vessel wall and myocardium enable MAPKp38 to mediate the breakdown of atherosclerotic plaque, attract platelets and release vasoregulatory

cytokines. As previously noted, physical trauma to the coronary arterial wall (e.g. stent implantation), would amplify the MAPKp38 mediated cascade involved with IL-6/cytokine signalling for secondary production of C-reactive protein (CRP) from the liver, which peaks 48 hours after percutaneous coronary intervention (PCI) (Melloni et al., 2012). It is also thought that MAPKp38 inhibition could potentially mediate vascular stabilization, due to the role of microvascular circulation in myocardial preservation during ACS. Furthermore, MAPKp38 is prominently involved in cardiomyocyte apoptosis. It is thus expected that losmapimod, a MAPKp38 inhibitor, may prevent remodelling after ACS (Melloni et al., 2012; Cheriyan et al., 2011).

In cases of myocardial injury, MAPKp38 can mediate cardiac fibroblast-based TGF signal transduction and therefore may have a critical involvement in cardiac fibrosis. Its inhibition can reduce interstitial and perivascular fibrosis. As such, losmapimod may promote cardiac relaxation, thus preventing detrimental remodelling. There is also evidence to suggest that MAPKp38 enables tropomyosin dephosphorylation, reducing cardiac contractility. The contractile element's calcium sensitivity is altered, rather than ATP use, which increases energy efficiency (Singh et al., 2010; Melloni et al., 2012).

1.4.6 p38 MAPK knockout mice

p38 α knockout mice

Defects in placental angiogenesis caused oxygen deprivation, malnutrition and death *in utero* for a number of p38 α null mice from a range of different backgrounds. Following E11.5, mice were backcrossed from (129/Sv X 129/J)F1 X C57BL/6 into a C57BL/6 background and this led to a reduction in the number of knockout embryos detected. Of the survivors, the homozygous offspring were infertile, whereas the heterozygous mice remained fertile. Foetal livers in the TG mice appeared underdeveloped and were paler. The mice overall also appeared paler. Their yolk sac appeared normal and only a small number of circulating erythrocytes were detected. The study used markers for hematopoietic cell types and stages of development, and found that CFU-E progenitors had reduced differentiation and expansion, although it was possible to correct this. These findings suggest that p38 α is required for both erythroid differentiation and Epo expression (Tamura et al. 2000; Adams et al. 2000; Mudgett et al. 2000).

The involvement of p38 α in cardiac function has been the subject of a number of studies. One study, of mice specifically generated with both p38 α alleles deleted, found reduced cardiac function at 6-8 weeks. This effect appeared to be more pronounced in mice from a C57BL/6

background than those with a FVB/N background (Kaiser et al., 2004). A different study, of heterozygous p38 α and p38 β mice at 6-8 weeks old found similar results to the previous study, but also noted that p38 α mice exhibited higher resistance to myocardial infarction. The study detected no changes in blood pressure (diastolic or systolic), heart weight or architecture, or LV pressures (Otsu et al. 2003; Braz et al. 2003). Cardiac-specific p38 $\alpha^{\Delta 40-83}$ floxed mice with a C57BL/6 background were generated to study cardiac ischaemia and specifically the effect of p38 α on hypertrophy and fibrosis. Externally, these KO mice appeared identical to WT mice. Cardiac structure and function appeared the same (detected via echocardiography and cardiac cauterization), but biomechanical stress (pressure overload) caused a different response to that exhibited by WT mice. These findings have been interpreted to indicate that survival is dependent on the kinase, but that this is not essential to hypertrophic heart growth (Nishida et al. 2004).

p38 β knockout mice

p38 β KO mice were generated and were found to exhibit normal birth frequency, fertility, thymocyte development and size. In fact, no health problems or phenotype were observed. These were crossbred with TNFDARE mice, which are susceptible to the development of inflammatory diseases. The offspring were found to be identical to the controls, indicating no significant involvement of p38 β in inflammatory diseases (Beardmore et al. 2005). A different study found that the lack of p38 β had no effect on either basal or insulin-mediated glucose uptake, suggesting that hormonal activated glucose transport also does not involve p38 β (Turban et al. 2005).

Heart function studies have also studied the involvement of p38 β . These found no increase in the survival of, or resistance to, myocardial infarction for heterozygous p38 $\beta^{+/-}$ mice compared with p38 $\alpha^{+/-}$ mice (Braz et al. 2003; Otsu et al. 2003). p38 β was found to play a more significant role in cardiomyocyte survival in response to biomechanical stress. TG mice were generated by crossbreeding dn14-3-3 with cardiac-specific forms of dnp38 α or dnp38 β . Mice with dn14-3-3 alone were unable to withstand cardiac pressure overload and died. However, dn14-3-3/dnp38 β mice all survived, and p38 α /dn14-3-3 mice exhibited a 60% survival rate (Zhang et al. 2003b).

p38 γ and p38 δ knockout mice. p38 γ and p38 δ mouse models have been generated in both single and double KO varieties. All appeared normal and were both viable and fertile (Beardmore et al. 2005; Sabio et al. 2005; Aouadi et al. 2006).

1.5 Exercise and cardiac rehabilitation

1.5.1 Effects of exercise on the immune system

Physical exercise has an important role to play in general health and wellbeing (Figure 1.7). The development and evolution of atherosclerosis is affected significantly by the activity of the immune system (Libby et al., 2009). Vascular endothelial cell signals recruit monocytes which, when activated, produce nitric oxide (NO), metalloproteinases, tumor necrosis factor α (TNF- α) and interferon- γ (Janeway et al., 2002). Proinflammatory cytokines are produced by T-lymphocytes activated by oxidised LDL cholesterol within the intima. It has been shown that exercise can affect these functions to lower rates of inflammation and thus slow down atherosclerotic progression. (Pynn et al., 2004 and Fukao et al., 2010)

C-reactive protein (CRP) is an acute-phase reactive protein, used as an inflammatory biomarker to predict cardiovascular disease and mortality (Kaptoge et al., 2010). Similarly, fibrinogen has been used to predict mortality in CAD patients (Danesh et al., 2005). Through use of these biomarkers, there is evidence to suggest that interleukin (IL) 6 and VCAM-1 aid more precise medical decision making (Lindmark et al., 2001). In elderly CAD patients, there is also an association with TNF- α , whereas increased concentration of IL-10 has been linked with cardiovascular risk reduction. It cannot be consistently shown that physical activity lowers CRP concentrations in all adults, although changes in CRP and other inflammatory biomarker concentrations have been found in CAD patients. (Oemrawsingh et al., 2011; Kelley and Kelley, 2006; Lavie et al., 2011).

The peripheral T cell compartment is susceptible to many changes as a result of the ageing process. Whilst the numbers of T-cells are similar between the elderly and the young, older people tend to display more late stage differentiation phenotypes ($\text{KLRG1}^+/\text{CD28}^-/\text{CD27}^-/\text{CD57}^+$) and specificity to antigenic determinants of specific viruses, including EBV and CMV. Healthy adults have a greater number of CD4^+ T cells than CD8^+ T cells (Agrawal et al., 2009). When this trend is found to be inverted, it is presumed that excessive clonal expansions of apoptosis resistant CD8^+ T cells have resulted in memory CD8^+ T cell inflation. Ageing causes a higher rate of defects in adaptive immune responses, which can significantly impair T cells' ability to secrete IL-2 and to proliferate in response to various stimuli. (Appay et al., 2008)

Many studies have demonstrated that physical exercise improves the body's functioning in all parameters and can lead to decreased risk of developing diseases, including infectious illnesses, age-related impairments and cardiovascular diseases. This in turn leads to increased longevity (Kodama, 2009). Spielmann et al. (2011) performed a study of 102 healthy men ages 18 to 61 years, and found that the training group showed an increased proportion of naïve CD8⁺ T-cells, and decreasing proportions of senescent/exhausted CD4⁺ and CD8⁺ T-cells. Nieman et al. (1993) undertook a study of 30 trained women, ages 72.3 to 74.7 years, which demonstrated increasing NK-cell cytotoxicity, increasing T-cell proliferation, constant lymphocyte counts, and decreasing frequency of URTI symptoms compared to a group of women with an untrained status. Ludlow and co-authors (2008) conducted a study on 69 men and women, ages 55.4 to 65.2 years, and the results showed increasing leukocyte telomere length in moderate exercisers. Ogawa et al. (2003) studied 62 to 64 year old subjects, including 9 trained and 12 untrained women; the trained women were members of a walking group, whilst the untrained women were sedentary. They concluded that IL-2⁺/CD8⁺ IL-4⁺/CD8⁺ and IL-4⁺/CD4⁺ T-cell numbers are increased and that IFN- γ :IL-4 ratio is constant.

In comparison to less physically active older people, those who exercise demonstrated greater T cell proliferative response to mitogens and depleted memory T cells and senescent T cells. Both Nieman et al. (1993) and Shinkai et al. (1995) found greater mitogen-induced T cell proliferation in aerobically conditioned older people. When adjusted for the indication that age may be of less importance than aerobic fitness change in terms of influencing T cell phenotypic shifts, the relationship between age and naïve or senescent T cells was not maintained.

When multiple doses of the mitogens concanavalin (Con A) and phorbol myristate acetate (PMA) were used, Woods et al. (1999) found that a 6-month supervised aerobic training programme increased T cell proliferation in previously sedentary elderly subjects on the same medication. The same group (Woods et al., 2003) then conducted a follow up study, which showed that age-related memory and naïve T cell ratio increase in mice, which may simply indicate a response to exercise training in mice; they suggested that the experiment needs further reestablishment and refinement with human subjects. Initial immune status may have a greater effect than previously thought. De Waard et al., (2007) conducted a study on mice with a large myocardial infarction, to investigate effect of early exercise training on myofilament function and effects on pump dysfunction in the left ventricle. They concluded that there was no clear effect in terms of left ventricular remodelling, but did however find

that early exercise after a large myocardial infarction can decrease dysfunction of the left ventricle. They explained this as a result of improvement in myofilament function via exercise training.

Furthermore, Fairey et al. (2005) found a positive correlation between aerobic exercise and T cell generation in postmenopausal women who had survived breast cancer. Shimizu et al. (2008) performed a 6-month aerobic exercise intervention on males and females between 61 and 76 years old, which resulted in increased numbers and percentages of CD4⁺ T-cells expressing CD28.

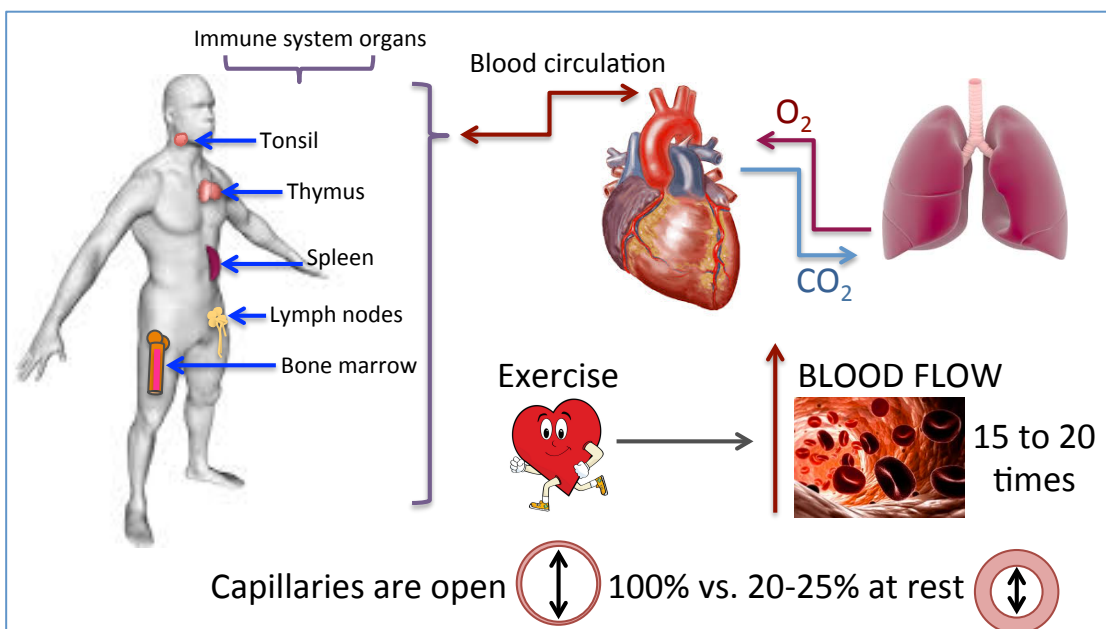


Figure 1.9. Interaction between exercise, cardiovascular system and the immune system.

Physical activity causes the capillaries to open by about 100% (compared to 20-25% at rest), leading to increased blood flow. This increase in blood flow interacts with cardiac input/output and the immune system organs.

1.5.2 Exercise and atherosclerosis

Animal models have been used to investigate the anti-atherogenic effect of exercise, which was shown to prevent and improve the outcome of cardiovascular diseases (Froelicher, 1972; Kramsch et al., 1981). ApoE^{-/-} mice were used to provide evidence of experimental atherosclerosis by induced fibro-fatty accumulation at the arterial walls. After forced mild to moderate exercise treatment, the development of atherosclerosis was suppressed in these mice (Okabe et al., 2006). It is therefore thought that in HFD-fed ApoE^{-/-} mice, a higher number of fatty acids are plasma oxidized and that nitric oxide synthase (eNOS), an endothelial isoform,

may be increasingly upregulated. Indeed, eNOS expression is stimulated in endothelial cells in response to HFD, and this is thought to be associated with plasma lipid peroxides (Ramasamy et al., 1998).

Many studies concluded that atherosclerosis progression was reduced by medium-term exercise over 6-9 weeks (Laufs et al., 2005; Okabe et al., 2007; Pellegrin et al., 2007). Mice who underwent long-term exercise developed a more stable plaque phenotype shown by decreased macrophage levels (Pellegrin et al., 2009).

Numerous atherosclerotic risk factors exist, including: obesity, intolerance to glucose, resistance to insulin, high blood pressure, low HDL-C and elevated triglyceride concentration. Physical exercise and weight loss can have a positive effect on many of these factors. For example, reduced LDL-C may lead to reduced HDL-C to a similar degree, which is associated with a reduction in ingested saturated fat (Stefanick et al., 1998). Exercise in humans can modify IL-6 and TNFalpha, both adipocytokine products, which regulate intercellular adhesion molecule-1 and vascular adhesion molecule-1 (Ziccardi et al., 2002). 52 exercise studies, lasting under 12 weeks and including 4700 participants underwent meta-analysis, and results demonstrated an average increase of 4.6% in HDL-C levels. LDL-C reduced by 5% and triglyceride by 3.7% (Leon and Sanchez, 2001). The HEalth, RIisk factors, exercise Training And GEnetics (HERITAGE) study is the largest of its type, involving 299 male and 376 female normolipidemic participants over a 5-month exercise training period (Leon et al., 2000). Male participants exhibited a 1.1mg/dl (3%) increase in HDL-C, a 0.9mg/dl (0.8%) decrease in LDL-C and a 5.9mg/dl (2.7%) decrease in triglycerides. Female participants showed a 1.4mg/dL (3%) increase in HDL-C, a 4.4mg/dL (4%) decrease in LDL-C and a 0.6mg/dL (0.6%) decrease in triglycerides. Subjects with baseline hypertriglyceridemia may be prone to greater HDL-C increases (Couillard et al., 2001).

1.5.3 Effects of exercise on telomerase activity and telomere length

Oxidative and psychological stresses have been shown to play a significant role in telomerase activity and to affect telomere length (Demissie et al., 2006; Epel et al., 2004; Epel et al., 2006). It has been suggested that low telomerase levels in leukocytes – and therefore shortened telomeres - may be a predictor of CVD risk (Epel et al., 2006). Many studies provide evidence of a positive link between exercise and telomerase activity and telomere lengths (Melk et al., 2014; Cherkas et al., 2008; Werner et al., 2009 and Kadi and Ponsot, 2010).

In a human study there was an overall positive correlation between leukocyte telomere length and maximal oxygen consumption ($r = 0.44$, $P < 0.01$) (LaRocca et al., 2010). Human leukocytes had longer telomeres in the healthy older exercise group compared to the sedentary group of the same age, while there was no effect of exercise on telomere length in the healthy younger group compared to young sedentary people (LaRocca et al., 2010). Other lifestyle factors, including BMI, smoking status and levels of physical exercise were correlated with telomere length (Song et al., 2010) and some studies have shown that negative lifestyle factors cause telomeres to shorten, resulting in damage to DNA. Moreover, exercise is associated with reduced oxidative DNA damage, whereas smoking increases this damage (Tamae et al., 2009). Athletes exhibit a noticeable increase in telomerase activity in mononuclear cells after exercise; in young people this was 2.5-fold and in middle-aged people, it was 1.8-fold. Moreover, peripheral blood mononuclear cell cultures (PBMNCs) had longer telomeres in older athletes compared to older people with sedentary lifestyles (Werner et al., 2009). Shorter telomeres are also associated with increased subjective psychological stress (Epel et al., 2004; Epel et al., 2006). Physical exercise was shown to enable a buffer between psychological stress and telomere length (Werner et al., 2009), and people experiencing low psychological stress were found to have longer telomeres and higher telomerase activity (Epel et al., 2004; Epel et al., 2006; Puterman et al., 2010). The level of exercise has a positive effect on telomere length. Moderate exercise levels lead to significantly increased telomere length in human PBMNCs compared with the lowest or highest levels of exercise, based on each subject's exercise energy expenditure (EEE). It is not thought that telomere length can be influenced by acute or short term exercise, as this does not provide strong enough stimulation (Ludlow et al., 2008). Telomerase has been shown to play a central role in telomere regulation and on survival proteins after exercise; the voluntary running exercise had no effect on $TERT^{-/-}$ mice (Werner et al., 2009).

1.5.4 Cardiac rehabilitation and its phases

Cardiac rehabilitation is critically important, in view of the high mortality rate associated with cardiovascular diseases. About 1.8 million lives are put at risk annually from cardiac diseases in Europe alone (British Heart Foundation: European cardiovascular disease statistics 2012). In the UK, approximately 170,000 patients are diagnosed with acute myocardial infarction every year, and around 2.3 million people are living with cardiovascular disease in the UK (British Heart Foundation 2012). Based on this, a cardiac exercise program, either as a preventative or rehabilitative measure, is of great importance. Cardiac rehabilitation is part of a comprehensive care package for cardiovascular patients (Wenger et al., 1995; Leon et al.,

2005). Such rehabilitation is a long-term program, tailored to both the patient's physiological and psychological needs, and requires a combination of daily exercise and education to modify the risk factors (Balady et al., 2000).

Numerous studies and associations increasingly agree that patients with ST elevation MI, non-ST elevation MI and all patients undergoing reperfusion will benefit from cardiac rehabilitation (British Association for Cardiovascular Prevention and Rehabilitation, 2012; National Institute for Health and Care Excellence (NICE), 2010a, 2010b, 2013; Piepoli et al., 2014; and Department of Health (DH) Cardiac rehabilitation commissioning pack, 2010).

Bethell et al. (2009) and Mampuya (2012) show that cardiac rehabilitation programs vary in frequency, intensity and duration between patients. Most cardiac exercise rehabilitation programs involve 2-3 sessions weekly for approximately 8 weeks (British Heart Foundation, 2014), whereas some may last for 3-6 months depending on the patient's condition, assessed during sessions medically supervised by a physical therapist (Mampuya, 2012; Menezes et al., 2014).

Cardiac exercise rehabilitation is able to decrease mortality. A systematic review of over 6000 MI patients found that patients involved in cardiac exercise rehabilitation showed a lower risk of all mortality causes, compared with patients who were not involved (Lawler et al., 2011). Another review over 10,000 patients concluded that cardiac exercise rehabilitation reduced overall mortality and cardiovascular mortality (Heran et al., 2011). In addition, cardiac exercise rehabilitation led to reduced hospital admissions. A review study conducted on 33 randomised controlled trials and involving over 4700 heart failure patients summarised that the cardiac exercise rehabilitation program reduced the risk of overall hospitalisation and its duration (Sagar et al., 2015). Furthermore, cardiac exercise rehabilitation improved quality of life and physiological wellbeing in general. A randomised controlled trial on over 3100 cardiac patients from 23 studies concluded that after cardiac exercise rehabilitation, psychological distress was greatly decreased, and serum cholesterol and systolic blood pressure both improved (Linden et al., 1996). Cardiac patients also reported lower rates of anxiety and depression after cardiac rehabilitation (Lavie and Milani, 2006). Cardiac patients *with* depression after cardiac exercise rehabilitation still had 59% lower mortality compared to those who did not participate in exercise rehabilitation (Milani et al., 2011).

Rehabilitation programs consist of three phases (British Heart Foundation, 2014; Bethell et al., 2009; Mampuya, 2012), the first of which begins in hospital as soon as the patient has reached a stable condition. This is known as Phase I (acute) and involves educating the patient

about their cardiac condition and how it can be managed through physical exercise. Very mild breathing and range-of-motion exercises are introduced to the patient in their bed, before moving on to walking and stair climbing at an appropriate time. This partly also serves as psychological preparation for increased exercise in general.

Following discharge from the hospital, the recovery stage (Phase II) is instigated. A range of interventions are brought about, including a structured exercise program under supervision, as well as further education with regard to weight loss and nutrition, smoking cessation, stress management and any other lifestyle changes. This phase lasts for three months and involves between 24 and 36 sessions of 60-90 minutes. These involve 20-30 minutes of exercise designed according to the patient's ECG responses, as well as supervisory observation. An instructor also delivers guided warm up and cool down exercise instructions. The activity level is gradually increased and the patient observed until they are able to undertake the exercise sessions safely and without supervision.

At this point, the patient will be familiar with the exercises and will have developed their own regime, based on their education and self-observations. This is the long-term maintenance stage (Phase III), which continues for the rest of the patient's life. Any issues are reported to the rehabilitation team, who provide counselling and further information as necessary.

1.6 Aims and hypothesis

Aim and hypothesis 1:

Aim

To develop an *in-vitro* model that determines lymphocyte proliferation as well as telomerase activity under chronic inflammation, and thus reflects the response of immune cells during atherosclerosis.

Hypothesis

I hypothesized that hyperoxia (40% oxygen saturation) would lead to enhanced oxidative stress and inflammation, which would in turn suppress telomerase activity and cell proliferation.

Aim and hypothesis 2:

Aim

The aim of this part of the project was to test *in vitro* whether the effect of p38 MAPK inhibition on T cells, important mediators of atherosclerosis, was a) dependent on telomerase, and b) would exert a beneficial effect even under oxidative stress.

Hypothesis

I hypothesized that inhibition of MAPK promotes T-cell proliferation dependent on telomerase activity under oxidative stress.

Aim and hypothesis 3:

Aim

It is well known that aerobic exercise has anti-atherogenic effects. Additionally, exercise in mice has been shown to induce telomere-stabilizing proteins in the arterial wall (Werner et al., 2008). Consequently, this chapter aims to:

- a) Study the effect of voluntary exercise on mice splenocytes.
- b) Establish the regulation of telomerase activity in atherosclerosis using an *mTert*-GFP⁺ x ApoE^{-/-} mouse model.

Hypothesis

I had hypothesized that the anti-atherogenic effects of exercise are co-dependent on telomerase and the immune system.

Aim and hypothesis 4:

Aim

This part of the project aims to identify the effect of cardiac rehabilitation on T-lymphocytes, regulatory T-cells, telomere length and telomerase activity in patients diagnosed with acute myocardial infarction (AMI).

Hypothesis

I hypothesized that the effects of cardiac exercise rehabilitation might be co-dependent on telomerase and the immune system.

CHAPTER 2. MATERIAL AND METHODS

2.1 Materials

2.1.1 Plasticware

- 96-, 24-, 6-well plates; 25cm²-flask (VWR European).
- PCR plates (VWR European).
- Tissue culture dishes (Thermo Fisher Scientific, Korea)
- Cell strainer 100μm (Nylon, USA)
- FACS tubes (FALCON a Corning brand, 352054, Mexico)
- Magnetic beads (Miltenyi Biotec)

2.1.2 Media, antibodies and chemicals

Fetal Bovine Serum (FBS) (Lonza) was brought up to 37°C then activated by heat via a 1h immersion in a water bath at 56°C. This was then aliquoted in sterile conditions for 50ml and frozen at -20°C.

Penicillin and streptomycin, under sterile conditions, 10,000 units/mL penicillin and 10 mg/mL streptomycin solution (Sigma-Aldrich).

Media RPMI 1640 (Gibco 21875-034) supplemented with 0.5 mM 2-mercaptoethanol (Sigma M7522), 25 mM Hepes Buffer (Gibco 15630-080), 10% FBS (PAA A15 151) and 30μg/ml of penicillin-streptomycin (Gibco 15070-063). Culture media were pre-warmed in a 37°C water bath (Grant Instruments, Jencons PLS, UK).

IL-2 (AE5212101, RD, USA) was prepared from frozen stock (-20°C) of 100μM/ml and added to a working concentration of 1.5μg/ml.

MAPK inhibitor BIRB 796 Doramapimod (Axon 1358) was prepared in DMSO (Sigma 472301) to working dilutions of 500nM.

Phosphate Buffered Saline (PBS) (Gibco 18912-014).

Dimethyl sulfoxide (DMSO) (472301 Sigma, USA).

Equipments were described in relevant chapter.

2.2 Methods

2.2.1 Mouse lines and Ethics statements

Ethical approval for the use of all mice was granted by Newcastle University's Local Ethical Review Committee and it was licensed by the UK Home Office (PPL 60/3864) for TERT mice, (PPL/60-3876) for *mTert*-GFP⁺ mice and (PPL/60/4553) for ApoE^{-/-}*mTert*-GFP⁺. All mice were housed in a single room with sawdust, paper bedding and ad libitum water access. They were kept at 20±2°C under a 12/12h light/dark photoperiod. All guiding principles for the care and use of laboratory animals were complied with.

2.2.1.1 TERT^{+/+} (C57BL/6), TERT^{-/-} and TERT^{+/−} mice

The TERT knockout (Figure 2.1) mouse line was purchased from Jackson Laboratory. TERT^{-/-} mice lines, strain: B6.129S-Tert, tm1Yjc/J (Chiang et al., 2004), on a C57BL/6 background were used. Breeding produced wild-type, first-generation (G1) knockout as well as heterozygote mice for the TERT genotypes. TERT^{-/-} mice and their wild type and heterozygote littermates were all purchased from Jackson Laboratory (USA).

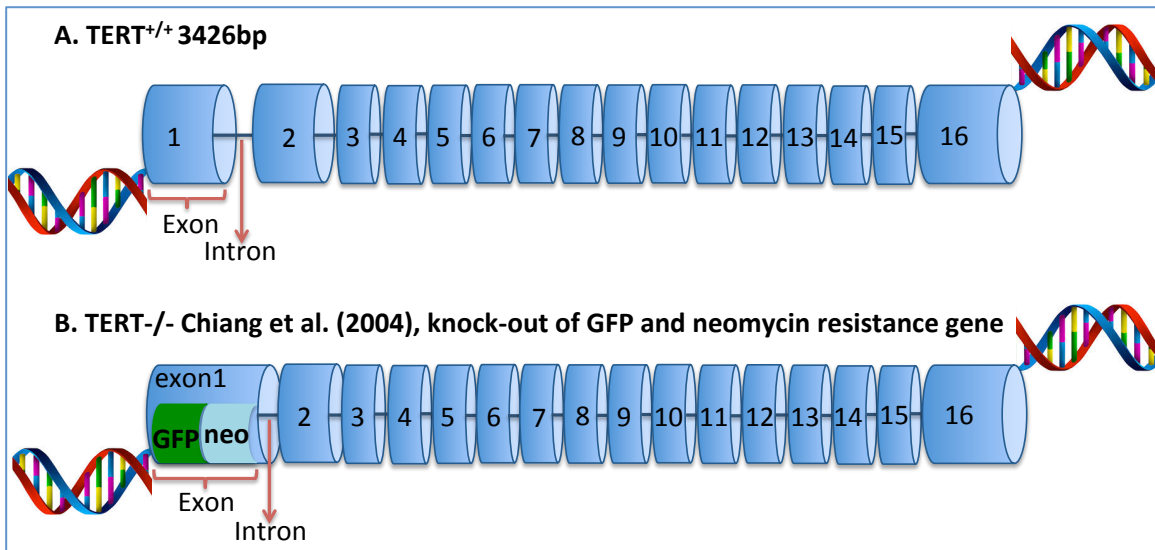


Figure 2.1. Illustration of wild type TERT gene and the TERT knockout construct (modified from Chiang 2004)

A. Comparison of wild type TERT DNA and **B.** the TERT^{-/-} constructs in mice. Wild type TERT^{+/+} contains 16 exons. The knockout described by Chiang et al (2004) contains a GFP and a neomycin-resistant gene (neo) inserted into exon 1. Chiang et al. (2004) performed a two-step construction process on TERT-deficient mice.

Step 1) A 6kb-mTERT genomic DNA fragment derived from strain 129 and containing exons 1 and 2 of the mTERT gene was used as the basis of a targeting vector, which was inserted into the pBluescript-KS vector at the EcoRI site (KS-tert). A BamHI-XbaI fragment excised from KS-tert was sub-cloned into pBluescript-KS vector (KS-BX). A unique enzyme restriction site (Xhol) in KS-BX was proximal to an ATG corresponding to the translation initiation code of the mTERT mRNA. Neomycin resistance and green fluorescent protein (GFP) genes were then inserted in the Xhol site to create a BamHI-XbaI DNA fragment with neomycin and GFP-resistant genes. This replaced the BamHI-XbaI fragment of KS-tert. An mTERT gene-targeting construct was created by inserting the thymidine kinase gene at a Not1 site outside of the genomic DNA fragment. **Step 2)** This was linearized using Sall, then electroporated into embryonic stem cells. Colonies that were resistant to G418 were isolated. A BamHI-XbaI fragment from KS-tert was used as a probe in the Southern blot analysis to identify embryonic stem cell colonies with homologous recombination events. Mutant mice were generated from these.

2.2.1.2 $mTert^{+/+}$ GFP⁺ mice

$mTert$ -GFP⁺ mice were generated (Figure 2.2) as a model in 2008 by Breault et al. to determine the expression of TERT in mice at the single-cell level (Briault et al., 2008). These transgenic were generated by integrating a GFP gene behind the mTERT promotor with the aim of getting an easier read-out of mTERT transcription in this mouse model. The construction of the mouse model is shown in figure 2.1.

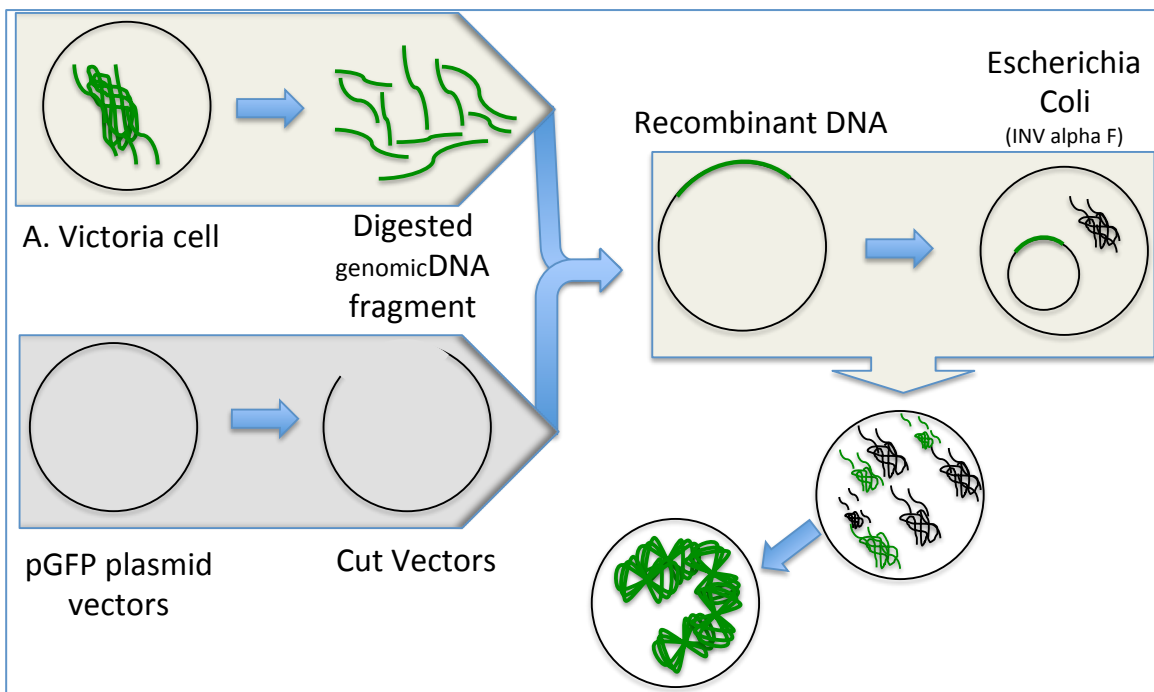


Figure 2.2. Illustration of the $mTert$ -GFP⁺ construct (Breault et al., 2008)

Genomic DNA fragments were digested from A.victoria cells, at the same time cut vectors applied on pGFP plasmid vectors. One strap of DNA was placed on the cutting part of the pGFP plasmid vectors to recombinant. This was then excised from the recombinant (E. Coli) DNA by electroporation to produce GFP⁺ cells. The $mTert$ -GFP plasmid was created and a linearised mTerT GFP transgene was electroporated into mouse (J1) embryonic stem cells. This was selected using G418 and screened for GFP expression. The transgene was created using the 4471 bp fragment of the $mTert$ gene promoter (accession number AF 121949). The fragment was amplified by PCR from genomic DNA, then digested using BamHI and HindIII. Part of the promoterless GFP vector was also digested. The remaining part was recombined with purified PCR fragment, then removed from the new recombinant DNA in (Excherichia coli) E. Coli by electroporation. A pure 129S1/SvIMJ background of $mTert$ -GFP was used because embryonic stem (ES) cells normally tend to express high telomerase activity (Breault et al., 2008 and Armstrong et al., 2000). In light of this, ES transgenesis (as opposed to pronuclear oocyte injection) was used to enable maximal transgene expression and to exclude transgene silenced clones following genomic integration.

Advantages and limitations of a GFP reporter mouse for measuring gene expression.

Principle and definition of a reporter system: Gene promoter activity (e.g. the TERT promoter) determines the level of gene expression. A reporter system is able to substitute gene coding sequences using that gene's promoter with a detectable reporter. One commonly used reporter is the fluorescence gene, GFP (other genes can also be used, such as luciferase or galactosidase). In this case, GFP intensity indicates the expression level of that promoter's gene. In my study (Nayef AL Zhrany, thesis, Chapters 3, 4 and 5) for example, I used the mTERT promoter with a GFP reporter gene behind it in order to determine the gene expression levels of the mTERT gene in mTERT reporter mice (Breault et al., 2008). The gene expression levels or transcriptional activity of a promoter is determined by the binding of various transcription factors. These can be activating or repressing. Examples for activating transcription factors for the TERT gene are Sp1, c-myc while inhibiting factors are mad and others.

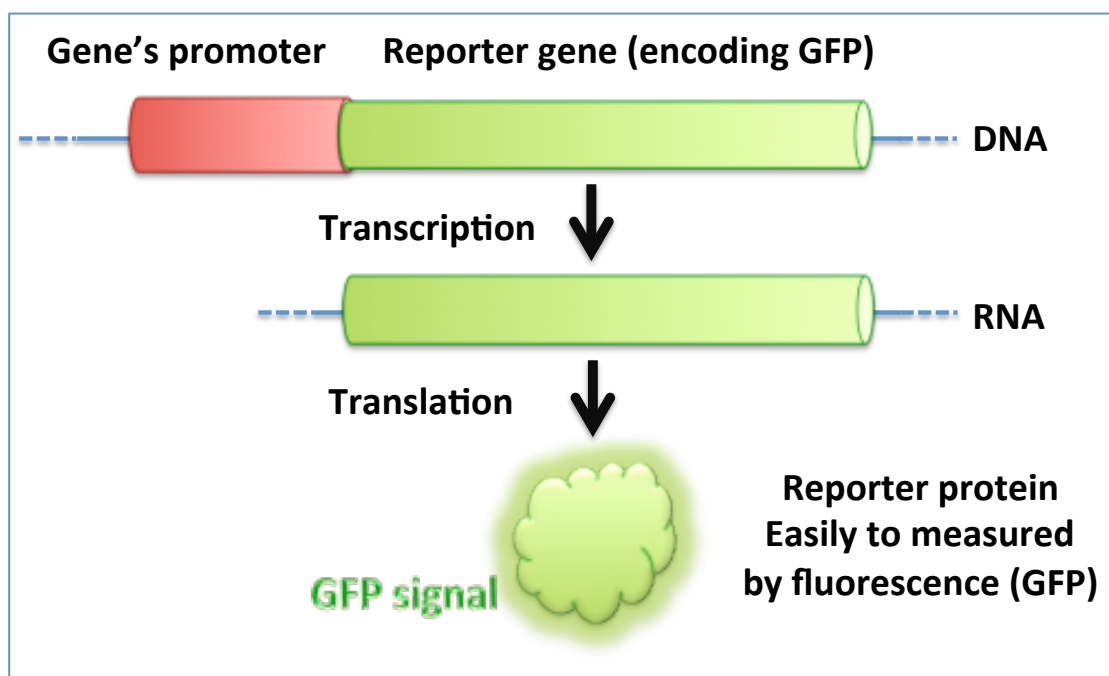


Figure 2.3. A diagram illustrating the principle of a reporter gene (modified from Wikipedia).

Advantages. The GFP reporter of gene expression has two advantages: i) direct observation of protein accumulation in single living cells is possible, prior to quantitative analysis and ii) It can be measured on a 'per-cell' basis.

i. Direct observation of protein accumulation in living cells prior to quantitative analysis

This is a significant advantage, as it enables the quantitative results to be reasonably approximated prior to flow cytometric analysis of the cells. Furthermore, this ability for direct observation of GFP accumulation enables the observer to empirically assess that GFP expression has occurred prior to the tasks involved in preparing the cells for analysis (Soboleski et al., 2005).

ii. Measurement of GFP expression on a cell-by-cell basis

This enables greater accuracy in assessing promoter activity in the cell population than alternative measurement techniques, which simply take an average value across the entire cell population for example when using RNA isolation and RT-PCR. Consequently, a more accurate picture is produced with the reporter assay. Flow cytometry then allows for mean and SD values to be quickly determined in different cell populations (for example, positive and negative for GFP). GFP fluorescence, measured by flow cytometry is especially powerful in comparing the expression of reporter genes across different cell populations (Soboleski et al., 2005).

Limitations of GFP as a reporter of gene expression

- i. One significant limitation of this method is that high intensity auto-fluorescence may be exhibited by tissues. This can result in unusually high background readings, which can confound the data interpretation.
- ii. Assessing gene expression events in real time may be affected also by GFP instability and degradation.
- iii. Cultured cells have to be transfected with the reporter system (usually plasmids) which is an overexpression and the expression levels of the gene also might vary depending on the integration site of the plasmid. For mouse model a transgenic mouse has to be generated which is time consuming and labourious.

2.2.1.3 ApoE^{-/-} mTert-GFP⁺ mice

ApoE null male and female mice (Piedrahita et al., 1992) were bred in order to maintain an ApoE^{-/-} mouse colony. Mice from this colony were crossed with *mTert*-GFP^{+/+} (Breault et al., 2008) mice, resulting in ApoE^{+-/-} *mTert*-GFP^{+-/-} mice. These were subsequently inbred to create ApoE^{-/-}, ^{-/+} and ^{+/+} mice. Of these, approximately 50% were *mTert*-GFP⁺ (Figure 2.3).

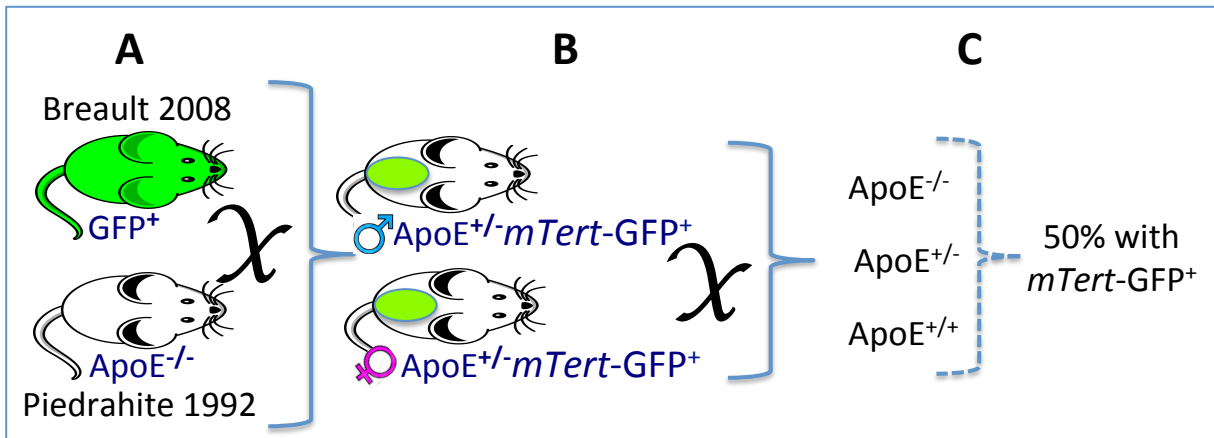


Figure 2.4. *ApoE*^{-/-}*mTert*-GFP⁺ mouse generation

Step A: Cross of *ApoE*^{-/-} mice with *mTert*-GFP⁺. **Step B:** Cross male *ApoE*^{+/-}*mTert*-GFP⁺ female with *ApoE*^{+/-}*mTert*-GFP⁺. **Step C:** Select appropriate mice (*ApoE*^{-/-}*mTert*-GFP⁺) for the experiment.

2.2.1.4 Mouse diet

All mouse groups in my PhD thesis were on a normal diet (ND) (Harlan, Teklad Global 19% Protein Extruded Rodent Diet) of 19% crude protein, 9% crude fat and 5% crude fibre. However some groups from *ApoE*^{-/-}*mTert*-GFP⁺ or *ApoE*^{+/-}*mTert*-GFP⁺ (assigned to the exercise programme or its control groups) received an adjusted calorie, high fat diet (HFD) containing 42% fat (Harlan, Rx:1591957, TD.88137).

2.2.2 Mouse dissection and isolation of spleen and thymus

After being euthanized (cervical dislocation), mouse bodies were dissected inside the tissue culture hood, under sterile conditions. Each body was placed on its back, a midline incision was made and the skin was retracted between the head and the thighs. A one-inch incision was made left of the peritoneal wall to reveal the spleen. This was gently separated from the body by tearing the connective tissue which lay behind it. An incision was made from the xiphoid to the neck and the ribs were gently cracked to enable retraction. This exposed the thymus, which sits just above the heart. Both lobes were excised as one part using curved forceps.

Both organs were macerated through a 100µm cell strainer (BD352360), then suspended in 10ml complete MACS buffer rinsing solution (phosphate buffered saline (pH 7.2), 2mM EDTA, and 0.5% MACS BSA stock solution). The suspension was pipetted at an angle and

layered over 5ml Ficoll Biochrom in a 15ml falcon tube by pipetting it with the tubes held at an angle. This was placed in a centrifuge at 800xg for 20 minutes at 20°C. Acceleration was set at full (9) and stopped without any deceleration. The suspension was separated and the Peripheral Blood Mononuclear Cell (PBMNCs) layer was removed to another 15ml tube and washed again in complete MACS buffer rinsing solution. This was spun down again for 10 minutes under the same conditions but this time with full deceleration (9), and the resulting pellet was re-suspended in fresh buffer solution. The process was repeated and the pellet was re-suspended once more, this time in complete RPMI medium for counting.

10 μ l of this suspension was diluted in 1:10 buffer (Figure 2.4), then mixed with 1:1 0.4% Trypan blue solution. 10 μ l of this mixture was loaded on to the edge of the cover glass of a Neubauer hemocytometer until capillary action ensured that the counting area was filled entirely. After 30 seconds had elapsed, the cells were counted. Now, the cells were ready for further use, either for culture, staining, or cryopreservation, as described later.

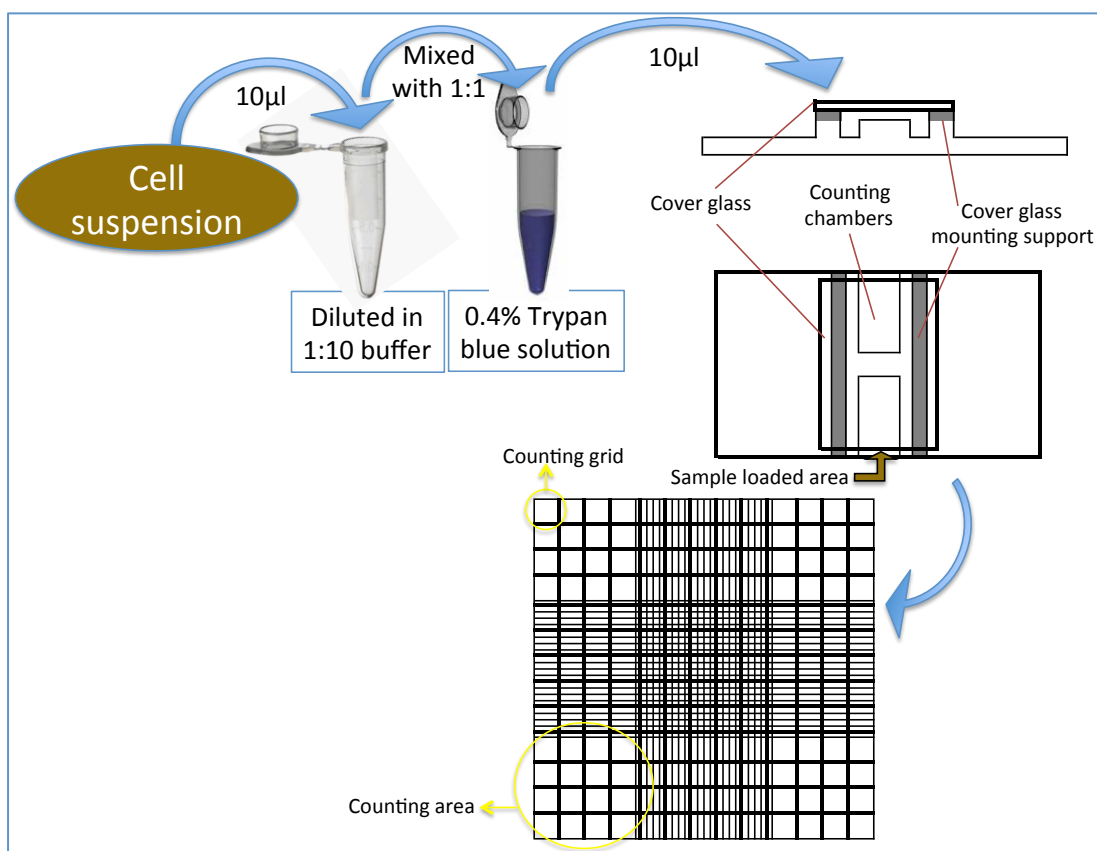


Figure 2.5. Cell counting steps:

10 μ l from cell suspension was diluted 1:10 in buffer, then mixed 1:1 with 0.4% Trypan blue solution. 10 μ l from this mixture was loaded at the edge of the cover glass.

2.2.3 Cryopreservation of cells

Cryopreservation at -80°C was used to maintain either human PBMNCs or mouse splenocytes as live cells. In the case of freezing live cells, RPMI 1640 [R0883 Sigma, USA] with 10% FBS and 10% DMSO, was used as freezing medium. To do this, cells were sedimented by centrifugation (800g for 10 minutes) and the supernatant was discarded. The media were then added at 100 μl per million cells. After mixing, the cells were transferred to a cryovial and stored in a cryo-container (Thermo Scientific, USA) to cool slowly at 1 degree per minute overnight at -80° . Afterwards, the cryovial was removed from the cryo-container and stored at -80° .

2.2.4 TCR stimulation

Activation of T-cell receptors of splenocytes was achieved in two ways (Figure 2.5), achieving either strong or moderate activation of the T-cell receptor. Coating wells with antibody results in less frequent contact of cells with the antibodies (moderate activation), while mixing micro-beads with cells leads to a 1:1 ratio between cells and antibodies.

- 1) Strong TCR activation. A micro-beads CD3e/CD28-Biotin T-cell expansion kit (Miltenyi Biotec, 130-093-627) was used at ratio of 1:1 (cells to beads) in RPMI 1640 medium. Anti-Biotin MACSibead particles were loaded with 100 μl of vortexed CD3e-Biotin and 100 μl CD28-Biotin in a 2ml tube. 300 μl of cold (4°C) complete Auto MACS rinsing solution (Phosphate buffered saline (pH 7.2), with 2mM EDTA and 0.5% MACS BSA stock solution) was mixed with the antibody mixture. Anti-Biotin MACSibead particles were homogenously resuspended and 500 μl was added to the antibody mixture, then incubated at 4°C for 2 hours before use with cells.
- 2) Moderate TCR activation. Plates were coated overnight with anti-CD3 (BD 553238) and anti-CD28 (BD 553295) antibodies at 1 $\mu\text{l}/\text{ml}$ PBS at 4°C .

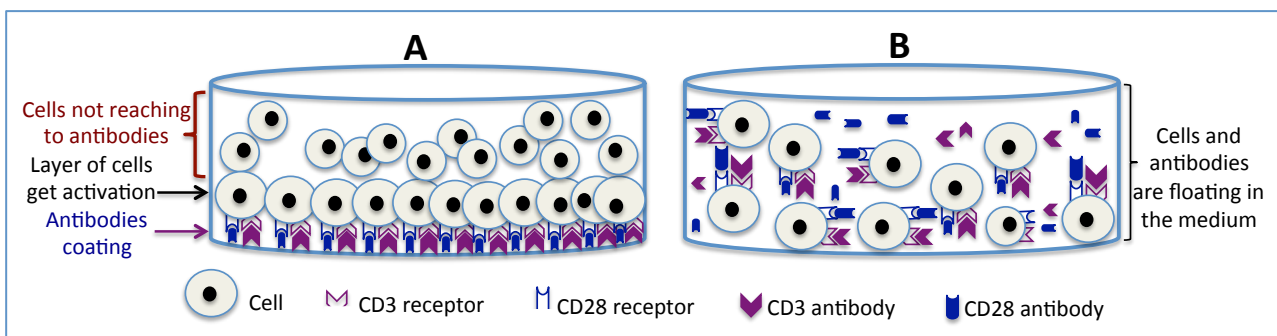


Figure 2.6. Two modes of splenocytes T-cell receptor activation in splenocytes

A: Moderate activation. As antibodies coated the well floor, the layer of cells which lay on the antibodies were activated, whilst the other cells had less frequent contact with the antibodies to activate.

B: Severe activation. As antibodies floated with the cells in the medium, this gave a high frequent contact between antibodies and cells to activate.

2.2.5 Mouse PBMNCs culture

A Ficoll-hypaque density gradient (using Biochrom AG Biocoll L 6113/5) was used to isolate PBMNCs from mouse spleens. Cells (2×10^6 /ml) were cultured in complete RPMI 1640 medium (Gibco 21875-034) supplemented with 0.5 mM 2-mercaptoethanol (Sigma M7522), 25 mM Hepes Buffer (Gibco 15630-080) and 10% fetal bovine serum (FBS) (PAA, A15 151). Different cell plates were incubated under different oxygen saturations (2.2.8) and activated using two stimulation types, as specified in each experiment description. All procedures were carried out in a sterile environment and under a cell culture hood.

2.2.5.1 Cell culture in 96-well plates

96-well plates were used only with pure CD4⁺ T-cell expansion under strong activation. CD4⁺ T-cells from either TERT^{+/+} or TERT^{-/-} mice were seeded at 2×10^5 cells/well (volume = 200 μ l/well) in a 96-well plate. CD4⁺ T-cells were generated by immunomagnetic bead-isolation from splenocytes, which were cultured at 2×10^6 /ml in a 24-well plate for 14 days (as described in 2.2.5.2) with anti-CD3 (BD 553238) and anti-CD28 (BD 553295) antibodies (prepared at 1 μ l/ml PBS). The medium was changed and 1.5 μ g/ml IL-2 was added every 2-3 days for all experiments. CD4⁺ T-cells were re-activated every 7 days (days 0, 7, 14, and 21) by adding CD3e/CD28-Biotin micro-beads at a 1:1 ratio (Miltenyi T-cell expansion kit). Cells were incubated under appropriate oxygen saturation (described in the experiment). For the control group, 1 μ l/ml DMSO was added, and 500nM/ml mitogen-activated protein kinases inhibitor (MAPKi, BIRB 796 Doramapimod, Axon 1358) was added to the treated group. CD4⁺ T-cells were split to a new well when they reached double their starting number. This continued until they reached 2×10^6 cells, after which cells were collected and transferred to 24-well plates.

2.2.5.2 Cell culture in 24-well plates

Cells were isolated from the spleen by Ficoll-hypaque density gradient. Splenocytes from any mouse independently of their genotype were then seeded at 2×10^6 /ml in a 24-well plate for different times, specified at each experiment. There were two types of activation: the first is called ‘moderate activation’, because the antibodies stick to the well bottom. The layer of cells which lies on top of the antibodies will activate, whilst the other cells get less frequent contact with the antibodies. In moderate activation, plates were coated overnight before the day of the experiment with anti-CD3 (BD 553238) and anti-CD28 (BD 553295) antibodies

(prepared at 1 μ l/ml PBS) at 4°C. The medium was changed and 1.5 μ g/ml and IL-2 was added every 2-3 days. For the control group, 1 μ g/ml of DMSO was added, whilst 500nM/ml MAPKi was added for treated group. Cells were incubated under the oxygen saturation described at each experiment.

The second type of activation is called strong activation, because the micro-antibodies were floated with the cells in the medium, giving cells high frequent contact with the antibodies for activation. In this type of activation, cells were seeded at 2 \times 10 6 /well/2ml; 1ml for cells and 1ml for CD3e/CD28-Biotin micro-beads at a 1:1 ratio (Miltenyi T-cell expansion kit). T-lymphocytes were activated every 7 days (days 0, 7, 14, and 21). The medium was changed and 1.5 μ g/ml of IL-2 was added every 2-3 days. For the control group, 1 μ l/ml DMSO was added and 500nM/ml MAPKi was added to the treated group. In strong activation, cells were split to a new well when they reached double the starting number. This continues until they reached 10 \times 10 6 cells, then cells were collected and transferred to 6-well plates.

2.2.5.3 Cell culture in 6-well plates

6-well plates were used after cell expansion in 24-well plates under strong activation. All 10 \times 10 6 cells were collected and mixed in one well of a 6-well plate. 50% of the suspension was spun down for 10 minutes at 800g. The medium was changed and 1.5 μ g/ml of IL-2 was added every 2-3 days. For the control group, 1 μ l/ml DMSO was added and 500nM/ml MAPKi was added to the treated group. Cells were split to a new well when their number doubled; this was done without spinning down, just adding new medium. This continued until cell numbers reached 24 \times 10 6 , after which they were transferred to a 25 cm 2 flask (50ml).

2.2.5.4 Cell culture in 25cm 2 flask

25cm 2 flasks were used after cell expansion in 6-well under strong activation. Cells were collected and mixed when they reached up to 24 \times 10 6 cells in one 25cm 2 flask. 50% of the suspension was spun down for 10 minutes at 800g. The medium was changed and 1.5 μ g/ml of IL-2 was added every 2-3 days. For the control group, 1 μ l/ml DMSO was added, and 500nM/ml MAPKi was added to the treated group. Cells were split into a new 25cm 2 flask when their number doubled without centrifugation.

2.2.6 Immunomagnetic sorting of mouse CD4⁺ T-cells

Mouse splenocytes derived from either a) the process described above at 2.2.2 or b) splenocytes were expanded for 14 days in coated 24-well plates overnight at 4°C with anti-CD3 (BD555338) and anti-CD28 (BD555727) antibodies; cells were seeded as 2x10⁶/well in 1ml of complete mouse medium RPMI 1640 (Gibco 21875-034) supplemented with 0.5 mM 2-mercaptoethanol (Sigma M7522), 25 mM Hepes Buffer (Gibco 15630-080), 10% FBS (PAA A15 151). DMSO (1µl/ml) was added at the zero time point, then every 2-3 days, along with a change of medium. Splenocytes were expanded under hypoxic conditions 3% O₂ saturation, 5% CO₂, and humidified air, at 37°C.

When the CD4⁺ purification stage was reached, cells were passed through a sterilized 30µm pre-separation filter (120-002-220) and counted. The splenocytes were pelleted again (300xg, 10minutes) and the supernatant completely discarded. The pellets were then re-suspended in cold complete Auto MACS rinsing solution (phosphate buffered saline (pH 7.2), 2mM EDTA, and 0.5% MACS BSA stock solution) at 90µl/10⁷ cells. Then CD4 (L3T4, 130-049-201) MicroBeads (10µl/10⁷ cells) were added and the mixture vortexed. Following incubation for 15 minutes at 4°C, the cells were rinsed again with the same solution, re-pelleted (300xg, 10minutes), then re-suspended in the Auto MACS solution, this time at 500µl/10⁸ cells.

A pre-prepared MS column (130-042-201), placed on a MiniMACS magnetic separator, was washed with 1ml of 4°C complete Auto MACS rinsing solution and cells were passed through. This process enabled the separation of unlabelled (CD4⁻) cells, which passed straight through, and CD4⁺ cells, which remained inside the column. The column was washed three times with 500µl of the Auto MACS solution, then removed from the magnetic separator. A further rinse with 1ml Auto MACS solution and plunging forced the remaining CD4⁺ T-cells into a pre-cooled collection tube. The process was then repeated to increase the sample's purity.

The CD4⁺ T-cells' purity was assessed by transferring 200µl of the final suspension to a fresh FACS tube for staining with CD4-PE-Cy (552775). This was then incubated for 20 minutes in zero light conditions and washed using the BD FACS Lyse/Wash Assistant (337146, USA). A compensated FACS Canto II, running FACS Diva software for 50,000 live events was used to analyse purification against negative controls. Dead cells were excluded as far as possible, based on scatter signals. All processes were carried out under sterile and ice-cold conditions.

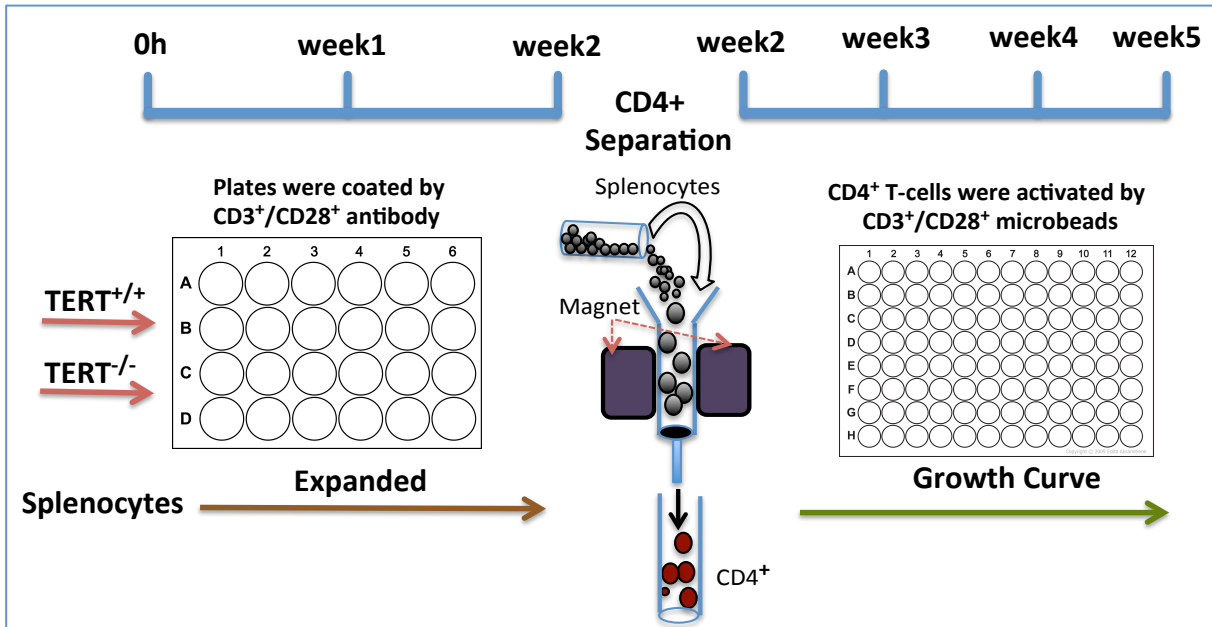


Figure 2.7. CD4⁺ T-cell purification after expansion

Splenocytes from both TERT^{+/+} and TERT^{-/-} mice were expanded for 2 weeks in 24-well plates coated with CD3⁺/CD28⁺ antibodies (moderate activation), then CD4⁺ cells were sorted using immunomagnetic separation (microbeads bind specifically to a CD4⁺ cell antigen and are retained in a magnetic field, whilst unlabelled cells pass through with buffer washes. Labelled cells are removed from the magnetic field and flushed out). Pure CD4⁺ cells are then ready to be used and activated with CD3⁺/CD28⁺ microbeads (strong activation) for 3 weeks to obtain the growth curve.

2.2.7 Long-term culture of splenocytes and CD4⁺ T-lymphocytes

Splenocytes were cultured in a 24-well plate (2×10^6 cells/2ml/well) and CD4⁺ T-cells were cultured in a 96-well plate (2×10^5 cells/200 μ l/well). Both sets of cultured cells were expanded using (50% volume) complete medium RPMI 1640. MACSibead mouse T-cell expansion beads (Miltenyi 130-093-627) were added to the remaining medium at a ratio of 1:1 beads per cell (i.e. 4×10^6 cells and 4×10^6 beads/2ml).

50% of the volume of each sample was transferred to a new well every 2-3 days and 50% fresh medium added, to maintain T-cell activation beads, without centrifugation. Cells were counted under a microscope, using the Neubauer chamber (hemocytometer) as described previously. 1.5 μ g/ml IL-2 and 500nM/ml MAPKi (Di Mitri et al., 2011) was added and cells were re-activated on a seven-day cycle. When the cell count reached 10×10^6 cells, the suspensions were collected, mixed and transferred to a 6-well plate. These were centrifuged to 50% volume and the supernatant aspirated. The cells were then re-suspended in fresh medium. When the cell count reached 24×10^6 in the 6-well plate, they were transferred to a

50ml (25cm²) culture flask and re-suspended in 50ml complete mouse medium for further cell culture expansion.

CD4⁺ T-cells underwent a similar process. When the cell count reached 2x10⁶, they were transferred to a 24-well plate (2x10⁶/2ml/well). Following this, the same process was used as for the splenocytes expansion.

2.2.8 Hypoxia, normoxia and hyperoxia

Hypoxia (3% O₂), normoxia (atmospheric 20% O₂) and hyperoxia (40% O₂) conditions were maintained throughout experiments using a Heraeus Hera Cell 150 incubator. A constant 5% CO₂ in humidified air at 37°C was maintained. Cell behaviour under oxidative stress was explored under hyperoxic conditions by introducing industrial O₂ to produce 40% oxygen saturation.

2.2.9 Quantification of TERT^{+/+} and *mTert*-GFP⁺ (cells) splenocytes, thymocytes and T-lymphocytes

Cells were harvested from the spleens and thymuses of both Tert^{+/+} and *mTert*-GFP⁺ mice. These were strained via a cell strainer (100µm, BD Falcon 50734-0004) and rinsed in complete Auto MACS rinsing solution (described above). Lymphocytes were isolated using Ficoll-Hypaque density gradient and washed twice, diluted to 2x10⁶/ml in complete RPMI 1640 mouse medium. 2x10⁶ cells from each genotype were transferred to FACS tubes and rinsed with 1ml of Auto MACS rinsing solution at time point zero. These were then centrifuged at 800xg for five minutes, and the supernatant discarded.

Fc (Fragment-crystallizable) receptor-mediated binding of unspecific epitopes was blocked using purified rat anti-mouse CD16/CD32 (Mouse BD Fc Blocking solution 553141). The pellets were then suspended in 100µl of the rinsing solution and 2µg mouse BD Fc Blocking solution purified anti-mouse CD16/CD32 per 2x10⁶ cells was added to the suspension, which was then incubated for 5 minutes at 4°C. The cells were then directly stained in the presence of Fc blocker using CD4-PE-Cy, CD8a-Pacific-Blue, CD11b-APC and CD45R (B220) PerCP antibodies. GFP expression in GFP mice was determined with no need for labelling because it is endogenously expressed. A compensated FACSCanto II, running FACSDiva software for 50,000 live events was used to measure the cell expression against negative controls (wild-type cells).

The remaining $\text{Tert}^{+/+}$ and $m\text{Tert-GFP}^+$ cells were cultured for 3, 5, 7, 10 and 14 days to 2×10^6 cells per well. 24-well plates were coated overnight, before the day of the experiment, with anti-CD3 (BD555338) and anti-CD28 (BD555727) antibodies at 4°C . MAPKi (500nM) and $1.5\mu\text{g/ml}$ IL-2 were added to cells at 0h, then at each medium change, every 2-3 days. Cells were then incubated under hypoxic conditions ($3\% \text{ O}_2$) and hyperoxic conditions ($40\% \text{ O}_2$). Cells were rinsed and counted at regular intervals (3, 5, 7, 10 and 14 days). 0.1% DMSO was added for control wells.

1ml of each mixture was spun down at 800xg for 5 minutes. Following aspiration of the supernatant, the pellet was stained with Fc blocking solution (Mouse BD Fc Block purified anti-mouse CD16/CD32, BD 553141) as described previously. Cells were then labelled with CD4-PE-Cy, CD8a-Pacific-Blue, CD11b-APC and CD45R (B220) PerCP antibodies for flow cytometric analysis. GFP expression was determined by endogenous expression, and other expressed antigen markers were measured as described previously (2.2.9).

2.2.9.1 Flow cytometry (FACS)

Flow cytometry was developed in the 1970s to enable quantitative analysis of single cells and is now widely used in research and industrial contexts. The technique is able to define phenotype expression, intracellular DNA/RNA measurements and other cell functions, including apoptosis. Flow cytometry involves a process of fluorescence-activated cell sorting (FACS) analysis, which was developed by BD Biosciences. Flow cytometry is able to distinguish individual particles according to internal complexity, size or granularity.

Three primary systems, optics, electronics and fluidics, make up the flow cytometer (Figure 2.7). Optics involves the use of lasers, lenses and a range of sensors to analyse samples; electronics converts these light signals to digital data for computational analysis; and fluidics uses hydrodynamic focusing of the sheath fluid to enable the optical analysis.

To explain this further; laser beams aimed at individual cells are either scattered or absorbed. When light at an appropriate wavelength is absorbed by the cell, it can then be re-emitted (fluorescence) if that cell contains naturally fluorescent particles. Another way for this to happen is if intracellular antigens become bound to fluorochrome antibodies. The detected data is then comprised of either forward-scattered (FSC, collected at an angle $<10^\circ$) or side-scattered (SSC, $= 90^\circ$) light, which is contingent on both the cell's internal complexity and its

size, as shown in (Figure 2.8). The data yielded by this technique reveals a large amount of information with regard to cells' physical properties.

Fluorochromes (fluorescent probes) may also be measured using flow cytometry, and a wide choice of (primarily monoclonal) antibodies is available on the market for use with a range of specific antigens. Peridinin Chlorophyll Protein (PerCP), Allophycocyanin (APC), Phycoerythrin with Cyanine (PE-Cy) and Pacific Blue are all popular choices for targeting cell content, e.g. DNA (Hoechst 33342 or propidium iodide (PI)). When light is absorbed by fluorochromes, this energises the electrons, making them unstable. Light of a longer wavelength is then emitted. That 'emission wavelength' reveals specific characteristics about the emitting molecule. Spectral overlaps may occur when more than one fluorochrome is used, and this must be taken into account when interpreting the results. The emitted photons are detected by a photomultiplier tube (PMT), which uses a photocathode to generate a corresponding voltage and consequently, a pulse. This pulse is then converted into a digital signal for data analysis by the computer, which records fluorescence quantity and intensity and can report this data in various graphical ways (Scheffold and Kern, 2000; Stewart, 2000; Bakke, 2001; Givan, 2001).

Table 2.1. Antibodies used in immunophenotyping of mouse splenocytes and thymocytes

Laser	Bandpass filter	Fluorochromes	Antibodies	Source	Catalogue number	Quantity (μl)
Blue 488nm	780/60	PE-Cy7	CD4	BD	552775	5μl
Blue 488nm	530/30	GFP	Genetically modified	Genetically modified
Violet 405nm	450/50	Pacific Blue	CD8a	BD	558108	5μl
Red 633nm	660/20	APC	CD11b	MACS	130-091-241	5μl
Blue 488nm	682/33	PerCP	CD45R (B220)	MACS	130-102-213	5μl

Splenocyte and thymocyte populations were prepared (at each time point for FACS) by addition of 5μl CD4 (PE-Cy7), 5μl CD8a (APC), 5μl CD11b (APC) and 5μl CD45R-B220 (PerCP) to 2x10⁶ cells after the cells were washed by centrifugation. Cells were then incubated in the dark at room temperature for 10 minutes before being washed using BD FACS lyse/wash assistant, and analysed in FACSCanto II 424 (BD, USA). The same steps were applied for *mTert*-GFP⁺ cells, but 5 colours were detected by FACS, as GFP was the extra one.

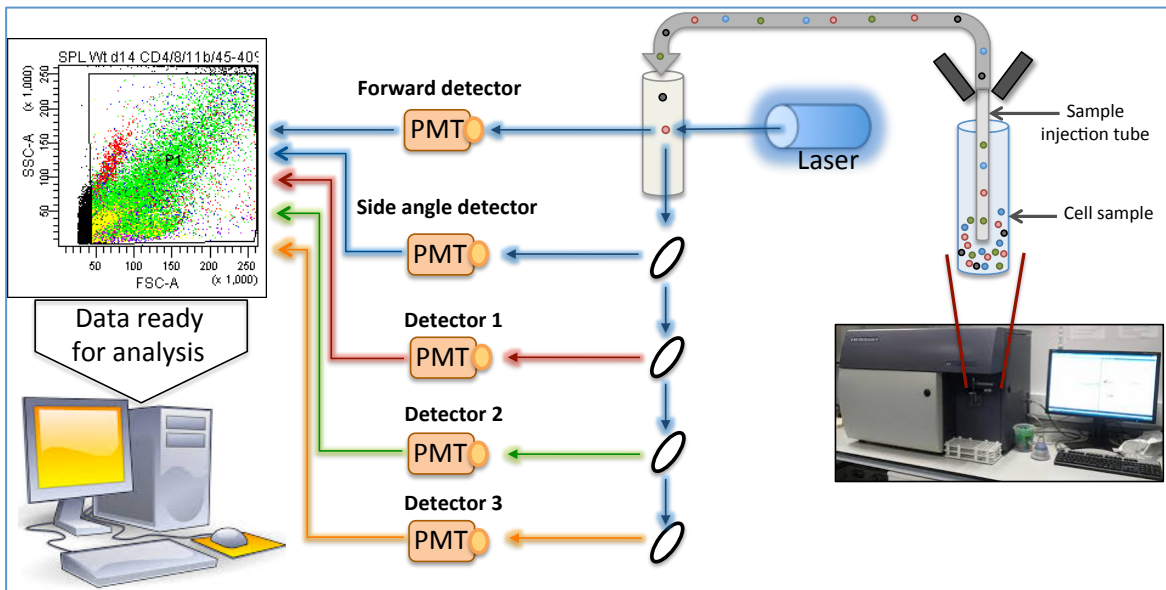


Figure 2.8. Flow cytometer principle

Laser analysis of cells in sheath fluid is carried out to identify different physical and fluorescent properties, using a range of lenses and sensors. The signal is transmitted via a photomultiplier tube (PMT) to a computer, where it is digitised and converted to data.

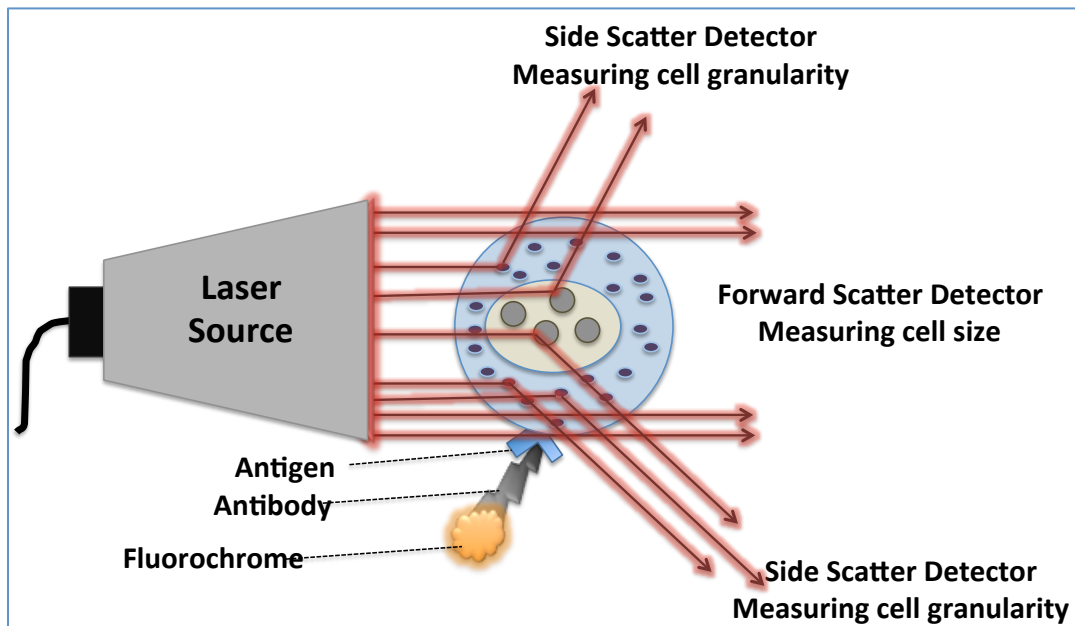


Figure 2.9. Flow cytometry analysis on single cell level: modified from (Dimmick, 2009)

Laser beams become diverted when they hit a cell. Relative directions of the forward scatter detector and side scatter detector and fluorescence of the fluorochromes.

2.2.9.2 Strategy for FACS gating of wild-type cells

Dying and dead cells were gated as accurately as possible from the main population of P1 events. B-cells (CD45R(B220)) and monocytes (CD11b) were discounted from the negative B-cell population. CD4⁺, CD8⁺, DP and DN cells were then determined and gated from negative monocytes. Fluorochromes of CD4⁺, CD8⁺, CD11b and CD45R(B220) were recorded and compared with negative controls from the same cell populations, with all other conditions remaining the same. In total, 50,000 live events were recorded using FACSCanto II, running FACSDiva software. These were then scored and analysed (Figure 2.9).

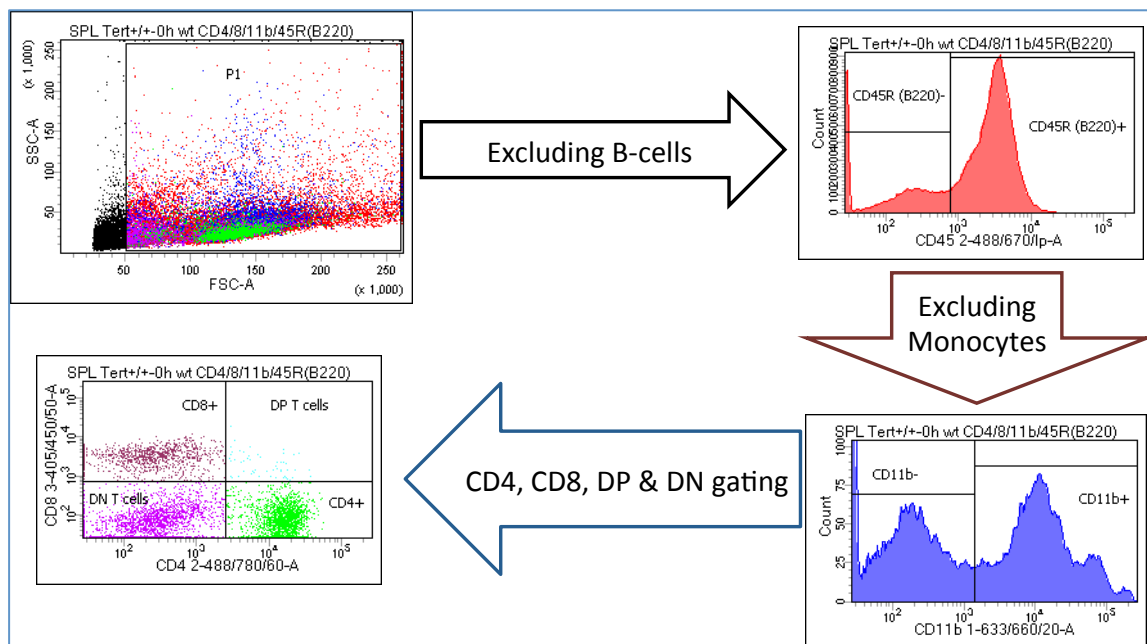


Figure 2.10. FACS gating strategy for wild-type cells

CD45R(B220) positive (B-cells) were gated from the main lymphocyte population (P1). CD11b positive (monocytes) were then gated from the CD45R(B220) negative (B-cell) population. Finally, CD4⁺, CD8⁺, DP and DN T-lymphocytes were gated from the CD11b negative (monocytes) population.

2.2.9.3 Strategy of FACS gating of *mTert*-GFP⁺ cells

The cells were gated in the main lymphocyte population as P1 events, excluding dying and dead cells as far as possible. Having excluded B-cells (CD45R(B200)) from lymphocyte (P1), monocytes (CD11b) were similarly discounted from the population of negative B-cells. GFP⁺ cells were gated from negative monocytes. Then, CD4⁺, CD8⁺, DP and DN cells were determined and gated from both GFP positive and GFP negative cells. Furthermore, GFP⁺ cells were gated in a positive population of B-cells and monocytes. GFP expression was measured against non-transgenic cell controls, and the remaining fluorochromes were

compared with negative controls from the same cell populations, with all other conditions remaining the same. In total, 50,000 live events were recorded using FACSCanto II, running FACSDiva software, which were then scored and analysed (Figure 2.10).

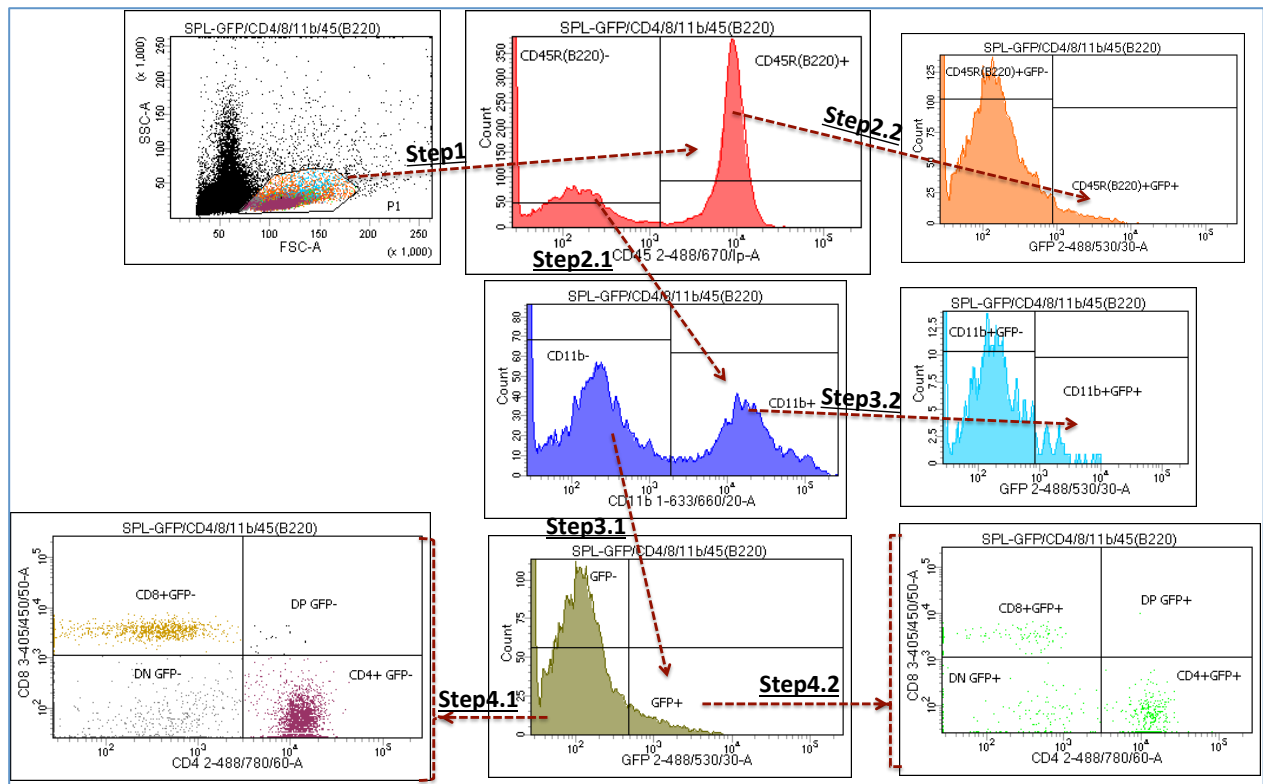


Figure 2.11. FACS gating strategy for *mTert*-GFP⁺ mice cells

Step 1: After gating and determining the lymphocyte population (P1), B-cells were excluded. **Step 2.1:** Monocytes were excluded from negative B-cells. **Step 2.2:** B-cell⁺GFP⁺ cells were determined from B-cells⁺. **Step 3.1:** GFP⁺ cells were excluded from negative monocytes. **Step 3.2:** Monocyte⁺GFP⁺ cells were determined from monocytes⁺. **Step 4.1:** T-cells (CD4⁺, CD8⁺, DP and DN cells) were determined and gated from negative GFP cells. **Step 4.2:** GFP⁺T-cells⁺ (CD4⁺, CD8⁺, DP and DN cells) were determined and gated from GFP positive cells.

2.2.10 Quantification of oxidative stress and mitochondrial membrane potential

These techniques were performed together with Dr. G. Saretzki at the Campus for Ageing and Vitality at Newcastle University, using splenocytes that I had prepared.

DHE staining

Dihydroethidium was purchased from Molecular Probes (Life Sciences). A working solution of 1:500 dilution was produced by adding 2µl of stock solution (5mM in DMSO) to 1ml of DMEM medium without serum. Mitochondrial superoxide levels were measured by staining $\approx 2 \times 10^5$ cells with 10µM DHE. This was left in total darkness at 37°C for 30 minutes, then incubated and spun for three minutes at 1800rpm. After discarding the supernatant, the cells were re-suspended in 3ml of DMEM. FL3 median fluorescence intensity was measured using

flow cytometry (Partec, Germany). Those cells that remained unstained were re-suspended in DMEM with FCS and measured at FL3. The resulting value was then subtracted from that of the stained cells.

Measurement of the mitochondrial permeability transition using JC-1 probe:

(5,5',6,6'-tetrachloro-1,1',3,3'-tetraethylbenzimidazolylcarbocyanine iodide, Molecular Probes, T3168)

Approximately 2×10^5 cells were pelleted and re-suspended in 300 μ l RPMI 1640. 200 μ l of JC-1 (1 μ l/ml in phenol red and supplement-free RPMI) was prepared, then mixed vigorously by pipette with the suspension, giving a JC-1 concentration of 1 μ g/ml.

Following incubation and centrifugation as above, the cells were then washed in cold PBS and re-suspended in 3ml PBS at room temperature. Cells were then measured for FL1 and FL3 fluorescence using flow cytometry. The amount of FL3 fluorescence of unstained cells was subtracted from FL1 and the ratio between FL3 and FL1 provided a measure for the membrane potential.

At low membrane potential or at concentrations below 0.1 μ M, the green fluorescent JC-1 probe exists as a monomer. At higher concentrations or higher membrane potentials, red JC-1 aggregates are formed by JC-1. These exhibit a broad excitation spectrum with a maximum emission at 590nm. The green fluorescent monomer emissions (absorption/emission maxima 510/527nm in water) can therefore be combined with the aggregate to yield various ratio measurements. In the case of flow cytometry, JC-1 can be excited at 488nm and detected in bivariate mode, using the green channel for the monomer and the red channel for the J-aggregate. Both measurements were performed in a Partec Flow cytometer (Partec, Muenster, Germany).

2.2.11 Quantification of telomerase activity by TRAP-PCR ELISA

(Roche, Switzerland)

Photometric enzyme immunoassay for determination of telomerase activity, using the Telomeric Repeat Amplification Protocol (TRAP):

This assay was performed by Dr. G. Saretzki (Institute for Cell and Molecular Biosciences at the Campus for ageing and Vitality at Newcastle University), using splenocytes that I had prepared.

Cultured cells were added to 1ml cryopreservation medium, then cooled to -80°C. The samples were later removed and thawed quickly by rubbing the tubes. These were then centrifuged for 5 minutes at 800xg (SIGMA 1-14, 134744, Germany) and the supernatant removed. The cells were washed in 1ml PBS, then pelleted at 800xg for 5 minutes.

Following re-suspension in 20µl pre-cooled Lysis reagent, the cells were retropipetted three times, then incubated on ice for 30 minutes. Protein content was measured using a Bradford assay and 500ng of protein was removed from each sample for the PCR reaction (using 2x PCR mix provided with the kit). The TRAP reaction was carried out using a thermal cycler (Hybaid) to perform a combined primer elongation/amplification reaction.

Table 2.2. TRAP reaction protocol

	Time	Temp	Cycles
Primer elongation	30min	25°C	1
Telomerase inactivation	5min	94°C	1
Amplification:			30
Denaturation	30s	94°C	
Annealing	30s	50°C	
Polymerization	90s	72°C	
	10min	72°C	1
Hold		4°C	

Hybridisation and ELISA procedure:

5µl of the amplification product was added to 20µl of denaturation reagent per sample in an Eppendorf tube, and incubated at 15-25°C for 10 minutes. 225µl of hybridization buffer was added and mixed by vortex in each tube. 100µl from each tube was then transferred to pre-coated MP modules (Roche), and covered with a self-adhesive foil to prevent evaporation. Following incubation on a 300rpm shaker at 37°C for 2 hours, the hybridization solution was removed and the wells were rinsed in 200µl (per well) of washing buffer. The process was repeated 4 times before completely removing the washing buffer.

100µl of Anti-DIG-POD working solution was added to each well. Once again, the MP was covered with foil and incubated on a 300rpm shaker at 18-22°C for 30 minutes. The wells were washed 5 times x 30s with 200µl of the same washing buffer. 100µl room temperature TMB substrate solution was added to each well. These were incubated for colour

development, shaking very slowly either manually or on a shaker at 50 rpm at 15°C - 25°C for around 15 minutes. 100µl of stop reagent was added to each well immediately after incubation, causing the reacted POD substrate to change colour from blue to yellow, maximizing sensitivity. Each sample's absorbance level was measured within the following 30 minutes using the Omega spectrophotometer microplate reader (BMG Labtech) at 450nm.

2.2.12 Total RNA isolation and cDNA synthesis

Total RNA isolation

Cultured cells were added to 1ml cryopreservation medium, then cooled to -80°C. The samples were later removed and thawed quickly by rubbing the tubes. These were then centrifuged for 5 minutes at 800xg (SIGMA 1-14, 134744, Germany) and the supernatant removed. The cells were washed in 1ml PBS, then pelleted at 800xg for 5 minutes. The pellets were thoroughly mixed with 1ml of TRIzol (155966026, Life Technologies, USA) and incubated at room temperature for 5 minutes. 250µl chloroform was added to the TRIzol mixture and the tubes were shaken vigorously for 15 seconds, then incubated for a further 5 minutes at room temperature. The samples were spun down at 10,000 rpm for 5 minutes and three layers were formed as follows: top layer: clear-aqueous, interphase layer: white precipitated DNA and bottom layer: pink organic phase.

The top of clear-aqueous layer was carefully extracted to a fresh 1.5ml eppendorf tube using a 200µl pipette (leaving about \geq 1mm behind to avoid DNA contamination). Top layer containing RNA was mixed gently with 550µl isopropanol and incubated for 5 minutes at room temperature. The cells were pelleted at 14,800 rpm for 30 minutes and the isopropanol removed by pipette. The pellets were then washed over ice with 1ml of 75% ethanol (Sigma, 7023, USA) in distilled water (Gibco, DNase/RNase Free, 10977-035, UK)

This mixture was centrifuged for 5 minutes at 9500 rpm and the ethanol was aspirated. The samples were then returned to ice, and any remaining ethanol was evaporated by keeping tubes open. To accelerate the process, the RNA pellets were centrifuged again at high speed (14,800 rpm) for 30 seconds and a 10µl pipette was used to carefully aspirate the remaining ethanol. 20µl of distilled water was added and gently mixed with the RNA pellet. The total RNA concentration was determined using a Thermo Scientific NanoDrop spectrophotometer (8-sample spectrophotometer, ND-8000 UV/Vis, 0319, USA).

One drop (3 μ l) of distilled water was pipetted on to the 8-sample pedestal and this was cleaned using Whatman paper after the sampling arm was closed for few seconds. ND-8000-V2.2.1 was operated, then nucleic-acid standard method was chosen following preparation and a blank measurement. One drop of (the same buffer that was used to dilute the RNA pellet) distilled water (Gibco, DNase/RNase free, 10977-035, UK) was loaded to lower sample pedestal. The sample type was then switched from DNA-50 to RNA-40 after the sampling arm was closed. The blank was measured and stored with DNase/RNase free distilled water. Both sample pedestals were cleaned again using Whatman paper. The lower sample pedestals were loaded with 2 μ l RNA samples and were then activated from the computer program. RNA concentration measurement was chosen and result was recorded as ng/ μ l.

The quality of the RNA concentration at ratio of 260/280 was determined using the RNA wavelength (260nm) and protein wavelength (280nm). Following this measurement, the sampling arm was opened and both pedestals were cleaned with distilled water and Whatman paper. The RNA samples were cryopreserved at -80°C for further use.

cDNA synthesis

A High Capacity cDNA Reverse Transcription kit (Applied Biosystems AB, 4368814, USA) was used to synthesise the first strand of cDNA. Kit reagents and RNA samples were thawed on ice separately. 500ng of RNA was diluted in cold distilled water in individual PCR tubes at up to 10 μ l/reaction. This was followed by adding 10 μ l/reaction of 2X reverse transcription (RT) master mix to the same PCR tube.

The master mix was prepared as 2 μ l of 10X RT reverse transcription buffer (4319981); 0.8 μ l of 25X dNTP Mix (100mM, 4367381, AB, UK); 2 μ l of 10X RT reverse transcription random primers (4319979, AB, USA); and 1 μ l of MultiScribe Reverse Transcriptase (1312125, AB, USA), mixed with 4.2 μ l of cold distilled water. The mixture was placed on ice and mixed via pipette. The mixture was then centrifuged (Eppendorf, centrifuge 5810R, Germany) at maximum speed for 1 minute to spin down the mixture and expel air bubbles. It was then either placed on ice until needed or loaded directly onto a thermal cycler (SENSOQUEST, Labcycler, Germany), which was programed for 4 steps as follows: 10 minutes at 25°C; 120

minutes at 37°C; 5 minutes at 85°C; then incubated at 4°C, using infinity as a time unit. The first strand of cDNA was stored at -20°C until required for further use.

2.2.13 Quantitative Polymerase Chain Reaction (q-PCR)

TaqMan Gene expression (Applied Biosystems 4369016, US) approaches was used to test gene expression of synthesised cDNA. First strand cDNA was synthesised from total RNA. This was isolated, then stored at -80°C. cDNA tubes were thawed on ice and separated completely from the Master Mix primers, using TaqMan to avoid any contamination.

TaqMan procedure

1µl 20X TaqMan gene expression assay was mixed with 10µl 2X TaqMan gene expression master mix to create the TaqMan Master Mix, which was used for a single reaction and diluted in 5µl of DNase/RNase-free water (gibco, DNase/RNase free, 10977-035, UK). Each single reaction was triplicated and aliquoted to either 96- or 384-well reaction plates. 4µl cDNA was then pipetted per single reaction, after cDNA was diluted with DNase/RNase-free water to 30ng for each sample. Each plate was loaded to an appropriate Real-Time PCR machine (the 96-well plate was run at Applied Biosystems 7500 fast real-time PCR system and 384-well plate was run at Applied Biosystems QuantStudio 7 flex) and both machines applied a standard run. Three stages of thermal cycling were conducted as follows:

- 1) Hold for 2 minutes at 50°C
- 2) Hold for 10 minutes at 95°C
- 3) 40 cycles of 95°C for 15 seconds followed by 1 minute at 60°C

Rn18s was used as housekeeping gene primer and gene expression was quantified against the no activation cell group as control for activation group. The activation group was used as a control for the treated group.

Table 2.3. Different specificities of studied primers

Primers (TaqMan)	Sequence 5'-3' Forward – Reverse “Information is not released by the company”	Annealing temperature (°C)
Rn18s	Mm03928990_g1, 1341105	72
IL-2	Mm00434256_M1, 1328535	72
IFN-gamma	Mm01168134_M1, 1340467	72

2.2.14 Quantification of mouse regulatory T-cells

1×10^6 splenocytes were centrifuged at 300g for 10 minutes and the supernatant was aspirated. Cells were then resuspended in $1 \times 10^6/90 \mu\text{l}$ of buffer. $10 \mu\text{l}$ of CD4-FITC and CD25 antibody was added to the suspension and mixed well (FoxP3-APC, 130-094-164, MACS). Cells were incubated at 4°C for 10 minutes in the dark, then washed in 1ml of buffer per 1×10^6 cells and centrifuged at 300g for 5 minutes at 4°C and the supernatant aspirated. 1×10^6 cells were resuspended in cold, fresh Fixation/Permeabilization Solution then mixed well. Cells were incubated for 30 min in the dark at 4°C . Cells were washed in 1ml of cold buffer per 1×10^6 , then centrifuged at 300g for 5 min at 4°C and the supernatant aspirated. Cells were washed in 1x Permeabilization Buffer per 1×10^6 cells, then centrifuged at 300g for 5 min at 4°C and the supernatant aspirated. Cells were then resuspended in $80 \mu\text{l}$ of cold 1x Permeabilization buffer, mixed well and incubated for 5 min at 4°C . $10 \mu\text{l}$ of Anti-FoxP3 antibody was added to the cells, which were mixed well and incubated for 30 min in the dark at 4°C . Cells were then washed in 1ml of cold 1x Permeabilization buffer and centrifuged at 300g for 5 min at 4°C and the supernatant aspirated. A wash-only programme was then used, involving BD FACS Lyse/Wash Assistant (337146, USA). T-cell surface marker expression was measured and scored against negative controls. 50,000 live events were scored and analysed using compensated FACSCanto II using FACSDiva software.

2.2.15 Voluntary wheel running of mice and quantification of running parameters with Spike2 (7.12) software

The computer system of voluntary wheel running mice and the facilities combined with it were created by Dr. Bill Chaudhry and modified from the University of Oxford (De Bono et al., 2006). Each exercise cage was provided with a 37.8 cm diameter angled rotating running track (Lillico, Surry, UK), fixed to a greased steel axle attached to a plank. The running wheels were angled to allow them to fit inside the smaller cages. Two magnets were affixed to the wheel and there a sensor was fixed to the cage. This sensor connected to the Transducer (MICRO3, 1401, CED, Cambridge, UK) which simultaneously monitored the individual rotations of up to 44 wheels. This transducer was connected to the computer (Figure 2.11). Each magnetic detection was recorded as a ‘tick’ on the computer system and was analysed by Spike 2 Cambridge Electronic Design (CED) software, version 7.12 (072866). This system recorded and saved each 24 hour cycle in a separate file. From the baseline activity data, the running parameters can be calculated as the duration of time continuously spent running, with maximum 5 second intervals between recorded wheel rotations. The distance was calculated

from the total number of wheel rotations multiplied by the wheel diameter (37.8 cm). The average speed in each 24-hour cycle is calculated by dividing the total distance travelled by the total duration of running time. Maximum speed was calculated as the fastest upper 99th percentile of all wheel rotations during a 24-hour period. Mice, food, water and the recording computer system were observed and monitored daily. The steel axle was greased once/twice a week if necessary. Mice and food were weighed weekly, and the mice ran voluntarily on the running wheel. Some mouse groups on HFD, another group on ND as described at 2.2.1.4.

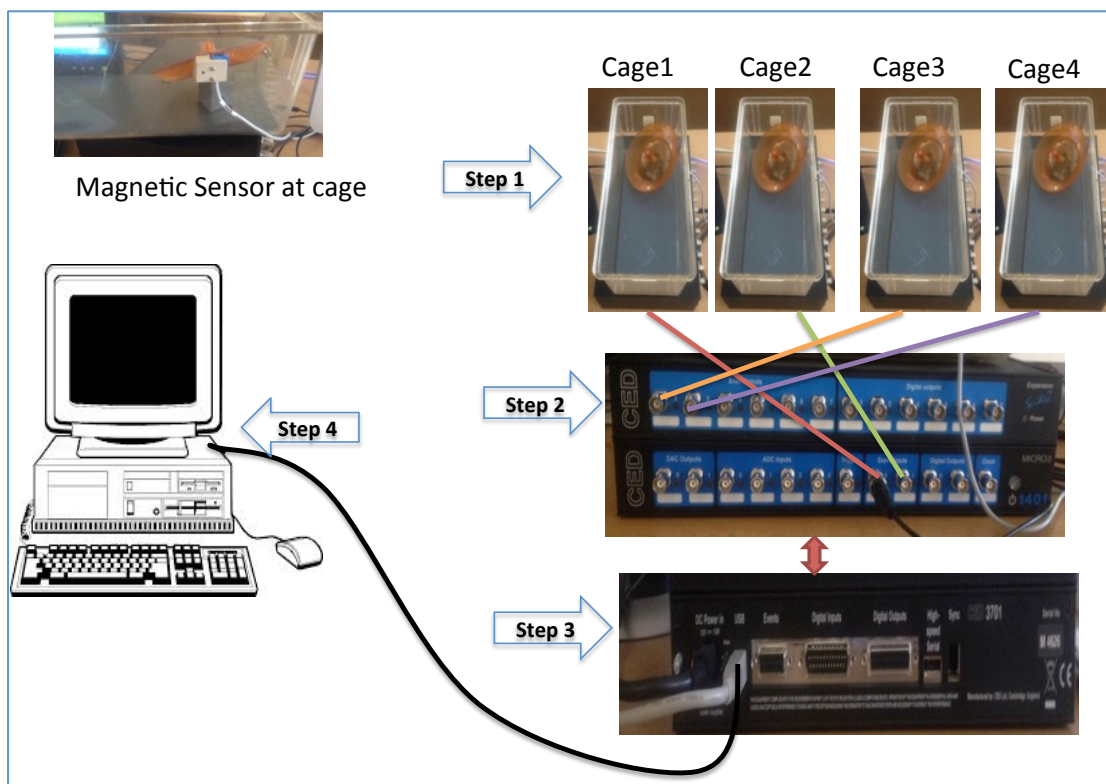


Figure 2.12. Illustration of the computer system for the mouse voluntary wheel running exercise

Step 1: Affix magnet to the outer wheel surface and the sensor on the outside of the cage, ensuring both are aligned for detection of the activity. **Step 2:** connect cages to the transducer, with each cage on a separate channel. **Step 3:** connect the transducer to the computer system. **Step 4:** computer system records the activity and analyses it using Spike 2 Cambridge Electronic Design (CED) software, version 7.12 (072866).

2.2.16 Patient recruitment, inclusion and exclusion criteria.

Ethical approval was granted by the National Research Ethics Service (NRES) North East Ethics Committee. NHS permissions were granted by the Newcastle University Hospitals NHS Trust (REC no: 15/EM/0072).

19 acute STEMI patients being treated with PPCI at the Freeman Hospital in Newcastle upon Tyne gave informed consent to take part in this study. Inclusion criteria were as follows: patients must be over 50 years old; they must have acute coronary syndrome (STEMI); they must be undergoing percutaneous coronary intervention (PCI) treatment; they must have blood samples taken within 24h of the PCI following the cardiac rehabilitation programme. Additionally, the coronary artery under investigation must be >3mm in diameter, and must be proximally occluded (TIMI flow grade 0-1) on admission, then reperfused (TIMI flow grade 2-3).

Exclusion criteria were as follows:

- 1) Immunological dysfunction (e.g. positive serology for HIV or hepatitis; acute or chronic inflammatory or neoplastic co-existing disease).
- 2) Haemodynamic instability, cardiogenic shock, unconsciousness.
- 3) Open (TIMI >1) culprit coronary artery during angiography.
- 4) Any other studies involving investigatory drugs within 30 days prior to this study.
- 5) Incapacity to consent verbally.
- 6) Non-cardiac condition resulting in life expectancy <1 year.

2.2.17 Accelerometer and GENEActive software for the analysis of daily activity in patients with myocardial infarction (MI)

An accelerometer (GENEActive) was used to objectively monitor each patient's daily physical activity. The device is waterproof, has a sampling frequency of 85.7Hz and measures in three dimensions (x, y and z axes), with a dynamic range of $\pm 8g$. The data are retained onboard, unfiltered on the MEMS chip. Acceleration is expressed in mg (where g = acceleration due to gravity = 9.81 m/s^2). The GENEActive and Actigraph accelerometers used in the NHANES survey (Troiano et al., 2014) were recently validated and strong agreement was found between the two devices measuring vector magnitude of wrist acceleration. Intra-class correlation was >0.95. Oxygen consumption variance was explained (>70%) across a range of activities and intensities (Hildebrand et al., 2014).

Each patient (with no contraindications, i.e. allergies to plastic or metal) was given the accelerometer (GeneActiv; Activiinsights Ltd., Kimbolton, Cambs, UK) twice; once at 24h after cardiac stent percutaneous coronary intervention (PCI) for 7 days (24-hour periods) consecutively, and once after 3 months of cardiac rehabilitation for the same amount of time. Accelerometers were fixed in the non-dominant hand and all accelerometers were sent back via pre-paid mail at the end of 7 days. Data was expressed in m/s² and the sample rate was 75Hz. Static periods were accounted for and corrected accordingly (Lukowics et al., 2004). The three raw signals (x, y, z) were used to calculate the Euclidian norm, or magnitude (-1g, negative numbers rounded to 0), which gave rise to the movement-related acceleration, expressed in milligrams (van Hees et al., 2013)

2.2.17.1 Accelerometer data processing and analysis

After the GENEActive software and accelerometer systems were set up, R-package (R Core Team, Vienna, Austria) was used to analyse the binary data, using GGIR software [<http://cran.r-project.org>] (van Hees et al., 2013) and was sent for further analysis at MOVELab (Newcastle University, Newcastle Upon Tyne, UK).

The average wrist acceleration magnitude (overall volume), time distribution across acceleration, and estimated time spent in 5 minute and 10 minute bouts of MVPA were used as summary measures. Detailed signal processing adhered to the following: verification of sensor calibration error using local gravity as a reference (van Hees et al., 2014) detection of sustained abnormally high values; non-wear detection; calculation of the vector magnitude of activity-related acceleration using the Euclidian Norm minus 1 g (ENMO: $\sqrt{x^2 + y^2 + z^2}$ - 1g) with any negative values rounded up to zero; exclusion of the first 10h and last 20h of the measurement (van Hees et al., 2013).

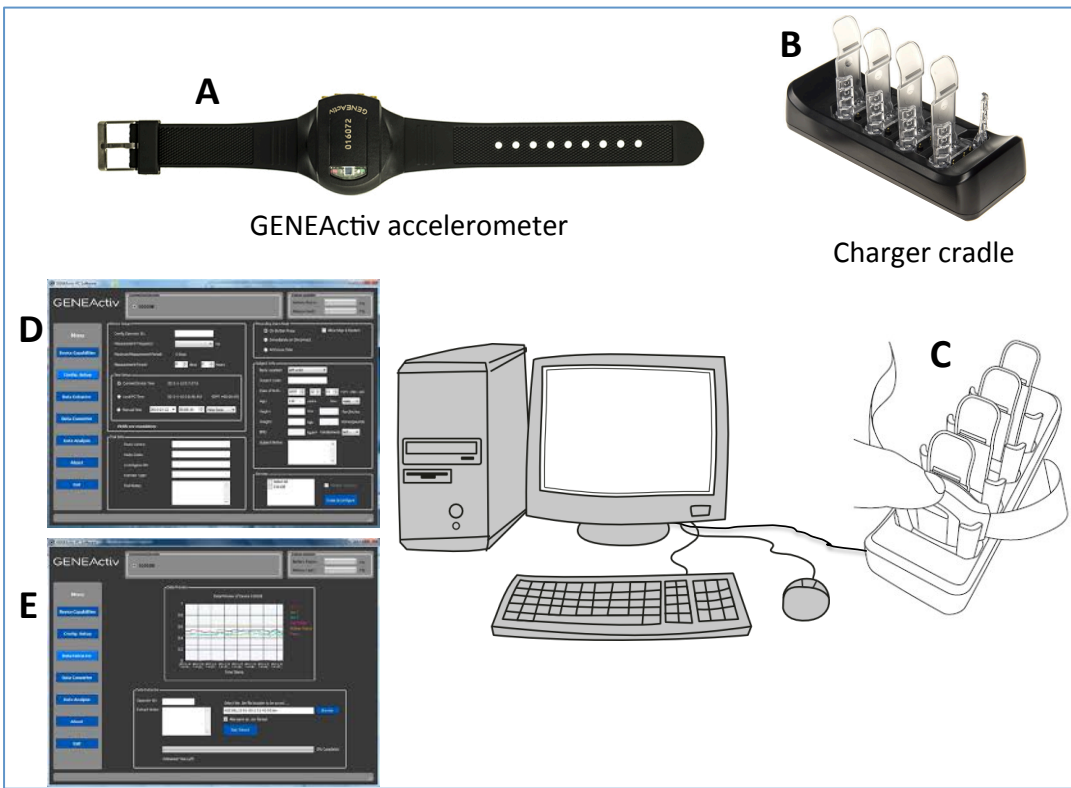


Figure 2.13. GENEActiv devices

A. GENEActiv accelerometer: given to participants to record and store daily physical activity. **B.** Charger cradle: used to connect the accelerometer to the computer system, **C.** The accelerometer is inserted into the cradle until a firm click is heard and the light flashes. **D.** GENEActiv software setup page, providing participant information (participant code, age, BMI, etc.), measurement frequency, time and recording start mode, etc. **E.** GENEActiv software data extraction page which shows a preview of the first few minutes of data collected and allows data to be downloaded to a chosen file location.

2.2.18 Cardiac rehabilitation programme

At the Freeman Hospital (Newcastle Upon Tyne, UK) all cardiac patients (15/EM/0072) went for cardiac rehabilitation, which was tailored according to the severity of each patient's condition and their need for recovery to normal daily activity and a productive life, to prevent further complications as per National Health Service (NHS) UK recommendations. Patients who participated in this study were diagnosed by a cardiologist with acute coronary syndrome (STEMI) and underwent percutaneous coronary intervention (PPCI). In accordance with NHS regulations, these patients underwent cardiac rehabilitation one week after myocardial infarction. In this study, we accepted any type of aerobic exercise as cardiac rehabilitation, but not as a strengthening exercise. There was variation in aerobic exercise between patients (table 2.4) and the exercise location differed between patients depending on where they live. The main goal here was to discover whether aerobic cardiac rehabilitation (for 3 months) had

an effect on telomerase activity, telomerase length and lymphocytes (immune cells), regardless of the type of aerobic exercise, duration of the session, location (place) of the exercise, and of the medical team who care for and observe the patient. The primary aim was to find out the potential benefit, and changes in clinical condition, after cardiac exercise rehabilitation vs. before cardiac exercise rehabilitation.

Table 2.4. Aerobic exercise types

Patient number	Type of Aerobic exercise	Rehabilitation centre
2	Walk and general activity	No
1	Walk and running	Yes
1	Walk and steps exercise	Yes
1	Stationary cycling	Yes
3	Aerobics classes	Yes

2.2.19 Human regulatory T-cells quantification

Whole fresh blood from patients with acute myocardial infarction (MI) was collected in 10ml heparinized vacutainer tubes 24-hours post-STEMI and 3 months post-heart attack. 100 μ l was transferred to a FACS tube (FALCON, 352054, Mexico) with two controls (Isotype control-PE and FMO-CD25 control, BD). All samples were incubated in the dark at room temperature for 20 minutes with 5 μ l anti-CD4-V500, 20 μ l anti-CD3-PerCP, BD. The test tube and isotype control tubes used 20 μ l anti-CD25-APC, whilst the control tube did not. Lysing solution: Pharm Lyse (BD, Pharm Lyse, 555899) was diluted 1:10 with water (Sigma, 7732-18-5), then 1ml of the diluted lysing reagent was added to all tubes. This was incubated for 15 minutes at room temperature in the dark. Lysing mixture was washed with 2ml/tube of 5% FBS (PAA, A15 151) in PBS, pH 7.4, then centrifuged at 500xg for 5 minutes and the supernatant was removed. The washing step was repeated and the pellet was gently resuspended in residual wash buffer. 2ml of human FoxP3 buffer A (BD, 560098), diluted 1:10 with (room temperature) water (Sigma, 7732-18-5), was added to cells and vortexed and then incubated for 10 minutes at room temperature in the dark. This was centrifuged at 500xg for 5 minutes and the fixative was removed gently by pipette. The pellet was then rinsed in 2ml 5% FBS in PBS and centrifuged for a further 5 minutes at 500xg. The supernatant was aspirated and the pellet was gently resuspended in residual wash buffer. Diluted Human FoxP3 buffer B (BD, 51-9005450) was mixed with diluted Human FoxP3 buffer A at ratio of 1:50 to create Human FoxP3 buffer C. 0.5ml of this was added to the cells to permeabilise them. This mixture was

incubated for 30 minutes at room temperature in the dark. The permeabilising mixture was washed with 2ml/tube of 5% FBS/PBS, pH 7.4, then centrifuged at 500xg for 5 minutes and the supernatant removed. The washing step was repeated.

20 μ l FoxP3-PE (BD, 560046) was added to test tube and FMO-CD25 control, whilst 20 μ l PE Mouse IgG1k Isotype Control (BD, 556027) was added to the Isotype control-PE tube. All tubes were gently shaken by vortex and incubated for 30 minutes at room temperature in the dark. Cells were then washed, using a wash only programme, using BD FACS Lyse/Wash Assistant (337146, USA). Expression of regulatory T-cell surface markers was scored against two negative controls. One tube was stained without CD25-APC and another tube stained with PE Mouse IgG1k Isotype Control instead of FoxP3. Compensated FACSCanto II utilising FACSDiva software was used. 30,000 CD3 $^{+}$ /CD4 $^{+}$ live events were scored for analysis.

Table 2.5. Antibodies and reagents used with human regulatory T-cells

Reagent	Source	Quantity (μ l)
CD3-PerCP	BD, 345766	20
CD4-V500	BD, 560768	20
CD25-APC	BD, 555434	5
FoxP3-PE	BD, 560046	20
PE Mouse IgG1k Isotype Control	BD, 556027	20
Human FoxP3 Buffer Set	BD, 560098	See above description
Lysing Buffer	BD, 555899	See above description

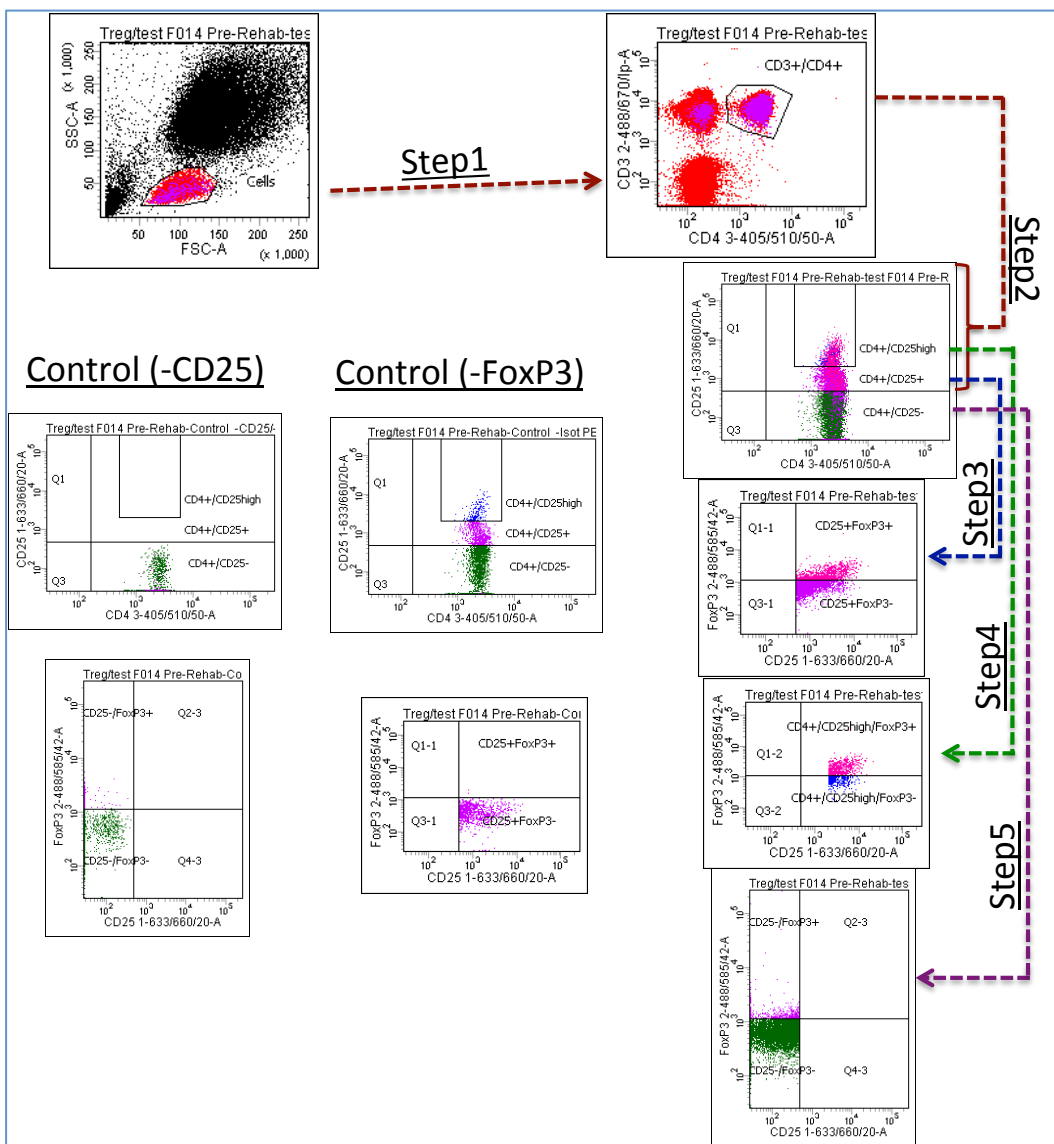


Figure 2.14. FACS gating strategy for human regulatory T-cells quantification

Step 1: After gating and determining the lymphocyte population (cells), $CD4^+$ T-lymphocytes ($CD3^+/CD4^+$) was gated. **Step 2:** $CD4^+CD25^+$ cells were determined from $CD4^+$ population. **Step 3:** $CD25^+FoxP3^+$ cells were determined from $CD4^+CD25^+$ population. **Step 4:** $CD4^+CD25^{+high}FoxP3^+$ cells were determined from $CD4^+CD25^{+high}$ population. **Step 5:** $CD25^-FoxP3^+$ cells were determined from $CD4^+CD25^-$ population. Two controls (-CD25 and -FoxP3) were used to quantify the Tregs.

2.2.20 Human whole blood TruCount

50 μ l of complete blood was placed in the centre of the TruCount tube by electronic reversal pipette. 10 μ l of BD Multitest 6-color (TBNK, 337166, BD) was added to a blood sample and mixed well by gently vortexing. The mixture was incubated at room temperature for 25 minutes in the dark. 1ml of (1:10) lysing buffer (555899, BD) was added to the blood mixture and incubated for 15 minutes at room temperature in the dark. The tube was then placed on a roller (SRT6, Stuart, UK) at room temperature in the dark for 5 minutes. The BD FACSCanto II software for TruCount was set up, using 7-color setup beads (BD, 335775). 500 μ l of Bead

diluent (BD FACS 7-colour setup B, Bead Diluent, 336565) was added to the 7-colour setup beads tube and mixed well by gentle vortex. This tube was run in FACSCanto II software to setup the system. When the setting passed, the sample tube was run and TruCount cells were calculated by software system.

2.2.21 Telomere length determination in human PBMNCs

The assay was performed by the Biomarker lab of the Institute of Neurosciences at the Campus for Ageing and Vitality, Newcastle University, using splenocytes that I had prepared.

The QiaAmp DNA mini Kit (QIAGEN, Hilden, Germany) was used to extract DNA from the PBMC. Quality and concentration was established using NanoDrop (ThermoScientific). Using a modified method, similar to that described by Martin-Ruiz et al., 2005, based on the abundance of telomeric template, telomere length was compared to a single copy gene (36B4), using the following primers: TelA (5' CGG TTT GTT TGG GTT TGG GTT TGG GTT TGG GTT TGG 3'); TelB (5' GGC TTG CCT TAC CCT TAC CCT TAC CCT TAC CCT TAC CCT TAC CCT CCT 3'); 36B4F (5' CAG CAA GTG GGA AGG TGT AAT CC 3') and 36B4R (5' CCC ATT CTA TCA TCA ACG GGT ACA A 3'). Plate-to-plate variation was accounted for by using three internal control DNA samples, whose telomere length was already known (10.4 kb, 3.9 kb and 2 kb), and each measurement was carried out three times, using an Applied Biosystems 7900HT Fast Real Time PCR system with 384-well capacity. The intra-assay variation coefficient was 2.7% (Martin-Ruiz et al., 2005).

2.2.22 Statistical analysis

Graphs from all test results were produced using GraphPad Prism version 6.0. All data are displayed as mean \pm standard error of the mean (sem) except where otherwise stated. A p-value of < 0.05 was considered statistically significant. The paired T-test and nonparametric tests (two-tailed), followed by the Wilcoxon matched-pairs signed rank test (confidence level of 95%) were used to compare two matching groups with one different parameter. An unpaired T-test and nonparametric test (two-tailed), followed by the Mann-Whitney test were used to compare two non-matching groups with one different parameter at a confidence level of 95%. Multiple groups, differing in just one parameter were compared using one-way ANOVA and Dunnett's test as post-hoc test. Multiple groups with two different parameters, represented at different time points, were compared using the two-way ANOVA, multiple comparisons, followed by a Tukey test. All n-numbers indicated for the different experiments (*in vitro* or *in vivo*) are independent biological repeats, either mice or cells derived from independent mice.

CHAPTER 3. Effect of mild chronic oxidative stress on proliferation and regulation of telomerase in splenocytes and CD4⁺ T-lymphocytes

3.1 Introduction

Atherosclerosis is a cardiovascular disease characterized by chronic inflammation and oxidative stress. Chronic oxidative stress has been implicated in atherosclerotic plaques and endothelial dysfunction that contributes to vascular inflammation (Guzik et al., 2006; Heitzer et al., 2001). Oxidative stress was found to enhance atherogenesis in the vascular wall, which may lead to inflammation or myocardial infarction (Sorescu et al., 2002).

Lymphocytes play an important role in atherosclerosis but its mechanisms are complicated, as some subsets accelerate atherosclerosis, whilst others are atheroprotective. Th1, Th2, Th17 and Tregs are the subset of CD4⁺ cells. CD4⁺ with CD8⁺ are components of T lymphocytes. From a population of T lymphocytes, CD4⁺ cells have a contradictory role with atherosclerosis, as Th1 secretes IFN- γ cytokines, which are proatherogenic (Frostegård et al., 1999). Th2 cells are associated with recovery from myocardial infarction (Frostegård et al., 1999; Engelbertsen et al., 2013). Recently, the study of B cells has identified a controversial role with atherosclerosis. B cells are of two main types: B1 and B2 (Ait-Oufella et al., 2010). B1 cells were classified as atheroprotective, secondary to the natural IgM antibodies produced (Perry et al., 2013; Chou et al., 2008). Some studies indicate that B2 cells are also atheroprotective (Caligiuri et al., 2002; Doran et al., 2012), whilst others argue that B2 cells are proatherogenic (Ait-Oufella et al., 2010; Kyaw et al., 2010).

3.2 Results

3.2.1 Hyperoxia induces oxidative stress and inflammation in lymphocytes

3.2.1.1 Hyperoxia induces oxidative stress in splenocytes and CD4⁺ T-cells

To study the effect of oxidative stress on cells, a 40% O₂ saturation level (hyperoxia) was chosen to create an oxidative stress environment in the culture. In order to analyse the level of ROS, oxidative stress was measured using dihydroethidium (DHE). DHE is cell-permeable and reacts with O₂⁻ to create ethidium, which exhibits red fluorescence when it binds to nuclear DNA (Benov et al., 1998; Zhao et al., 2003). Cells were cultured (tert^{+/+} and tert^{-/-} splenocytes for \geq 20 days and CD4⁺ T-cells for 10 days), then stained with DHE as described at (2.2.10).

40% oxygen saturation (hyperoxia) produced significant (P<0.01) oxidative stress in both genotypes, Tert^{+/+} and Tert^{-/-} (figure 3.1A), compared to Tert^{+/+} hypoxia (3% O₂). There were no significant changes between 3% O₂ Tert^{+/+} vs. 3% O₂ Tert^{-/-}. The cell genotype also has no effect on oxidative stress. 40% O₂ produced significantly (P<0.05) greater oxidative stress with Tert^{+/+} CD4⁺ T-cell (figure 3.1B), compared to Tert^{+/+} 3% O₂. Finally, Hyperoxia (40% O₂) saturation is an in-vitro model to increase oxidative stress.

3.2.1.2 The effect of hyperoxia on mitochondrial membrane potential levels in splenocytes and CD4⁺ T-cells

As found in the previous experiment, hyperoxia (40% O₂ saturation) increased oxidative stress *in vitro*, highlighting the importance of mitochondria as its dysfunction leads to increased oxidative stress (Dexter et al., 1989; Zhang et al., 1999). Mitochondria are ordinarily associated with cellular energy production, but also serve functions beyond this role. Mitochondrial membrane potential measurements have indicated a role in both normal cell function and cell death (Škárka and Oštádal, 2002; Adams et al., 2000). Oxidative stress can be controlled *in vitro*. In human fibroblasts, increasing oxidative stress accelerates telomere shortening in replicating DNA, whereas decreasing oxidative stress has the opposite effect, resulting in an increased cell lifespan (von Zglinicki et al., 1995; Saretzki et al., 2003). Induction of telomere damage results in mitochondrial dysfunction and consequently senescence within a dividing cellular population (Passos et al., 2007; Saretzki, 2009).

This experiment was therefore designed to establish the extent to which mitochondrial function under ROS production may affect cell proliferation. The JC-1 fluorescence ratio was used to measure the mitochondrial membrane potential levels as described at (2.2.10). These properties are important because the physiological function of the respiratory chain ATP relies on mitochondrial membrane potential (Joshi and Bakowska, 2011).

Splenocytes from either wild-type $\text{Tert}^{+/+}$ or $\text{Tert}^{-/-}$ mice were cultured for ≥ 20 days and CD4^+ T cells from $\text{Tert}^{+/+}$ (wild-type) mice were cultured for 10 days. Figure 3.2A shows no significant effect of the increased oxidative stress in this experiment on mitochondrial membrane potential levels for both genotypes. The same result was found with $\text{tert}^{+/+}$ CD4^+ T-cells (figure 3.2B). In conclusion, oxidative stress produced secondary to 40% oxygen saturation does not seem to be associated with mitochondrial membrane potential levels in splenocytes and CD4^+ T lymphocytes.

3.2.1.3 Oxidative stress produces inflammation in mice splenocytes

An imbalance between free radical production, reactive metabolites, oxidants and antioxidants is known as ‘oxidative stress’, which may cause damage to biomolecules, cells, and potentially an entire organism (Duracková, 2008). Oxidative stress, among other factors, including biological, chemical and physical, may cause chronic inflammation (Bartsch and Nair, 2006). $\text{IFN-}\gamma$ is a key proatherogenic cytokine, expressed in arterial plaques during inflammation (Frostegård et al., 1999).

The goal for this experiment was to establish whether oxidative stress caused by hyperoxia (40% O_2 saturation) leads to inflammation, by measuring transcription of $\text{IFN-}\gamma$. Splenocytes were cultured for 3 days, then $\text{IFN-}\gamma$ transcription was measured by RT-PCR at day 1, 2 and 3, as described at (2.2.13).

Figure 3.3 shows that the $\text{IFN-}\gamma$ mRNA transcription declined between day one and day three under hypoxia (3% O_2 saturation), whereas it increased under hyperoxia (40% O_2 saturation). At day 3, there was a significant ($P<0.05$) difference in the level of $\text{IFN-}\gamma$ mRNA transcription between 3% and 40% O_2 saturation, with the hyperoxic condition yielding a 15.3-fold increase. From this we can conclude that the oxidative stress produced under hyperoxia also induces inflammation. 40% oxygen saturation (hyperoxia) provides a suitable *in vitro* model to produce inflammation. Furthermore, it seems that 3% oxygen saturation also initially induces inflammation, but it is reduced by day 3, while under 40% oxygen saturation the inflammation response seems to remain constant.

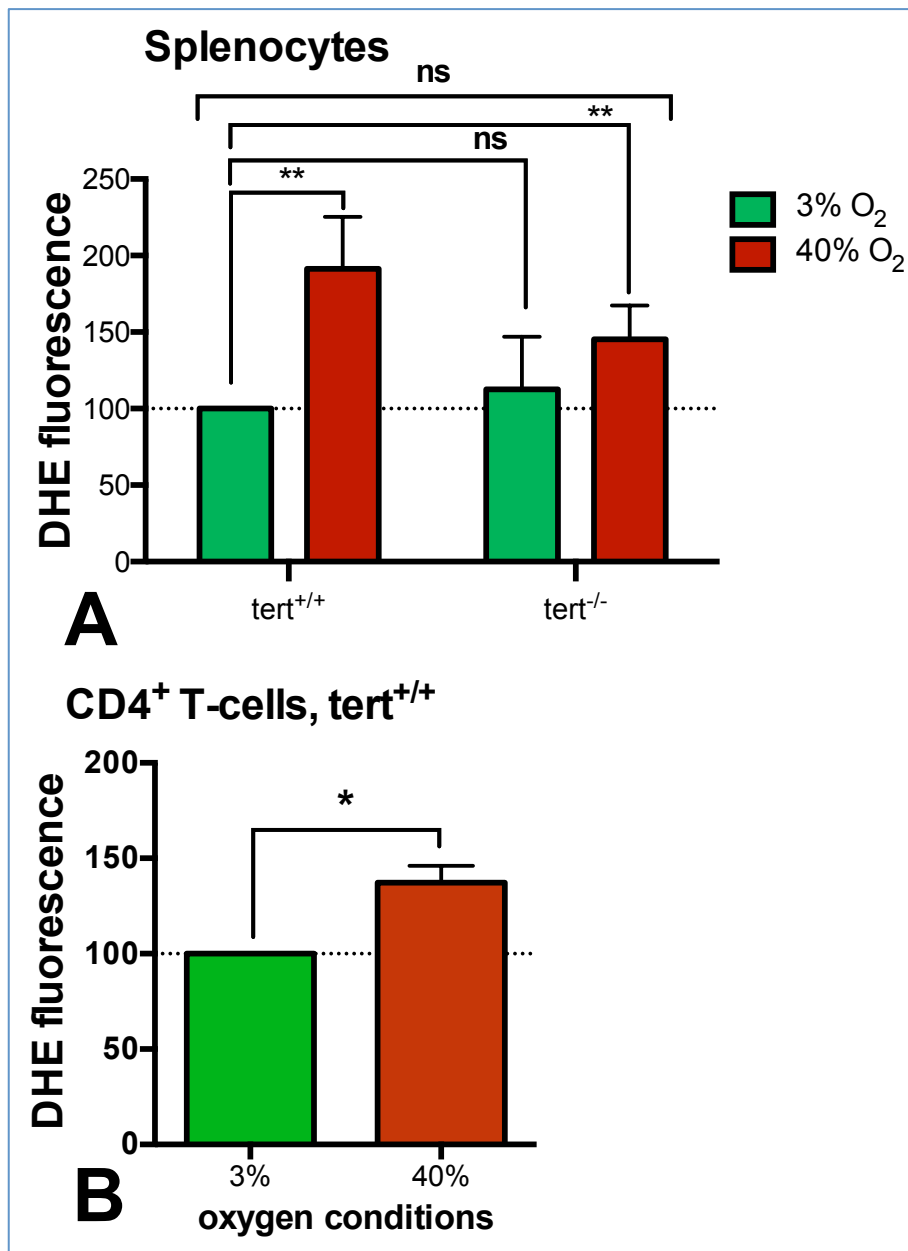
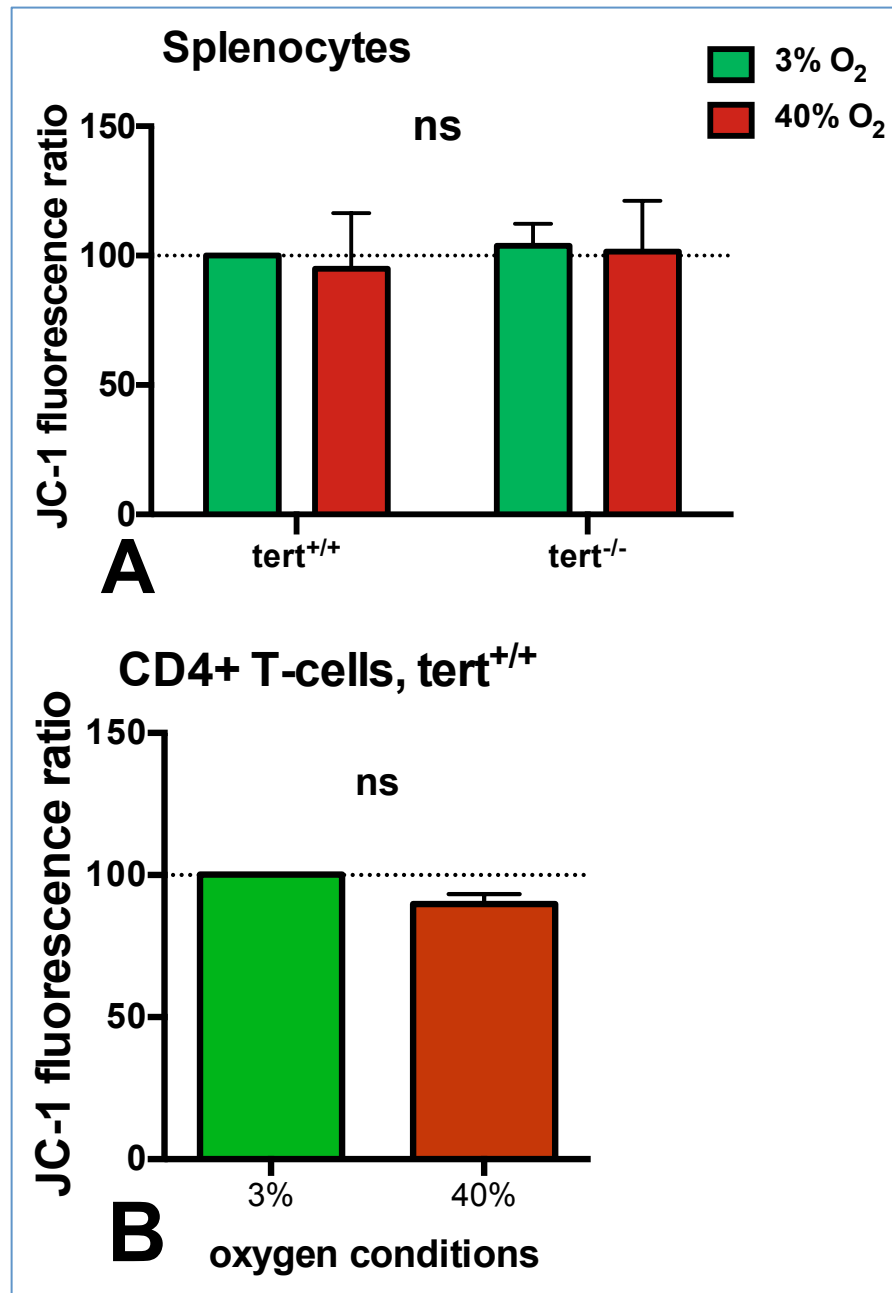


Figure 3.1. Oxidative stress levels as measured by dihydroethidium (DHE) fluorescence.

A-B. Plates were coated with anti-CD3 and anti-CD28 antibodies (prepared at 1 μ l/ml PBS). Medium was changed and 1.5 μ g/ml IL-2 was added every 2-3 days for all experiments. Cells were cultured under 3% and 40% oxygen saturation. **A.** Splenocytes from either Tert^{+/+} or Tert^{-/-} mice were seeded at 2 \times 10⁶/ml in a 24-well plate. Splenocytes were cultured for \geq 20 days (n=4). **B.** CD4⁺ T cells from wild-type (Tert^{+/+}) mice were seeded at 2 \times 10⁵ cells/well (volume = 200 μ l/well) in a 96-well plate. CD4⁺ T-cells were generated by immunomagnetic bead-isolation from splenocytes and cultured for 10 days (n=3). TERT^{+/+} under 3% O₂ was used as 100%. All values are displayed as mean \pm sem. *P<0.05, **P<0.01 for comparison between oxygen saturation levels using 2-way ANOVA for **A**, and two-tailed unpaired t test for **B**.



A-B. Plates were coated with anti-CD3 and anti-CD28 antibodies (prepared at 1 μ l/ml PBS). Medium was changed and 1.5 μ g/ml IL-2 was added every 2-3 days for all experiments. Cells were cultured under 3% and 40% oxygen saturation.

A. Splenocytes from either wild-type Tert^{+/+} or Tert^{-/-} mice were seeded at 2 \times 10⁶/ml in a 24-well plate. Splenocytes were cultured for \geq 20 days (n=4). **B.** CD4⁺ T cells from wild-type (Tert^{+/+}) mice were seeded at 2 \times 10⁵ cells/well (volume = 200 μ l/well) in a 96-well plate. CD4⁺ T-cells were generated by immunomagnetic bead-isolation from splenocytes and cultured for 10 days (n=3). All values are displayed as mean \pm sem. (ns) no significant for comparison between oxygen saturation levels using 2-way ANOVA for **A**, and two-tailed unpaired t test for **B**.

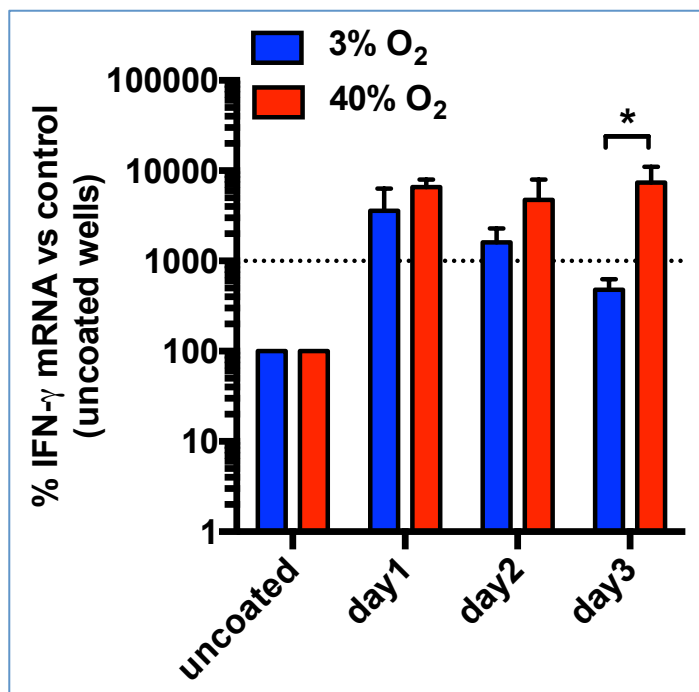


Figure 3.3. Oxidative stress enhances transcription of IFN-gamma mRNA.

Splenocytes from wild-type (*Tert*^{+/+}) mice were seeded at 2×10^6 /ml in a 24-well plate. Splenocytes were cultured for 3 days. Plates were coated with anti-CD3 and anti-CD28 antibodies. Control cells grew on uncoated wells. Cells were cultured under 3% (hypoxia) and 40% (hyperoxia) oxygen saturation. All values are displayed as mean \pm sem (n=3). *P<0.05 for comparison between oxygen saturation levels using two-tailed unpaired t test.

3.2.2 Hyperoxia suppresses splenocyte proliferation by a telomerase dependent mechanism

3.2.2.1 Effects of telomerase and oxidative stress on splenocyte proliferation

Having confirmed that hyperoxia leads to increased oxidative stress (Figure 3.1) and inflammation, I next sought to investigate how this affects the proliferation of lymphocytes. In order to test this I used a hyperoxic 40% oxygen saturation and compared this to 3% oxygen saturation. Mouse splenocytes were cultured and T-cells specifically activated with anti-CD3e/anti-CD28 micro-beads. As shown in figure 3.4, splenocytes proliferated under 3% oxygen saturation from 2×10^6 /well on day zero to $55.7 \pm 4.6 \times 10^6$ /well after 28 days. Interestingly, under hyperoxic conditions cell proliferation was diminished significantly, resulting in $38.4 \pm 0.73 \times 10^6$ /well after 28 days ($P < 0.0001$).

Telomerase has been shown play a crucial role in cell proliferation (Martin-Rivera et al., 1998), especially in lymphocytes (Buchkovich and Greider, 1996). To investigate the role of telomerase in oxygen dependent inhibition of proliferation, I isolated splenocytes from telomerase deficient mice ($\text{TERT}^{-/-}$). As expected, $\text{TERT}^{-/-}$ cells proliferated almost 2.4-fold less under 3% oxygen saturation compared to $\text{TERT}^{+/+}$ cells ($22.9 \pm 4.2 \times 10^6$ /well vs. $55.7 \pm 4.6 \times 10^6$ /well, respectively, $P < 0.0001$) (Figure 3.4). Surprisingly, there was no further decrease in proliferation under 40% oxygen saturation in the $\text{TERT}^{-/-}$ cells, as present in $\text{TERT}^{+/+}$ cells, suggesting that the effect of hyperoxia and oxidative stress on T-cell proliferation is dependent on telomerase.

Altogether, $\text{TERT}^{+/+}$ splenocytes showed maximal proliferation under 3% O_2 culture condition, expanding about 30-fold over 28 days. $\text{TERT}^{-/-}$ splenocytes only expanded 10-fold over the same time period. Surprisingly, this was independent of oxygen conditions, suggesting that the effect of hyperoxia on cell growth is telomerase or at least TERT -dependent. This experiment also confirmed that T-lymphocytes can proliferate without the presence of telomerase.

3.2.2.2 Effect of telomerase and oxidative stress on proliferation of different splenocyte subsets

Splenocytes consist of a range of different cell populations with different roles and immune functions. These include T-cells, B-cells and monocytes. In the previous experiment (Figure 3.4), splenocytes were expanded in culture and their proliferation monitored. Now I aimed to find out whether there are differences in proliferation between cell types, especially when

only T-cells (CD4⁺ and CD8⁺ cells) were activated. This experiment was designed to study the proliferation behaviour of a subpopulation of T-cells and also to discover the effect of T-cell activation on other splenocyte subsets.

Although the previous experiment (Figure. 3.4) showed that hyperoxia had a suppressive effect on activated splenocytes, I wanted to know whether this effect was directed at a specific subpopulation of splenocytes. Since mouse splenocytes consist mainly of B-lymphocytes, T-lymphocytes and monocytes, I used specific antibodies and flow cytometry to identify which population was affected. Activation of splenocytes with anti-CD3/CD28 antibody leads primarily to proliferation of CD4⁺ T-lymphocytes (from $0.08\pm0.004\times10^6/\text{well}$ to $20.5\pm2.4\times10^6/\text{well}$, a 267-fold increase over 2 weeks ($P<0.0001$), under 3% oxygen saturation and to $11.75\pm1.4\times10^6/\text{well}$ under hyperoxia (40% oxygen saturation), $P<0.01$, (Figure 3.5A). A significant increase in cell number was observed from day 7 ($P<0.05$) 3% $O_2 = 5.5\pm0.72\times10^6/\text{well}$ vs. 40% $O_2 = 2.3\pm0.12\times10^6/\text{well}$ and again at day 10, $11.6\pm1.3\times10^6/\text{well}$ under 3% O_2 vs. $5.8\pm1.3\times10^6/\text{well}$ under 40% O_2 ($P<0.001$). Furthermore, there was a trend for increase – although this did not reach statistical significance (ns) - between 3% and 40% oxygen saturation which started from day 5 ($2.5\pm0.72\times10^6/\text{well}$ vs. $0.98\pm0.36\times10^6/\text{well}$). From this, we can conclude that with time, an interaction between cells presumably by secreted cytokines leads to an increase in cell proliferation. CD8⁺ T-cells (Figure 3.5B) proliferate less than CD4⁺ T-cells, also without significant difference in proliferation between 3% and 40% (hyperoxia) oxygen saturation.

However, CD8⁺ T-cells (Figure 3.5B) are cytotoxic and require a pathogen in order to be activated, whilst CD4⁺ T-cells are helper cells which stimulate other cells to carry out their function. Consequently, CD4⁺ T-cells proliferate more.

Double positive (DP), CD4⁺CD8⁺ T-cells, (Figure 3.5 C) proliferate under 3% oxygen saturation 0.62-fold more than under 40% oxygen saturation 0.07-fold (ns). Double negative (DN) proliferated significantly ($P<0.01$) more under hyperoxia 8.5-fold vs. 3.2-fold under hypoxia (Figure 3.5D).

B-lymphocytes (Figure 3.5 E) and monocytes (Figure 3.5 F) proliferated as well, but also, like CD8⁺ cells, to a far lesser degree than CD4⁺ (1.09-fold for B-cells and 1.04-fold for monocytes, both in favour of 3% oxygen saturation). Interestingly, hyperoxia only affected proliferation of CD4⁺ T-cells, but not monocytes or B-lymphocytes. In summary, I found that hyperoxia suppressed CD4⁺ T-cell proliferation.

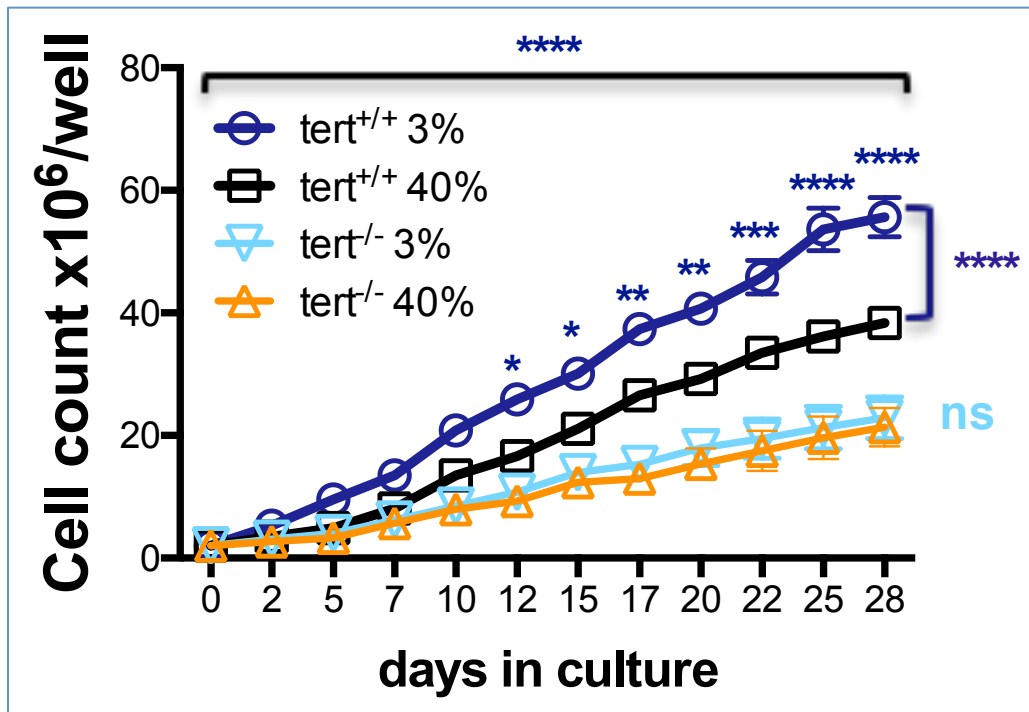


Figure 3.4. Proliferation of splenocytes depends on the level of oxygen saturation and the presence of telomerase (TERT)

Splenocytes from Tert^{+/+} and Tert^{-/-} mice were seeded at 2x10⁶/well (volume = 2ml/well) in a 24-well plate. Medium was changed and 1.5µg/ml IL-2 was added every 2-3 days for all experiments. T lymphocytes were re-activated every 7 days (days 0, 7, 14, and 21 if necessary) by adding CD3e/CD28-Biotin micro-beads at a 1:1 ratio (Miltenyi T-cell expansion kit). Cells were cultured either under 3% oxygen saturation or under 40% (hyperoxia) oxygen saturation. Growth curves were generated by counting a 10µl aliquot of cells in the Neubauer chamber. All values are displayed as mean±sem (n=4 Tert^{+/+} and n=3 Tert^{-/-}). *P<0.05, **P<0.01, ***P<0.001, ****P<0.0001 for comparison between 3% vs. 40% oxygen saturation using 2-way ANOVA.

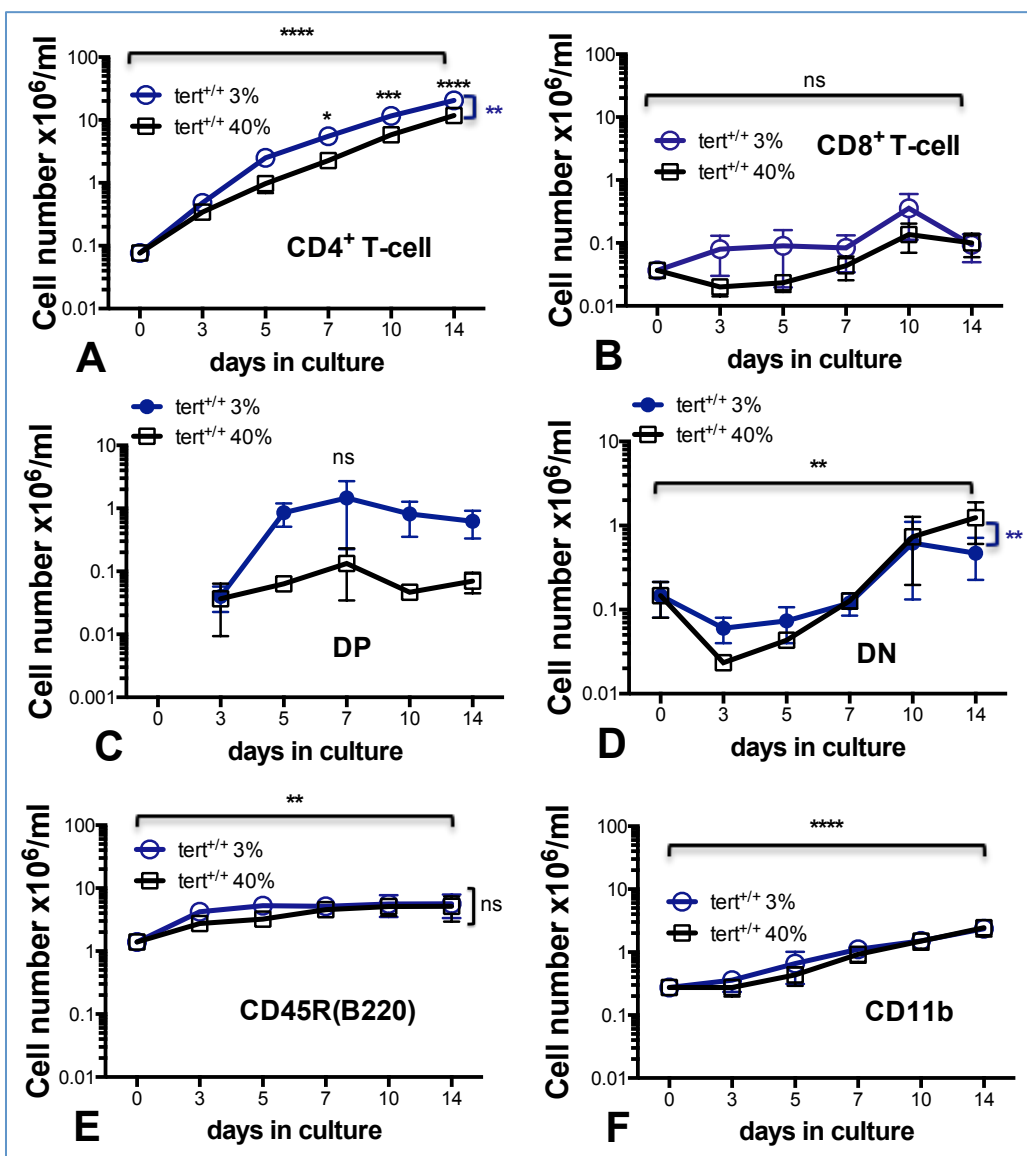


Figure 3.5. Long-term culture and growth curves of different splenocyte subpopulations under different oxygen saturation levels with strong activation

Wild-type splenocytes were seeded at 2×10^6 cells/ml in a 24-well plate. Cells were cultured over 14 days using anti-CD3 and anti-CD28 antibodies; $1.5\mu\text{g}/\text{ml}$ IL-2 was added and media was changed every 2-3 days, under 3% and 40% (hyperoxia) O_2 . At each time point of this experiment (0h, d3, d5, d7, d10, d14), cells were stained for CD45R, Cd11b, CD4 T-cells and CD8 T-cells to determine the proportions of each cell type in the sample. **A:** total CD4⁺ T-cells number/splenocytes, **B:** total CD8⁺ T-cell number/splenocytes, **C:** DP T-cells number/splenocytes, **D:** DN cells/splenocytes, **E:** total B-cells number/splenocytes, and **F:** total monocytes number/splenocytes. All values are displayed as mean \pm SEM ($n=3$). * $P<0.05$, ** $P<0.01$, *** $P<0.001$, **** $P<0.0001$ for comparison between 3% vs. 40% oxygen saturation using 2-way ANOVA.

3.2.3 Role of telomerase in CD4⁺ T-cell proliferation

In this subchapter my aim was to understand the contribution of telomerase to proliferation of T-lymphocytes at under 3% and at 40% (hyperoxia) oxygen saturation.

The previous experiment (Figure 3.5) suggested that the interaction between CD4⁺ T-cells, CD8⁺ T-cells, B-cells and monocytes plays an important role in cell proliferation and survival. This was particularly the case for B-cells and monocytes, which proliferate and survive similarly under both oxygen saturations (3% and 40%). This could be explained by the effect of cytokines, secreted by other splenocytes (Th2 cells secrete IL-4, which activate B-cells; Th1 cells secrete IL-2 and IFN-gamma, which activate monocytes. IFN-gamma also activates B-cells, and B-cells secrete TGF-beta and IL-4, activating Th1 cells and monocytes).

I noticed that CD4⁺ T-cells proliferated more strongly than CD8⁺ T-cells in spite of similarities in cell receptors, activation and conditions. The reason for this difference might be that CD8⁺ T-cells respond less to T-cell receptor ligation compared to antigen-stimulation, however, the latter was not used in my experiment. In contrast, CD4⁺ T-cells can be activated by ligation of their CD3 and CD28 T-cell receptor and co-receptor. This raised the question how CD4⁺ T-cells would react under the same stimulation and oxygen concentration, provided they would be cultured on their own. To answer this question, the following experiment was undertaken.

Splenocytes (Tert^{+/+} and Tert^{-/-}) were expanded for 2 weeks under 3% oxygen saturation, as this yielded the highest proliferation rate, which also correlates to the highest telomerase activity. Cells were harvested on day 14, then purified through a magnetic separator. 2 x 10⁵/well CD4⁺ T-cells were cultured in a 96-well plate for 20 days under hypoxia (3% oxygen saturation) and hyperoxia (40% oxygen saturation). I found (Figure 3.6) that CD4⁺ (Tert^{+/+}) T-cells proliferated strongly under 3% O₂ culture conditions (P<0.0001), but not hyperoxic conditions (at day 20, cell numbers reached 3.5±0.11 x 10⁶/well and 2.1±0.18 x 10⁶/well respectively, from 2 x 10⁵/well at day zero).

To investigate the effect of TERT on CD4⁺ T-cell proliferation, TERT^{-/-} mouse cells were used under the same conditions and treatment. As figure 3.6 shows, there was proliferation independent of telomerase for Tert^{-/-} CD4⁺ T-cells from 2 x 10⁵/well to 1.47 x 10⁶/well and 1.3 x 10⁶/well at day 20 (ns) under 3% and 40% oxygen saturation. However, these increasing cell numbers were unaffected by 3% O₂ or 40% (hyperoxia) O₂, which was similar to whole

splenocytes TERT^{-/-} (Figure 3.4). This result suggests that telomerase mainly plays a role in cell proliferation in either isolated CD4+ cells or whole splenocytes. I also noticed that the TERT^{+/+} CD4⁺ T-cells seemed to require interaction with other cells for proliferation, because all splenocytes (figure 3.4) increased in number under 40% oxygen saturation after day 10, compared to TERT^{-/-} under both conditions (Tert^{+/+} 40% = 13.5×10^6 /well, Tert^{-/-} with 3% O₂= 8.5×10^6 /well, TERT^{-/-} with 40% O₂= 7.97×10^6 /well (ns) at day 10).

The trend for cell numbers in this experiment at day 17 was: Tert^{+/+} with 40% O₂ = 1.7×10^6 /well; Tert^{-/-} with 3% O₂ = 1.3×10^6 /well; and Tert^{-/-} with 40% O₂ = 1.3×10^6 /well. All are not significant except Tert^{+/+} with 40% O₂ vs. Tert^{-/-} with 40% O₂ in which telomerase had a significant effect (P<0.05) on cell proliferation under hyperoxia (40% oxygen saturation). Furthermore, in Tert^{-/-}, oxygen conditions had no effect on cell proliferation under 3% O₂ = 1.47×10^6 /well and under 40% O₂ = 1.3×10^6 /well at day 20 compared to 2×10^5 /well at day zero.

After time and in the presence of telomerase, CD4⁺ T-cells may benefit from cytokines. Indeed, at day 20 there was a significant increase in cell numbers under 40% oxygen saturation (Tert^{+/+} 2.1×10^6 /well compared to Tert^{-/-} with 3% oxygen saturation 1.6×10^6 /well (P<0.01)). I also noticed that by day 20, CD4⁺ T-cells increased from 2×10^5 /well in the presence of Tert^{+/+} under 40% oxygen saturation = 2.1×10^6 /well and Tert^{-/-} under the same oxygen saturation 40% = 1.5×10^6 /well (P<0.0001).

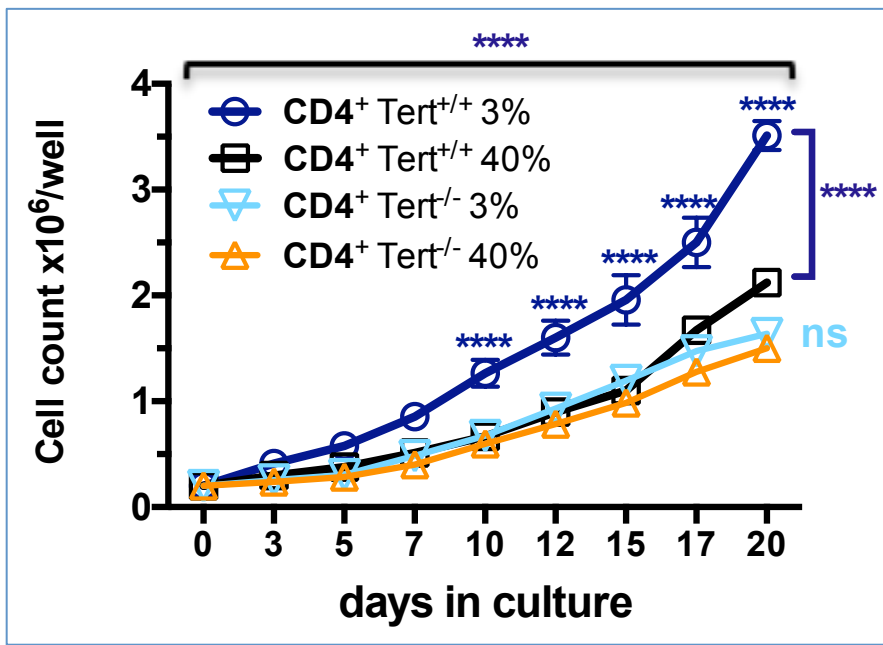


Figure 3.6. The influence of TERT⁺⁺ and oxidative stress on long-term culture and growth curve of CD4⁺ T-cells

CD4⁺ T cells from either TERT⁺⁺ or TERT⁻ mice were seeded at 2x10⁵ cells/well (volume = 200µl/well) in a 96-well plate. CD4⁺ T-cells were generated by immunomagnetic bead-isolation from splenocytes, which were cultured for 14 days with anti-CD3 and anti-CD28 antibodies. Medium was changed and 1.5µg/ml IL-2 was added every 2-3 days for all experiments. CD4⁺ T cells were activated every 7 days (days 0, 7, 14, and 21 if necessary) by adding CD3e/CD28-Biotin micro-beads at a 1:1 ratio (Miltenyi T-cell expansion kit). Cells were cultured either under 3% or under 40% (hyperoxia) oxygen saturation. Growth curves were generated by counting a 10µl aliquot of cells in the Neubauer chamber. All values are displayed as mean±sem (n=3). ****P<0.0001 for comparison between 3% vs. 40% oxygen saturation using 2-way ANOVA.

3.2.4 *mTert-GFP⁺* (telomerase reporter) mice used to investigate the regulation of telomerase in lymphocytes

3.2.4.1 Effect of oxidative stress on splenocyte proliferation from transgenic *mTert-GFP⁺* mice

The *mTert-GFP⁺* mice in this chapter were genotyped by another laboratory colleague, Dr. Gavin Richardson, IGM, Newcastle University.

The aim was to investigate the regulation of telomerase in living cells as well as at a single cell level, based on the findings of previous experiments (3.3.4) in which telomerase plays an important role in cell proliferation. To establish the expression of the TERT gene in live cells *mTert-GFP⁺* reporter mice were used. Splenocytes were expanded for 14 days. A single-cell suspension was purified from transgenic *mTert-GFP⁺* and wild-type splenocytes. Finally, GFP⁺ expression was detected by flow cytometry and proliferation determined under different oxygen concentrations.

Figure 3.7 shows that splenocytes with moderate activation of the *mTert-GFP⁺* reporter also proliferate more under 3% O₂ saturation than under 40% O₂ saturation, from 2x10⁶/well at day zero to 7.7±1.2x10⁶/well and 5.3±0.4x10⁶/well at day 14 (P<0.001) with O₂ saturation having a significant effect (P<0.05). Regardless of the activation level, splenocyte proliferation was suppressed under oxidative stress, while strong activation correlated with a greater proliferation under both levels of O₂ saturation. With strong activation (Figure 3.4), cells expanded 15-fold at day 14 (28-fold by the end of experiment, at day 28) compared to 4-fold (at day 14) with moderate activation (in this experiment) under 3% O₂ saturation. Also under 40% O₂ saturation, I could see that cells were expanded about 11-fold at day 14 (and about 19-fold by the end of experiment, day 28) with strong stimulation (Figure 3.4) compared to about 3-fold at day 14 with moderate stimulation (Figure 3.7).

3.2.4.2 Effect of oxidative stress on proliferation of subsets of transgenic *mTert-GFP⁺* splenocytes

As mentioned previously, interactions between different cell types within a splenocyte population seem to play a critical role in terms of proliferation based on various cytokines secreted by cells which also leads to the activation of other cell types.

Figure 3.8A shows that the proliferation behaviour of CD4⁺ T-cells under moderate activation of the *mTert-GFP⁺* is similar to the previous experiment (figure 3.5A) under strong activation.

CD4⁺ T-cells proliferated about 54-fold ($P<0.0001$) under 3% O₂ saturation, from $0.11\pm0.02\times10^6/\text{well}$ to $6.13\pm1.47\times10^6/\text{well}$ and, under 40% O₂ saturation, about 35-fold ($P<0.0001$) from $0.11\pm0.02\times10^6/\text{well}$ to $3.92\pm0.6\times10^6/\text{well}$ at day 14 (Figure 3.8A). The difference between 3% O₂ saturation and 40% O₂ saturation was found to be significant at day 14 ($P<0.01$). The significant changes between the two O₂ saturations in cell proliferation numbers started from day 10 ($P<0.05$). At 3% O₂ saturation (day 10), CD4⁺ T-cells reached $5.5\pm0.8\times10^6/\text{well}$ and at 40% O₂ saturation, CD4⁺ T-cells reached $3.6\pm0.7\times10^6/\text{well}$. Also, the effect of O₂ saturation was significant ($P<0.05$) between 3% and 40% at day 10.

Compared to CD4⁺ T-cells, the cytotoxic CD8⁺ T-cells (both came from the same original T-lymphocytes and both have the same receptors) showed the same behaviour under moderate activation (figure 3.8B) compared to strong stimulation (figure 3.5B). This may be due to the cytotoxic function of CD8⁺ T-cells requiring a pathogen to be activated more. However, figure 3.8B shows that at day 3 there was a significantly higher ($P<0.0001$) proliferation under 3% O₂ saturation with $0.46\pm0.1\times10^6/\text{well}$ compared to $0.1\pm0.04\times10^6/\text{well}$ under 40% O₂ saturation from $0.05\pm0.01\times10^6/\text{well}$ at day zero. Also, with moderate stimulation, there was a significant ($P<0.001$) effect for O₂ saturation between 3% and 40% (Figure 3.8B).

Figure 3.8C shows the total GFP⁺ cell proliferation under 3% O₂ saturation with $0.36\pm0.14\times10^6/\text{well}$ as significant ($P<0.01$) compared to 40% O₂ saturation with $0.07\pm0.04\times10^6/\text{well}$ by day 14 from $0.04\pm0.015\times10^6/\text{well}$ at day zero. The majority of proliferation happened at day 3 under 3% O₂ saturation, during which cell numbers reached $0.8\pm0.1\times10^6/\text{well}$ compared to $0.15\pm0.04\times10^6/\text{well}$ under 40% O₂ saturation ($P<0.0001$). However, since we found that hyperoxia (40% O₂ saturation) suppressed telomerase activity (see figure 3.10) that might explain the lower cell proliferation under hyperoxia.

There is no clear explanation for the differences in results of B-cell proliferation shown in figure 3.8D in this experiment compared to the previous experiment (Figure 3.5E). Here we can see that by the end of experiment, the B-cells had decreased to a lower level than at the beginning of the experiment. However, at day 5 there was a significantly ($P<0.05$) lower proliferation under 40% O₂ saturation ($0.92\pm0.33\times10^6/\text{well}$) compared to 3% O₂ saturation ($0.5\pm0.14\times10^6/\text{well}$) from ($0.58\pm0.1\times10^6/\text{well}$ at day zero). There was also a significant decrease in total cell number between the start of the experiment ($0.58\pm0.1\times10^6/\text{well}$) and the end of the experiment (3% O₂ saturation = $0.2\pm0.07\times10^6/\text{well}$; 40% O₂ saturation = $0.33\pm0.2\times10^6/\text{well}$). This may be related to the type of activation since B-cells require strong

activation as in the previous experiment (Figure 3.5E) in order to survive. The mouse genotype may have an effect on B-cells, which are from *mTert*-GFP⁺ mice (compared to wild-type mice, figure 3.5E). There was no significant of O₂ saturation on B-cell proliferation.

What is surprising is that monocytes exhibited the same proliferation behaviour under moderate activation (shown in figure 3.8E) as they did under strong stimulation (Figure 3.5F). The influence of O₂ saturation was not significant on monocyte proliferation. In addition, there was a slight trend for monocytes to proliferate (almost similarly) under both types of O₂ saturation (3% O₂ saturation = $0.16 \pm 0.1 \times 10^6$ /well and 40% O₂ saturation = $0.19 \pm 0.08 \times 10^6$ /well, both from $0.11 \pm 0.007 \times 10^6$ /well at day zero). In this case, there may have been some benefit yielded by cytokines secreted by other cells.

3.2.4.3 Oxidative stress downregulates transgenic *mTert*-GFP⁺ expression in splenocytes

The following experiment was created to explore how telomerase activity in a single live cell would be affected by oxidative stress. *mTert*-GFP⁺ mice were chosen on the basis of their telomerase reverse transcriptase, indicated by green fluorescent protein (GFP) (Breault, et al., 2008). Furthermore, the expression of mouse telomerase reverse transcriptase is very close to telomerase activity in terms of regulation (Greenberg et al., 1998). GFP⁺ expression was measured against (wild-type) negative controls using a compensated FACSCanto II running FACSDiva software.

Figure 3.9A shows that the total GFP⁺ cell proliferation under 3% O₂ saturation with $0.36 \pm 0.14 \times 10^6$ /well was significantly different ($P < 0.01$) compared to under 40% O₂ saturation with $0.07 \pm 0.04 \times 10^6$ /well by day 14, from $0.04 \pm 0.015 \times 10^6$ /well at day zero. The majority of proliferation happened at day 3 under 3% O₂ saturation. Cell numbers reached $0.8 \pm 0.1 \times 10^6$ /well, compared to $0.15 \pm 0.04 \times 10^6$ /well under 40% O₂ saturation with $P < 0.0001$ at day 3. However, we found (Figure 3.10) that 40% O₂ saturation suppressed telomerase activity, which might be the reason for the decrease in cell proliferation.

To find out which subpopulation of GFP⁺ cells proliferated most, the reporter GFP⁺ cells were classified by FACSDiva software related to the majority population subset of splenocytes used in this study (CD4⁺, CD8⁺, CD11b and CD45R (B220)).

Figure 3.9B shows that $\text{GFP}^+\text{CD4}^+$ cells exhibit proliferation behaviour closer to the total GFP^+ cells than the other cell populations shown in figures 3.9C, 3.9D, and 3.9E. A single cell expression percentage was generated based on the cell count per well at each time point. $\text{GFP}^+\text{CD4}^+$ cells proliferated from $0.016\pm 0.008 \times 10^6/\text{well}$ at day zero to $0.2\pm 0.13 \times 10^6/\text{well}$ under 3% O_2 saturation and $0.051\pm 0.05 \times 10^6/\text{well}$ under 40% O_2 saturation (ns). At day 10, cells had proliferated significantly ($P<0.01$) ($0.3\pm 0.1 \times 10^6/\text{well}$ under 3% O_2 saturation and $0.02\pm 0.006 \times 10^6/\text{well}$ under 40% O_2 saturation). The major proliferation took place at day 3 ($P<0.001$). Cells reached $0.34\pm 0.05 \times 10^6/\text{well}$ under 3% O_2 saturation and $0.06\pm 0.02 \times 10^6/\text{well}$ under 40% O_2 saturation. O_2 saturation significantly affects telomerase expression. Figure 3.9 shows $\text{GFP}^+\text{CD4}^+$ telomerase expression ($P<0.01$), $\text{GFP}^+\text{CD8}^+$ telomerase expression ($P<0.01$), $\text{GFP}^+\text{B-cells}^+$ telomerase expression ($P<0.01$) and $\text{GFP}^+\text{monocytes}^+$ ($P<0.05$).

3.2.4.4 Oxidative stress represses telomerase activity in splenocytes

By experimenting with *mTert-GFP⁺* mice, we found that GFP^+ expression disclosed information about telomerase presence at a single cell level. From this, we concluded that telomerase expression is diminished at 40% O_2 saturation. Telomerase plays a crucial role in cell division and proliferation (Greenberg et al., 1999). To ensure that GFP^+ expression *in vivo* correlates with telomerase activity, and also to find the effect of oxidative stress on telomerase activity, I expanded splenocytes for two weeks to assess the role of oxidative stress on telomerase activity during splenocyte proliferation. Telomerase activity was measured by TRAP-PCR ELISA as described in 2.2.10. Negative (*Tert*^{-/-}) and positive controls (3T3 cells) were used (figure 3.10A). Figure 3.10B shows that under oxidative stress, telomerase activity diminished after day 5, whilst the maximum activity occurred at day 3, increasing by about 1.6-fold. Conversely, telomerase activity under 3% O_2 saturation reached a significant ($P<0.01$) maximum activity at day 5, increasing by 3.9-fold vs. 1.4-fold under 40% O_2 saturation. Telomerase activity under hypoxia (3% O_2) fluctuated after day 5 but remained high compared to zero hours and under hyperoxia (40% O_2) until the end of the experiment at day 14. Telomerase activity under hypoxia (3% O_2) was significantly ($P<0.05$) higher, increasing by 2.2-fold compared to 0.09-fold under oxidative stress (40% O_2). There is a statistically significant ($P<0.0001$) difference between hypoxia (3% O_2) and hyperoxia (40% O_2). Time also played a significant ($P<0.0001$) role in terms of telomerase activity under hypoxia (3% O_2). In conclusion, we can infer that oxidative stress is one factor that may decrease cell proliferation due to telomerase suppression. Furthermore, we can conclude that 40% O_2 saturation is an appropriate lab condition to model physiological oxidative stress.

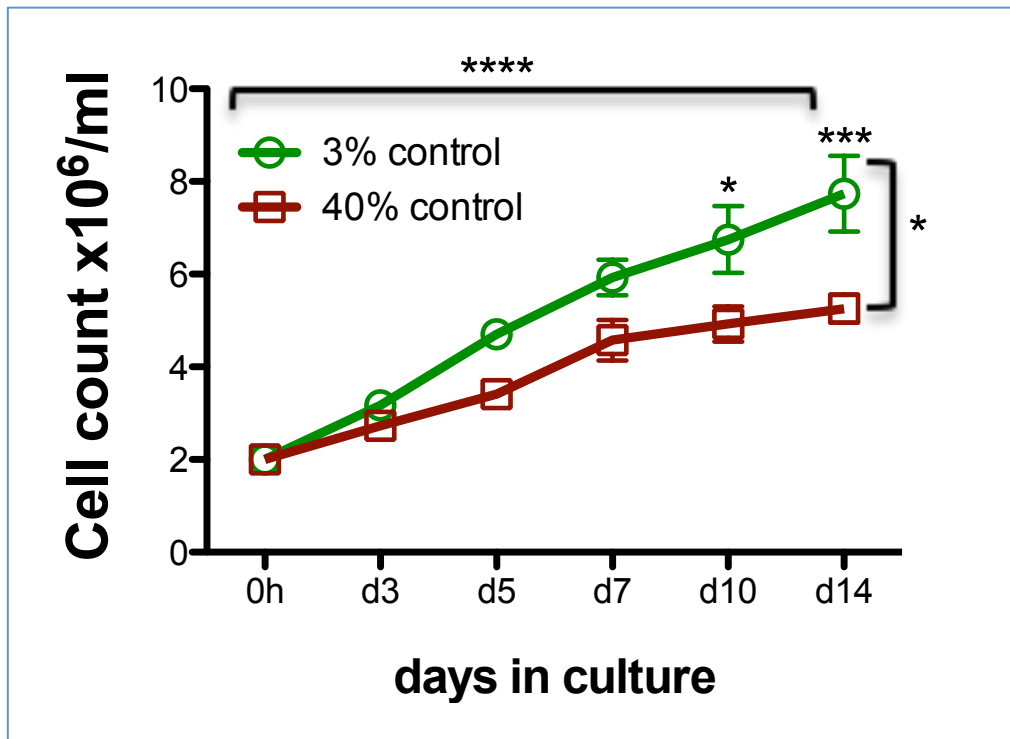


Figure 3.7. Splenocytes from transgenic *mTert*-GFP⁺ grow better under 3% than 40% oxygen saturation

Splenocytes from transgenic *mTert*-GFP⁺ mice were seeded at 2x10⁶/ml in a 24-well plate, and the plate was coated with anti CD3 and CD28 antibodies. Medium was changed and 1.5 μ g/ml IL-2 was added every 2-3 days for all experiments. Cells were cultured either under 3% or under 40% (hyperoxia) oxygen saturation for 14 days. All values are displayed as mean \pm sem (n=4). *P<0.05, ***P<0.001, ****P<0.0001 for comparison between 3% vs. 40% oxygen saturation using 2-way ANOVA.

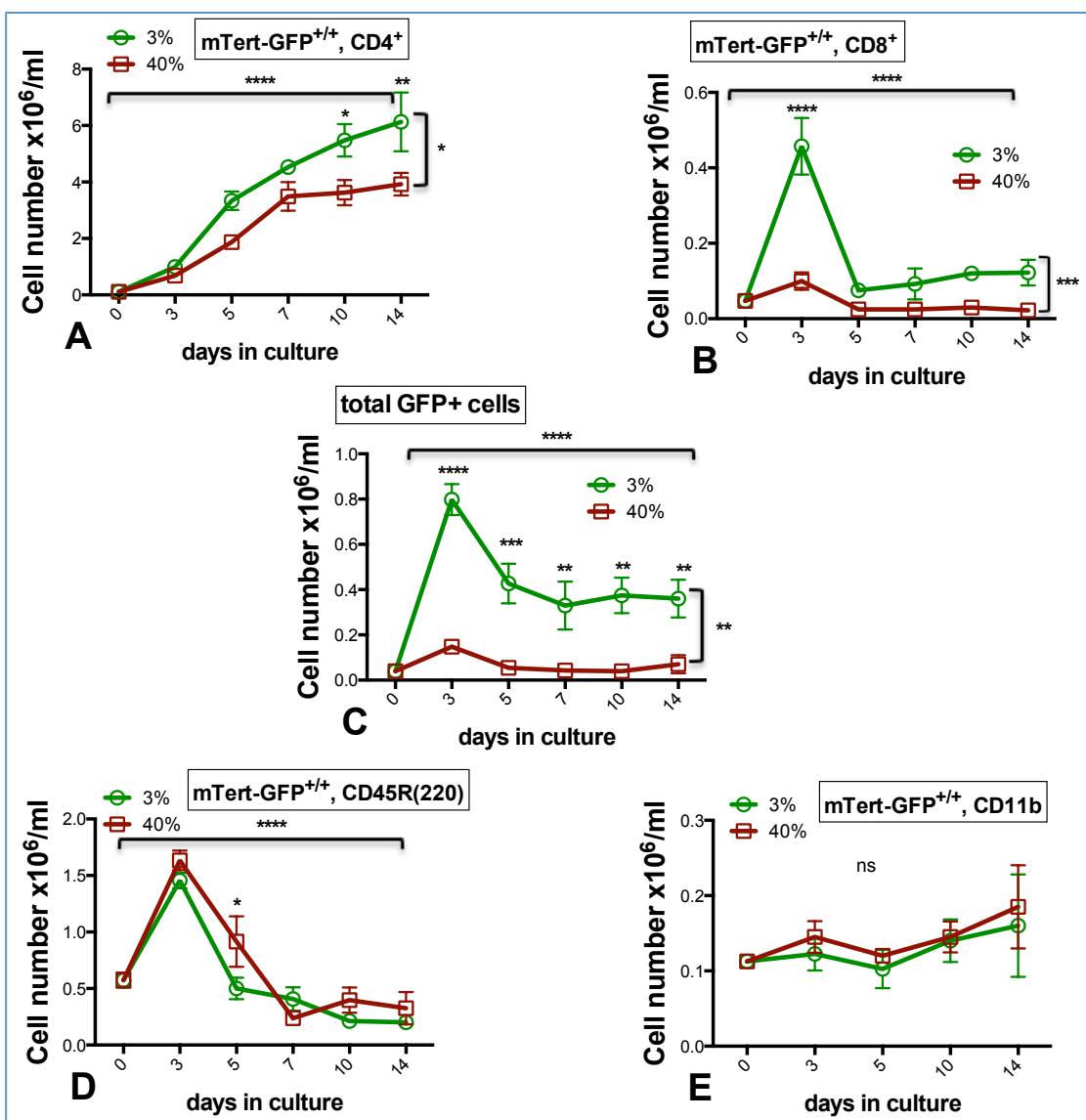


Figure 3.8. Long-term growth curves of different lymphocyte subsets from transgenic *mTert-GFP*⁺ mice splenocytes under different oxygen saturation

Splenocytes from *mTert-GFP*⁺ reporter mice were seeded at 2×10^6 /ml in 24-well plates (coated by CD3 and CD28 antibodies overnight) for 14 days and on days 3, 5, 7, 10 and 14. The cells were then cultured in 3% and 40% incubator oxygen saturation. Then, at each time point, expression of the GFP⁺ reporter relative to surface markers CD45R B220, CD11b, CD4⁺ and CD8⁺ was measured against wild-type and (unstained) negative controls using a compensated FACSCanto II running FACSDiva software; 50,000 live events were analysed to determine the proportion of T-cell types. **A:** CD4⁺ T-cell number/splenocytes, **B:** CD8⁺ T-cell number/splenocytes, **C:** total GFP⁺ cell number/splenocytes, **D:** B-cell number/splenocytes, **E:** monocytes number/splenocytes. All values are displayed as mean \pm sem (n=4). * P<0.05, **P<0.01, *** P<0.001, **** P<0.0001 for comparison between 3% vs. 40% oxygen saturation using 2-way ANOVA.

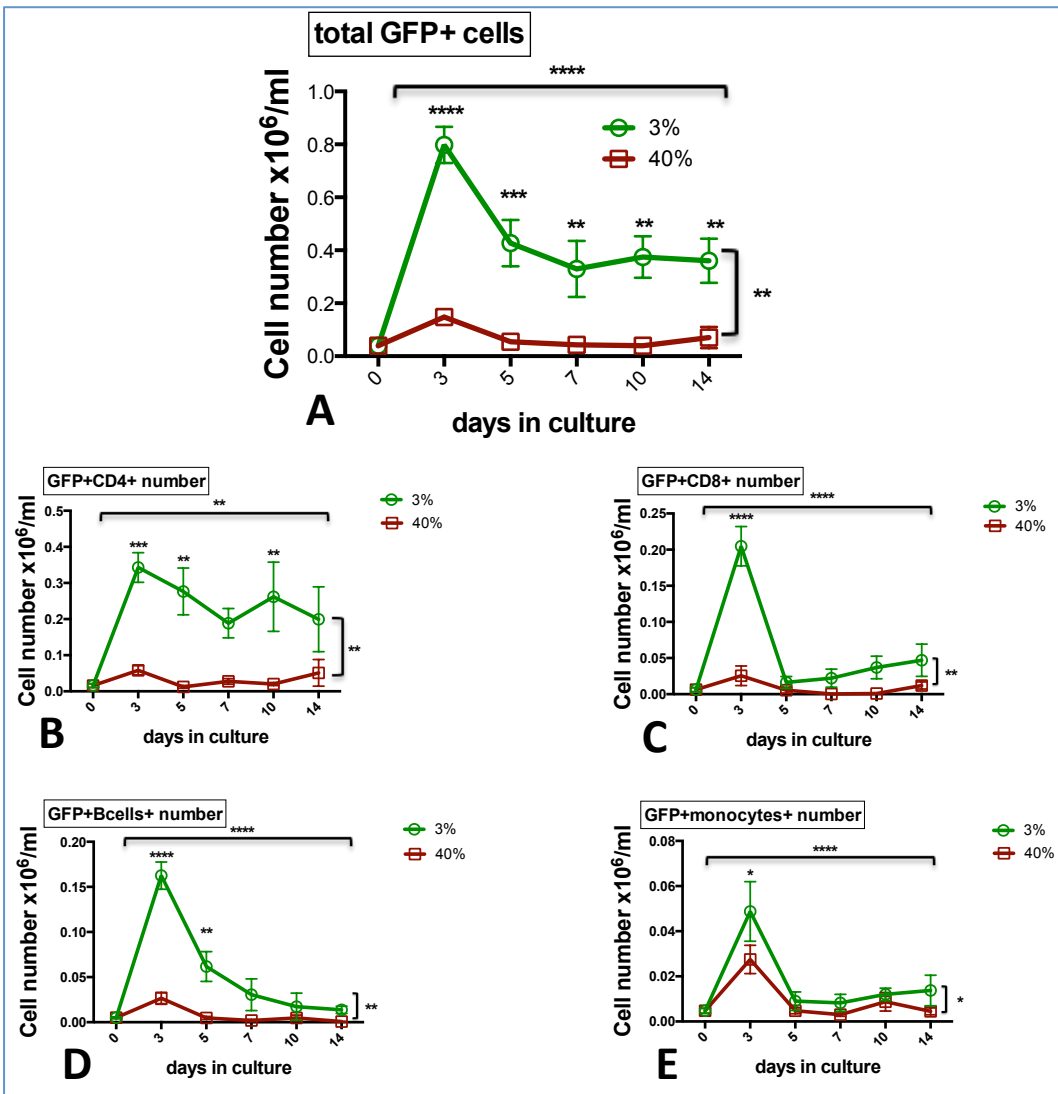


Figure 3.9. Number of GFP⁺ cells in each splenocyte subset that express TERT gene from transgenic *mTert*-GFP⁺ mice

Splenocytes from *mTert*-GFP⁺ reporter mice were seeded at $2 \times 10^6/\text{ml}$ in 24-well plates (coated by CD3 and CD28 antibodies overnight) for 14 days and on days 3, 5, 7, 10 and 14. The cells were then cultured in 3% and 40% incubator oxygen saturation. Then, at each time point, surface marker expression of genetically GFP relative to CD45R, CD11b, CD4⁺ and CD8⁺ was measured against negative controls using a compensated FACSCanto II running FACSDiva software; 50,000 live events were analysed to determine the proportion of T-cell types. **A:** total GFP⁺ cells number (splenocytes), **B:** total GFP⁺CD4⁺ cells number, **C:** total GFP⁺CD8⁺ cells number GFP⁺, **D:** total GFP⁺B-cell⁺ number, **E:** total GFP⁺monocytes⁺ number/ GFP⁺ cells. All values are displayed as mean \pm sem (n=4). * P<0.05, ** P<0.01, *** P<0.001, ****P<0.0001 for comparison between 3% vs. 40% oxygen saturation using 2-way ANOVA.

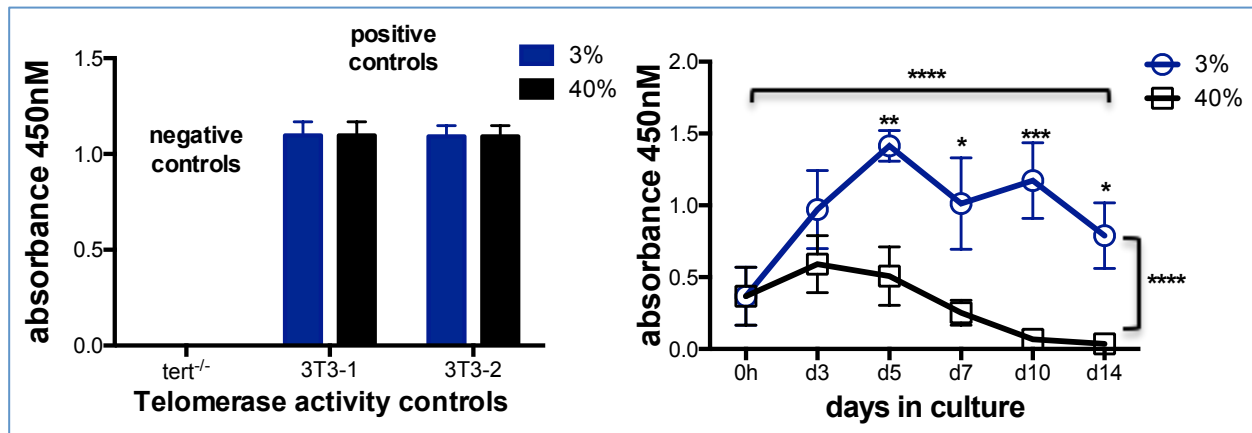


Figure 3.10. Telomerase activity in splenocytes from wild-type mice is higher under 3% than under 40% oxygen saturation

Wild-type mice splenocytes were generated and then seeded at 2×10^6 /ml in a 24-well plate at day 0, on plates coated overnight at 4°C with anti CD3 and CD28 antibodies. Medium was changed and 1.5 $\mu\text{g}/\text{ml}$ IL-2 was added every 2-3 days, under 3% and 40% oxygen saturation. Cells were harvested at the indicated time points (days 3, 5, 7, 10 and 14), and cryopreserved at -80°C . TRAP-PCR was run with 500ng protein loaded for splenocytes and 100ng for 3T3 cells (positive control). **A:** controls, **B:** Telomerase activity under 3% and 40% O₂ saturation. All values are displayed as mean \pm sem (n=5). * P<0.05, ** P<0.01, *** P<0.001, **** P<0.0001 for comparison of 3% vs. 40% oxygen saturation using 2-way ANOVA.

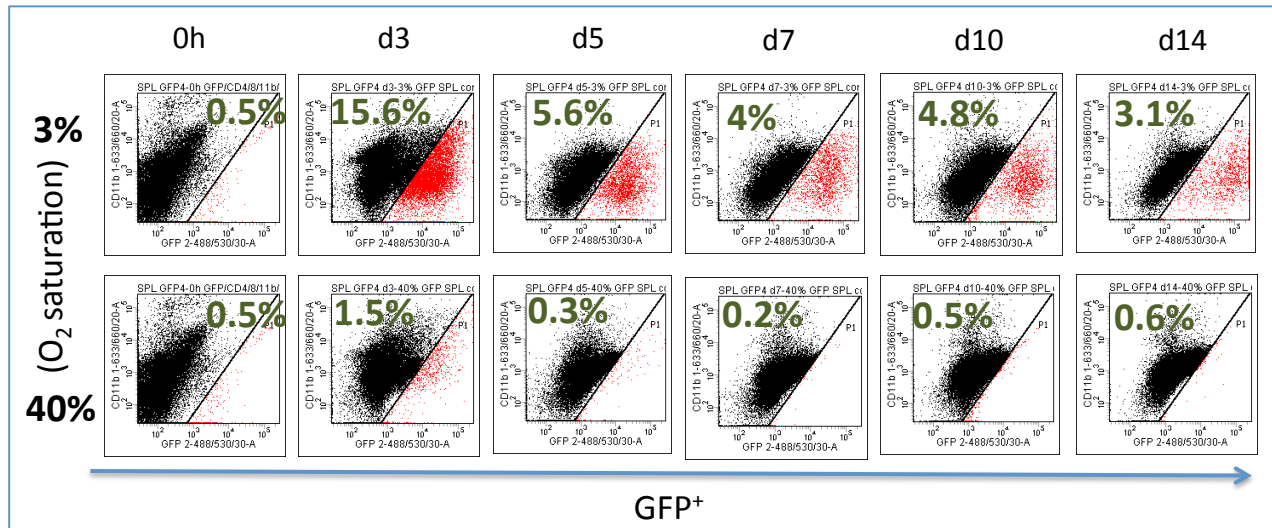


Figure 3.11. Percentage of GFP⁺ cells from *mTert*-GFP⁺ mice that were cultured under different oxygen saturation, presented as a FACS dot plot

Splenocytes from *mTert*-GFP⁺ reporter mice were seeded at 2×10^6 /ml in 24-well plates (coated by CD3 and CD28 antibodies overnight) for 14 days. The cells were then cultured in 3% and 40% incubator oxygen saturation. Then, at each time point, on days 3, 5, 7, 10 and 14 surface marker expression of genetically GFP relative to CD45R (B220), CD11b, CD4⁺ and CD8⁺ was measured against negative controls using a compensated FACSCanto II running FACSDiva software; 50,000 live events were analysed to determine the percentage of GFP⁺ cells to all splenocytes. Red dots = GFP⁺ cells. (n=4)

3.2.5 Telomerase confers resistance to cell death in splenocytes

In this final subchapter, I describe attempts to establish the role of telomerase or TERT in the ability of lymphocytes to resist cell death. Telomerase activation is linked with a range of processes, including immune cell activation, expansion of bone marrow blood cell progenitors and embryonic cell proliferation. Conversely, telomerase inhibition is associated with apoptosis, cellular senescence and degenerative diseases (Hahn et al., 1999; Mitchell et al., 1999; Wyllie et al., 2000; Zhang et al., 1999).

As in all previous experiments within this project, 50% of the medium (serum) was changed every 2 to 3 days. IL-2 and DMSO were also added when the medium was changed. These play a role in cell survival and proliferation. In order to analyse the effect of serum, IL-2 and DMSO starvation on telomerase activity and cell proliferation, 20% O₂ saturation was used, which produced significant oxidative stress compared to 3% oxygen saturation (figure 3.12). Splenocytes (tert^{+/+} and tert^{-/-}) were cultured in coated plates for 28 days, with no medium change or additions. To ensure the emerging environment had no effect, the oxidative stress level was measured between both genotypes (tert^{+/+} and tert^{-/-}) and both conditions (medium change and no medium change) using dihydroethidium (DHE) fluorescence.

Figure 3.13A shows that telomerase seems to play a critical role in cell survival, especially for CD4⁺ T-cells. The tert^{+/+} cell numbers were 2.2-fold greater than tert^{-/-} ($12.6 \pm 1.56 \times 10^6$ /well vs. $5.65 \pm 1.1 \times 10^6$ /well respectively) ($P < 0.01$). For B-cells, the tert^{+/+} cell numbers were 1.8-fold more than tert^{-/-} ($4.05 \pm 0.14 \times 10^6$ /well vs. $2.27 \pm 0.44 \times 10^6$ /well) ($P < 0.01$). In monocytes, the tert^{+/+} cell numbers were 1.7-fold greater than tert^{-/-} ($1.7 \pm 0.06 \times 10^6$ /well vs. $1.01 \pm 0.11 \times 10^6$ /well) ($P < 0.001$). Furthermore, there was a positive trend in favour of tert^{+/+} cells compared to tert^{-/-} (ns): in CD8⁺ T-cells ($0.06 \pm 0.01 \times 10^6$ /well vs. $0.04 \pm 0.01 \times 10^6$ /well) and in DN ($0.09 \pm 0.02 \times 10^6$ /well vs. $0.04 \pm 0.02 \times 10^6$ /well). We can conclude from this that telomerase not only leads to cell division and proliferation, or cell survival with normal nutrition, but also influences cell survival under starvation conditions.

Figure 3.13B shows that there was no significant effect on oxidative stress level whether the medium was changed or not, nor when genotype tert^{+/+} under 20% oxygen saturation with medium change was used as 100% compared with other groups (Tert^{+/+} with no medium change, Tert^{-/-} with medium change and Tert^{-/-} with no medium change all under 20% O₂). This also ensured that no effect came from potential physiological changes in the mitochondrial membrane, which can affect oxidative phosphorylation and hence ATP

generation by cells. In this instance, the JC-1 fluorescence ratio (FL3/FL1) was used to measure the mitochondrial membrane potential. Figure 3.13C shows no significant effect relating to either medium changes (or not) or genotype ($\text{tert}^{+/+}$, $\text{tert}^{-/-}$). $\text{tert}^{+/+}$ under 3% O_2 was used as 100% to compare with other groups ($\text{tert}^{+/+}$ with no medium change, $\text{tert}^{-/-}$ with medium change and $\text{tert}^{-/-}$ with no medium change all under 20% O_2).

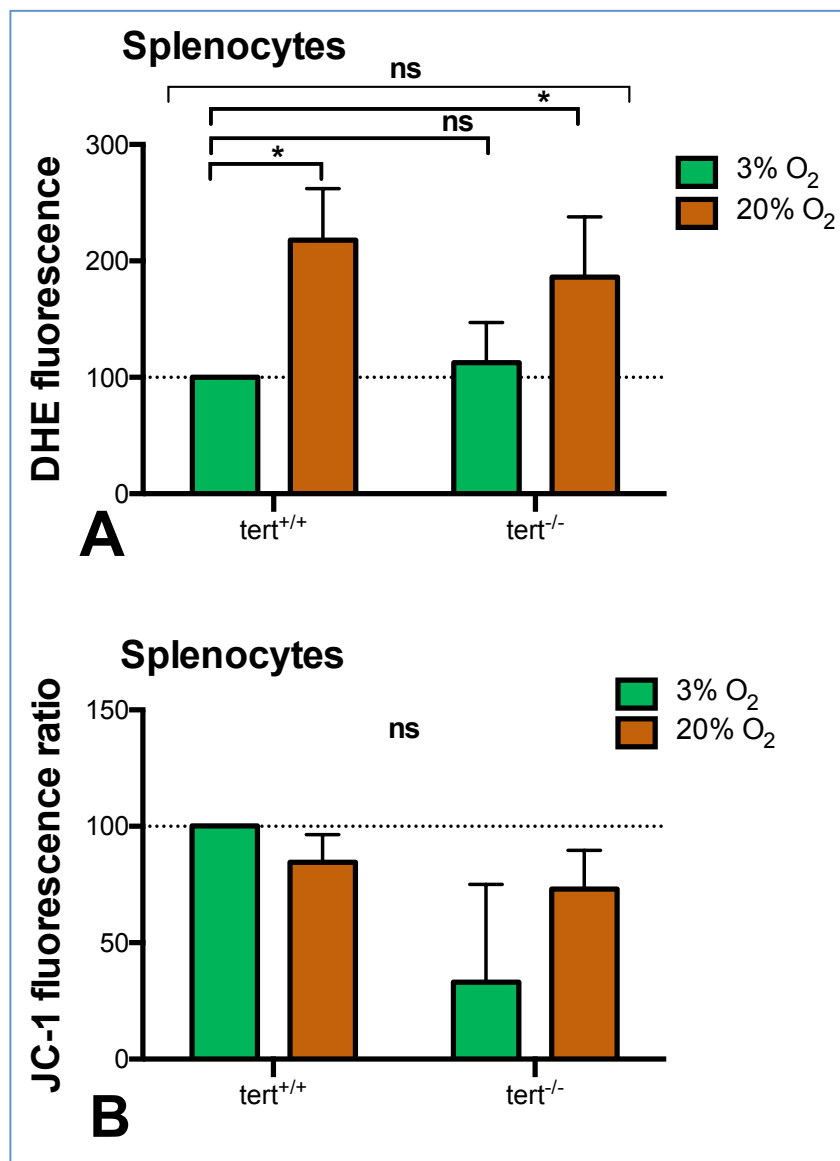


Figure 3.12. Measurement of oxidative stress levels and mitochondrial membrane potential levels under 20% oxygen saturation.

A, B. Splenocytes from either wild-type $\text{tert}^{+/+}$ or $\text{tert}^{-/-}$ mice were seeded at $2 \times 10^6/\text{ml}$ in a 24-well plate. Splenocytes were cultured for ≥ 20 days ($n=4$). Plates were coated with anti-CD3 and anti-CD28 antibodies. Medium was changed and $1.5\mu\text{g}/\text{ml}$ IL-2 was added every 2-3 days for all experiments. Cells were cultured under 3% and 20% oxygen saturation. **A.** Oxidative stress levels were measured by dihydroethidium (DHE) fluorescence. **B.** Mitochondrial membrane potential levels measured by JC-1 fluorescence ratio FL3/FL1. All values are displayed as mean \pm sem ($n=4$). * $P<0.05$ for comparison between oxygen saturation levels using 2-way ANOVA.

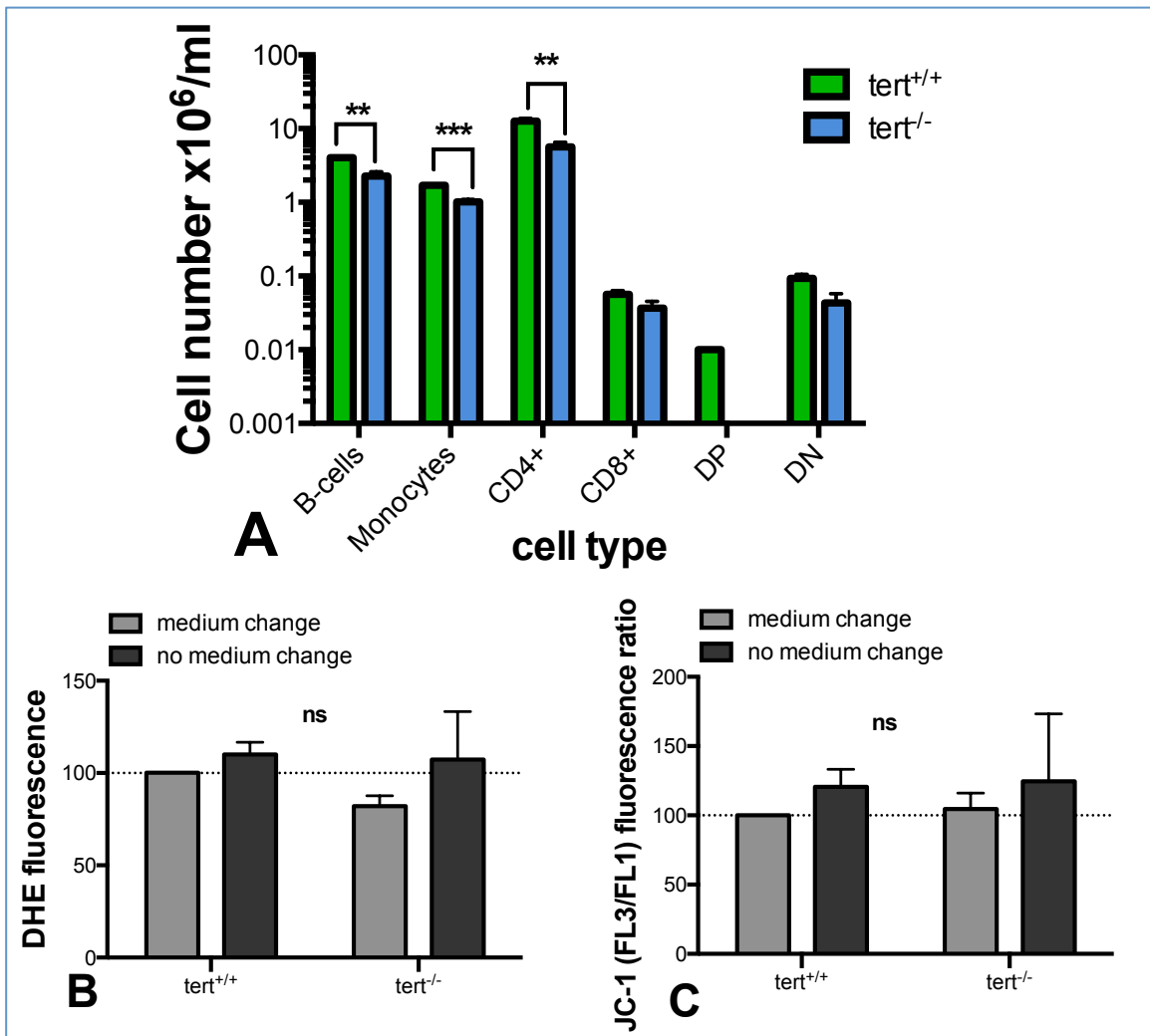


Figure 3.13. Telomerase positive cells survive better than telomerase negative cells under normoxia

Splenocytes from Tert^{+/+} and Tert^{-/-} mice were seeded at 10x10⁶ cells/well in a 6-well plate (5ml/well). Cells were cultured over 28 days using anti-CD3 and anti-CD28 antibodies. 1.5µg/ml IL-2 was added at the start time, after which no IL-2 was added or media changed during the 28 days. Cells were incubated under 20% O₂. At the end of experiments (day 28): **(A)** splenocytes were stained with four colours, CD45R(B220), Cd11b, CD4⁺ and CD8⁺, to determine the proportions of each cell type in a sample. Also cell viability (bright field only) was measured using a Tali image-based cytometer (Invitrogen), with a Tali cellular analysis slide (20µl), splenocytes were stained with dead cell red and incubated one minute. **(B)** Tert^{+/+} vs. Tert^{-/-} splenocytes oxidative stress levels were measured by dihydroethidium (DHE) fluorescence with and without medium change at day 28. **(C)** Tert^{+/+} vs. Tert^{-/-} splenocytes mitochondrial membrane potential levels were measured by JC-1 fluorescence ratio with and without medium change at day 28. All values are displayed as mean±sem (n=3). ** P<0.01 for comparison between 3% vs. 20% oxygen saturation using 2-way ANOVA.

3.3 Discussion

In this study, I used three different oxygen saturations; 3%, 20% and 40%. I found that under hypoxia (3% oxygen saturation) cells grew faster, lived longer and showed lower stress, compared to either 20% (normoxia) or 40% (hyperoxia) O₂. This is in accordance with the finding of others who had shown improved growth and less damage under hypoxia compared to normoxia or hyperoxia in other cell systems and species (human and mouse cells) (Richter et al., 1972; von Zglinicki et al., 1995; Parrinello et al., 2003).

One of the early studies on fetal tissues of mice and rat demonstrated that cell numbers increased under low oxygen percentage (1-3% O₂) (Richter et al., 1972). The lifespan of human fibroblasts increased under 10% O₂, compared to 20% O₂ saturation (Packer and Fuehr, 1977). Mouse primary embryonic fibroblasts were cultured under 3% vs. 20% oxygen saturation for 28 days. Under 3% O₂, the senescence effect that usually happens under 20% O₂ after 28 days of culture was not apparent (Parrinello et al., 2003). In another study, 3% O₂ was used as hypoxia vs. 18% O₂ as normoxia. The 3% O₂ hypoxia induced cell proliferation and differentiation in rat mesangial cells, specialized cells around blood vessels in the kidneys (Sahai et al., 1997). 3% oxygen saturation also enhanced vascular cell proliferation compared to 21% oxygen saturation (Humar et al., 2002). According to Lopez-Barneo et al. (2001), the boundary between physiological and non-physiological hypoxia is blurred; any physiological response may be considered adaptive and can be either brought about by, or reversed by, induced hypoxia (3–5% O₂). In a more recent review, McKeown (2014) suggested a 2-6% range of oxygen saturation is likely to be deemed physiological hypoxia. She also suggested some definitions, for example: phyoxia (physiological oxygen level) between 4-7.5% O₂ and physiological hypoxia from 1-5% O₂. Based on these, the 3% O₂ saturation is in hypoxia range, not in phyoxia range. Therefore, the term ‘hypoxia’ will refer to the 3% oxygen saturation used in this study.

In this study, 40% O₂ (hyperoxia) and 20% O₂ (normoxia) significantly induced oxidative stress in splenocytes and CD4⁺ T-cells. It is known that normoxia induces oxidative stress in mouse primary cells and they are much more sensitive to oxidative stress than human cells (Parrinello et al., 2003). Here, it caused inflammation in mouse splenocytes under both 3% and 40% O₂, but under hyperoxia, the inflammation level was stable at all time points and was at a significantly higher level compared to 3% O₂. Inflammation levels declined from day 1 to day 3 by 7.5-fold (ns) under 3% O₂. This finding is supported by a study on human fibroblasts, which concluded that 40% oxygen saturation decreased the proliferation of

fibroblasts and also decreased telomere length, suggesting that 40% O₂ is a good model for senescence in human cells (von Zglinicki et al., 1995).

Furthermore, a study on rats suggested that 40% O₂ or higher for 24h or more enhanced oxidative stress by increasing the level of derivatives of reactive oxygen metabolites (dROMs) (Nagatomo et al., 2012). Oxidative stress was found to enhance atherogenesis in the vascular wall, which may lead to inflammation or myocardial infarction (Sorescu et al., 2002). Chronic oxidative stress has been implicated in atherosclerotic plaques and endothelial dysfunction, which contributes to vascular inflammation (Guzik et al., 2006; Heitzer et al., 2001). Moreover, the effect of oxidative stress on cell proliferation seems to be TERT-dependent. T-lymphocytes from TERT^{-/-} proliferated equally badly under both hypoxia and hyperoxia in comparison to T-lymphocytes from TERT^{+/+}, which proliferated more under hypoxia than under hyperoxia. This finding aligned with previous studies which also demonstrated the vital role of telomerase in cell proliferation (Martin-Rivera et al., 1998), especially in lymphocytes (Buchkovich and Greider, 1996). From my results, analysis of both, *mTert*-GFP^{+/+} expression and telomerase activity, confirmed that oxidative stress under hyperoxia suppressed telomerase activity. In long term cell culture, and without medium changes under normoxia (20% oxygen saturation), telomerase positive splenocytes survived about twice as well compared with Tert^{-/-} and showed a significant (P<0.0001) proliferation increase and survival for CD4⁺ Tert^{+/+} (more than 10x10⁶ compared with about 5x10⁶ CD4⁺ Tert^{-/-}) after 28 days in culture.

CHAPTER 4. Effect of MAPK inhibition/inhibitor (MAPKi) on splenocytes and CD4⁺ T-lymphocytes under chronic mild oxidative stress

4.1 Introduction

Previous studies have shown that telomerase activity and survival following TCR activation was enhanced by the inhibition of p38 MAPK signalling in CD4⁺ T-lymphocytes (Di Miti et al, 2011). Furthermore, treatment of hypercholesterolaemic patients with a selective p38 α/β Mitogen-activated protein kinase inhibitor (MAPKi) (losmapimod; GW856553) significantly improved endothelial dysfunction and vascular inflammation, making p38 a novel target for patients with cardiovascular disease (Cherian et al, 2011).

MAPKi has been shown to reduce IFN- γ secretion *in-vitro*, causing less inflammation (Ranjbaran et al, 2007). Therefore MAPKp38 inhibition could stabilize atherosclerotic plaque, decrease the atherogenic process itself (Melloni et al, 2012; Cherian et al, 2011), decrease myocardial apoptosis and improve post-ischaemic cardiac function (Ma et al, 1999). The aim for this experiment was to test whether inhibition of MAPK in CD4 T-cells affects proliferation in a telomerase-dependent way under culture conditions, with or without increased oxidative stress.

4.2 Results

4.2.1 Effect of MAPKi on IFN-gamma mRNA transcription under oxidative stress

I have shown in the previous chapter that oxidative stress induces transcription of IFN-gamma mRNA in splenocytes (Figure 3.3). IFN-gamma is known to suppress T-cell proliferation (Krenger et al., 1996). MAPKi has been shown to reduce IFN-gamma secretion *in vitro*, causing less inflammation (Sarov-Blat et al., 2010; Cherian et al., 2011). This experiment sought to find out the effect of MAPKi on IFN-gamma mRNA transcription under oxidative stress. Splenocytes were expanded and cultured for 3 days under hypoxia (3% O₂) and hyperoxia (40% O₂). One group was treated with (500nM/ml) MAPKi, the other remained as a control as described at (2.2.5). Figure 4.1 shows that the level of IFN-gamma in cells treated with 500nM/ml MAPKi was increased at day 1 and day 2, then at day 3 the level of IFN-gamma transcription was almost the same as on day 3 under hypoxia (3% oxygen) saturation.

At day 3 under hyperoxia (40% oxygen saturation) the level of IFN-gamma mRNA transcript in cells treated with 500nM/ml MAPKi declined significantly ($P<0.05$); about 18-fold compared to the same cells not treated with MAPKi. At the same time point, there was a significant ($P<0.05$) difference between hypoxia and hyperoxia; about 15.3-fold, both untreated with MAPKi. Furthermore, there was no significant change (1.2-fold) in levels of IFN-gamma transcription between cells under hypoxia and hyperoxia treated with MAPKi. Based on this finding, I can conclude that 500nM MAPKi/ml seems to down-regulate IFN-gamma production under oxidative stress, which could lead to decreased inflammation *in vitro*.

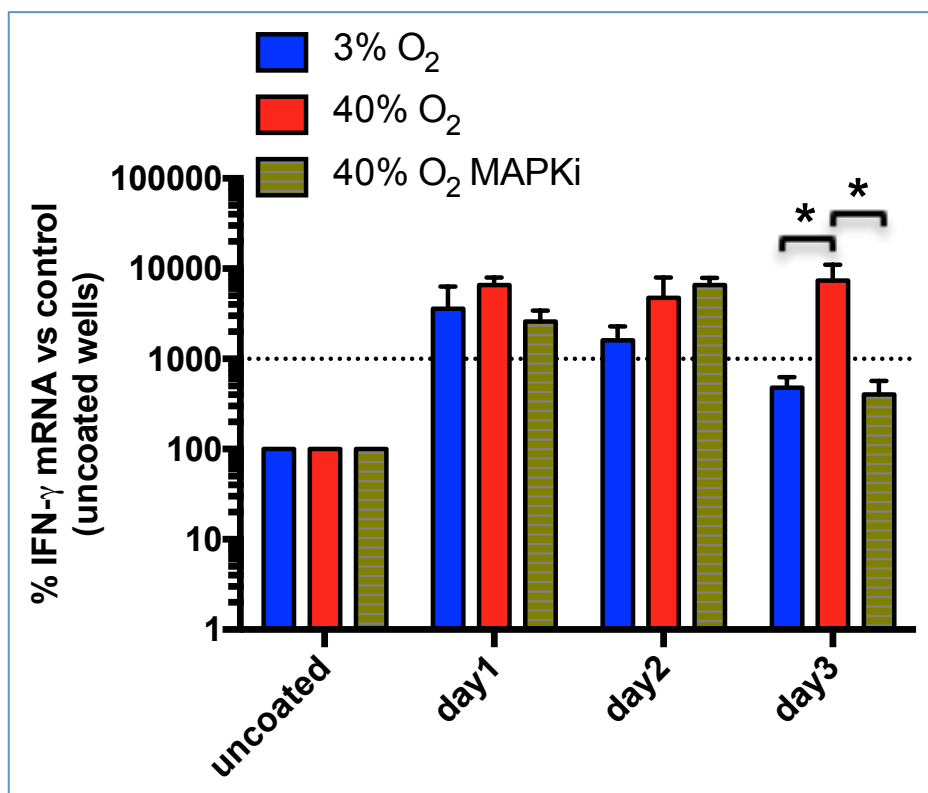


Figure 4.1. MAPKi regulates transcription of IFN-gamma mRNA in splenocytes under oxidative stress.

Splenocytes from wild-type ($\text{Tert}^{+/+}$) mice were seeded at $2 \times 10^6/\text{ml}$ in a 24-well plate. Splenocytes were cultured for 3 days. Plates were coated with anti-CD3 and anti-CD28 antibodies. Control cells were grown on uncoated wells. Cells were cultured under 3% (hypoxia) and 40% (hyperoxia) oxygen saturation. All values are displayed as mean \pm sem ($n=3$). $^*P<0.05$, for comparison between oxygen saturation levels using two-tailed unpaired t test.

4.2.2 Effect of MAPK inhibition on splenocyte proliferation under oxidative stress

4.2.2.1 Effect of MAPK inhibition on lymphocyte proliferation under oxidative stress

I have shown in figure 3.4 that oxidative stress suppresses proliferation of splenocytes and CD4⁺ T-cells. With the next experiment, I wanted to find out the effect of p38 MAPKi on cell proliferation under oxidative stress. Splenocytes were expanded under both oxygen conditions, 3% and 40%, as described previously. Cells were treated with 500nM/ml p38 MAPKi vs. control cells. Figure 4.2 shows that the positive effect of MAPKi on TERT^{+/+} splenocytes was comparable between 3% O₂ (1.7-fold) and 40% O₂ (1.4-fold) (ns), implying that oxygen saturation with MAPKi had no significant effect on splenocyte proliferation, which is the opposite of what was shown in the previous experiment (Figure 3.4). With MAPKi treatment, the suppressive effect of oxidative stress (40% O₂ saturation) on splenocyte proliferation disappeared. This may be secondary to IFN- γ that was regulated by MAPKi under hyperoxia as seen in figure 4.1. There is no significant positive effect for MAPKi on TERT^{-/-} splenocytes, but I could not detect any cell proliferation secondary to the MAPKi effect. Neither under 3% O₂ nor under 40% did cell numbers change between day 2 and day 28. In fact, comparing the effect of MAPKi between TERT^{+/+} vs. TERT^{-/-} under the same oxygen conditions, I noticed that, under hypoxia the MAPKi has a significant (P<0.01) effect on TERT^{+/+} cell numbers (1.5-fold) vs. TERT^{-/-} starting from day 15 and continuing to be significant until the end of experiment at day 28 (1.8-fold) in favour of TERT^{+/+} (P<0.0001). Under hyperoxia, the significant changes between TERT^{+/+} and TERT^{-/-} from day 12 onwards were 1.5-fold in favour of TERT^{+/+} (P<0.05) and continued until the end of experiment at day 28 (1.8-fold (P<0.0001)).

Altogether, MAPKi seemed to counteract the oxidative stress produced by hyperoxia by decreasing the IFN- γ secreted by cells. Also, MAPKi enhances splenocyte proliferation both under hypoxia and under hyperoxia. The MAPKi effect is telomerase-dependent.

4.2.2.2 Effect of MAPK inhibition on proliferation of lymphocyte subsets under oxidative stress

The majority of cell populations within splenocytes are CD4⁺ T-lymphocytes, CD8⁺ T-lymphocytes, B-lymphocytes and monocytes, all of which serve different immunological roles and functions. Figure 4.2 shows that MAPKi enhances splenocyte proliferation under

both hypoxia and hyperoxia. The following experiment was established to discover which type of splenocyte subset proliferated more under hypoxia vs. hyperoxia when treated with MAPKi.

Splenocytes were cultured under 3% and 40% oxygen saturation and both treated with 500nM MAPKi as described previously (2.2.5). Control samples without MAPKi were cultured under both oxygen conditions as a baseline to identify the impact of MAPKi on cells. Figure 4.3 shows that all major splenocyte populations demonstrated the same effect on cell number under both oxygen saturations, which might suggest that MAPKi led to a neutralizing of the oxidative stress produced by hyperoxia. Furthermore, there were no significant changes in cell proliferation between hypoxia and hyperoxia (figures 4.3B-F) in CD8⁺ T-cells, DP, DN, B-lymphocytes and monocytes, indicating that MAPKi plays a beneficial role with cells under oxidative stress. Figure 4.3A shows a significant effect of MAPKi between day 3 (first day of effect) and day 14 (final day of experiment), under both oxygen saturations (1.2-fold under hypoxia 3% O₂ and 1.4-fold under hyperoxia 40% O₂, P<0.05). This supports the conclusion that MAPKi keeps cells healthy under hyperoxia (40% O₂), and neutralised the effect of IFN-gamma secreted under oxidative stress. CD4⁺ T-cells demonstrated the most significant effect from MAPKi under both oxygen conditions.

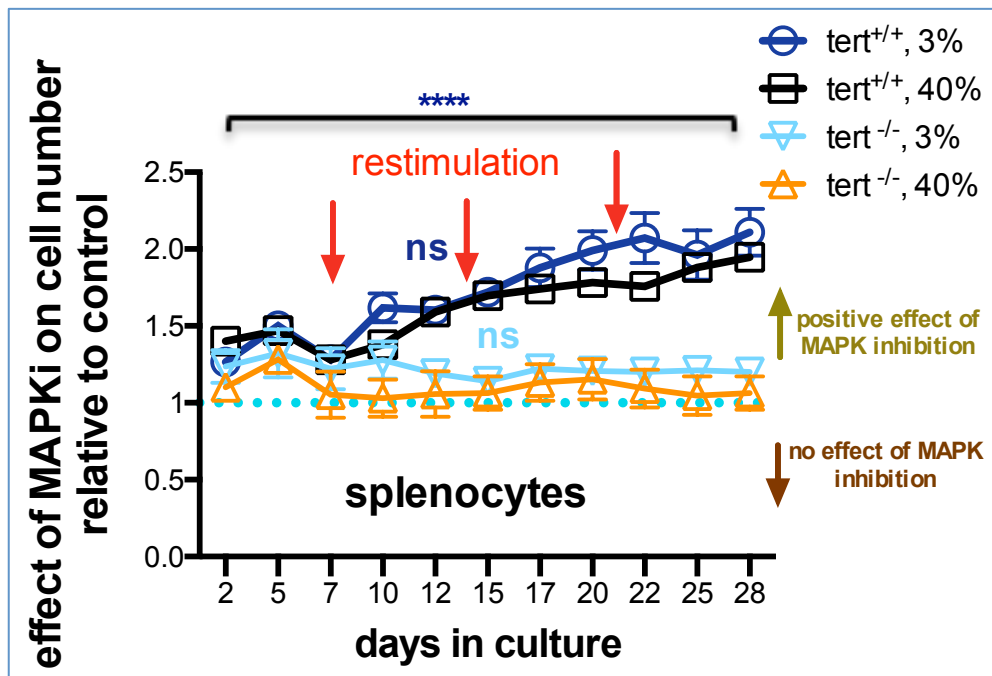


Figure 4.2. Long-term culture and growth curve of splenocytes treated with 500nM MAPKi under different oxygen saturations

Splenocytes from Tert^{+/+} and Tert^{-/-} mice were seeded at 2×10^6 /well (volume = 2ml/well) in a 24-well plate. Medium was changed, 500nM/ml MAPKi and 1.5 μ g/ml IL-2 were added every 2-3 days for all experiments. T lymphocytes were activated every 7 days (days 0, 7, 14, and 21 if necessary) by adding CD3e/CD28-Biotin micro-beads at a 1:1 ratio (Miltenyi T-cell expansion kit). Cells were cultured either under 3% (hypoxia) or under 40% (hyperoxia) oxygen saturation. Effect of MAPKi on cells number was calculated as relative to individual control for each group (without MAPKi). All values are displayed as mean \pm sem (Tert^{+/+} (3% n=4), (40% n=3), Tert^{-/-} n=3)). **** P<0.0001 for comparison of 3% vs. 40% oxygen saturation using two-way ANOVA.

Table 4.1. Primary cell counts ($\times 10^6$) of splenocyte growth curve from TERT^{+/+} mice cultured under 3% oxygen saturation.

Days in culture	3% O ₂ , control ($\times 10^6$)				3% O ₂ , 500nM MAPKi ($\times 10^6$)			
	Mouse 1	Mouse 2	Mouse 3	Mouse 4	Mouse 1	Mouse 2	Mouse 3	Mouse 4
0	2	2	2	2	2	2	2	2
2	5.85	5.35	4.9	5.14	7.55	6.93	5.56	6.87
5	10.55	9.8	8.75	9.13	14.5	15.13	13.76	13.95
7	14.88	13.13	12.88	13	18.38	17.19	16.45	16.93
10	23.28	21.31	18.12	20.56	37.75	35.98	29.25	31.88
12	28.68	25.5	24.25	25.17	43.5	43.41	38	40.85
15	32.75	31.25	27	29.45	56.88	55.25	45.51	49.65
17	41.25	40.88	32.13	35.1	80.2	75.1	59.2	65.54
20	45.68	43.25	35.08	38.9	93.63	84.13	69.98	76.12
22	52.08	48.12	39.25	44	113.5	99.5	79.88	87.11
25	63.41	53.35	46.85	51.04	128.4	107.93	88.1	97.14
28	64.53	56.12	49.99	52	137.8	124.05	99.45	108.1

Table 4.2. Primary cell counts ($\times 10^6$) of splenocyte growth curve from TERT^{+/+} mice cultured under 40% oxygen saturation.

Days in culture	40% O ₂ , control ($\times 10^6$)			40% O ₂ , 500nM MAPKi ($\times 10^6$)		
	Mouse 1	Mouse 2	Mouse 3	Mouse 1	Mouse 2	Mouse 3
0	2	2	2	2	2	2
2	3.7	3.61	3.13	4.91	5.1	4.6
5	5.13	4.95	4.58	7.65	7.13	6.76
7	8.3	8.11	7.87	10.5	11.2	9.42
10	14	13.65	12.92	19.87	17.25	18.61
12	17.12	16.74	15.97	26.75	25.48	27
15	21.73	20.45	21.1	39.13	34.23	33.95
17	27.83	25.52	26.4	50.7	46.75	41.13
20	30.25	29.15	28.25	57.13	51.8	47.46
22	34.1	34	32.35	62.88	58.2	55.13
25	36.25	37.09	35.15	71.7	65.02	67.14
28	38.7	39.11	37.25	78.22	71.98	73.72

Table 4.3. Primary cell counts ($\times 10^6$) of splenocyte growth curve from TERT^{-/-} mice cultured under 3% oxygen saturation.

Days in culture	3% O ₂ , control ($\times 10^6$)			3% O ₂ , 500nM MAPKi ($\times 10^6$)		
	Mouse 1	Mouse 2	Mouse 3	Mouse 1	Mouse 2	Mouse 3
0	2	2	2	2	2	2
2	2.74	2.9	3.7	2.92	4.1	4.5
5	3.41	3.45	5.22	3.57	5.87	6.54
7	4.69	5.21	8.75	5.78	7.2	9.81
10	7.03	7.3	11.24	9.75	9.11	13.85
12	10.45	8.5	13.25	12.12	11	15.2
15	12.8	11.3	17.85	14.79	14.24	18.74
17	14.44	11.7	19.85	18.19	16.87	21.17
20	17.21	13.4	23.24	20.1	19.24	25.75
22	18.54	14.5	25.5	20.9	22.5	26.94
25	20.3	15.87	27.81	23.24	25.21	29.22
28	22.1	17.4	29.21	25.25	26.7	30.45

Table 4.4. Primary cell counts ($\times 10^6$) of splenocyte growth curve from TERT^{-/-} mice cultured under 40% oxygen saturation.

Days in culture	40% O ₂ , control ($\times 10^6$)			40% O ₂ , 500nM MAPKi ($\times 10^6$)		
	Mouse 1	Mouse 2	Mouse 3	Mouse 1	Mouse 2	Mouse 3
0	2	2	2	2	2	2
2	2.45	2.4	3.21	2.63	2.7	3.54
5	2.91	2.8	4.28	4.04	3.9	4.91
7	4.64	4.6	7.9	4.67	4.91	8.45
10	6.75	6.7	10.46	6.8	6.9	10.95
12	8.71	7	12.25	8.99	7	13.6
15	10.98	10.05	16.11	11.57	10.97	16.96
17	11.5	10.1	17.28	14	11.3	18.81
20	13.4	12.25	20.4	17.16	13	22.87
22	15.5	13.13	23.87	18.1	14.45	24.85
25	18.32	14.4	26.25	19.21	15.37	27.15
28	20.6	16.2	27.2	22.75	16.95	28.27

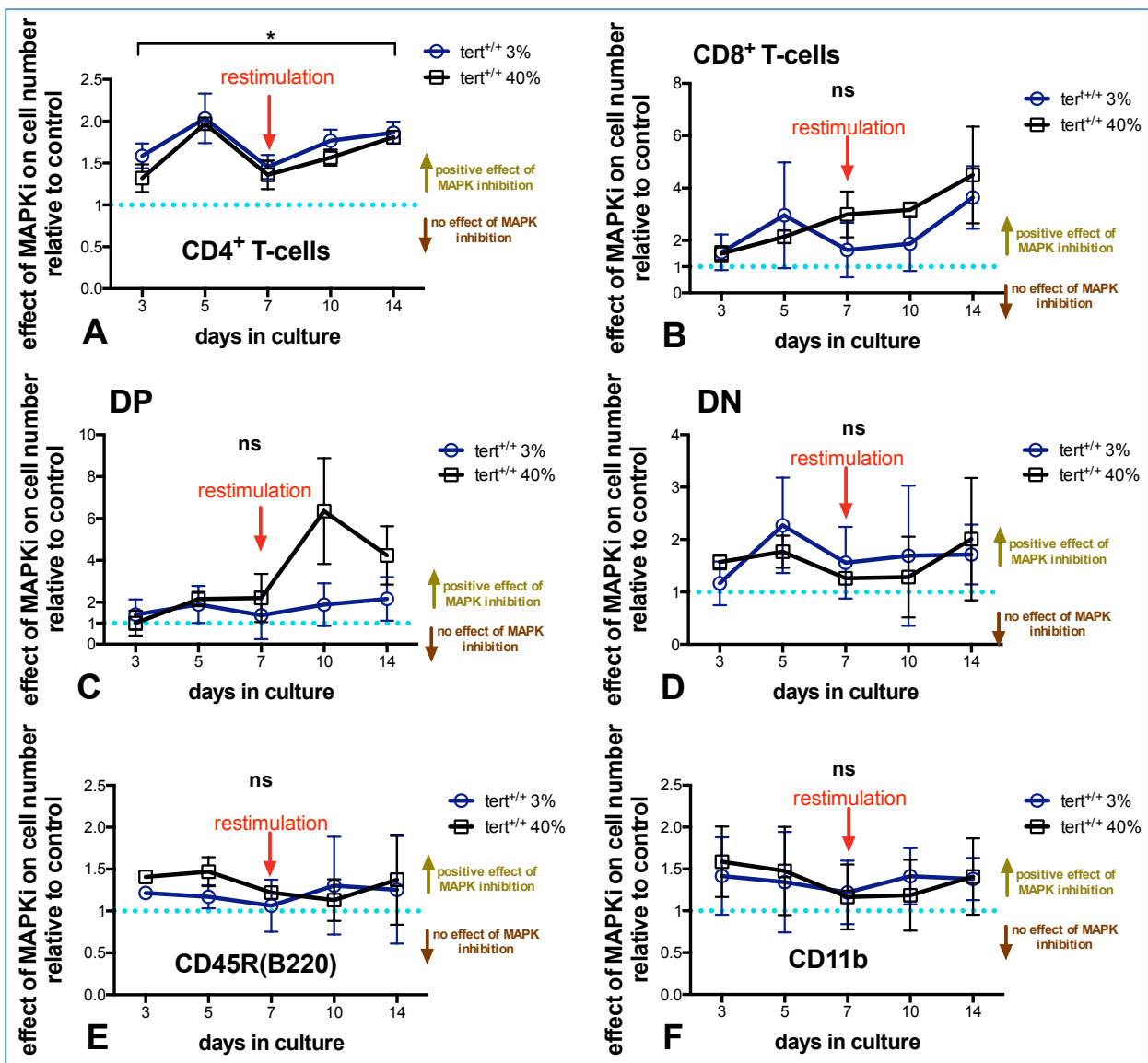


Figure 4.3. Long-term culture and growth curve of splenocyte subsets treated with 500nM MAPKi under different oxygen saturations.

Wild-type splenocytes were seeded at 2×10^6 cells/ml in a 24-well plate. Cells were cultured over 14 days; 500nM MAPKi and 1.5 μ g/ml IL-2 were added, and medium was changed every 2-3 days, under 3% and 40% O₂ saturation. Effect of MAPKi on cell number was calculated as relative to control. **A:** effect of MAPKi on CD4 T-cell number relative to control, **B:** effect of MAPKi on CD8 T-cell number relative to control, **C:** effect of MAPKi on DP T-cell number relative to control, **D:** effect of MAPKi on DN cells relative to control, **E:** effect of MAPKi on B-cell number relative to control, and **F:** effect of MAPKi on monocyte number relative to control. All values are displayed as mean \pm SEM (n=3). * P<0.05 for comparison of 3% vs. 40% oxygen saturation using 2-way ANOVA.

4.2.3 Effect of MAPK inhibition on splenocyte telomerase expression (*mTert*-GFP⁺) and telomerase activity under oxidative stress

4.2.3.1 Effect of MAPK inhibition on *mTert*-GFP⁺ reporter lymphocyte proliferation under oxidative stress

The *mTert*-GFP⁺ mice in this chapter were genotyped by another laboratory colleague, Dr. Gavin Richardson, IGM, Newcastle University.

The telomerase complex has various components, including the catalytic subunit, telomerase reverse transcriptase (TERT). TERT is distinct from other components in that it is transcriptionally regulated (Blackburn, 2005). According to Stewart et al. (2002), there is increasing evidence underlining the critical function of TERT in cell proliferation and differentiation. Ahmed et al. (2008) found that TERT also plays key roles in apoptosis and protection against oxidative stress, by entering mitochondria. Others have described a binding of TERT to mitochondrial DNA (Haendeler et al., 2009). There is a close correlation between *mTert*-GFP reporter expression and native mTert mRNA transcripts and telomerase activity in the tissue systems investigated (Montgomery et al, 2011; Stadtfeld et al., 2008).

As the expression of GFP⁺ cells driven by native mouse TERT promoter shows a high correlation with telomerase activity, I used splenocytes from *mTert*-GFP⁺ mice to test the expression of TERT when treated with MAPK inhibitor under hypoxia (3% O₂) and hyperoxia (40% O₂). Figure 4.4 shows a positive effect of MAPKi on *mTert*-GFP⁺ splenocytes proliferation at oxygen saturations of 3% and 40% respectively. However this effect was significant (P<0.01) under 3% O₂ (1.3-fold), compared to 40% O₂ at day 3. This increase continued, reaching a peak at day 10 (P<0.001) by 1.3-fold in favour of 3% vs. 40% O₂ saturation at the same day. At day 14 (the end of experiment) there remained a significant (P<0.05) effect under hypoxia of a 1.2-fold increase compared to hyperoxia. The reason for the difference in significance between hypoxia and hyperoxia may be the type of cell activation (described at figure 2.5), as in this experiment moderate activation was used whilst strong activation was used in experiments (4.2.2.1 and 4.2.2.1). Alternatively, it may be related to a different mouse genotype. Altogether, the MAPKi had a positive effect under both hypoxia and hyperoxia in *mTert*-GFP⁺ splenocytes.

4.2.3.2 Effect of MAPK inhibition on proliferation of lymphocyte subsets from *mTert*-GFP⁺ mice under oxidative stress

Splenocytes consist of T-lymphocytes, B-lymphocytes and monocytes as a majority population. I conducted this experiment to find out which lymphocyte subset has the greatest proliferation following MAPK inhibitor treatment under oxidative stress vs. hypoxia. Figure 4.5A shows that the CD4⁺ T-cells benefited the most from MAPKi treatment under both oxygen saturation conditions, especially under hyperoxia, which was significant ($P<0.05$) from (no effect) day 3 (first day testing the MAPKi effect) to day 14 (end of experiment), increasing by 1.4-fold. Also, under hypoxia MAPKi had a significant positive effect on cell proliferation at day 3 ($P<0.05$) by 1.5-fold and day 7 ($P<0.01$) by 1.4-fold, compared to hyperoxia 40% O₂. A positive effect was also observed on GFP⁺ expression under both oxygen saturation conditions that was non-significant (figure 4.5C); this supports the conclusion that the effect of MAPKi was telomerase-dependent. Figure 4.5B shows a positive trend of MAPKi on CD8⁺ T-cells under both hypoxia and hyperoxia (ns). B-cells (figure 4.5D) and monocytes (figure 4.5E) showed a similar trend under both oxygen conditions, but by the end of the experiments (day 14) there was no effect of MAPKi on these cells under 3% O₂, whereas the positive trend continued over the whole experiment under 40% O₂.

In conclusion, it seems that MAPK inhibitor treatment has a positive effect on cell proliferation under oxidative stress. This effect was present in splenocytes/CD4⁺ T-cells from *mTert*-GFP⁺ mice (different genotype), and the majority of proliferation is generated by CD4⁺ T-cells under both oxygen saturations.

4.2.3.3 Effect of MAPK inhibition on telomerase activation in splenocytes under oxidative stress

Inhibition of p38 MAPK activated the telomerase activity of CD4⁺ T-cells after TCR activation (Di Mitri et al., 2011). This experiment was conducted to evaluate the effect of MAPKi on telomerase activity in splenocytes under oxidative stress vs. hypoxia. Splenocytes were expanded under both 3% and 40% oxygen saturation as described at (2.2.5). Telomerase activity was quantified at different time points using TRAP ELISA as described at (2.2.11).

Figure 4.6 shows a trend for a positive effect of MAPKi on telomerase activity under hypoxia which seems to be stable during the experiment. There is no clear explanation for the absence of any effect of MAPKi on telomerase activity under hyperoxia at the beginning of experiments (days 3, 5 and 7). By day 10 a positive effect was also observed under hyperoxia

(2.1-fold compared to telomerase activity at day zero). This positive trend continued until it became significant ($P<0.05$) at day 14 by 2.9-fold compared to hypoxia (3% O₂) at day 14, and by 3.7-fold compared to telomerase activity at day zero ($P<0.01$). Compared to *mTert*-GFP⁺ telomerase expression at figure 4.5C and to the splenocyte proliferation experiments under hypoxia and hyperoxia at figure 4.4, I noticed that the number of cells and also the telomerase expression in GFP⁺ cells under hyperoxia was less than under hypoxia, whilst the telomerase activity after time (days 10 and 14) under hyperoxia was higher than under hypoxia.

This implies that under hyperoxia, even when the number of cells or expression of telomerase are lower, MAPKi maintains these low cell numbers, and expression of telomerase is more active under disadvantaged conditions of oxidative stress, to enable cell survival.

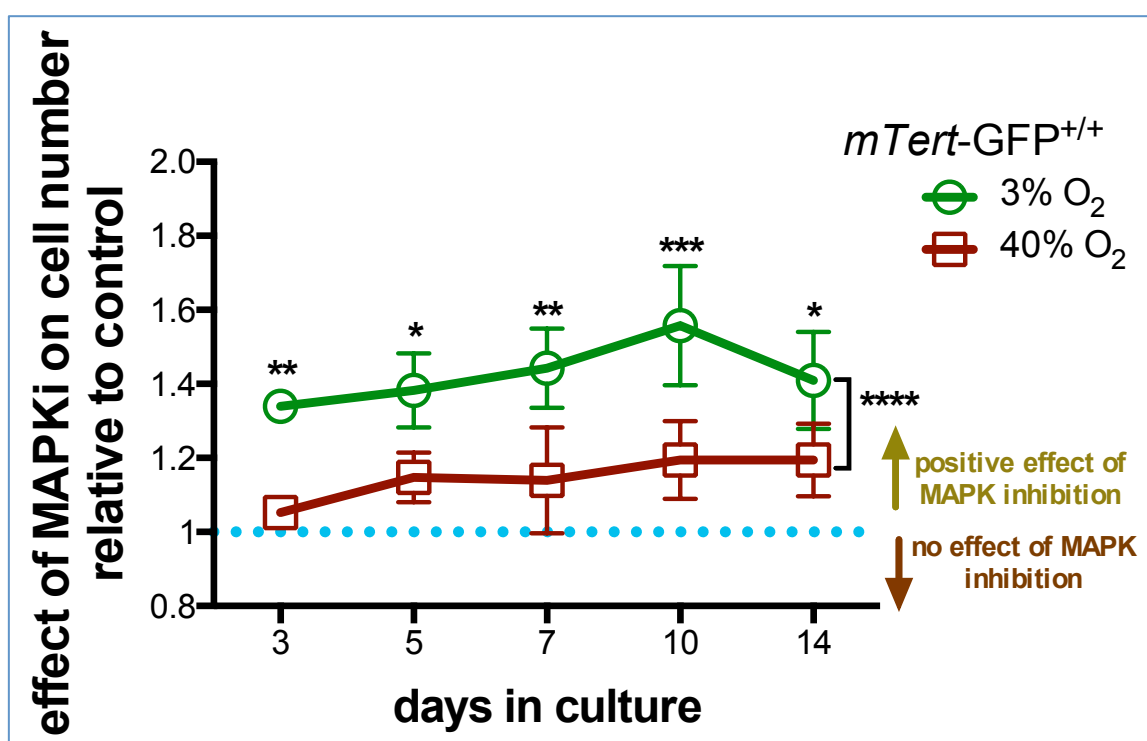


Figure 4.4. Long-term culture and growth curve of splenocytes from transgenic *mTert*-GFP⁺ mice treated with 500nM MAPKi under different oxygen saturations.

Splenocytes from transgenic *mTert*-GFP⁺ mice were seeded at 2x10⁶/ml in a 24-well plate and coated overnight at 4°C with anti CD3 and CD28 antibodies (prepared at 1μl/ml PBS). Medium was changed, 1.5μg/ml IL-2 and 500nM MAPKi were added every 2-3 days for all experiments. Cells were cultured either under 3% (hypoxia) or under 40% (hyperoxia) oxygen saturation for 14 days. Effect of MAPKi on cell number was calculated as relative to control. All values are displayed as mean±sem (n=4). * $P<0.05$, ** $P<0.01$, *** $P<0.001$, **** $P<0.0001$ for comparison between 3% vs. 40% oxygen saturation using 2-way ANOVA.

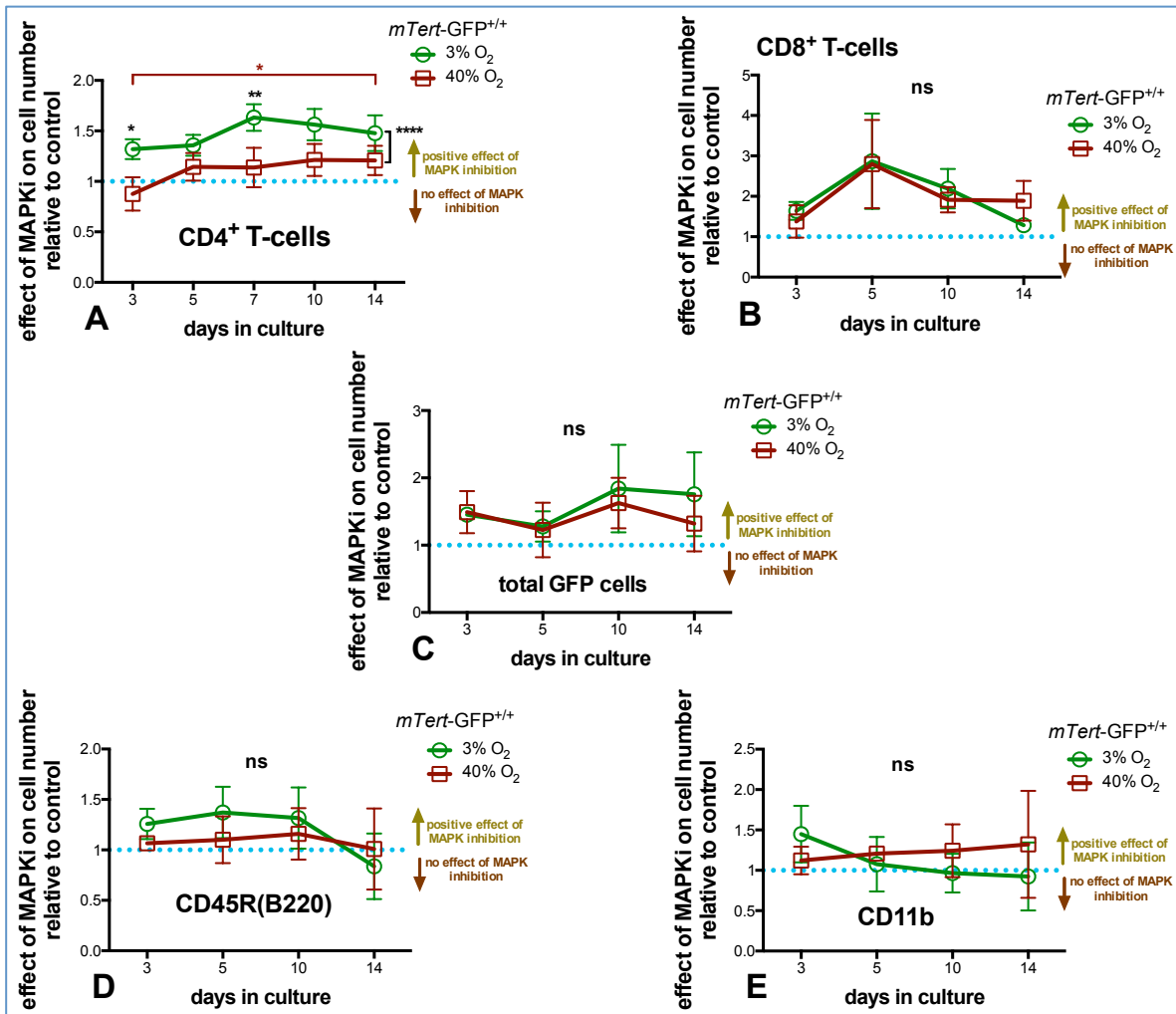


Figure 4.5. Long-term growth curve of T-cells from transgenic *mTert-GFP*⁺ mouse splenocytes treated with 500nM MAPKi under different oxygen saturations.

Splenocytes from *mTert-GFP*⁺ reporter mice were seeded at 2×10^6 /ml in 24-well plates coated with CD3 and CD28 antibodies overnight for 14 days. The cells were then cultured in incubators with 3% and 40% oxygen saturation. Medium was changed, 1.5 μ g/ml IL-2 and 500nM MAPKi were added every 2-3 days for all experiments. Then, at each time point (days 3, 5, 7, 10 and 14), cells were harvested and surface marker expression of native GFP relative to CD45R, CD11b, CD4⁺ and CD8⁺ was measured against negative controls using a compensated FACSCanto II running FACSDiva software; 50,000 live events were analysed to determine the proportion of T-cell types. Effect of MAPKi on cells number was calculated as relative to control. **A:** effect of MAPKi on CD4 T-cells number relative to control, **B:** effect of MAPKi on CD8 T-cell number relative to control, **C:** effect of MAPKi on GFP cells number relative to control, **D:** effect of MAPKi on B-cell number relative to control, **E:** effect of MAPKi on monocytes number relative to control. All values are displayed as mean \pm sem (n=4). * P<0.05, ** P<0.01, *** P<0.0001 for comparison between 3% vs. 40% oxygen saturation using 2-way ANOVA.

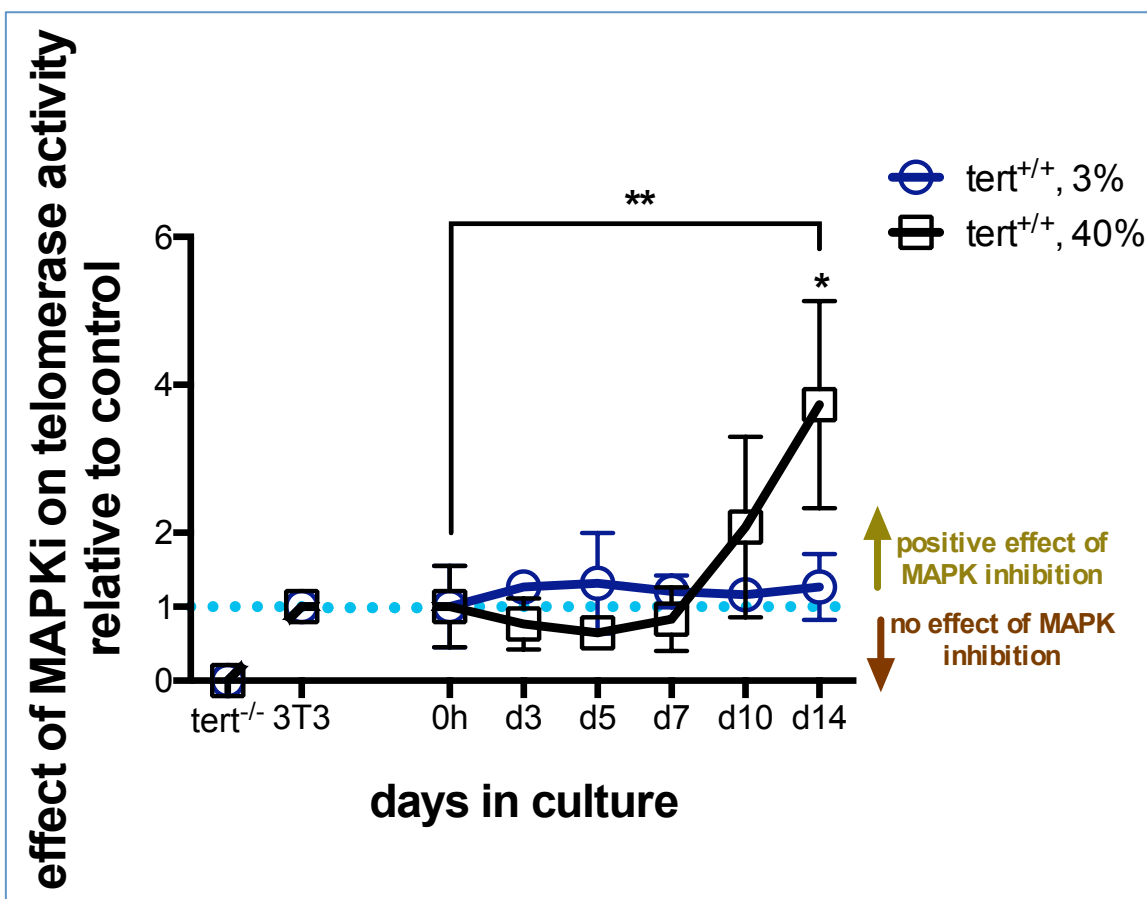


Figure 4.6. MAPKi treatment rescues telomerase activity in wild-type mice splenocytes treated under hyperoxia

Splenocytes from wild-type mice were generated by seeding 2×10^6 /ml in a 24-well plate at day 0, and plates were coated overnight at 4°C with anti CD3 and CD28 antibodies. Medium was changed; 500nM MAPKi and 1.5 $\mu\text{g}/\text{ml}$ IL-2 were added every 2-3 days, under 3% and 40% oxygen saturation. Cells were harvested at each time point (days 3, 5, 7, 10 and 14), then cells were cryopreserved at -80°C . TRAP-PCR was run with 500ng protein loaded and 100ng for 3T3 (positive control). Effect of MAPKi on telomerase activity was calculated relative to its control. All values are displayed as mean \pm sem (n=5). *P<0.05, ** P<0.01 for comparison of 3% vs. 40% oxygen saturation using 2-way ANOVA.

Table 4.5. Primary results of mouse splenocyte telomerase activity measured by TRAP-ELISA (absorbance 450nM)

Days in culture	Mouse 1	Mouse 2	Mouse 3	Mouse 4	Mouse 5
3% O₂, control					
0h	1.1	0.125	0	0.5	0.11
d3	0	1.639	0.862	1.2	1.15
d5	0.082	0.684	1.11	0.015	0.65
d7	1.87	0.023	1.323	1.25	0.6
d10	1.8	0.245	1.531	1.09	1.2
d14	0.44	1.198	0.142	0.8	1.37
3% O₂, 500nM MAPKi					
0h	1.1	0.125	0	0.5	0.11
d3	1.198	1.679	0.731	1.2	1.35
d5	0.006	1.352	1.659	0.2	0.135
d7	1.943	0.643	1.33	1.25	0.95
d10	1.692	1.711	0.961	1.25	1.2
d14	1.761	1.756	0.345	0.065	1.085
40% O₂, control					
0h	1.1	0.125	0	0.5	0.11
d3	0.153	1.072	0.095	0.7	0.93
d5	1.554	1.375	1.745	1.15	1.25
d7	0.569	0.3	0.171	0.15	0.07
d10	0.067	0	0.121	0.14	0.01
d14	0.032	0.04	0.11	0	0
40% O₂, 500nM MAPKi					
0h	1.1	0.125	0	0.5	0.11
d3	0.073	0.867	0.003	0.325	1
d5	1.626	1.021	0.11	0.71	1.11
d7	0	0.533	0.111	0	0.4
d10	0	0.12	0.131	0	0.45
d14	0.319	0.085	0.033	0.17	0.072

4.2.4 Effect of MAPK inhibition on the proliferation of activated pure CD4⁺ T-cells under oxidative stress

Splenocytes were expanded for 14 days as described at (2.2.7), then CD4⁺ T-cells were purified by immunomagnetic bead-isolation as described at (2.2.6), to find the effect of MAPK inhibitor on CD4⁺ T-cell proliferation under hyperoxia. Figure 4.7 shows that a significant (P<0.0001) positive effect of MAPKi on TERT^{+/+} CD4⁺ T-cell proliferation under hypoxia from day 5 (1.36-fold) until the end of the experiment at day 15 (1.56-fold), compared to hyperoxia. But under oxidative stress, MAPKi had a positive effect on CD4⁺ T-cells similar to the positive effect of MAPKi on TERT^{-/-} samples (under both oxygen saturation conditions).

There was no effect of MAPKi on cell proliferation in TERT^{-/-} CD4⁺ T-cells under hypoxia and hyperoxia. This suggests that the effect of MAPKi on TERT^{+/+} CD4⁺ T-cells under hyperoxia is not telomerase-dependent and may, due to the lack of cytokines secreted by other splenocytes, improve TERT^{+/+} CD4⁺ T-cells more strongly under oxidative stress and increase survival rates.

Taking all this information together, I can conclude that the effect of MAPKi was telomerase-dependent in the presence of other splenocytes in the subset (e.g. B-cells and monocytes) and that it interacted with its secretion (cytokines).

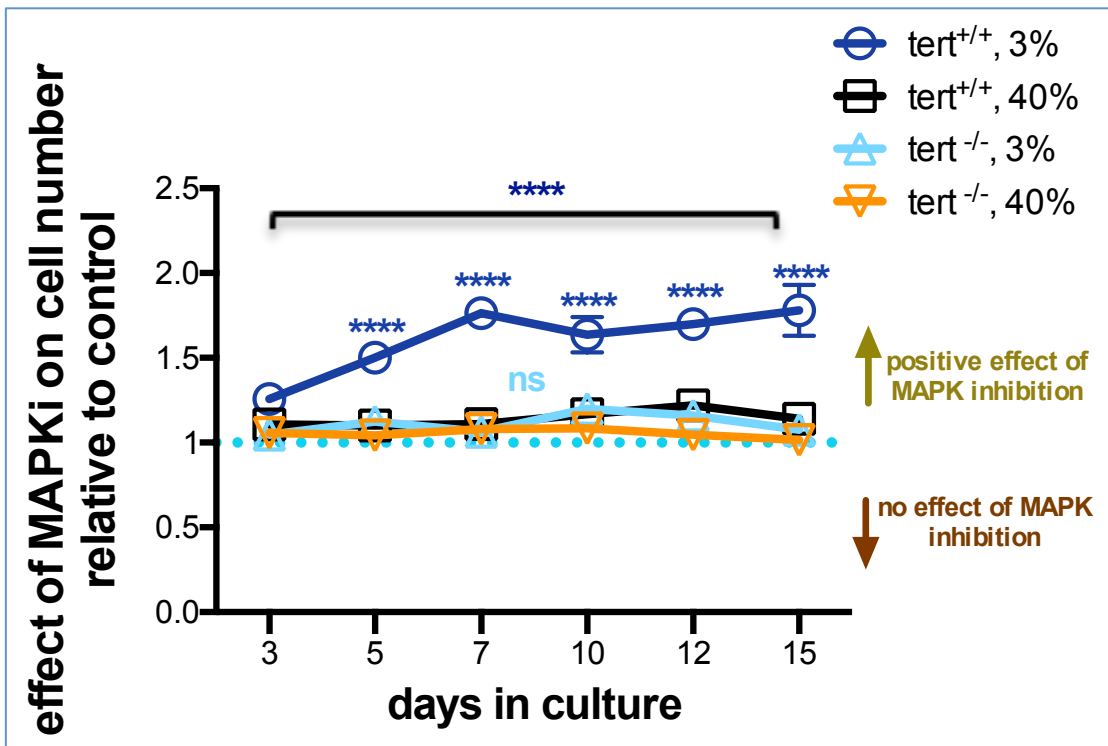


Figure 4.7. MAPKi improves proliferation of pure CD4⁺ T-cells under 3% oxygen in a TERT dependent manner

CD4⁺ T cells from either Tert^{+/+} or Tert^{-/-} mice were seeded at 2x10⁵ cells/well (volume = 200µl/well) in a 96-well plate. CD4⁺ T-cells were generated by immunomagnetic bead-isolation from splenocytes, which were cultured for 14 days with anti-CD3 and anti-CD28 antibodies. Medium was changed, 500nM/ml MAPKi and 1.5µg/ml IL-2 were added every 2-3 days for all experiments. T lymphocytes were activated every 7 days (days 0, 7, 14, and 21 if necessary) by adding CD3e/CD28-Biotin micro-beads at a 1:1 ratio (Miltenyi T-cell expansion kit). Cells were cultured either under 3% (hypoxia) or under 40% (hyperoxia) oxygen saturation. Effect of MAPKi on cell numbers was calculated as relative to individual control (no MAPKi) for each group. All values are displayed as mean±sem (n=3). **** P<0.0001 for comparison of 3% vs. 40% oxygen saturation using two-way ANOVA.

4.3 Discussion

As described in chapter 3, hyperoxia induced oxidative stress, which led to decreased T-cell proliferation, suppressed telomerase activity, and enhanced transcription of IFN- γ mRNA. In this chapter, splenocytes were treated with mitogen-activated protein kinase inhibitor (MAPKi) under oxidative stress (40% O₂) as well as under hypoxia (3% O₂). I found MAPKi significantly reduced IFN- γ levels under hyperoxia, indicating that MAPKi might resist or prevent the effect of oxidative stress on cell proliferation under hyperoxia. By day 3, the IFN- γ levels were almost equal under both hypoxia and hyperoxia. This matches previous studies which found that MAPKi can reduce IFN- γ secretion *in vitro*, causing less inflammation (Sarov-Blat et al., 2010; Cheriyan et al., 2011).

The second significant finding here is that lymphocytes from TERT^{+/+} mice proliferated almost equally under both hypoxia and hyperoxia when MAPKi was used. This suggests that the suppressive effect of oxidative stress on cell proliferation might be inhibited by MAPKi under hyperoxia. However, with TERT^{-/-} mice, the positive effect of MAPKi was almost equal under both oxygen conditions and there was no change in proliferation pattern relative to the control group under either 3% or 40% oxygen saturation (figure 4.2 and figure 4.7). This suggests that the effect of MAPKi on cell proliferation required the presence of TERT. When I explored the effect of MAPKi on splenocyte subsets (when CD4⁺ T-cells are purified), I found a positive effect under both oxygen saturations, with no significant changes on cell proliferation numbers. This is contrary to the significant changes in splenocyte proliferation (chapter 3) when MAPKi was not present. The most apparent effect of MAPKi was generated by CD4⁺ T-cells under both hypoxia and hyperoxia. From this, we can conclude that MAPKi maintains splenocytes and CD4⁺ T-cell health under hyperoxic conditions might be through counteracting the effect of IFN- γ , which is produced under conditions of oxidative stress. MAPK inhibition enhanced CD4⁺ T-cell proliferation (figure 4.7) only under hypoxia when using purified CD4⁺ T-cells.

MAPK inhibition seems to exert a trend toward higher telomerase activity (figure 4.6) in the TRAP qPCR (ns). Under hyperoxia, MAPK inhibition enhanced telomerase activity by day 10, showing significantly increased telomerase activity by day 14 (P<0.05). The proliferative effect of the MAPK inhibitor seems to be telomerase-dependent. Atherosclerotic plaques may be more stable under MAPKp38 inhibition, which would consequently slow down the atherogenesis, inhibit myocardial apoptosis and ultimately benefit post-ischaemic myocardial cardiac function (Ma et al., 1999). IFN- γ secretion has been shown to be reduced by p38

MAPKi, resulting in decreased inflammation in human coronary artery rings (Ranjbaran et al, 2007), reduced myocardial apoptosis, and better post-ischaemic cardiac function (Ma et al, 1999). CD4⁺ T-cell survival following TCR activation is greatly increased when p38 signalling is inhibited, and telomerase activity was also enhanced in these cells (Di Mitri et al., 2011). When the p38 signalling pathway is blocked, both cell proliferation and telomerase activity are increased following human T-cell stimulation (Di Mitri et al., 2011). When p53 is activated, both senescence and DNA damage are increased as a result of oxidative stress (Liu and Xu, 2011). When DNA damage occurs, p38 MAPK is activated, which leads to pRb/p16 and p53 pathway activation, both of which contribute to the progression of senescence (Passos et al., 2010; Freund et al., 2011; Iwasa et al., 2003). Following CD4⁺ T-cell stimulation, both telomerase activity and proliferation were seen to be increased (Di Mitri et al., 2011). Furthermore, it has been shown that p38 MAPK inhibition can increase mitochondrial mass, which leads to better mitochondrial function and possibly improved proliferation (Henson et al., 2014).

CHAPTER 5. Effect of voluntary exercise on telomerase and regulatory T-lymphocytes in mice

5.1 Introduction

Good health is closely linked with regular physical exercise. In humans, aerobic exercise is associated with reduced cardiovascular risk (Tanasescu et al., 2002) and, in the presence of cardiovascular disease, with lower mortality rates (Jolliffe et al., 2001; Piepoli et al., 2014; Taylor et al., 2004). More broadly, a wide range of conditions including cancer (Juarranz et al., 2002), osteoporosis (Kemmler et al., 2004) and depression (Blumenthal et al., 1999) are positively affected by physical exercise. Furthermore, telomere length and telomerase activity increase in PBMNCs in sedentary middle-aged men after 3 months of exercise for telomerase activity, and after 4 months for telomere length (Melk et al., 2014). In a murine model, male wild-type (C57BL/6) mice had a significantly decreased body weight after 5 weeks of voluntary wheel running exercise compared to the sedentary male group mice. Decreasing body weight was not significant in female mice compared to the sedentary female group. In contrast, female mice ran faster and longer than male mice on the voluntary wheel running exercise. Furthermore, the absolute heart rate was significantly increased in the female group under exercise compared to the non-exercise female group. In the male exercising group, this increase was not significant (De Bono et al., 2006).

Various complex diseases have been studied at a molecular level in genetically modified mouse models. In this chapter I employed apolipoprotein (ApoE) knockout *mTert*-GFP⁺ and other mouse genotypes, which have been used to study the effects of exercise on atherosclerosis (Okabe et al., 2006). It is known that atherosclerosis in ApoE^{-/-} mice is caused by accumulation of fat inside the capillaries, when a high fat diet is consumed (Mahley, 1988; Piedrahita et al., 1992). Our combined ApoE^{-/-}*mTert*-GFP⁺ mice were bred in our laboratory, to investigate telomerase activity and expression under different diet and exercise regimes.

5.2 Results

5.2.1 Effect of voluntary wheel running exercise on C57BL/6 wild-type mice

5.2.1.1 Variability and spatial pattern of speed and duration during voluntary wheel running exercise on C57BL/6 wild-type mice

As C57BL/6 strain mice are widely used in physiological and genetic mouse studies (De Bono et al., 2006; Mekada et al., 2009), I also used them in this experiment. Small groups were used initially, to test our computer system and the running facilities. These were created by Dr. Bill Chaudhry and modified from De Bono et al. (2006), as described at 2.2.15. 2 male and 2 female 8-week old C57BL/6 mice were individually provided with an angled wheel running exercise. After 3 weeks of voluntary wheel running, monitored by digital odometers activated by wheel rotation (Enduro 2), both genders had reached over 4 hours of exercise per day (Figure 5.1A).

However, the female mice spent more time on the running wheel, especially in the second half of experimental period (days 13 to 22). Males peaked at 5 hours of exercise per day, while females reached up to 7 hours. There was a significant (2.1-fold, $P<0.05$) increase in terms of time spent running for the female group (from 3.1 hours to 6.5 hours at the end of exercise). The male group ($P<0.05$) increased their exercise by 1.3-fold, from 3.8 hours at the beginning of the experiment to 4.9 hours at the end of experiment.

During the exercise period, female mice ran larger distances than the males (Figure 5.1B) especially in the second half of the experiment (females ran 18.3 km per 24 hours ($P<0.0001$), increasing by 5.2-fold, while males reached 13.4 km per 24 hours, increasing by 2.8-fold).

The average running speed for both groups (Figure 5.1C) almost reached the same level during the exercise period, without significant changes between either of them. However, there were significant changes for individual groups between starting average speed and the end-point average speed (2.5-fold for the female group ($P<0.0001$) and 2.2-fold in the male group ($P<0.0001$)).

Figure 5.1D shows the maximum speed at the upper 99.9th percentile of the interval histogram. By the end of exercising, the female mice reached 35 ± 0.13 km/h and the males reached 25 ± 2.2 km/h ($P<0.0001$) in 24 hours.

5.2.1.2 Diurnal pattern of TERT^{+/+} wild-type mice on voluntary wheel running exercise

Running activity was recorded continuously (in-second frames), which allowed analysis of individual diurnal exercise patterns. Both male and female mice ran almost exclusively during the dark time (Figure 5.2). However, the females' average wheel rotation (speed) was higher per hour than male mice, especially at night (ns). From this, we can conclude that the computerised recording system of voluntary wheel running exercise is a good and sufficient measure to determine mouse activity at all times, including night time. Mice are a good model for voluntary wheel running exercise and have a nocturnal tendency. Female mice were more active than male mice.

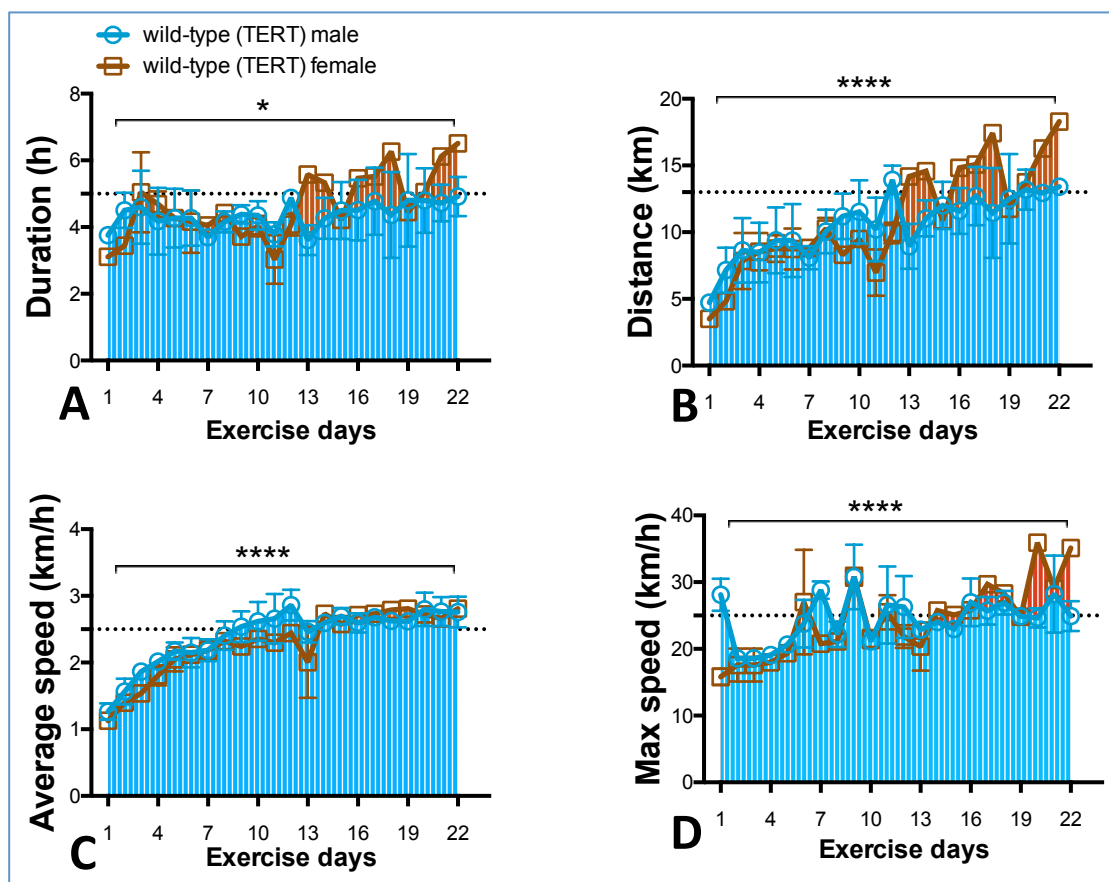


Figure 5.1. Daily running parameters for TERT^{+/+} wild-type mice:

TERT^{+/+} wild-type mice were subjected to a voluntary wheel running exercise (using a computerized system to record and analyse individual wheel rotations) for 3 weeks. 2 male and 2 female mice were used, both on normal diet. **A**: mean daily time (h) spent wheel running, defined as continuous exercise with a maximum interval between detected wheel rotations of 5 seconds. **B**: mean daily running distance (km) calculated by wheel circumference x the total of wheel rotations. **C**: mean daily average speed (km/h) calculated by the total distance run/total running time during each 24-hours period. **D**: mean daily maximum speed (km/h), the speed at the upper 99th percentile of wheel rotation speeds from all individual wheel rotation time intervals in a 24-hours period. All values are displayed as a standard deviation (SD). * P<0.05, **** P<0.0001 for comparison of male group vs. female group using two-way ANOVA.

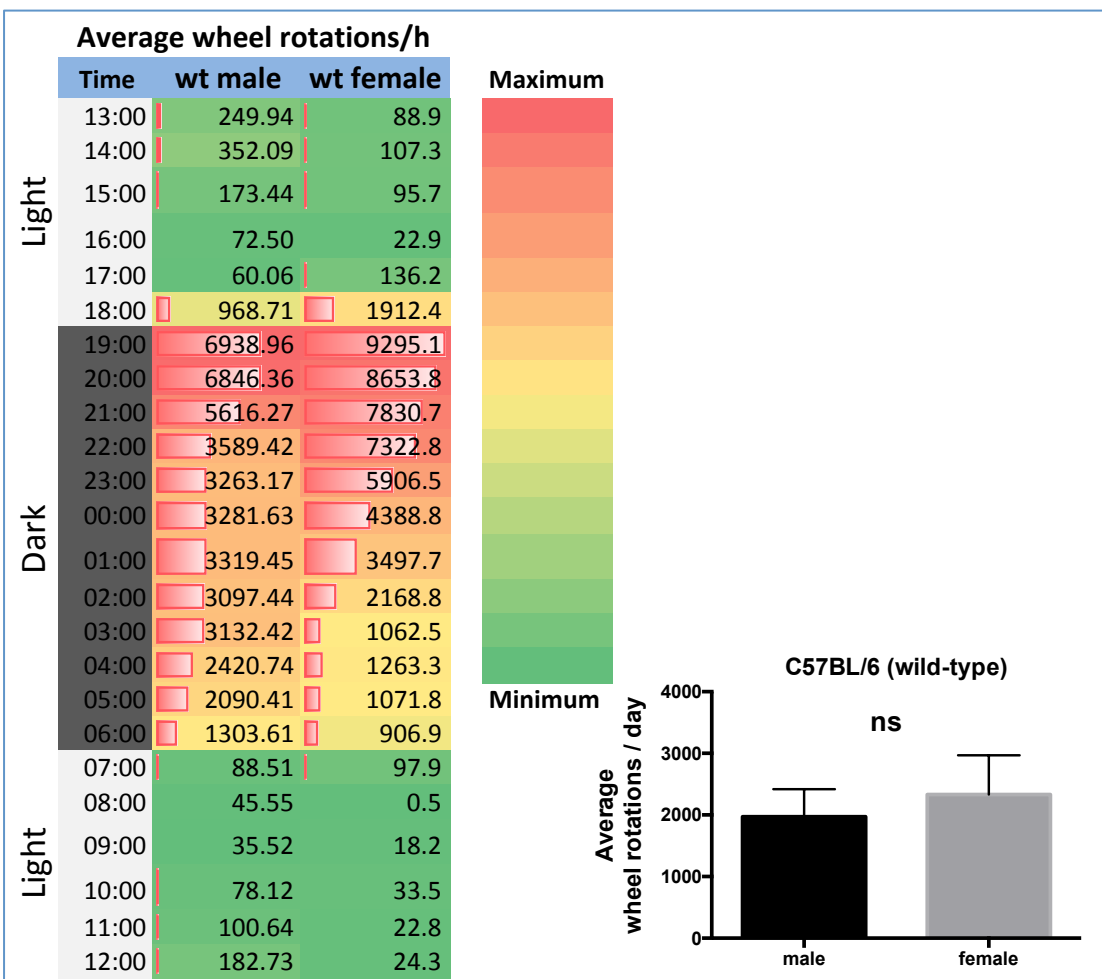


Figure 5.2 Diurnal patterns of average wheel rotations per hour for TERT^{+/+} wild-type mice

TERT^{+/+} wild-type (C57BL/6) mice on voluntary wheel running exercise for 3 weeks. 2 male mice vs. 2 female mice, both on a normal diet. Number of wheel rotations per hour were averaged for each group. All values are displayed as a standard deviation (SD). No significant (ns) for comparison of male vs. female average wheel rotations using unpaired T-test, two-tailed.

5.2.2 Effect of voluntary wheel running exercise on TERT^{+/−} (heterozygous) mice

5.2.2.1 Variability and spatial pattern of speed and duration during voluntary wheel running exercise on TERT^{+/−} (heterozygous) mice

The main goal for this chapter is to find the effect of exercise on telomerase activity and to further test our computerised recording system of voluntary wheel running exercise. This was conducted on TERT-heterozygous mice as these mice were available from Dr. Gabriele Saretzki's lab, and also since using these it was possible to investigate the effect of heterozygous telomerase deficiency on mouse activity. 5 female TERT heterozygous mice were randomly entered into the study as the exercising group for 7 weeks, vs. 5 female TERT heterozygous mice randomly selected as the control group (no exercise). Both groups were on a normal diet and 7-9 months old. Figure 5.3A shows that these mice started at 2.5 hours exercise per day. It is very noticeable that the time spent exercising varied considerably from mouse to mouse and from day to day until they peaked at day 23 and spent about 6 hours exercising per day. Following this, the peak declined to a trough of 2.8 hours at day 34, which is still higher than the first day's run. This decline came after about 3 weeks of increasing the duration of running. I suspected that the mice required some recovery time for the second increasing running duration, which continued until the end of the study, reaching 4.54 hours of exercising during a 24-hour period.

Figure 5.3B shows the variation in distance covered during the experiment, which started from about 2.94 km per day, peaking at day 23 (15.2 km during 24 hours), then declining to a trough of 5.4km at day 34. Then after a prospective recovery stage, the distance covered increased until the end of experiment, reaching about 10.8 km.

Average speed (Figure 5.3C) reached 2.51 km/h (peak) at day 23, which started from 1.01 km/h at day one and reached 2.43 km/h at the end of experiment. Maximum speed (Figure 5.3D) almost reached 25 km/h on most days. However, it started from 18.6 km/h at day one and reached about 21.6 km/h by the final day.

Together with the 7-9 month old mice, at some points mice might have needed some recovery time before starting to do more running. Furthermore, the computerised monitoring system generated clear data regarding the activity of individual mice.

5.2.2.2 Diurnal pattern of TERT^{+/−} (heterozygous) mice on voluntary wheel running exercise

Figure 5.4 shows the circadian pattern of wheel rotation during each hour per day. However, the mice do more voluntary activity at night time; this activity disappears during day time (light). The peak of average number of wheel rotations was at 3772.7 rotations per 24 hours.

5.2.2.3 Effect of voluntary wheel running exercise on weight of TERT^{+/−} (heterozygous) mice

During the voluntary wheel running exercise, mice were weighed weekly, whilst the control group (no exercise) was only weighed at the beginning and end of the study. Both groups were on a normal diet. Figure 5.5 shows a significant ($P<0.05$) difference in body weight between the exercising group (26.24 ± 2.4 g) and the control group (28.84 ± 0.87 g) by the end of study. However, the exercising group showed a decrease in body weight, especially during the first two weeks of exercise. Body weight then increased, but not far from original weight (26.14 ± 2.7 g) vs. (26.24 ± 2.4 g) at the end of study (ns). There was a significant ($P<0.05$) weight increase for non-exercise mice (26.94 ± 1.41 g at the start vs. 28.84 ± 0.87 g at the end of study). Finally, after 7 weeks of voluntary wheel running, the exercise led to control weight in TERT^{+/−} mice.

5.2.2.4 Effect of voluntary wheel running exercise on splenocyte numbers in TERT^{+/−} (heterozygous) mice

After 7 weeks, both groups were dissected and splenocytes isolated. After washing, cells were counted using the Neubauer chamber as described under 2.2.2. Figure 5.6 shows a non-significant trend for an increase in splenocyte numbers for the training group ($28.1\pm1.2 \times 10^6$ cells vs. $25.4\pm2 \times 10^6$ cells for the control group). Under voluntary wheel running exercise, no major changes in lymphocyte numbers were observed in spleens from TERT^{+/−} mice.

5.2.2.5 Effect of voluntary wheel running exercise on splenocyte subpopulations of TERT^{+/−} (heterozygous) mice

Splenocytes were phenotyped into the main populations by flow cytometer as described in 2.2.9.2. There was a trend towards an increased percentage in favour of the training group for CD4⁺ T-cells (Figure 5.7A), $9.5\pm0.9\%$ per spleen vs. $8.4\pm0.5\%$ per spleen in the non-training group (ns) and for CD8⁺ T-cells (Figure 5.7B), $5.3\pm0.5\%$ per spleen vs. $4.3\pm1.04\%$ per spleen in the non-training group (ns). Furthermore, there were some trends in the percentage of

double positive (DP) T-cells (Figure 5.7C), double negative (DN) T-cells (Figure 5.7D), B-cells (Figure 5.7E) and monocytes (Figure 5.7F) between both groups. Thus, in summary, there were no significant differences detected for any splenocyte subset under exercise compared to the non-exercise group.

5.2.2.6 Effect of voluntary wheel running exercise on splenocyte regulatory T-cells of TERT^{+/−} mice

Immune function in mice was found to be enhanced by regular moderate physical activity, such as the wheel-running exercise. Previous studies showed that T-cell mediated immunity, Th1 response and NK cell activity were potentiated in response to exercise in both humans and animals (Sugiura et al., 2001; Davis et al., 2004; Murphy et al., 2004).

The purpose of this experiment was to determine the effect of voluntary wheel running exercise on the percentage of regulatory T-cells in TERT^{+/−} mice. Splenocytes from exercise trained mice were isolated and T-cell surface markers were stained and detected by FACS as described at 2.2.9. Figure 5.8A shows a trend towards an increase in percentage of CD4⁺FoxP3⁺ cells 2.4±0.4% per spleen for the exercise group vs. 2±0.4% per spleen for the non-exercise group. Figure 5.8B shows a trend for an increase in percentage of CD4⁺CD25⁺ in favour of the exercise group (0.35±0.04% per spleen vs. 0.33±0.03% per spleen in the non-exercise group). The same trend is noticeable for the percentage of CD4⁺FoxP3⁺CD25⁺ (figure 5.8C), increasing by 0.94±0.06% per spleen vs. 0.89±0.08% per spleen in the non-exercise group. However, this trend disappeared for the percentage of CD4⁺FoxP3[−]CD25⁺ 12.1±0.98% per spleen vs. 12.1±0.49% per spleen for the non-exercise group (figure 5.8D). Thus, in summary, in these mice, there was no clear effect on regulatory T-cells (as they are healthy mice) and the benefit of running exercise may be converted to physiological muscle strength (this was observed for mice on exercise, but not measured here) and blood circulation improvement (Baltgalvis et al., 2012; Hayes and Williams, 1998).

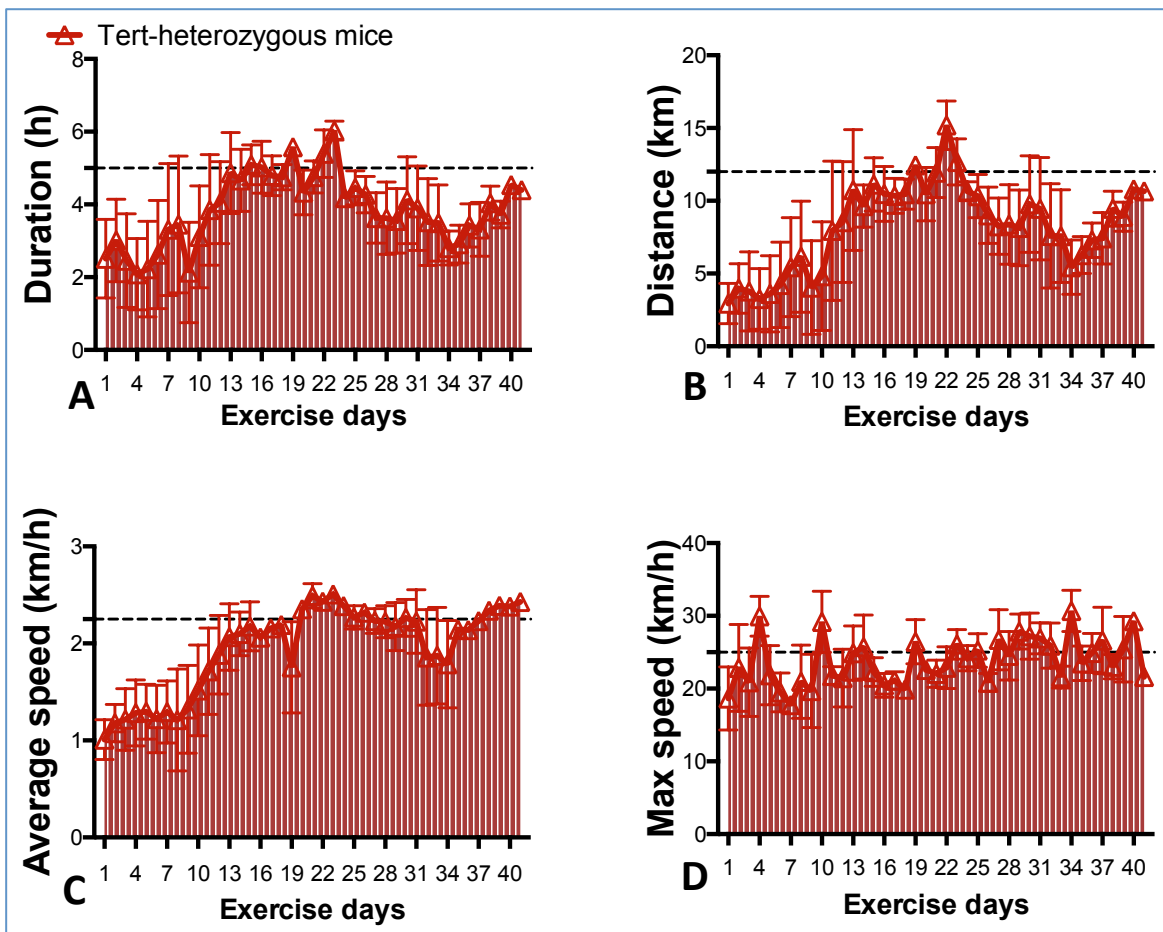


Figure 5.3. Daily running parameters for $\text{TERT}^{+/-}$ (heterozygous) mice

$\text{TERT}^{+/-}$ (heterozygous) mice were subjected to a voluntary wheel running exercise (using a computerized system to record and analyse individual wheel rotations) for 7 weeks. 5 female mice on exercise with a normal diet. **A:** mean daily time (h) spent wheel running, defined as continuous exercise with a maximum interval between detected wheel rotations of 5 seconds. **B:** mean daily running distance (km) calculated by wheel circumference x the total of wheel rotations. **C:** mean daily average speed (km/h) calculated by the total distance run/total running time during each 24-hour period. **D:** mean daily maximum speed (km/h), the speed at the upper 99th percentile of wheel rotation speeds from all individual wheel rotation time intervals in a 24-hour period. All values are displayed as mean \pm sem.

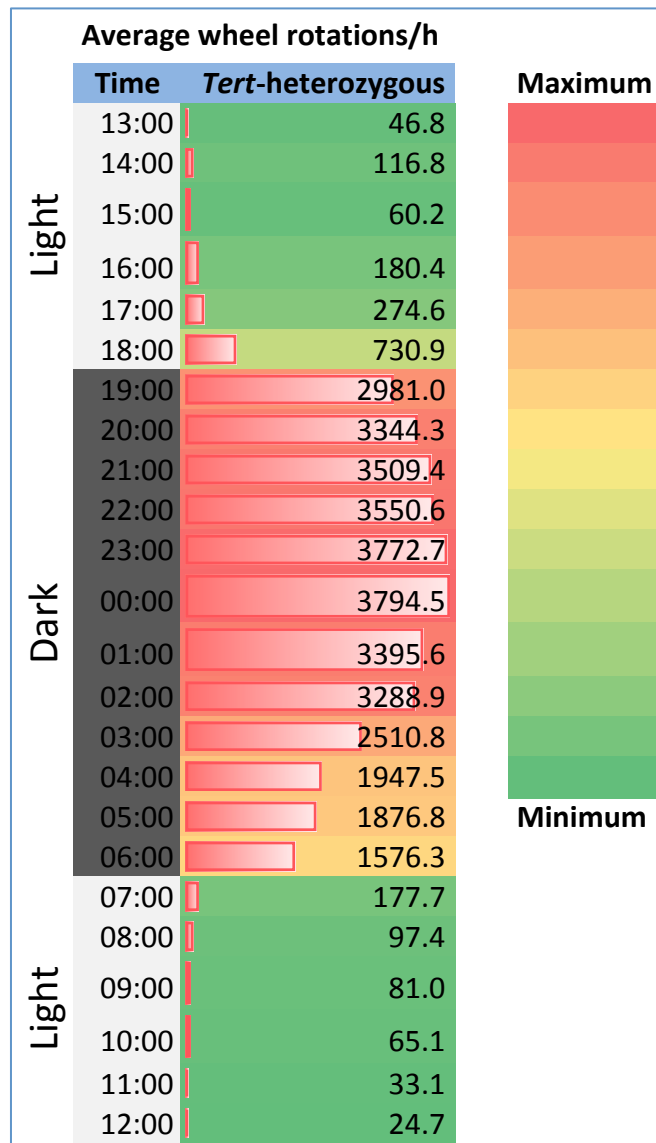


Figure 5.4. Diurnal pattern of average wheel rotations per hour for TERT⁺⁻ (heterozygous) mice

Heterozygous TERT⁺⁻ mice on voluntary wheel running exercise for 7 weeks. 5 female mice on exercise, with a normal diet. Numbers of wheel rotations per hour were averaged for the group.

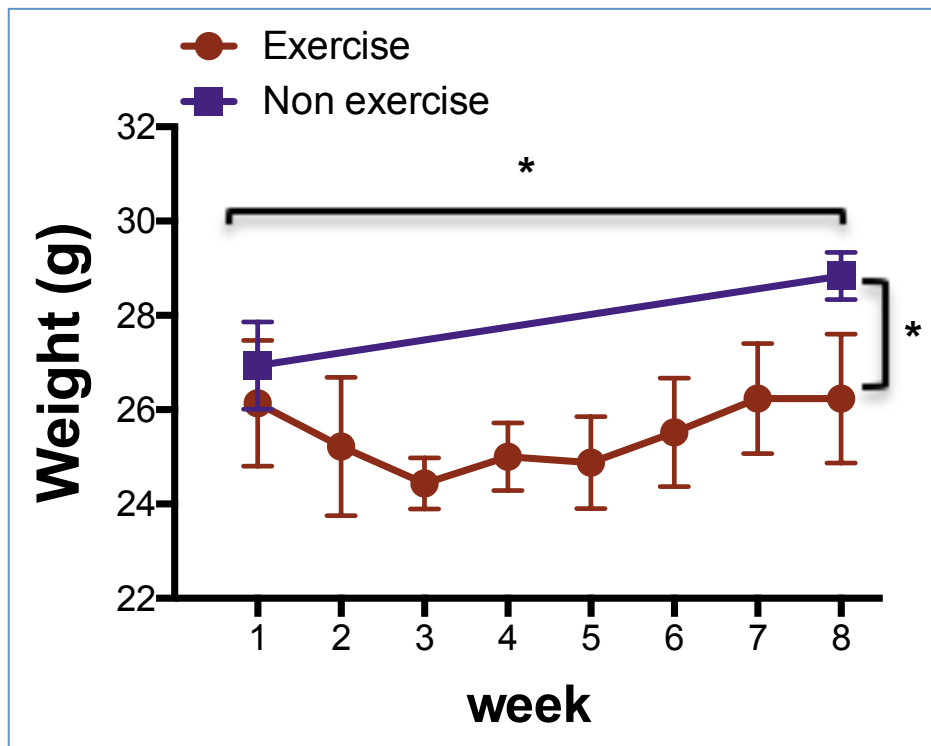


Figure 5.5. Body weight of TERT-heterozygous mice

TERT^{+/−} (heterozygous) mice on the voluntary wheel running exercise for 7 weeks. 5 female mice on exercise vs. 5 female mice with no exercise, both on a normal diet. Body weight was measured for the exercising group each week, but only at the beginning and the end of study for control group. All values are displayed as mean±sem. * P<0.05 for comparison of body weight for the exercise group vs. no exercise group using paired t-test, two-tailed.

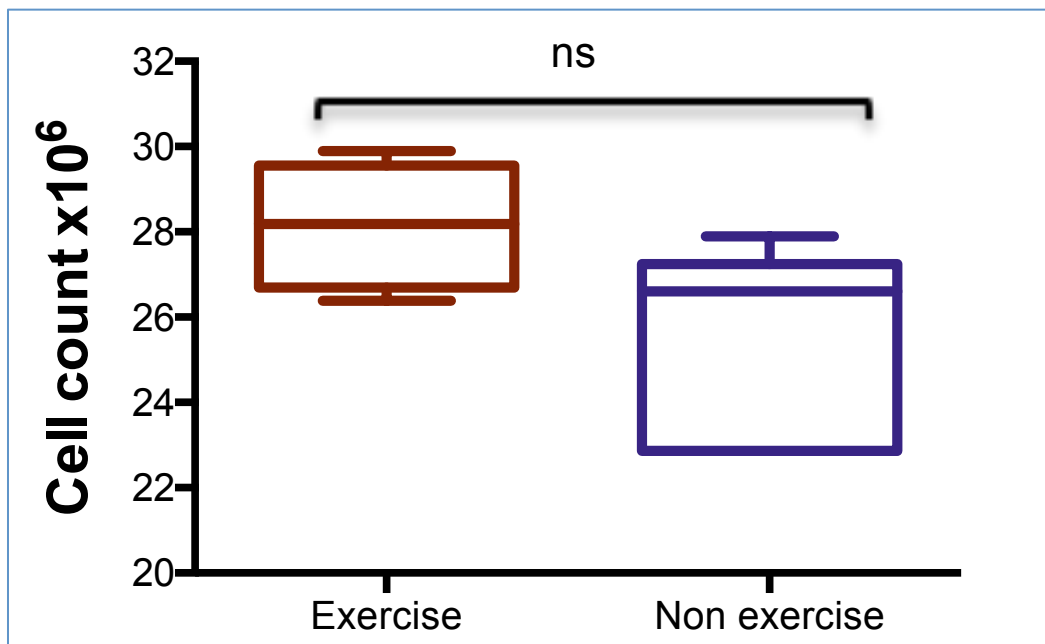


Figure 5.6. Splenocyte numbers of $\text{TERT}^{+/-}$ heterozygous mice with and without exercise

$\text{TERT}^{+/-}$ (heterozygous) mice on voluntary wheel running exercise for 7 weeks. 5 female mice on exercise vs. 5 female mice with no exercise, both on a normal diet. Cells were mixed with 1:1 0.4% Trypan blue solution and splenocyte numbers counted. All values are displayed as mean \pm sem. No significant (ns) for comparison of splenocyte numbers between exercising group vs. non-exercising group using unpaired t-test, two-tailed.

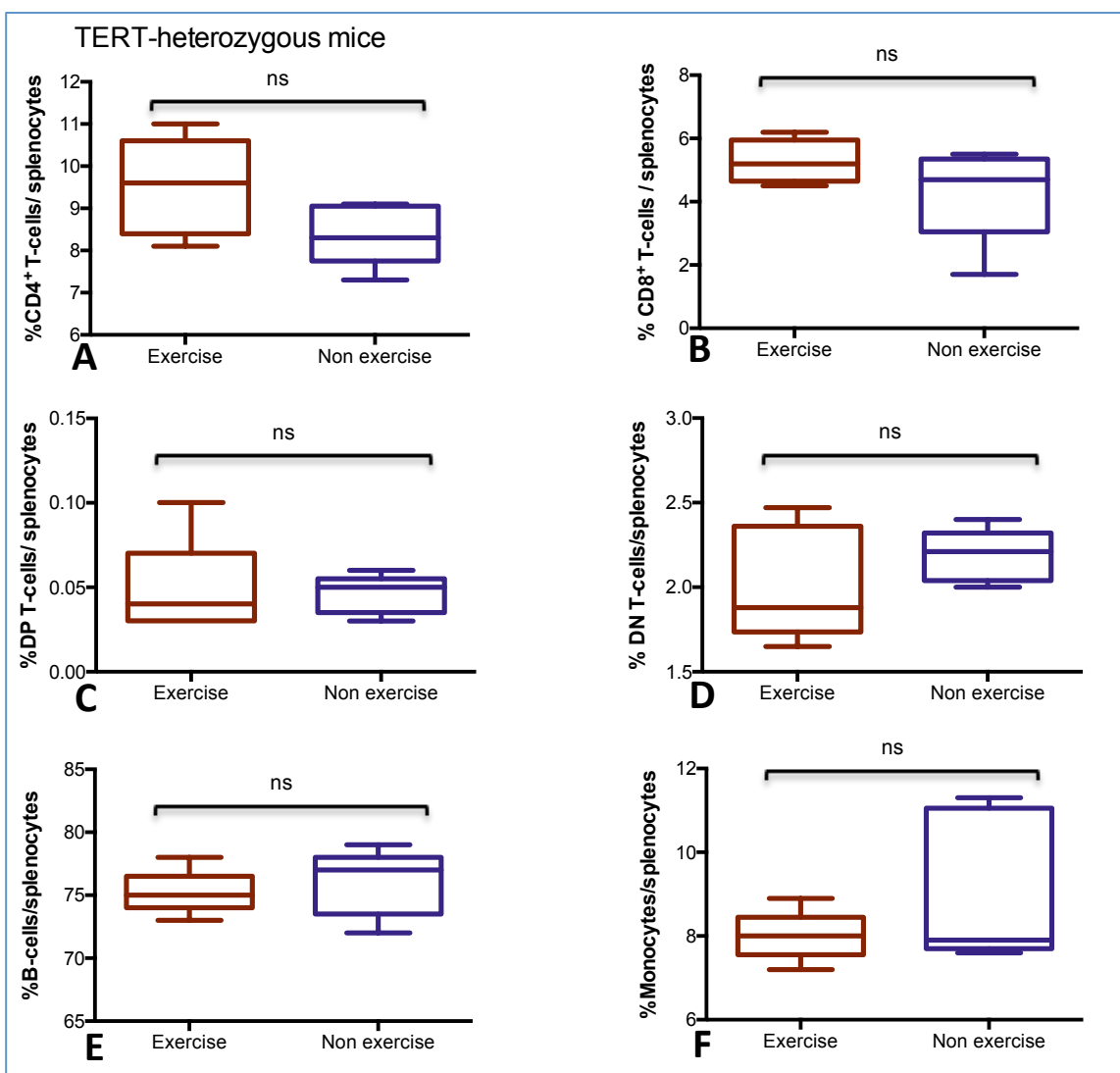


Figure 5.7. Percentage of splenocyte subsets of TERT^{+/−} heterozygous mice with and without exercise.

TERT^{+/−} (heterozygous) mice on voluntary wheel running exercise for 7 weeks. 5 female mice on exercise vs. 5 female mice with no exercise, both on a normal diet. Splenocytes were isolated by Ficoll-hypaque density gradient and cells were stained with the antibodies as described at 2.2.8. **A:** %CD4⁺ T-cells/splenocytes, **B:** %CD8⁺ T-cells/splenocytes, **C:** %DP T-cells/splenocytes, **D:** %DN T-cells/splenocytes, **E:** %B-cells/splenocytes and **F:** %Monocytes/splenocytes. All values are displayed as mean±sem. No significant (ns) for comparison of exercise group vs. non-exercise group using unpaired t-test, two-tailed.

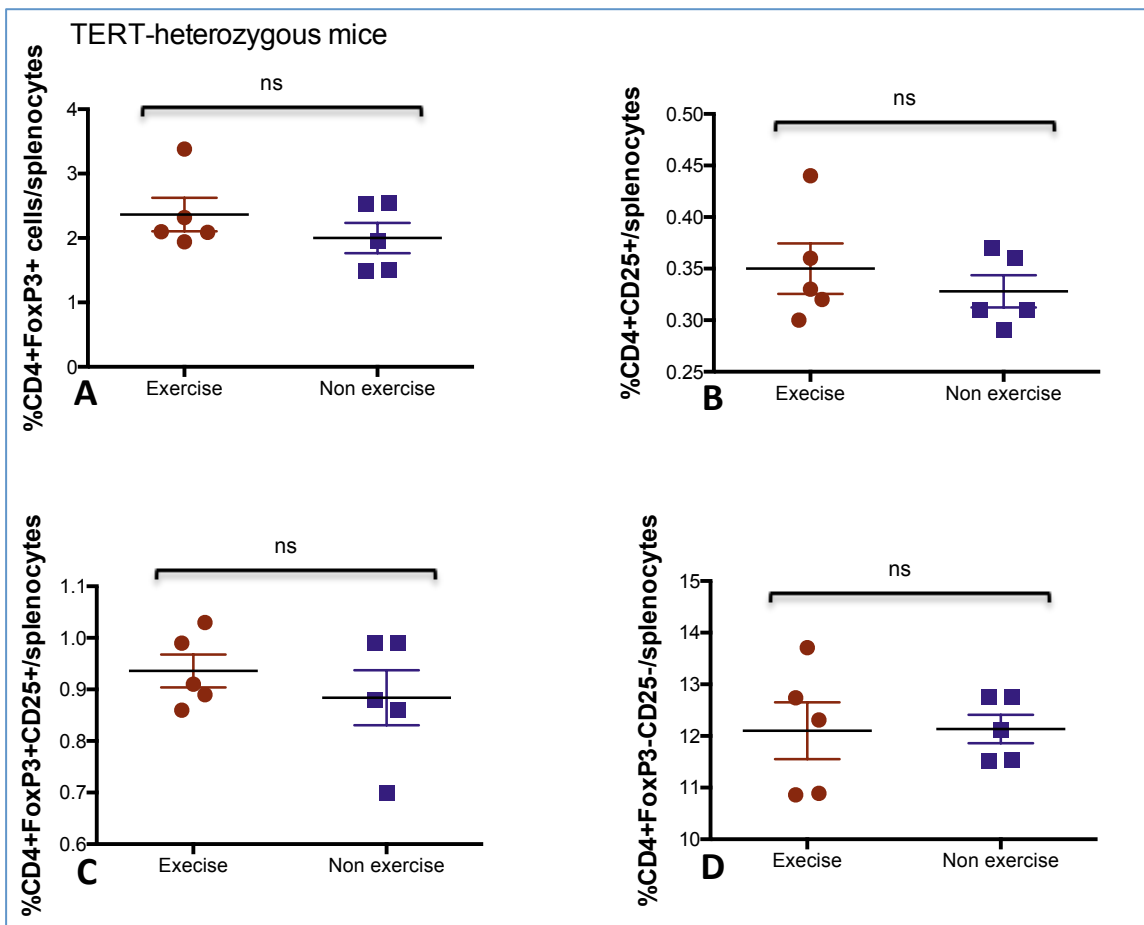


Figure 5.8. Percentage of regulatory T-cells in $\text{TERT}^{+/-}$ mice during exercise

$\text{TERT}^{+/-}$ (heterozygous) mice on voluntary wheel running exercise for 7 weeks. 5 female mice on exercise vs. 5 female mice without exercise, both on a normal diet. Cells were isolated by Ficoll-hypaque density gradient and cells were stained with beads as described at 2.2.14. **A:** percentage of $\text{CD4}^+\text{FoxP3}^+$ cells/splenocytes, **B:** percentage of $\text{CD4}^+\text{CD25}^+$ /splenocytes, **C:** percentage of $\text{CD4}^+\text{FoxP3}^+\text{CD25}^+$ /splenocytes and **D:** percentage of $\text{CD4}^+\text{FoxP3}^-\text{CD25}^-$ /splenocytes. All values are displayed as mean \pm sem. No significant (ns) for comparison of exercise group vs. non-exercise group using unpaired t-test, two-tailed.

5.2.3 Effects of voluntary wheel running exercise on *mTert*-GFP⁺ mice

5.2.3.1 Variability and spatial pattern of speed and duration during voluntary wheel running exercise on *mTert*-GFP⁺ mice

The *mTert*-GFP⁺ mice in this sub-chapter were genotyped by another laboratory colleague, Dr. Karim Bennaceur, IGM, Newcastle University.

mTert-GFP⁺ mice are genetically modified to contain a telomerase (mTERT) expression reporter. Therefore, in this experiment, 6 female mice were assigned to the voluntary wheel running exercise group vs. 6 female mice assigned to the control group (no exercise). Both groups were on a normal diet and were 2-3 months old. Performance varied between mice as well as from day to day. Figure 5.9A shows the time mice spent with running exercise, which started below 2 hours per day, then varied from 2-2½ hours per day. The distance travelled (Figure 5.9B) by these mice started at less than 2 km per 24 hours and reached up to 5 km per 24 hours by the end of the experiment. The average speed (Figure 5.9C) started from about 1 km/h at day one, reaching 1.75 km/h at the end of experiment. The maximum speed (Figure 5.9D) for *mTert*-GFP⁺ mice started at around 35 km/h at the beginning of experiment and reached around 20 km/h by the end of the experiment. These mice spent a significant time exercising, but this was not what I expected based on the previous two groups.

5.2.3.2 Diurnal pattern of *mTert*-GFP⁺ mice on voluntary wheel running exercise

From wheel average rotation at figure 5.10, during the 5 weeks of exercising, the 6 female mice spent more time running during the night (in the dark). Maximum wheel rotation was at the beginning of the night, then gradually decreased until the lights were turned on.

5.2.3.3 Effect of voluntary wheel running exercise on body weights of *mTert*-GFP⁺ mice

After 5 weeks of voluntary wheel running exercise, the weight of mice under exercise decreased from 21.5±1.4g at the first two weeks to 20.7±0.9g. It then returned to the starting weight at week four (by 21.65±0.98g), then plateaued during the last two weeks of the experiment at 21.7±0.8g. On the other hand, the non-exercising group started from 21.5±0.5g then gradually increased (P<0.05), reaching 22.8±0.7g by the end of the experiment. In conclusion, exercising can lead to loss and control of weight.

5.2.3.4 Effect of voluntary wheel running exercise on splenocyte numbers in *mTert*-GFP⁺ mice

Cells were isolated from the spleen at the end of experiments by Ficoll-hypaque density gradient. Splenocytes were counted under the microscope using a Neubauer chamber (described at 2.2.2) for both exercising and non-exercising groups. There was no significant change in splenocyte numbers after exercising ($28\pm0.9 \times 10^6$ /spleen) compared to the control group ($26.6\pm2.3 \times 10^6$ /spleen) by the end of the experiment. However, there is a trend towards increasing numbers for the exercising group. In contrast, there is a high variation in cell numbers from spleen to spleen in the control group ($26.6\pm2.3 \times 10^6$ /spleen) vs. a smaller variation (<0.99) for the exercising group.

5.2.3.5 Effect of voluntary wheel running exercise on splenocyte subpopulations of *mTert*-GFP⁺ mice

The aim of this experiment was to determine the effect of exercise on telomerase expression, as these mice have a telomerase reporter, as well as T-lymphocytes, B-lymphocytes and monocytes, which form the main splenocyte population. Cells were isolated from mice and stained with the respective antibodies as described under 2.2.8. For CD4⁺ T-cells (Figure 5.13A) and CD8⁺ T-cells (Figure 5.13B), there were no significant changes under exercise compared to the control group. The same was noticed for GFP⁺ cells (Figure 5.13C); there was no significant change on TERT expression in GFP⁺ cells, just a trend toward increasing GFP⁺ cell numbers for the exercising group. However, a significant ($P<0.05$) response was observed for B-lymphocytes (Figure 5.13D) after the voluntary wheel running exercise ($19.1\pm0.79 \times 10^6$ /spleen) vs. ($17.2\pm1.7 \times 10^6$ /spleen) for the control group. B-cells may be differentiated into plasma cells, which produce antibodies and are released into the blood, or memory cells which remain in circulation for a long time and may respond to an antigen subsequently (Ozaki et al., 2004), so further investigation is required to find out which subset of B-cells responds to exercise. Monocytes (Figure 5.13E) also did not show any response to the running exercise.

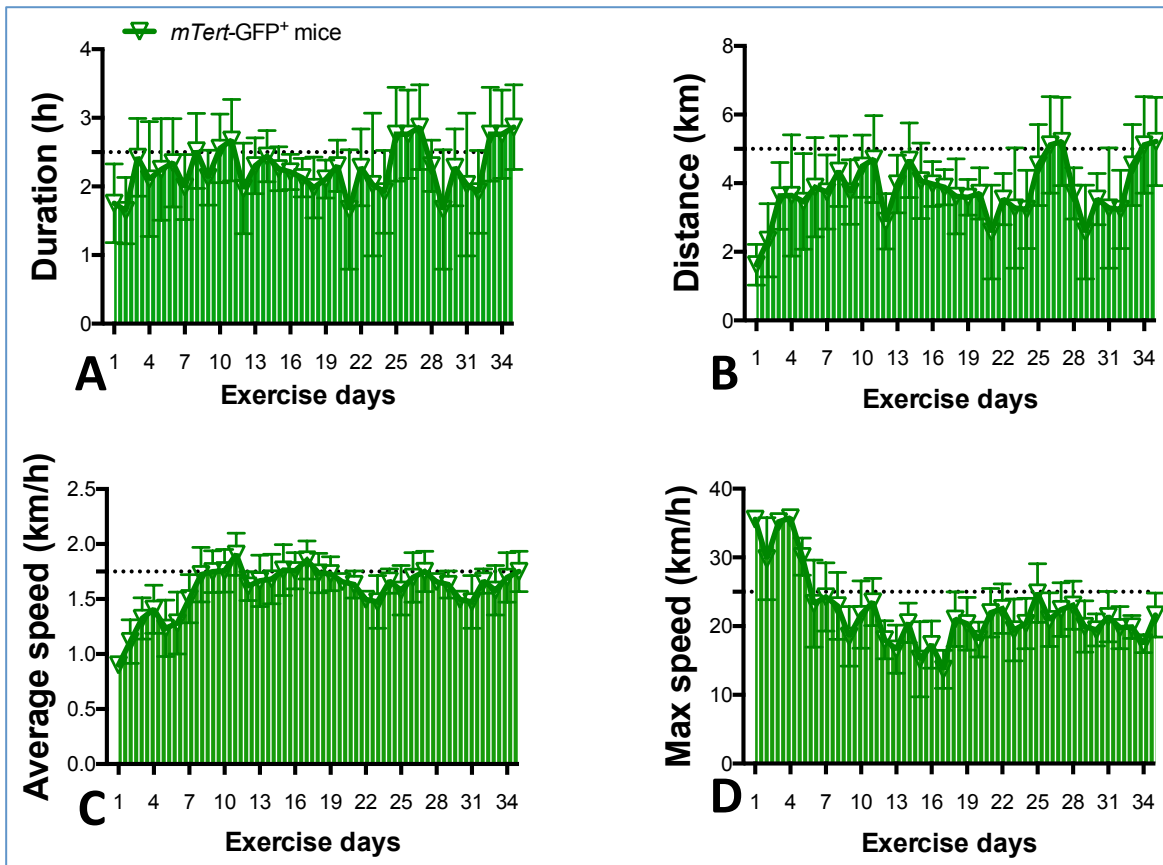


Figure 5.9. Daily running parameters for *mTert-GFP⁺* mice

mTert-GFP⁺ mice were subjected to voluntary wheel running exercise (using a computerized system to record and analyse individual wheel rotations) for 5 weeks. 6 female mice, exercising and on a normal diet. **A:** mean daily time (h) spent wheel running, defined as continuous exercise with a maximum interval between detected wheel rotations of 5 seconds. **B:** mean daily running distance (km) calculated by wheel circumference x the total of wheel rotations. **C:** mean daily average speed (km/h) calculated by the total distance run/total running time during each 24-hours period. **D:** mean daily maximum speed (km/h), the speed at the upper 99th percentile of wheel rotation speeds from all individual wheel rotation time intervals in a 24-hours period. All values are displayed as mean±sem.

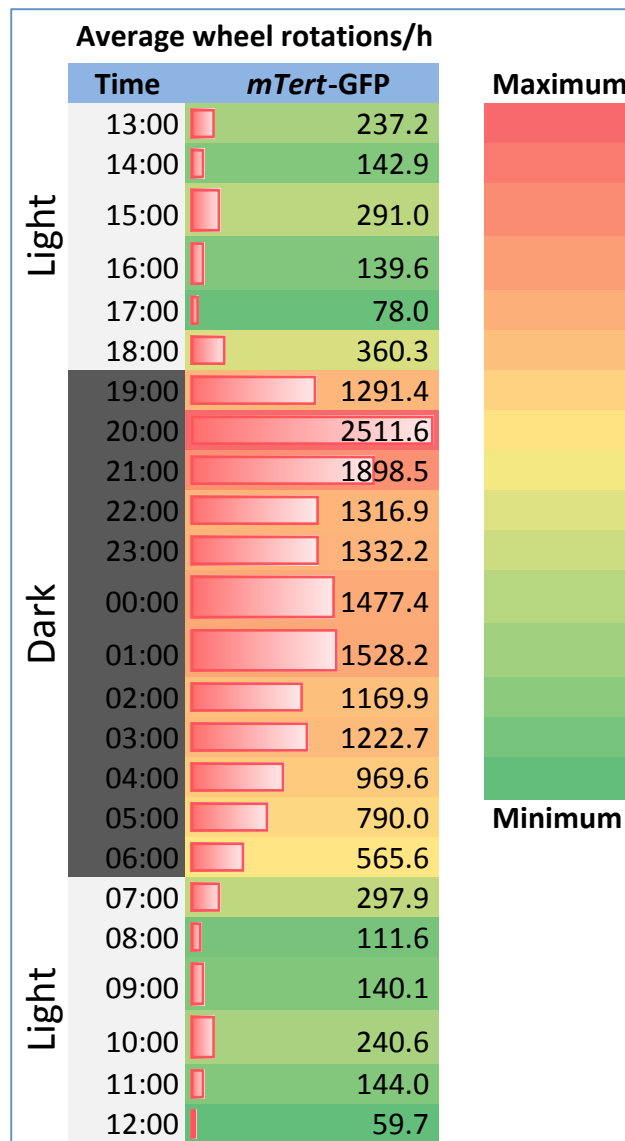


Figure 5.10. Diurnal pattern of average wheel rotations per hour for *mTert-GFP*⁺ mice

mTert-GFP⁺ mice on voluntary wheel running exercise for 5 weeks. 6 female mice exercising and on a normal diet. Numbers of wheel rotations per hour were averaged for the group.

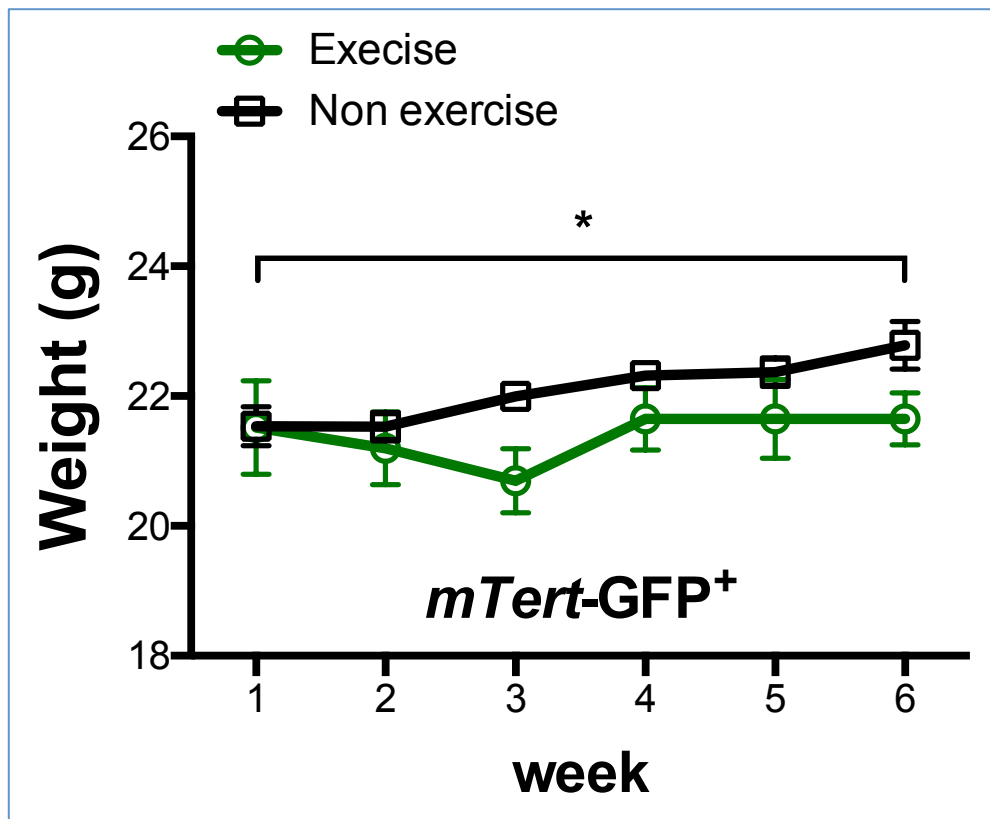


Figure 5.11 Body weight of *mTert-GFP⁺* mice with and without exercise

mTert-GFP⁺ mice on the voluntary wheel running exercise for 5 weeks. 6 female mice on exercise vs. 6 female mice with no exercise, both on a normal diet. Weight was measured weekly for both groups. All values are displayed as mean \pm sem. * P<0.05 for comparison of exercise group vs. no exercise group using two-way ANOVA.

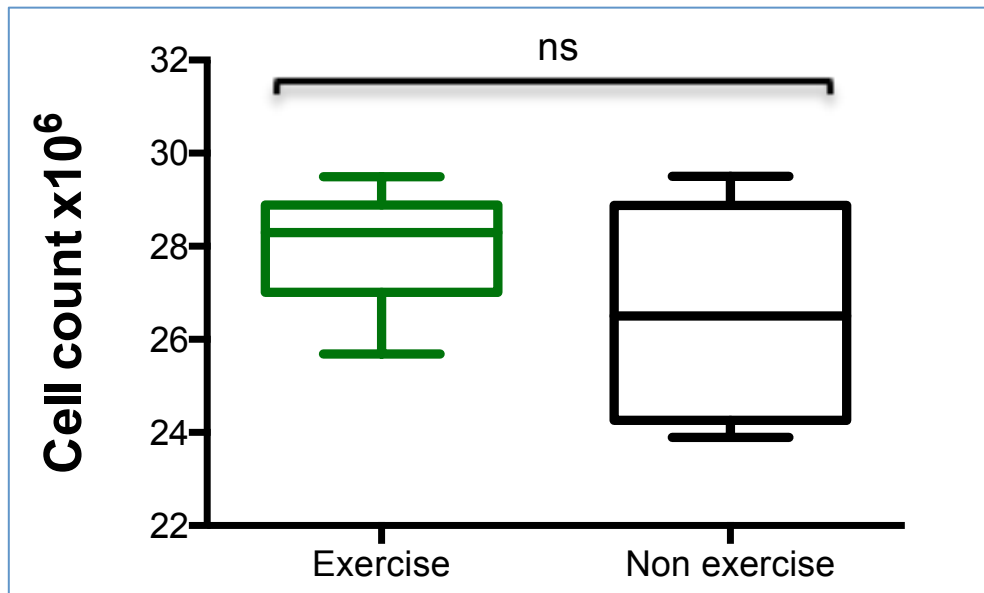


Figure 5.12. Number of splenocytes from *mTert-GFP⁺* mice with and without exercise

mTert-GFP⁺ mice on voluntary wheel running exercise for 5 weeks. 6 female mice on exercise vs. 6 female mice without exercise, both on a normal diet. Cells were mixed with 1:1 0.4% Trypan blue solution and splenocyte numbers counted. All values are displayed as mean \pm sem. (ns) no significant for comparison of exercising group vs. non exercising group using unpaired t-test, two-tailed.

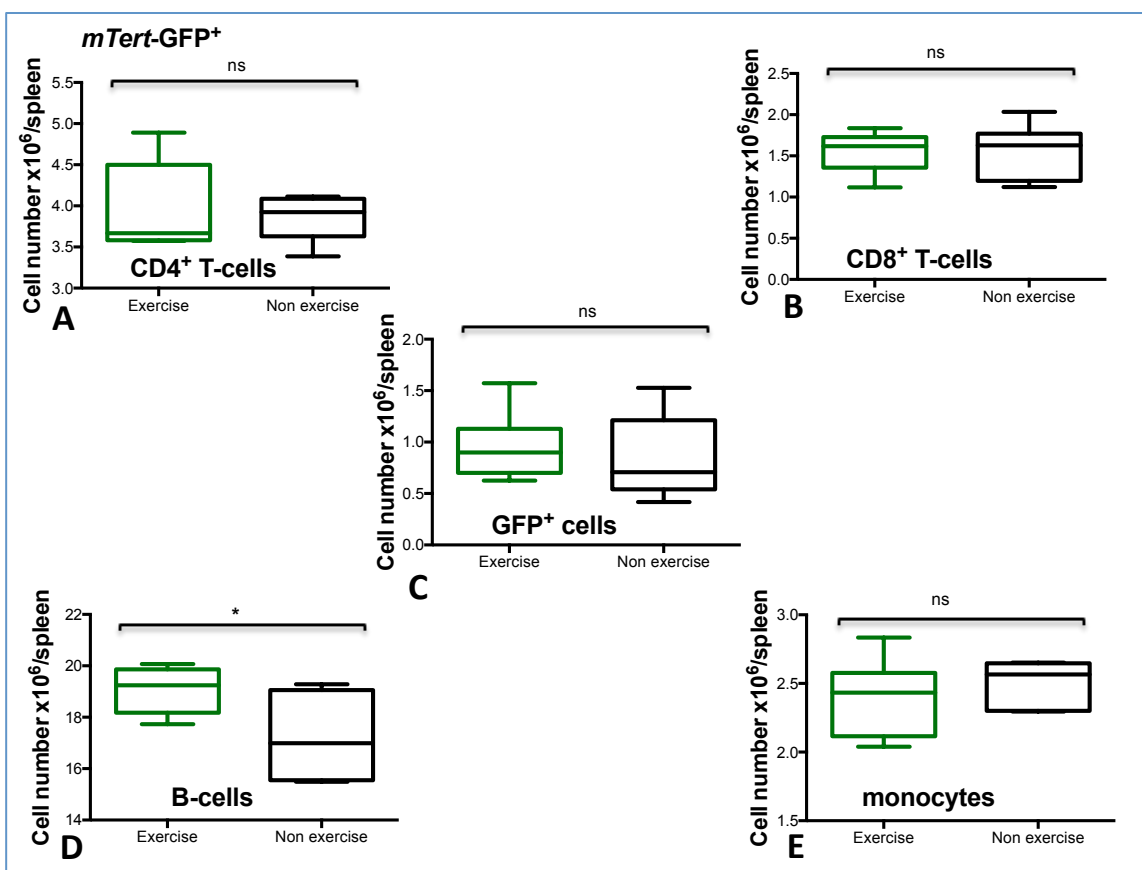


Figure 5.13. Percentage of splenocyte subpopulations in *mTert-GFP⁺* mice with and without exercise

mTert-GFP⁺ mice on voluntary wheel running exercise for 5 weeks. 6 female mice on exercise vs. 6 female mice with no exercise, both on a normal diet. Cells were isolated by Ficoll-hypaque density gradient and stained with antibodies as described at 2.2.8. **A:** percentage of CD4⁺ T-cells/splenocytes, **B:** percentage of CD8 T-cells/splenocytes, **C:** percentage of GFP⁺ cells/splenocytes, **D:** percentage of B-cells/splenocytes and **E:** percentage of monocytes/splenocytes.

All values are displayed as mean \pm sem. * P<0.05 for comparison of exercise group vs. non-exercise group using unpaired t-test, two-tailed.

5.2.4 Effect of voluntary wheel running exercise on $\text{ApoE}^{-/-}\text{mTert-GFP}^+$ mice

5.2.4.1 Variability and spatial pattern of speed and duration during voluntary wheel running exercise on $\text{ApoE}^{-/-}\text{mTert-GFP}^+$ mice

The mTert-GFP^+ mice in this sub-chapter were genotyped by another laboratory colleague, Dr. Karim Bennaceur, whilst the $\text{ApoE}^{-/-}$ mice were genotyped by Natasha Curley, PhD student with Prof. Deborah Henderson and Dr. Bill Chaudhry's team, IGM, Newcastle University.

Mice body weight and calorie intake in this sub-chapter were recorded weekly by myself and by Natasha Curley, PhD student from Prof. Deborah Henderson and Dr. Bill Chaudhry's team. The vascular phenotype of these mice and how it was affected by exercise will be studied by Prof. Deborah Henderson and Dr. Bill Chaudhry's team (Natasha Curley, PhD student), IGM, Newcastle University.

Apolipoprotein E (ApoE) is a protein-coding gene, from which the protein generated combines with fat to create a lipoprotein. ApoE is a very low density lipoprotein, involved in removing cholesterol from the bloodstream (Daniels et al., 2009). In 1992, the first line of ApoE-knockout mice was generated and these have since become the most used model for research on atherosclerosis. ApoE-knockout mice develop a high degree of atherosclerosis, rendering them ideal for research on the disease, and contributing towards vital new theories around atherosclerosis, namely that it is an inflammatory disease (Zhang et al., 1992; Williams et al., 2002; Knouff et al., 1999). Furthermore, atherosclerotic plaques were found to be stabilized in $\text{ApoE}^{-/-}$ mice after long term exercise (Pellegrin et al., 2009).

Mouse telomerase reverse transcriptase (mTert)-GFP- transgenic mice (see chapters 3 and 4 and others: Breault et al., 2008; Armstrong et al., 2000; Richardson et al., 2012) provide a model which can be used to determine TERT expression and presence *in vivo* and on a single cell level, which is thought to correlate well with its activity in several tissues (Breault et al., 2008; Armstrong et al., 2000). As $\text{ApoE}^{-/-}$ mice provide a good model for lipid accumulation and plaque build up in atherosclerosis development (Candido et al., 2002; Patel et al., 2001), we decided to generate a new mouse genotype: $\text{ApoE}^{-/-}\text{mTert-GFP}^+$, which can accumulate lipid (atherosclerosis) and report telomerase, through crosses between $\text{ApoE}^{+/-}$ (heterozygous) and mTert-GFP^+ as described at 2.2.1.3. Ultimately, this would enable us to establish the role of telomerase specific to cells in atherosclerotic conditions. I had hypothesized that the exercise effects would increase the telomerase activity of lymphocytes.

ApoE^{-/-}*mTert*-GFP⁺ mice were assigned to the voluntary wheel running exercise as two groups; one with a high fat diet (HFD) and another on normal diet (ND). Another two groups were assigned to no exercise (control group), one on a HFD and the other on ND. Furthermore, ApoE^{+/+}*mTert*-GFP⁺ mice were used as a control group for (ApoE^{-/-}). These mice had no exercise and again, one group was given a HFD and the other ND (table 5.1).

Table 5.1. Groups of ApoE^{-/-}*mTert*-GFP⁺ and ApoE^{+/+}*mTert*-GFP⁺ mice

	<i>mTert</i> -GFP ⁺		
	Exercise	No exercise	
	ApoE ^{-/-}	ApoE ^{+/+}	
High fat diet	n= 4 mice	n= 4 mice	n= 3 mice
Normal diet	n= 4 mice	n= 4 mice	n= 4 mice

During 16 weeks of voluntary wheel running exercise, both HFD and ND groups reached up to 5 hours (Figure 5.14A) of running per 24 hours. However, there was a clear variation in exercise duration between mice and also from day to day. There was no significant change in time spent exercising between the two groups based on their diet, although there was a trend towards increased duration for the HFD group. Running duration gradually increased during the first 3 weeks for both groups. The HFD group started at about 2.2h per 24 hours, reaching up to 4.2h of running per 24 hours (P<0.0001) after 3 weeks. The ND group started at 2.2h, reaching up to 5.3h per 24 hours (P<0.0001). After this first peak for each group, the duration gradually fluctuated up and down until a second peak was reached at day 51. The HFD reached up to about 5.3h/24h (P<0.0001) and the ND about 5.2h/24h (P<0.0001). By the end of the experiment, mice in both groups spent about the same time running as when they started, around 2.2h/24h for each group.

The distance moved (Figure 5.14B) during the first 3 weeks gradually increased, peaking at day 17, at 11.6 km/24h. The ND group started at 3.97 km/24h at day one (P<0.001), but the HFD group continued to increase until reaching its first peak at day 32, of 12.96 km/24h, up from about 3kh/24h at day one (P<0.001). After the first peak for each group there was a variation in distance moved between mice as well as from day to day, which may be related to the recovery period required before starting training again. It is clear that the HFD group ran the greater distance compared to the ND group at almost all time points in the second half of experiment, and this may be due to the higher energy in their diet.

Figure 5.14C shows that the average speed reached by the HFD group was greater than that of the ND group (ns). The HFD group almost reached 2.25 km/h at several time points, while the ND group reached only 1.75 km/h at the majority of time points.

The maximum speed (Figure 5.14D) was almost equal for both groups until the last quarter of the experimental period, when a sudden drop was observed in the ND group for a few days, before returning to the maximum speed again.

5.2.4.2 Diurnal pattern of $\text{ApoE}^{-/-}\text{mTert-GFP}^+$ mice on voluntary wheel running exercise

According to the average wheel rotation for individual hours, it was obvious that the mice ran for longer and moved greater distances during night time when it was dark.

However, $\text{ApoE}^{-/-}\text{mTert-GFP}^+$ mice in the HFD group performed more average wheel rotations (over 927.3 ± 215.5 /day vs. over 733.1 ± 170 /day for the ND group ($P<0.01$)).

5.2.4.3 Effect of voluntary wheel running exercise on body weight of $\text{ApoE}^{-/-}\text{mTert-GFP}^+$ mice

During this experiment, mice in all groups were weighed, as was their food intake. The lowest body weights were recorded for the groups on exercise (Figures 5.3i and ii). As expected, all groups gained weight during the study as they started young, at 4 weeks old. Body weights increased significantly for all groups between day one and the last day (table 5.2).

Table 5.2. Body weight of $\text{ApoE}^{-/-}\text{mTert-GFP}^+$ and $\text{ApoE}^{+/+}\text{mTert-GFP}^+$ mice

Groups		Exercise	Diet	Average 1 st weight	Average end weight	P value	
mTert-GFP^+	$\text{ApoE}^{-/-}$	YES	HFD (i)	13.7 ± 1.8	25.75 ± 2.53	$P<0.0001$	
			ND (ii)	16.13 ± 2.88	24 ± 4.15	$P<0.0001$	
		NO	HFD (iii)	17.13 ± 1.88	30.88 ± 4.43	$P<0.0001$	
	$\text{ApoE}^{+/+}$		ND (iv)	17.37 ± 1.83	28.18 ± 1.58	$P<0.0001$	
			HFD (v)	18.73 ± 2.71	31.98 ± 2.08	$P<0.0001$	
			ND (vi)	15.48 ± 1.33	29.38 ± 2.34	$P<0.0001$	

Calorie intake was measured as ‘weight of food eaten multiplied with calorie intake of high fat diet’; (weight of food eaten = weight of food given – weight of food left; calorie intake of high fat diet is 4.5 kCal/g) to ensure any changes in weight were not due to poor nutrition, irrespective of exercise. Figure 5.16B shows that all groups had the same average food intake during the study, with no significant changes between them. There was a trend towards

increase in body weight for normal diet in the exercise $\text{ApoE}^{-/-}\text{mTert-GFP}^+$ group (ns). Under exercise, there were no significant changes between groups (i and ii). In terms of food type, the HFD group gained more weight than the ND group (ns). There was a significant ($P<0.05$) change in weight between ND on exercise (ii) compared to the HFD non-exercise group (iii) for $\text{ApoE}^{-/-}\text{mTert-GFP}^+$ mice.

ApoE protein binds to lipids to form lipoproteins. Its function is to package and carry cholesterol in the bloodstream, thereby playing a role in cholesterol level maintenance. Based on the results with exercise and an absence of ApoE, diet does not appear to cause any significant changes in our study (with exercise eat what you want). Furthermore, in the presence of ApoE, mice gain more weight than the exercising mice without ApoE, regardless of diet.

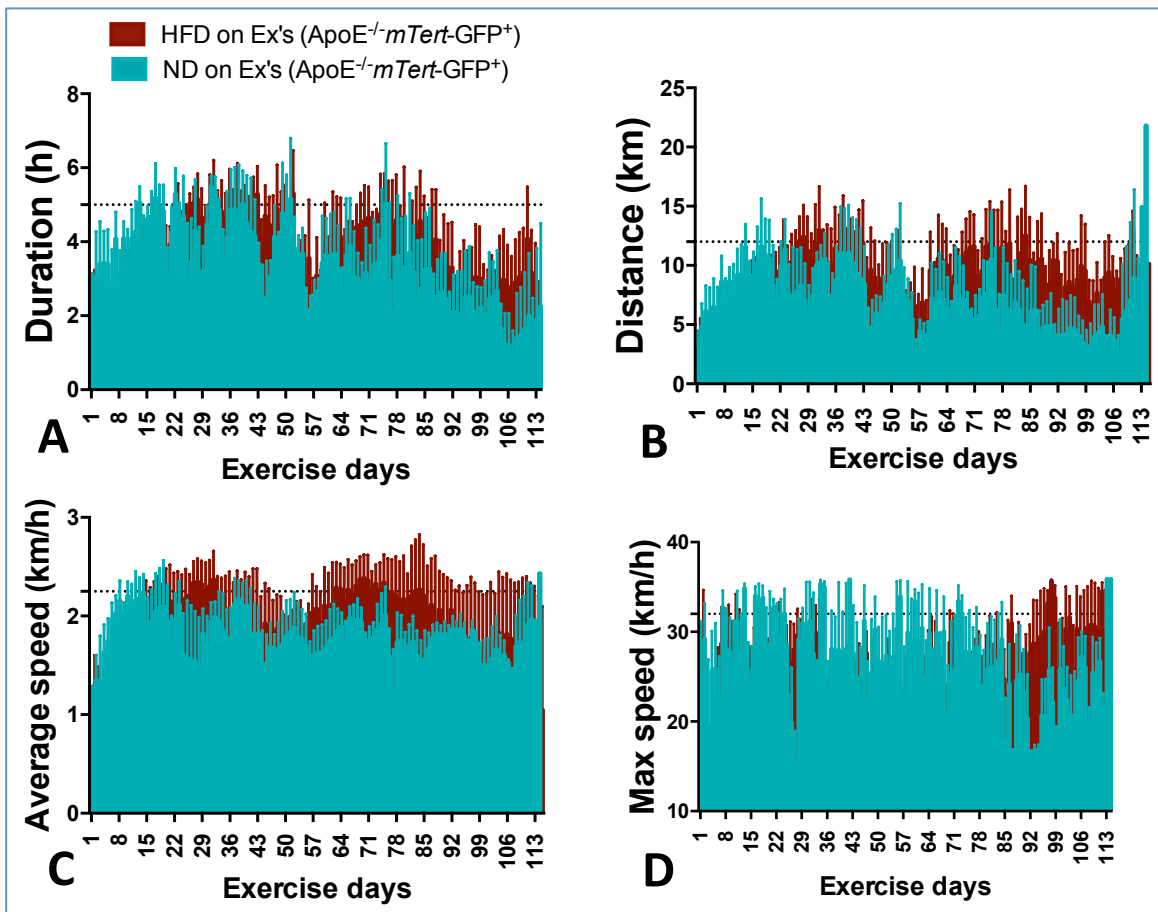


Figure 5.14. Daily running parameters for *ApoE*^{-/-}*mTert-GFP*⁺ mice

ApoE^{-/-}*mTert-GFP*⁺ mice were subjected to a voluntary wheel running exercise (using a computerized system to record and analyse individual wheel rotations) for 16 weeks. 4 mice on HFD vs. 4 mice on ND. **A:** mean daily time (h) spent wheel running, defined as continuous exercise with a maximum interval between detected wheel rotations of 5 seconds. **B:** mean daily running distance (km) calculated by wheel circumference x total of wheel rotations. **C:** mean daily average speed (km/h) calculated by the total distance run/total running time during each 24-hour period. **D:** mean daily maximum speed (km/h), the speed at the upper 99th percentile of wheel rotation speeds from all individual wheel rotation time intervals in a 24-hour period. All values are displayed as mean±sem. For comparison of HFD group vs. ND group using two-way ANOVA.

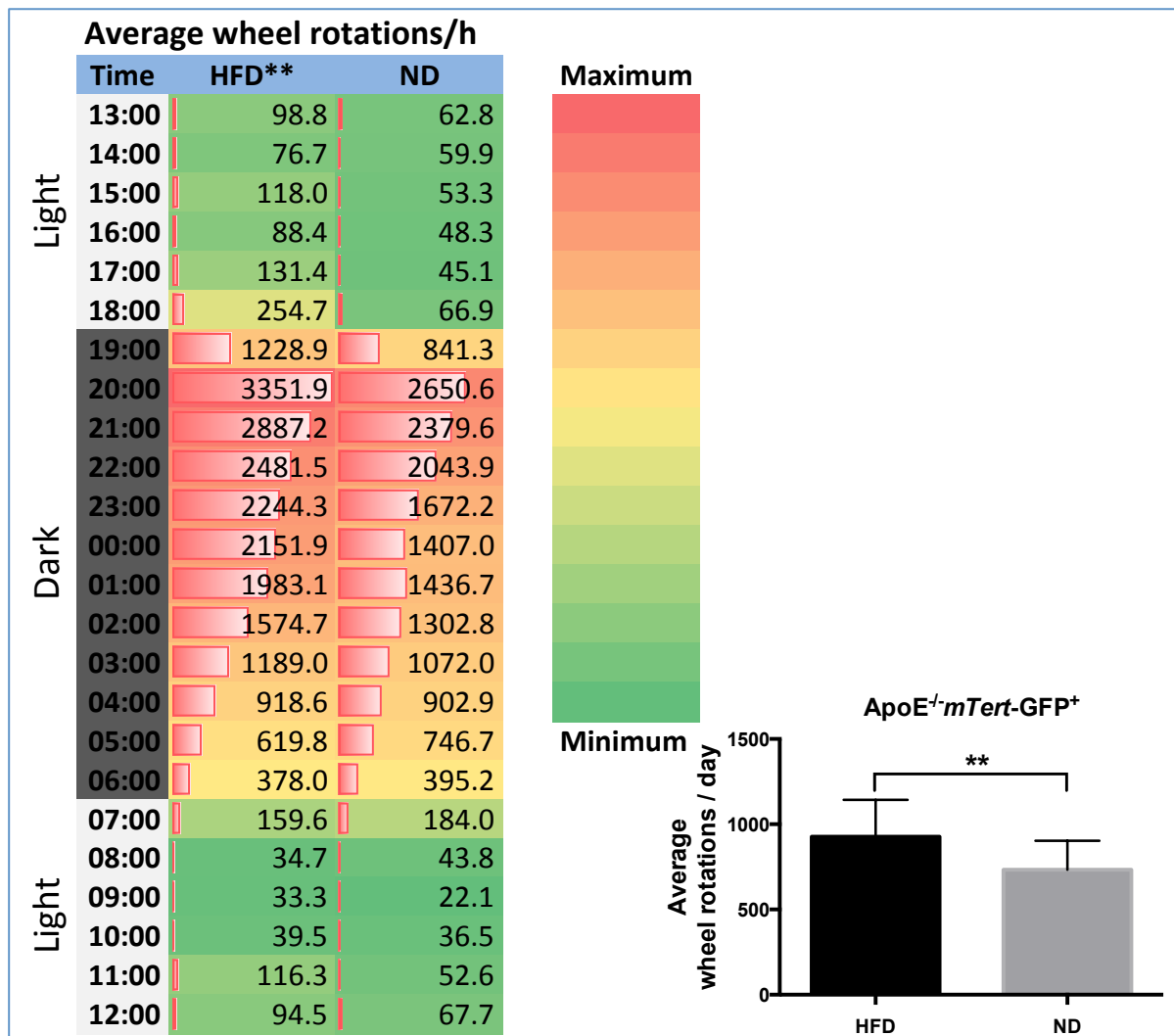


Figure 5.15 Diurnal pattern of average wheel rotations per hour for ApoE^{-/-}mTert-GFP⁺ mice

ApoE^{-/-}mTert-GFP⁺ mice on voluntary wheel running exercise for 16 weeks. 4 mice on high fat diet vs. 4 mice on normal diet. Number of wheel rotations per hour were averaged for each group. High fat diet (HFD) group ran further, especially in dark period. All values are displayed as mean±sem. ** P<0.01 for comparison of HFD vs. ND wheel average rotation using unpaired T-test, two-tailed.

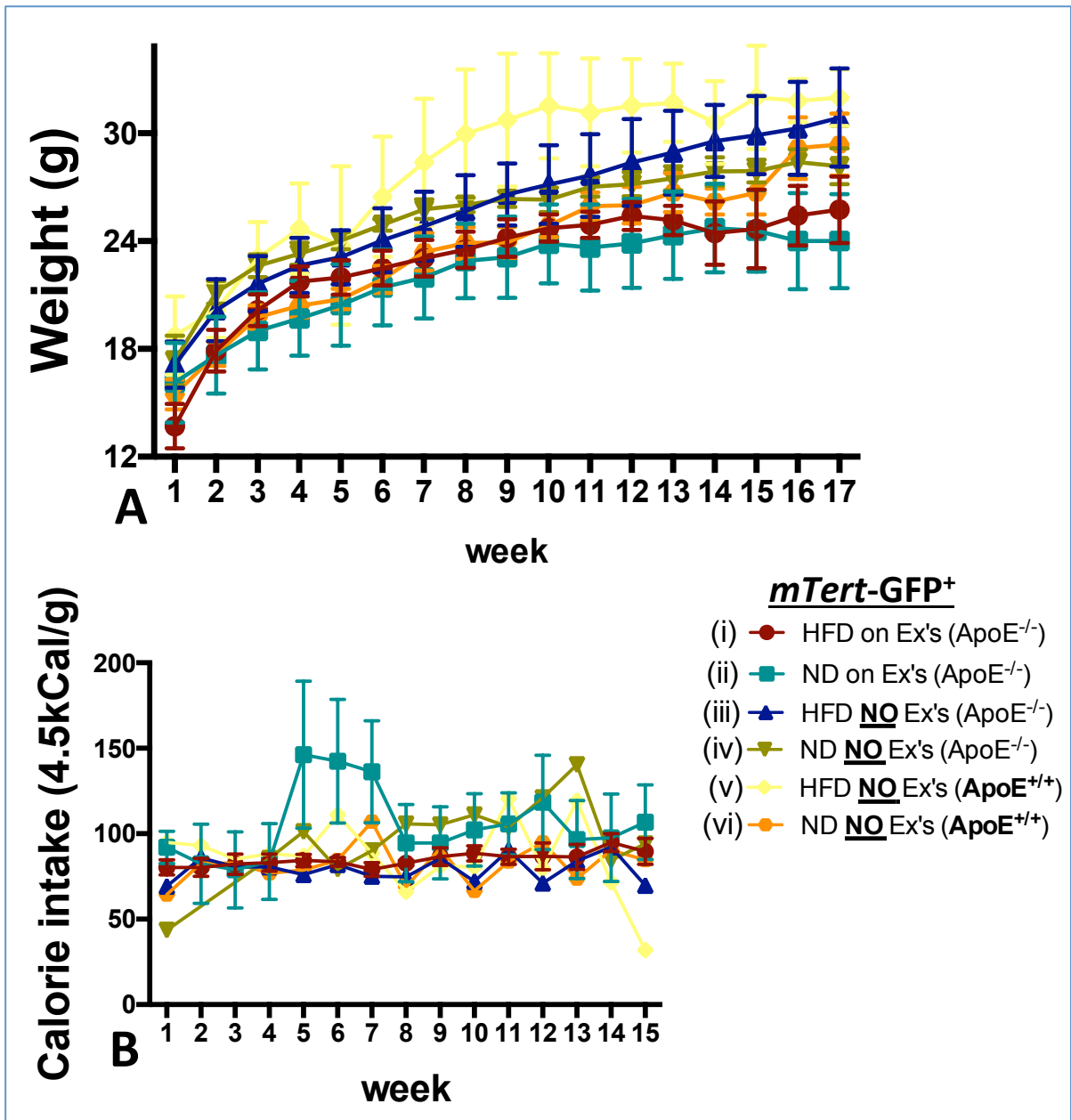


Figure 5.16. Body weight and calorie intake for $\text{ApoE}^{-/-}\text{mTert-GFP}^+$ and $\text{ApoE}^{+/+}\text{mTert-GFP}^+$ mice on different diets with and without exercise

$\text{ApoE}^{-/-}\text{mTert-GFP}^+$ mice on voluntary wheel running exercise for 16 weeks (4 mice on HFD (i) vs. 4 mice on ND (ii)), all vs. no exercise groups (4 mice on HFD (iii) vs. 4 mice on ND (iv)), in addition to groups of $\text{ApoE}^{+/+}\text{mTert-GFP}^+$ mice (3 mice on HFD (v) vs. 4 mice on ND (vi)). **A:** Body weight was measured weekly for all groups. **B:** Calorie intake was measured for all groups. All values are displayed as mean \pm sem. * $P<0.05$, ** $P<0.01$, *** $P<0.001$, **** $P<0.0001$ for comparison between HFD vs. ND and exercise vs. no exercise on $\text{ApoE}^{-/-}\text{mTert-GFP}^+$ mice using 2-way ANOVA multiple comparisons. Also, 2-way ANOVA multiple comparisons were used to compare between HFD vs. ND and $\text{ApoE}^{-/-}\text{mTert-GFP}^+$ vs. $\text{ApoE}^{+/+}\text{mTert-GFP}^+$ mice.

5.2.4.4 Effect of voluntary wheel running on telomerase activity in $\text{ApoE}^{-/-} \text{mTert-GFP}^+$ mice

Telomerase reverse transcriptase (TERT) plays an important role in cell division. Also, PBMNCs telomere lengths significantly increased under moderate exercise (Ludlow et al., 2008). Aerobic exercise reverses arterial inflammation with ageing in mice (Lesniewski et al, 2011). In humans, telomere length and telomerase activity increases in PBMNCs in middle-aged men with sedentary lifestyles after exercising for 4 months (Melk et al., 2014). This part of the experiment was designed to identify the effect of exercise on telomerase activity under either HFD or ND on modified genotype $\text{ApoE}^{-/-} \text{mTert-GFP}^+$ mice and also in $\text{ApoE}^{+/+} \text{mTert-GFP}^+$ mice.

Firstly, I compared diet and exercise in $\text{ApoE}^{-/-}$ mice (Figure 5.17 - purple section). Under exercise, HFD had a significant effect on telomerase activity 1.54 ± 0.02 vs. 0.91 ± 0.15 for ND group ($P < 0.05$). Exercise induced significantly ($P < 0.001$) higher telomerase activity than HFD without exercise in the same diet group (exercise = 1.54 ± 0.02 vs. 0.4 ± 0.18 = no exercise). HFD with exercise led to significantly ($P < 0.01$) higher telomerase activity compared to the ND group without exercise (0.68 ± 0.14).

Secondly, I compared between $\text{ApoE}^{-/-}$ vs. $\text{ApoE}^{+/+}$ mice on both diets but without exercise (Figure 5.17 - brown section). Under HFD without exercise, $\text{ApoE}^{-/-}$ mice had a trend towards higher telomerase activity than $\text{ApoE}^{+/+}$ mice (ns). In general, the $\text{ApoE}^{+/+}$ groups had a trend towards lower telomerase activity than $\text{ApoE}^{-/-}$ groups (ns).

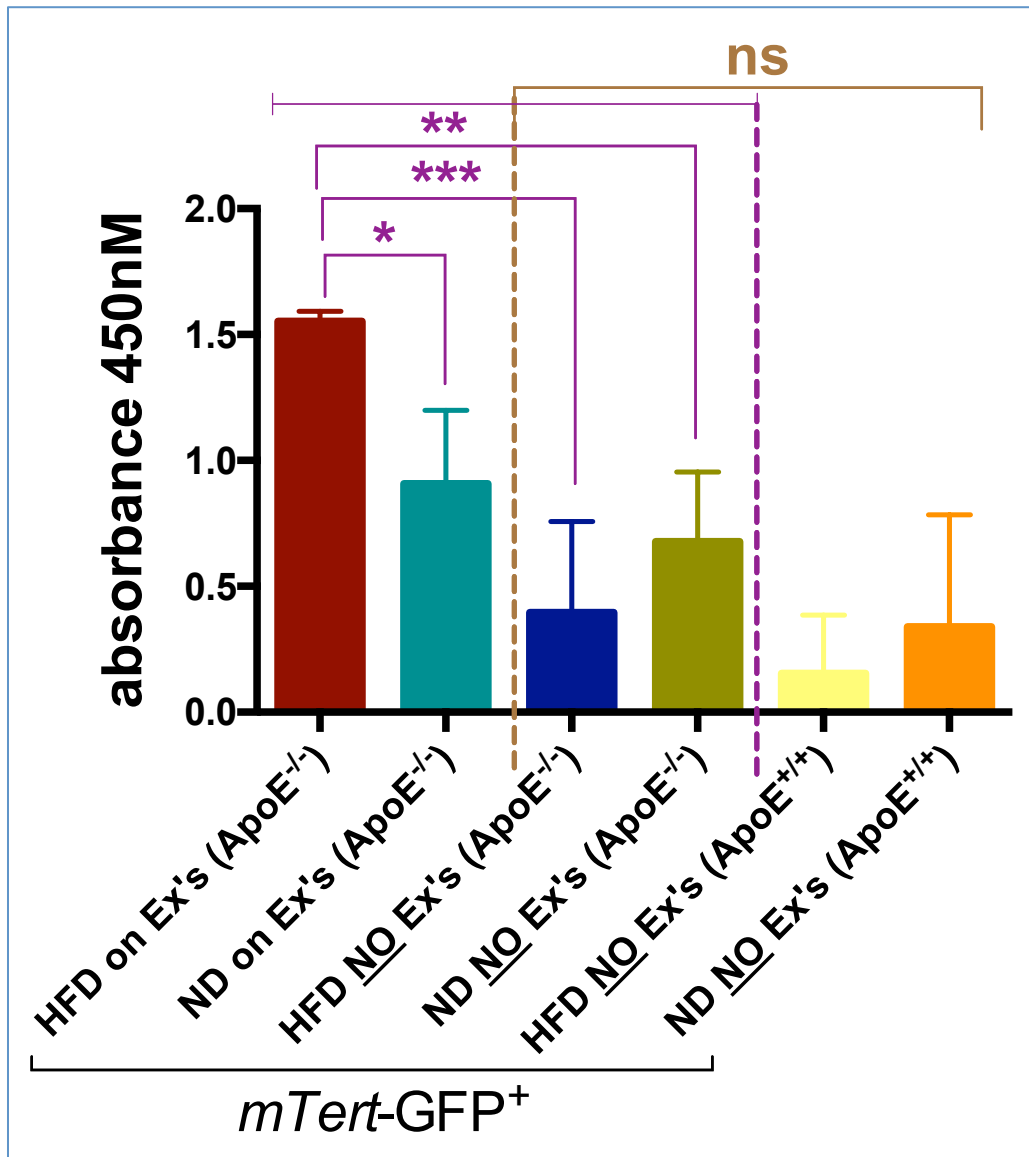


Figure 5.17. Telomerase activity for $\text{ApoE}^{-/-}m\text{Tert-GFP}^+$ and $\text{ApoE}^{+/-}m\text{Tert-GFP}^+$ mice on different diets with and without exercise

2 groups of $\text{ApoE}^{-/-}m\text{Tert-GFP}^+$ mice on the voluntary wheel running exercise for 16 weeks, 4 mice on HFD vs. 4 mice on ND. 2 groups of $\text{ApoE}^{-/-}m\text{Tert-GFP}^+$ mice with no exercise, 4 mice on HFD vs. 4 mice on ND. 2 groups of $\text{ApoE}^{+/-}m\text{Tert-GFP}^+$ with no exercise, 3 mice on HFD vs. 4 mice on ND. Telomerase activity was measured for each mouse in each group. All values are displayed as mean \pm sem. * $P<0.05$, ** $P<0.01$, *** $P<0.001$ for comparison between HFD vs. ND and exercise vs. no exercise on $\text{ApoE}^{-/-}m\text{Tert-GFP}^+$ mice using 2-way ANOVA multiple comparisons (purple section). 2-way ANOVA multiple comparisons (brown section) were also used to compare between HFD vs. ND and $\text{ApoE}^{-/-}m\text{Tert-GFP}^+$ vs. $\text{ApoE}^{+/-}m\text{Tert-GFP}^+$ mice. The TRAP assay was performed by Dr. Gabriele Saretzki NU, ICaMB, using splenocyte pellets that I had prepared as described above.

5.2.4.5 Effect of voluntary wheel running on splenocyte numbers in $\text{ApoE}^{-/-}$ $mTert$ - GFP^+ mice

The purpose of the next experiment was to find out if there is any effect of exercise or diet on the number of splenocytes. Also, I wanted to find out whether there was an effect of diet type on splenocyte number in mice with a functioning $\text{ApoE}^{+/+}$ gene. Splenocytes were counted using a Neubauer hemocytometer after being isolated by Ficoll-hypaque density gradient and washed as described at 2.2.2.

In groups of $\text{ApoE}^{-/-}$ $mTert$ - GFP^+ mice (Figure 5.18 - purple section), there was no significant change in splenocyte numbers as a result of exercising. However, under HFD, splenocytes showed an increasing trend ($42 \pm 2.16 \times 10^6/\text{spleen}$ compared to the exercising group $36.26 \pm 4.45 \times 10^6/\text{spleen}$ (ns)). The same trend was found under ND; splenocyte numbers increased ($36.35 \pm 1.44 \times 10^6/\text{spleen}$ compared to the exercising group $32.6 \pm 5.8 \times 10^6/\text{spleen}$ (ns)).

In the non-exercise groups (Figure 5.18 - brown section), there was a significant ($P < 0.05$) increase in splenocyte numbers (42 ± 2.16) when ApoE was knocked out and under HFD, compared to the group on ND and in the presence of $\text{ApoE}^{+/+}$. In summary, there was no significant change on splenocyte numbers for $\text{ApoE}^{-/-}$ $mTert$ - GFP^+ or $\text{ApoE}^{-/-}$ $mTert$ - GFP^+ mice under all conditions.

5.2.4.6 Effect of voluntary wheel running on splenocyte B-cell numbers in $\text{ApoE}^{-/-}$ $mTert$ - GFP^+ mice

The goal for this experiment was to find out whether exercise has an effect on mice under different diets regarding splenocyte sub-populations. To achieve this goal, cells were stained with 4 antibodies as described at 2.2.9, and subjected to flow cytometry. Surprisingly, the B-cell population was affected the most under exercise (Figure 5.19 - purple section). Under exercise, B-cells significantly ($P < 0.001$) decreased with ND ($13.1 \pm 0.31 \times 10^6/\text{spleen}$ compared to $20.16 \pm 0.82 \times 10^6/\text{spleen}$ for the HFD group). B-cells in the exercise group on ND ($13.1 \pm 0.31 \times 10^6/\text{spleen}$) decreased significantly ($P < 0.0001$) when compared to the no exercise group with HFD ($22.7 \pm 1.18 \times 10^6/\text{spleen}$) and also when compared with the ND no exercise group $20.3 \pm 1.11 \times 10^6/\text{spleen}$ ($P < 0.001$).

When I compared the effect of the HFD without exercise on B-cell numbers in both ApoE^{-/-} and ApoE^{+/+} (Figure 5.19 - brown section), there was no significant change in cell numbers. However, there was a trend towards increasing numbers between the same diet groups when comparing ApoE^{-/-} with ApoE^{+/+}. B-cell numbers were decreased under exercise with ND, suggesting that HFD increases B-cell numbers, while exercise counteracts this increase.

5.2.4.7 Effect of voluntary wheel running on CD8⁺ T-cell numbers in ApoE^{-/-} *mTert*-GFP⁺ mice

On T-lymphocyte levels, surprisingly, CD8⁺ T-cells significantly ($P<0.05$) decreased under exercise with HFD ($0.95\pm0.14 \times 10^6/\text{spleen}$) compared to the non-exercising group on ND ($2.48\pm0.39 \times 10^6/\text{spleen}$). However, there were no significant changes between the other groups. The main thing to notice here (Figure 5.20, compared with Figure 5.19) is that B-cell numbers increased under the running exercise with HFD compared to ND with exercise. However, CD8⁺ T-cell numbers decreased under the running exercise with HFD compared to ND with exercise. We noticed these opposing increases and decreases between B-cells and CD8⁺ T-cells in all groups, with some variation for ApoE^{-/-} *mTert*-GFP⁺ mice.

5.2.4.8 Effect of voluntary wheel running on GFP⁺ B-cell numbers in ApoE^{-/-} *mTert*-GFP⁺ mice

There was no significant change in the total number of GFP⁺ cell (Figure 5.22D) under all conditions, as these cells reflect telomerase-positive. However, total GFP⁺ cells have different subsets (GFP⁺CD4⁺, GFP⁺CD8⁺, GFP⁺B-cell and GFP⁺monocytes⁺), and figure 5.21 shows that GFP⁺B-cell number decreases significantly ($P<0.05$) ($0.11\pm0.011 \times 10^6/\text{spleen}$ in HFD with exercise, compared to ND without exercise ($0.16\pm0.011 \times 10^6/\text{spleen}$)). B-cell with telomerase expression shows a significant ($P<0.01$) decrease in the exercising group ($0.083\pm0.01 \times 10^6/\text{spleen}$), compared to the non-exercising group ($0.16\pm0.011 \times 10^6/\text{spleen}$) both on ND. This significant ($P<0.01$) decrease was noticed when comparing the exercising group on ND ($0.083\pm0.01 \times 10^6/\text{spleen}$) vs. the non-exercising group on HFD ($0.15\pm0.015 \times 10^6/\text{spleen}$).

On the other hand, when comparing ApoE^{-/-} (HFD vs. ND) vs. ApoE^{+/+} (HFD vs. ND), both non-exercising (Figure 5.21 - brown section), there were no significant changes between all groups except ApoE^{+/+} groups. There was a significant ($P<0.05$) decrease in GFP⁺B-cell numbers in ND without exercise ($0.058\pm0.025 \times 10^6/\text{spleen}$), compared to HFD non-exercise

in the same genotype ($\text{ApoE}^{+/+}$), of $0.363 \pm 0.17 \times 10^6$ /spleen. Finally, the number of B-cells that express telomerase increased in $\text{ApoE}^{-/-}$ without exercise. Exercising seems to decrease the number of active telomerase-expressing B-cells under both types of diet, but more with ND.

5.2.4.9 Effect of voluntary wheel running on other splenocyte subset numbers in $\text{ApoE}^{-/-} mTert-\text{GFP}^+$ mice

Splenocytes include T-lymphocytes, B-lymphocytes and monocytes as a major population within the spleen. B-cells are shown in figure 5.19. T-lymphocytes also contain further subsets (CD4^+ , CD8^+ , DP and DN). In figure 5.20, CD8^+ T-cells are displayed. Here, we can see the other T-lymphocyte subsets, CD4^+ (Figure 5.22A), DP (Figure 5.22B) and DN (Figure 5.22C). There were no significant changes between any of the groups under different exercise or diet conditions, and different genotypes have no effect on these cells. Figure 5.22D shows the total GFP^+ cells, as these cells express active telomerase, but here also there was no significant change between all groups. Monocyte numbers (Figure 5.22E) show no significant changes under any effect for all groups.

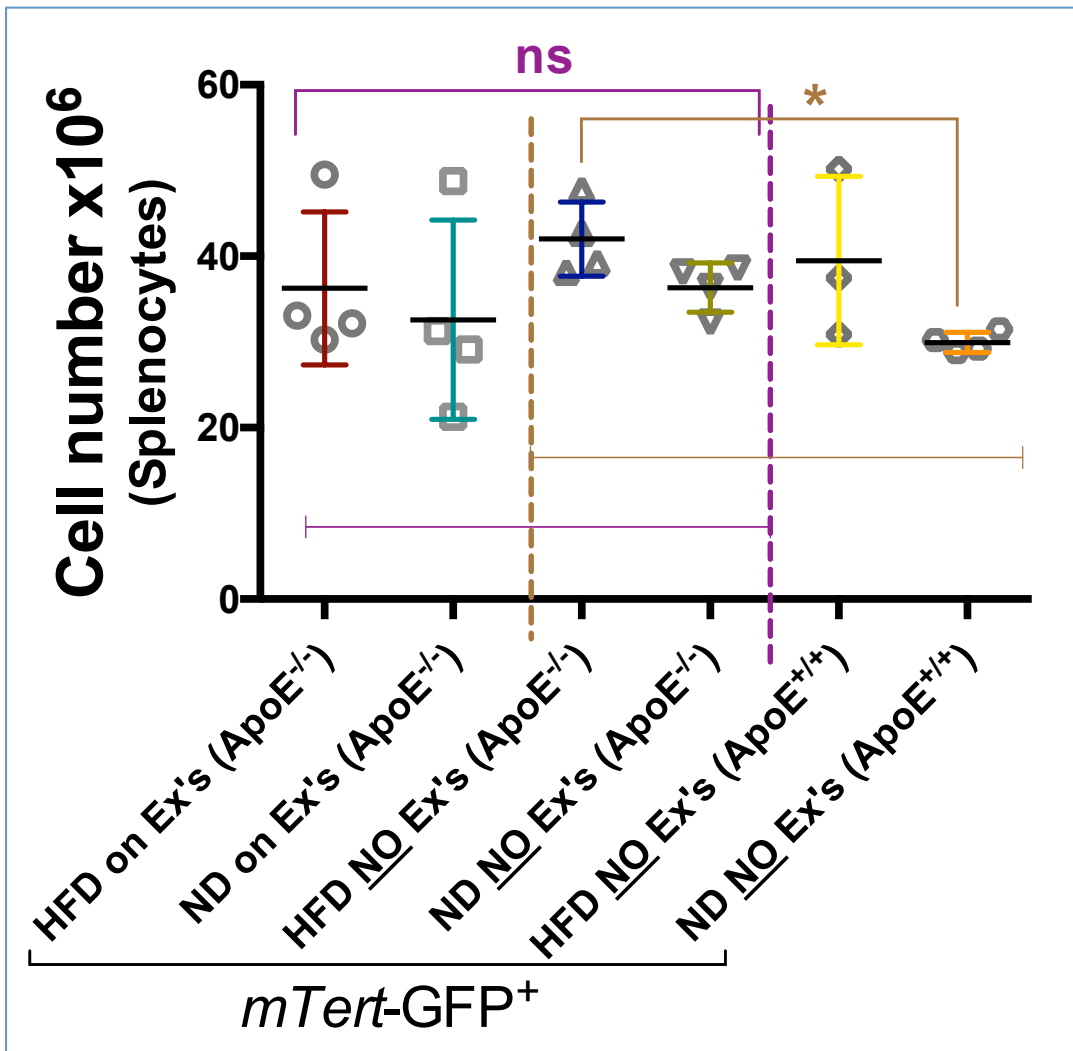


Figure 5.18. Splenocyte numbers for $\text{ApoE}^{-/-}mTert\text{-GFP}^+$ and $\text{ApoE}^{+/-}mTert\text{-GFP}^+$ mice on different diets with and without exercise

2 groups of $\text{ApoE}^{-/-}mTert\text{-GFP}^+$ mice on the voluntary wheel running exercise for 16 weeks, 4 mice on HFD vs. 4 mice on ND. 2 groups of $\text{ApoE}^{-/-}mTert\text{-GFP}^+$ mice with no exercise, 4 mice on HFD vs. 4 mice on ND. 2 groups of $\text{ApoE}^{+/-}mTert\text{-GFP}^+$ with no exercise, 3 mice on HFD vs. 4 mice on ND. Splenocytes were counted for each mouse in each group. All values are displayed as mean \pm sem. * $P<0.05$ for comparison between HFD vs. ND and exercise vs. no exercise on $\text{ApoE}^{-/-}mTert\text{-GFP}^+$ mice using 2-way ANOVA multiple comparisons (purple section). 2-way ANOVA multiple comparisons (brown section) were also used to compare between HFD vs. ND and $\text{ApoE}^{-/-}mTert\text{-GFP}^+$ vs. $\text{ApoE}^{+/-}mTert\text{-GFP}^+$ mice.

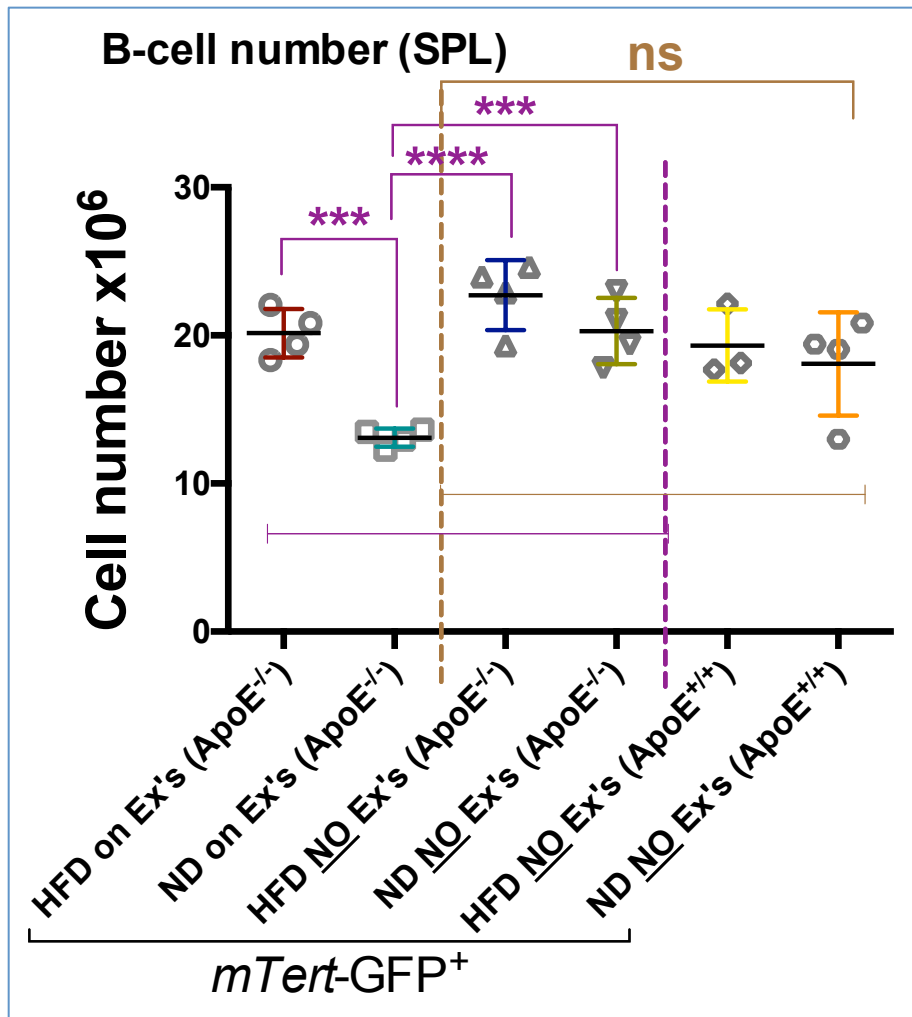


Figure 5.19. B-cell (splenocytes) numbers for $\text{ApoE}^{-/-}\text{mTert-GFP}^+$ and $\text{ApoE}^{+/-}\text{mTert-GFP}^+$ mice on different diets with and without exercise

2 groups of $\text{ApoE}^{-/-}\text{mTert-GFP}^+$ mice on the voluntary wheel running exercise for 16 weeks; 4 mice on HFD vs. 4 mice on ND. 2 groups of $\text{ApoE}^{-/-}\text{mTert-GFP}^+$ mice with no exercise, 4 mice on HFD vs. 4 mice on ND. 2 groups of $\text{ApoE}^{+/-}\text{mTert-GFP}^+$ with no exercise, 3 mice on HFD vs. 4 mice on ND. B-cell numbers were gated and counted for each mouse.

All values are displayed as mean \pm sem. *** $P<0.001$, **** $P<0.0001$ for comparison between HFD vs. ND and exercise vs. no exercise on $\text{ApoE}^{-/-}\text{mTert-GFP}^+$ mice using 2-way ANOVA multiple comparisons (purple section). 2-way ANOVA multiple comparisons (brown section) were also used to compare between HFD vs. ND and $\text{ApoE}^{-/-}\text{mTert-GFP}^+$ vs. $\text{ApoE}^{+/-}\text{mTert-GFP}^+$ mice.

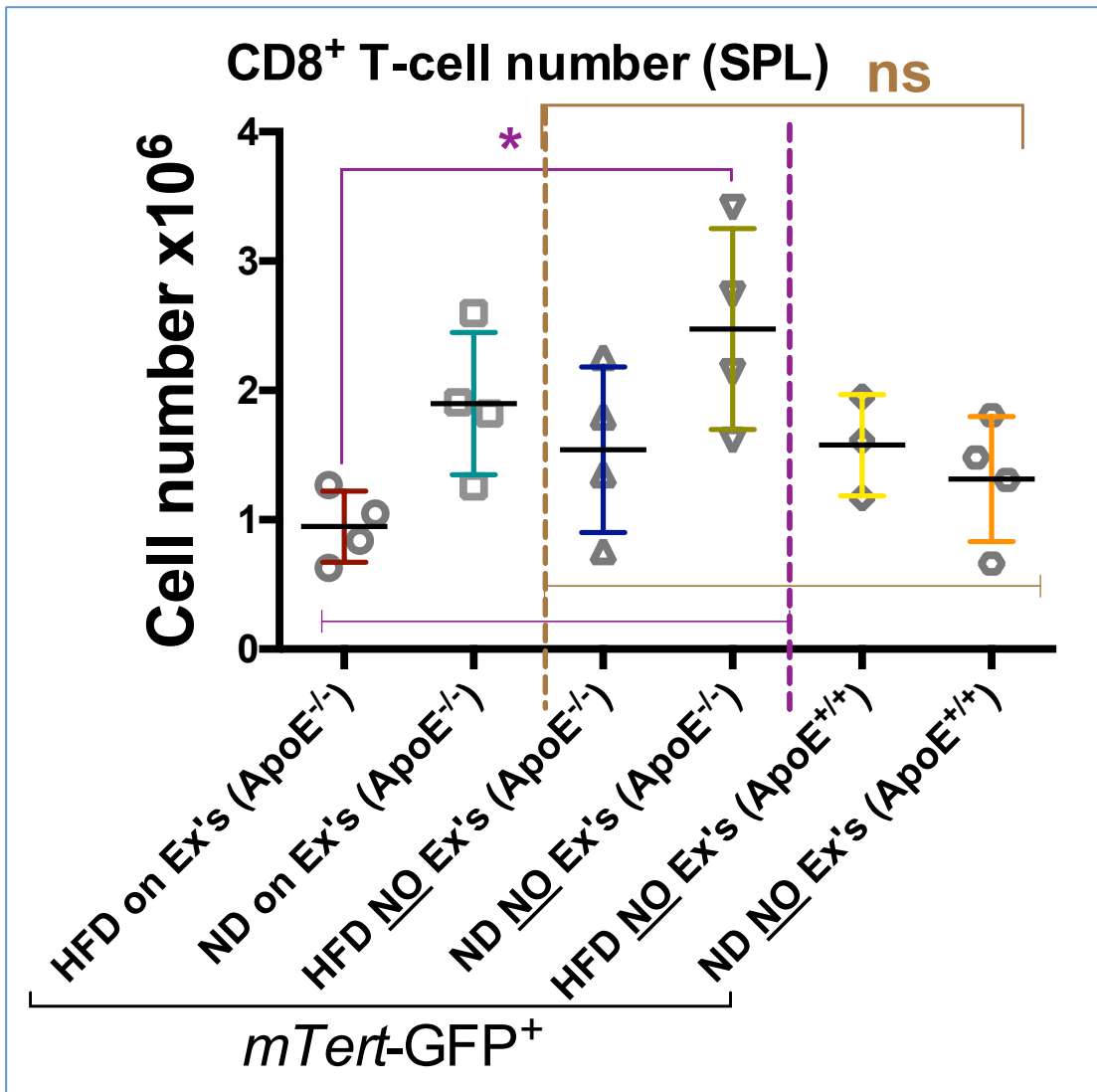


Figure 5.20. CD8⁺ T-cell (splenocyte) numbers for ApoE^{-/-}*mTert-GFP*⁺ and ApoE^{+/-}*mTert-GFP*⁺ mice on different diets with and without exercise

2 groups of ApoE^{-/-}*mTert-GFP*⁺ mice on the voluntary wheel running exercise for 16 weeks, 4 mice on HFD vs. 4 mice on ND. 2 groups of ApoE^{-/-}*mTert-GFP*⁺ mice with no exercise, 4 mice on HFD vs. 4 mice on ND. 2 groups of ApoE^{+/-}*mTert-GFP*⁺ with no exercise, 3 mice on HFD vs. 4 mice on ND. CD8⁺ T-cell (spleen) numbers were counted for each mouse. All values are displayed as mean±sem. * P<0.05 for comparison between HFD vs. ND and exercise vs. no exercise on ApoE^{-/-}*mTert-GFP*⁺ mice using 2-way ANOVA multiple comparisons (purple section). 2-way ANOVA multiple comparisons (brown section) were also used to compare between HFD vs. ND and ApoE^{-/-}*mTert-GFP*⁺ vs. ApoE^{+/-}*mTert-GFP*⁺ mice.

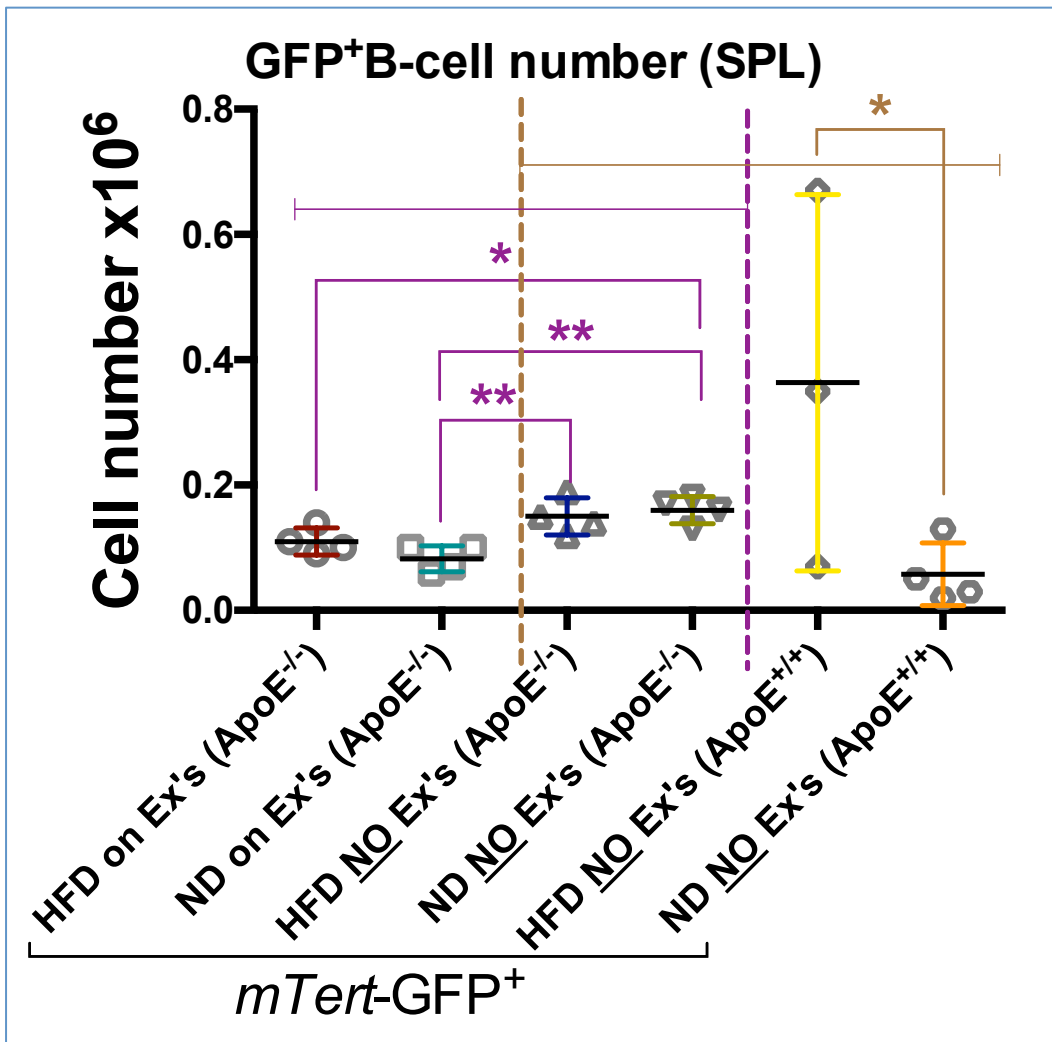


Figure 5.21. GFP^+ B-cell (splenocytes) numbers for $\text{ApoE}^{-/-}\text{mTert-GFP}^+$ and $\text{ApoE}^{+/+}\text{mTert-GFP}^+$ mice on different diets with and without exercise

2 groups of $\text{ApoE}^{-/-}\text{mTert-GFP}^+$ mice on the voluntary wheel running exercise for 16 weeks, 4 mice on HFD vs. 4 mice on ND. 2 groups of $\text{ApoE}^{-/-}\text{mTert-GFP}^+$ mice with no exercise, 4 mice on HFD vs. 4 mice on ND. 2 groups of $\text{ApoE}^{+/+}\text{mTert-GFP}^+$ with no exercise, 3 mice on HFD vs. 4 mice on ND. GFP^+ B-cells from spleen number was counted for each mouse. All values are displayed as mean \pm sem. * $P<0.05$, ** $P<0.01$ for comparison between HFD vs. ND and exercise vs. no exercise on $\text{ApoE}^{-/-}\text{mTert-GFP}^+$ mice using 2-way ANOVA multiple comparisons (purple section). 2-way ANOVA multiple comparisons (brown section) were also used to compare between HFD vs. ND and $\text{ApoE}^{-/-}\text{mTert-GFP}^+$ vs. $\text{ApoE}^{+/+}\text{mTert-GFP}^+$ mice.

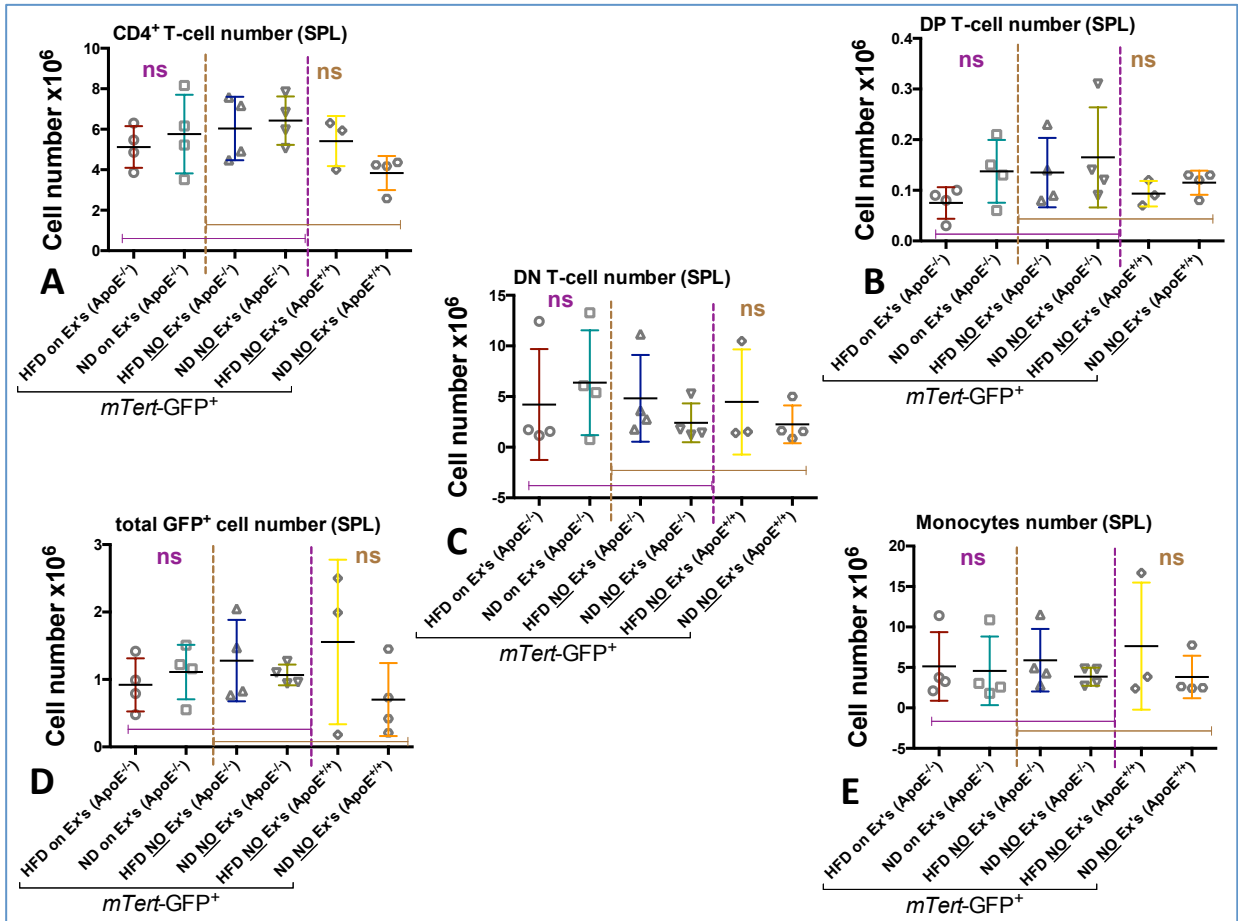


Figure 5.22. Number of other splenocyte subsets from ApoE^{-/-} mTert-GFP⁺ and ApoE^{+/+} mTert-GFP⁺ mice on different diets with and without exercise

2 groups of ApoE^{-/-} mTert-GFP⁺ mice on the voluntary wheel running exercise for 16 weeks, 4 mice on HFD vs. 4 mice on ND. 2 groups of ApoE^{-/-} mTert-GFP⁺ mice with no exercise, 4 mice on HFD vs. 4 mice on ND. 2 groups of ApoE^{+/+} mTert-GFP⁺ with no exercise, 3 mice on HFD vs. 4 mice on ND. **A:** CD4⁺ T-cell (spleen) number were counted for each mouse. **B:** DP T-cell (spleen) number. **C:** DN T-cell (spleen) number. **D:** GFP⁺ splenocyte number and **E:** Monocytes (spleen) number. All values are displayed as mean \pm sem. * P<0.05, ** P<0.01, *** P<0.001, **** P<0.0001 for comparison between HFD vs. ND and exercise vs. no exercise on ApoE^{-/-} mTert-GFP⁺ mice using 2-way ANOVA multiple comparisons (purple section). 2-way ANOVA multiple comparisons (brown section) were also used to compare between HFD vs. ND and ApoE^{-/-} mTert-GFP⁺ vs. ApoE^{+/+} mTert-GFP⁺ mice.

5.2.4.10 Effect of voluntary wheel running on percentage of B-cells (thymocytes) in *ApoE^{-/-} mTert-GFP⁺* mice

Bone marrow yields committed lymphoid progenitors, which make their way towards the thymus. During the early stage, committed T-cells do not express a T-cell Receptor (TCR) and these are deemed ‘double-negative thymocytes’ (DN; no CD4 or CD8) (Godfrey et al., 1993). When these are successfully expressed (pre-TCR), cells proliferate extensively during the transition from DN4 to double-positive (DP). Cortical epithelial cells, which express MHC class I and II molecules, related to self-peptides, then interact with the TCR⁺CD4⁺CD8⁺ (DP) thymocytes (Robey et al., 1994; von Boehmer et al., 1989). T-lymphocytes mature in the thymus, so we investigated the cell population in this organ to identify the effect of exercise, diet and genotype on T-cells. Thymocytes were isolated by Ficoll-hypaque density gradient. I also assumed the presence of a B-cell population in the thymus and cells were stained by CD45R (B220) together with other antibodies as described at 2.2.8. Thymic B-cells exist in small numbers in the thymus (Fehervari, 2013) and the sub-population was gated and separated from the other population by flow cytometry. Surprisingly, there was an excess of B-lymphocytes in the thymus (Figure 5.23). Furthermore, there was a significant ($P<0.05$) decrease in B-cell percentage (Figure 5.23 - purple section) under training ($1.25\pm0.25\%$ per thymocyte compared to $5.25\pm0.85\%$ per thymocyte, both on normal diet). On the other section (Figure 5.23 - brown section) there were no significant changes between all groups under all conditions on the percentage of B-cells at the thymus.

5.2.4.11 Effect of voluntary wheel running on percentage of total GFP⁺ (thymocytes) in *ApoE^{-/-} mTert-GFP⁺* mice

Green fluorescent protein (GFP⁺) positive cells correlate to cells that express the telomerase expression number at a cellular level. This expression indicates the percentage of telomerase present and of telomerase activity (Breault et al., 2008; Armstrong et al., 2000; Richardson et al., 2012). In this experiment, total GFP⁺ cell percentage was used as a read-out for telomerase protein expression, and we also sought to find the effect of exercise and other effects on both mouse genotypes on cell telomerase levels. Figure 5.24 (purple section) shows a significant ($P<0.05$) decrease in GFP⁺ percentage under exercise with HFD ($0.798\pm0.22\%$ per thymus vs. $1.965\pm0.35\%$ per thymus for the non-exercising group with ND).

When comparing the *ApoE^{-/-}* vs. *ApoE^{+/+}* groups, both on the non-exercise program and fed with HFD vs. ND (figure 5.24 - brown section), there was no significant effect between all groups under all conditions. Surprisingly, in the spleen, the telomerase expression on B-cells

was significantly higher under exercise with HFD compared to ND with exercise. However, in the thymus (figure 5.24), the percentage of these cells was the lowest compared to all groups, except ND without exercise, in which both percentages were very similar (“ApoE^{-/-} mTert-GFP⁺” HFD exercise group = % 0.798±0.22 per thymus vs. “ApoE^{+/+} mTert-GFP⁺” ND non-exercise group = % 0.76±0.31 per thymus).

The percentage of total GFP⁺ expression in the thymus was very close to the CD8⁺ T-cell number at the spleen. From this, and because CD8⁺ T-cells are most commonly found in the thymus, the percentage of expression at the thymus matches the number of CD8⁺ T-cells.

5.2.4.12 Effect of voluntary wheel running on percentage of CD4⁺ T-cells (thymocytes) in ApoE^{-/-} *mTert-GFP*⁺ mice

CD4⁺ T-cells mature and develop in the thymus. They are a subset of T-lymphocytes called T helper cells. This experiment was designed to ascertain whether exercise and diet have an effect on CD4⁺ T-cells in the thymus for both genotypes (ApoE^{-/-}, and ApoE^{+/+}) *mTert-GFP*⁺ mice. Figure 5.25 (purple section) shows that exercise with HFD does not change the percentage of CD4⁺ T-cells in the thymus 10±2.48% per vs. 7.5±0.5% for exercising group under ND (ns). Under the same diet without exercise, this trend became significant (P<0.05), but in favour of (ApoE^{-/-}) ND no exercise (20±3.29% per thymocyte compared to (ApoE^{-/-}) HFD no exercise, 10.5±1.5% per thymocyte). Furthermore, this increase in CD4⁺ T-cell percentage (20±3.29% per thymocyte) for group ApoE^{-/-} *mTert-GFP*⁺ under ND without exercise was significant (P<0.01) compared to the exercising group with ND (7.5±0.5% per thymocyte). It was also significant (P<0.05) compared to the exercising group with HFD (10±2.48% per thymocyte).

Figure 5.25 (brown section) shows that in ApoE^{+/+} *mTert-GFP*⁺ mice (both groups without exercise), there was a trend towards an increase in CD4⁺ T-cells in favour of the ND group (9.25±0.25% vs. 7±2% for the HFD group, ns). When comparing these groups (ApoE^{+/+}) with (ApoE^{-/-}) no exercise, there was a significant (P<0.05) increase in CD4⁺ T-cell percentage in favour of ApoE^{-/-} *mTert-GFP*⁺ on ND without exercise (20±3.29% per thymocyte compared to the same diet and no exercise, but ApoE^{+/+} *mTert-GFP*⁺ mice, 9.25±0.25% per thymocyte). ApoE^{-/-} *mTert-GFP*⁺ on ND without exercise (20±3.29% per thymocyte), the increasing percentage for CD4⁺ T-cells was significant (0.01) compared to ApoE^{+/+} *mTert-GFP*⁺ group on HFD without exercise (7±2% per thymocyte).

5.2.4.13 Effect of voluntary wheel running on percentage of DP T-cells and other Thymocyte subsets in $\text{ApoE}^{-/-} \text{mTert-GFP}^+$ mice

Double positive (DP) T-cells represent one stage of progress through the development of thymocytes. This phenotype follows DN ($\text{CD4}^- \text{CD8}^-$) cells and precedes the final mature T-cells either $\text{CD4}^+ \text{CD8}^-$ or $\text{CD4}^- \text{CD8}^+$ (Li et al., 2007; Haynes et al., 2000). This experiment was designed to identify the effect of all variables in this study on the extent of DP T-cells in the thymus.

Figure 5.26 (purple section) shows that there were no significant changes between all groups. However, under exercise, there was a trend towards increase in favour of the ND $\text{ApoE}^{-/-} \text{mTert-GFP}^+$ group ($73 \pm 3.9\%$ per thymus vs. $65.75 \pm 7.9\%$ per thymus for the HFD $\text{ApoE}^{-/-} \text{mTert-GFP}^+$ group). Without exercise, the increasing percentage was in favour of HFD $\text{ApoE}^{-/-} \text{mTert-GFP}^+$ ($64.75 \pm 5.41\%$ per thymus vs. $51.75 \pm 2.32\%$ per thymus for the ND $\text{ApoE}^{-/-} \text{mTert-GFP}^+$ no exercise group).

On other hand, figure 5.26 (brown section) shows a significant ($P < 0.05$) decrease of DP T-cell percentage ($51.75 \pm 2.32\%$ per thymus, ND $\text{ApoE}^{-/-} \text{mTert-GFP}^+$ no exercise group compared to $71 \pm 2.1\%$ per thymus, HFD $\text{ApoE}^{+/+} \text{mTert-GFP}^+$ no exercise group). Also, the ND $\text{ApoE}^{-/-} \text{mTert-GFP}^+$ no exercise group had a significant ($P < 0.05$) decrease of DP T-cell percentage ($51.75 \pm 2.32\%$ per thymus vs. $68.75 \pm 3.47\%$ per thymus, ND $\text{ApoE}^{+/+} \text{mTert-GFP}^+$ no exercise group).

CD8^+ T-cells (Figure 5.27A), DN T-cells (Figure 5.27B) and monocytes (Figure 5.27C) comprise the majority sub-population at the mouse thymus. However, these sub-populations showed no significant changes between cells under all conditions (exercise, diet and mouse genotype).

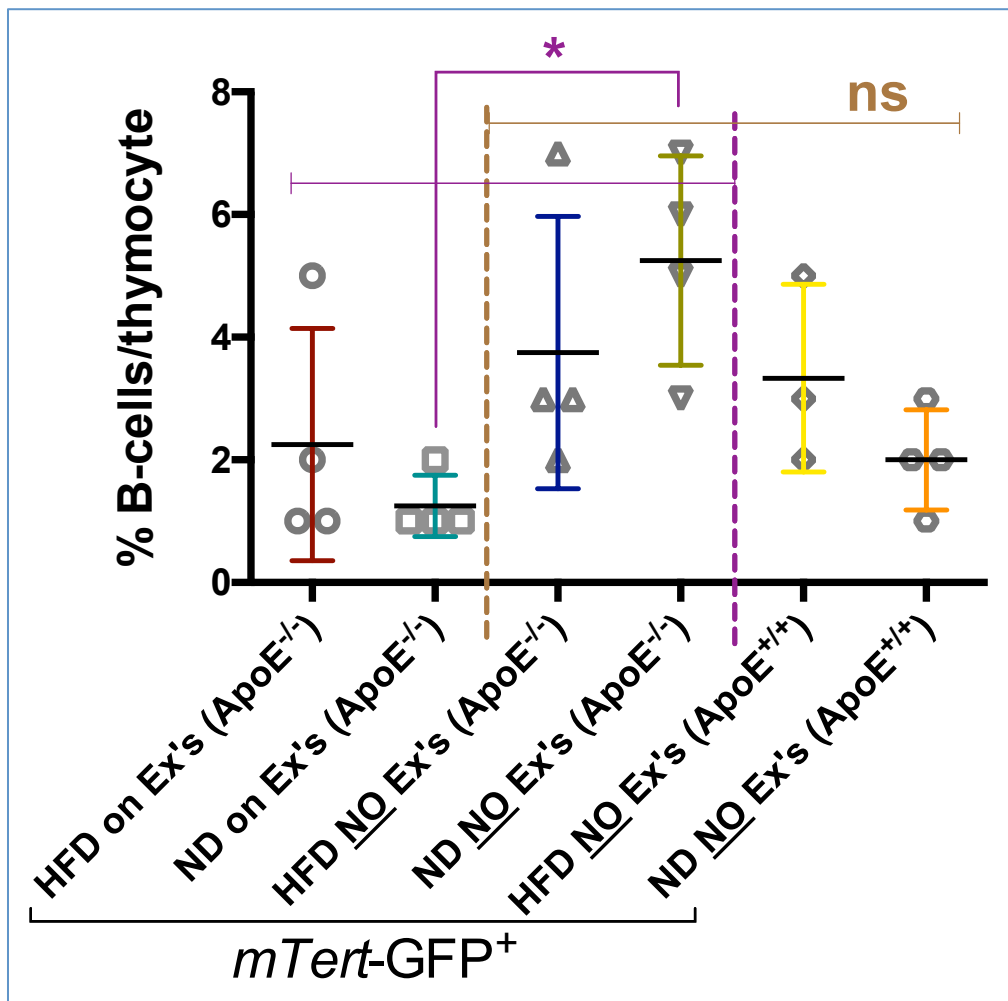


Figure 5.23 Percentage of B-cells in the thymus of $\text{ApoE}^{-/-}\text{mTert-GFP}^+$ and $\text{ApoE}^{+/-}\text{mTert-GFP}^+$ mice on different diets with and without exercise

2 groups of $\text{ApoE}^{-/-}\text{mTert-GFP}^+$ mice on the voluntary wheel running exercise for 16 weeks, 4 mice on HFD vs. 4 mice on ND. 2 groups of $\text{ApoE}^{-/-}\text{mTert-GFP}^+$ mice with no exercise, 4 mice on HFD vs. 4 mice on ND. 2 groups of $\text{ApoE}^{+/-}\text{mTert-GFP}^+$ with no exercise, 3 mice on HFD vs. 4 mice on ND. Percentage of B-cell⁺ per thymocyte. All values are displayed as mean \pm sem. * $P<0.05$ for comparison between HFD vs. ND and exercise vs. no exercise on $\text{ApoE}^{-/-}\text{mTert-GFP}^{+/-}$ mice using 2-way ANOVA multiple comparisons (purple section). 2-way ANOVA multiple comparisons (brown section) were also used to compare between HFD vs. ND and $\text{ApoE}^{-/-}\text{mTert-GFP}^+$ vs. $\text{ApoE}^{+/-}\text{mTert-GFP}^+$ mice.

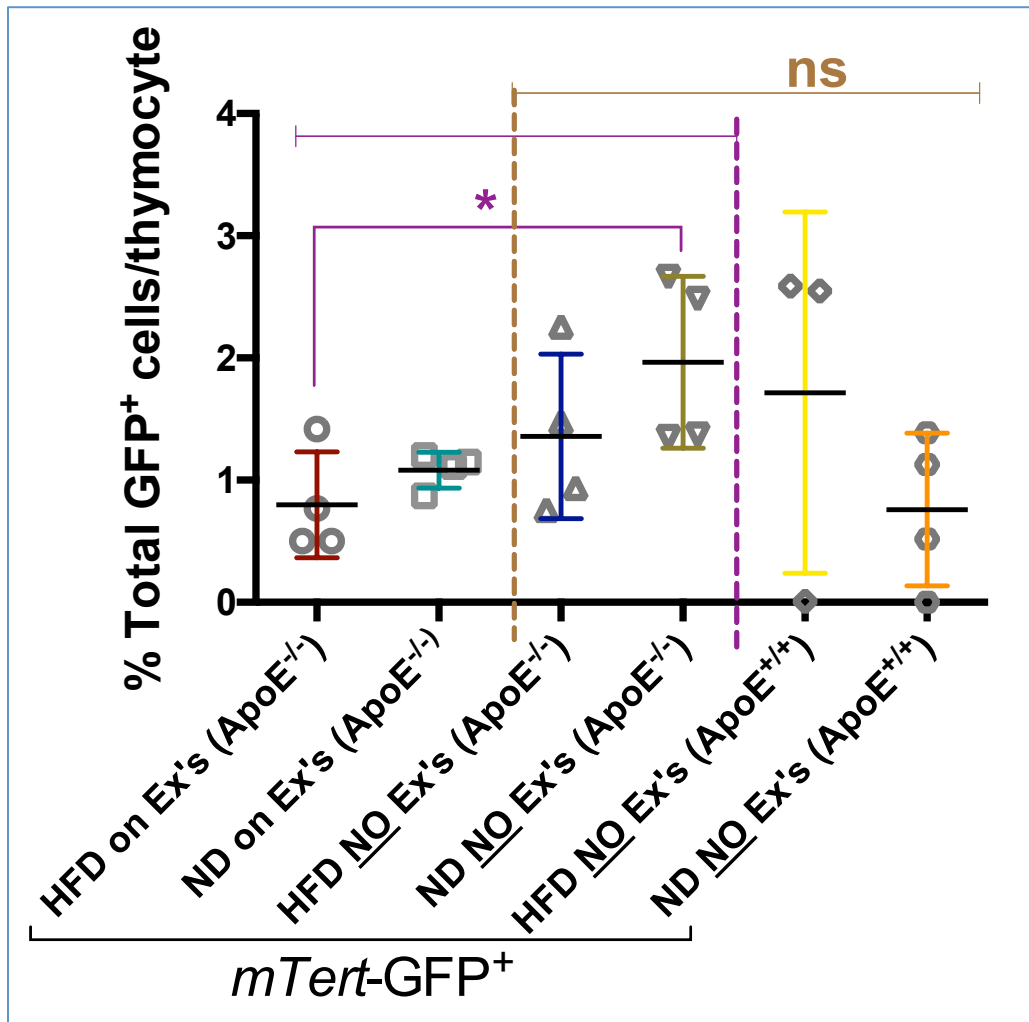


Figure 5.24. Percentage of total GFP⁺ cells in the thymus of ApoE^{-/-}*mTert-GFP⁺* and ApoE^{+/+}*mTert-GFP⁺* mice on different diets with and without exercise

2 groups of ApoE^{-/-}*mTert-GFP⁺* mice on the voluntary wheel running exercise for 16 weeks, 4 mice on HFD vs. 4 mice on ND. 2 groups of ApoE^{-/-}*mTert-GFP⁺* mice with no exercise, 4 mice on HFD vs. 4 mice on ND. 2 groups of ApoE^{+/+}*mTert-GFP⁺* with no exercise, 3 mice on HFD vs. 4 mice on ND. Percentage of total GFP⁺ per thymocyte. All values are displayed as mean±sem. * P<0.05 for comparison between HFD vs. ND and exercise vs. no exercise on ApoE^{-/-}*mTert-GFP⁺* mice using 2-way ANOVA multiple comparisons (purple section). 2-way ANOVA multiple comparisons (brown section) were also used to compare between HFD vs. ND and ApoE^{-/-}*mTert-GFP⁺* vs. ApoE^{+/+}*mTert-GFP⁺* mice.

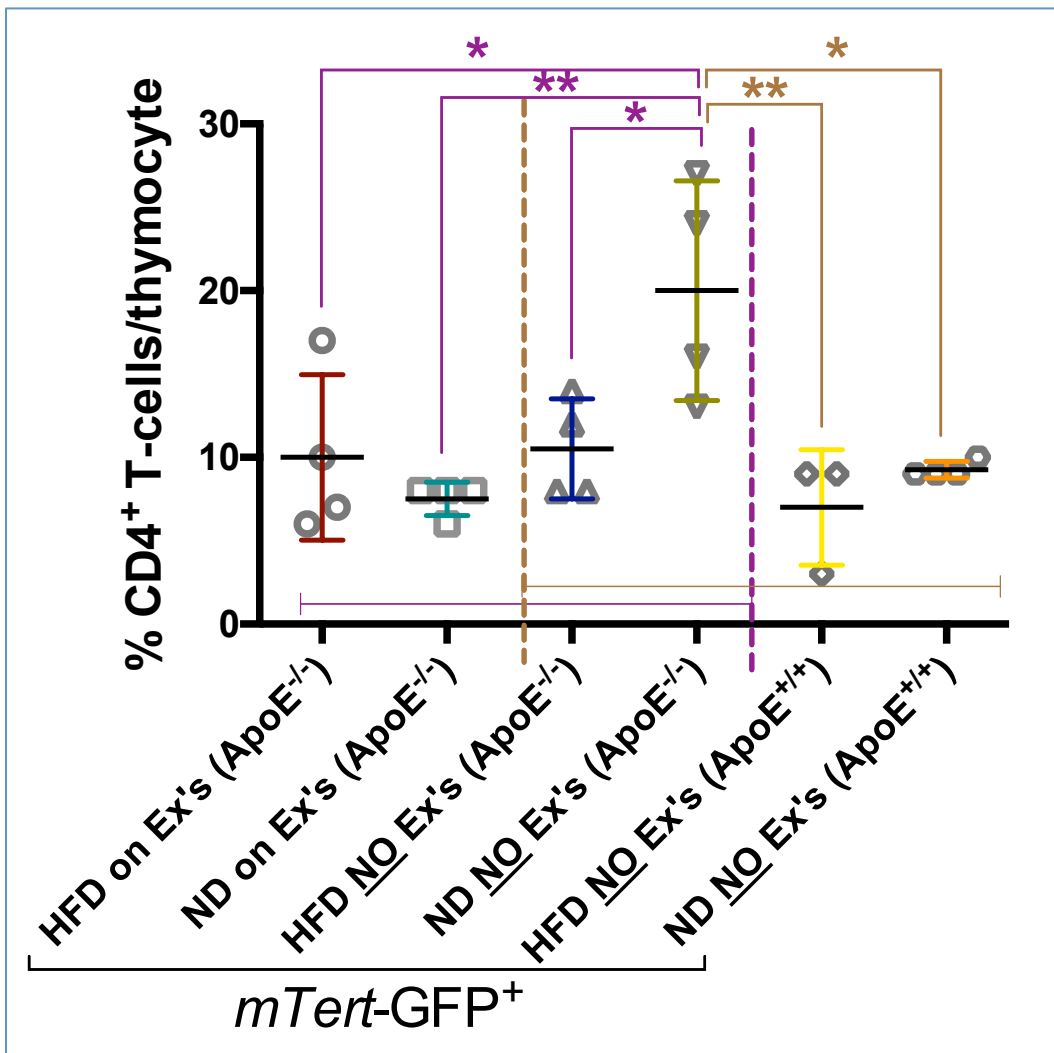


Figure 5.25. Percentage of CD4⁺ T-cells in the thymus of ApoE^{-/-}*mTert-GFP*⁺ and ApoE^{+/-}*mTert-GFP*⁺ mice on different diets with and without exercise

2 groups of ApoE^{-/-}*mTert-GFP*⁺ mice on the voluntary wheel running exercise for 16 weeks, 4 mice on HFD vs. 4 mice on ND. 2 groups of ApoE^{-/-}*mTert-GFP*⁺ mice with no exercise, 4 mice on HFD vs. 4 mice on ND. 2 groups of ApoE^{+/-}*mTert-GFP*⁺ with no exercise, 3 mice on HFD vs. 4 mice on ND. Percentage of CD4⁺ T-cell per thymocyte. All values are displayed as mean \pm sem. * P<0.05, ** P<0.01 for comparison between HFD vs. ND and exercise vs. no exercise on ApoE^{-/-}*mTert-GFP*⁺ mice using 2-way ANOVA multiple comparisons (purple section). 2-way ANOVA multiple comparisons (brown section) were also used to compare between HFD vs. ND and ApoE^{-/-}*mTert-GFP*⁺ vs. ApoE^{+/-}*mTert-GFP*⁺ mice.

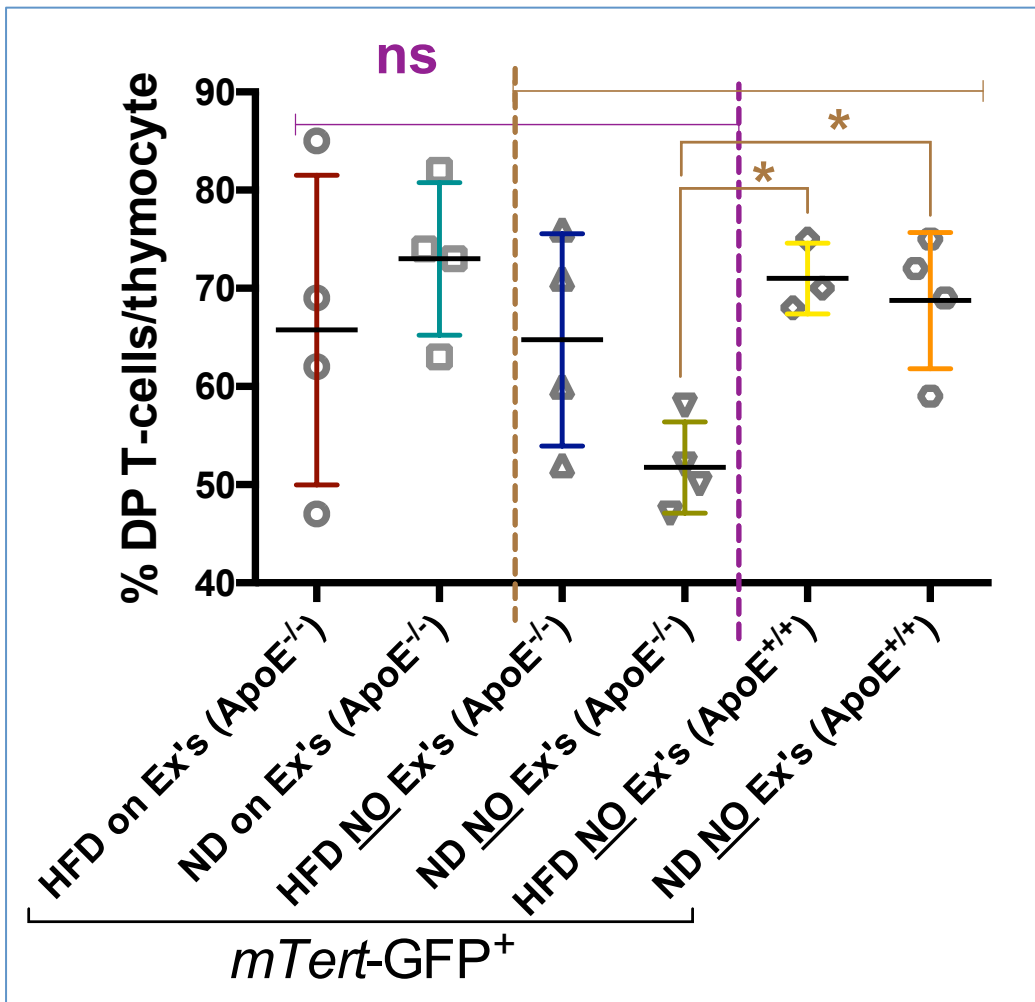


Figure 5.26. Percentage of DP T-cells in the thymus of $\text{ApoE}^{-/-}m\text{Tert-GFP}^+$ and $\text{ApoE}^{+/-}m\text{Tert-GFP}^+$ mice on different diets with and without exercise

2 groups of $\text{ApoE}^{-/-}m\text{Tert-GFP}^+$ mice on the voluntary wheel running exercise for 16 weeks, 4 mice on HFD vs. 4 mice on ND. 2 groups of $\text{ApoE}^{-/-}m\text{Tert-GFP}^+$ mice with no exercise, 4 mice on HFD vs. 4 mice on ND. 2 groups of $\text{ApoE}^{+/-}m\text{Tert-GFP}^+$ with no exercise, 3 mice on HFD vs. 4 mice on ND. Percentage of DP T-cell per thymocyte. All values are displayed as mean \pm sem. * $P<0.05$ for comparison between HFD vs. ND and exercise vs. no exercise on $\text{ApoE}^{-/-}m\text{Tert-GFP}^+$ mice using 2-way ANOVA multiple comparisons (purple section). 2-way ANOVA multiple comparisons (brown section) were also used to compare between HFD vs. ND and $\text{ApoE}^{-/-}m\text{Tert-GFP}^+$ vs. $\text{ApoE}^{+/-}m\text{Tert-GFP}^+$ mice.

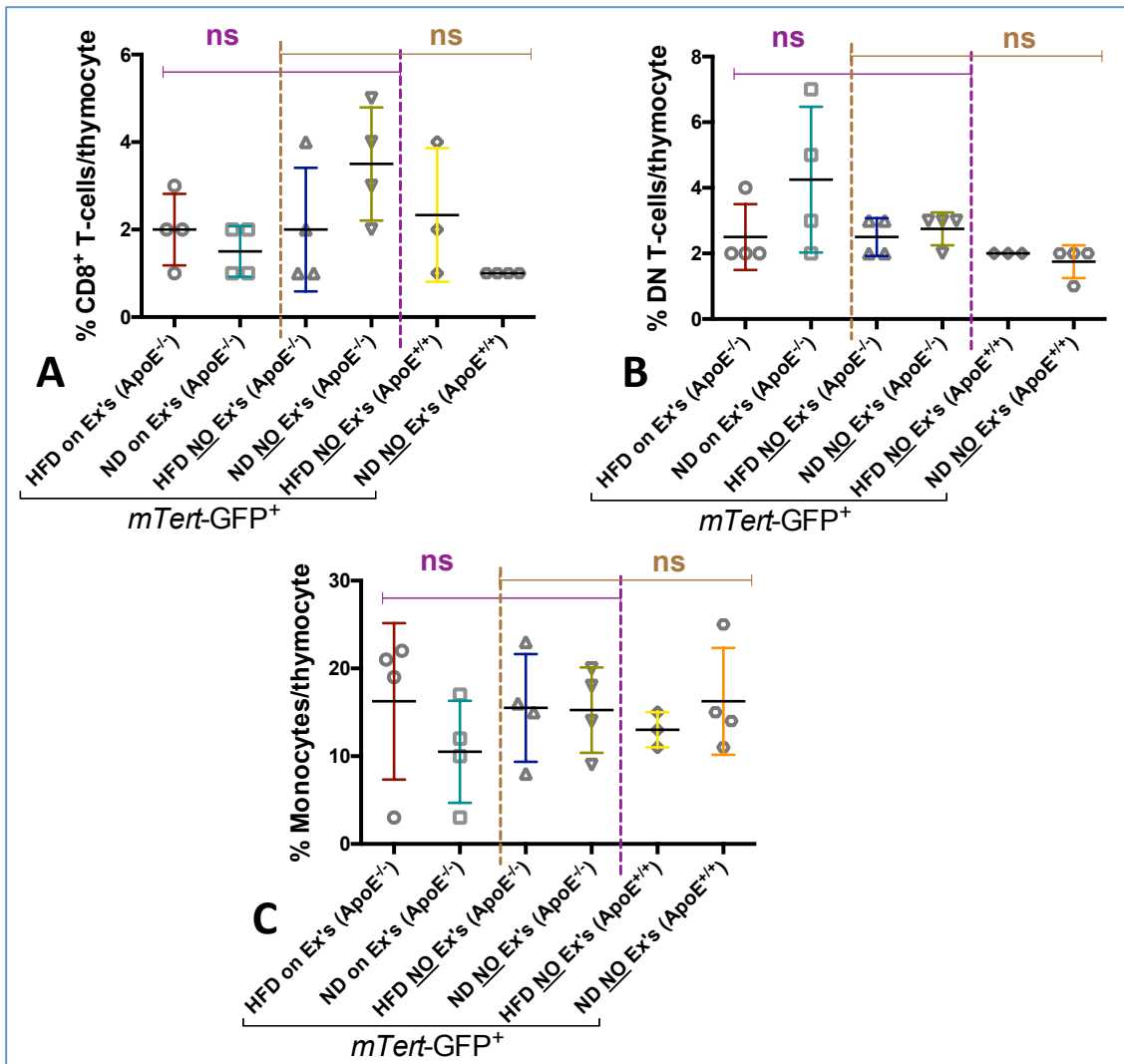


Figure 5.27. Percentages of other thymocyte subsets of ApoE^{-/-}*mTert-GFP*⁺ and ApoE^{+/+}*mTert-GFP*⁺ mice on different diets with and without exercise

2 groups of ApoE^{-/-}*mTert-GFP*⁺ mice on the voluntary wheel running exercise for 16 weeks, 4 mice on HFD vs. 4 mice on ND. 2 groups of ApoE^{-/-}*mTert-GFP*⁺ mice with no exercise, 4 mice on HFD vs. 4 mice on ND. 2 groups of ApoE^{+/+}*mTert-GFP*⁺ with no exercise, 3 mice on HFD vs. 4 mice on ND. **A:** percentage of CD8⁺ T-cells per thymocyte, **B:** percentage of DN T-cells per thymocyte, **C:** percentage of monocytes per thymocyte. All values are displayed as mean±sem. No significant (ns) for comparison between HFD vs. ND and exercise vs. no exercise on ApoE^{-/-}*mTert-GFP*⁺ mice using 2-way ANOVA multiple comparisons (purple section). 2-way ANOVA multiple comparisons (brown section) were also used to compare between HFD vs. ND and ApoE^{-/-}*mTert-GFP*⁺ vs. ApoE^{+/+}*mTert-GFP*⁺ mice.

5.3. Discussion

This study confirmed that voluntary wheel running is a good model for investigating mouse exercise. The design gives mice the freedom to run as per their physiological need. Being voluntary, it also works at the molecular level, because it is non-stressful and therefore does not disrupt normal activity patterns. 4 different mouse genotypes were used: TERT^{+/+} (C57BL/6), TERT⁺⁻, *mTert*-GFP⁺ and ApoE^{-/-}*mTert*-GFP⁺. All exhibited almost the same diurnal activity.

Weight and activity

As expected, mouse bodyweight decreased after the running exercise, compared to the non-exercise groups and this was significant in some cases. This finding supports previous studies (De Bono et al., 2006; Turner et al., 2005; Bernstein, 2003 and Allen et al., 2001). Female TERT^{+/+} mice were found to be more active and spent more time exercising compared to male mice. This was also found by De Bono et al. (2006).

ApoE^{-/-}*mTert*-GFP⁺ mice on a high fat diet (HFD) were more active in terms of both duration and distance, compared to mice of the same genotype on a normal diet (ND), both on voluntary exercise. These groups, on either HFD or ND gained less bodyweight in comparison to non-exercising HFD or ND groups. The average calorie intake by ApoE^{-/-}*mTert*-GFP⁺ mice on training with HFD was similar to ApoE^{-/-}*mTert*-GFP⁺ mice without exercise either on HFD or ND. ApoE^{-/-}*mTert*-GFP⁺ mice on training with ND consumed more calories compared to those on a HFD or those without exercise either on HFD or ND. This may be related either to ApoE deficiency, or because the opportunity to do more voluntary wheel exercise resulted in a loss of some bodyweight. Moreover, HFD mice may have been more active compared to ND mice because they had more energy. There was no significant change in the bodyweight for ApoE^{-/-}*mTert*-GFP⁺ exercising mice for both HFD and ND.

ApoE plays an important role in lipoprotein metabolism. Both chylomicrons and VLDL remnants (derived from diet and liver respectively) are cleared through a process that relies in part on ApoE. Studies by Mahley (1988) and Piedrahite et al. (1992) on ApoE deficient (ApoEKO) mice demonstrated for the first time a viable model for hyperlipidemia and atherosclerosis. The decrease in bodyweight after exercise was demonstrated by Pellegrin et al. (2009), who found that swimming exercise for 6 months led to significantly decreased bodyweight in ApoE^{-/-} mice compared to a sedentary group. In addition, their data showed that 6 months of swimming exercise stabilized atherosclerosis progression (Pellegrin et al.,

2009). However, other studies concluded that the exercise led to decreased atherosclerosis extension in ApoE^{-/-} mice (Laufs et al., 2005; Pellegrin et al., 2009; Okabe et al., 2007).

Lymphocyte ‘shifts’

Splenocyte numbers were measured in all groups and there was no significant trend towards increased cell numbers in the exercising groups. A range of other studies, using various designs, protocols, exercise regimes, species and tissues have found similar results in regard to immune cell levels following voluntary exercise (Woods et al., 2000; Woods et al., 2003; Hoffman-Goetz et al., 1992; Macneil and Hoffman-Goetz, 1993 and Jonsdottir et al., 1997). In conclusion, exercise does not seem to change splenocyte numbers. Interestingly, I found opposing increases and decreases between B-cell numbers and CD8⁺ T-cell numbers in all groups with some variation for ApoE^{-/-} *mTert*-GFP⁺ mice.

TERT heterozygous mice exhibited a trend toward increased CD4⁺ and CD8⁺ T-lymphocytes (ns) for the exercise group compared to the non-exercise group. However, the other subpopulations (double positive, double negative, B-cells and monocytes) seemed to decrease in cell numbers for the exercise group compared to the non-exercise group. A similar increase in T-lymphocytes was observed by Woods et al. (2003), who found that Balb/cByJNia mouse strains after 4 months of exercise provided a good model for immunology and cardiovascular research. Injecting BALB/c mice with mineral oil causes plasmacytoma production, which leads to monoclonal antibody production. In young mice, this caused, naïve and memory T-lymphocyte production from splenocytes to return to normal. They also found the ratio of naïve to memory T-lymphocytes increased after exercise training in old mice, as exercise maintained absolute naïve T-cell numbers vs. memory T-cell numbers (Woods et al., 2003). The percentage of regulatory T-cells trended towards increasing (ns) compared to the non-exercise group. This gave the impression that there was an effect on blood circulation, which allowed these cells to circulate and proliferate, leading to an increase in percentage. We used healthy mice and the benefit of the running exercise may convert to physiological muscle strength (this was observed but not measured). Because Tregs play an important role in activating or suppressing immune system function (Parsons et al., 2007; Akbari et al., 2003) and because the immune system functionality is normal for these mice, we did not find any significant changes between the exercising and control groups.

mTert-GFP⁺ mice showed no significant changes in cell numbers for CD4⁺ and CD8⁺ T-cells, or in monocyte numbers between the exercising and non-exercising groups. I found a trend towards an increase in GFP⁺ cells expressing telomerase activity (ns). This may arise from

increased blood circulation due to exercise, which plays a role in cell proliferation and may improve telomerase function (expression).

The trend towards increased splenocyte numbers favoured the non-exercise control group in the ApoE^{-/-} *mTert*-GFP⁺ groups. This may be secondary to ApoE deficiency, which puts these mice under high risk of lipid accumulation and cardiovascular complications (Candido et al., 2002; Patel et al., 2001). Also, the ApoE^{-/-} *mTert*-GFP⁺ mice group on HFD with exercise expressed significantly lower numbers of GFP⁺B-cells⁺ compared to the non-exercise ND group, and trended towards decreased GFP⁺B-cell⁺ expression compared to the non-exercise HFD group. This may be related to the humoral immunity classification of Ig producing B-cells (Berkowska et al., 2011).

ApoE^{-/-} *mTert*-GFP⁺ mice under exercise exhibited increased B-cell numbers in the HFD group and decreased B-cell numbers in the ND group. CD8⁺ T-cell numbers decrease in the HFD group and increased in the ND group. Similar trends were observed for ApoE^{-/-} *mTert*-GFP⁺ mice without exercise; the B-cell numbers increased for the HFD group and decreased in the ND group, whilst CD8⁺ T-cell numbers decreased for the HFD group and increased in the ND group. Ig production by B-cells plays a key role in humoral immunity. Conversely, CD8⁺ T-cells are cytotoxic and therefore contribute to the cellular immune response (Berkowska et al., 2011). Further study is required to establish the relationship between B-cells and CD8⁺ T-cells in atherosclerosis.

Interestingly, I found a significant increase in B-cell numbers for the exercising group ($19.1 \pm 0.79 \times 10^6$ /spleen) vs. the control group ($17.2 \pm 1.7 \times 10^6$ /spleen). The increase of circulating B-cells was reported after sprinting exercise (Gray et al., 1993; Nieman, et al., 1995). B-cells produce immunoglobulins (Ig) and play a role in humoral immunity (Berkowska et al., 2011). They differentiate into antibody-producing plasma cells or circulating memory cells (Ozaki et al., 2004). Further studies would be required to determine which type of B-cell responds to exercise.

I found B-cells⁺ at the mouse thymus organ. This was also demonstrated by Fehervari (2013), who found a small population of thymic B-cells at the thymus. The percentage of total GFP⁺ expression in the thymus is very close to the CD8⁺ T-cell number at the spleen. From this, and because CD8⁺ T-cells are most commonly found in the thymus, this percentage of expression at the thymus matches the number of CD8⁺ T-cells.

Telomerase

My study supports the idea that the effect of exercise on telomeres might be mediated in some way by telomerase and the TERT protein. Experiments using murine tissues have indicated that TERT may form part of a chromatin remodelling complex or act as a transcription factor (Park et al., 2009). These findings strongly support the idea that phenotype ageing can be inhibited in immune, vascular and cardiac cells, due to the connection between exercise and a supportive cellular environment which prevents telomere shortening. Furthermore, Ludlow et al. (2012) trained a CAST/Ei mice strain for 11 months on voluntary wheel running and found increased telomerase activity after exercise in mouse skeletal muscle.

Telomerase is the enzyme that protects and elongates the telomeres at each chromosome end of the DNA. The effect of exercise on TERT expression and telomere-related proteins was determined by comparing TERT deficient mice with wild type mice (Werner et al., 2009; Werner et al., 2008). Both groups underwent the voluntary wheel running exercise and it was concluded that exercise had no effect on cell-cycle-checkpoint kinase 2 (Chk2), tumour suppressor protein p16, tumour suppressor protein p53 or telomere repeat binding factor 2 (TRF2) for the TERT^{-/-} group compared to the TERT^{+/+} group. In contrast, 3 weeks of running exercise significantly increased cardiac telomerase activity by more than twofold in wild type mice, as well as TERT expression in the heart compared to the sedentary group. In addition, cardiac telomere-stabilising proteins increased in wild-type mice doing voluntary exercise. P53, P16 and Chk2 mRNA expression was significantly reduced after 3 weeks of voluntary running compared to the control groups. In humans, telomerase activity in PBMNCs significantly increased by 2.5-fold in young athletes and by 1.8-fold in middle-aged athletes compared to sedentary individuals. Young participants exhibited non-significant changes in lymphocyte telomere lengths between athletes and untrained groups, but older people in the control group showed significant telomere shortening compared to the trained older group and younger groups either with or without training (Werner et al., 2009; Werner et al., 2008). *mTert-GFP⁺* are telomerase reporter mice. There were no significant changes for telomerase expression in all GFP⁺ cells.

I found that telomerase activity significantly increased in ApoE^{-/-}*mTert-GFP⁺* mice on exercise and HFD, compared to no exercise and ND. However, there was no significant change in the bodyweight for ApoE^{-/-}*mTert-GFP⁺* mice under exercise for both HFD and ND. I also demonstrated a significant effect on telomerase activity when ApoE^{-/-}*mTert-GFP⁺* mice on exercise were compared with the no exercise group, both on HFD. On exercise, telomerase

activity increased significantly (by 3.9-fold), indicating that ApoE^{-/-}*mTert*-GFP⁺ mice without exercise may suffer from the HFD as they are ApoE deficient, whilst the ApoE^{-/-}*mTert*-GFP⁺ mice on exercise benefit from exercise to reduce the lipids that may accumulate secondary to HFD and ApoE deficiency. ApoE^{-/-} mice on HFD developed atherosclerosis (Meir and Leitersdorf, 2004). In contrast, aerobic exercise is able to reverse arterial inflammation with ageing in mice (Lesniewski et al, 2011). Human studies in leukocytes showed that decreased telomere length is associated with the development of atherosclerosis (Ogami et al., 2004; Benetos et al., 2004; Obana et al., 2003 and Samani et al., 2001). Thus, it is possible that by increasing telomerase activity during exercise, telomeres might become stabilised as shown by others previously (Melk et al., 2014). Thus one could expect one of the beneficial effects of exercise to be a delay in atherosclerosis. However, this was evident only under HFD in ApoE-/- mice. However, telomerase expression in B-cells in ApoE^{-/-}*mTert*-GFP⁺ mice decreased significantly in cell numbers for the exercise group with ND compared to both groups (HFD and ND) without exercise.

Finally, using the ApoE^{-/-}*mTert*-GFP⁺ mouse model of atherosclerosis, we accelerate the effects of the disease by feeding these mice a high fat diet (HFD). Surprisingly, this treatment did not change telomerase activity in splenocytes. This contradicts the results from Gizard et al., (2011) who found increased vascular telomerase activity in a different mouse model (LDLR^{-/-} mice) on a HFD. This discrepancy might be explained by either the different mouse models or the different cell type used to measure telomerase activity (Gizard et al., 2011). However, applying exercise to our ApoE^{-/-}*mTert*-GFP⁺ mice under HFD resulted in increased telomerase activity in splenocytes, while a normal diet (ND) did not yield this effect (Chapter 5). Exercise has been associated with improved cardiovascular health (Werner et al., 2008, 2009; Sallam and Laher, 2016). The cardiovascular benefits of exercise have been frequently attributed to the reduction of many classical cardiovascular risk factors including blood lipid, inflammation and oxidative stress (Sallam and Laher, 2016). Oxidative stress and inflammation are also caused by HFD and I found in the *in vitro* experiments that hyperoxia inhibited splenocyte telomerase activity (Chapter 3). Atherosclerosis development is closely linked with oxidative stress and inflammation while exercise has been shown to decrease oxidative stress by upregulating the antioxidant defense and reducing inflammation markers including IFN γ and TNF α (Sallam and Laher, 2016). Therefore, increased splenocyte telomerase activity during exercise may be linked to decreased oxidative stress and inflammation. However, we did not measure these parameters in the mouse model in order to draw direct conclusions. My data of increased telomerase activity after exercise (chapter 5),

correspond to those from Melk et al., (2014) who found longer telomeres increased telomerase activity after 3 months of exercise in human PBMNCs from middle-age sedentary males and those of Werner et al., (2009) who found increased telomerase activity and longer telomere length in PBMCs of athletes after exercise. The same group demonstrated on a mouse model that the beneficial effect of exercise on the decrease of senescence markers in vascular cells was dependent on the presence of telomerase since the effects were absent in TERT^{-/-} mice (Werner et al., 2008). Taken together, all these results including our own findings of increased telomerase activity in ApoE^{-/-}*mTert*-GFP⁺ mice during exercise and HFD compared to ApoE^{-/-}*mTert*-GFP⁺ mice without exercise and on HFD suggest that telomerase activity may mediate the benefit of exercise on telomere length. However, the underlying mechanism is yet to be investigated in more detail.

CHAPTER 6. Effect of cardiac rehabilitation on telomerase activity and regulatory T-lymphocytes in patients following acute myocardial infarction

6.1 Introduction

Heart disease patients can benefit from being offered cardiac rehabilitation, which is a complex and tailored blend of lifestyle and nutritional education as well as a physical training programme (Wenger et al., 1995; Morris and Froelicher, 1991). Levels of telomerase activity directly affect telomere length, which is associated with oxidative stress and an increased risk of cardiac diseases (Epel et al., 2004; Epel et al., 2006; Demissie et al., 2006) and indeed, shortening of leukocyte telomeres has been implicated as a risk factor for myocardial infarction (MI) (Zee et al., 2009). Cardiovascular diseases are associated with low telomerase activity in PBMNCs (Epel et al., 2006). A study by Melk et al. (2014) found that healthy middle-aged men who had a previously sedentary lifestyle exhibited increased telomerase activity and telomere lengths following a three-month programme of physical activity. Naïve T-cells differentiate into separate subpopulations when stimulated by antigens and cytokines. These subpopulations include T-helper (Th) cells and $CD4^+CD25^+FOXP3^+$ regulatory (Treg) T-cells. 5-10% of all peripheral $CD4^+$ cells are Tregs and these are critical to the maintenance and induction processes involved in immune homeostasis (Chen et al., 2003; Fontenot et al., 2003). Tregs also govern target T-cells and antigen presenting cells (APCs), which inhibit T-cell proliferation and cytokine expression by secreting inhibitory cytokines, including transforming growth factor beta (TGF- β) and IL-10. These have an immunosuppressant effect (Sakaguchi, 2005) and also suppress atherosclerosis (Robertson et al., 2003; Mallat et al., 2001). Telomere maintenance is influenced at a molecular level by TERT mRNA up-regulation (Codd et al., 2013). miRNAs are regulated through physical exercise and this in turn influences the expression of the genes which control telomere homeostasis (Chilton et al., 2014). This sheds some light on the relationships between exercise, telomere length in PBMNCs and health improvement (Chilton et al., 2014).

6.2 Results

6.2.1 Accelerometer-based physiological response to cardiac rehabilitation

6.2.1.1 Effect of cardiac exercise rehabilitation on patients' weight and BMI

In my study, average weight of the 19 patients who participated was 84 ± 3.7 kg and it was 81.8 ± 3.1 kg for the 8 patients who attended the post-cardiac exercise rehabilitation test (Figure 6.1A). However, when the comparison was performed for the 8 patients who attended pre- and post-exercise tests, a non-significant trend toward decrease was noticed in favour of post-cardiac rehabilitation (84 ± 3.7 kg vs. 86.5 ± 4.7 kg for pre-cardiac exercise rehabilitation) (Figure 6.1B). Figure 6.1C shows that the BMI result from all 19 patients who participated in the pre-rehabilitation test and those 8 patients who participated in the post-rehabilitation test. There was no significant decrease in BMI after the cardiac exercise rehabilitation programme among the 8 patients who underwent both pre- and post-cardiac exercise rehabilitation tests (Figure 6.1D).

6.2.1.2 Effect of cardiac rehabilitation on daily physical activity

The accelerometer data were extracted by Dr. Sarah Charman, MoveLab, Newcastle University, using accelerometers that I had prepared and collected from patients. Data were analysed by me.

An accelerometer is a movement sensor which objectively measures the intensity of both physical activity and the relaxation period (Jakovljevic et al., 2014). This device has been used in various forms since 1920 as a measurement of acceleration (Walter, 2007). The GENEActiv monitor was worn by our patients at the wrist of the non-dominant hand for 7 days, as previously described by Jakovljevic et al. (2014) for 24 hours per day. The device was used to time the participants' pre-cardiac exercise rehabilitation programme, followed by their post-cardiac exercise rehabilitation programme, as described at (2.2.17). Figure 6.2A shows the average daily physical activity measured in acceleration (mg), (mg is 1000 gal, gal is galileo = 1cm/sec^2), which was 5.3 ± 0.9 mg for the pre-rehabilitation patients (14 individuals) and 23.8 ± 2.6 mg for the post-rehabilitation patients (7 individuals). The significant ($P < 0.05$) increase in intensity of acceleration movement was noticed when the comparison applied only to the 6 patients who underwent both pre- and post-cardiac exercise rehabilitation testing (Figure 6.2B). I found the intensity was 26 ± 1.6 mg for post-exercise group vs. 15.5 ± 1 mg for pre-exercise group. The cardiac exercise rehabilitation programme can therefore lead to improvement of daily activity.

6.2.1.3 Time spent per day in moderate to vigorous physical activity (MVPA)

Studies have shown that after cardiac rehabilitation, the capacity and duration of exercise was improved (Tyni-Lenne et al., 1998; Cheetham et al., 2002). Time spent on exercise is one parameter that can indicate improvement levels. I measured the time patients spent each day doing MVPA, as shown in figure 6.3A. The 14 patients at the pre-rehabilitation stage spent 35.3 ± 5 min/day and the 7 patients after the cardiac rehabilitation programme spent 91.9 ± 15.2 min/day. A significant ($P < 0.05$) increase in time spent on daily MVPA was found with the 6 patients (Figure 6.3B) who engaged in both pre- and post-rehabilitation testing (35.6 ± 5.8 min/day before exercise rehabilitation, compared to 104 ± 10.8 min/day after the exercise rehabilitation programme).

6.2.1.4 Daily physical activity as acceleration distribution

The daily activity for patients was measured as acceleration distribution and this was divided into units of 50mg intensity for pre- and post-exercise programmes. The activity distribution was different from patient to patient during the day-night period. This intensity was averaged for all monitoring over 7 days. Figure 6.4 shows the results from the groups of 14 patients pre-rehabilitation and 7 patients post-rehabilitation, whilst figure 6.5 shows the comparison between 6 patients who underwent the test pre- and post-rehabilitation after MI. In figure 6.4, most of the daytime was spent with low intensity (0-50mg) activity - about 1320 ± 10.2 min/day for the pre-rehabilitation group and 1222 ± 28.2 min/day for the post-rehabilitation group. This means that the post-rehabilitation group spent more time on moderate and vigorous activity per day. After the rehabilitation programme, the patients started to spend about 83.6 ± 14.9 min/day on moderate activity, with an intensity of 50-150mg and 54.4 ± 6.8 min/day before rehabilitation with about half an hour difference per day. Conversely, the patients who spent 18.1 ± 3.3 min/day on vigorous activity had an intensity of 150-250mg and 4.6 ± 0.7 min/day for before the exercise program, with about 13.5 min/day spent on vigorous activity.

When only the 6 patients who underwent both tests (pre- and post-) were considered (figure 6.5), I noticed that before cardiac rehabilitation, these patients spent significantly ($P < 0.05$) more time in low intensity activity 0-50mg by 1320 ± 11.7 min/day vs. 1196 ± 13.2 min/day for the same patients after cardiac rehabilitation. The moderate (50-150mg) daily activity for these 6 patients was increased significantly ($P < 0.001$) from 54.3 ± 9.8 min/day for pre-rehabilitation vs. 95.8 ± 14.3 min/day for the same patients after exercise rehabilitation. The

time spent on vigorous (150-250mg) activity for the same patients was significantly ($P<0.001$) increased to 20.6 ± 3.3 min/day post-cardiac exercise rehabilitation from 4.5 ± 1 min/day pre-cardiac exercise rehabilitation. It seems clear that after cardiac rehabilitation, physical activity was increased and the intensity of exercise was significantly increased.

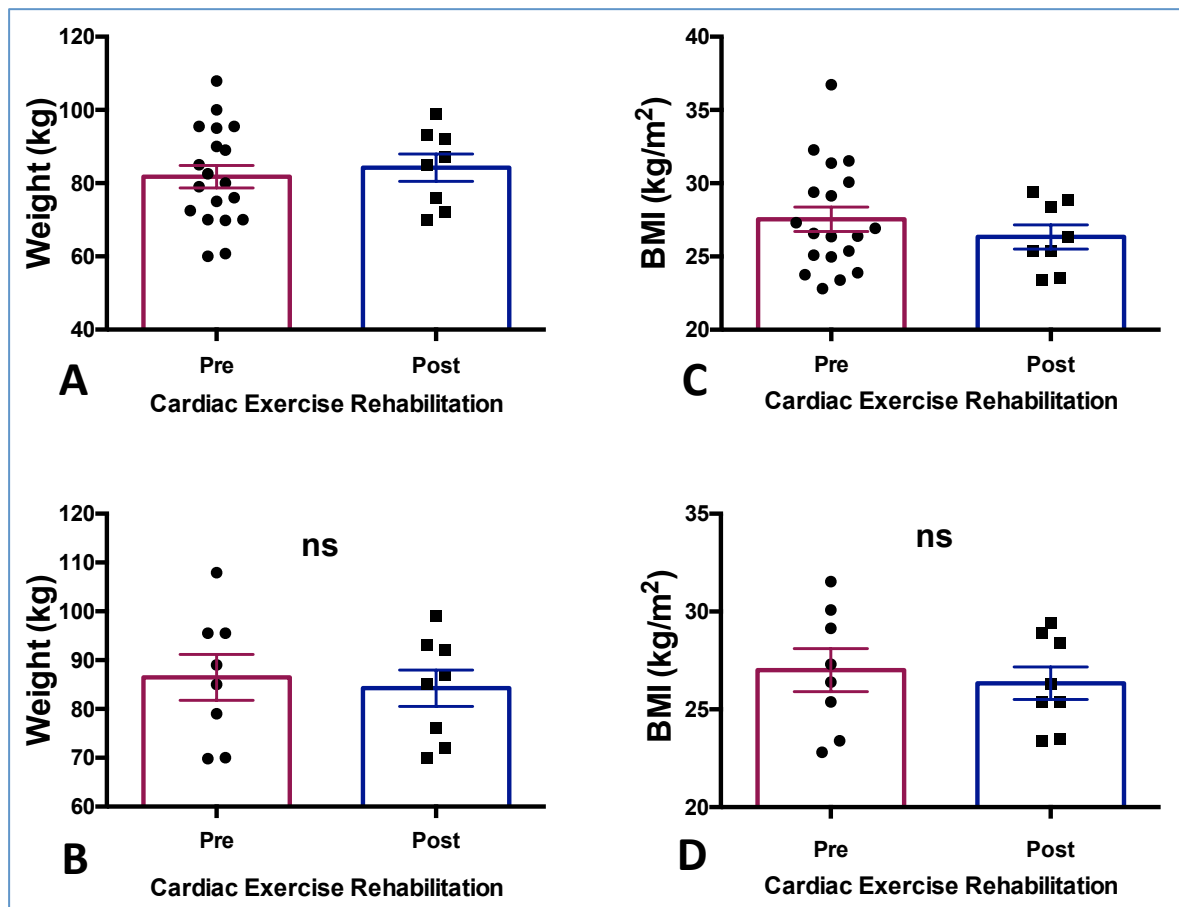


Figure 6.1. Cardiac patients' weight and BMI pre- and post-cardiac exercise rehabilitation.

Weight (kg) and BMI (kg/m^2) were measured before and after cardiac exercise rehabilitation. **A:** Weight (kg) for all patients involved in the study, **B:** Weight (kg) for 8 patients involved in both pre- and post- examination, **C:** BMI (kg/m^2) for all patients involved in the study, **D:** BMI (kg/m^2) for 8 patients involved in both Pre- and Post-examination. All values are displayed as mean \pm sem. (ns) not significant for comparison between Pre- and Post-cardiac exercise rehabilitation using a two-tailed paired t-test for **B, D**.

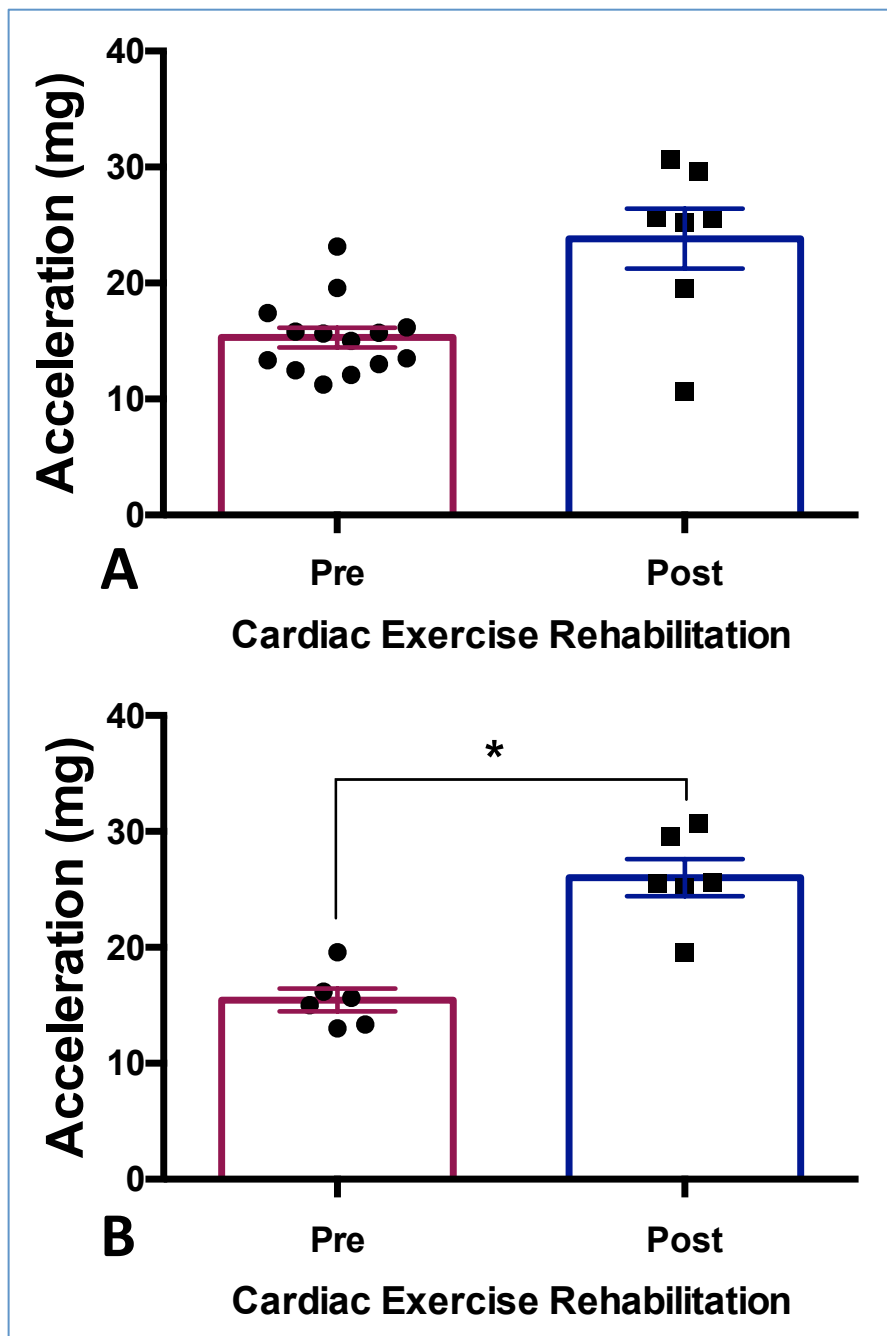


Figure 6.2. Acceleration for cardiac patients pre- and post-cardiac exercise rehabilitation

The wrist accelerometer was used to determine the daily physical activity by acceleration. **A:** The comparison between all patients with valid data for 24h/7days. 14 patients pre-cardiac exercise rehabilitation vs. 7 patients post- cardiac exercise rehabilitation. **B:** The comparison between the patients with valid data for 24h/7days attending both tests. 6 patients pre- and post-cardiac exercise rehabilitation. All values are displayed as mean \pm sem. * $P<0.05$ for comparison between pre- and post-cardiac exercise rehabilitation using a two-tailed paired t-test for **B**.

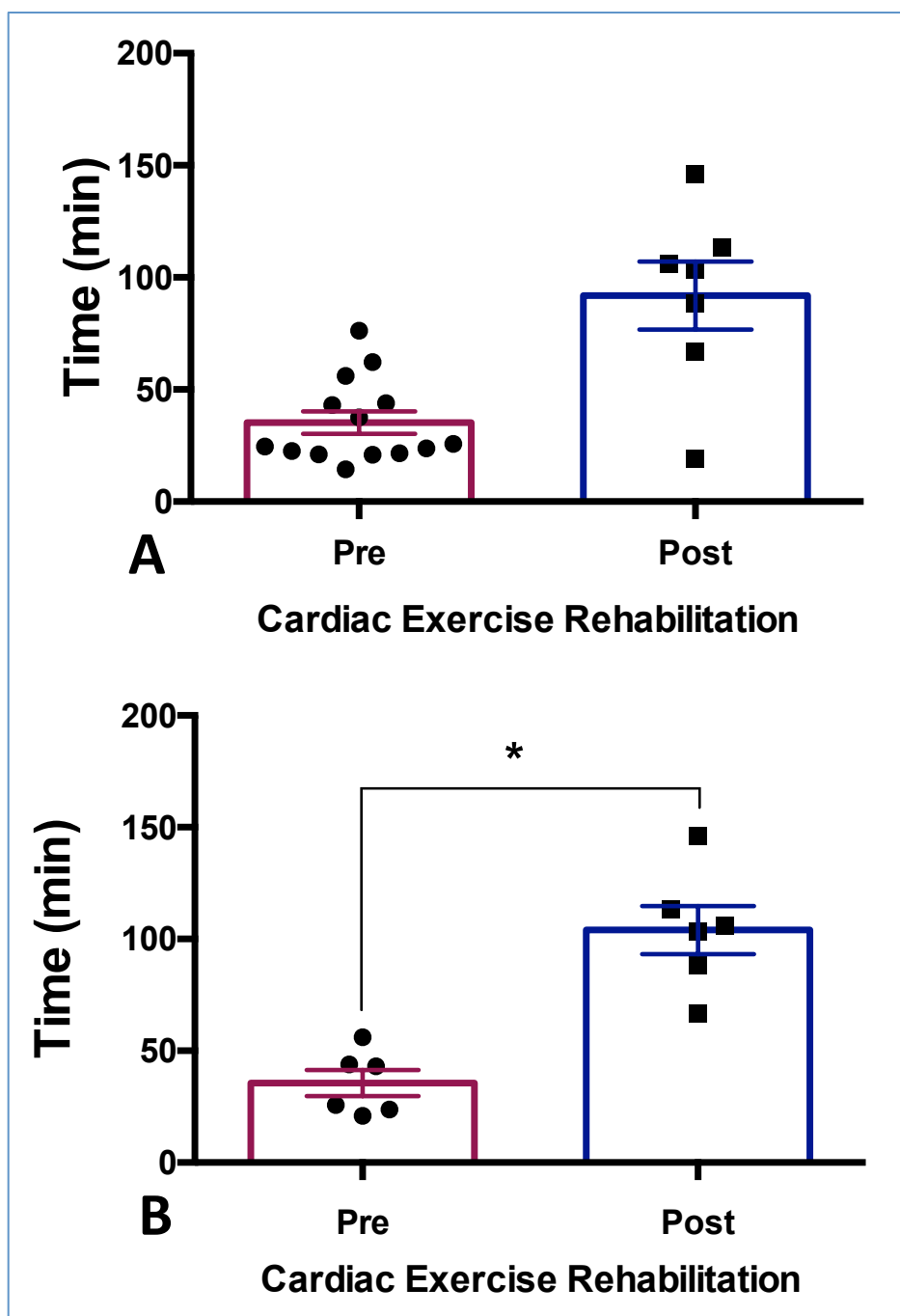


Figure 6.3. Time spent per day in moderate to vigorous physical activity (MVPA) for pre- and post-cardiac exercise rehabilitation.

A: The comparison between all patients with valid data for 24h/7days. 14 patients pre-cardiac exercise rehabilitation vs. 7 patients post-cardiac exercise rehabilitation.

B: The comparison between the patients with valid data for 24h/7days attending both tests, 6 patients pre- and post-cardiac exercise rehabilitation. All values are displayed as mean \pm sem. * $P<0.05$, ** $P<0.01$ for comparison between pre- and post-cardiac exercise rehabilitation using a two-tailed unpaired t-test for **A** and a paired t-test for **B**.

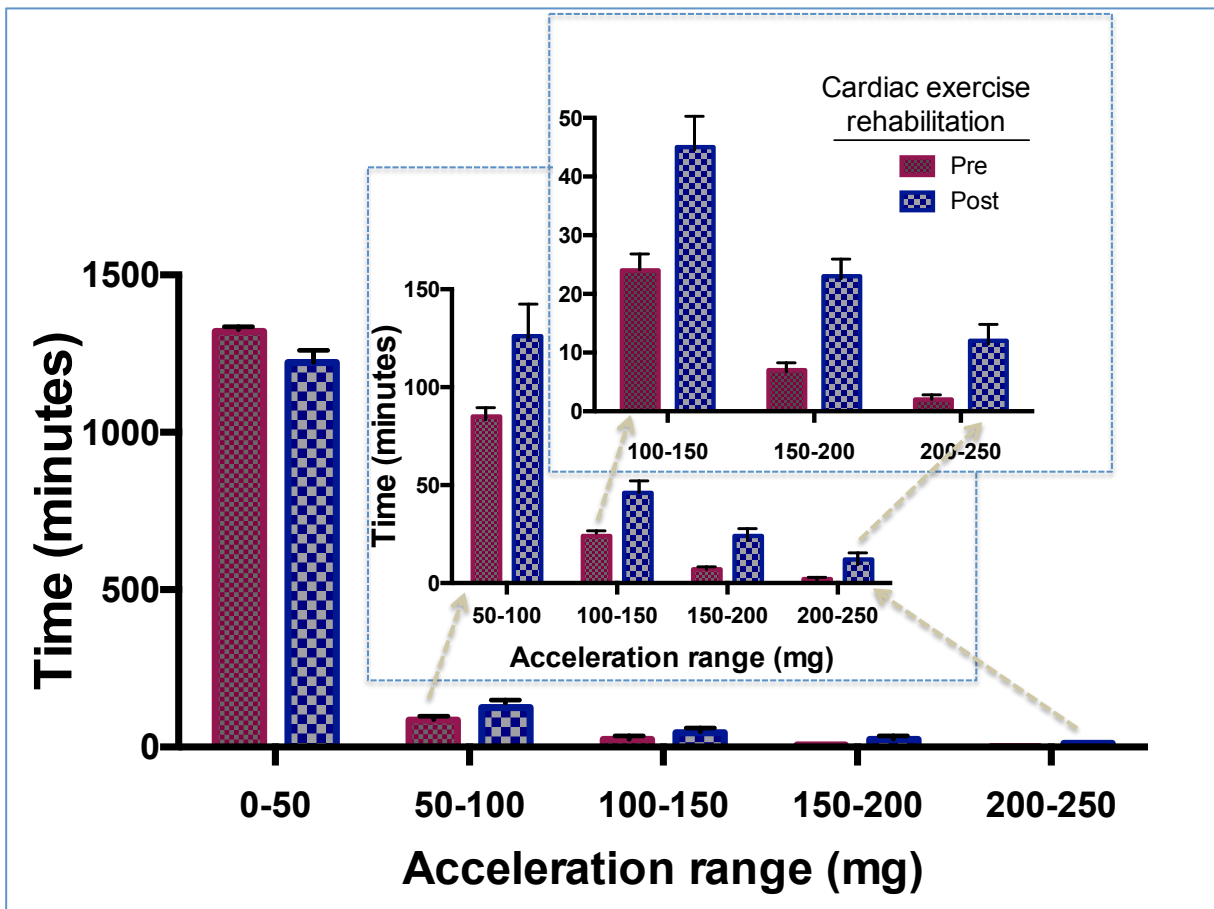


Figure 6.4. Acceleration distribution of time spent in 50 mg units-intensity for pre- and post-cardiac exercise rehabilitation.

All daily activity for each patient was recorded and divided into 50mg units (intensity) for 24h/7 days. In each 50mg unit, the average for all patients/7days was calculated for 14 patients pre-cardiac exercise rehabilitation and 7 patients post-cardiac exercise rehabilitation. All values are displayed as mean \pm sem.

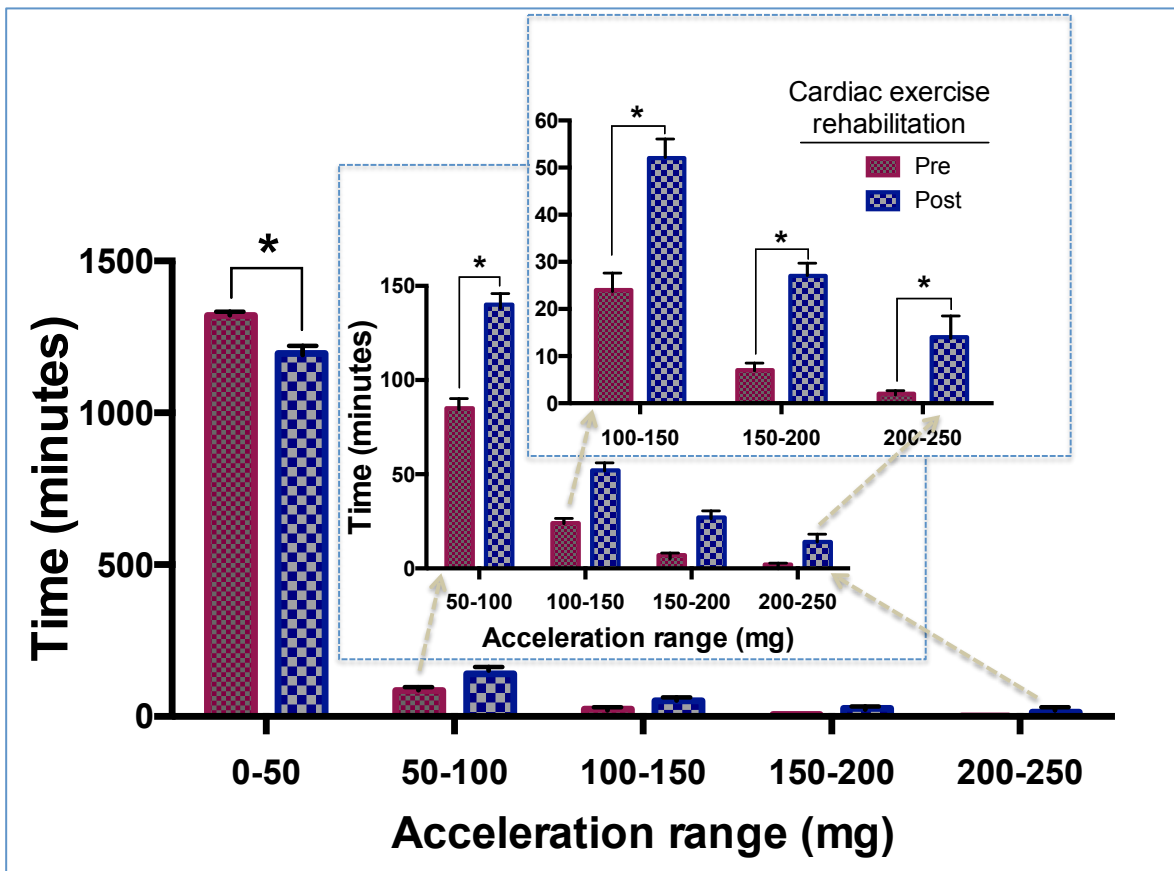


Figure 6.5. Acceleration distribution of time spent in 50 mg units-intensity for pre- and post-cardiac exercise rehabilitation.

All daily activity for each patient was recorded and divided into 50mg units (intensity) for 24h/7 days. In each 50mg unit, the average for all patients/7days was calculated for 6 patients pre-cardiac exercise rehabilitation and 6 patients post-cardiac exercise rehabilitation. All values are displayed as mean \pm sem. *P<0.05 for comparison between pre- and post-cardiac exercise rehabilitation using a two-tailed paired t-test.

6.2.2 Effect of cardiac rehabilitation on lymphocyte subsets

6.2.2.1 Effect of cardiac rehabilitation on T-lymphocytes

All 19 patients in this chapter were recruited and blood taken for pre-cardiac rehabilitation stage by Marilena Giannoudi, post graduated medical student, Newcastle University, whilst the blood were taken for post-cardiac rehabilitation by Dr. Suzanne Cormack, IGM, Newcastle University.

Lymphocytes Th1 and Th17/Th1 significantly increase in peripheral blood after myocardial infarction (Cheng et al., 2008; Methé et al., 2005 and Zhao et al., 2011). The circulating frequency of CD4⁺ T-cells increases in patients with established atherosclerosis or with high risk factors of cardiovascular diseases (Dumitriu et al., 2009). In mouse models, $\gamma\delta$ T-cells, $\alpha\beta$ CD4⁺ T-cells, NK T-cells and B-cells were detected in the myocardium after myocardial infarction, and $\gamma\delta$ T-cells remain present for days afterwards (Yan et al., 2012; Yan et al., 2013). To find the effect of cardiac exercise rehabilitation on T-lymphocytes, PBMNCs were 24h after primary percutaneous coronary intervention (PPCI) and also after the cardiac rehabilitation exercise program described at (2.2.20). Figure 6.6A shows the absolute T-cell numbers after cardiac rehabilitation (1241 ± 143 cells/ μ l) and (1764 ± 258 cells/ μ l) for all patients in the pre-rehabilitation group. This decrease in total T-lymphocytes was significant ($P=0.03$) in comparison to the 8 patients tested before (2174 ± 578 cells/ μ l) and after (1241 ± 143 cells/ μ l) rehabilitation (Figure 6.6B). However, this significance disappeared when I applied the sensitivity analysis (omitting the single outlier) $P=0.08$.

6.2.2.2 Effect of cardiac rehabilitation on CD4⁺ and CD8⁺ T-lymphocytes

Figure 6.7A illustrates the CD4⁺ T-cell levels when all participants were considered, 910 ± 119.2 cells/ μ l compared to 1261 ± 192.9 cells/ μ l for the pre-rehabilitation group. However, when comparing only patients who underwent blood sampling before and after cardiac rehabilitation, 8 patients, (Figure 6.7B), this decrease in CD4⁺ T-cell numbers was significantly ($P=0.02$) in favour of the post-rehabilitation group by 910 ± 119.2 cells/ μ l vs. 1610 ± 429.7 cells/ μ l for pre-rehabilitation exercise group. Furthermore, this significance of CD4⁺ T-cells remained even after I applied the sensitivity analysis (omitting the single outlier) $P=0.02$). Figure 6.7C shows the CD8⁺ T-cell numbers pre-cardiac rehabilitation (491.2 ± 72.9 cells/ μ l) and after cardiac exercise rehabilitation (287.6 ± 57.5 cells/ μ l). Figure 6.7D shows a non-significant trend towards decreased CD8⁺ T-cell numbers post-cardiac exercise (287.6 ± 57.5 cells/ μ l vs. 552.4 ± 144.1 cells/ μ l) for the same patients before the rehabilitation programme.

Double positive (DP) T-cell numbers, figure 6.8A illustrates the DP T-cell numbers from all patients who participated in this study, with an average of (28.2±9.2 cells/µl) before the exercise programme and (23.5±14.7 cells/µl) after the exercise programme. When a comparison was performed for the patients who had taken part in both pre- and post-rehabilitation (Figure 6.8B), there was a significant ($P<0.05$) decrease in DP T-cell numbers in favour of the post-cardiac rehabilitation programme (23.5±14.7 cells/µl compared to 38.4±22.2 cells/µl for the pre-cardiac rehabilitation programme). Figures 6.8C and 6.8D compare the ratio of CD4⁺/CD8⁺ T-cells between pre- and post-cardiac exercise rehabilitation programmes, showing no change was noticed between these.

In conclusion, the rehabilitation exercise programme had a positive effect in decreasing T-lymphocytes and their subsets after myocardial infarction. These cells are ordinarily increasingly recruited to the affected myocardium (Methe et al., 2005; Zhao et al., 2011).

6.2.2.3 Effect of cardiac rehabilitation on other lymphocyte subsets

Figures 6.6-6.8 illustrates the effect of cardiac exercise rehabilitation on T-lymphocytes and their subsets. This experiment was performed to discover to what extent the other lymphocyte subsets were affected by exercise. Figure 6.9A shows all lymphocyte subsets (T-cells, B-cells and NK-cells) for all patients. There was a decrease in all lymphocyte numbers after exercise (1771±215.9 cells/µl) and (2319±339.6 cells/µl) before exercise programme. When compared with the 8 patients who took part in pre- and post-rehabilitation blood tests (Figure 6.9B), the same non-significant decrease by 1771±215.9 cells/µl after the exercise programme compared to 2883±770.4 cells/µl for before exercise program. Figure 6.9C shows that the B-lymphocyte numbers for all participants in the pre-rehabilitation group (347.3±72.4 cells/µl) and (262.4±53 cells/µl) for post-cardiac rehabilitation. The non-significant decrease in B-cell numbers was noticed only when compared with the 8 pre- and post-exercise program patients (figure 6.9D). Natural Killer (NK) lymphocyte numbers are illustrated as an average of 173.7±22.5 cells/µl for the pre-rehabilitation group and 260.1±46.8 cells/µl for the post-cardiac rehabilitation (figure 6.9E). A non-significant increase was noticed for the 8 patients (Figure 6.9F) pre-rehabilitation 260.1±46.8 cells/µl compared to 230.8±44.3 cells/µl for before exercise program.

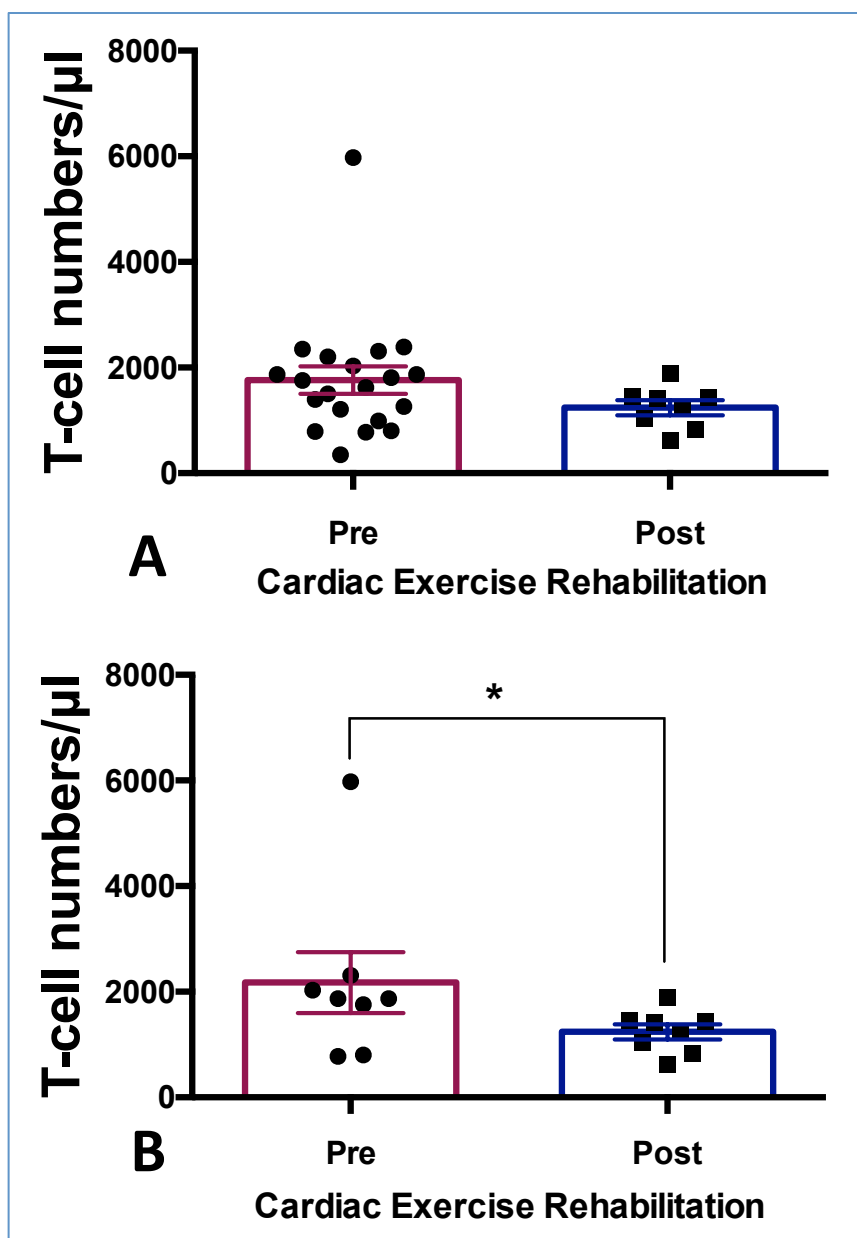


Figure 6.6. Total T-lymphocyte absolute numbers pre- and post-cardiac exercise rehabilitation

PBMNCs TruCount using FACSCanto II software was applied to determine the absolute number for each cell population. **A:** Total T-cell number/μl for all patients involved in the study, **B:** Total T-cell number/μl for 8 patients involved in both Pre- and Post-examination. All values are displayed as mean \pm sem. * $P<0.05$ for comparison between pre- and post-cardiac exercise rehabilitation using a two-tailed paired t-test for **B**.

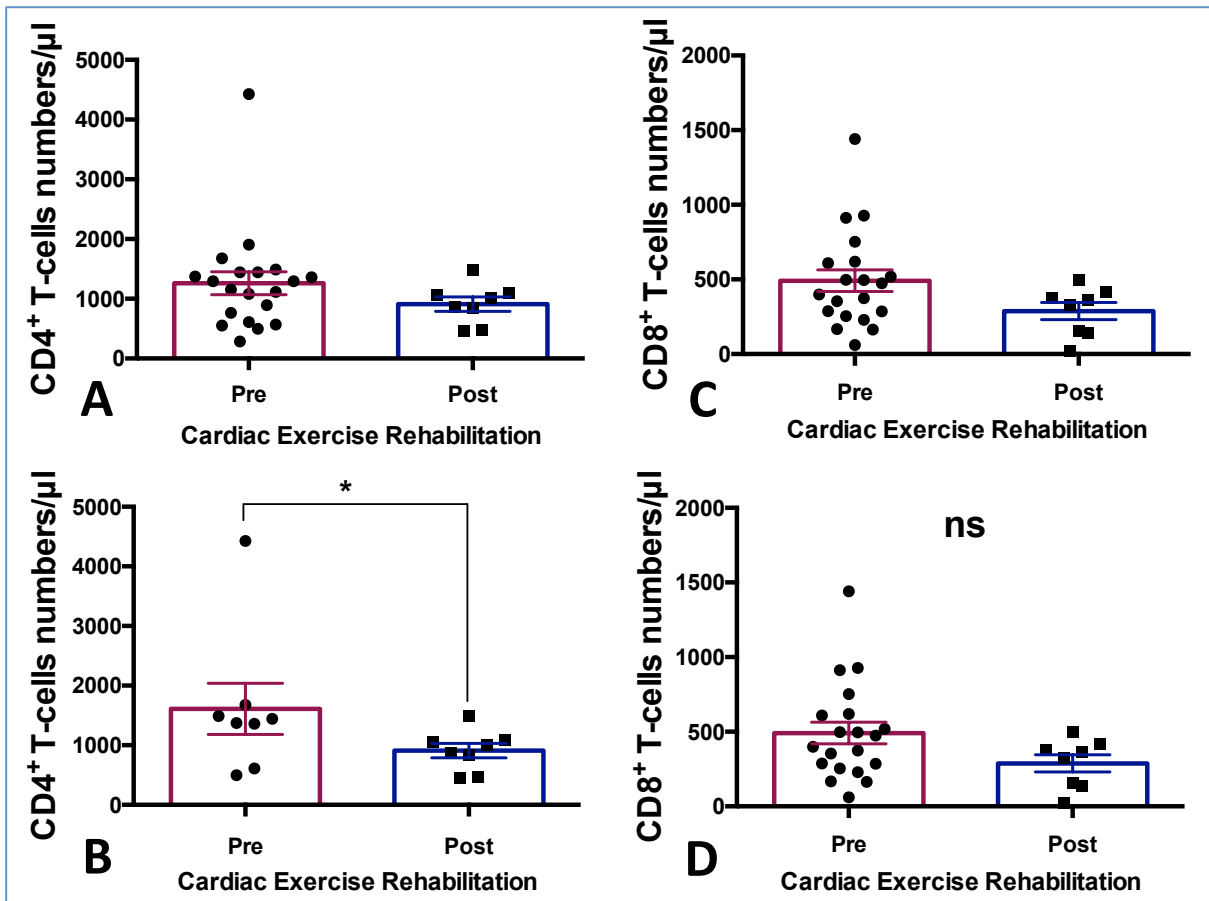


Figure 6.7. Absolute numbers of CD4⁺ and CD8⁺ T-lymphocytes pre- and post-cardiac exercise rehabilitation

PBMNCs TruCount using FACSCanto II software was applied to determine the absolute numbers for each cell population. **A:** CD4⁺ T-cell numbers/μl for all patients involved in the study, **B:** CD4⁺ T-cell numbers/μl for 8 patients involved in both Pre- and Post-examination, **C:** CD8⁺ T-cell numbers/μl for all patients involved in the study, **D:** CD8⁺ T-cell numbers/μl for 8 patients involved in both Pre- and Post-examination. All values are displayed as mean±sem. *P<0.05 for comparison between pre- and post-cardiac exercise rehabilitation using a two-tailed paired t-test for **B, D**.

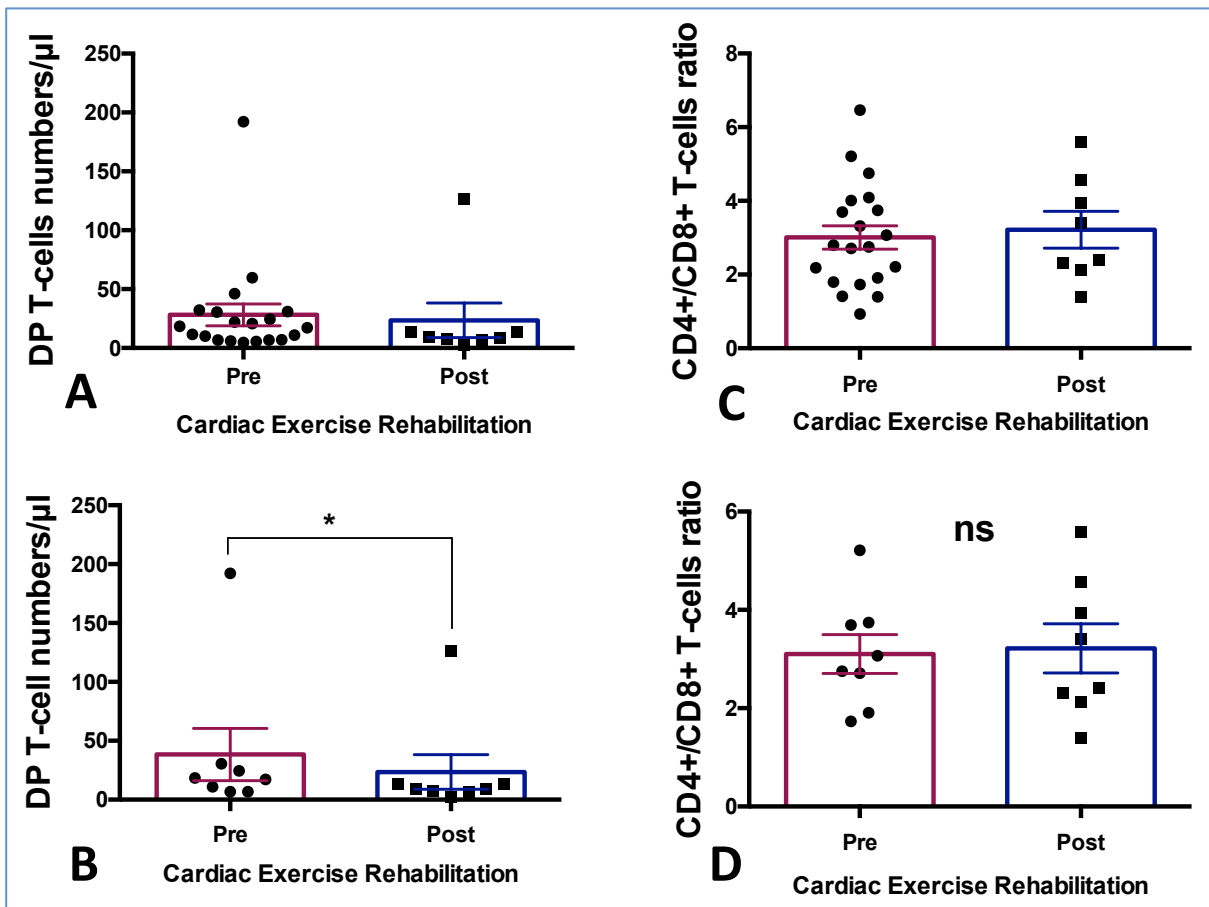


Figure 6.8. DP T-lymphocytes absolute number and CD4 $^{+}$ /CD8 $^{+}$ T-cells ratio pre- and post-cardiac exercise rehabilitation

PBMNCs TruCount using FACSCanto II software was applied to determine the absolute number for each cell population. **A:** DP T-cell numbers/ μ l for all patients involved in the study, **B:** DP T-cell numbers/ μ l for 8 patients involved in both Pre- and Post-examination, **C:** CD4 $^{+}$ /CD8 $^{+}$ T-cell ratio for all patients involved in the study and **D:** CD4 $^{+}$ /CD8 $^{+}$ T-cell ratio for 8 patients involved in both Pre- and Post-examination. All values are displayed as mean \pm sem. *P<0.05 for comparison between pre- and post-cardiac exercise rehabilitation using a two-tailed paired t-test for **B, D**.

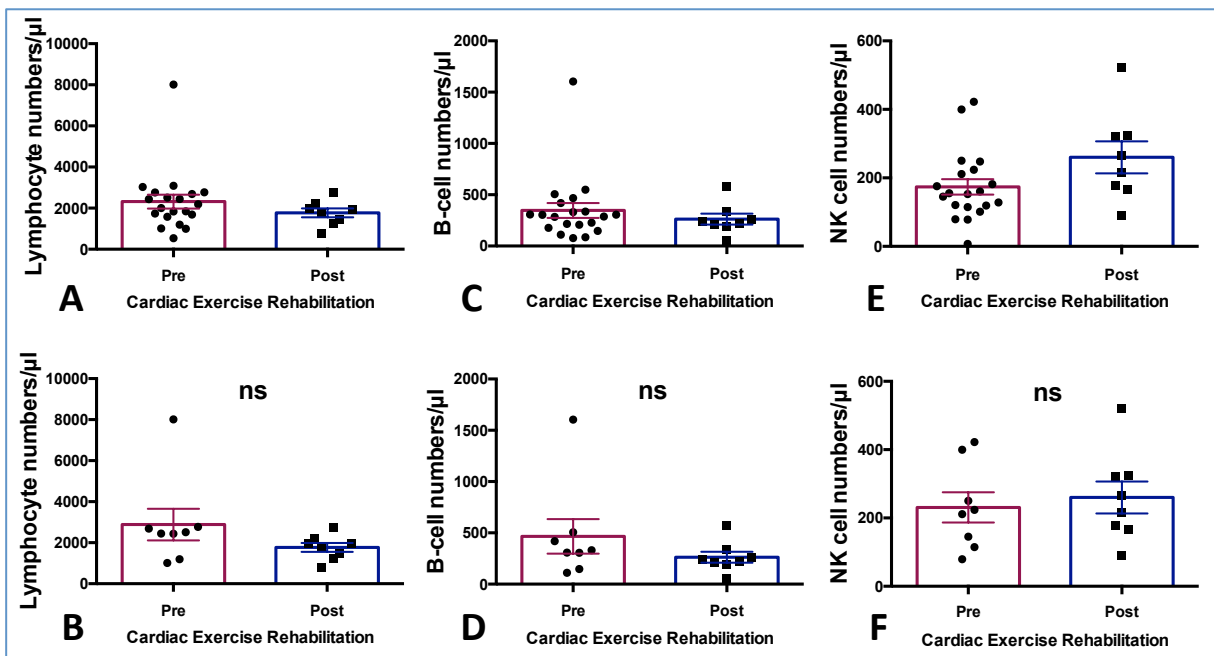


Figure 6.9. Absolute numbers of other lymphocyte types pre- and post-cardiac exercise rehabilitation

PBMNCs TruCount using FACSCanto II software was applied to determine the absolute number for each cell population. **A:** All lymphocyte numbers/µl for all patients involved in the study, **B:** All lymphocyte numbers/µl for 8 patients involved in both Pre- and Post-examination, **C:** B-cell numbers/µl for all patients involved in the study, **D:** B-cell numbers/µl for 8 patients involved in both Pre- and Post-examination, **E:** NK-cell numbers/µl for all patients involved in the study, **F:** NK-cell numbers/µl for 8 patients involved in both Pre- and Post-examination. All values are displayed as mean \pm sem. (ns) not significant for comparison between pre- and post-cardiac exercise rehabilitation using a two-tailed paired t-test for **B, D, F**.

6.2.3. Effect of cardiac rehabilitation on regulatory T-cells

Stimulation by antigens and cytokines differentiates naïve T-cells into distinct subpopulations, which include: T-helper (Th) cells as well as CD4⁺CD25⁺FOXP3⁺ regulatory T (Treg) cells. Tregs play a key role in immune homeostasis and tolerance, including maintenance and induction, and make up 5-10% of all peripheral CD4⁺ cells (Chen et al., 2003; Fontenot; 2003). Antigen presenting cells (APCs) and target T-cells are regulated through Tregs, which consequently inhibit both cytokine production and T-cell proliferation. Tregs secrete transforming growth factor (TGF)- β , IL-10 and other inhibitory cytokines, which suppress the immune system (Sakaguchi, 2005) and also atherosclerosis (Robertson et al., 2003; Mallat et al., 2001). Patients with ST-segment elevation MI were found to have higher levels of Tregs circulating in their bloodstream (Ammirati et al., 2010).

To investigate the effect of exercise rehabilitation on regulatory T-cells in patients with MI, Tregs were quantified pre- and post-cardiac exercise rehabilitation using flow cytometry (described at 2.2.19). Figure 6.10A shows the percentage of Tregs with high CD25 expression for all patients who participated in the study (the percentage of Tregs after exercise at 0.22 \pm 0.1% and 1.5 \pm 0.2% before exercise). A significant ($P<0.01$) decrease was noted for the 8 patient results post-rehabilitation 0.2 \pm 0.1% compared to 1.4 \pm 0.4% pre-rehabilitation (figure 6.10B). At low CD25⁺ expression for all patients (Figure 6.10C), Treg percentage was 4.2 \pm 0.6% before cardiac rehabilitation and 0.7 \pm 0.2% after cardiac rehabilitation. For the 8 patients the decrease in Treg percentage was significant ($P<0.001$) post-cardiac exercise rehabilitation (Figure 6.10D) (0.7 \pm 0.2% vs. 4.5 \pm 1% for pre-cardiac rehabilitation). Figure 6.10E shows that CD4⁺/FoxP3⁺ without any expression for CD25⁺ cells (CD4⁺/CD25⁻/FoxP3⁺), was 3.7 \pm 0.8% for all patients who participated in the pre-exercise programme and 0.5 \pm 0.1% of the post-exercise programme. A study has shown FoxP3 expression in CD4⁺CD25⁻ T-cells (Khattari et al., 2003). Figure 6.10F compares Treg cells with negative CD25⁺ cells for the 8 patients who had the pre- and post- test. A significant decrease in the percentage of Tregs was noticed in favour of post-rehabilitation patients (0.5 \pm 0.1% compared to 3.5 \pm 1% for pre-rehabilitation patients).

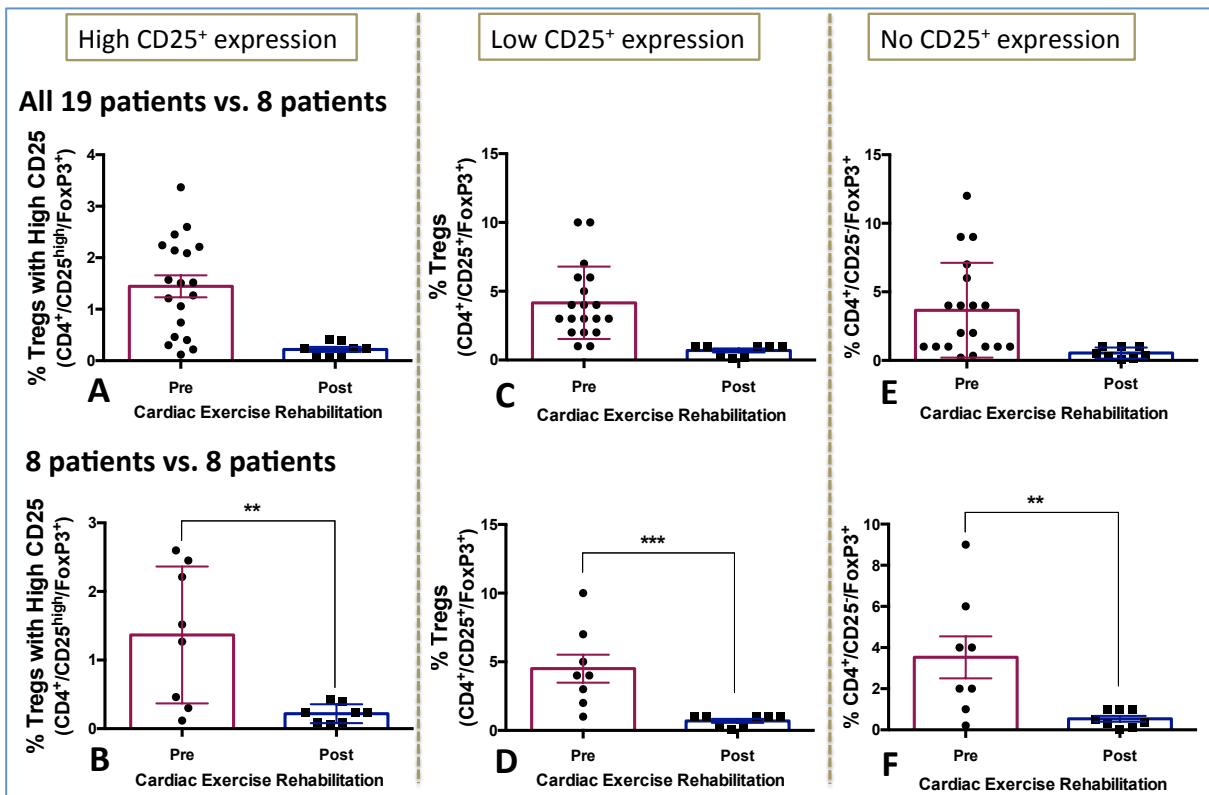


Figure 6.10. Percentage of regulatory T-cells pre- and post-cardiac exercise rehabilitation

The percentage of regulatory T-cells from PBMNCs was measured using FACSCanto II. **A:** Percentage of Treg expression with high expression of CD25 for all patients, **B:** Percentage of Treg expression with high expression of CD25 for the 8 patients involved in both Pre- and Post-examination, **C:** Percentage of Treg expression with low expression of CD25 for all patients, **D:** Percentage of Treg expression with low expression of CD25 for the 8 patients involved in both Pre- and Post-examination, **E:** Percentage of Treg expression with non-CD25 expression for all patients, **F:** Percentage of Treg expression with non-CD25 expression for the 8 patients involved in both pre- and post-examination. All values are displayed as mean \pm sem. **P<0.01, ***P<0.001, ****P<0.0001 for comparison between Pre- and Post-cardiac exercise rehabilitation using a two-tailed paired t-test for **B, D, F**.

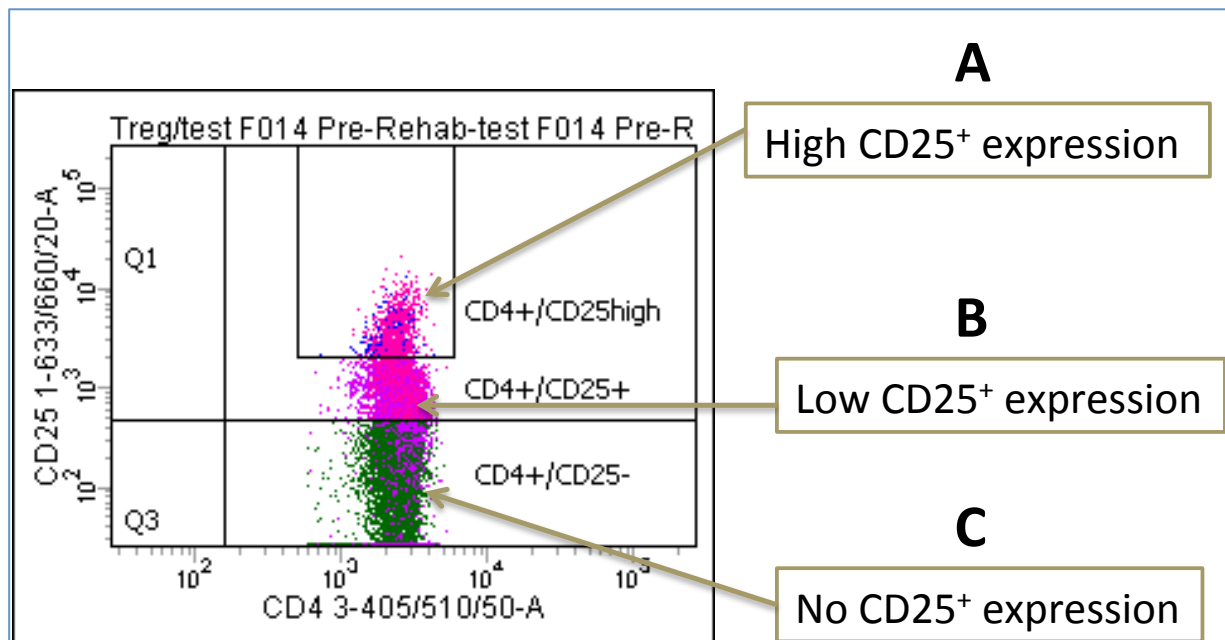


Figure 6.11. Illustration of the detection and gating of the two levels of CD25⁺ expression

Gating of CD25⁺ expression. **A:** High CD25⁺ expression. **B:** Low CD25⁺ expression. **C:** No CD25⁺ expression (negative).

6.2.4 Effect of cardiac rehabilitation on telomerase activity and telomere length

6.2.4.1 Effect of cardiac rehabilitation on telomerase activity

Low telomerase activity in PBMNCs has been found to be related to cardiovascular diseases (Epel et al., 2006). Telomerase activity and telomere length among PBMNCs increased after 3 months of physical activity in healthy middle-aged men with a sedentary lifestyle (Melk et al., 2014). This experiment was designed to find the effect of cardiac exercise rehabilitation on telomerase activity for patients following acute MI. PBMNCs were measured after 24 hours of catheterization and following the cardiac rehabilitation programme. Telomerase activity was measured by TRAP ELISA as described at 2.2.11. Figure 6.12A shows the difference in telomerase activity before and after cardiac exercise in all 19 patients and in the 8 patients who attended the post-cardiac rehabilitation test. There is no significant difference in telomerase activity before and after cardiac exercise when compared with the 8 patients who attended both the pre- and post-rehabilitation tests (figure 6.12B).

6.2.4.2 Effect of cardiac rehabilitation on telomere length

Telomeres are found at the end of chromosomes and plays an important role in cell division (Hayflick, 1965). Telomeres shorten with each cell division until their length reaches a critical level and the cell stops replicating (Benetos et al., 2001). Telomere length and telomerase activity have been shown to contribute to cardiac diseases and oxidative stress (Epel et al., 2004; Epel et al., 2006; Demissie et al., 2006). This study was conducted to find the effect of cardiac exercise rehabilitation on telomere length in acute MI patients. Telomere length was measured, as described at 2.2.21. Figure 6.13A shows the telomere length results for pre-cardiac exercise rehabilitation, with a TS ratio of 0.6147 ± 0.044 for all 19 patients and post-cardiac exercise rehabilitation with a ratio of 0.6125 ± 0.07 for 8 patients. Telomere length apparently trends toward increase for pre-cardiac exercise rehabilitation (0.6638 ± 0.043 vs. 0.6125 ± 0.07 for post-cardiac exercise rehabilitation (ns)) when compared with the 8 patients who did both pre- and post- tests (Figure 6.13B).

Figure 6.14A shows that in all 19 patients, cells with shorter telomeres exhibited higher telomerase activity during the pre-rehabilitation exercise. Currently, very little is known about this correlation, but it is believed that it demonstrates that telomerase activity is required to prevent telomere shortening. The signalling mechanism between short telomeres and telomerase also remains unknown, although the involvement of TERRA mechanisms, or ATM or TRF1 signalling has been suggested (Redon et al., 2010, Tong et al., 2015).

However, figure 6.14B indicates that following rehabilitation exercise, this relationship might be reversed; patients with longer telomeres exhibited higher telomerase activity. These findings were also observed in patients who did both the pre-rehabilitation and post-rehabilitation tests (n=8), as seen in figures 6.14C.

From these findings, we can conclude that rehabilitation exercise might be able to invert the negative correlation between telomere length and telomerase activity. However, a much larger sample size is required to confirm this suggestion.

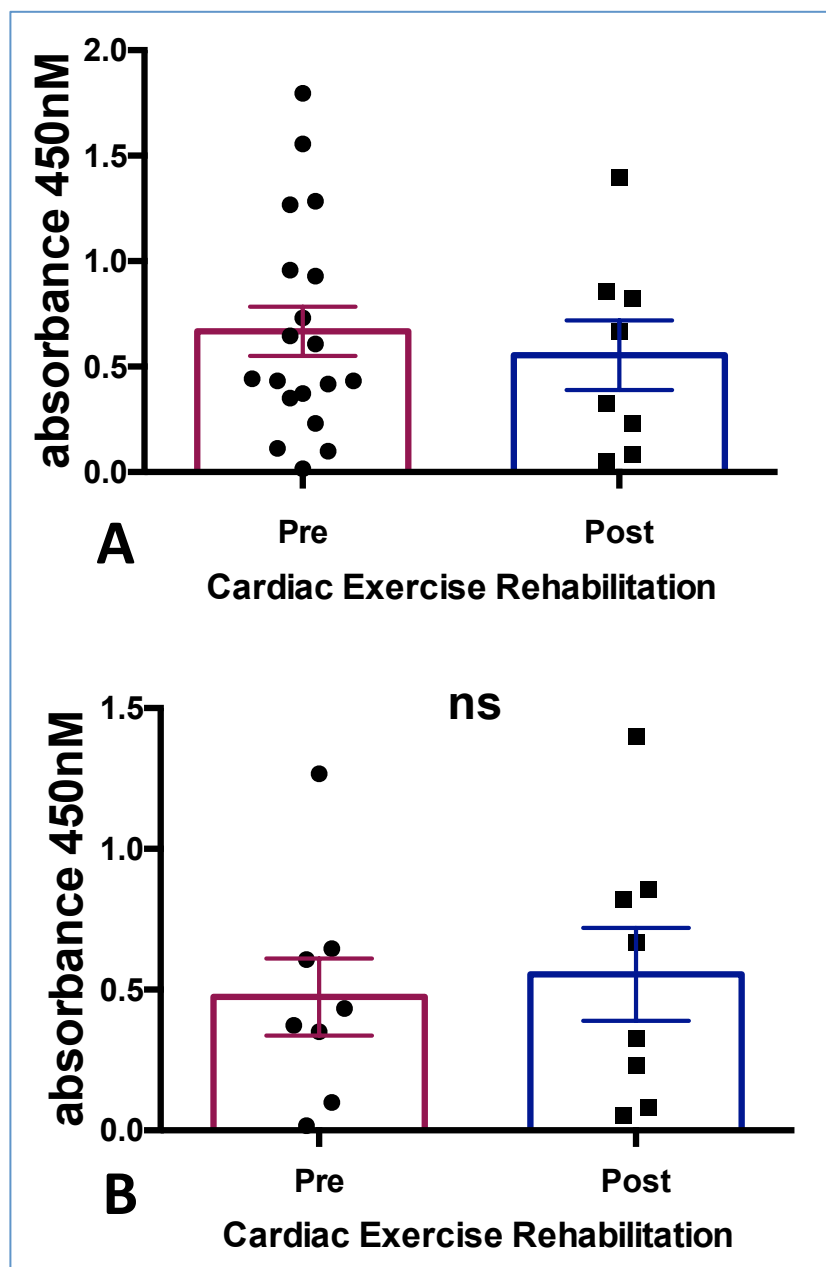


Figure 6.12. Telomerase activity in PBMNCs for MI patients pre- and post-cardiac exercise rehabilitation

Telomerase activity was measured for MI patients both pre- and post-cardiac exercise rehabilitation. All values are displayed as mean \pm sem. (ns) not significant for comparison between pre- and post-cardiac exercise rehabilitation using a two-tailed paired t-test for B.

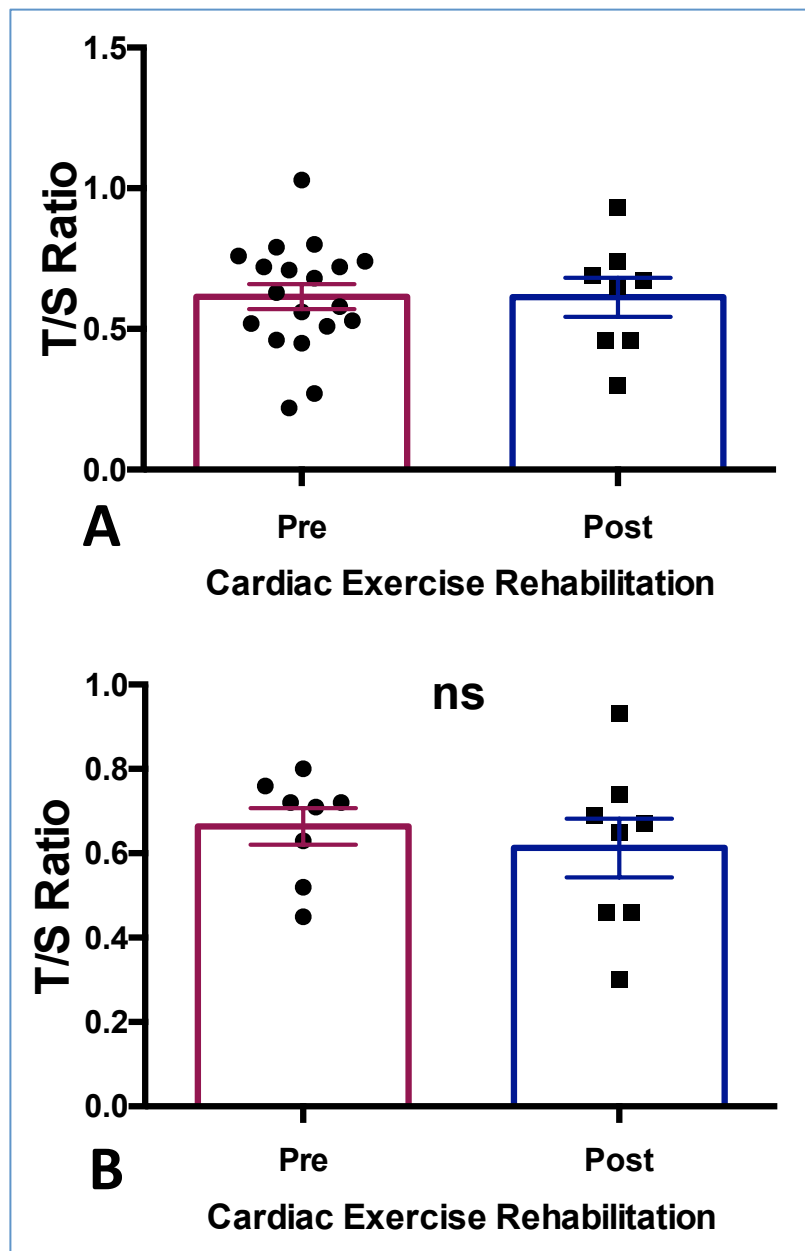


Figure 6.13. Telomere length in PBMNCs for MI patients pre- and post-cardiac exercise rehabilitation.

Telomere length was measured as ratio of the telomere length to the single copy gene. All values are displayed as mean \pm sem. (ns) not significant for comparison between pre- and post-cardiac exercise rehabilitation using a two-tailed paired t-test for **B**.

Patients with low telomerase activity were not able to maintain telomere length, while those with high or medium telomerase activity were able to maintain or even elongate their telomere length.

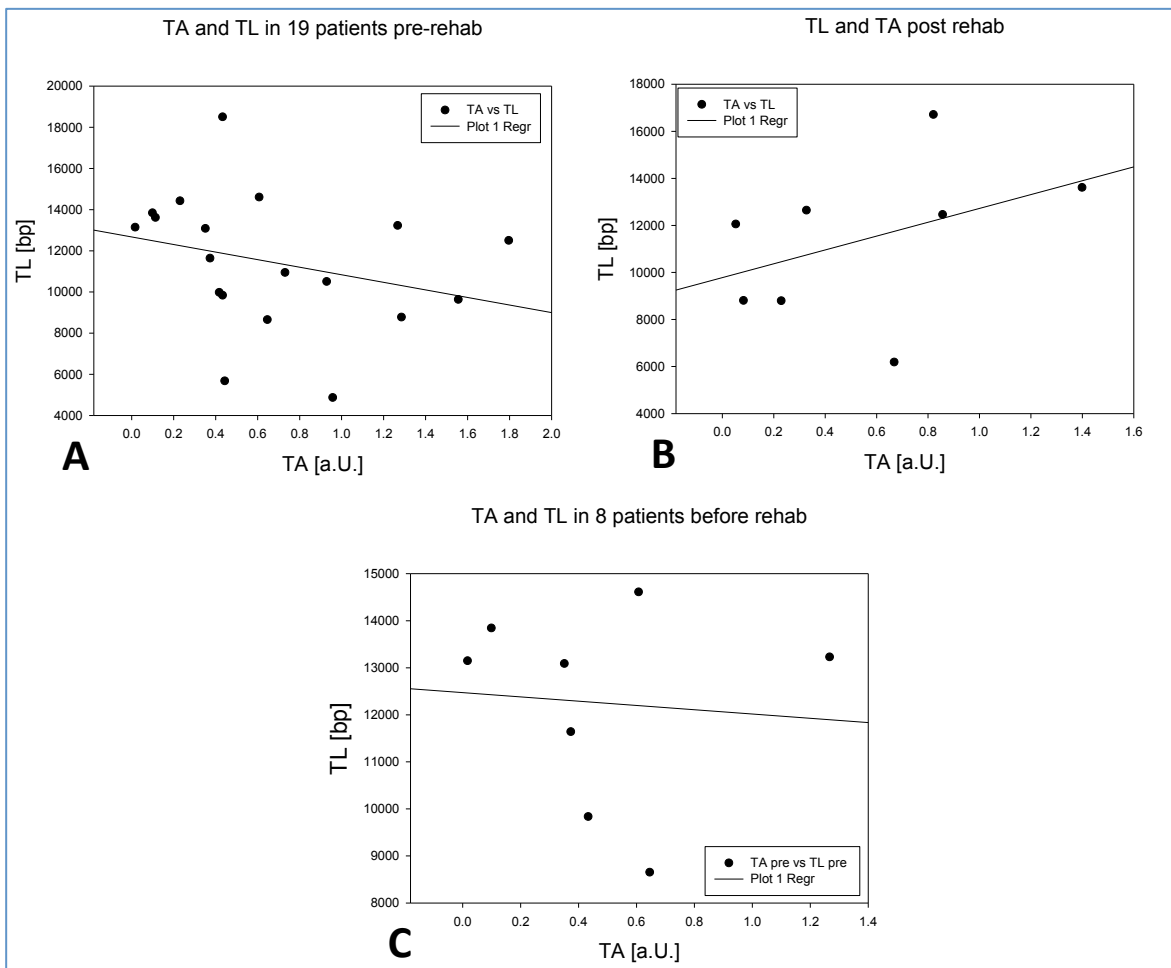


Figure 6.14. Relationship between telomere length (TL) and telomerase activity (TA) in PBMNCs for MI patients with pre- and post-cardiac exercise rehabilitation.

A: Relationship between TA and TL for 19 patients who underwent the pre-cardiac exercise rehabilitation test. **B:** Relationship between TA and TL for 8 patients who underwent the post-cardiac exercise rehabilitation test. **C:** Relationship between TA and TL for 8 patients who underwent the pre-cardiac exercise rehabilitation test. Correlation was performed by Dr. G. Saretzki using SIGMA Plot.

6.3. Discussion

Acute myocardial infarction (AMI) patients who underwent cardiac rehabilitation exhibited a non-significant trend toward decreased body weight and BMI (measured as weight/height²). Figure 6.1A shows that body weight increased after cardiac rehabilitation. This was because the pre-rehabilitation group included female patients. Our result was not significant in term of decreased body weight after 12 weeks of cardiac exercise rehabilitation, but it does correspond to results from Kraemer et al. (1997), who studied 31 healthy participants either with or without specific exercise training programmes for 12 weeks and observed a significant decrease in body weight after 6 weeks of exercise. Additionally, they found a significant reduction in high-density lipoprotein cholesterol (HDL-C) levels in both groups without exercise (hypocaloric low-fat diet group, and high diet group), whilst low-density lipoprotein cholesterol (LDL-C) levels reduced in the exercise group (Kraemer et al., 1997). Several studies recognized that high LDL-C levels were associated with increased MI risk, and this risk was decreased with high HDL-C levels (Duffy et al., 2012; Sniderman et al., 2012; Murphy et al., 2009, Smith et al., 2006). Furthermore, Leon and Sanchez's (2001) review of 51 studies involving a total of 4700 participants found that physical training for more than 12 weeks yielded increased HDL-C levels and decreased LDL-C and triglyceride levels (Leon and Sanchez, 2001). This confirms work by Stefanick et al., 1998, which stated that physical exercise leads to decreased LDL-C levels and increased HDL-C levels.

In this study, the post-cardiac rehabilitation test was conducted with patients 6-9 months after MI, which had included 3 months of cardiac exercise rehabilitation. Physical exercise improved daily physical activity, confirming the findings of a study by Luszczynska and Sutton (2006), which found continued exercise 8 months after MI to be a major predictor of physical activity compared to a non-continuous exercise group. Following cardiac rehabilitation, patients usually maintain the exercise regime so as not to relapse through lack of exercise (Sullum et al., 2000; Scholz et al., 2005). The authors referred to this patient maintenance as 'self-efficacy'. This was noticed in our study as well, as patients reported that they were still training on the rehabilitation programme. In our study, I found that time spent doing moderate to vigorous physical activity increased by 2.6-fold after cardiac exercise rehabilitation ($P=0.0074$). These findings were demonstrated by other studies; that exercise rehabilitation leads to improved daily activity for cardiac patients (Tyni-Lenna et al., 1998) and improves both their capacity to exercise and their cardiac output (Cheetham et al., 2002). In our study (figures 6.4 and 6.5), patients spent less time in low intensity daily activity (0-50mg) including sleep and relaxation, after cardiac exercise rehabilitation this. Some of this

time was spent in high acceleration movement, whilst some of it averaged as moderate to vigorous (daily) physical activity.

T-lymphocytes in this study decreased after cardiac exercise rehabilitation. This was significant for the patients who underwent blood sampling before and after cardiac rehabilitation, however, in my results when I applied the sensitivity analysis the decrease of T-lymphocytes was no longer significant. In contrast, I still found a significant decrease in CD4⁺ T-cells (which remained after the sensitivity analysis), but not in CD8⁺ T-cells after exercise rehabilitation. Moreover, this was also detected in the double positive population of CD4⁺CD8⁺ T-cells. This significant decrease in CD4⁺ T-cell numbers had a positive effect on patient health following cardiac exercise rehabilitation. The circulating frequency of CD4⁺ T-cells increases in patients with established atherosclerosis or with high cardiovascular disease risk factors (Dumitriu et al., 2009). Lymphocytes Th1 and Th17/Th1 significantly increase in peripheral blood after MI (Cheng et al., 2008; Methé et al., 2005 and Zhao et al., 2011). In mouse models, $\gamma\delta$ T-cells, $\alpha\beta$ CD4⁺ T-cells, NK T-cells and B-cells were detected in the myocardium after MI, and $\gamma\delta$ T-cells remain present for days thereafter (Yan et al., 2012; Yan et al., 2013). The trend toward decreased B-cells is close to the T-cells pattern. However, natural-killer (NK) cells showed a trend towards an increase after cardiac exercise rehabilitation (ns). This result is consistent with a study performed to characterize NK cell activity in relation to AMI, which found significantly decreased baseline NK cell activity on days 1, 3, 7 and 14, and at 6-weeks among AMI patients compared to a control group (Klarlund et al., 1987). It was found that NK cell activity could be increased by using interferon, interleukin and indomethacin, although it was never completely restored to its original levels (Klarlund et al., 1987). NK cells exhibit the greatest lymphocyte subset increase in activity among all lymphocyte subsets, of up to 200% above resting levels, for high intensity, brief duration exercise (Nielsen et al., 1996) and longer duration exercise (Mackinnon et al., 1988). These increases in cell activity are observed during, or immediately following the exercise activity, and return to resting levels in the hours and days following the exercise (Berk et al., 1990; Mackinnon et al., 1988; Shek et al., 1995). A positive correlation has been found between NK cell levels and exercise intensity (Nieman, et al., 1993 and Tvede et al., 1993).

My results also demonstrated a significant reduction in Treg percentages at PBMNCs. As we found earlier in this study, CD4⁺ T-cells decreased significantly in pre- and post-cardiac exercise rehabilitation. Tregs are a subset of CD4⁺ and their decrease was confirmed by the CD4⁺ T-cell results. Treg cell numbers were increased and recruited to infarct area in

experimental MI mice, leading to a decrease in the inflammation which may occur after MI, helping to improve function and remodel the infarct area (Dobaczewski et al., 2010; Sharir et al., 2014; Saxena et al., 2014). A review study by Hofmann and Frantz (2015) demonstrated that inflammation is one complication of MI. Tregs were increased post MI, as anti-inflammatory cells may improve healing (Hofmann and Frantz, 2015). Based on this, and our results showing a decline in Tregs after cardiac rehabilitation, overall it may suggest that there was no inflammation - or at least the inflammation level decreased, which led to decreased Tregs. Also, cardiac function appeared to stabilize in MI mice, as increased Tregs play a role in preventing cardiac dysfunction (Tang et al., 2012). Tregs secrete transforming growth factor beta (TGF- β), IL-10 and other inhibitory cytokines, which suppress the immune system (reviewed in Sakaguchi, 2005) and also atherosclerosis (Robertson et al., 2003; Mallat et al., 2001). Patients with ST-segment elevation MI were found to have higher levels of circulatory Tregs (Ammirati et al., 2010). Our results showed that Treg cell expression significantly decreased with high CD25 $^{+}$ expression, low CD25 $^{+}$ expression and with no CD25 $^{+}$ expression (Khatri et al., 2003). This finding supports the idea that Tregs play a key role in immune homeostasis and tolerance, including maintenance and induction. They make up 5-10% of all peripheral CD4 $^{+}$ cells (Chen et al., 2003; Fontenot et al., 2003). Antigen presenting cells (APCs) and target T-cells are regulated through Tregs, which consequently inhibits both cytokine production and T-cell proliferation (reviewed in Sakaguchi, 2005).

My study showed that there were no significant changes either on telomere length or telomerase activity for patients between pre- and post-cardiac exercise rehabilitation. There was a non-significant trend towards an increase in telomerase activity for 8 vs. 8 patients after cardiac rehabilitation and this matched a study which demonstrated that low telomerase activity and telomere length is a risk factor of cardiovascular diseases (Epel et al., 2006). Our study conducted on MI patients may have required a longer time to notice a significant improvement in telomere length. The study by Melk et al. (2014) concluded that telomerase activity and telomere length among PBMNCs increased after 3 months of physical activity in healthy middle-aged men with a sedentary lifestyle.

MY study found a positive correlation between telomere length and telomerase activity. Patients exhibiting low telomerase activity also exhibited shorter telomeres, whilst patients whose telomerase activity was medium or high exhibited the ability to maintain or even extend their telomeres. Telomere length and telomerase activity contributes to cardiac diseases and oxidative stress (Epel et al., 2004; Epel et al., 2006; Demissie et al., 2006).

CHAPTER 7. GENERAL DISCUSSION

7.1 Telomerase regulation under hyperoxia and hypoxia *in vitro*

Firstly I established an *in vitro* model of oxidative stress and inflammation condition by culturing lymphocytes and monocytes under hyperoxic conditions. My results showed that hyperoxia (40% O₂ saturation) and normoxia (20% O₂ saturation) induced oxidative stress (measured with DHE in a flow cytometer) in mouse splenocytes and CD4⁺ T-cells from both TERT^{+/+} and TERT^{-/-} mice respectively, compared with hypoxia (3% O₂ saturation). I also found that hyperoxia induced a persistantly high IFN-gamma production in cultured mouse splenocytes, whereas under hypoxia, IFN-gamma production decreased from day one to day three. The main finding was the decrease of T-cell proliferation under hyperoxic conditions, which was dependent on the presence of TERT and telomerase activity. A study by von Zglinicki et al. (1995) showed that the proliferation of human fibroblasts under hyperoxic conditions was reduced compared to normoxia. This decrease in proliferation correlated to an accelerated telomere shortening caused by single strand damage in the telomerase due to increased oxidative stress under hyperoxia (von Zglinicki et al., 1995). It was also noted that hyperoxia can cause telomeres to reduce to lengths similar to that found in senescence. Consequently, hyperoxic conditions may also be used as a model for senescence. Furthermore, both the ageing process and hyperoxia cause increased generation of intracellular oxygen free radicals (Gille and Joenje, 1992; Sohal and Brunk, 1992; Shigenaga et al., 1994). Single-strand breaks and other DNA damage are mediated by the presence of free radicals, even under normoxic conditions (Fraga et al., 1990). The p53-dependent cell cycle exit pathway has been shown to rely on DNA strand breaks (Nelson and Kastan, 1994) and the same pathway has been found to mediate proliferation inhibition during senescence (Shay et al., 1993; Bond et al., 1994; Passos et al., 2010).

My study observed the effect of oxidative stress on both telomerase activity and cell proliferation, proposing two potential mechanisms, for the decrease in proliferation in cells that have telomerase activity. Telomere maintenance is affected by oxidative stress in two ways: 1) DNA damage is induced in telomerase negative fibroblasts, resulting in increased telomere shortening (Petersen et al., 1998); 2) oxidative stress causes telomerase to be exported from nuclei to mitochondria (Ahmed et al., 2008; Haendeler et al., 2009), thus preventing it from maintaining telomeres in the nucleus in hTERT over-expressing fibroblasts (Ahmed et al., 2008). However, nothing is known about this mechanism in lymphocytes.

My study found that hyperoxia decreased telomerase activity, however, it is not known whether telomerase/TERT was exported out of the nucleus. A study by Santos et al. (2004) has demonstrated that the TERT sequence contains a mitochondrial localisation signal which causes TERT to localise at mitochondrial sites. Furthermore, exclusion from the nucleus of both ectopically overexpressed TERT, as well as endogenous TERT in endothelial cells, has been shown to be stress dependent (Haendeler et al., 2004) and is therefore not solely due to overexpression itself. The large nucleus to cytoplasm ratio found in lymphocytes makes it technically difficult to analyse the exclusion of telomerase from the nucleus. Furthermore, studies by Akiyama (2003) and Kawauchi (2005) have shown Akt phosphorylation on serine 227 of the TERT protein to induce telomerase activity. T-cell (CD8⁺) senescence causes this phosphorylation to decline (Plunkett et al., 2007), suggesting that oxidative stress may be involved in reduced telomerase activity by reducing the activity of Akt responsible for this telomerase activating phosphorylation. Proving this hypothesis would however require further study.

Under hypoxia, it has been observed that cells grow more quickly, live longer and exhibit fewer stress indicators (Richter et al., 1972; Packer and Fuehr, 1977; Parrinello et al., 2003). The cells in my study were mouse splenocytes and T-cells, and in accordance with findings from Parrinello et al. (2003), these showed signs of significant oxidative stress under conditions of normoxia and hyperoxia. Inflammation levels, reflected by IFN- γ production at the RNA level, were higher under hyperoxia. A study by von Zglinicki et al. (1995) showed that 40% oxygen saturation led to senescence after human fibroblast proliferation was suppressed and telomere length decreased. Our study confirmed decreased splenocyte and lymphocyte proliferation at 40% O₂. Telomere length was not analysed in mouse models in my study because the incubation times under hyperoxia were very short and the telomeres in mouse cells are very long. However, our group did use the flow-FISH technique to find that telomere length changed in TERC knockout splenocytes in comparison with wild-type littermates (Bennaceur et al., 2014; Al-Ajmi et al., 2014). The study on mouse ageing by Hewitt et al. (2012) suggests that telomere damage as a potential cause of cell senescence and ageing may also implicate telomere influence in decreased proliferation.

Hyperoxia (40% O₂ saturation) is a model for inducing oxidative stress, which may lead to a number of health outcomes in different cell types. These include; atherogenesis in vascular walls, which is linked to inflammation or an enhanced risk of myocardial infarction (Sorescu et al., 2002); the formation of atherosclerotic plaques; and endothelial dysfunction, which also leads to inflammation (Guzik et al., 2006; Heitzer et al., 2001).

Telomerase plays a critical role in cell proliferation. In our study, the absence of TERT was found to diminish the effects of oxidative stress, with TERT^{-/-} T-lymphocytes exhibiting the same low proliferation levels under both hypoxia and hyperoxia. My study also found that *mTert*-GFP⁺ expression and telomerase activity in splenocytes were suppressed under hyperoxia and that telomerase expression was significantly higher under conditions of hypoxia. I speculate that hyperoxia might enhance IFN- γ mRNA transcription and inflammation in general (Kudo et al., 2012, González-Muniesa et al., 2015), which leads to suppressed T-cell proliferation and decreased *mTert*-GFP⁺ expression under 40% O₂. Our group has demonstrated that decreased telomerase activity in unstimulated PBMCs is caused by increased inflammation in patients with acute cardiovascular infarction (acute stemi), but further study is required to confirm a direct causal relationship (Bennaceur et al., 2014).

7.2 Effects of mitogen-activated protein kinases inhibition (MAPKi) on telomerase under oxidative stress

In my results MAPK inhibition down-regulated IFN-gamma production under oxidative stress at the same level under hypoxia by day 3. Splenocyte proliferation increased equally under hypoxia and hyperoxia. This may be related to decreased inflammation *in vitro*, as IFN-gamma is a pro-inflammatory cytokine (Prasanna et al., 2010), and IFN-gamma is produced as a key proatherogenic cytokine expressed in arterial plaques (Frostegård et al., 1999). This is secondary to the fact that IFN-gamma reduces CD8 T-lymphocyte generation, largely during the immune response to foreign antigens, by limiting proliferation of IL-2 producing CD4⁺ T cells. As suggested by Hidalgo et al. (2005), a feedback loop is generated, in which IFN-gamma is produced by effectors to inhibit production of IL-2. In turn, this suppresses the production of CD8⁺ T cells.

Sarov-Blat et al. (2010) and Cherian et al. (2011) found that IFN- γ secretion *in vitro* was reduced by the presence of MAPKi, resulting in less inflammation. Studies on IFN- γ secretion from human atherosclerotic coronary artery rings cultured with IL-12/IL-18 yielded decreased production of IFN- γ after treatment with MAPKi, including reduced inflammation (Ranjbaran et al, 2007).

My results showed that the effect of MAPKi seemed to be telomerase-dependent, as there was no increase in proliferation in TERT^{-/-} mice splenocytes under either oxygen saturation when cells were treated with MAPK inhibitor compared to untreated cells. Furthermore, telomerase expression, reflected by the percentage of GFP⁺ cells from *mTert*-GFP⁺ mice increased when

these cells were treated with the MAPK inhibitor, and was diminished when cells were cultured under hyperoxia without MAPK inhibitor treatment.

The study of MAPK inhibition under hyperoxia found telomerase activity increased by day 10, and this became significant by day 14 (2.9-fold, $P<0.05$), in comparison to hypoxia. MAPKi therefore seems to be dependent on both TERT and also interaction between cells. The same proliferation pattern was observed in purified CD4⁺ T-cells from both TERT^{+/+} and TERT^{-/-} under hyperoxia. Under MAPKi treatment, no proliferation was observed in either hypoxic or hyperoxic conditions. Cell proliferation was seen to be the same for all splenocyte subsets and TERT^{+/+} when treated with MAPKi in both hypoxic and hyperoxic conditions (1.4-fold and 1.6-fold respectively at day 28 compared to day 2). This improvement in cell proliferation, telomerase (TERT) expression and telomerase activity may relate to the blocking of the p38 signalling pathway, which was found to lead to increased cell proliferation and increased telomerase activity after stimulation in human T-cells (Di Mitri et al., 2011).

p38 MAPK signalling plays a key role in senescence and in pro-inflammatory cytokine production by T-cells, including: IL-1 β , TNF- α , and IL-6 (Iwasa et al., 2003; Rincón and Pedraza-Alva, 2003; Zarubin and Han, 2005). The p38 pathway is also involved in the response to oxidative stress induced by mild hyperoxia, which inhibits fibroblast proliferation and in addition activates p53, which shortens telomeres. As stated earlier, hyperoxic conditions *in vitro* may be used as a model for senescence (von Zglinicki et al., 1995). My data demonstrated that hyperoxic conditions led to decreased T-cell proliferation, which is linked to reduced telomerase expression and activity. This association can be partially reversed by blocking the p38 pathway under oxidative stress. This result is a confirmation of findings by A. Akbar's group (Di Mitri et al., 2011, Henson et al., 2015).

DNA damage activates p38 MAPK, which plays an important role in senescence induction by activating the pRb/p16 and p21/p53 pathways (Freund et al., 2011; Iwasa et al., 2003; Passos et al., 2010). Increased telomerase activity and proliferation were noticed after CD4⁺ T-cells were stimulated (Di Mitri et al., 2011). A study showed that inhibition of p38 MAPK improves mitochondrial function with increasing mitochondrial mass, which, it has been suggested, may improve proliferation (Passos et al., 2010; Henson et al., 2014).

Mouse CD4⁺ T-cells exhibit separate pathways for IL-12/IL-18 and TCR signalling. The former depends on p38 MAPK activation, whilst the latter relies on calcineurin activity (Yang et al., 2001). Studies in organ culture have shown that inhibition of p38 MAPK has a greater

effect on stabilizing and limiting the atherosclerotic human coronary artery rings than rapamycin, which is an mTOR (mammalian target of rapamycin) inhibitor. These findings are echoed in experiments on the inhibition of IFN- γ production via IL-12. IFN- γ secretion has been shown to be reduced by p38 MAPKi, resulting in decreased inflammation in human coronary artery rings cultured with IL-12/IL-18 (Kusaba et al., 2005; Ranjbaran et al., 2007).

7.3 Voluntary wheel running exercise increases telomerase activity in splenocytes in mice

In this part of my thesis, I subjected mice from different genetic backgrounds to voluntary wheel running exercise. As expected, mice were mainly exercising during night-time. Our computerised voluntary wheel running system proved to be a reliable monitor of exercise activity in mouse models. My study's most important finding was that splenocytes from $\text{ApoE}^{-/-}\text{mTert-GFP}^+$ mice on high fat diet (HFD) and exercise showed increased telomerase activity by 3.9-fold ($P<0.001$) in comparison to cells from the non-exercising group. Telomerase activity increased by 1.7-fold ($P<0.05$) for the HFD exercise group compared to the normal diet (ND) exercise group. Thus, there seems to be an interaction between diet, exercise and telomerase activity. However, the underlying mechanisms are still unknown.

In theory, the possibility of an unspecific silencing of GFP reporter exists. However, I do not think it occurred in my experiment because the amount of GFP^+ cells in the growth-curve (Figure 3.8C – page 121) measuring the mTERT transcription is identical to the telomerase activity measured by TRAP-ELISA (Figure 3.10 – page 123). This means that the downregulation of the mTERT promoter in the GFP^+ cells from the transgenic mice shows the same as the decrease in telomerase activity measured by TRAP assay. Furthermore, within the GFP^+ population, the number of $\text{GFP}^+\text{CD4}^+$ cells (Figure 3.9B – page 122) shows a growth-curve almost identical to the two previous results. Thus, most of the changes (less mTERT transcription and less telomerase activity) are mainly due to the downregulation of these 2 parameters in CD4^+ cells. Consequently, I did not observe any unspecific decrease of the reporter, but rather a specific change due to transcriptional changes of the mTERT promoter.

$\text{ApoE}^{-/-}\text{mTert-GFP}^+$ mice on HFD and exercise showed a 1.5-fold ($P<0.001$) increase in B-cells in comparison to ND. A similar pattern was seen with the ND exercise group in comparison to both the HFD and ND non-exercise groups (1.7-fold with $P<0.0001$ and 1.6-fold with $P<0.001$ respectively).

Telomerase activity was increased in splenocytes by exercise. However, we do not know whether this increase contributes to the enhanced cell division rates in ApoE^{-/-} *mTert*-GFP⁺ mice. We also speculate that these parameters might contribute to the slowing of atherosclerotic plaque development. Other animal models have shown that atherosclerosis can be slowed to a large extent by voluntary exercise in ApoE^{-/-} under HFD (Fukao et al., 2010). These authors show reduction in white adipose tissue weight and improved endothelial function as possible mechanisms. In general, exercise can reduce inflammation (Petersen and Pedersen, 2005; Ringseis et al., 2015). It has been shown that a TNF- α independent pathway enables muscle cells to produce IL-6 during exercise, which causes other anti-inflammatory cytokines (e.g. IL-1ra and IL-10) to enter the blood circulation. Similarly, TNF- α , a pro-inflammatory cytokine, is inhibited by exercise (Petersen and Pedersen, 2005).

It has been suggested by Moustardas et al. (2014) that reduction in atherosclerotic plaque size is connected with matrix-metalloproteinases and their inhibitors, MMP/TIMP, and in particular, their balance following exercise. Proteolytic enzyme inhibition and infiltration of inflammatory cells into the plaque are suggested as a mechanism by which plaque development might be reduced. Further to this, the plaque could be stabilised by combined exercise and statin treatment (Moustardas et al., 2014).

A study by Cardinot et al. (2016) found that atherosclerotic plaques could be modified via exercise in mice, resulting in a more stable phenotype. Both the preventative and therapeutic exercise protocols caused the collagen content of plaques to increase, and the preventative protocol also caused fat content to decrease. The precise causal mechanism for this is not yet established, but a number of processes were implicated. For example, increased collagen deposition is caused by reduced CD40 expression (Cardinot et al., 2016). Regular exercise is widely considered by clinical researchers to induce an anti-inflammatory response, protecting against atherosclerosis (Szostak and Laurant, 2011; Petersen and Pedersen, 2005), and experimental models have yielded similar results. Exercise appears to reduce the inflammatory response in various areas, including the hypothalamus (Moreira et al., 2013; Yi et al., 2012), adipose tissue (Medeiros et al., 2011; Ringseis et al., 2015), aortic valve (Matsumoto et al., 2010) and even within the atherosclerotic plaque (Matsumoto et al., 2013). *In vitro* results from our study confirmed that inflammation (IFN-gamma production) suppressed splenocyte and T-lymphocyte proliferation, as well as telomerase activity under hyperoxia (40% oxygen saturation), whilst cells proliferated more with activated telomerase activity when treated with a MAPK inhibitor under the same oxygen conditions.

Telomere repeat binding factor (TRF2) expression is increased by exercise in wild-type mice, and this was shown to prevent doxorubicin-induced cardiac apoptosis (Werner et al., 2008). The effect was not observed in TERT^{-/-} mice, however. From this, we can infer that when telomerase is not present, telomere-stabilising proteins are inhibited and cardiac apoptosis increases.

Splenocyte numbers did not increase significantly among the exercising groups. Other studies also found this, including Woods et al. (2000, 2003), Hoffman-Goetz et al. (1992), Macneil and Hoffman-Goetz (1993) and Jonsdottir et al. (1997). Woods et al. (2003) concluded that 4 months of aerobic exercise on a treadmill was the ideal duration, allowing manipulation and quantification of the intensity and duration of exercise. (Our study also measured intensity and duration of exercise). However, they found that the percentage of CD4⁺ and CD8⁺ splenic T-cells was unchanged by exercise compared to the control group, although the number of splenocytes in the spleen had decreased significantly after exercise. The non-exercising ApoE^{-/-}*mTert*-GFP⁺ control groups exhibited an increase in splenocyte numbers, and it is thought this may be connected with ApoE deficiency, which is linked to lipid accumulation and cardiovascular complications (Zhang et al., 1992; Williams et al., 2002; Knouff et al., 1999).

A non-significant increase in numbers of CD4⁺ and CD8⁺ T-lymphocytes was observed in the exercised TERT heterozygous group. Other subpopulations however (DP, DN, B-cells and monocytes) decreased in the exercise group. Woods et al. (2003) found T-lymphocyte numbers, in 2 year old specific pathogen-free (SPF) inbred male Balb/cByJ mice increased following 4 months of exercise, enabling restoration of their levels to those of young mice. Older mice exhibited increased numbers of naïve (as opposed to memory) T-lymphocytes after exercise. Furthermore, regulatory T-cells were seen in my study to increase following exercise, suggesting that increased blood circulation might have enhanced the proliferation of these cells. I observed increased physiological muscle strength in our exercised mice (not measured). In spite of the important role played by Tregs in immune activation or suppression, our mice were healthy, and to my best knowledge had normal immune function. No significant difference was observed between the exercise and non-exercise groups.

No significant difference was observed in CD4⁺, CD8⁺ T-cell or monocyte numbers in *mTert*-GFP⁺ mice between exercise and non-exercise groups. I did, however, observe a trend (ns) towards increased telomerase activity in GFP⁺ cells for the exercise group, possibly due to higher blood circulation levels. Other studies indicate that exercise had no effect on cell-

cycle-checkpoint kinase 2 (Chk2), tumour suppressor protein p16, tumour suppressor protein p53, or telomere repeat binding factor 2 TRF2 for TERT^{-/-} mice compared to TERT^{+/+} after 21 days of short-term voluntary running exercise (Werner et al., 2008, 2009). Telomerase protects and elongates telomeres at each chromosome end, and therefore the effect of exercise on telomerase activity is of great importance. Our findings, combined with previous studies (Werner et al., 2008, 2009), add credibility to the idea that telomerase might mediate the effect of exercise on telomeres. Findings by Park et al. (2009) suggest that TERT may act as a transcription factor or may be a component within a chromatin remodelling complex. Consequently, there is a possible connection between exercise and a supportive cellular environment for immune, vascular and cardiac cells, which could be significant in preventing oxidative stress and its complications. A study by Ludlow et al. (2012), which found increased telomerase activity in skeletal muscle of CAST/Ei (wild-derived short telomere) mice after 11 months of voluntary exercise, shows that exercise might have a positive effect on telomerase activity. Telomeres exhibited reduced shortening in the liver and cardiac tissues of mice who underwent exercise. These findings correspond to my experiments, in which I analysed telomerase activity (but not telomerase lengths) in splenocytes. In both studies, telomerase activity was maintained after exercise, which suggests that exercise might have a positive effect on telomere length.

The *mTert*-GFP⁺ exercise group exhibited significantly increased B-cell numbers after exercise compared to the control group. Supporting results from human studies were reported by Gray et al. (1993) who found the percentage of plasma cells (effector B-cells) significantly increased post interval exercise in young trained men. B-cells serve many functions, including immunoglobulin (Ig) production and humoral immunity (Berkowska et al., 2011), differentiating into antibody-producing plasma cells, or circulating memory cells (Ozaki et al., 2004).

Diet was critical to our murine study. A high fat diet enabled ApoE^{-/-}*mTert*-GFP⁺ mice to run further and for longer. The exercising mice also gained less body weight on HFD compared to non-exercising mice on HFD, in spite of having a similar average calorie intake. Exercising ApoE^{-/-}*mTert*-GFP⁺ mice on a normal diet consumed more calories than other ApoE^{-/-}*mTert*-GFP⁺ groups on average. Whilst this may be connected to the loss in body weight, it could also be associated with ApoE deficiency. As expected, HFD mice had more energy and were therefore more active. Pellegrin et al. (2009) found that not only did exercise (swimming) cause decreased body weight in ApoE^{-/-} mice, but that it also stabilised the progression of atherosclerosis. This is supported by a number of other studies (Laufs et al., 2005; Pellegrin et al., 2007 and Okabe et al., 2006). Laufs et al., (2005) used male wild-type and ApoE^{-/-} mice

on a voluntary wheel running exercise for 6 weeks, and a control group from each genotype randomly. They found that oxidative stress was increased in aortic tissue for the wild-type control group compared to the wild-type exercise group. Importantly, his finding implicates that exercise decreases oxidative stress which could, in accordance with my *in vitro* findings that oxidative stress decreases telomerase activity, that the latter was increased by exercise via a decrease in oxidative stress. Following 6 weeks on a HFD, the control group of ApoE^{-/-} mice exhibited atherosclerotic lesions in the aortic root and ascending aorta. Conversely, the exercising group did not exhibit such lesions. A twofold increase in vascular superoxide levels was found in HFD ApoE^{-/-} mice with no exercise compared to HFD wild-type mice with no exercise (Laufs et al., 2005).

Pellegrin et al., (2007) divided male ApoE^{-/-} mice on HFD for 9 weeks into two groups. One group underwent a swimming exercise for 9 weeks, and one group was a control. The swimming group was found to have significantly fewer atherosclerotic lesions in the aortic roots compared to the control group.

Okabe et al. (2006) forced 6-week old ApoE^{-/-} mice to undertake swimming exercise in a warm water bath (37°C) for 20min/day, 3 times/week for 2 months. A second group undertook the exercise for 4 months. Each of these two groups had its own (non-exercising) control. It was concluded that both exercise periods decreased the development of experimental atherosclerosis in ApoE^{-/-} mice compared to the non-exercising groups. It was also suggested that exercise may increase the level of plasma oxidized fatty acids in mice on HFD, and further upregulate the endothelial isoform of nitric oxide synthase.

ApoE^{-/-}*mTert*-GFP⁺ mice on exercise and HFD exhibited increased telomerase activity in splenocytes, but there was no significant change in body weight for either this group or the ND group, compared to non-exercise groups. HFD-fed mice exhibited increased telomerase activity with exercise, indicating that the HFD combined with exercise has a significant effect on increasing telomerase activity. This suggests that the ApoE^{-/-}*mTert*-GFP⁺ mice might benefit from exercise to reduce the lipids that accumulate as a result of the HFD and the ApoE deficiency. Meir and Leitersdorf (2004) found that ApoE^{-/-} mice on HFD developed atherosclerosis, and a subsequent study, by Lesniewski et al. (2011) showed that aerobic exercise reversed arterial inflammation with ageing. Human leukocyte studies have associated shorter telomeres with the onset of atherosclerosis (Ogami et al., 2004; Benetos et al., 2004; Obana et al., 2003 and Samani et al., 2001). Exercise might lead to increased telomerase activity and consequently maintained telomere length. However I did not measure telomere length in my study involving mice, in view of their known long lengths.

No significant changes were found in TERT expression in all GFP⁺ cells isolated from *mTert*-GFP⁺ mice. However, the number of telomerase-positive lymphocytes among peripheral blood mononuclear cells was found to decrease with age (Bennaceur et al., 2014), which could be a consequence of lesser proliferation among immune cells. In my results, TERT expression was determined on a single cell level, whilst telomerase activity was measured from a cell pellet in our experiments. Telomerase activity increased in ApoE^{-/-}*mTert*-GFP⁺ mice on exercise with HFD. However, in the *mTert*-GFP⁺ mice experiment, no significant effect of exercise was observed on TERT expression. Despite the fact that GFP⁺ cells only report TERT expression, a number of other mechanisms are known to regulate telomerase activity, such as post-transcriptional TERT modification. In lymphocytes, telomerase activity is regulated by Akt phosphorylation of TERT on serine 227 (Akiyama et al., 2003 and 2004). Akt expression and phosphorylation can be increased by exercise, resulting in decreased apoptosis and improved cardiac function (Zhang et al., 2007). Conversely, using a PI3K kinase inhibitor reversed these beneficial effects, revealing some insights and opening up potential for further investigation into the connection between cardiac function and exercise (Zhang et al., 2007). From this, it can be speculated that telomerase activity might be upregulated during exercise due to increased Akt activity.

B-cell number in ApoE^{-/-}*mTert*-GFP⁺ mice decreased significantly for the ND exercise group in comparison with the ND and HFD no-exercise groups. ApoE deficient mice on HFD also expressed fewer GFP⁺B-cells (*mTert*-GFP⁺B-cells expression) in comparison with the ND and HFD non-exercise groups. This is thought to be connected with Ig-producing B-cells' humoral immunity function (effector B-cells) (Berkowska et al., 2011). However, a human study conducted on young male athletes demonstrated that the concentration of effector B-cells increased in PBMNCs after exercise (Gray et al., 1993). B-cell numbers increased in both ND and HFD without exercise, and may lead to accelerated atherosclerosis in ApoE^{-/-}. Ig production plays a vital role in humoral immunity and our study showed opposing increases and decreases between B-cells and CD8⁺ T-cells in all ApoE^{-/-}*mTert*-GFP⁺ groups. B-cells were also found in the mouse thymuses. The relationship between B-cells and CD8⁺ cells is, to my knowledge, not established, and requires further investigation.

7.4 Cardiac exercise rehabilitation reduces Tregs in PBMNCs after myocardial infarction (MI) in humans

Acute myocardial infarction (AMI) patients who had undergone cardiac rehabilitation showed reduced regulatory T-cell percentages at PBMNCs by 6.8-fold ($P<0.001$). There may be an association here with decreased inflammation levels that increased after AMI, and Tregs recruitment and proliferation at the infarct site. Although my study found no significant effect of exercise in human patients on telomerase activity, I hesitate to draw firm conclusions on this issue in view of the low sample number involved. Whilst the sample number is an obvious limitation, the study may nevertheless be of value as a pilot study for larger experiments.

Patients with AMI who performed a programme of cardiac rehabilitation generally exhibit a trend towards decrease in body weight and BMI. Kraemer et al. (1997), in their study of 31 healthy patients on a 12-week exercise training programme, found significantly reduced body weight after 6 weeks, as well as significantly reduced HDL-C levels in the non-exercise groups (with both a LFD and HFD). The opposite was found for LDL-C, which was reduced with exercise. The benefits of exercise are therefore obvious regarding cardiovascular risk, as LDL-C is associated with a high risk of MI (Duffy et al., 2012; Sniderman et al., 2012; Murphy et al., 2009 and Smith et al., 2006). A review of 51 studies on physical training across 4700 participants (18 to 80 years old men) who successfully completed their exercise programme (about 60% of all participants) found that the exercise programme increased HDL-C levels and decreased LDL-C and triglyceride levels (Leon and Sanchez, 2001).

My study investigated the effects of 6-9 months of post-cardiac rehabilitation in 8 MI patients, which included 3 months of physical training exercise. It was found that the exercise component increased the likelihood of patients being physically active 8 months following MI (Luszczynska and Sutton, 2006). The exercise regime is usually maintained to prevent relapse, which has been referred to as 'self-efficacy'. Self-efficacy was observed in our study, which found that the time spent doing moderate to vigorous physical activity increased by 2.6-fold after cardiac exercise rehabilitation. My study found that patients often spent less time doing low intensity activity and more time doing moderate to vigorous daily activity and had more time for recovery.

Our study also measured T-lymphocytes both before and after cardiac rehabilitation, finding a significant decrease for patients who underwent cardiac exercise rehabilitation, but when sensitivity analysis was applied (omitting the single outlier) the decrease of T-lymphocytes

after cardiac rehabilitation was not significant. More specifically, I found CD4⁺ T-cells decreased significantly also with sensitivity analysis (omitting the single outlier), but not CD8⁺ T-cells. This yields a benefit to the patient's health, as a higher frequency of CD4⁺ T-cells is associated with higher atherosclerosis or cardiovascular disease risk factors (Dumitriu et al., 2009). Other studies found that Th1 and Th17/Th1 lymphocytes increased significantly following MI (Cheng et al., 2008; Methe et al., 2005 and Zhao et al., 2011). In mice, $\gamma\delta$ T-cells, $\alpha\beta$ CD4⁺ T-cells, NK T-cells and B-cells were detected in the myocardium following MI. Furthermore, $\gamma\delta$ T-cells can remain in the peripheral blood for many days (Yan et al., 2012, 2013).

Cardiac exercise rehabilitation also caused a trend towards increase in numbers of NK cells compared to pre cardiac exercise rehabilitation in my study. Klarlund et al. (1987) found that interferon, interleukin and indomethacin could increase NK cell activity, but never quite restore it to pre-AMI levels. High intensity exercise was found to increase the amount of NK cells among lymphocyte subsets by up to 200% (Nielsen et al., 1996; Mackinnon et al., 1988), but these levels returned to normal within a few hours of the exercise. Exercise intensity and NK cell levels are positively correlated (Nieman et al., 1993; Tvede et al., 1993).

As mentioned earlier, we found a significant decrease in CD4⁺ T-cells following cardiac exercise rehabilitation. This was also indicative of a drop in Treg percentages. In murine models, when Treg numbers increase, inflammation following MI was found to decrease, which benefits the recovery of the infarct area through remodelling, as Tregs play a role in suppressing inflammation (Dobaczewski et al., 2010; Sharir et al., 2014; Saxena et al., 2014). Inflammation is a complication associated with MI, so if this is reduced, then recovery outcomes improve (Hofmann and Frantz, 2015). The decrease in Tregs found in our experiments could be due to decreased inflammation. Tang et al. (2012) also found a negative correlation between increased Treg numbers and cardiac dysfunction. This was due to the secretion of TGF-beta, IL-10 and other inhibitory cytokines, which suppressed the immune system (reviewed in Sakaguchi, 2005) and also suppressed atherosclerosis (Robertson et al., 2003; Mallat et al., 2001). A study by Ammirati et al. (2010) found increased Treg levels in ST-elevated MI patients, and I found that high CD25 expression, low CD25 expression, and no CD25 expression (Khattri et al. 2003), caused a significant decrease in Treg cell expression after cardiac exercise rehabilitation. Tregs make up 5-10% of all peripheral CD4⁺ cells, and the above findings emphasise the critical role they play in immune homeostasis, tolerance, maintenance and induction. A review by Sakaguchi (2005) emphasised that Tregs

also have a role in regulating APCs and target T-cells, inhibiting cytokine production and T-cell proliferation.

I found no significant changes in telomerase activity or telomere length between pre- and post-cardiac exercise rehabilitation patients in our study. However, our study found a trend towards increased telomerase activity in some patients following cardiac rehabilitation, suggesting that exercise has a beneficial effect on telomerase activity. This confirms findings by Melk et al. (2014), as well as studies by Werner et al. (2008 and 2009), which suggested that telomerase activity may reflect the benefit of exercise on telomere length. This is confirmed in our own findings of increased telomerase activity in $\text{ApoE}^{-/-}\text{mTert-GFP}^+$ mice during exercise and HFD compared to $\text{ApoE}^{-/-}\text{mTert-GFP}^+$ mice without exercise and on HFD.

A study by Epel et al. (2006) established a link between telomerase activity, telomere length and cardiovascular disease, but did so without using an exercise program. Their study found a correlation between low telomerase activity and risk factors for cardiovascular disease (CVD). These include: an unhealthy lipid profile, high glucose levels during fasting, high systolic blood pressure, increased adipose in the abdomen, composite Metabolic Syndrome variable and of course, smoking. However, a correlation with telomere length was only found with increased catecholamine and cortisol levels. The authors proposed that low levels of telomerase in leukocytes may indicate potential risk of CVD and might potentially cause decreased telomere length. My research may require more time and a greater number of patients to establish any significant changes in telomerase activity and increase in telomere length. Melk et al. (2014) found that 6 months of physical exercise could increase telomere length and telomerase activity even at earlier time points in PBMNCs among healthy but previously sedentary middle-aged men.

My study found a trend for a positive correlation between telomerase activity and telomere length. Telomere length is maintained, and can even be increased, among patients who exhibit medium or high telomerase activity (Melk et al., 2014). Cardiac diseases and oxidative stress are heavily influenced by telomerase activity and telomere length (Epel et al., 2006; Demissie et al., 2006; Ludlow et al 2012; Werner et al., 2008 and 2009).

7.5 Limitations of my study

My study of GFP positive lymphocytes (chapters 3,4 and 5) may be prone to the following limitations:

The *mTERT*-GFP⁺ reporter system only detects changes in mTERT expression levels. However, it is not known if telomerase activity will also increase as a result of transcriptional TERT activation. In general, it is known that telomerase activity is regulated on many different levels and transcriptional control of TERT is only one of these. Nevertheless, changes in transcription levels have often been reported as resulting in changes in telomerase activity (Breault et al., 2008). However, in my study we used the *mTERT*-GFP⁺ reporter cells as an additional method of measuring telomerase activity directly using the TRAP assay. In page/chapter we showed that there was a positive correlation between the TRAP assay results of telomerase activity in splenocytes and the GFP expression level in splenocytes from *mTert*-GFP⁺ mice.

In the mouse study, unavailability of the mouse ApoE^{-/-}*mTert*^{-/-} genotype made it impossible to establish how much the presence of TERT contributed to the effects of exercise and diet.

Unfortunately, I made an error in the cryopreservation of the ApoE^{-/-}*mTert*-GFP⁺ mouse serum, and consequently these samples could not be used to establish lipid accumulation levels and the extent to which the exercise and diet contributed to lipid accumulation in the presence and absence of the ApoE gene.

I realised late in the study that 20% oxygen saturation would be a more useful saturation to determine the effects of oxidative stress on splenocytes and CD4⁺ T-cells, especially with MAPKi.

In the human study, patient numbers were low for many reasons. For example, some patients' conditions did not fit my inclusion criteria; some patients left the study or did not use the accelerometer correctly; and some patients were unable to attend the post-cardiac rehabilitation test. In addition, I was not able to involve a control group (healthy participants) due to time limitations.

7.6 Future experiments:

Given the time and opportunity, I would like to find out:

1. The effect of MAPK inhibition on splenocytes under 20% oxygen saturation. Also, I would like to establish the effect of MAPK inhibition on splenocytes expanded under 40% oxygen saturation for at least two weeks without MAPK inhibitor treatment. Following transfer to 3% oxygen saturation some cells would be treated with MAPK inhibitor, whilst others would not. This might establish possible effects of MAPK inhibition on splenocytes under oxidative stress and inflammation conditions (taken from 40% O₂ in the previous two weeks), and would also find the extent to which oxygen saturation itself contributes to decrease the IFN-gamma and oxidative stress.
2. It would be interesting to analyse how oxidative stress decreases telomerase activity and whether it is directly regulated by decreased Akt activity. Likewise, it would be interesting to analyse whether TERT is also excluded from the nucleus in lymphocytes by using immuno-fluorescence staining of TERT and/or Western blot analysis after cell fractionation.
3. I would like to explore the extent to which telomerase might be affected by exercise and diet in ApoE^{-/-}Tert^{-/-} and ApoE^{+/+}Tert^{-/-} mice.
4. In the human study, I would have liked to increase the number of MI patients to get a higher power and statistical significances for the potential effects of exercise on telomerase activity and telomere length.
5. I would be interested to use a control group of healthy participants, some of whom would be assessed for exercise and others not, in parallel with MI patients undergoing the rehabilitation programme, to ascertain how Tregs, B-cells and CD8 T-cells respond to exercise in different groups.
6. I would like to isolate (pre- and post-rehabilitation) B-cells and CD8⁺ T-cells from MI patients and from healthy (with and without exercise) groups, to study these cells' behaviour under different oxygen saturations.

REFERENCES

Abreu, E., Aritonovska, E., Reichenbach, P., Cristofari, G., Culp, B., Terns, R. M., Lingner, J. and Terns, M. P. (2010) 'TIN2-tethered TPP1 recruits human telomerase to telomeres in vivo', *Mol Cell Biol.*, 30, pp. 2971–2982.

Acuto, F. and Michel, F. (2003) 'CD28-mediated co-stimulation: a quantitative support for TCR signalling', *Nature Review Immunology*, 3, pp. 939–51.

Adaikalakoteswari, A., Balasubramanyam, M., Ravikumar, R., Deepa, R. and Mohan, V. (2007) 'Association of telomere shortening with impaired glucose tolerance and diabetic macroangiopathy', *Atherosclerosis*, 195(1), pp. 83–9.

Adams R.H., Porras A., Alonso G., Jones M., Vintersten K., Panelli S., Valladares A., Perez L., Klein R., Nebredda A.R. (2000) 'Essential role of p38a MAP kinase in placental but not embryonic cardiovascular development'. *Mol Cell* 6(1), pp. 109–116

Adams, J. W., Pagel, A. L., Means, C. K., Oksenbergs, D., Armstrong, R. C. and Brown, J. H. (2000) 'Cardiomyocyte apoptosis induced by G_αq signaling is mediated by permeability transition pore formation and activation of the mitochondrial death pathway', *Circ Res.*, 87, pp. 1180–1187.

Adibzadeh, M., Mariani, E., Bartoloni, C., Beckman, I., Lighthart, G., Remarque, E., Shall, S., Solana, R., Taylor, G. M., Barnett, Y. and Pawelec, G. (1996) 'Lifespan of T lymphocytes', *Mech Ageing Dev*, 91, pp. 145–54.

Agrawal, A., Tay, J., Ton, S., Agrawal, S. and Gupta, S. (2009) 'Increased reactivity of dendritic cells from aged subjects to self-antigen, the human DNA', *J Immunol*, 182, pp. 1138–45.

Ahmed, S., Passos, J. F., Birket, M. J., Beckmann, T., Brings, S., Peters, H., Birch-Machin, M. A., von Zglinicki, T. and Saretzki, G. (2008) 'Telomerase does not counteract telomere shortening but protects mitochondrial function under oxidative stress', *J Cell Sci.*, 121, pp. 1046–53.

Ait-Oufella, H., Herbin, O., Bouaziz, J. D., Binder, C. J., Uyttenhove, C., Laurans, L., Taleb, S., Van Vré, E., Esposito, B., Vilar, J., Sirvent, J., Van Snick, J., Tedgui, A., Tedder, T. F. and Mallat, Z. (2010) 'B cell depletion reduces the development of atherosclerosis in mice', *J Exp Med*, 207, pp. 1579–1587.

Ait-Oufella, H., Salomon, B. L., Potteaux, S., Robertson, A. K., Gourdy, P., Zoll, J., Merval, R., Esposito, B., Cohen, J. L., Fisson, S., Flavell, R. A., K Hansson, G., Klatzmann, D., Tedgui A. and Mallat Z. (2006) 'Natural regulatory T cells control the development of atherosclerosis in mice', *Nat Med*, 12, pp. 178–80.

Akbar, A. N. and Vukmanovic-Stejic, M. (2007) 'Telomerase in T lymphocytes: use it and lose it?', *J Immunol*, 178, pp. 6689–94.

Akbari, O., Stock, P., DeKruyff, R. H. and Umetsu, D. T. (2003) 'Role of regulatory T cells in allergy and asthma', *Curr Opin Immunol*, 15, pp. 627–33.

Akiyama, M., Hideshima, T., Hayashi, T., Tai, Y. T., Mitsiades, C. S., Mitsiades, N., Chauhan, D., Richardson, P., Munshi, N. C. and Anderson, K. C. (2003) 'Nuclear factor-kappaB p65 mediates tumor necrosis factor alpha-induced nuclear translocation of telomerase reverse transcriptase protein', *Cancer Res.*, 63, pp. 18-21.

Akiyama, M., Hideshima, T., Hayashi, T., Tai, Y.T., Mitsiades, C. S., Mitsiades, N., Chauhan, D., Richardson, P., Munshi, N. C. and Anderson, K. C. (2002) 'Cytokines modulate telomerase activity in a human multiple myeloma cell line', *Cancer Research*, 62, pp. 3876–3882.

Akiyama, M., Yamada, O., Hideshima, T., Yanagisawa, T., Yokoi, K., Fujisawa, K., Eto, Y., Yamada, H. and Anderson K.C. (2004) 'TNFalpha induces rapid activation and nuclear translocation of telomerase in human lymphocytes', *Biochem. Biophys. Res. Commun.*, 316, pp. 528–532

Al-Ajmi, N., Saretzki, G., Miles, C. and Spyridopoulos, I. (2014) 'Dietary restriction ameliorates haematopoietic ageing independent of telomerase, whilst lack of telomerase and short telomeres exacerbate the ageing phenotype', *Experimental Gerontology*, 58, pp. 113-119.

Alberola-Illa, J., Hogquist, K. A., Swan, K. A., Bevan, M. J. and Perlmuter, R. M. (1996) 'Positive and negative selection invoke distinct signaling pathways', *The Journal of Experimental Medicine*, 184, pp. 9–18.

Alcorta, D. A., Xiong, Y., Phelps, D., Hannon, G., Beach, D. and Barrett, J. C. (1996) 'Involvement of the cyclin-dependent kinase inhibitor p16 (INK4a) in replicative senescence of normal human fibroblasts', *Proc. Natl. Acad. Sci. U. S. A.*, 93, pp. 13742–13747.

Allen, D. L., Harrison, B. C., Maass, A., Bell, M. L., Byrnes, W. C. and Leinwand, L. A. (2001) 'Cardiac and skeletal muscle adaptations to voluntary wheel running in the mouse', *J Appl Physiol*, 90, pp. 1900–08.

Allsopp, R. C., Vaziri, H., Patterson, C., Goldstein, S., Younglai, E. V., Futcher, A. B., Greider, C. W. and Harley, C. B. (1992) 'Telomere length predicts replicative capacity of human fibroblasts' *Proc Natl Acad Sci U S A.*, 89(21), pp. 10114-10118.

Ammirati, E., Cianflone, D., Banfi, M., Vecchio, V., Palini, A., De Metrio, M., Marenzi, G., Panciroli, C., Tumminello, G., Anzuini, A., Palloshi, A., Grigore, L., Garlaschelli, K., Tramontana, S., Tavano, D., Airoldi, F., Manfredi, A. A., Catapano, A. L. and Norata, G. D. (2010) 'Circulating CD4+CD25hiCD127lo regulatory T-Cell levels do not reflect the extent or severity of carotid and coronary atherosclerosis', *Arterioscler Thromb Vasc Biol*, 30, pp. 1832-41.

Ancelin, K., Brunori, M., Bauwens, S., Koering, C. E., Brun, C., Ricoul, M., Pommier, J. P., Sabatier, L. and Gilson, E. (2002) 'Targeting assay to study the cis functions of human telomeric proteins: evidence for inhibition of telomerase by TRF1 and for activation of telomere degradation by TRF2', *Mol. Cell. Biol.*, 22, pp. 3474–3487.

Anderson, T. J., Gerhard, M. D., Meredith, I. T., Charbonneau, F., Delagrange, D., Creager, M. A., Selwyn, A. P. and Ganz, P. (1995) 'Systemic nature of endothelial dysfunction in atherosclerosis', *Am J Cardiol.*, 75(6), pp. B71–4.

Andersson, J., Libby, P. and Hansson, G. K. (2010) 'Adaptive immunity and atherosclerosis', *Clin. Immunol.*, 134, pp. 33–46.

Aouadi, M., Binetruy, B., Caron, L., LeMarchand-Brustel, Y. and Bost, F. (2006) 'Role of MAPKs in development and differentiation: lessons from knockout mice', *Biochimie*, 88(9), pp. 1091–1098.

Appay, V., van Lier, R. A., Sallusto, F. and Roederer, M. (2008) 'Phenotype and function of human T lymphocyte subsets: consensus and issues', *Cytometry A.*, 73, pp. 975–83.

Armstrong, L., Lako, M., Lincoln, J., Cairns, P. M. and Hole, N. (2000) 'mTert expression correlates with telomerase activity during the differentiation of murine embryonic stem cells', *Mech Dev.*, 97, pp. 109–116.

Babcock, G. T. (1999) 'How oxygen is activated and reduced in respiration', *Proc Natl Acad Sci USA.*, 96, pp. 13114–13117.

Bakke, A. (2001) 'The principles of flow cytometry', *Lab Medicine*, 32, pp. 207–211.

Balady, G. J., Ades, P. A., Comoss, P., Limacher, M., Piña, I. L., Southard, D., Williams, M. A. and Bazzarre, T. (2000) 'Core components of cardiac rehabilitation/ secondary prevention programs: a statement for healthcare professionals from the American Heart Association and the American Association of Cardiovascular and Pulmonary Rehabilitation Writing Group', *Circulation*, 102, pp. 1069–73.

Baltgalvis, K. A., Call, J. A., Cochrane, G. D., Laker, R. C., Yan, Z. and Lowe, D. A. (2012) 'Exercise training improves plantarflexor muscle function in mdx mice', *Med Sci Sports Exerc.*, in press.

Banik, S.S., Counter, C.M. (2004) 'Characterization of interactions between PinX1 and human telomerase subunits hTERT and hTR', *J Biol Chem*, 279, pp.51745–51748.

Bartsch, H. and Nair J. (2006) 'Chronic inflammation and oxidative stress in the genesis and perpetuation of cancer: role of lipid peroxidation, DNA damage, and repair', *Langenbecks Arch. Surg.*, 391, pp. 499–510.

Beardmore, V. A., Hinton, H. J., Ftychi, C., Apostolaki, M., Armaka, M., Darragh, J., McIlrath, J., Carr, J. M., Armit, L. J., Clacher, C., Malone, L., Kollias, G. and Arthur, J. S. C. (2005) 'Generation and characterization of p38b (MAPK11) gene-targeted mice', *Mol Cell Biol.*, 25(23), pp. 10454–10464.

Beissert, S., Schwarz, A. and Schwarz, T. (2006) 'Regulatory T cells', *J Invest Dermatol*, 126, pp. 15–24.

Benetos, A., Gardner, J., P., Zureik, M., Labat, C., Xiaobin, L., Adamopoulos, C. Temmar, M., Bean, K. E., Thomas, F. and Aviv, A. (2004) 'Short telomeres are associated with increased carotid atherosclerosis in hypertensive subjects', *Hypertension*, 43, pp. 182–185.

Benetos, A., Okuda, K., Lajemi, M., Kimura, M., Thomas, F., Skurnick, J., Labat, C., Bean, K. and Aviv, A. (2001) 'Telomere length as an indicator of biological aging: the gender effect and relation with pulse pressure and pulse wave velocity', *Hypertension*, 37(2 Pt 2), pp. 381–5.

Bennaceur, K., Atwill, M., Al Zhrany, N., Hoffmann, J., Keavney, B., Breault, D., Richardson, von Zglinicki, T., Saretzki, G. and Spyridopoulos, I. (2014) 'Atorvastatin induces T cell proliferation by a telomerase reverse transcriptase (TERT) mediated mechanism', *Atherosclerosis*, 236(2), pp. 312–320.

Benov, L., Sztejnberg, L. and Fridovich, I. (1998) 'Critical evaluation of the use of hydroethidine as a measure of superoxide anion radical', *Free Radic Biol Med*, 25(7), pp. 826–31.

Bentz, G. L. and Yurochko, A. D. (2008) 'Human CMV infection of endothelial cells induces an angiogenic response through viral binding to EGF receptor and beta1 and beta3 integrins', *Proc Natl Acad Sci U S A*, 105, pp. 5531–5536.

Benzie, I. F. (2000) 'Evolution of antioxidant defence mechanisms', *Eur J Nutr*, 39, pp. 53–61.

Berk, L. S., Nieman, D. C., Youngberg, W. S., Arabatzis, K., Simpson-Westerberg, M., Lee, J. W., Tan, S. A. and Eby, W.C. (1990) 'The effect of long endurance running on natural killer cells in marathoners', *Med Sci Sports Exerc*, 22(2), pp. 207-12.

Berkowska, M.A., Driessen, G.J., Bikos, V., Grosserichter-Wagener, C., Stamatopoulos, K., Cerutti, A. He, B., Biermann, K., Lange, J. F., van der Burg, M., van Dongen, J. J. and van Zelm, M. C. (2011) 'Human memory B cells originate from three distinct germinal center-dependent and-independent maturation pathways', *Blood*, 118, pp. 2150-2158.

Bernstein, D. (2003) 'Exercise assessment of transgenic models of human cardiovascular disease', *Physiol Genomics*, 13, pp. 217–26.

Bethell, H., Lewin, R. and Dalal, H. (2009) 'Cardiac rehabilitation in the United Kingdom', *Heart*, 95, pp. 271–5.

Beyer, A. L. and Osheim, Y. N. (1988) 'Splice site selection, rate of splicing, and alternative splicing on nascent transcripts', *Genes & development*, 2, pp. 754–765.

Beyer, M. and Schultz, J. L. (2006) 'Regulatory T cells in cancer', *Blood*, 108, pp. 804–11.

Bilsland, A. E., Stevenson, K., Atkinson, S., Kolch, W., Keith, W. N., (2006) 'Transcriptional repression of telomerase RNA gene expression by c-Jun-NH2-kinase and Sp1/Sp3', *Cancer Res.*, 66, pp. 1363–1370.

Binder, C. J. Hartvigsen, K., Chang, M. K., Miller, M., Broide, D., Palinski, W., Curtiss, L. K., Corr, M., Witztum, J. L. (2004) 'IL-5 links adaptive and natural immunity specific for epitopes of oxidized LDL and protects from atherosclerosis', *J Clin Invest*, 114, pp. 427–37.

Blackburn, E. H. (2005) 'Telomeres and telomerase: their mechanisms of action and the effects of altering their functions', *FEBS Lett*, 579, pp. 859 – 862.

Blasco, M. A., Lee, H. W., Hande, M. P., Samper, E., Lansdorp, P. M., DePinho, R. A., and Greider, C. W. (1997) 'Telomere shortening and tumor formation by mouse cells lacking telomerase RNA', *Cell*, 91, pp. 25–34.

Blum, A. and Yeganeh, S. (2003) 'The role of T-lymphocyte subpopulations in acute myocardial infarction', *Eur J Intern Med*, 14, pp. 407–10.

Blumenthal, J. A., Babyak, M. A., Moore, K. A., Craighead, W. E., Herman, S., Khatri, P., Waugh, R., Napolitano, M. A., Forman, L. M., Appelbaum, M., Doraiswamy, P. M. and Krishnan, K. R. (1999) 'Effects of exercise training on older patients with major depression', *Arch Intern Med*, 159, pp. 2349 –56.

Boag, S. E., Das, R., Shmeleva, E. V., Bagnall, A., Egred, M., Howard, N., Bennaceur, K., Zaman, A., Keavney, B. and Spyridopoulos, I. (2015) 'T lymphocytes and fractalkine contribute to myocardial ischemia/reperfusion injury in patients', *Journal of Clinical Investigation*, 125(8), pp. 3063-3076.

Bodi, V., Sanchis, J., Llacer, A., Fáfila, L., Núñez, J., Pellicer, M., Bertomeu, V., Ruiz, V. and Chorro, F. J. (2005) 'Multimarker risk strategy for predicting one-month and one-year major events in non-ST elevation acute coronary syndromes. Assessment of troponin I, myoglobin, C-reactive protein, fibrinogen and homocysteine', *Am Heart J*, 149, pp. 268–74.

Boehm, U., Klamp, T., Groot, M. and Howard, J. C. (1997) 'Cellular responses to interferongamma', *Annual Review of Immunology*, 15, pp. 749–95.

Bond, J. A., Wyllie, F. S. and Wynford-Thomas, D. (1994) 'Escape from senescence in human diploid fibroblasts induced directly by mutant p53', *Oncogene*, 9, pp. 1885–1889.

Bonilla, F. A. and Oettgen, H. C. (2010) 'Adaptive immunity', *The Journal of Allergy and Clinical Immunology*, 125, pp. 33–40.

Braz, J. C., Bueno, O. F., Liang, Q., Wilkins, B. J., Dai, Y. S., Parsons, S., Braunwart, J., Glascock, B. J., Klevitsky, R., Kimball, T. F., Hewett, T. E. and Molkentin, J. D. (2003) 'Targeted inhibition of p38 MAPK promotes hypertrophic cardiomyopathy through upregulation of calcineurinNFAT signaling', *J Clin Investigat*, 111(10), pp. 1475–1486.

Breault, D. T., Min, I. M., Carlone, D. L., Farilla, L. G., Ambruzs, D. M., Henderson, D. E., Algra, S., Montgomery, R. K., Wagers, A. J. and Hole, N. (2008) 'Generation of mTert-GFP mice as a model to identify and study tissue progenitor cells', *Proc Natl Acad Sci USA*, 105(30), pp. 10420–5.

Brigelius-Flohé, R. and Maiorino, M. (2013) 'Glutathione peroxidases', *Biochim. Biophys. Acta* 1830, pp. 3289–3303.

British Association for Cardiovascular Prevention and Rehabilitation. (2012) BACPR standards and core components for cardiovascular disease prevention and rehabilitation 2012, 2nd ed., UKBACPR.

British Heart Foundation. (2012) European cardiovascular disease statistics 2012. www.bhf.org.uk/publications/statistics/european-cardiovascular-disease-statistics-2012.

British Heart Foundation. (2014) Heart statistics. www.bhf.org.uk/research/heart-statistics.

British Heart Foundation. (2014) The National Audit of Cardiac Rehabilitation: annual statistical report 2014, British Heart Foundation, 2014. www.bhf.org.uk/~media/files/publications/research/nacr_2014.pdf.

Brown, J. P., Wei, W. and Sedivy, J. M. (1997) 'Bypass of senescence after disruption of p21CIP1/WAF1 gene in normal diploid human fibroblasts', *Science*, 277, pp. 831–834.

Buchkovich, K. J. and Greider, C. W. (1996) 'Telomerase regulation during entry into the cell cycle in normal human T cells', *Mol Biol Cell*, 7, pp. 1443–54.

Buchner, N., Zschauer, T. C., Lukosz, M., Altschmied J., Haendeler, J. (2010) 'Downregulation of mitochondrial telomerase reverse transcriptase induced by H₂O₂ is Src kinase dependent', *Exp Gerontol*, 45, pp. 558-62.

Cairney, C. J., and Keith, W. N. (2008) 'Telomerase redefined: integrated regulation of hTR and hTERT for telomere maintenance and telomerase activity', *Biochemie*, 90, pp. 13–23.

Caligiuri, G., Nicoletti, A., Poirier, B. and Hansson, G. K. (2002) 'Protective immunity against atherosclerosis carried by B cells of hypercholesterolemic mice', *J Clin Invest*, 109, pp. 745–753.

Caliguri, G. and Nicoletti, A. (2006) 'Lymphocytes responses in acute coronary syndromes: lack of regulation spawns deviant behaviour', *Eur Heart J*, 27, pp. 2485–6.

Candido, R., Jandeleit-Dahm, K. A., Cao, Z., Nesteroff, S. P., Burns, W. C., Twigg, S. M., Dilley, R. J., Cooper, M. E. and Allen, T. J. (2002) 'Prevention of accelerated atherosclerosis by angiotensin-converting enzyme inhibition in diabetic apolipoprotein E-deficient mice', *Circulation*, 106, pp. 246–253.

Cardinot, T. M., Lima, T. M., Moretti, A. I., Koike, M. K., Nunes, V. S., Cazita, P. M., Krieger, M. H., Brum, P. C., Souza, H. P. (2016) 'Preventive and therapeutic moderate aerobic exercise programs convert atherosclerotic plaques into a more stable phenotype', *Life Sci.*, 153, pp. 163-70.

Cargnello, M. and Roux, P. P. (2011) 'Activation and function of the MAPKs and their substrates, the MAPK-activated protein kinases', *Microbiol. Mol. Biol. Rev.*, 75, pp. 50–83.

Carnaud, C., Lee, D., Donnars, O., Park, S. H., Beavis, A., Koezuka, Y. and Bendelac, A. (1990) 'Cutting edge: cross-talk between cells of the innate immune system: NKT cells rapidly activate NK cells', *Journal of Immunology*, 163, pp. 4647–50.

Cawthon, R. M., Smith, K. R., O'Brien, E., Sivatchenko, A. and Kerber, R. A. (2003) 'Association between telomere length in blood and mortality in people aged 60 years or older', *Lancet*, 361, pp. 393–395.

Cemerski, S., van Meerwijk, J. P. and Romagnoli, P. (2003) 'Oxidative-stress-induced T lymphocyte hyporesponsiveness is caused by structural modification rather than proteasomal degradation of crucial TCR signalling molecules', *Eur J Immunol*, 33, pp. 2178–85.

Chandra, K., Syed, S. A., Abid, M., Sweety, R. and Najam, A. K. (2015) 'Protection Against FCA Induced Oxidative Stress Induced DNA Damage as a Model of Arthritis and In vitro Anti-arthritis Potential of *Costus speciosus* Rhizome Extract' *International Journal of Pharmacognosy and Phytochemical Research*, 7 (2), pp. 383–389.

Cheetham, C., Green, D., Collis, J., Dembo, L. and O'Driscoll, G. (2002) 'Effect of aerobic and resistance exercise on central hemodynamic responses in chronic heart failure', *J Appl Physiol*, 93, pp. 175–80.

Chen, J. L. and Greider, C. W. (2003) 'Determinants in mammalian telomerase RNA that mediate enzyme processivity and cross-species incompatibility', *EMBO J.*, 22(2), pp. 304-14.

Chen, W. Jin, W., Hardegen, N., Lei, K. J., Li, L., Marinos, N., McGrady, G. and Wahl, S. M. (2003) 'Conversion of peripheral CD4+CD25- naive T cells to CD4+CD25+ regulatory T cells by TGF- β induction of transcription factor Foxp3', *J Exp Med*, 198, pp. 1875–86.

Cheng, C. F., Juan, S. H., Chen, J. J., Chao, Y. C., Chen, H. H., Lian, W. S., Lu, C. Y., Chang, C. I., Chiu, T. H., Lin, H. (2008) 'Pravastatin attenuates carboplatin-induced cardiotoxicity via inhibition of oxidative stress associated apoptosis', *Apoptosis*, 13, pp. 883–894.

Cheng, X., Liao, Y. H., Ge, H. Li, B., Zhang, J., Yuan, J., Wang, M., Liu, Y., Guo, Z., Chen, J., Zhang, J. and Zhang, L. (2005) 'TH1/TH2 functional imbalance after acute myocardial infarction: coronary arterial inflammation or myocardial inflammation', *J Clin Immunol*, 25, pp. 246–53.

Cheriyan, J., Webb, A., Sarov-Blat, L., Elkhawad, M., Wallace, S., Mäki-Petäjä, K., Collier, D., Morgan, J., Fang, Z., Willette, R., Lepore, J., Cockcroft, J., Sprecher, D. and Wilkinson, I. (2011) 'Inhibition of p38 Mitogen-activated protein kinase improves nitric oxide-mediated vasodilatation and reduces inflammation in hypercholesterolemia', *Circulation*, 123, pp. 515–23.

Cherkas, L. F., Hunkin, J. L., Kato, B. S., Richards, J. B., Gardner, J. P., Surdulescu, G. L., Kimura, X., Lu, X., Spector, T. D. and Aviv, A. (2008) 'The association between physical activity in leisure time and leukocyte telomere length', *Arch Intern Med*, 168, pp. 154–8.

Chiang, Y. J., Hemann, M. T., Hathcock, K. S., Tessarollo, L., Feigenbaum, L., Hahn, W. C. and Hodes, R. J. (2004) 'Expression of telomerase RNA template, but not telomerase reverse transcriptase, is limiting for telomere length maintenance in vivo', *Mol Cell Biol*, 24(16), pp. 7024-31.

Chilton, W. L., Marques, F. Z., West, J. Kannourakis, G. Berzins, S. P. O'Brien, B. J. Charchar, F. J. (2014) 'Acute exercise leads to regulation of telomere-associated genes and microRNA expression in immune cells', *PLoS One*, 9(4), article ID e92088.

Chou, M. Y., Hartvigsen, K., Hansen, L. F., Fogelstrand, L., Shaw, P. X., Boullier, A., Binder, C. J. and Witztum, J. L. (2008) 'Oxidation-specific epitopes are important targets of innate immunity', *J Intern Med*, 263, pp. 479–88.

Chu, T. W., D'Souza, Y. and Autexier, C. (2015) 'The insertion in fingers domain in human telomerase can mediate enzyme processivity and telomerase recruitment to telomeres in a TPP1-dependent manner', *Mol Cell Biol.*, 36, pp. 210–222.

Chung, J., Khadka, P. and Chung, I. K. (2012) 'Nuclear import of hTERT requires a bipartite nuclear localization signal and Akt-mediated phosphorylation', *J. Cell Sci.*, 125, pp. 2684–2697.

Codd, V., Nelson, C. P., Albrecht, E., Mangino, M., Deelen, J. et al. (2013) 'Identification of seven loci affecting mean telomere length and their association with disease', *Nat Genet*, 45, pp. 422–7.

Colgin, L. M. Wilkinson, C., Englezou, A., Kilian, A., Robinson, M. O. and Reddel, R. R. (2000) 'The hTERTalpha splice variant is a dominant negative inhibitor of telomerase activity', *Neoplasia*, 2, pp. 426–432.

Cong, Y. and Shay, J. W. (2008) 'Actions of human telomerase beyond telomeres', *Cell Res.* 2008 Jul;18(7), pp. 725–32.

Cong, Y. S., and Bacchetti, S. (2000) 'Histone deacetylation is involved in the transcriptional repression of hTERT in normal human cells', *J. Biol. Chem.*, 275, pp. 35665–35668.

Cong, Y. S., Wen, J. and Bacchetti, S. (1999) 'The human telomerase catalytic subunit hTERT: organization of the gene and characterization of the promoter', *Hum. Mol. Genet.*, 8, pp. 137–142.

Cong, Y. S., Wright, W. E., Shay, J. W. (2002) 'Human telomerase and its regulation', *Microbiol. Mol. Biol. Rev.*, 66, pp. 407–25

Cook, B. D., Dynek, J. N., Chang, W., Shostak, G. and Smith, S. (2002) 'Role for the related poly (ADP-Ribose) polymerases tankyrase 1 and 2 at human telomeres', *Mol. Cell. Biol.*, 22, pp. 332–342.

Couillard, C., Després, J. P., Lamarche, B., Bergeron, J., Gagnon, J., Leon, A. S., Rao, D. C., Skinner, J. S., Wilmore, J. H., Bouchard, C. (2001) 'Effects of endurance exercise training on plasma HDL cholesterol levels depend on levels of triglycerides: evidence from men of the Health, Risk Factors, Exercise Training and Genetics (HERITAGE) Family Study', *Arterioscler Thromb Vasc Biol.*, 21, PP. 1226–1232.

Counter, C.M., Hahn, W.C., Wei, W., Caddle, SD., Beijersbergen, RL., Lansdorp, PM., Sedivy, J.M., Weinberg, R.A. (1998) 'Dissociation among in vitro telomerase activity, telomere maintenance, and cellular immortalization', *Proc. Natl. Acad. Sci. U. S. A.*, 95, pp. 14723–14728.

Cybulsky, M. I., Iiyama, K., Li, H. Li, H., Zhu, S., Chen, M., Iiyama, M., Davis, V., Gutierrez-Ramos, J., Connelly, P. W. and Milstone, D. S. (2001) 'A major role for VCAM-1, but not ICAM-1, in early atherosclerosis', *J Clin Invest*, 107, pp. 1255–1262.

d'Adda di Fagagna, F., Reaper, P. M., Clay-Farrace, L., Fiegler, H., Carr, P., Von Zglinicki, T., Saretzki, G., Carter, N. P. and Jackson, S. P. (2003) 'A DNA damage checkpoint response in telomere-initiated senescence', *Nature* 426, pp. 194–198.

Dahlgren, C. and Karlsson, A. (1999) 'Respiratory burst in human neutrophils', *J Immunol Methods*, 232, pp. 3–14.

Danesh, J., Lewington, S., Thompson, S. G. et al. (2005) 'Plasma fibrinogen level and the risk of major cardiovascular diseases and nonvascular mortality: an individual participant meta-analysis', *JAMA*, 294, pp. 1799–809.

Daniels, T. F., Killinger, K. M., Michal, J. J., Wright Jr, R. W. and Jiang Z (2009) 'Lipoproteins, cholesterol homeostasis and cardiac health', *Int J Biol Sci.*, 5(5), pp. 474–488.

Darr, D., Dunston, S., Faust, H. and Pinnell, S. (1996) 'Effectiveness of antioxidants (vitamin C and E) with and without sunscreens as topical photoprotectants', *Acta Derm Venereol*, 76, pp. 264–8.

Davis, J. M., Murphy, E. A., Brown, A. S., Carmichael, M. D., Ghaffar, A. and Mayer, E. P. (2004) 'Effects of moderate exercise and oat $\{\beta\}$ -glucan on innate immune function and susceptibility to respiratory infection', *Am J Physiol Regul Integr Comp Physiol.*, 286, pp. R366–R372.

De Bono, J. P., Adlam, D., Paterson, D. J. and Channon, K. M. (2006) 'Novel quantitative phenotypes of exercise training in mouse models', *Am J Physiol Regul Integr Comp Physiol*, 290, pp. R926–R934.

De Caterina, R., Libby, P., Peng, H. B., Thannickal, V. J., Rajavashisth, T. B., Gimbrone, M. A. Jr., Shin, W. S. and Liao, J. K. (1995) 'Nitric oxide decreases cytokine-induced endothelial activation: nitric oxide selectively reduces endothelial expression of adhesion molecules and proinflammatory cytokines', *J Clin Invest*, 96, pp. 60–8.

de Jesus, B. B., Schneeberger, K., Vera, E., Tejera, A., Harley, C. B. and Blasco, M. A. (2011) 'The telomerase activator TA-65 elongates short telomeres and increases health span of adult/old mice without increasing cancer incidence', *Aging Cell*, 10(4), pp. 604–21.

de Lange, T. (2002) 'Protection of mammalian telomeres', *Oncogene*, 21, pp. 532–540.

de Lange, T. (2005) 'Shelterin: the protein complex that shapes and safeguards human telomeres', *Genes Dev.*, 19, pp. 2100–2110.

de Lange, T., and Petrini, J. (2000) 'A new connection at human telomeres: association of the Mre11 complex with TRF2', *Cold Spring Harb. Symp. Quant. Biol.*, 65, pp. 265–273.

De Servi, S., Mariani, M., Mariani, G. and Mazzone, A. (2005) 'C-reactive protein increase in unstable coronary disease. Cause or effect?', *J Am Coll Cardiol*, 46, pp. 1496–502.

De Waard, M. C., van der Velden, J., Bito, V., Ozdemir, S., Biesmans, L., Boontje, N. M., Dekkers, D. H., Schoonderwoerd, K., Schuurbiers, H. C., de Crom, R., Stienen, G. J., Sipido, K. R., Lamers, J. M. and Duncker, D. J. (2007) 'Early exercise training normalizes myofilament function and attenuates left ventricular pump dysfunction in mice with a large myocardial infarction', *Circ. Res.*, 100, pp. 1079–1088.

Deacon, K., Mistry, P., Chernoff, J., Blank, J. L. and Patel, R. (2003) 'p38 Mitogen-activated protein kinase mediates cell death and p21-activated kinase mediates cell survival during chemotherapeutic drug-induced mitotic arrest', *Mol Biol Cell*, 14, pp. 2071–2087.

Demissie, S., Levy, D., Benjamin, E. J., Cupples, L. A., Gardner, J. P., Herbert, A. and Aviv, A. (2006) 'Insulin resistance, oxidative stress, hypertension, and leukocyte telomere length in men from the Framingham Heart Study', *Aging Cell*, 5, pp. 325–30.

Department of Health (DH). (2010) 'Cardiac rehabilitation commissioning pack'. http://webarchive.nationalarchives.gov.uk/20130107105354/http://www.dh.gov.uk/en/Publicationsandstatistics/Publications/PublicationsPolicyAndGuidance/Browsable/DH_117504.

Devasagayam, T, Tilak, J. C., Boloor, K. K., Sane Ketaki, S., Ghaskadbi Saroj, S. and Lele, R. D. (2004) 'Free Radicals and Antioxidants in Human Health: Current Status and Future Prospects', *Journal of Association of Physicians of India (JAPI)*, 52, pp. 796.

Dexter, D. T., Carter, C. J., Wells, F. R., Javoy-Agid, F., Agid, Y., Lees, A., Jenner, P. and Marsden, C. D. (1989) 'Basal lipid peroxidation in substantia nigra is increased in Parkinson's disease', *JNeurochem*, 52, pp. 381-389.

Di Mitri, D., Azevedo, R., Henson, S., Libri, V., Riddell, N., Macaulay, R., Kipling, D., Soares, M., Battistini, L. and Akbar, A. (2011) 'Reversible senescence in human CD4+CD45RA+CD27- memory T cells', *J Immunol.*, 187(5), pp. 2093-2100.

Dimmick, I. (2009) 'Flow Cytometry', in Maxwell, M. H.-F. a. P. (ed.) *Advanced Techniques in Diagnostic Cellular Pathology*. Chichester, UK: John Wiley & Sons Ltd.

Dobaczewski, M., Xia, Y., Bujak, M., Gonzalez-Quesada, C. and Frangogiannis, N. G. (2010) 'CCR5 signaling suppresses inflammation and reduces adverse remodeling of the infarcted heart, mediating recruitment of regulatory T cells', *Am J Pathol*, 176, pp. 2177-87.

Doran, A. C., Lipinski, M. J., Oldham, S. N. Garmey, J. C., Campbell, K. A., Skaflen, M. D., Cutchins, A., Lee, D. J., Glover, D. K., Kelly, K. A., Galkina, E. V., Ley, K., Witztum, J. L., Tsimikas, S., Bender, T. P. and McNamara, C. A. (2012) 'B-cell aortic homing and atheroprotection depend on Id3', *Circ Res*, 110, pp. e1-12.

Dragu, R., Khoury, S., Zuckerman, R., Suleiman, M., Mutlak, D., Agmon, Y., Kapeliovich, M., Beyar, R., Markiewicz, W., Hammerman, H. and Aronson, D. (2008) 'Predictive value of white blood cell subtypes for long-term outcome following myocardial infarction', *Atherosclerosis*, 196, pp. 405-12.

Dröge, W. (2002) 'Free radicals in the physiological control of cell function', *Physiol Rev*, 82, pp. 47-95.

Ducloux, D., Challier, B., Saas, P., Tiberghien, P. and Chalopin, J. M. (2003) 'CD4 cell lymphopenia and atherosclerosis in renal transplant recipients', *J Am Soc Nephrol*, 14, pp. 767-72.

Duffy, D., Holmes, D. N., Roe, M. T. and Peterson, E. D. (2012) 'The impact of high density lipoprotein cholesterol levels on long-term outcomes after non-ST-elevation myocardial infarction', *Am Heart J*, 163, pp. 705-713.

Dumitriu, I. E., Araguas, E. T., Baboonian, C. and Kaski, J. C. (2009) 'CD4+ CD28 null T cells in coronary artery disease: when helpers become killers', *Cardiovasc Res.*, 81, pp. 11-9.

Dunne, P. J., Belaramani, L. Fletcher, J. M. de Mattos, S. F. Lawrenz, M. Soares, M. V. Rustin, M. H. Lam, E. W. Salmon, M. and Akbar, A. N. (2005) 'Quiescence and functional reprogramming of Epstein-Barr virus (EBV)-specific CD8 T cells during persistent infection', *Blood*, 106, pp. 558 -565.

Duracková, Z. (2008) 'Oxidants, antioxidants and oxidative stress', In: Gvozdjáková, A., Ed., Mitochondrial Medicine, Springer Science Business Media, New York, pp. 19-54.

Dyson, N., Howley, P. M., Munger, K. and Harlow, E. (1989) 'The human papilloma virus-16 E7 oncoprotein is able to bind to the retinoblastoma gene product', *Science* 243, pp. 934-937.

Effros, R. B., Dagarag, M. and Valenzuela, H. F. (2003) 'In vitro senescence of immune cells', *Exp Gerontol*, 38, pp. 1243-9.

Egan, E. D. and Collins, K. (2012) 'Biogenesis of telomerase ribonucleoproteins', *RNA*, 18(10), pp. 1747-59.

Emili, A., Greenblatt, J. and Ingles, C. J. (1994) 'Species-specific interaction of the glutamine-rich activation domains of Sp1 with the TATA box-binding protein', *Mol. Cell. Biol.*, 14, pp. 1582-1593.

Engelbertsen, D., Andersson, L., Ljungrantz, I., Wigren, M., Hedblad, B., Nilsson, J. and Björkbacka, H. (2013) 'T-helper 2 immunity is associated with reduced risk of myocardial infarction and stroke', *Arterioscler Thromb Vasc Biol*, 33, pp. 637-44.

Englert, C. (1998) 'WT1-more than a transcription factor? ', *Trends Biochem. Sci.*, 23, pp. 389-393.

Epel, E. S., Blackburn, E. H., Lin, J., Dhabhar, F. S., Adler, N. E., Morrow, J. D. and Cawthon, R. M. (2004) 'Accelerated telomere shortening in response to life stress', *Proceedings of the National Academy of Sciences of the United States of America*, 101, pp. 17312-5.

Epel, E. S., Lin, J., Wilhelm, F. H., Wolkowitz, O. M., Cawthon, R., Adler, N. E. and Blackburn, E. H. (2006) 'Cell aging in relation to stress arousal and cardiovascular disease risk factors', *Psychoneuroendocrinology*, 31, pp. 277-87.

Evans, S. K., and Lundblad, V. (2000) 'Positive and negative regulation of telomerase access to the telomere', *J Cell Sci.*, 113, pp. 3357-3364.

Fairey, A. S., Courneya, K. S., Field, C. J., Bell, G. J., Jones, L. W. and Mackey, J. R. (2005) 'Randomized controlled trial of exercise and blood immune function in postmenopausal breast cancer survivors', *J Appl Physiol*, 98, pp. 1534-40.

Fehervari, Z. (2013) 'Thymic B cells', *Natural Immunology*, 14(12), p. 1211.

Feng, J., Funk, W. D., Wang, S. -S., Weinrich, S. L., Avilion, A. A., Chiu, C. -P., Adams, R. R., Chang, E., Allsopp, R. C., Yu, J., Le, S., West, M. D., Harley, C. B., Andrews, W. H., Greider, C. W. and Villeponteau, B. (1995) 'The RNA component of human telomerase', *Science*, 269, pp. 1236-1241.

Finkelman, F. D., Katona, I. M., Mosmann, T. R. and Coffman, R. L. (1988) 'IFN-gamma regulates the isotypes of Ig secreted during in vivo humoral immune responses', *Journal of Immunology*, 140, pp. 1022-7.

Fitzpatrick, A. L., Kronmal, R. A., Gardner, J. P., Psaty, B. M., Jenny, N. S., Tracy, R. P., Walston, J., Kimura, M. and Aviv, A. (2007) 'Leukocyte telomere length and cardiovascular disease in the cardiovascular health study', *Am J Epidemiol*, 165, pp. 14-21.

Fletcher, J. M., Vukmanovic-Stejic, M., Dunne, P. J., Birch, K. E., Cook, J. E., Jackson, S. E., Salmon, M., Rustin, M. H. and Akbar, A. N. (2005) 'Cytomegalovirus-specific CD4 T cells in healthy carriers are continuously driven to replicative exhaustion', *J. Immunol*, 175, pp. 8218 - 8225.

Foks, A. C., Frodermann, V., ter Borg, M., Habets, K. L., Bot, I., Zhao, Y., van Eck, M., van Berkel, T. J., Kuiper, J. and van Puijvelde, G. H. (2011) 'Differential effects of regulatory T cells on the initiation and regression of atherosclerosis', *Atherosclerosis*, 218, pp. 53-60.

Fontenot, J. D., Gavin M. A. and Rudensky A. Y. (2003) 'Foxp3 programs the development and function of CD4+CD25+ regulatory T cells', *Nat Immunol*, 4, pp. 330-6.

Foote, C. S., Valentine, J. S., Greenberg, A. and Liebman, J. F. (1985) 'Active Oxygen in Chemistry', Chapman and Hall, New York.

Fraga, C. G., Shigenaga, M. K., Park, J. W., Degan, P. and Ames, B. N. (1990) 'Oxidative damage to DNA during aging: 8-hydroxy-2'-deoxyguanosine in rat organ DNA and urine', *Proc Natl Acad Sci U S A*, 87, pp. 4533-7.

Fransen, M., Nordgren, M., Wang, B. and Apanases, O. (2012) 'Role of peroxisomes in ROS/RNS-metabolism: implications for human disease', *Biochim. Biophys. Acta* 1822, pp. 1363-1373.

Freund, A., Patil, CK. and Campisi, J. (2011) 'p38MAPK is a novel DNA damage response-independent regulator of the senescence-associated secretory phenotype', *EMBO J.*, 30(8), pp. 1536-1548.

Fridovich, I. (1995) 'Superoxide radical and superoxide dismutases', *Annu Rev Biochem.*, 64, pp. 97-112.

Froelicher, V. F. (1972) 'Animal studies of effect of chronic exercise of the heart and atherosclerosis: A review', *Am. Heart J.*, 84, pp. 496-506.

Frostegård, J., Ulfgren, A. K., Nyberg, P., Hedin, U., Swedenborg, J., Andersson, U. and Hansson, G. K. (1999) 'Cytokine expression in advanced human atherosclerotic plaques: dominance of pro-inflammatory (Th1) and macrophage-stimulating cytokines', *Atherosclerosis*, 145, pp. 33-43.

Fukao, K., Shimada, K., Naito, H., Sumiyoshi, K., Inoue, N., Iesaki, T., Kume, A., Kiyanagi, T., Hiki, M., Hirose, K., Matsumori, R., Ohsaka, H., Takahashi, Y., Toyoda, S., Itoh, S., Miyazaki, T., Tada, N. and Daida, H. (2010) 'Voluntary exercise ameliorates the progression of atherosclerotic lesion formation via anti-inflammatory effects in apolipoprotein E-deficient mice', *J Atheroscler Thromb*, 17, pp. 1226-36.

Fukao, T., Matsuda, S. and Koyasu, S. (2000) 'Synergistic effects of IL-4 and IL-18 on IL-12-dependent IFN-gamma production by dendritic cells', *Journal of Immunology*, 164, pp. 64-71.

Gaffen, S. L. and Liu, K. D. (2004) 'Overview of interleukin-2 function, production and clinical applications', *Cytokine*, 28, pp. 109–23.

Gaffen, S. L., Wang, S. and Koshland, M. E. (1996) 'Expression of the immunoglobulin J chain in a murine B lymphoma is driven by autocrine production of interleukin 2', *Cytokine*, 8, pp. 513–24.

Galkina, E. and Ley, K. (2009) 'Immune and inflammatory mechanisms of atherosclerosis', *Annual Review of Immunology*, 27, pp. 165–197.

Garrity, P. A., Chen, D., Rothenberg, E. V. and Wold, B. J. (1994) 'Interleukin-2 transcription is regulated in vivo at the level of coordinated binding of both constitutive and regulated factors', *Molecular & Cellular Biology*, 14, pp. 2159–69.

Gershon, R. K., Cohen, P., Hencin, R. and Liebhaber, S. A. (1972) 'Suppressor T cells', *J Immunol*, 108, pp. 586–90.

Gewin, L. and Galloway, D. A. (2001) 'E box-dependent activation of telomerase by human papillomavirus type 16 E6 does not require induction of c-myc', *J. Virol.*, 75, pp. 7198–7201.

Gibson, W. J. and Gibson, C. M. (2006) 'The association of impaired myocardial perfusion and monocytosis with late recovery of left ventricular function following primary percutaneous coronary intervention', *Eur Heart J*, 27, pp. 2487–8.

Gille, H., Kortenjann, M., Thomae, O., Moomaw, C., Slaughter, C., Cobb, M. H. and Shaw P. E. (1995) 'ERK phosphorylation potentiates Elk-1-mediated ternary complex formation and transactivation', *EMBO J.*, 14, pp. 951–962.

Gille, J. J. and Joenje, H. (1992) 'Cell Culture Models for Oxidative Stress: Superoxide and Hydrogen Peroxide vs. Normobaric Hyperoxia', *Mutat. Res.*, 275, pp. 405–414.

Givan, A. L. (2001) 'Principles of flow cytometry: an overview', *Methods Cell Biol*, 63, pp. 19–50.

Gizard, F., Heywood, E. B., Findeisen, H. M., Zhao, Y., Jones, K. L., Cudejko, C., Post, G. R., Staels, B. and Bruemmer, D. (2011) 'Telomerase activation in atherosclerosis and induction of telomerase reverse transcriptase expression by inflammatory stimuli in macrophages', *Arterioscler. Thromb. Vasc. Biol.*, 31, pp. 245–252.

Godfrey, P., Rahal, J. O., Beamer, W. G., Copeland, N. G., Jenkins, N. A. and Mayo, K. E. (1993) 'GHRH receptor of little mice contains a missense mutation in the extracellular domain that disrupts receptor function', *Nat Genet.*, 4(3), pp. 227–32.

Gol-Ara, M., Jadidi-Niaragh, F., Sadria, R., Azizi, G. and Mirshafiey, A. (2012) 'The role of different subsets of regulatory T cells in immunopathogenesis of rheumatoid arthritis', *Arthritis*, 2012, p. 805875.

Goldstrohm, A. C., Greenleaf, A. L. and Garcia-Blanco, M. A. (2001) 'Co-transcriptional splicing of pre-messenger RNAs: considerations for the mechanism of alternative splicing', *Gene*, 277, pp. 31–47.

González-Muniesa, P., Garcia-Gerique, L., Quintero, P., Arriaza, S., Lopez-Pascual, A. and Martinez, J. A. (2015) 'Effects of Hyperoxia on Oxygen-Related Inflammation with a Focus on Obesity', *Oxid Med Cell Longev.*, pp. 8957827.

Goronzy, J. J. and Weyand, C. M. (2006) 'Immunosoppression in atherosclerosis. Mobilizing the opposition within', *Circulation*, 114, pp. 1901–4.

Gotsman, I., Grabie, N., Dacosta, R., Sukhova, G., Sharpe, A. and Lichtman, A. H. (2007) 'Proatherogenic immune responses are regulated by the PD-1/ PD-L pathway in mice', *J Clin Invest*, 117, pp. 2974–2982.

Gotsman, I., Grabie, N., Gupta, R., Dacosta, R., MacConmara, M., Lederer, J., Sukhova, G., Witztum, J. L., Sharpe, A. H. and Lichtman, A. H. (2006) 'Impaired regulatory T-cell response and enhanced atherosclerosis in the absence of inducible costimulatory molecule', *Circulation*, 114, pp. 2047–55.

Grandori, C., Cowley, S.M., James, L.P. and Eisenman, R.N. (2000) 'The Myc/Max/Mad network and the transcriptional control of cell behavior', *Annu. Rev. Cell. Dev. Biol.*, 16, pp. 653–699.

Granucci, F., Vizzaderelli, C., Pavelka, N., Feau, S., Persico, M., Virzi, E., Rescigno, M., Moro, G. and Riccardi-Castagnoli, P. (2001) 'Inducible IL-2 production by dendritic cells revealed by global gene expression analysis', *Nature Immunology*, 2(9), pp. 882–8.

Gray, A. B., Telford, R. D. and Weidemann, M. J. (1993) 'Endocrine response to intense interval exercise', *Eur J Appl Physiol*, 66(4), pp. 366–71.

Greenberg, R. A., Allsopp, R. C., Chin, L., Morin, G. B. and DePinho, R. A. (1998) 'Expression of mouse telomerase reverse transcriptase during development, differentiation and proliferation', *Oncogene*, 16, pp. 1723–1730.

Greenberg, R. A., O'Hagan, R. C., Deng, H., Xiao, Q., Hann, S. R., Adams, R. R., Lichtsteiner, S., Chin, L., Morin, G. B. and De, R. A. (1999) 'Telomerase reverse transcriptase gene is a direct target of c-Myc but is not functionally equivalent in cellular transformation', *Oncogene*, 18, pp. 1219–1226.

Greider, C. W. (1999) 'Telomeres do D-loop-T-loop', *Cell*, 97(4), pp. 419–422.

Greider, C. W. and Blackburn, E. H. (1989) 'A telomeric sequence in the RNA of Tetrahymena telomerase required for telomere repeat synthesis', *Nature*, 337, pp. 331–337.

Griffith, J. D., Comeau, L., Rosenfield, S., Stansel, R. M., Bianchi, A., Moss, H. and de Lange, T. (1999) 'Mammalian telomeres end in a large duplex loop', *cell*, 95, pp. 503–514.

Griffith, J., Bianchi, A. and de Lange, T. (1998) 'TRF1. promotes parallel pairing of telomeric tracts in vitro', *J. Mol. Biol.*, 278, pp. 79–88.

Griffiths, H. R. (2005) 'ROS as signalling molecules in T cells – evidence for abnormal redox signalling in the autoimmune disease, rheumatoid arthritis', *Redox Rep*, 10, pp. 273–80.

Groyer, E., Nicoletti, A., Ait-Oufella, H., Khallou-Laschet, J., Varthaman, A., Gaston, A. T., Thaunat, O., Kaveri, S. V., Blatny, R., Stockinger, H., Mallat, Z. and Caligiuri, G. (2007) 'Atheroprotective effect of CD31 receptor globulin through enrichment of circulating regulatory T-cells', *J Am Coll Cardiol*, 50, pp. 344–50.

Gu, L., Okada, Y., Clinton, S. K., Gerard, C., Sukhova, G. K., Libby, P. and Rollins, B. J. (1998) 'Absence of monocyte chemoattractant protein-1 reduces atherosclerosis in low-density lipoprotein-deficient mice', *Mol Cell*, 2, pp. 275–81.

Guzik, T. J., Sadowski, J., Guzik, B., Jopek, A., Kapelak, B., Przybylowski, P., Wierzbicki, K., Korbut, R., Harrison, D. G. and Channon, K. M. (2006) 'Coronary artery superoxide production and nox isoform expression in human coronary artery disease', *Arterioscler Thromb Vasc Biol*, 26, pp. 333–9.

Haendeler, J., Dröse, S., Büchner, N., Jakob, S., Altschmied, J., Goy, C., Spyridopoulos, I., Zeiher, A. M., Brandt, U. and Dimmeler, S. (2009) 'Mitochondrial telomerase reverse transcriptase binds to and protects mitochondrial DNA and function from damage' *Arterioscler Thromb Vasc Biol*, 29, pp. 929–35.

Haendeler, J., Hoffmann, J., Brandes, R., Zeiher, A. and Dimmeler, S. (2003b) 'Hydrogen peroxide triggers nuclear export of telomerase reverse transcriptase via Src kinase family dependent phosphorylation of tyrosine 707', *Mol Cell Biol*, 23, pp. 4598 – 4610.

Haendeler, J., Hoffmann, J., Diehl, J. F., Vasa, M., Spyridopoulos, I., Zeiher, A. M. and Dimmeler, S. (2004) 'Antioxidants inhibit nuclear export of telomerase reverse transcriptase and delay replicative senescence of endothelial cells', *Circ Res*, 94, pp. 768–75.

Haendeler, J., Hoffmann, J., Rahman, S., Zeiher, A. M. and Dimmeler, S. (2003a) 'Regulation of telomerase activity and anti-apoptotic function by protein-protein interaction and phosphorylation', *FEBS Lett*, 536, pp. 180–6.

Hahn, W. C., Counter, C. M., Lundberg, A. S., Beijersbergen, R. L., Brooks, M. W. and Weinberg, R. A. (1999) 'Inhibition of telomerase limits the growth of human cancer cells', *Nature*, 400, pp. 464–468.

Halliwell, B. and Gutteridge, J. M. C. (1990) 'The antioxidants of human extracellular fluids', *Arch Biochem Biophys*, 280, pp. 1–8.

Halliwell, B. and Gutteridge, J. M. C. (2006) 'Free Radicals in Biology and Medicine', Ed 4, Clarendon Press, Oxford.

Han, D., Williams, E. and Cadenas, E. (2001) 'Mitochondrial respiratory chain-dependent generation of superoxide anion and its release into the intermembrane space', *The Biochemical Journal*, 353(Pt 2), pp. 411–6.

Hansson, G. K. (2005) 'Inflammation, atherosclerosis, and coronary artery disease', *N Engl J Med*, 352, pp. 1685–95.

Hansson, G. K. and Libby, P. (2006) 'The immune response in atherosclerosis: a double-edged sword', *Nature Review Immunology*, 6, pp. 508–19.

Hara, E., Smith, R., Parry, D., Tahara, H., Stone, S. and Peters, G. (1996) 'Regulation of p16CDKN2 expression and its implications for cell immortalization and senescence', *Mol. Cell. Biol.*, 16, pp. 859–867.

Harley, C. B., Futcher, A. B. and Greider, C. W. (1990) 'Telomeres shorten during ageing of human fibroblasts', *Nature*, 345, pp. 458–460.

Harley, C. B., Liu, W., Blasco, M., Vera, E., Andrews, W. H., Briggs, L.A. and Raffaele, J. M. (2011) 'A natural product telomerase activator as part of a health maintenance program', *Rejuvenation Res.*, 14(1), pp. 45–56.

Hartley, C. J., Reddy, A. K., Madala, S., Martin-McNulty, B., Vergona, R., Sullivan, M. E., Halks-Miller, M., Taffet, G. E., Michael, L. H., Entman, M. L. and Wang, Y. X. (2000) 'Hemodynamic changes in apolipoprotein E-knockout mice', *Am J Physiol Heart Circ Physiol.*, 279(5), pp. H2326–34.

Hathcock, K. S., Weng, N. P., Merica, R., Jenkins, M. K. and Hodes, R. J. (1998) 'Antigen-dependent regulation of telomerase activity in murine T cells', *J Immunol*, 160, pp. 5702–6.

Hathcock, K.S., Chiang, Y. and Hodes, R.J. (2005) 'In vivo regulation of telomerase activity and telomere length', *Immunol. Rev.*, 205, pp. 104–113.

Hayes, A., Williams, D. A. (1998) 'Contractile function and low-intensity exercise effects of old dystrophic (mdx) mice', *Am J Physiol*, 274, pp. C1138–C1144.

Hayflick, L. (1965) 'The limited in vitro lifetime of human diploid cell strains', *Exp Cell Res.*, 37, pp. 614–636.

Hayflick, L., (2000) 'The illusion of cell immortality', *Br. J. Cancer*, 83, pp. 841– 846.

Hayflick, L., Moorhead, P. S., (1961) 'The serial cultivation of human diploid cell strains', *Exp. Cell Res.*, 25, pp. 585–621.

Haynes, L., Eaton, S. M. and Swain, S. L. (2000) 'The defects in effector generation associated with aging can be reversed by addition of IL-2 but not other related gamma(c)-receptor binding cytokines', *Vaccine*, 18(16), pp. 1649-53.

Heitzer, T., Schlinzig, T., Krohn, K., Meinertz, T. and Munzel, T. (2001) 'Endothelial dysfunction, oxidative stress, and risk of cardiovascular events in patients with coronary artery disease', *Circulation*, 104, pp. 2673–78.

Henle, E. S., Han, Z., Tang, N., Rai, P., Luo, Y. and Linn, S. (1999) 'Sequence-specific DNA cleavage by Fe2+-mediated fenton reactions has possible biological implications', *J Biol Chem.*, 274(2), pp. 962-71.

Henson, S. M., Lanna, A., Riddell, N. E., Franzese, O., Macaulay, R., Griffiths, S. J., Puleston, D. J., Watson, A. S., Simon, A. K., Tooze, S. A. and Akbar, A. N. (2014) 'p38 signaling inhibits mTORC1- independent autophagy in senescent human CD8⁺ T cells', *J Clin Invest*, 124, pp. 4004–16.

Henson, S. M., Macaulay, R., Riddell, N. E., Nunn, C. J. and Akbar, A. N. (2015) 'Blockade of PD-1 or p38 MAP kinase signaling enhances senescent human CD8(+) T-cell proliferation by distinct pathways', *Eur J Immunol.*, 45(5), pp. 1441-51.

Heran, B. S., Chen, J. M., Ebrahim, S., Moxham, T., Oldridge, N., Rees, K. Thompson, D. R. and Taylor, R. S. (2011) 'Exercise-based cardiac rehabilitation for coronary heart disease', *Cochrane Database Syst Rev*, 7, article ID. CD001800.

Herbig, U. and Sedivy, J. M. (2006) 'Regulation of growth arrest in senescence: telomere damage is not the end of the story', *Mech. Ageing Dev.*, 127, pp. 16-24.

Herbig, U., Jobling, W. A., Chen, B. P., Chen, D. J. and Sedivy, J. M. (2004) 'Telomere shortening triggers senescence of human cells through a pathway involving ATM, p53, and p21(CIP1), but not p16(INK4a)', *Mol. Cell*, 14, pp. 501-513.

Hewitt, G., Jurk, D., Marques, F. D., Correia-Melo, C., Hardy, T., Gackowska, A., Anderson, R., Taschuk, M., Mann, J. and Passos, J. F. (2012) 'Telomeres are favoured targets of a persistent DNA damage response in ageing and stress-induced senescence', *Nat. Commun.*, 3, p. 708.

Hidalgo, L. G., Urmson, J. and Halloran, P. F. (2005) 'IFN-gamma decreases CTL generation by limiting IL-2 production: A feedback loop controlling effector cell production', *American Journal of Transplantation*, 5, pp. 651-661.

Hildebrand, M., VAN Hees, V. T., Hansen, B. H. and Ekelund, U. (2014) 'Age group comparability of raw accelerometer output from wrist- and hip-worn monitors', *Med Sci Sports Exerc.*, 46, pp. 1816-1824.

Ho, I. C., Kim, J. I., Szabo, S. J. and Glimcher, L. H. (1999) 'Tissue-specific regulation of cytokine gene expression', *Cold Spring Harbour Perspectives in Biology*, 64, pp. 573-84.

Hoey, T., Weinzierl, R. O., Gill, G., Chen, J. L., Dynlacht, B. D. and Tjian, R. (1993) 'Molecular cloning and functional analysis of Drosophila TAF110 reveal properties expected of coactivators', *Cell*, 72, pp. 247-260.

Hoffman-Goetz, L., Macneil, B., Arumugam, Y. and Randallsimpson, J. (1992) 'Differential effects of exercise and housing condition on murine natural killer cell activity and tumor growth', *Int J Sports Med*, 13, pp. 167-171.

Hoffmann, J. and Spyridopoulos, I. (2011) 'Telomere length in cardiovascular disease: new challenges in measuring this marker of cardiovascular aging', *Future Cardiol*, 7(6), pp. 789-803.

Hoffmann, J. and Spyridopoulos, I. (2015) 'Senescent cytotoxic T cells in acute myocardial infarction: innocent bystanders or the horsemen of apocalypse?', *Cellular & Molecular Immunology*, 12(4), pp. 510-512.

Hoffmann, J., Shmeleva, E. V., Boag, S. E., Fiser, K., Bagnall, A., Murali, S., Dimmick, I., Pircher, H., Martin-Ruiz, C., Egred, M., Keavney, B., von Zglinicki, T., Das, R., Todryk, S. and Spyridopoulos, I. (2015) 'Myocardial Ischemia and Reperfusion Leads to Transient CD8 Immune Deficiency and Accelerated Immunosenescence in CMV-Seropositive Patients', *Circulation Research*, 116(1), pp. 87-98.

Hofmann, U. and Frantz, S. (2015) 'Role of lymphocytes in myocardial injury, healing, and remodeling after myocardial infarction', *Circ Res*, 116, pp. 354–67.

Holt, N. E., Zigmantas, D., Valkunas, L., Li, X. P., Niyogi, K. K. and Fleming, G. R. (2005) 'Carotenoid cation formation and the regulation of photosynthetic light harvesting', *Science*, 307, pp. 433–436.

Hooijberg, E., Ruizendaal, J. J., Snijders, P. J., Kueter, E. W., Walboomers, J. M. and Spits, H. (2000) 'Immortalization of human CD8+ T-cell clones by ectopic expression of telomerase reverse transcriptase', *J Immunol*, 165, pp. 4239–45.

Horne, B. D., Anderson, J. L., John, J. M. Weaver, A., Bair, T. L., Jensen, K. R., Renlund, D. G., Muhlestein, J. B; Intermountain Heart Collaborative Study Group (2005) 'Which white blood cell subtypes predict increased cardiovascular risk?', *J Am Coll Cardiol*, 45, pp. 1638–43.

Hotchkiss, R. S. and Karl, I. E. (2003) 'The pathophysiology and treatment of sepsis', *N Engl J Med*, 348, pp. 138–50.

Howard, M. T., Lee, M. P., Hsieh, T. -S. and Griffith, J. D. (1991) 'Drosophila topoisomerase II-DNA interactions are affected by DNA structure', *J. Mol. Biol.*, 217, pp. 53-62.

Hrdlicková, R., Nehyba, J. and Bose H. R. Jr. (2012) 'Alternatively spliced telomerase reverse transcriptase variants lacking telomerase activity stimulate cell proliferation', *Molecular and cellular biology*, 32, pp. 4283– 4296.

Humar, R., Kiefer, F. N., Berns, H., Resink, T. J. and Battegay, E. J. (2002) 'Hypoxia enhances vascular cell proliferation and angiogenesis in vitro via rapamycin (mTOR)-dependent signaling', *FASEB J*, 16, pp. 771–80.

Huzen, J., Wong, L. S., van Veldhuisen, D. J., Samani, N. J., Zwinderman, A. H., Codd, V., Cawthon, R. M., Benus, G. F., van der Horst, I. C., Navis, G., Bakker, S. J., Gansevoort, R. T., de Jong, P. E., Hillege, H. L., van Gilst, W. H., de Boer, R. A. and van der Harst, P. (2014) 'Telomere length loss due to smoking and metabolic traits', *J Intern Med*, 275, pp. 155–163.

Ide, T., Tsuji, Y., Ishibashi, S. and Mitsui, Y. (1983) 'Reinitiation of host DNA synthesis in senescent human diploid cells by infection with Simian virus 40', *Exp. Cell Res.*, 143, pp. 343–349.

Iwasa, H., Han, J., Ishikawa, F. (2003) 'Mitogen-activated protein kinase p38 defines the common senescence-signalling pathway', *Genes Cells*, 8(2), pp. 131–144.

Jakovljevic, D. G., McDiarmid, A., Hallsworth, K., Seferovic, P. M., Ninkovic, V. M., Parry, G., Schueler, S., Trenell, M. I. and MacGowan, G. A. (2014) 'Effect of Left Ventricular Assist Device Implantation and Heart Transplantation on Habitual Physical Activity and Quality of Life', *The American Journal of Cardiology*, 114(1), pp. 88–93.

Janeway, C. A. and Medzhitov, R. (2002) 'Innate immune recognition', *Annu Rev Immunol*, 20, pp. 197–216.

Janeway, C. A. J. (1992) 'The T cell receptor as a multicomponent signalling machine: CD4/CD8 coreceptors and CD45 in T cell activation', *Annual Review of Immunology*, 10, pp. 645–74.

Janknecht, R., (2004) 'On the road to immortality: hTERT upregulation in cancer cells', *FEBS Lett.*, 564, pp. 9–13.

Jolliffe, J. A., Rees, K., Taylor, R. S., Thompson, D., Oldridge, N. and Ebrahim, S. (2001) 'Exercise-based rehabilitation for coronary heart disease', *Cochrane Database Syst Rev.*, (1), article ID. CD001800.

Jonsdottir, I. H., Hoffman, P. and Thoren, P. (1997) 'Physical exercise, endogenous opioids and immune function', *Acta Physiol Scand*, 640, pp. 47–50.

Joshi, D. C. and Bakowska, J. C. (2011) 'Determination of mitochondrial membrane potential and reactive oxygen species in live rat cortical neurons', *J. Vis. Exp.*, pp. 1-4.

Juarranz, M., Calle-Puron, M. E., Gonzalez-Navarro, A., Regidor-Poyatos, E., Soriano, T., Martinez-Hernandez, D., Rojas, V. D. and Guinee, V. F. (2002) 'Physical exercise, use of Plantago ovata and aspirin, and reduced risk of colon cancer', *Eur J Cancer Prev.*, 11, pp. 465–472.

Jurica, M. S. and Moore, M. J. (2003) 'Pre-mRNA splicing: awash in a sea of proteins' *Molecular cell*, 12, pp. 5– 14.

Kadi, F. and Ponsot, E. (2010) 'The biology of satellite cells and telomeres in human skeletal muscle: effects of aging and physical activity', *Scand J Med Sci Sports*, 20, pp. 39-48.

Kaiser, R. A., Bueno, O. F., Lips, D. J., Doevedans, P. A., Jones, F., Kimball, T. F. and Molkentin, J. D. (2004) 'Targeted inhibition of p38 mitogen-activated protein kinase antagonizes cardiac injury and cell death following ischemia reperfusion in vivo', *J Biol Chem.*, 279(15), pp. 15524–15530.

Kane, L. P., Andres, P. G., Howland, K. C., Abbas, A. K. and Weiss, A. (2001) 'Akt provides CD28 costimulatory signal for up-regulation of IL-2 and IFN γ but not TH2 cytokines', *Nat. Immunol.*, 2, pp. 37–44.

Kang, S. S., Kwon, T., Kwon, D. Y. and Do, S. I. (1999) 'Akt protein kinase enhances human telomerase activity through phosphorylation of telomerase reverse transcriptase subunit', *J. Biol. Chem.*, 274, pp. 13085–13090.

Kaptoge, S., Di Angelantonio, E., Lowe, G., Pepys, M. B., Thompson, S. G., Collins, R. and Danesh, J. (2010) 'C-reactive protein concentration and risk of coronary heart disease, stroke, and mortality: an individual participant meta-analysis', *Lancet*, 375, pp. 132–140.

Karlseder, J., Broccoli, D., Dai, Y., Hardy, S. and de Lange, T. (1999) 'p53- and ATM-dependent apoptosis induced by telomeres lacking TRF2', *Science*, 283, pp. 1321–1325.

Karlseder, J., Smogorzewska, A. and de Lange, T. (2002) 'Senescence induced by altered telomere state, not telomere loss', *Science*, 295, pp. 2446–2449.

Karnoub, A. E. and Weinberg, R. A. (2008) 'Ras oncogenes: split personalities', *Nat. Rev. Mol. Cell. Biol.*, 9, pp. 517–531.

Kasic, T., Colombo, P., Soldani, C. Kasic, T., Colombo, P., Soldani, C., Wang, C. M., Miranda, E., Roncalli, M., Bronte, V. and Viola, A. (2011) 'Modulation of human T-cell functions by reactive nitrogen species', *Eur J Immunol*, 41, pp. 1843–49.

Kastan, M. B. and Bartek, J. (2004) 'Cell-cycle checkpoints and cancer', *Nature*, 432, pp. 316–323.

Katayama, Y., Battista, M., Kao, W. M., Hidalgo, A., Peired, A. J., Thomas, S. A., Frenette, P. S. (2006) 'Signals from the sympathetic nervous system regulate hematopoietic stem cell egress from bone marrow', *Cell*, 124, pp. 407–21.

Kawagoe, J., Ohmichi, M., Takahashi, T., Ohshima, C., Mabuchi, S., Takahashi, K., Igarashi, H., Mori-Abe, A., Saitoh, M., Du, B., Ohta, T., Kimura, A., Kyo, S., Inoue, M. and Kurachi, H. (2003) 'Raloxifene inhibits estrogen-induced up-regulation of telomerase activity in a human breast cancer cell line', *J. Biol. Chem.*, 278, pp. 43363–43372.

Kawauchi, K., Ihjima, K. and Yamada, O. (2005) 'IL-2 Increases human telomerase reverse transcriptase activity transcriptionally and posttranslationally through phosphatidylinositol 3'-kinase/Akt, heat shock protein 90, and mammalian target of rapamycin in transformed NK cells', *J Immunol*, 174, pp. 5261–5269.

Kelley, G. A. and Kelley, K. S. (2006) 'Effects of aerobic exercise on C-reactive protein, body composition, and maximum oxygen consumption in adults: a meta-analysis of randomized controlled trials', *Metabolism*, 55, pp. 1500–7.

Kemmler, W., Lauber, D., Weineck, J., Hensen, J., Kalender, W. and Engelke, K. (2004) 'Benefits of 2 years of intense exercise on bone density, physical fitness, and blood lipids in early postmenopausal osteopenic women: results of the Erlangen Fitness Osteoporosis Prevention Study (EFOPS)', *Arch Intern Med.*, 164, pp. 1084–1091.

Keul, P., Tolle, M., Lucke, S., von Wnuck, L. K., Heusch, G., Schuchardt, M., van der Giet, M. and Levkau, B. (2007) 'The sphingosine-1-phosphate analogue FTY720 reduces atherosclerosis in apolipoprotein E-deficient mice', *Arterioscler Thromb Vasc Biol*, 27, pp. 607–13.

Kharbanda, S., Kumar, V., Dhar, S., Pandey, P., Chen, C., Majumder, P., Yuan, Z.M., Whang, Y., Strauss, W., Pandita, T.K., Weaver, D. and Kufe, D. (2000) 'Regulation of the hTERT telomerase catalytic subunit by the c-Abl tyrosine kinase', *Curr. Biol. : CB.*, 10, pp. 568–575.

Khattri, R., Cox, T., Yasayko, S. A. and Ramsdell, F. (2003) 'An essential role for Scurfin in CD4+CD25+ T regulatory cells', *Nat Immunol*, 4, pp. 337–42.

Kilian, A., Bowtell, D. D., Abud, H. E., Hime, G. R., Venter, D. J., Keese, P. K., Duncan, E. L., Reddel, R. R. and Jefferson, R. A. (1997) 'Isolation of a candidate human telomerase catalytic subunit gene, which reveals complex splicing patterns in different cell types', *Human molecular genetics*, 6, pp. 2011–2019.

Kilic, T., Ural, D., Ural, E., Yumuk, Z., Agacdiken, A., Sahin, T., Kahraman, G., Kozdag, G., Vural, A. and Komsuoglu, B. (2006) 'Relation between proinflammatory to anti-inflammatory cytokine ratios and long-term prognosis in patients with non-ST elevation acute coronary syndrome', *Heart*, 92, pp. 1041–6.

Killar, L., MacDonald, G., West, J., Woods, A. and Bottomly, K. (1987) 'Cloned Ia restricted T cells that do not produce IL4/BSF-1 fail to help antigen specific B cells', *J. Immunol.*, 138, pp. 1674–79.

Kim, S. H., Kaminker, P. and Campisi, J. (1999) 'TIN2, a new regulator of telomere length in human cells', *Nat. Genet.*, 23, pp. 405–412.

Kimura, A., Ohmichi, M., Kawagoe, J., Kyo, S., Mabuchi, S., Takahashi, T., Ohshima, C., Arimoto-Ishida, E., Nishio, Y., Inoue, M., Kurachi, H., Tasaka, K. and Murata, Y. (2004) 'Induction of hTERT expression and phosphorylation by estrogen via Akt cascade in human ovarian cancer cell lines' *Oncogene*, 23, pp. 4505–4515.

King, M. R., Ismail, A. S., Davis, L. S. and Karp, D. R. (2006) 'Oxidative stress promotes polarization of human T cell differentiation toward a T helper 2 phenotype', *J Immunol*, 176, pp. 2765–72.

Klarlund, K., Pedersen, B. K., Theander, T. G. and Andersen, V. (1987) 'Depressed natural killer cell activity in acute myocardial infarction', *Clinical and Experimental Immunology*, 70(1), pp. 209–16.

Klingelhutz, A. J., Foster, S. A. and McDougall, J. K. (1996) 'Telomerase activation by the E6 gene product of human papillomavirus type 16', *Nature*, 380, pp. 79–82.

Knouff, C., Hinsdale, M. E., Mezdour, H., Altenburg, M. K., Watanabe, M., Quarfordt, S. H., Sullivan, P. M., and Maeda, N. (1999) 'ApoE structure determines VLDL clearance and atherosclerosis risk in mice', *J Clin Invest.*, 103, pp. 1579–1586.

Kodama, S., Saito, K., Tanaka, S., Maki, M., Yachi, Y., Asumi, M., Sugawara, A., Totsuka, K., Shimano, H., Ohashi, Y., Yamada, N. and Sone ,H. (2009) 'Cardiorespiratory fitness as a quantitative predictor of all-cause mortality and cardiovascular events in healthy men and women: a meta analysis', *JAMA*, 301(19), pp. 2024–2035.

Kotsias, F., Hoffmann, E., Amigorena, S. and Savina, A. (2013) 'Reactive oxygenspecies production in the phagosome: impact on antigen presentationin dendritic cells', *Antioxid Redox Signal.*, 18, pp. 714–729.

Kovalenko, O. A., Caron, M. J., Ulema, P., Medrano, C., Thomas, A. P., Kimura, M., Bonini, M. G., Herbig, U. and Santos, J. H. (2010) 'A mutant telomerase defective in nuclear-cytoplasmic shuttling fails to immortalize cells and is associated with mitochondrial dysfunction', *Aging Cell*, 9, pp. 203–19.

Kraemer, W. J., Volek, J. S., Clark, K. L., Gordon, S. E., Incledon, T., Puhl, S. M., Triplett-McBride, N. T., McBride, J. M., Putukian, M. and Sebastianelli, W. J. (1997) 'Physiological adaptations to a weight-loss dietary regimen and exercise programs in women', *J Appl Physiol*, 83, pp. 270–9.

Kramsch, D. M., Aspen, A. I., Abramowitz, B. M., Kreimendahl, T. and Hood, W. B. Jf. (1981) 'Reduction of coronary atherosclerosis by moderate conditioning exercise in monkeys on an atherogenic diet', *N. Engl. J. Med.*, 305(1), pp. 483-89.

Krenger, W., Falzarano, G., Delmonte, J. Jr, Snyder, K. M., Byon, J. C. and Ferrara, J. L. (1996) 'Interferon-gamma suppresses T-cell proliferation to mitogen via the nitric oxide pathway during experimental acute graft-versus-host disease', *Blood*, 88(3), pp. 1113-21.

Kudo, M., Ogawa, E., Kinose, D., Haruna, A., Takahashi, T., Tanabe, N., Marumo, S., Hoshino, Y., Hirai, T., Sakai, H., Muro, S., Date, H. and Mishima, M. (2012) 'Oxidative stress induced Interleukin-32 mRNA expression in human bronchial epithelial cells', *Respir Res.*, 13, p. 19.

Kusaba, H., P. Ghosh, R. Derin, M. Buchholz, C. Sasaki, K. Madara, and D. L. Longo. (2005) 'Interleukin-12-induced interferon- production by human peripheral blood T cells is regulated by mammalian target of rapamycin (mTOR) ', *J. Biol. Chem.*, 280, pp. 1037-1043.

Kyaw, T., Tay, C., Khan, A., Dumouchel, V., Cao, A., To, K., Kehry, M., Dunn, R., Agrotis, A., Tipping, P., Bobik, A. and Toh, B. H. (2010) 'Conventional B2 B cell depletion ameliorates whereas its adoptive transfer aggravates atherosclerosis', *J Immunol*, 185, pp. 4410-9.

Kyo, S., and Inoue, M. (2002) 'Complex regulatory mechanisms of telomerase activity in normal and cancer cells: how can we apply them for cancer therapy?', *Oncogene*, 21, pp. 688-697.

Kyo, S., Takakura, M., Kanaya, T., Zhuo, W., Fujimoto, K., Nishio, Y., Orimo, A. and Inoue, M. (1999) 'Estrogen activates telomerase', *Cancer Res.*, 59, pp. 5917-5921.

Kyo, S., Takakura, M., Kohama, T. and Inoue, M. (1997) 'Telomerase activity in human endometrium', *Cancer Res.*, 57, pp. 610-614.

Kyo, S., Takakura, M., Taira, T., Kanaya, T., Itoh, H., Yutsudo, M., Ariga, H., and Inoue, M. (2000) 'Sp1 cooperates with c-Myc to activate transcription of the human telomerase reverse transcriptase gene (hTERT) ', *Nucleic Acids Res.*, 28, pp. 669-677.

La Rocca, T. J., Seals, D. R. and Pierce, G. L. (2010) 'Leukocyte telomere length is preserved with aging in endurance exercise-trained adults and related to maximal aerobic capacity', *Mechan Ageing Develop.*, 131, pp. 165-167.

Laky, K., Fleischacker, C. and Fowlkes, B. J. (2006) 'TCR and Notch signaling in CD4 and CD8 T-cell development', *Immunological Reviews*, 209, pp. 274-83.

LaRocca, T. J. Seals, D. R. Pierce G. L. (2010) 'Leukocyte telomere length is preserved with aging in endurance exercise-trained adults and related to maximal aerobic capacity', *Mechanisms of Ageing and Development*, 131, pp. 165-167.

Laufs, U., Wassmann, S., Czech, T., Münzel, T., Eisenhauer, M., Böhm, M. and Nickenig, G. (2005) 'Physical inactivity increases oxidative stress, endothelial dysfunction, and atherosclerosis', *Arterioscler Thromb Vasc Biol.*, 25, pp. 809-14.

Lavie, C. J. and Milani, R. V. (2006) 'Adverse psychological and coronary risk profiles in young patients with coronary artery disease and benefits of formal cardiac rehabilitation', *Arch Intern Med*, 166, pp. 1878–83.

Lavie, C. J., Church, T. S., Milani, R. V. and Earnest, C. P. (2011) 'Impact of physical activity, cardiorespiratory fitness, and exercise training on markers of inflammation', *J Cardiopulm Rehabil Prev*, 31, pp. 137–145.

Lawler, P. R., Filion, K. B. and Eisenberg, M. J. (2011) 'Efficacy of exercise-based cardiac rehabilitation post-myocardial infarction: a systematic review and meta-analysis of randomized controlled trials', *Am Heart J*, 162, pp. 571–584.

Lee, R. T., Yamamoto, C., Feng, Y., Potter-Perigo, S., Briggs, W. H., Landschulz, K. T., Turi, T. G., Thompson, J. F., Libby, P. and Wight, T. N. (2001) 'Mechanical strain induces specific changes in the synthesis and organization of proteoglycans by vascular smooth muscle cells', *J Biol Chem*, 276, pp. 13847–51.

Leon, A. and Sanchez, O. (2001) 'Response of blood lipids to exercise training alone or combined with dietary intervention', *Med Sci Sports Exerc*, 33(6), pp. S502–15.

Leon, A. S., Rice T, Mandel, S., Després, J. P., Bergeron, J., Gagnon, J., Rao, D. C., Skinner, J. S., Wilmore, J. H. and Bouchard, C. (2000) 'Blood lipid response to 20 weeks of supervised exercise in a large biracial population: the HERITAGE Family Study', *Metabolism*, 49, pp. 513-520.

Leon, S., Franklin, B. A., Costa, F., Balady, G. J., Berra, K. A., Stewart, K. J., Thompson, P. D., Williams, M. A. and Lauer, M. S. (2005) 'Cardiac rehabilitation and secondary prevention of coronary heart disease: an American Heart Association scientific statement from the Council on Clinical Cardiology (Subcommittee on Exercise, Cardiac Rehabilitation, and Prevention) and the Council on Nutrition, Physical Activity, and Metabolism', *Circulation*, 111, pp. 369–76.

Lesniewski, L. A., Durrant, J. R., Connell, M. L., Henson, G. D., Black, A. D., Donato, A. J. and Seals, D. R. (2011) 'Aerobic exercise reverses arterial inflammation with ageing in mice', *Am J Physiol Heart Circ Physiol*, 301, pp. H1025–32.

Levy, M. Z., Allsopp, R. C., Futcher, A. B., Greider, C. W. and Harley, C. B. (1992) 'Telomere end-replication problem and cell aging', *J Mol Biol*, 225, pp. 951–960.

Li, H., Cybulsky, M. L., Gimbrone, M. A. Jr. and Libby, P. (1993) 'An atherogenic diet rapidly induces VCAM-1, a cytokine-regulatable mononuclear leukocyte adhesion molecule, in rabbit endothelium', *Arterioscler Thromb*, 13, pp. 197–204.

Li, M. O., Wan, Y. Y. and Flavell, R. A. (2007) 'T Cell-Produced Transforming Growth Factor- β 1 Controls T Cell Tolerance and Regulates Th1- and Th17-Cell Differentiation', *Immunity*, 26, pp. 579–591.

Li, X., Fang, P., Mai, J., Choi, E. T., Wang, H. and Yang, X. F. (2013) 'Targeting mitochondrial reactive oxygen species as novel therapy for inflammatory diseases and cancers', *Journal of Hematology & Oncology*, 6(19), p. 19.

Libby, P. (2001) 'Current concepts of the pathogenesis of the acute coronary syndromes', *Circulation*, 104, pp. 365–72.

Libby, P., Geng, Y.-J., Aikawa, M., Schoenbeck, U., Mach, F., Clinton, S. K., Sukhova, G. K. and Lee, R. T. (1996) 'Macrophages and atherosclerotic plaque stability', *Curr Opin Lipidol*, 7, pp. 330–5.

Libby, P., Ridker, P. M. and Hansson, G. K. (2009) 'Inflammation in atherosclerosis: from pathophysiology to practice', *J Am Coll Cardiol*, 54, pp. 2129–38.

Lin, J. and Blackburn, E. H. (2004) 'Nucleolar protein PinX1p regulates telomerase by sequestering its protein catalytic subunit in an inactive complex lacking telomerase RNA', *Genes Dev.*, 18, pp. 387–396.

Lin, J., Jin, R., Zhang, B., Yang, P.X., Chen, H., Bai, Y.X., Xie, Y., Huang, C. and Huang, J. (2007) 'Characterization of a novel effect of hPinX1 on hTERT nucleolar localization', *Biochem. Biophys. Res. Comm.*, 353, pp. 946–952.

Linden, W., Stossel, C. and Maurice, J. (1996) 'Psychosocial interventions for patients with coronary artery disease: a meta-analysis', *Arch Intern Med*, 156, pp. 745–52.

Lindmark, E., Diderholm, E., Wallentin, L. and Siegbahn, A. (2001) 'Relationship between interleukin 6 and mortality in patients with unstable coronary artery disease: effects of an early invasive or noninvasive strategy', *JAMA*, 286, pp. 2107–13.

Lingner, J., Hughes, T. R., Shevchenko, A., Mann, M., Lundblad, V. and Cech, T. R. (1997) 'Reverse transcriptase motifs in the catalytic subunit of telomerase', *Science*, 276, pp. 561–567.

Liu, D. and Xu, Y. (2011) 'p53, oxidative stress, and aging. Antioxid', *Redox Signal*, 15, pp. 1669–1678.

Liu, J. P. (1999) 'Studies of the molecular mechanisms in the regulation of telomerase activity', *FASEB*, 13, pp. 2091–104.

Liu, K., Hodes, R. J. and Weng, N. (2001) 'Cutting edge: telomerase activation in human T lymphocytes does not require increase in telomerase reverse transcriptase (hTERT) protein but is associated with hTERT phosphorylation and nuclear translocation', *J. Immunol.*, 166, pp. 4826 – 4830.

Liu, Y., Imanishi, T., Ikejima, H., Tsujioka, H., Ozaki, Y., Kuroi, A., Okochi, K., Ishibashi, K., Tanimoto, T., Ino, Y., Kitabata, H. and Akasaka T. (2010) 'Association between circulating monocyte subsets and in-stent restenosis after coronary stent implantation in patients with ST-elevation myocardial infarction', *Circ J*, 74, pp. 2585–91.

Liuzzo, G., Goronzy, J. J., Yang, H., Kopecky, S. L., Holmes, D. R., Frye, R. L. and Weyand, C. M. (2000) 'Monoclonal T-cell proliferation and plaque instability in acute coronary syndromes', *Circulation*, 101, pp. 2883–8.

Liuzzo, G., Biasucci, L. M., Trotta, G., Brugaletta, S., Pinnelli, M., Digianuario, G., Rizzello, V., Rebuzzi, A. G., Rumi, C., Maseri, A. and Crea, F. (2007) 'Unusual CD4+CD28null T lymphocytes and recurrence of acute coronary events', *J Am Coll Cardiol*, 50, pp. 1450–8.

Lopez-Barneo, J., Pardal, R. and Ortega-Saenz, P. (2001) 'Cellular mechanism of oxygen sensing', *Annu Rev Physiol*, 63, pp. 259–87.

Lorenz, M., Saretzki, G., Sitte, N., Metzkow, S. and von Zglinicki, T. (2001) 'BJ fibroblasts display high antioxidant capacity and slow telomere shortening independent of hTERT transfection', *Free Radic. Biol. Med.*, 31, pp. 824–831.

Los, M., Dröge, W., Stricker, K., Baeuerle, P. A. and Schulze-Osthoff, K. (1995) 'Hydrogen peroxide as a potent activator of T lymphocyte functions', *Eur J Immunol*, 25, pp. 159–65.

Lou, Z., and Chen, J. (2006) 'Cellular senescence and DNA repair', *Exp Cell Res.*, 312, pp. 2641–2646.

Ludewig, B., Freigang, S., Jäggi, M., Kurrer, M. O., Pei, Y. C., Vlk, L., Odermatt, B., Zinkernagel, R. M. and Hengartner, H. (2000) 'Linking immune-mediated arterial inflammation and cholesterol induced atherosclerosis in a transgenic mouse model', *Proc Natl Acad Sci USA*, 97, pp. 12752–7.

Ludlow, A. T., Witkowski, S., Marshall, M. R., Wang, J., Lima, L. C., Guth, L. M., Spangenburg, E. E. and Roth, S. M. (2012) 'Chronic exercise modifies age-related telomere dynamics in a tissue-specific fashion', *The Journals of Gerontology*, 67(9), pp. 911–26.

Ludlow, A. T., Zimmerman, J. B., Witkowski, S., Hearn, J. W., Hatfield, B. D. and Roth, S. M. (2008) 'Relationship between physical activity level, telomere length, and telomerase activity', *Med Sci Sports Exerc*, 40, pp. 1764–71.

Lukowicz, P., Ward, J., Junker, H., Stager, M., Troster, G., Atrash, A. and Starner, T. (2004) 'Reconizing workshop activity using body worn microphones and accelerometers Pervasive Computing', (Lecture Notes in Computer Science vol 3001) (Berlin: Springer), pp 18–32.

Luszczynska, A. and Sutton, S. (2006) 'Physical activity after cardiac rehabilitation: Evidence that different types of self-efficacy are important in maintainers and relapsers', *Rehabilitation Psychology*, 51(4), pp. 314–21.

Ma, X. L., Kumar, S., Gao, F., Louden, C. S., Lopez, B. L., Christopher, T. A., Wang, C., Lee, J. C., Feuerstein, G. Z. and Yue, T. (1999) 'Inhibition of p38 mitogen-activated protein kinase decreases cardiomyocyte apoptosis and improves cardiac function after myocardial ischemia and reperfusion', *Circulation*, 99(13), pp. 1685–91.

Mach, F., Sauty, A., Iarossi, A., Sukhova, G. K., Neote, K., Libby, P. and Luster, A. D. (1999) 'Differential expression of three T lymphocyte-activating CXC chemokines by human atheroma-associated cells', *J Clin Invest*, 104, pp. 1041–50.

Mach, F., Schönbeck, U., Sukhova, G. K., Atkinson, E. and Libby, P. (1998) 'Reduction of atherosclerosis in mice by inhibition of CD40 signalling', *Nature*, 394, pp. 200–3.

Mackinnon, L. T., Chick, T. W., Van Es, A. and Tomasi, T. B. (1988) 'The effect of exercise on secretory and natural immunity', *Adv Exp Med Biol.*, 216A, pp. 869–76.

Macneil, B. and Hoffman-Goetz, L. (1993) 'Chronic exercise enhances in vivo and in vitro cytotoxic mechanisms of natural immunity in mice', *J Appl Physiol* 74, pp. 388–95.

Maffia, P., Zinselmeyer, B. H., Ialenti, A., Kennedy, S., Baker, A. H., McInnes, I. B., Brewer, J. M. and Garside, P. (2007) 'Images in cardiovascular medicine. Multiphoton microscopy for 3-dimensional imaging of lymphocyte recruitment into apolipoprotein-E-deficient mouse carotid artery', *Circulation*, 115, pp. e326–28.

Mahley, R. W. (1988) 'Apolipoprotein E: cholesterol transport protein with expanding role in cell biology', *Science*, 240, pp. 622–30.

Maier, B., Gluba, W., Bernier, B., Turner, T., Mohammad, K., Guise, T., Sutherland, A., Thorner, M. and Scrable, H. (2004) 'Modulation of mammalian life span by the short isoform of p53', *Genes Dev.*, 18, pp. 306–319.

Maini, M. K., Soares, M. V. D., Zilch, C. F., Akbar, A. N. and Beverly, P. C. L. (1999) 'Virus-induced CD8+ T-cell clonal expansion is associated with telomerase up-regulation and telomere length preservation: a mechanism for rescue from replicative senescence', *J Immunol*, 162, pp. 4521–6.

Major, A. S., Fazio, S. and Linton, M. F. (2002) 'B-lymphocyte deficiency increases atherosclerosis in LDL receptor-null mice', *Arterioscler Thromb Vasc Biol*, 22, pp. 1892–8.

Makarov, V. L., Hirose, Y., and Langmore, J. P. (1997) 'Long G tails at both ends of human chromosomes suggest a C strand degradation mechanism for telomere shortening', *Cell*, 88(5), pp. 657–666.

Mallat, Z., Ait-Oufella, H. and Tedgui A. (2007) 'Regulatory T-cell immunity in atherosclerosis', *Trends Cardiovasc Med*, 17(4), pp. 113–8.

Mallat, Z., Gojova, A., Brun, V., Esposito, B., Fournier, N., Cottrez, F., Tedgui, A. and Groux, H. (2003) 'Induction of a regulatory T cell type 1 response reduces the development of atherosclerosis in apolipoprotein E-knockout mice', *Circulation*, 108, pp. 1232–37.

Mallat, Z., Gojova, A., Marchiol-Fournigault, C., Esposito, B., Kamaté, C., Merval, R., Fradelizi, D. and Tedgui, A. (2001) 'Inhibition of transforming growth factor- β signaling accelerates atherosclerosis and induces an unstable plaque phenotype in mice', *Circ Res*, 89, pp. 930–4.

Mampuya, W. M. (2012) 'Cardiac rehabilitation past, present and future: an overview', *Cardiovasc Diagn Ther*, 2, pp. 38–49.

Mariani, M., Fetiveau, R., Rossetti, E., Poli, A., Poletti, F., Vandoni, P., D'Urbano, M., Cafiero, F., Mariani, G., Klersy, C. and De Servi S. (2006) 'Significance of total and differential leucocyte count in patients with acute myocardial infarction treated with primary coronary angioplasty', *Eur Heart J*, 27, pp. 2511–5.

Martens, U. M., Zijlmans, J. M., Poon, S. S., Dragowska, W., Yui, J., Chavez, E. A., Ward, R. K. and Lansdorp, P. M. (1998) 'Short telomeres on human chromosome 17p', *Nat Genet*, 18(1), pp. 76–80.

Martín-Rivera, L., Herrera, E., Albar, J. P. and Blasco, M. A. (1998) 'Expression of mouse telomerase catalytic subunit in embryos and adult tissues', *Proc Natl Acad Sci USA*, 95(18), pp. 10471–6.

Martin-Ruiz, C. M., Gussekloo, J., van Heemst, D., von Zglinicki, T. and Westendorp, R. G. (2005) 'Telomere length in white blood cells is not associated with morbidity or mortality in the oldest old: a population-based study', *Aging Cell*, 4(6), pp. 287-90.

Matsumoto, A., Manthey, H. D., Marsh, S. A., Fassett, R. G., de Haan, J. B., Matsumoto, A., Manthey, H. D., Marsh, S. A., Fassett, R. G., de Haan, J. B., Rolfe, B. E. and Coombes, J. S. (2013) 'Effects of exercise training and RhoA/ROCK inhibition on plaque in ApoE^{-/-} mice', *Int. J. Cardiol.*, 167, pp. 1282-1288.

Matsumoto, Y., Adams, V., Jacob, S., Mangner, N., Schuler, G. and Linke A. (2010) 'Regular exercise training prevents aortic valve disease in low-density lipoprotein-receptordeficient mice', *Circulation* 121, pp. 759-767.

Matsushita, H., Chang, E., Glassford, A. J., Cooke, J. P., Chiu, C. P. and Tsao, P. S. (2001) 'eNOS activity is reduced in senescent human endothelial cells: Preservation by hTERT immortalization', *Circ Res*, 89(9), pp. 793-8.

McKeown, S. R. (2014) 'Defining normoxia, physoxia and hypoxia in tumours—implications for treatment response', *The British Journal of Radiology*, 87(1035), p. 20130676.

Medeiros, C., Frederico, M.J., da Luz, G., Pauli, J.R., Silva, A.S., Pinho, R. A., Velloso, L. A., Ropelle, E. R. and De Souza, C. T. (2011) 'Exercise training reduces insulin resistance and upregulates the mTOR/p70S6k pathway in cardiac muscle of diet-induced obesity rats', *J. Cell. Physiol.* 226, pp. 666-674.

Meir, K. S. and Leitersdorf, E. (2004) 'Atherosclerosis in the apolipoprotein-E-deficient mouse: a decade of progress', *Arterioscler Thromb Vasc Biol*, 24, pp. 1006-14.

Mekada, K., Abe, K., Murakami, A., Nakamura, S., Nakata, H., Moriwaki, K., Obata, Y. and Yoshiki, A. (2009) 'Genetic differences among C57BL/6 substrains', *Exp. Anim.*, 58, pp. 141-149.

Melk, A., Tegtbur, U., Hilfiker-Kleiner, D., Eberhard, J., Saretzki, G., Eulert, C., Kerling, A., Nelius, A. K., Homme, M., Strunk, D., Berliner, D., Rontgen, P., Kuck, M., Bauersachs, J., Hilfiker, A., Haverich, A., Bara, C. and Stiesch, M. (2014) 'Improvement of biological age by physical activity', *Int J Cardiol*, 176, pp. 1187-9.

Melloni, C., Sprecher, D. MD, Sarov-Blat, L., Patel, M., Heitner, J., Hamm, C., Aylward, P., Tanguay, J., DeWinter, R., Marber, M., Lerman, A., Hasselblad, V., Granger, C. and Newby, L. (2012) 'The Study Of LoSmapimod Treatment on inflammation and InfarCt size (SOLSTICE): Design and rationale', *Am Heart J*, 164, pp. 646-653.e3.

Meloche, S., and Pouyssegur, J. (2007) 'The ERK1/2 mitogen-activated protein kinase pathway as a master regulator of the G1- to S-phase transition', *Oncogene*, 26, pp. 3227-3239.

Menezes, A. R., Lavie, C. J., Milani, R. V., Forman, D. E., King, M. and Williams, M. A. (2014) 'Cardiac rehabilitation in the United States', *Prog Cardiovasc Dis*, 56, pp. 522-9.

Methe, H., Brunner, S., Wiegand, D., Nabauer, M., Koglin, J. and Edelman, E. R. (2005) 'Enhanced T-helper-1 lymphocyte activation patterns in acute coronary syndromes', *J Am Coll Cardiol*, 45, pp. 1939-45.

Milani, R. V., Lavie, C. J., Mehra, M. R. and Ventura, H. O. (2011) 'Impact of exercise training and depression on survival in heart failure due to coronary heart disease', *Am J Cardiol*, 107, pp. 64–8.

Minamino, T. and Komuro, I. (2007) 'Vascular cell senescence: contribution to atherosclerosis', *Circ Res*, 100(1) pp. 15-26.

Minamino, T. and Kourembanas, S. (2001) 'Mechanisms of telomerase induction during vascular smooth muscle cell proliferation', *Circ. Res.*, 89, pp. 237–243.

Minamino, T., Miyauchi, H., Yoshida, T., Ishida, Y., Yoshida, H. and Komuro, I. (2002) 'Endothelial cell senescence in human atherosclerosis: role of telomere in endothelial dysfunction', *Circulation*, 105(13), pp. 1541-4.

Misiti, S., Nanni, S., Fontemaggi, G., Cong, Y. S., Wen, J., Hirte, H. W., Piaggio, G., Sacchi, A., Pontecorvi, A., Bacchetti, S. and Farsetti, A. (2000) 'Induction of hTERT expression and telomerase activity by estrogens in human ovary epithelium cells', *Mol. Cell. Biol.*, 20, pp. 3764–3771.

Mitchell, J. R., Cheng, J. and Collins, K. (1999) 'A box H/ACA small nucleolar RNA-like domain at the human telomerase RNA 3' end', *Mol. Cell. Biol.*, 19, pp. 567–576.

Miyazaki, T., Liu, Z. J., Kawahara, A., Minami, Y., Yamada, K., Tsujimoto, Y., Barsoumian, E. L., Permutter, R. M. and Taniguchi, T. (1995) 'Three distinct IL-2 signaling pathways mediated by bcl-2, c-myc, and lck cooperate in hematopoietic cell proliferation', *Cell*, 81, pp. 223–31.

Moghaddam, A. E., Gartlan, K. H., Kong, L. and Sattentau, Q. J. (2011) 'Reactive carbonyls are a major Th2-inducing damage-associated molecular pattern generated by oxidative stress', *J Immunol*, 187, pp. 1626–33.

Montgomery, S. H. Capellini, I. Venditti, C. Barton, R. A. and Mundy N. I. (2011) 'Adaptive evolution of four microcephaly genes and the evolution of brain size in anthropoid primates', *Molecular Biology and Evolution*, 28, pp 625 – 638.

Mor, A., Luboshits, G., Planer, D. Keren, G. and George, J. (2006) 'Altered status of CD4+CD25+ regulatory T cells in patients with acute coronary syndromes', *Eur Heart J*, 27, pp. 2530–7.

Moreira, E.L., Aguiar Jr. A.S., de Carvalho C.R., Santos D.B., de Oliveira, J., de Bem, A. F., Xikota, J. C., Walz, R., Farina, M. and Prediger, R. D. (2013) 'Effects of lifestyle modifications on cognitive impairments in a mouse model of hypercholesterolemia', *Neurosci. Lett.* 541, pp. 193–198.

Morris, C. K. and Froelicher, V. F. (1991) 'Cardiovascular benefits of physical activity', *Herz*, 16, pp. 222–36.

Mosmann, T. R., Kobie, J. J., Lee, F. E. and Quataert, S. A. (2009) 'T helper cytokine patterns: defined subsets, random expression, and external modulation', *Immunologic Research*, 45, pp. 173–84.

Mougiakakos, D., Johansson, C. C. and Kiessling, R. (2009) 'Naturally occurring regulatory T cells show reduced sensitivity toward oxidative stress-induced cell death', *Blood*, 113, pp. 3542–5.

Mougiakakos, D., Johansson, C. C., Jitschin, R., Böttcher, M. and Kiessling, R. (2011) 'Increased thioredoxin-1 production in human naturally occurring regulatory T cells confers enhanced tolerance to oxidative stress', *Blood*, 117, pp. 857–61.

Moustardas, P., Kadoglou, N. P., Katsimpoulas, M., Kapelouzou, A., Kostomitsopoulos, N., Karayannacos, P. E., Kostakis, A., Liapis, C. D. (2014) 'The complementary effects of atorvastatin and exercise treatment on the composition and stability of the atherosclerotic plaques in ApoE knockout mice', *PLoS One*, 9(9), Article ID. e108240.

Mudgett, J. S., Ding, J., Guh-Siesel, L., Chartrain, N. A., Yang, L., Gopal, S. and Chen, M. M. (2000) 'Essential role for p38a mitogen-activated protein kinase in placental angiogenesis', *Proc Natl Acad Sci.*, 97(19), pp. 10454–10459.

Muller, F. (2000) 'The nature and mechanism of superoxide production by the electron transport chain: Its relevance to aging', *Journal of the American Aging Association*, 23 (4), pp. 227–53.

Murphy, E. A., Davis, J. M., Brown, A. S., Carmichael, M. D., Van Rooijen, N., Ghaffar, A. and Mayer, E. P. (2004) 'Role of lung macrophages on susceptibility to respiratory infection following short-term moderate exercise training', *Am J Physiol Regul Integr Comp Physiol.*, 287, pp. R1354–R1358.

Murphy, S. A., Cannon, C. P., Wiviott, S. D., McCabe, C. H. and Braunwald, E. (2009) 'Reduction in recurrent cardiovascular events with intensive lipid-lowering statin therapy compared with moderate lipid-lowering statin therapy after acute coronary syndromes from the PROVE IT-TIMI 22 (Pravastatin or Atorvastatin Evaluation and Infection Therapy-Thrombolysis in Myocardial Infarction 22) trial', *J Am Coll Cardiol*, 54, pp. 2358–62.

Nagatomo, F., Fujino, H., Kondo, H. and Ishihara, A. (2012) 'Oxygen concentration-dependent oxidative stress levels in rats', *Oxid Med Cell Longev*, 2012, p. 381763.

Nagel, T., Resnick, N., Atkinson, W. J. Dewey, C. F. Jr., Gimbrone, M. A. Jr. (1994) 'Shear stress selectively upregulates intercellular adhesion molecule-1 expression in cultured human vascular endothelial cells', *J Clin Invest*, 94, pp. 885–91.

Naito, T. and Taniuchi, I. (2010) 'The network of transcription factors that underlie the CD4 versus CD8 lineage decision', *International Immunology*, 22, pp. 791–6.

Nakamura, T. M., Morin, G. B., Chapman, K. B., Weinrich, S. L., Andrews, W. H., Lingner, J., Harley, C. B. and Cech, T. R. (1997) 'Telomerase catalytic subunit homologs from fission yeast and human', *Science*, 277, pp. 955–959.

Nandakumar, J. and Cech, T. R. (2013) 'Finding the end: recruitment of telomerase to telomeres', *Nat Rev Mol Cell Biol.*, 14, pp. 69–82.

National Institute for Health and Care Excellence. (2010a) Management of chronic heart failure in adults in primary and secondary care (clinical guidance 108), NICE. www.nice.org.uk/guidance/cg108.

National Institute for Health and Care Excellence. (2010b) The early management of unstable angina and non-ST-segment-elevation myocardial infarction (clinical guidance 94), NICE. www.nice.org.uk/guidance/cg94.

National Institute for Health and Care Excellence. (2013) Secondary prevention in primary and secondary care for patients following a myocardial infarction (clinical guidance 172), NICE.

Nelson, G. and von Zglinicki, T. (2013) 'Monitoring DNA damage during cell senescence', *Methods Mol Biol.*, 965, pp. 197-213.

Nelson, W. G. and Kastan, M. B. (1994) 'DNA strand breaks: the DNA template alterations that trigger p53-dependent DNA damage response pathways' *Mol. Cell. Biol.*, 14, pp. 1815-1823.

Nickoloff, B. J. and Turka, L. A. (1994) 'Immunological functions of non-professional antigen presenting cells: new insights from studies of T-cell interactions with keratinocytes', *Immunology Today*, 15, pp. 464-9.

Niebauer, J., Maxwell, A. J., Lin, P. S., Tsao, P. S., Kosek, J., Bernstein, D. and Cooke, J. P. (1999) 'Impaired aerobic capacity in hypercholesterolemic mice: partial reversal by exercise training', *Am J Physiol.*, 276(4 Pt 2), pp. H1346-54.

Nielsen, C., Fischer, E. and Leslie, R. (2000) 'The role of complement in the acquired immune response', *Immunology*, 100(1), pp. 4-12.

Nielsen, H. B., Secher, N. H., Kappel, M., Hanel, B. and Pedersen, B. K. (1996) 'Lymphocyte, NK and LAK cell responses to maximal exercise', *Int J Sports Med.*, 17, pp. 60-5.

Nieman, D. C., Henson, D. A., Gusewitch, G., Warren, B. J., Dotson, R. C., Butterworth, D. E. and Nehls-Cannarella, S. L. (1993) 'Physical activity and immune function in elderly women', *Med Sci Sports Exerc.*, 25, pp. 823-31.

Nieman, D. C., Henson, D. A., Sampson, C. S., Herring, J. L., Suttles, J., Conley, M. Stone, M. H., Butterworth, D. E. and Davis, J. M. (1995) 'Acute immune response to exhaustive resistance exercise', *International Journal of Sports Medicine*, 16, pp. 322-8.

Nikolich-Zugich, J., Slifka, M. K. and Messaoudi, I. (2004) 'The many important facets of Tcell repertoire diversity', *Nature Review Immunology*, 4, pp. 123-32.

Nilsen, T. W. and Graveley, B. R. (2010) 'Expansion of the eukaryotic proteome by alternative splicing' *Nature*, 463, pp. 457-463.

Nimse, S. B. and Dilipkumar, P. (2015) 'Free radicals, natural antioxidants and their reaction mechanisms', *Royal Soc. Chem. Adv.*, 5, pp. 27986-28006.

Nishida, K., Yamaguchi, O., Hirotani, S., Hikoso, S., Higuchi, Y., Watanabe, T., Takeda, T., Osuka, S., Morita, T., Kondoh, G., Uno, Y., Kashiwase, K., Taniike, M., Nakai, A., Matsumura, Y., Chien, K. R., Takeda, J., Hori, M. and Otsu, K. (2004) 'p38a mitogen-activated protein kinase plays a critical role in cardiomyocyte survival but not in cardiac

hypertrophic growth in response to pressure overload', *Mol Cell Biol.*, 24(24), pp. 10611–10620.

Nofer, J. R., Bot, M., Brodde, M., Taylor, P. J., Salm, P., Brinkmann, V., van Berkel, T., Assmann, G. and Biessen, E. A. (2007) 'FTY720, a synthetic sphingosine 1 phosphate analogue, inhibits development of atherosclerosis in low-density lipoprotein receptor-deficient mice', *Circulation*, 115, pp. 501–8.

Núñez, J., Núñez, E., Bodí, V., Sanchis, J., Miñana, G., Mainar, L., Santas, E., Merlos, P., Rumiz, E., Darmofal, H., Heatta, A. M. and Llacer, A. (2008) 'Usefulness of the neutrophil to lymphocyte ratio in predicting long-term mortality in ST segment elevation myocardial infarction', *Am J Cardiol*, 101, pp. 747–52.

Núñez, J., Núñez, E., Sanchis, J., Bodí, V. and Llacer, A. (2006) 'Prognostic value of leukocytosis in acute coronary syndromes: the Cinderella of the inflammatory markers', *Curr Med Chem*, 13, pp. 2113–8.

Obana, N., Takagi, S., Kinouchi, Y., Tokita, Y., Sekikawa, A., Takahashi, S., Hiwatashi, N., Oikawa, S. and Shimosegawa, T. (2003) 'Telomere shortening of peripheral blood mononuclear cells in coronary disease patients with metabolic disorders', *Intern Med*, 42, pp. 150–3.

Oemrawsingh, R. M., Lenderink, T., Akkerhuis, K. M., Heeschen, C., Baldus, S., Fichtlscherer, S., Hamm, C. W., Simoons, M. L. and Boersma, E. (2011) 'Multimarker risk model containing troponin-T, interleukin 10, myeloperoxidase and placental growth factor predicts long-term cardiovascular risk after non-ST-segment elevation acute coronary syndrome', *Heart*, 97, pp. 1061–6.

Ogami, M., Ikura, Y., Ohsawa, M., Matsuo, T., Kayo, S., Yoshimi, N. Hai, E., Shirai, N., Ehara, S., Komatsu, R., Naruko, T. and Ueda, M. (2004) 'Telomere shortening in human coronary artery diseases', *Arterioscler Thromb Vasc Biol*, 24, pp. 546–50.

Ogawa, K., Oka, J., Yamakawa, J. Higuchi M. (2003) 'Habitual exercise did not affect the balance of type 1 and type 2 cytokines in elderly people', *Mech Aging Dev.*, 124, pp. 951–6.

Oguchi, K., Tamura, K., Takahashi, H. (2004) 'Characterization of *Oryza sativa* telomerase reverse transcriptase and possible role of its phosphorylation in the control of telomerase activity', *Gene*, 342, pp. 57–66.

Oh, S., Song, Y. H., Yim, J. and Kim, T. K. (2000) 'Identification of Mad as a repressor of the human telomerase (hTERT) gene', *Oncogene*, 19, pp. 1485–1490.

Oh, S., Song, Y., Yim, J. and Kim, T. K. (1999) 'The Wilms' tumor 1 tumor suppressor gene represses transcription of the human telomerase reverse transcriptase gene', *J. Biol. Chem.*, 274, pp. 37473–37478.

Okabe, T. A., Shimada, K., Hattori, M., Murayama, T., Yokode, M., Kita, T. and Kishimoto, C. (2007) 'Swimming reduces severity of atherosclerosis in apolipoprotein E deficient mice by antioxidant effects', *Cardiovasc. Res.*, 74, pp. 537–545.

Okabe, T., Kishimoto, C., Murayama, T., Yokode, M. and Kita, T. (2006) 'Effects of exercise on the development of atherosclerosis in apolipoprotein E-deficient mice', *Exp Clin Cardiol*, 11(4), pp. 276–9.

Olofsson, P. S., Söderström, L. A., Wågsäter, D., Sheikine, Y., Ocaya, P., Lang, F., Rabu, C., Chen, L., Rudling, M., Aukrust, P., Hedin, U., Paulsson-Berne, G., Sirsjö, A. and Hansson, G. K. (2008) 'CD137 is expressed in human atherosclerosis and promotes development of plaque inflammation in hypercholesterolemic mice', *Circulation*, 117, pp. 1292–1301.

Olovnikov, A. M. (1996) 'Telomeres, telomerase, and aging: origin of the theory', *Exp Gerontol.*, 31, pp. 443–48.

Otani, T., Nakamura, S., Toki, M., Motoda, R., Kurimoto, M. and Orita, K. (1999) 'Identification of IFN-gamma-producing cells in IL-12/IL-18-treated mice', *Cellular Immunology*, 198, pp. 111–9.

Otsu, K., Yamashita, N., Nishida, K., Hirotani, S., Yamaguchi, O., Watanabe, T., Hikoso, S., Higuchi, Y., Matsumura, Y., Maruyama, M., Sudo, T., Osada, H. and Hori, M. (2003) 'Disruption of a single copy of the p38a MAP kinase gene leads to cardioprotection against ischemia-reperfusion', *Biochem Biophys Res Commun*, 302(1), pp. 56–60.

Ozaki, K., Spolski, R., Ettinger, R., Kim, H. P., Wang, G. Qi, C. F., Hwu, P., Shaffer, D. J., Akilesh, S., Roopenian, D. C., Morse, H. C., Lipsky, P. E., Leonard, W. J. (2004) 'Regulation of B cell differentiation and plasma cell generation by IL-21, a novel inducer of Blimp-1 and Bcl-6', *J Immunol*, 173, pp. 5361–7.

Packer, L. and Fuehr, K. (1977) 'Low oxygen concentration extends the lifespan of cultured human diploid cells', *Nature*, 267, pp. 423–5.

Park, J. I., Venteicher, A. S., Hong, J. Y., Choi, J., Jun, S., Shkreli, M., Chang, W., Meng, Z., Cheung, P., Ji, H., McLaughlin, M., Veenstra, T. D., Nusse, R., McCrea, P. D. and Artandi, S. E. (2009) 'Telomerase modulates Wnt signalling by association with target gene chromatin', *Nature*, 460, pp. 66–72.

Parrinello, S., Samper, E., Krtolica, A., Goldstein, J., Melov, S. and Campisi, J. (2003) 'Oxygen sensitivity severely limits the replicative lifespan of murine fibroblasts', *Nat Cell Biol.*, 5(8), pp. 741–7.

Parsons, J. P., Kaeding, C., Phillips, G., Jarjoura, D., Wadley, G. and Mastronarde, J. G. (2007) 'Prevalence of exercise induced bronchospasm in a cohort of varsity college athletes', *Med Sci Sports Exerc*, 39, pp. 1487–92.

Pashkow, F. J. (2011) 'Oxidative stress and inflammation in heart disease: do antioxidants have a role in treatment and/or prevention?', *Int J Inflam.*, 2011, p. 514623.

Pasqui, A. L., Di Renzo, M., Bova, G. Bruni, F., Puccetti, L., Pompella, G. and Auteri, A. (2003) 'T cell activation and enhanced apoptosis in non-ST elevation myocardial infarction', *Clin Exp Med*, 3, pp. 37–44.

Passos, J. F. Saretzki, G. Ahmed, S. Nelson, G. Richter, T. Peters, H. Wappler, I. Birket, M. Harold, G. Schaeuble, K. Birch-Machin, M. A. Kirkwood, T. B. L. and von Zglinicki T.

(2007) 'Mitochondrial dysfunction accounts for the stochastic heterogeneity in telomere-dependent replicative senescence', *PLoS Biol.*, 5, pp. 1138–1151.

Passos, J. F., Nelson, G., Wang, C., Richter, T., Simillion, C., Proctor, C. J., Miwa, S., Olijslagers, S., Hallinan, J., Wipat, A., Saretzki, G., Rudolph, K. L., Kirkwood, T. B. and von Zglinicki, T. (2010) 'Feedback between p21 and reactive oxygen production is necessary for cell senescence', *Mol Syst Biol.*, 6, article ID. e347.

Passos, J. F., Saretzki, G. and von Zglinicki, T. (2007) 'DNA damage in telomeres and mitochondria during cellular senescence: is there a connection? ', *Nucleic Acids Res.*, 35, pp. 7505–7513.

Patel, S., Thelander, E., Hernandez, M., Montenegro, J., Hassing, H., Burton, C., Mundt, S., Hermanowski-Vosatka, A., Wright S., Chao, Y. and Detmers, P. (2001) 'ApoE(–/–) mice develop atherosclerosis in the absence of complement component C5', *Biochem. Biophys. Res. Commun.*, 286, pp. 164–170.

Paulsson, G., Zhou, X., Tornquist, E. and Hansson, G. K. (2000) 'Oligoclonal T cell expansions in atherosclerotic lesions of apolipoprotein E-deficient mice', *Arterioscler Thromb Vasc Biol.*, 20, pp. 10–7.

Pellegrin, M., Berthelot, A., Houdayer, C., Gaume, V., Deckert, V. and Laurant, P. (2007) 'New insights into the vascular mechanisms underlying the beneficial effect of swimming training on the endothelial vasodilator function in apolipoprotein E-deficient mice', *Atherosclerosis*, 190, pp. 35–42.

Pellegrin, M., Miguët-Alfonsi, C., Bouzourene, K., Aubert, J. F., Deckert, V., Berthelot, A., Mazzolai, L. and Laurant, P. (2009) 'Long-term exercise stabilizes atherosclerotic plaque in ApoE knockout mice', *Med Sci Sports Exerc.*, 41, pp. 2128–35.

Pereira, T. M., Nogueira, B. V., Lima, L. C., Porto, M. L., Arruda, J. A., Vasquez, E. C. and Meyrelles, S. S. (2010) 'Cardiac and vascular changes in elderly atherosclerotic mice: the influence of gender', *Lipids Health Dis.*, 9, p. 87.

Pericuesta, E., Ramirez, M. A., Villa-Diaz, A., Relano-Gines, A., Torres, J. M., Nieto, M., Pintado, B. and Gutierrez-Adan, A. (2006) 'The proximal promoter region of mTert is sufficient to regulate telomerase activity in ES cells and transgenic animals', *Reprod Biol Endocrinol.*, 4, p. 5.

Perry, H. M., Oldham, S. N., Fahl, S. P., Que, X., Gonen, A., Harmon, D. B., Tsimikas, S., Witztum, J. L., Bender, T. P. and McNamara, C. A. (2013) 'Helix-loop-helix factor inhibitor of differentiation 3 regulates interleukin-5 expression and B-1a B cell proliferation', *Arterioscler Thromb Vasc Biol.*, 33, pp. 2771–9.

Perussia, B., Dayton, E. T., Fanning, V., Thiagarajan, P., Hoxie, J. and Trinchieri, G. (2001) 'Inducible IL-2 production by dendritic cells revealed by global gene expression analysis', *Nature Immunology*, 2, pp. 882–8.

Petersen, A. M. and Pedersen, B. K. (2005) 'The anti-inflammatory effect of exercise' *J Appl Physiol*, 98, pp. 1154–1162.

Petersen, S., Saretzki, G. and von Zglinicki, T. (1998) 'Preferential accumulation of single-stranded regions in telomeres of human fibroblasts', *Exp Cell Res.*, 239(1), pp. 152-60.

Piedrahita, J. A., Zhang, S. H., Hagaman, J. R., Oliver, P. M. and Maeda, N. (1992) 'Generation of mice carrying a mutant apolipoprotein E gene inactivated by gene targeting in embryonic stem cells', *Proc Natl Acad Sci USA.*, 89, pp. 4471-4475.

Piepoli, M. F., Corrà, U., Adamopoulos, S., Benzer, W., Bjarnason-Wehrens, B., Cupples, M., Dendale, P., Doherty, P., Gaita, D., Höfer, S., McGee, H., Mendes, M., Niebauer, J., Pogosova, N., Garcia-Porrero, E., Rauch, B., Schmid, J. P. and Giannuzzi, P. (2014) 'Endorsed by the Committee for Practice Guidelines of the European Society of Cardiology. Secondary prevention in the clinical management of patients with cardiovascular diseases. Core components, standards and outcome measures for referral and delivery: a policy statement from the cardiac rehabilitation section of the European Association for Cardiovascular Prevention & Rehabilitation', *Eur J Prev Cardiol.*, 21, pp. 664-81.

Piedrahita, J. A., Zhang, S. H., Hagaman, J. R., Oliver, P. M. and Maeda, N. (1992) 'Generation of mice carrying a mutant apolipoprotein E gene inactivated by gene targeting in embryonic stem cells', *Proc. Natl. Acad. Sci. USA.*, 89, pp. 4471-4475.

Plump, A. S., Smith, J. D., Hayek, T., Aalto-Setälä, K., Walsh, A., Verstuyft, J. G., Rubin, E. M. and Breslow, J. L. (1992) 'Severe hypercholesterolemia and atherosclerosis in apolipoprotein E-deficient mice created by homologous recombination in ES cells', *Cell*, 71(2), pp. 343-53.

Plunkett F. J., Soares, M. V., Annels, N., Hislop, A., Ivory, K., Lowdell, M., Salmon, M., Rickinson, A., Akbar, A. N. (2001) 'The flow cytometric analysis of telomere length in antigen-specific CD8+ T cells during acute Epstein–Barr virus infection', *Blood*, 97, pp. 700-7.

Plunkett, F. J., Franzese, O., Finney, H. M., Fletcher, J. M., Belaramani, L. L., Salmon, M., Dokal, I., Webster, D., Lawson, A. D. G. and Akbar A. N. (2007) 'The loss of telomerase activity in highly differentiated CD8+CD28-CD27-T cells is associated with decreased Akt (Ser473) phosphorylation', *J Immunol*, 178, pp. 7710-7719.

Plunkett, F. J., Franzese, O., Finney, H. M., Fletcher, J. M., Belaramani, L. L., Salmon, M., Dokal, I., Webster, D., Lawson, A. D. G. and Akbar, A. N. (2007) 'The loss of telomerase activity in highly differentiated CD8+CD28-CD27-T cells is associated with decreased Akt (Ser473) phosphorylation', *J Immunol*, 178, pp. 7710-7719.

Prasanna, S. J., Gopalakrishnan, D., Shankar, S. R., and Vasandan, A. B. (2010) 'Pro-inflammatory cytokines, IFNgamma and TNFalpha, influence immune properties of human bone marrow and Wharton jelly mesenchymal stem cells differentially', *PLoS One*, 5, Article ID. e9016.

Pugh, B. F., and Tjian, R. (1991) 'Transcription from a TATA-less promoter requires a multi-subunit TFIID complex', *Genes Dev.*, 5, pp. 1935-1945.

Puterman, E., Lin, J., Blackburn, E., O'Donovan, A., Adler, N. and Epel E. (2010) 'The power of exercise: Buffering the effect of chronic stress on telomere length', *PLoS One*, 5, Article ID. e10837.

Pynn, M., Schäfer, K., Konstantinides, S. and Halle, M. (2004) 'Exercise training reduces neointimal growth and stabilizes vascular lesions developing after injury in apolipoprotein e-deficient mice', *Circulation*, 109, pp. 386–92.

Ramasamy, R., Trueblood, N. A. and Schaefer, S. (1998) 'Metabolic effects of aldose reductase inhibition during low-flow ischemia and reperfusion', *Am. J. Physiol.*, 275, pp. H195–H203.

Ranjbaran, H., Sokol, S., Gallo, A., Eid, R., Iakimov, A., D'Alessio, A., Kapoor, J., Akhtar, S., Howes, C., Aslan, M., Pfau, S., Pober, J. and Tellides, G. (2007) 'An inflammatory pathway of IFN- γ production in coronary atherosclerosis', *J Immunol*, 178, pp. 592–604.

Reardon, C. A. Blachowicz, L., White, T., Cabana, V., Wang, Y., Lukens, J., Bluestone, J. and Getz, G. S. (2001) 'Effect of immune deficiency on lipoproteins and atherosclerosis in male apolipoprotein E-deficient mice', *Arterioscler Thromb Vasc Biol*, 21, pp. 1011–6.

Redon, S., Reichenbach, P. and Lingner, J. (2010) 'The non-coding RNA TERRA is a natural ligand and direct inhibitor of human telomerase', *Nucleic Acids Res*, 38, pp. 5797–5806.

Reed, J. R., Vukmanovic-Stejic, M., Fletcher, J. M., Soares, M. V., Cook, J. E., Orteu, C. H., Jackson, S. E., Birch, K. E., Foster, G. R., Salmon, M., Beverley, P. C., Rustin, M. H., and Akbar, A. N. (2004) 'Telomere erosion in memory T cells induced by telomerase inhibition at the site of antigenic challenge in vivo', *J. Exp. Med.*, 199, pp. 1433–1443.

Richardson, G. D., Breault, D., Horrocks, G., Cormack, S., Hole, N. and Owens, W. A. (2012) 'Telomerase expression in the mammalian heart', *FASEB J*, 26, pp. 4832–4840.

Richter, A., Sanford, K. K. and Evans, V. J. (1972) 'Influence of oxygen and culture media on plating efficiency of some mammalian tissue cells', *J Nat Cancer Inst*, 49, pp. 1705–12.

Rimer, J., Cohen, I. and Friedman, N. (2014) 'Do all creatures possess an acquired immune system of some sort?', *BioEssays*, 36(3), pp. 273–281.

Rincón, M. and Pedraza-Alva, G. (2003) 'JNK and p38 MAP kinases in CD4+ and CD8+ T cells', *Immunol. Rev.*, 192, pp. 131–142.

Ringseis, R., Eder, K., Mooren, F. C. and Krüger, K. (2015) 'Metabolic signals and innate immune activation in obesity and exercise', *Exerc Immunol Rev.*, 21, pp. 58–68.

Robbins, D. J., Zhen, E., Owaki, H., Vanderbilt, C. A., Ebert, D., Geppert, T. D. and Cobb, M. H. (1993) 'Regulation and properties of extracellular signal-regulated protein kinases 1 and 2 in vitro', *J. Biol. Chem.*, 268, pp. 5097–5106.

Robertson, A. K. and Hansson, G. K. (2006) 'T cells in atherogenesis: for better or for worse?', *Arterioscler Thromb Vasc Biol*, 26, pp. 2421–32.

Robertson, A. K., Rudling, M., Zhou, X., Gorelik, L., Flavell, R. A. and Hansson, G. K. (2003) 'Disruption of TGF-beta signaling in T cells accelerates atherosclerosis', *J Clin Invest*, 112, pp. 1342–50.

Robey, E. (1999) 'Regulation of T cell fate by Notch', *Annual Review of Immunology*, 17, pp. 283–95.

Robey, E., Itano, A., Fanslow, W. C. and Fowlkes, B. J. (1994) 'Constitutive CD8 expression allows inefficient maturation of CD41 helper T cells in class II major histocompatibility complex mutant mice', *J. Exp. Med.*, 179, pp. 1997–2004.

Roca, X., Krainer, A. R. and Eperon, I. C. (2013) 'Pick one, but be quick: 5' splice sites and the problems of too many choices' *Genes & development*, 27, pp. 129–144.

Rodier, F. and Campisi, J. (2011) 'Four faces of cellular senescence', *J. Cell Biol.*, 192, pp. 547–556.

Rohde, V., Sattler, H.P., Bund, T., Bonkhoff, H., Fixemer, T., Bachmann, C., Lensch, R., Unteregger, G., Stoeckle, M. and Wullich, B. (2000) 'Expression of the human telomerase reverse transcriptase is not related to telomerase activity in normal and malignant renal tissue', *Clin. Cancer Res.*, 6, pp. 4803–4809.

Ross, R. (1999) 'Atherosclerosis is an inflammatory disease', *Am Heart J.*, 138(5 Pt 2), pp. S419–20.

Rössig, L., Flichtlscherer, S., Heeschen, C., Berger, J., Dimmeler, S. and Zeiher, A. M. (2004) 'The pro-apoptotic serum activity is an independent mortality predictor of patients with heart failure', *Eur Heart J.*, 25, pp. 1620–5.

Rossmann, A., Henderson, B., Heidecker, B., Seiler, R., Fraedrich, G., Singh, M., Parson, W., Keller, M., Grubeck-Loebenstein, B. and Wick, G. (2008) 'T-cells from advanced atherosclerotic lesions recognize hHSP60 and have a restricted T-cell receptor repertoire', *Exp Gerontol.*, 43, pp. 229–37.

Rouse, J. and Jackson, S. P. (2002) 'Interfaces between the detection, signaling, and repair of DNA damage', *Science*, 297, pp. 547–551.

Rouse, J., Cohen, P., Trigon, S., Morange, M., Alonso-Llamazares, A., Zamanillo, D., Hunt, T. and Nebreda, A. R. (1994) 'A novel kinase cascade triggered by stress and heat shock that stimulates MAPKAP kinase-2 and phosphorylation of the small heat shock proteins', *Cell*, 78, pp. 1027–1037.

Roux, P. P., Shahbazian, D., Vu, H., Holz, M. K., Cohen, M. S., Taunton, J., Sonenberg, N., Blenis, J. (2007) 'RAS/ERK signaling promotes site-specific ribosomal protein S6 phosphorylation via RSK and stimulates cap-dependent translation', *J. Biol. Chem.*, 282, pp. 14056–14064.

Rudolph, M. G., Stanfield, R. L. and Wilson, I. A. (2006) 'How TCRs bind MHCs, peptides, and coreceptors', *Annual Review of Immunology*, 24, pp. 419–66.

Rufer, N., Migliaccio, M., Antonchuk, J., Humphries, R. K., Roosnek, E. and Lansdorp, P. M. (2001) 'Transfer of the human telomerase reverse transcriptase (TERT) gene into T lymphocytes results in extension of replicative potential', *Blood*, 98, pp. 597–603.

Sabio, G., Arthur, J. S. C., Kuma, Y., Peggie, M., Carr, J., MurrayTait, V., Centeno, F., Goedert, M., Morrice, N. A. and Cuenda, A. (2005) 'p38c regulates the localisation of SAP97 in the cytoskeleton by modulating its interaction with GKAP', *EMBO J.*, 24(16), pp. 1134–1145.

Sadava, D. (2007) *Life: the science of biology*, 8th edn., New York, W. H. Freeman and Company.

Saebøe-Larsen, S., Fossberg, E. and Gaudernack, G. (2006) 'Characterization of novel alternative splicing sites in human telomerase reverse transcriptase (hTERT): analysis of expression and mutual correlation in mRNA isoforms from normal and tumour tissues', *BMC Mol Biol.*, 7, p. 26.

Sagar, V. A., Davies, E. J., Briscoe, S., Coats, A. J., Dalal, H. M., Lough, F. Rees, K. Singh, S. and Taylor, R. S. (2015) 'Exercise-based rehabilitation for heart failure: systematic review and meta-analysis', *Open Heart*, 2, Article ID. e000163.

Sahai, A., Mei, C., Zavosh, A. and Tannen, R. L. (1997) 'Chronic hypoxia induces LLC-PK1 cell proliferation and dedifferentiation by the activation of protein kinase C', *Am J Physiol*, 272(6 Pt 2), pp. F809–F815.

Sakaguchi H, Nishio N, Hama A, Kawashima, N., Wang, X., Narita, A., Doisaki, S., Xu, Y., Muramatsu, H., Yoshida, N., Takahashi, Y., Kudo, K., Moritake, H., Nakamura, K., Kobayashi, R., Ito, E., Yabe, H., Ohga, S., Ohara, A. and Kojima, S. (2014) 'Peripheral blood lymphocyte telomere length as a predictor of response to immunosuppressive therapy in childhood aplastic anemia', *Haematologica*, 99, pp. 1312–1316.

Sakaguchi, S. (2004) 'Naturally arising CD4+ regulatory T cells for immunologic self-tolerance and negative control of immune responses', *Annu Rev Immunol*, 22, pp. 531–62.

Sakaguchi, S. (2005) 'Naturally arising Foxp3-expressing CD25+CD4+ regulatory T cells in immunological tolerance to self and non-self', *Nature Immunol*, 6, pp. 345–52.

Sakaguchi, S., Ono, M., Setoguchi, R., Yagi, H., Hori, S., Fehervari, Z., Shimizu, J., Takahashi, T. and Nomura, T. (2006) 'Foxp3+CD25+CD4+ natural regulatory T cells in dominant self-tolerance and autoimmune disease', *Immunol Rev*, 212, pp. 8–27.

Sallam, N. and Laher, I. (2016) 'Exercise Modulates Oxidative Stress and Inflammation in Aging and Cardiovascular Diseases', *Oxid Med Cell Longev*, 2016, article ID. 7239639.

Samani, N. J., Boulby, R., Butler, R., Thompson, J. R. and Goodall, A. H. (2001) 'Telomere shortening in atherosclerosis', *Lancet*, 358, pp. 472–3.

Santos, J. H., Meyer, J. N., Skorvaga, M., Annab, L. A., Van Houten, B. (2004) 'Mitochondrial hTERT exacerbates free-radical-mediated mtDNA damage' *Aging Cell*, 3, pp. 399–411.

Santos, J. H., Meyer, J. N., Van Houten, B. (2006) 'Mitochondrial localization of telomerase as a determinant for hydrogen peroxide-induced mitochondrial DNA damage and apoptosis' *Hum Mol Genet.*, 15, pp. 1757–68.

Saretzki, G. (2009) 'Telomerase, mitochondria and oxidative stress', *Exp Gerontol*, 44, pp. 485–92.

Saretzki, G. (2014) 'Extra-telomeric functions of human telomerase: cancer, mitochondria and oxidative stress', *Curr Pharm Des*, 20, pp. 6386–403.

Saretzki, G., Murphy, M. P. and von Zglinicki, T. (2003) 'MitoQ counteracts telomere shortening and elongates lifespan of fibroblasts under mild oxidative stress', *Aging Cell*, 141, p. 143.

Saretzki, G., Sitte, N., Merkel, U., Wurm, R. E., von Zglinicki, T. (1999) 'Telomere shortening triggers a p53-dependent cell cycle arrest via accumulation of G-rich single stranded DNA fragments', *Oncogene*, 18, pp. 5148–5158.

Sarov-Blat, L., Morgan, J. M., Fernandez, P., James, R., Fang, Z., Hurle, M. R. Baidoo, C., Willette, R. N., Lepore, J. J., Jensen, S. E. and Sprecher, D. L. (2010) 'Inhibition of p38 mitogen-activated protein kinase reduces inflammation after coronary vascular injury in humans', *Arterioscler Thromb Vasc Biol*, 30(11), pp. 2256–63.

Saxena, A., Dobaczewski, M., Rai, V., Haque, Z., Chen, W., Li, N. and Frangogiannis N. G. (2014) 'Regulatory T cells are recruited in the infarcted mouse myocardium and may modulate fibroblast phenotype and function', *Am J Physiol Heart Circ Physiol*, 307, pp. H1233–H1242.

Scheffold, A. and Kern, F. (2000) 'Recent developments in flow cytometry', *J Clin Immunol*, 20(6), pp. 400-7.

Schmidt, J. C., Dalby, A. B., Cech, T. R. (2014) 'Identification of human TERT elements necessary for telomerase recruitment to telomeres', *Elife*, 3, article ID. e03563.

Schmidt, U., Basyuk, E., Robert, M. C., Yoshida, M., Villemin, J. P., Auboeuf, D., Aitken, S. and Bertrand, E. (2011) 'Real-time imaging of cotranscriptional splicing reveals a kinetic model that reduces noise: implications for alternative splicing regulation' *The Journal of cell biology*, 193, pp. 819–829.

Scholz, U., Sniehotta, F. F. and Schwarzer, R. (2005) 'Predicting physical exercise in cardiac rehabilitation: the role of phase-specific self-efficacy beliefs', *Journal of Sport and Exercise Psychology*, 27, pp. 135–51.

Sedelnikova, O. A., Horikawa, I., Zimonjic, D. B., Popescu, N. C., Bonner, W. M. and Barrett, J. C. (2004) 'Senescent human cells and ageing mice accumulate DNA lesions with unrepairable double-strand breaks', *Nat. Cell Biol.*, 6, pp. 168–170.

Seimiya, H., Sawada, H., Muramatsu, Y., Shimizu, M., Ohko, K., Yamane, K. and Tsuruo, T. (2000) 'Involvement of 14-3-3 proteins in nuclear localization of telomerase', *EMBO J.*, 19, pp. 2652-61.

Sharir, R., Semo, J., Shimoni, S., Ben-Mordechai, T., Landa-Rouben, N., Maysel-Auslender, S., Shaish, A., Entin-Meer, M., Keren, G. and George, J. (2014) 'Experimental myocardial infarction induces altered regulatory T cell hemostasis, and adoptive transfer attenuates subsequent remodeling', *PLoS ONE*, 9(12), article ID. e113653.

Shay, J. W., Wright, W. E. and Werbin, H. (1993) 'Toward a molecular understanding of human breast cancer: a hypothesis', *Breast Cancer Res Treat*, 25, pp. 83–94.

Shek, P. N., Sabiston, B. H., Buguet, A. and Radomski, M. W. (1995) 'Strenuous exercise and immunological changes', *International Journal of Sports Medicine*, 16, pp. 466-474.

Shigenaga, K. K., Tory, M. H. and Bruce, N. A. (1994) 'Oxidative damage and mitochondrial decay in ageing', *Proceedings of National Science Academy*, 91, pp. 10771-10778.

Shilo, Y. (2003) 'ATM and related protein kinases: safeguarding genomic integrity', *Nat. Rev. Cancer*, 3, pp. 155–168.

Shiloh, Y. (2003) 'ATM and related protein kinases: safeguarding genome integrity', *Nat. Rev. Cancer*, 3, pp. 155–168.

Shimizu, K., Kimura, F., Akimoto, T., Akama, T., Tanabe, K., Nishijima, T., Kuno, S. and Kono, I. (2008) 'Effect of moderate exercise training on T-helper cell subpopulations in elderly people', *Exerc Immunol Rev*, 14, pp. 24–37.

Shinkai, S., Kohno, H., Kimura, K., Komura, T., Asai, H., Inai, R., Oka, K., Kurokawa, Y. and Shephard, R. (1995) 'Physical activity and immune senescence in men', *Med Sci Sports Exerc*, 27, pp. 1516–26.

Shmeleva, E. V., Boag, S. E., Murali, S., Bennaceur, K., Das, R., Egred, M., Purcell, I., Edwards, R., Todryk, S. and Spyridopoulos, I. (2015) 'Differences in immune responses between CMV-seronegative and -seropositive patients with myocardial ischemia and reperfusion Immunity', *Inflammation and Disease*, 3(2), pp. 56-70.

Sies, H. (1997) 'Oxidative stress: oxidants and antioxidants', *Exp Physiol*, 82, pp. 291–5.

Singh, D., Smyth, L., Borrill, Z., Sweeney, L. and Tal-Singer, R. (2010) 'A randomized, placebo-controlled study of the effect of the p38 MAPK inhibitor SB-681323 on blood biomarkers of inflammation in COPD patients', *J Clin Pharm.*, 50, pp. 94–100.

Singhapol, C., Pal, D., Czapiewski, R., Porika, M., Nelson, G. and Saretzki, G. C. (2013) 'Mitochondrial telomerase protects cancer cells from nuclear DNA damage and apoptosis', *PLoS One*, 8(1), article ID. e52989.

Sitte, N. and von Zglinicki, T. (2003) 'Free radical production and antioxidant defense: a primer', *Kluwer Academic Publishers*, pp. 1-10.

Sitte, N., Saretzki, G. and von Zglinicki, T. (1998) 'Accelerated telomere shortening in fibroblasts after extended periods of confluence', *Free Radic Biol Med.*, 24(6), pp. 885-93.

Škárka, L. and Osštádal, B. (2002) 'Mitochondrial membrane potential in cardiac myocytes', *Physiol Res.*, 51, pp. 425-434.

Smith-Garvin, J. E., Koretzky, G. A. and Jordan, M. S. (2009) 'T cell activation', *Annual Review of Immunology*, 27, pp. 591–619.

Smith, J. D., Trogan, E., Ginsberg, M. Grigaux, C., Tian, J. and Miyata, M. (1995) 'Decreased atherosclerosis in mice deficient in both macrophage colony-stimulating factor (op) and apolipoprotein E', *Proc Natl Acad Sci USA.*, 92, pp. 8264–8.

Smith, S. C. Jr, Allen, J., Blair, S. N., Bonow, R. O., Brass, L. M., Fonarow, G. C., Grundy, S. M., Hiratzka, L., Jones, D., Krumholz, H. M., Mosca, L., Pearson, T., Pfeffer, M. A. and Taubert, K. A. (2006) 'AHA/ACC guidelines for secondary prevention for patients with

coronary and other atherosclerotic vascular disease: 2006 update endorsed by the National Heart, Lung, and Blood Institute', *J Am Coll Cardiol*, 47, pp. 2130–9.

Smith, S., Giri, I., Schmitt, A. and de Lange, T. (1998) 'Tankyrase, a poly (ADP-ribose) polymerase at human telomeres', *Science*, 282, pp. 1484–1487.

Smogorzewska, A. and de Lange, T. (2004) 'Regulation of telomerase by telomeric proteins', *Annu. Rev. Biochem.*, 73, pp. 177–208.

Smogorzewska, A. and De Lange, T. (2002) 'Different telomere damage signaling pathways in human and mouse cells', *EMBO J.*, 21, pp. 4338–4348.

Smogorzewska, A., van Steensel, B., Bianchi, A., Oelmann, S., Schaefer, M. R., Schnapp, G. and de Lange, T. (2000) 'Control of human telomere length by TRF1 and TRF2', *Mol. Cell. Biol.*, 20, pp. 1659–1668.

Smucker, E. J. and Turchi, J. J. (2001) 'TRF1 inhibits telomere C-strand DNA synthesis in vitro', *Biochemistry*, 40, pp. 2426–2432.

Sniderman, A., Thanassoulis, G., Couture, P., Williams, K., Alam, A. and Furberg, C. D. (2012) 'Is lower and lower better and better? A re-evaluation of the evidence from the Cholesterol Treatment Trialists', Collaboration meta-analysis for low-density lipoprotein lowering', *J Clin Lipidol*, 6, pp. 303–9.

Soboleski, M. R., Oaks, J. and Halford, W. P. (2005) 'Green fluorescent protein is a quantitative reporter of gene expression in individual eukaryotic cells', *FASEB J.*, 19, pp. 440–442.

Sohal, R. S. and Brunk, U. T. (1992) 'Mitochondrial production of pro-oxidants and cellular senescence', *Mutat. Res.*, 275, pp. 295–304.

Sohal, R. S., Sohal, B. H. and Orr, W. C. (1995) 'Mitochondrial superoxide and hydrogen peroxide generation, protein oxidative damage, and longevity in different species of life', *Free Rad Biol Med.*, 19, pp. 499–504.

Son, N. H., Murray, S., Yanovski, J., Hodes, R. J. and Weng, N. P. (2000) 'Lineage-specific telomere shortening and unaltered capacity for telomerase expression in human T and B lymphocytes with age', *J Immunol*, 165, pp. 1191–6.

Song, Z., Von Figura, G., Liu, Y., Kraus, J. M., Torrice, C., Dillon, P., Rudolph-Watabe, M., Ju, Z., Kestler, H. A., Sanoff, H. and Lenhard Rudolph, K. (2010) 'Lifestyle impacts on the aging-associated expression of biomarkers of DNA damage and telomere dysfunction in human blood', *Aging Cell*, 9, pp. 607–615.

Sorescu, D., Weiss, D., Lassegue, B., Clempus, R. E., Szocs, K., Sorescu, G. P., Valppu, L., Quinn, M. T., Lambeth, J. D., Vega, J. D., Taylor, W. R. and Griendling, K. K. (2002) 'Superoxide production and expression of Nox family proteins in human atherosclerosis', *Circulation*, 105, pp. 1429–35.

Sosa, Torres, M. E., Saucedo-Vázquez, J. P. and Kroneck, P. M. (2015) 'Chapter 1, Section 3 The dark side of dioxygen' In Kroneck PM, Torres ME. *Sustaining Life on Planet Earth*:

Metalloenzymes Mastering Dioxygen and Other Chewy Gases. Metal Ions in Life Sciences 15. Springer, pp. 1–12.

Spielmann, G., McFarlin, B. B., Connor, D. P. O., Smith, P. J., Pircher, H. and Simpson, R. J. (2011) 'Aerobic fitness is associated with lower proportions of senescent blood T-cells in man', *Brain Behav Immun*, 25, pp. 1521–9.

Spyridopoulos, I. and von Zglinicki, T. (2014), 'Telomere length predicts cardiovascular disease', *British Medical Journal*, 349, article ID. g4373.

Spyridopoulos, I. Hoffmann, J., Aicher, A., Brümmendorf, T. H., Doerr, H. W., Zeiher, A. M. and Dimmeler, S. (2009) 'Accelerated telomere shortening in leukocyte subpopulations of patients with coronary heart disease: role of cytomegalovirus seropositivity', *Circulation*, 120, pp. 1364–1372.

Spyridopoulos, I., Erben, Y., Brummendorf, T. H. Haendeler, J., Dietz, K., Seeger, F., Kissel, C. K., Martin, H., Hoffmann, J., Assmus, B., Zeiher, A. M. and Dimmeler, S. (2008) 'Telomere gap between granulocytes and lymphocytes is a determinant for hematopoietic progenitor cell impairment in patients with previous myocardial infarction', *Arterioscler Thromb Vasc Biol.*, 28(5), pp. 968–74.

Spyridopoulos, I., Hoffmann, J., Aicher, A., Brümmendorf, T. H., Doerr, H. W., Zeiher, A. M. and Dimmeler, S. (2009) 'Accelerated telomere shortening in leukocyte subpopulations of patients with coronary heart disease: role of cytomegalovirus seropositivity', *Circulation*, 120(14), pp. 1364–72.

Spyridopoulos, I., Martin-Ruiz, C., Hilkens, C., Yadegarf, M. E., Isaacs, J., Jagger, C., Kirkwood, T. and von Zglinicki, T. (2016) 'CMV-seropositivity and T-cell senescence predict increased cardiovascular mortality in octogenarians - results from the Newcastle 85+ studyAging', *Cell*, 15(2), pp. 389–392.

Stadtfeld, M., Maherali, N., Breault, D. T. and Hochedlinger, K. (2008) 'Defining molecular cornerstones during fibroblast to iPS cell reprogramming in mouse', *Cell Stem Cell*, 2, pp. 230–240.

Stefanick, M. L., Mackey, S., Sheehan, M., Ellsworth, N., Haskell, W. L. and Wood, P. D. (1998) 'Effects of diet and exercise in men and postmenopausal women with low levels of HDL cholesterol and high levels of LDL cholesterol', *N Engl J Med*, 339, pp. 12–20.

Steinert, S., Shay, J. W. and Wright, W. E. (2000) 'Transient expression of human telomerase extends the life span of normal human fibroblasts', *Biochem. Biophys. Res. Commun.*, 273, pp. 1095–1098.

Steppich, B. A., Moog, P., Matissek, C. Wisnioski, N., Kühle, J., Joghetaei, N., Neumann, F. J., Schomig, A. and Ott, I. (2007) 'Cytokine profiles and T cell function in acute coronary syndromes', *Atherosclerosis*, 190(2), pp. 443–51.

Stewart, C. C. (2000) 'Multiparameter flow cytometry', *J Immunoassay*, 21(2-3), pp. 255–72.

Stewart, S. A., Hahn, W. C., O'Connor, B. F., Banner, E. N., Lundberg, A. S., Modha, P., Mizuno, H., Brooks, M. W., Fleming, M., Zimonjic, D. B., Popescu, N. C. and Weinberg, R.

A. (2002) 'Telomerase contributes to tumorigenesis by a telomere length-independent mechanism', *Proc. Natl. Acad. Sci. USA.*, 99, pp. 12606–12611.

Stone, J. D., Chervin, A. S. and Kranz, D. M. (2009) 'T-cell receptor binding affinities and kinetics: impact on T-cell activity and specificity', *Immunology*, 126, pp. 165–76.

Sugiura, H., Sugiura, H., Nishida, H., Inaba, R., Mirbod, S. M. and Iwata, H. (2001) 'Effects of different durations of exercise on macrophage functions in mice', *J Appl Physiol.*, 90, pp. 789–794.

Sullum, J., Clark, M. M. and King, T. K. (2000) 'Predictors of exercise relapse in a college population', *Journal of American College Health*, 48, pp. 175–80.

Surh, C. D., and Sprent, J. (2005) 'Regulation of mature T cell homeostasis', *Semin. Immunol.*, 17, pp. 183–191.

Suzuki, H., Shinkai, Y., Granger, L. G., Alt, F. W., Love, P. E. and Singer, A. (1997) 'Commitment of immature CD4+8+ thymocytes to the CD4 lineage requires CD3 signaling but does not require expression of clonotypic T cell receptor (TCR) chains', *The Journal of Experimental Medicine*, 186, pp. 17–23.

Swandfager, W., Herrmann, N., Cornish, S., Mazereeuw, G., Marzolini, S., Sham, L., Lanctôt, K. L. (2012) 'Exercise intervention and inflammatory markers in coronary artery disease: a meta-analysis', *Am Heart J.*, 163, pp. 666–676.

Szostak, J. and Laurant, P. (2011) 'The forgotten face of regular physical exercise: a 'natural' anti-atherogenic activity', *Clin Sci (Lond)*, 121, pp. 91–106.

Takai, H., Smogorzewska, A. and de Lange, T. (2003) 'DNA damage foci at dysfunctional telomeres', *Curr Biol.*, 13(17), pp. 1549–56.

Takaoka, M., Nagata, D., Kihara, S., Shimomura, I., Kimura, Y., Tabata, Y., Saito, Y., Nagai, R. and Sata, M. (2009) 'Periadventitial adipose tissue plays a critical role in vascular remodeling', *Circ Res*, 105, pp. 906–11.

Taleb, S., Herbin, O., Ait-Oufella, H., Verreth, W., Gourdy, P., Barateau, V., Merval, R., Esposito, B., Clément, K., Holvoet, P., Tedgui, A. and Mallat, Z. (2007) 'Defective leptin/leptin receptor signaling improves regulatory T cell immune response and protects mice from atherosclerosis', *Arterioscler Thromb Vasc Biol.*, 27, pp. 2691–8.

Tamae, K., Kawai, K., Yamasaki, S., Kawanami, K., Ikeda, M., Takahashi, K., Miyamoto, T., Kato, N. and Kasai, H. (2009) 'Effect of age, smoking and other lifestyle factors on urinary 7-methylguanine and 8-hydroxydeoxyguanosine', *Cancer Sci.*, 100, pp. 715–721.

Tamura, K., Sudo T., Senftleben, U., Dadak, A. M., Johnson, R. and Karin, M. (2000) 'Requirement for p38a in erythropoietin expression: a role for stress kinases in erythropoiesis', *Cell* 102(2), pp. 221–231.

Tanaka, M., Kyo, S., Takakura, M., Kanaya, T., Sagawa, T., Yamashita, K., Okada, Y., Hiyama, E. and Inoue, M. (1998) 'Expression of telomerase activity in human endometrium is localized to epithelial glandular cells and regulated in a menstrual phase-dependent manner correlated with cell proliferation', *Am. J. Pathol.*, 153, pp. 1985–1991.

Tanasescu, M., Leitzmann, M. F., Rimm, E. B., Willett, W. C., Stampfer, M. J. and Hu, F. B. (2002) 'Exercise type and intensity in relation to coronary heart disease in men', *JAMA*, 288(16), pp. 1994–2000.

Tang, T. T., Yuan, J., Zhu, Z. F., Zhang, W. C., Xiao, H., Xia, N., Yan, X. X., Nie, S. F., Liu, J., Zhou, S. F., Li, J. J., Yao, R., Liao, M. Y., Tu, X., Liao, Y. H. and Cheng, X. (2012) 'Regulatory T cells ameliorate cardiac remodeling after myocardial infarction', *Basic Res Cardiol*, 107, p. 232.

Taylor, R. S., Brown, A., Ebrahim, S., Jolliffe, J., Noorani, H., Rees, K., Skidmore, B., Stone, J. A., Thompson, D. R. and Oldridge, N. (2004) 'Exercise-based rehabilitation for patients with coronary heart disease: systematic review and meta-analysis of randomized controlled trials', *Am J Med.*, 116(10), pp. 682-92.

Tennyson, C. N., Klamut, H. J. and Worton, R. G. (1995) 'The human dystrophin gene requires 16 hours to be transcribed and is cotranscriptionally spliced', *Nature genetics*, 9(2), pp. 184–190.

Thorén, F. B., Betten, A., Romero, A. I. and Hellstrand, K. (2007) 'Cutting edge: antioxidative properties of myeloid dendritic cells: protection of T cells and NK cells from oxygen radical-induced inactivation and apoptosis', *J Immunol*, 179, pp. 21–5.

Tong, A. S., Stern, J. L., Sfeir, A., Kartawinata, M., de Lange, T., Zhu, X. D., and Bryan, T. M. (2015) 'ATM and ATR signaling regulate the recruitment of human telomerase to telomeres', *Cell Rep.*, 13(8), pp. 1633-1646.

Topper, J. N., Cai, J., Falb, D., and Gimbrone, M. A. Jr. (1996) 'Identification of vascular endothelial genes differentially responsive to fluid mechanical stimuli: cyclooxygenase-2, manganese superoxide dismutase, and endothelial cell nitric oxide synthase are selectively up-regulated by steady laminar shear stress', *Proc Natl Acad Sci USA*, 93, pp. 10417–22.

Troiano, R. P., McClain, J. J., Brychta, R. J. and Chen, K. Y. (2014) 'Evolution of accelerometer methods for physical activity research', *Br J Sports Med.*, 48, pp. 1019–23.

Turban, S., Beardmore, V. A., Carr, J. M., Sakamoto, K., Hajduch, E., Arthur, J. S. C. and Hundal, H. S. (2005) 'Insulin-stimulated glucose uptake does not require p38 mitogen-activated protein kinase in adipose tissue or skeletal muscle', *Diabetes*, 54(11), pp. 3161–3168.

Turner, M. J., Kleeberger, S. R. and Lightfoot, J. T. (2005) 'Influence of genetic background on daily running-wheel activity differs with aging', *Physiol Genomics*, 22, pp. 76–85.

Tvede, N., Kappel, M., Halkjaer-Kristensen, J., Galbo, H. and Pedersen, B. K. (1993) 'The effect of light, moderate and severe bicycle exercise on lymphocyte subsets, natural and lymphokine activated killer cells, lymphocyte proliferative response and interleukin 2 production', *Int J Sports Med.*, 14(5), pp. 275-82.

Tyner, S. D., Venkatachalam, S., Choi, J., Jones, S., Ghebranious, N., Igelmann, H., Lu, X., Soron, G., Cooper, B., Brayton, C., Hee Park, S., Thompson, T., Karsenty, G., Bradley, A. and Donehower, L. A. (2002) 'p53 mutant mice that display early ageing-associated phenotypes', *Nature* 415, pp. 45–53.

Tyni-Lenne, R., Gordon, A., Europe, E., Jansson, E. and Sylven, C. (1998) 'Exercise-based rehabilitation improves skeletal muscle capacity, exercise tolerance, and quality of life in both women and men with chronic heart failure', *J Card Fail*, 4(1), pp. 9–17.

Ulaner, G. A. and Giudice, L. C. (1997) 'Developmental regulation of telomerase activity in human fetal tissues during gestation', *Mol Hum Reprod*, 3, pp. 769–773.

Ulaner, G. A., Hu, J. F., Vu, T. H., Giudice, L. C. and Hoffman, A. R. (1998) 'Telomerase activity in human development is regulated by human telomerase reverse transcriptase (hTERT) transcription and by alternate splicing of hTERT transcripts', *Cancer Res*, 58(18), pp. 4168–72.

Ulaner, G. A., Hu, J. F., Vu, T. H., Oruganti, H., Giudice, L. C. and Hoffman, A. R. (2000) 'Regulation of telomerase by alternate splicing of human telomerase reverse transcriptase (hTERT) in normal and neoplastic ovary, endometrium and myometrium', *International Journal of Cancer*, 85, pp. 330–335.

Underwood, D. C., Osborn, R. R., Bochnowicz, S., Webb, E. F., Rieman, D. J., Lee, J. C., Romanic, A. M., Adams, J. L., Hay, D. W. and Griswold, D. E. (2000) 'SB 239063, a p38 MAPK inhibitor, reduces neutrophilia, inflammatory cytokines, MMP-9, and fibrosis in lung', *Am J Physiol Lung Cell Mol Physiol*, 279, pp. L895–902.

Valavanidis, A., Vlachogianni, T. and Fiotakis C. (2009) '8-hydroxy-2'-deoxyguanosine (8-OHdG): A critical biomarker of oxidative stress and carcinogenesis', *J Environ Sci Health C Environ Carcinog Ecotoxicol Rev.*, 27, pp. 120–39.

Valenzuela, H. F. and Effros, R. B. (2002) 'Divergent telomerase and CD28 expression patterns in human CD4 and CD8 T cells following repeated encounters with the same antigenic stimulus', *Clinical Immunology*, 105, pp. 117–25.

Van der Merwe, P. A. and Dushek, O. (2011) 'Mechanisms for T cell receptor triggering', *Nature Review Immunology*, 11, pp. 47–55.

Van Hees, V. T., Fang, Z., Langford, J., Assah, F., Mohammad, A., da Silva, I. C., Trenell, M. I., White, T., Wareham, N. J. and Brage, S. (2014) 'Autocalibration of accelerometer data for free-living physical activity assessment using local gravity and temperature: an evaluation on four continents', *J Appl Physiol*, 117, pp. 738–44.

Van Hees, V. T., Gorzelnik, L., Dean León, E. C., Eder, M., Pias, M., Taherian, S., Ekelund, U., Renström, F., Franks, P. W., Horsch, A. and Brage, S. (2013) 'Separating movement and gravity components in an acceleration signal and implications for the assessment of human daily physical activity', *PLoS One*, 8(4), article ID. e61691.

van Puijvelde, G. H., van Es, T., van Wanrooij, E. J., Habets, K. L., de Vos, P. van der Zee, R., van Eden, W., van Berkel, T. J. and Kuiper, J. (2007) 'Induction of oral tolerance to HSP60 or an HSP60-peptide activates T cell regulation and reduces atherosclerosis', *Arterioscler Thromb Vasc Biol*, 27, pp. 2677–83.

van Steensel, B., and de Lange, T. (1997) 'Control of telomere length by the human telomeric protein TRF1', *Nature*, 385, pp. 740–743.

Veldman, T., Horikawa, I., Barrett, J. C. and Schlegel, R. (2001) 'Transcriptional activation of the telomerase hTERT gene by human papillomavirus type 16 E6 oncoprotein', *J. Virol.*, 75, pp. 4467–4472.

Venteicher, A. S. and Artandi, S. E. (2009) 'TCAB1: driving telomerase to Cajal bodies', *Cell Cycle*, 8, pp. 1329–1331.

von Boehmer, H., Teh, H. S. and Kisielow, P. (1989) 'The thymus selects the useful, neglects the useless and destroys the harmful', *Immunol. Today*, 10, pp. 57–61.

von Zglinicki, T., and Martin-Ruiz, C. M. (2005) 'Telomeres as biomarkers for ageing and age-related diseases', *Curr. Mol. Med.*, 5, pp. 197–203.

von Zglinicki, T., Pilger, R. and Sitte, N. (2000) 'Accumulation of single-strand breaks is the major cause of telomere shortening in human fibroblasts', *Free Radic. Biol. Med.*, 28, pp. 64–74.

von Zglinicki, T., Saretzki, G., Docke, W. and Lotze, C. (1995) 'Mild hyperoxia shortens telomeres and inhibits proliferation of fibroblasts: a model for senescence?', *Exp Cell Res*, 220, pp. 186–93.

von Zglinicki, T., Saretzki, G., Ladhoff, J., d'Adda di Fagagna, F. and Jackson, S. P. (2005) 'Human cell senescence as a DNA damage response', *Mech. Ageing Dev.*, 126, pp. 111–117.

Vukmanovic-Stejic, M., Zhang, Y., Cook, J. E., Fletcher, J. M., McQuaid, A., Masters, J. E., Rustin, M. H., Taams, L. S., Beverley, P. C., Macallan, D. C., and Akbar, A. N. (2006) 'Human CD4CD25hiFoxp3 regulatory T cells are derived by rapid turnover of memory populations in vivo', *J. Clin. Invest.*, 116, pp. 2423–2433.

Wallace, D. L., M. Berard, M. V. Soares, J. Oldham, J. E. Cook, A. N. Akbar, D. F. Tough, and P. C. Beverley. (2006) 'Prolonged exposure of naive CD8 T cells to interleukin-7 or interleukin-15 stimulates proliferation without differentiation or loss of telomere length', *Immunology*, 119, pp. 243–253.

Wang, F. and Lei, M. (2011) 'Human telomere POT1-TPP1 complex and its role in telomerase activity regulation', *Methods Mol Biol.*, 735, pp. 173–187.

Wang, F., Podell, E. R., Zaug, A. J., Yang, Y., Baciu, P., Cech, T. R., Lei, M. (2007) 'The POT1-TPP1 telomere complex is a telomerase processivity factor', *Nature*, 445, pp. 506–510.

Wang, Y. –X., Halks-Miller, M., Vergona, R., Sullivan, M. E., Fitch, R., Mallari, C., Martin-McNulty, B., da Cunha, V., Freay, A., Rubanyi, G. M. and Kauser, K. (2000) 'Increased aortic stiffness assessed by pulse wave velocity in apolipoprotein E-deficient mice', *Am J Physiol Heart Circ Physiol.*, 278(2), pp. H428–34.

Wang, Y. X. (2005) 'Cardiovascular functional phenotypes and pharmacological responses in apolipoprotein E deficient mice', *Neurobiol Aging*, 26, pp. 309–16.

Wang, Z., Rhee, D. B., Lu, J., Bohr, C. T., Zhou, F., Vallabhaneni, H., de Souza-Pinto, N. C. and Liu, Y. (2010) 'Characterization of oxidative guanine damage and repair in mammalian telomeres', *PLoS Genet.*, 6, article ID. e1000951.

Watson, J. D. (1972) 'Origin of concatameric T4 DNA', *Nature*, 239, pp. 197–201.

Wellinger, R. J., Ethier, K., Labrecque, P., and Zakian, V. A. (1996) 'Evidence for a new step in telomere maintenance', *Cell*, 85(3), pp. 423–433.

Weng, N. P., Palmer, L. D., Levine, B. L., Lane, H. C., June, C. H. and Hodes, R. J. (1997) 'Tales of tails: regulation of telomere length and telomerase activity during lymphocyte development, differentiation, activation and aging', *Immunol Rev*, 160, pp. 43–54.

Weng, N. P., Hathcock, K. S. and Hodes, R. J. (1998) 'Regulation of telomere length and telomerase in T and B cells: a mechanism for maintaining replicative potential', *Immunity*, 9, pp. 151–7.

Weng, N. P., Levine, B. L., June, C. H. and Hodes, R. J. (1995) 'Human naive and memory T lymphocytes differ in telomeric length and replicative potential', *Proc Natl Acad Sci USA*, 92, pp. 11091–4.

Weng, N. P., Liu, K. Catalfamo, M. Li, Y. and Henkart, P. A. (2002) 'IL-15 is a growth factor and an activator of CD8 memory T cells', *Ann. NY Acad. Sci.*, 975, pp. 46–56.

Weng, N., Levine, B. L., June, C. H., and Hodes, R. J. (1996) 'Regulated expression of telomerase activity in human T lymphocyte development and activation', *J. Exp. Med.*, 183, pp. 2471–2479.

Wenger, N. K., Froelicher, E. S., Smith, L. K., Ades, P. A., Berra, K., Blumenthal, J. A., Certo, C. M. E., Dattilo, A. M., Davis, D., DeBosk, R. F., Drozda, J. P., Fletcher, B. J., Franklin, B. A., Gaston, H., Greenland, P., McBride, P. E., McGregor, C. G. A., Oldridge, N. B., Piscatella, J. C. and Rogers, F. J. (1995) *Cardiac Rehabilitation. Clinical Practice Guideline No. 17*. Rockville, Md: US Department of Health and Human Services, Public Health Service, Agencies for Health Care Policy and Research, and the National Heart, Lung, and Blood Institute, ACHCPR Publication No. 96-0672.

Werner, C., Furster, T., Widmann, T. Pöss, J., Roggia, C., Hanhoun, M., Scharhag, J., Büchner, N., Meyer, T., Kindermann, W., Haendeler, J., Böhm, M. and Laufs, U. (2009) 'Physical exercise prevents cellular senescence in circulating leukocytes and in the vessel wall', *Circulation*, 120(24), pp. 2438–47.

Werner, C., Gensch, C., Poss, J., Haendeler, J., Bohm, M. and Laufs, U. (2011) 'Pioglitazone activates aortic telomerase and prevents stress-induced endothelial apoptosis', *Atherosclerosis*, 216, pp. 23–34.

Werner, C., Hanhoun, M., Widmann, T., Kazakov, A., Semenov, A., Pöss, J., Bauersachs, J., Thum, T., Pfreundschuh, M., Müller, P., Haendeler, J., Böhm, M. and Laufs, U. (2008) 'Effects of physical exercise on myocardial telomere-regulating proteins, survival pathways, and apoptosis', *J Am Coll Cardiol*, 52, pp. 470–82.

Werness, B. A., Levine, A. J. and Howley, P. M. (1990) 'Association of human papillomavirus types 16 and 18 E6 proteins with p53', *Science*, 248, pp. 76–79.

Whitmarsh, A. J. and Davis, R. J. (1996) 'Transcription factor AP-1 regulation by mitogen-activated protein kinase signal transduction pathways' *J. Mol. Med.*, 74, pp. 589–607.

Widmann, C., Gibson, S., Jarpe, M. B. and Johnson, G. L. (1999) 'Mitogen-activated protein kinase: conservation of a three-kinase module from yeast to human', *Physiol Rev*, 79(1), pp. 143–80.

Wikipedia: https://en.wikipedia.org/wiki/Reporter_gene

Williams, H., Johnson, J. L., Carson, K. G. S., and Jackson, C. L. (2002) 'Characteristics of intact and ruptured atherosclerotic plaques in brachiocephalic arteries of apolipoprotein E knockout mice', *Arterioscler Thromb Vasc Biol.*, 22, pp. 788–792.

Wong, J. M., Kusdral, L. and Collins, K. (2002) 'Subnuclear shuttling of human telomerase induced by transformation and DNA damage', *Nat. Cell Biol.*, 4, pp. 731–736.

Woods, J. A., Ceddia, M. A., Wolters, B. W., Evans, J. K., Lu, Q. and McAuley, E. (1999) 'Effects of 6 months of moderate aerobic exercise training on immune function in the elderly', *Mech Ageing Dev*, 109, pp. 1–19.

Woods, J. A., Ceddia, M. A., Zack, M. D., Lowder, T. W. and Lu, Q. (2003) 'Exercise training increases the naive to memory T cell ratio in old mice', *Brain Behav Immun*, 17, pp. 384–92.

Woods, J., Lu, Q., Ceddia, M. A. and Lowder, T. (2000) 'Special feature for the Olympics: effects of exercise on the immune system: exercise-induced modulation of macrophage function', *Immunol Cell Biol*, 78, pp. 545–53.

Wyllie, F. S., Jones, C. J., Skinner, J. W., Haughton, M. F., Wallis, C., Wynford-Thomas, D., Faragher, R. G. and Kipling, D. (2000) 'Telomerase prevents the accelerated cell ageing of Werner syndrome fibroblasts', *Nat Genet*, 24, pp. 16–17.

Xin, H., Liu, D., Wan, M., Safari, A., Kim, H., Sun, W., O'Connor, M. S. and Songyang, Z. (2007) 'TPP1 is a homologue of ciliate TEBP-beta and interacts with POT1 to recruit telomerase', *Nature*, 445, pp. 559–562.

Xiong, J., Armato, M. A. and Yankee, T. M. (2011) 'Immature single-positive CD8+ thymocytes represent the transition from Notch-dependent to Notch-independent T-cell development', *International Immunology*, 23, pp. 55–64.

Xu, D., Popov, N., Hou, M., Wang, Q., Bjorkholm, M., Gruber, A., Menkel, A. R. and Henriksson, M. (2001) 'Switch from Myc/Max to Mad1/Max binding and decrease in histone acetylation at the telomerase reverse transcriptase promoter during differentiation of HL60 cells', *Proc. Natl. Acad. Sci. USA*, 98, pp. 3826–3831.

Yan, X., Anzai, A., Katsumata, Y., Matsuhashi, T., Ito, K., Endo, J., Yamamoto, T., Takeshima, A., Shinmura, K., Shen, W., Fukuda, K. and Sano, M. (2013) 'Temporal dynamics of cardiac immune cell accumulation following acute myocardial infarction', *J Mol Cell Cardiol*, 62, pp. 24–35.

Yan, X., Shichita, T., Katsumata, Y., Matsuhashi, T., Ito, H., Ito, K., Anzai, A., Endo, J., Tamura, Y., Kimura, K., Fujita, J., Shinmura, K., Shen, W., Yoshimura, A., Fukuda, K. and Sano, M. (2012) 'Deleterious effect of the IL-23/IL-17A axis and $\gamma\delta T$ cells on left ventricular remodeling after myocardial infarction', *J Am Heart Assoc.*, 1(5), article ID. e004408.

Yan, Z. and Banerjee, R. (2010) 'Redox remodeling as an immunoregulatory strategy', *Biochemistry*, 49, pp. 1059–66.

Yan, Z., Garg, S. K. and Banerjee, R. (2010) 'Regulatory T cells interfere with glutathione metabolism in dendritic cells and T cells', *J Biol Chem*, 285, pp. 41525–32.

Yang, J., H. Zhu, T. L. Murphy, W. Ouyang, and K. M. Murphy. (2001) 'IL-18- stimulated GADD45 β required in cytokine-induced, but not TCR-induced, IFN- production', *Nat. Immunol*, 2, pp. 157–164.

Yang, Z., Zingarelli, B. and Szabo, C. (2000) 'Crucial role of endogenous interleukin-10 production in myocardial ischemia/reperfusion injury', *Circulation*, 101, pp. 1019–26.

Yasutomo, K., Doyle, C., Miele, L., Fuchs, C. and Germain, R. N. (2000) 'The duration of antigen receptor signalling determines CD4+ versus CD8+ T-cell lineage fate', *Nature*, 4040, pp. 506–10.

Yi, C.X., Al-Massadi, O., Donelan, E., Lehti, M., Weber, J., Ress, C., Trivedi, C., Müller, T. D., Woods, S. C. and Hofmann S. M. (2012) 'Exercise protects against high-fat diet-induced hypothalamic inflammation', *Physiol. Behav.* 106, pp. 485–490.

Yi, X., White, D. M., Aisner, D. L., Baur, J. A., Wright, W. E. and Shay, J. W. (2000) 'An alternate splicing variant of the human telomerase catalytic subunit inhibits telomerase activity', *Neoplasia*, 2, pp. 433–440.

Young, H. A. and Hardy, K. J. (1995) 'Role of interferon-gamma in immune cell regulation', *Journal of Leukocyte Biology*, 58, pp. 373–81.

Yu, J. J. and Gaffen, S. L. (2008) 'Interleukin-17: a novel inflammatory cytokine that bridges innate and adaptive immunity', *Frontiers in Biosciences*, 13, pp. 170–7.

Zal, B., Kaski, J. C., Arno, G. Akiyu, J. P., Xu, Q., Cole, D., Whelan, M., Russell, N., Madrigal, J. A., Dodi, I. A. and Baboonian, C. (2004) 'Heat-shock protein 60-reactive CD4 +CD28null T cells in patients with acute coronary syndromes', *Circulation*, 109, pp. 1230–5.

Zarubin, T. and Han, J. (2005) 'Activation and signaling of the p38 MAP kinase pathway', *Cell Res.*, 15, pp. 11–18.

Zee, R. Y., Michaud, S. E. and Ridker, P. M. (2009) 'Mean telomere length and risk of incident venous thromboembolism: a prospective, nested case-control approach', *Clin Chim Acta*, 406, pp. 148–50.

Zee, R.Y., Michaud, S. E., Germer, S. and Ridker, P. M. (2009) 'Association of shorter mean telomere length with risk of incident myocardial infarction: a prospective, nested case-control approach', *Clin Chim Acta*, 403, pp. 139–41.

Zhang, J., Perry, G., Smith, M. A., Robertson, D., Olson, S. J., Graham, D. G. and Montine, T. J. (1999) 'Parkinson's disease is associated with oxidative damage to cytoplasmic DNA, RNA in substantia nigra neurons', *Am J Pathol*, 154, pp. 1423–1429.

Zhang, K. R., Liu, H. T., Zhang, H. F., Zhang, Q. J., Li, Q. X., Yu, Q. J., Guo, W. Y., Wang, H. C. and Gao, F. (2007) 'Long-term aerobic exercise protects the heart against ischemia/reperfusion injury via PI3 kinase-dependent and akt-mediated mechanism', *Apoptosis*, 12, pp. 1579–1588.

Zhang, P., Chan, S. L., Fu, W., Mendoza, M. and Mattson, M. P. (2003) 'TERT suppresses apoptosis at a premitochondrial step by a mechanism requiring reverse transcriptase activity and 14-3-3 protein-binding ability', *FASEB J.*, 17, pp. 767-9.

Zhang, S. H., Reddick, R. L., Piedrahita, J. A., Maeda, N. (1992) 'Spontaneous hypercholesterolemia and arterial lesions in mice lacking apolipoprotein E', *Science*, 258, pp. 468-471.

Zhao, H., Kalivendi, S., Zhang, H., Joseph, J., Nithipatikom, K., Vasquez-Vivar, J. and Kalyanaraman, B. (2003) 'Superoxide reacts with hydroethidine but forms a fluorescent product that is distinctly different from ethidium: potential implications in intracellular fluorescence detection of superoxide', *Free Radic Biol Med*, 34(11), pp. 1359–68.

Zhao, Z., Wu, Y., Cheng, M., Ji, Y., Yang, X., Liu, P., Jia, S. and Yuan, Z. (2011) 'Activation of Th17/Th1 and Th1, but not Th17, is associated with the acute cardiac event in patients with acute coronary syndrome', *Atherosclerosis*, 217, pp. 518–524.

Zhong, X-P., Guo, R., Zhou, H., Liu, C. and Wan, C-K. (2008) 'Diacylglycerol kinases in immune cell function and self-tolerance', *Immunological Reviews*, 224, pp. 249-264.

Zhou, X. Z. and Lu, K. P. (2001) 'The Pin2/TRF1-interacting protein PinX1 is a potent telomerase inhibitor', *Cell*, 107, pp. 347–359.

Zhou, X., Nicoletti, A., Elhage, R. and Hansson, G. K. (2000) 'Transfer of CD4+ T cells aggravates atherosclerosis in immunodeficient apolipoprotein E knockout mice', *Circulation*, 102, pp. 2919–22.

Zhou, X., Paulsson, G., Stemme, S. and Hansson, G. K. (1998) 'Hypercholesterolemia is associated with a T helper (Th) 1/Th2 switch of the autoimmune response in atherosclerotic apo E-knockout mice', *J Clin Invest*, 101, pp. 1717–25.

Zhu, J. and Paul, W. E. (2008) 'CD4 T cells: fates, functions, and faults', *Blood*, 112, pp. 1557–69.

Zhu, J., Jankovic, D., Grinberg, A., Guo, L., and Paul, W. E. (2006) 'Gfi-1 plays an important role in IL-2- mediated Th2 cell expansion', *Proceedings of the National Academy of Sciences of the United States of America*, 103, pp. 18214–18219.

Zhuang, X.Y. and Yao, Y. G. (2013) 'Mitochondrial dysfunction and nuclear-mitochondrial shuttling of TERT are involved in cell proliferation arrest induced by G-quadruplex ligands', *FEBS Lett.*, 587, pp. 1656-62.

Ziccardi, P., Nappo, F., Giugliano, G., Esposito, K., Marfella, R., Cioffi, M., D'Andrea, F., Molinari, A. M. and Giugliano, D. (2002) 'Reduction of inflammatory cytokine concentrations and improvement of endothelial function in obese women after weight loss over one year', *Circulation*, 105, pp. 804–809.